ACCELERATORS: ENGINES FOR TRAVERSING A LARGE AND OFTEN DIFFICULT LANDSCAPE*

Andrew M. Sessler
Lawrence Berkeley National Laboratory, Berkeley, CA 94720, USA
Dedicated, with fond memories, to Dieter Moehl and Andre Lebedev

Abstract

The many applications of accelerators are presented, with pictures and comments, upon the machines and the results obtained with them. Attention is then given to possible future applications, and some remarks are made on the future development of accelerators. In short, the presentation should serve as an introduction to the Conference itself where there shall be many – wonderfully detailed – contributions to all of this.

INTRODUCTION

In this paper I will try to show – all in only five pages – the breadth of accelerator types and, more importantly, the many uses (applications) of particle accelerators. For a number of decades, starting in about 1930, accelerators were used primarily for nuclear and then high-energy physics. This wasn't exclusively true, for even in the 1930's Lawrence was employing his cyclotrons for medical purposes, but it was almost exclusively true.

However, now-a-days accelerators are widely used for many different purposes. Essentially all these accelerators are of a type particularly chosen for the application and specially designed to the particular use. This short report can't possibly go into the details --- which is the heart of the subject (and the topic of many contributions at this Conference) – but can only show the general sweep and extent of these applications. Nevertheless, it should prove interesting, especially to the many deep into the details of some particular application, to look broadly and see how extensive is the range of application of particle accelerators.

TYPES OF ACCELERATORS

There are some 30,000 accelerators in the world and these are of the six major types, or small modifications of these types. That is there are electrostatic machines, cyclotrons, linacs, betatrons, synchrotrons or colliders. We are all rather familiar with modern versions of these machines, but perhaps not many of us have looked back at their humble beginnings. In Fig. 1 is shown the very beginning; namely the first electrostatic machine that was able to fulfill Rutherford's dream, which was to achieve artificial radioactivity.

Looking to the future – and surely – the future will contain ever-more of the types mentioned; there may well be two very different accelerators. The first is an accelerator of muons. True, this may be a linac or a synchrotron at its heart, and culminate in a collider, but the handling of the short lifetime muon would seem to justify considering this a new type of accelerator. Muons are diffusely produced in hadron collisions, so they must be captured and "cooled" into a beam; a non-trivial task. A section of the proposed 2D cooling channel is incorporated in the experimental demonstration of cooling: Muon Ionization Cooling Experiment (MICE). This is an international collaboration and is underway at the Rutherford-Appleton Laboratories.

The second is the use of lasers and plasmas as accelerators. Effort is this direction has gone on for decades, and 1 GeV of acceleration has been achieved, but much still remains to be accomplished before the method produces a practical accelerator. Two methods are under particular study; a wakefield accelerator at SLAC and a laser/plasma accelerator at LBNL. Of course there is activity in many other places.

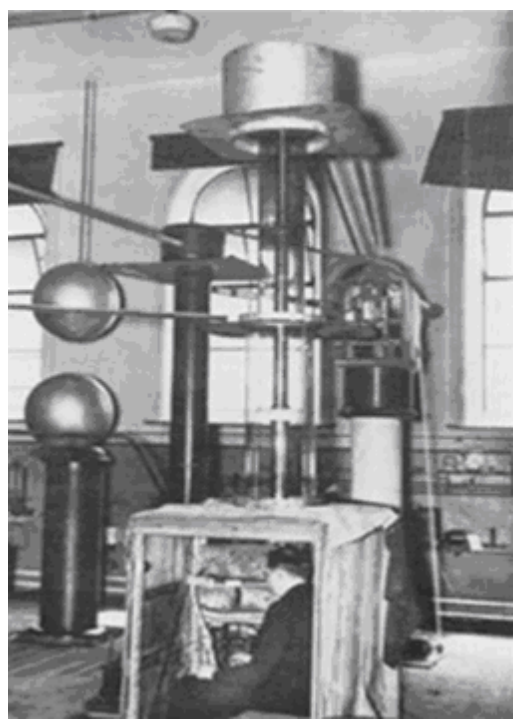

Figure 1: The first electrostatic accelerator. The original Cockcroft-Walton installation at Cavendish Laboratory in Cambridge. Walton is sitting in the observation cubicle (experimental area) immediately below the acceleration tube.

* This work was supported by the Director, Office of Science, and Program Office of High Energy Physics, of the U.S. Department of Energy under Contract No. DE-AC02-05-H11231.

ISBN 978-3-95450-125-0

NICA PROJECT AT JINR

N. Agapov, V. Kekelidze, R. Lednicky, V. Matveev, I. Meshkov*,
A. Sorin, G. Trubnikov, JINR, Russia

Abstract

The project of Nuclotron-based Ion Collider fAcility NICA/MPD (MultiPurpose Detector) under development at JINR (Dubna) is presented. The general goals of the project are providing of colliding beams for experimental studies of both hot and dense strongly interacting baryonic matter and spin physics (in collisions of polarized protons and deuterons). The first program requires providing of heavy ion collisions in the energy range of $\sqrt{s_{NN}} = 4 \div 11$ GeV at average luminosity of $L = 1 \cdot 10^{27}$ cm^{-2}·s^{-1} for $^{197}Au^{79+}$ nuclei. The polarized beams mode is proposed to be used in energy range of $\sqrt{s_{NN}} = 12 \div 27$ GeV (protons) at luminosity of $L \geq 1 \cdot 10^{30}$ cm^{-2}·s^{-1}. The key issue of the Project is application of cooling methods – stochastic and electron ones. The report contains description of the facility scheme and characteristics in heavy ion operation mode, status and plans of the project development.

NUCLOTRON-M & NICA PROJECT

The **N**uclotron-based **I**on **C**ollider f**A**cility (NICA) [1] is a new accelerator complex (Fig. 1) being constructed at JINR. It is aimed to provide collider experiments with*)

- heavy ions $^{197}Au^{79+}$ at $\sqrt{s_{NN}} = 4 \div 11$ GeV (1÷4.5 GeV/u ion kinetic energy) at average luminosity of $1 \cdot 10^{27}$ cm^{-2}·s^{-1} (at $\sqrt{s_{NN}} = 9$ GeV);
- light-heavy ions colliding beams of the same energy range and luminosity;
- polarized beams of protons $\sqrt{s} = 12 \div 27$ GeV (5÷12.6 GeV kinetic energy) and deuterons $\sqrt{s_{NN}} = 4 \div 13.8$ GeV (2÷5.9 GeV/u ion kinetic energy) at average luminosity $\geq (1 \div 10) \cdot 10^{30}$ cm^{-2}·s^{-1}.

The proposed facility consists of the following elements (Fig. 1):

– "*Old*" *injector* (pos. 1): set of light ion sources including source of polarized protons and deuterons and Alvarez-type linac LU-20*);

– "*New*" *injector* (pos. 2, under construction): ESIS-type ion source that provides $^{197}Au^{31+}$ ions of the intensity of $2 \cdot 10^9$ ions per pulse of about 7 μs duration at repetition rate up to 50 Hz and linear accelerator consisting of RFQ and RFQ Drift Tube Linac (RFQ DTL) sections. The linac accelerates the ions at $A/q \leq 8$ up to the energy of 6 MeV/u at efficiency not less than 80 %.

– *Booster-synchrotron* housed inside Synchrophasotron yoke (pos. 3). The Booster (pos. 4) has superconducting (SC) magnetic system that provides maximum magnetic rigidity of 25 T·m at the ring circumference of 215 m. It is equipped with electron cooling system that allows to provide cooling of the ion beam in the energy range from injection energy up to 100 MeV/u. The maximum energy of $^{197}Au^{31+}$ ions accelerated in the Booster is of 600 MeV/u. Stripping foil placed in the transfer line from the Booster to the Nuclotron allows to provide the stripping efficiency at the maximum Booster energy not less than 80 %.

– *Nuclotron* – SC proton synchrotron (pos. 5) has maximum magnetic rigidity of 45 T·m and the circumference of 251.52 m provides the acceleration of completely stripped $^{197}Au^{79+}$ ions up to the experiment energy in energy range of 1÷4.5 GeV/u and protons up to maximum energy of 12.6 GeV.

– *Transfer line* (pos. 6) transports the particles from Nuclotron to Collider rings.

– *Two SC collider rings* (pos. 8) of racetrack shape have maximum magnetic rigidity of 45 T·m and the circumference of about 400 m. The maximum field of SC dipole magnets is 1.8 T. For luminosity preservation an electron and stochastic cooling systems will be constructed.

– *Two detectors* – MultiPurpose Detector (*MPD*, pos. 9) and Spin Physics Detector (*SPD*, pos. 10) are located in opposite straight sections of the racetrack rings.

– *Two transfer lines* transport particle beams extracted from Booster (pos. 11) and Nuclotron (pos. 12) to the new research area, where fixed target experiments both basic and applied character will be placed.

The NICA parameters (Table below) allow us to reach the goals of the project formulated above.

One of NICA accelerators – Nuclotron is used presently for fixed target experiments on extracted beams (Fig. 1, pos. 7).

This program is planned to be developed further and will be complementary to that one to be performed at Collider in heavy ions beam mode operation. The program includes experimental studies on relativistic nuclear physics, spin physics in few body nuclear systems (with polarized deuterons) and physics of flavours. At the same time, the Nuclotron beams are used for research in radiobiology and applied research.

*Corresponding author: meshkov@jinr.ru

ISBN 978-3-95450-125-0

LASER-PLASMA ACCELERATION – TOWARDS A COMPACT X-RAY LIGHT SOURCE AND FEL

Andrei Seryi, John Adams Institute for Accelerator Science, UK

Abstract

Advances in many scientific and technical fields depend on availability of instruments, which can probe the structure of materials or molecules on unprecedented levels of spatial or temporal resolution. Many of such instruments are based on accelerators of charged particles, with particular examples of synchrotron radiation light sources and coherent X-ray Free Electron Lasers. The high cost of such facilities, however, preclude wide spread of such instruments. Modern accelerator science witnesses emergence of a new direction – compact x-ray sources are coming to the scene, enabled by the synergy of accelerators and lasers, where high gradient laser-plasma acceleration can significantly reduce the size and cost of the facilities. Compact x-ray sources will be developed in the nearest future and will share their scientific and market niche with large national scale x-ray facilities. The compact sources will in particular be suitable for placement in universities and medical or technological centres. The compact x-ray light sources are being developed by many centres in UK. Development of compact x-ray FEL is a promising topic for scientific and technological collaboration between UK and Russia, where expertise of partners will cross-fertilize their ability to solve scientific and technological challenges.

ACCELERATOR SCIENCE AND TECHNOLOGICAL PROGRESS

Science is a driver for the economy. This is a commonly accepted statement —however, the mechanisms of the impact are complicated and their analysis is necessary not only from a philosophical point of view, but also in order to optimize research priorities and define the strategy for technological innovation.

Particle accelerators have already impacted many areas of our lives via their medical and industrial use, and in research instruments. Tens of millions of patients receive accelerator-based diagnoses and treatment each year around the world, and the total annual market value for all products that are treated or inspected by accelerators is more than US$500B [1]. Approximately 30% of the Nobel Prizes in physics, as well as many in other areas, are directly connected to the use of accelerators [2].

The ideas that enabled use of accelerators in everyday life and industry were developed decades ago; therefore, new ideas will be essential for ensuring the future impact of this field. Analysis of the mechanisms how accelerator science affects the economy and technological progress is needed in order to make predictions and optimise the future directions of research. In the text presented below in this section, we follow the approach and views expressed by the author earlier in [3], [4] and [5].

One of the attempts to analyze the model for research and technology transfer was done by the famous Vannevar Bush, who, during the WWII, was instrumental in reorganizing the research and science community according to the needs of that difficult time. Vannevar Bush's post-war report, "Science, the Endless Frontier", prepared for the USA President, has defined the post-war scientific policy in the USA and in many other countries for decades to come.

In this report, Bush describes what will later be called a one-dimensional or linear model for research and technology transfer. In this report, Bush, in particular, claims that research that is more basic is less applied and vice versa. According to Bush, applied research invariably drives out pure if the two are mixed, and therefore basic research must be completely isolated from considerations of use.

Correspondingly, the dynamic linear model of technology transfer looks like a pipeline wherein government funding stimulates basic research, which then in turn feeds to applied research, which then results in technology and product development, with eventual benefits for the society.

These views of the relationship between basic science and technological innovation have since then been analyzed, criticized, and a new model has been developed.

The contradiction between these linear models and practice can be illustrated via the example of accelerator science and technology. The invention of the so-called "strong focusing" in the fifties was a revolutionary change in accelerator technology. It enabled numerous applications. This invention may have come about as a result of pure fundamental interest— however it was developed as a result of the pursuit of a certain concrete goal, and was made possible due to certain technologies available at that time.

A new model of research and technology transfer was suggested by Donald Stokes, who worked on the Advisory Committee on Research for the USA National Science Foundation. In his report to NSF, and in the book he subsequently published [6], Donald Stokes argued against Bush's linear model and introduced the notion of use-inspired research, of "research with consideration to use", which redefined the paradigm of the relationship between basic science and technological innovation.

To illustrate his views, Donald Stokes suggested considering research on a two-dimensional plane, where the axis are fundamental knowledge impact and consideration of use.

A characteristic example of a purely fundamental scientific pursuit is the research works of Niels Bohr on the structure of nuclei, while the other examples are

ISBN 978-3-95450-125-0

DESIGN AND SIMULATION OF PRACTICAL ALTERNATING-PHASE-FOCUSED (APF) LINACS – SYNTHESIS AND EXTENSION IN TRIBUTE TO PIONEERING RUSSIAN APF RESEARCH

R. A. Jameson, Inst. Angewandte Physik, Goethe Uni Frankfurt, Max-von-Laue Str. 1, Frankfurt-am-Main, Germany

Abstract

A high fraction of the cost and complexity of conventional linacs lies in the use of magnetic transverse focusing. The strong-focusing effect of alternating patterns (sequences) of gap phases and amplitudes – known as Alternating-Phase-Focusing (APF) – can produce both transverse and longitudinal focusing from the rf field. APF has undeservedly been deemed largely impractical because simple schemes have low acceptances, but sophisticated schemes have produced short sequence APFs with good acceptances and acceleration rates that are now used in a number of practical applications. Suitable sequence design has been difficult, without direct theoretical support, inhibiting APF adoption. By synthesizing reported details and adding new physics and optimization technique, a new, general method for designing practical APF linacs is demonstrated, using simple dynamics and no space charge – incorporation of space-charge and more accurate elements is straight-forward. APF linacs can now be another practical approach in the linac designer's repertoire. APF can be used in addition to conventional magnetic focusing, and could be useful in minimizing the amount of additional magnetic focusing needed to handle a desired amount of beam current.

ALTERNATING PHASE FOCUSING

Particles exposed to an rf field in a gap may receive focusing or defocusing forces in the transverse and longitudinal directions, according to the phase and amplitude of the gap field. Arranging a sequence of gaps in some particular manner, termed here an "APF sequence", can provide large simultaneous transverse and longitudinal acceptances with high acceleration rates and good emittance preservation.

Typical transverse focusing and energy gain per unit length (dW/dz) forces over the full 360° range of rf phase (phi) are shown in Fig. 1.

There is no adequate theory for determining an APF sequence with acceleration. There are some APF linacs in operation, but their designs were laboriously produced by hand, and the sequences are short. Further APF development has also been hindered by a misconception that APF acceptances are necessarily small.

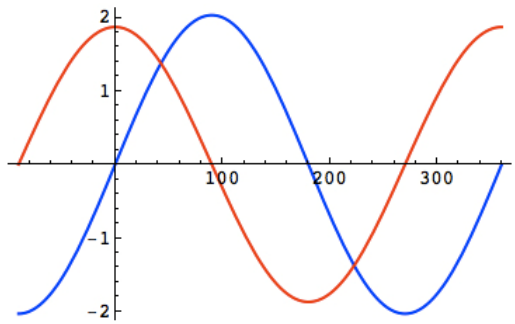

Fig. 1. Typical longitudinal acceleration (red) and transverse focusing forces (blue) over the full 360° range of phi.

THE APF SEQUENCE, AND SYNTHESIS OF A GENERAL METHOD

The most sophisticated work was realized in the USSR during the 1960's-1980's [1,2, and culminated in the "Garaschenko Sequence" [3], a 51-cell synchronous phase sequence for a 0.0147-1.0 MeV/u (factor 68), $_{238}U^{7+}$(qom=1/24), 6.8m, 25 MHz uranium-ion linac shown in Fig. 2, resulting from a complicated nonlinear optimization procedure to find the maximum longitudinal and transverse acceptances. The longitudinal acceptance was larger than for a typical RFQ.

A nonlinear optimization program must be given good enough starting points that it can converge to the correct optimum. Here the preliminary sequence was based on the extant schemes and a successfully operating APF linac at Dubna, which set out the general properties of the sequence in six separate focusing periods of 6-13 gaps and different spacings in each.

The great value of this paper is not that it helps find a good initial sequence, but that *it shows the form of an optimized sequence.* From this, we can draw very useful general conclusions. In particular, the full ±90° range can be used for high acceleration rate, and the period is extended as acceleration occurs to maintain the focusing strength, as with magnetic focusing.

During the next decades, work continued, especially in Russia by V.V. Kushin, V.K. Baev, and S. Minaev, who was a leading practitioner of actual APF designs until his death in 2010 and who influenced many extent APF designs. However, Minaev noted in [4] that "there is no theory for optimization of drift tube array so far" (i.e., for determining the underlying sequence); this is still the situation at this date. Summarizing details from the literature leads to a practical design method [5].

ISBN 978-3-95450-125-0

STATUS OF ELECTRON-POSITRON COLLIDER VEPP-2000*

D. Berkaev, A. Borisov, Yu. Garinov, A. Kirpotin, I. Koop,
A. Lysenko, I. Nesterenko, A. Otboyev, E. Perevedentsev, Yu. Rogovsky, A. Romanov,
P. Shatunov, D. Shwartz, A. Skrinsky, Yu. Shatunov#
Budker INP SB RAS, Novosibirsk, Russia

Abstract

The main goal of VEPP-2000 construction is to measure the cross sections of hadron production in e^+e^- annihilations and to collect an integral luminosity about few inverse femtobarns in the energy range 0.4 – 2 GeV. To reach these goals, the Round Beam Concept (RBC) was realized at VEPP-2000 collider. RBC requires equal emittances, equal small fractional tunes, equal beta functions at the IP, no betatron coupling in the arcs [1]. Such an approach results in conservation of the longitudinal component of particle's angular momentum. As a consequence, it yields an enhancement of dynamical stability, even with nonlinear effects from the beam-beam force taken into account.

The first beam was injected in VEPP-2000 machine 5 years ago and RBC was successfully tested at VEPP-2000 in 2008 [2]. Two experimental seasons in 2010-2012 were performed with two detectors SND and CMD3 in the energy range between 500 and 1000 MeV. Now, the total luminosity accumulated at VEPP-2000 is near to the final result of the VEPP-2M collider. The single bunch luminosity of 3×10^{31} $cm^{-2}s^{-1}$ was achieved together with a maximum beam-beam tuneshift as high as 0.15. At present, the work is in progress to increase the rate of positron delivery and upgrade the booster ring BEP for the beam transfer up to the top collider energy of 1 GeV.

COLLIDER OVERVIEW

The VEPP-2000 electron-positron collider has to operate in the beam energy range 0.2 – 1 GeV. It was constructed at the place of its predecessor VEPP-2M, using the existing beam production chain of accelerators: ILU – a pulsed RF cavity with a voltage of 2.5 MeV, a 250 MeV synchrotron B-3M and a booster storage ring BEP with the maximum beam energy of 800 MeV (see Fig. 1). The lattice of VEPP-2000 has a two-fold symmetry with two experimental straight sections of 3m length, where Cryogenic Magnetic Detector and Spherical Neutral Detector are located. Two other long straights (2.5m) are designed for injection of beams and RF cavity, and 4 short technical straight sections accommodate triplets of quadrupole magnets (max. gradient 50 T/m). To avoid dispersion in the detectors, RF cavity and injection straights, a pair of dipoles together with the triplet in between constitute 4 achromats. Chromaticity corrections are performed by two families of sextupole magnets located in the technical straight section, where the dispersion is high.

Design parameters of the collider are given in Table 1.

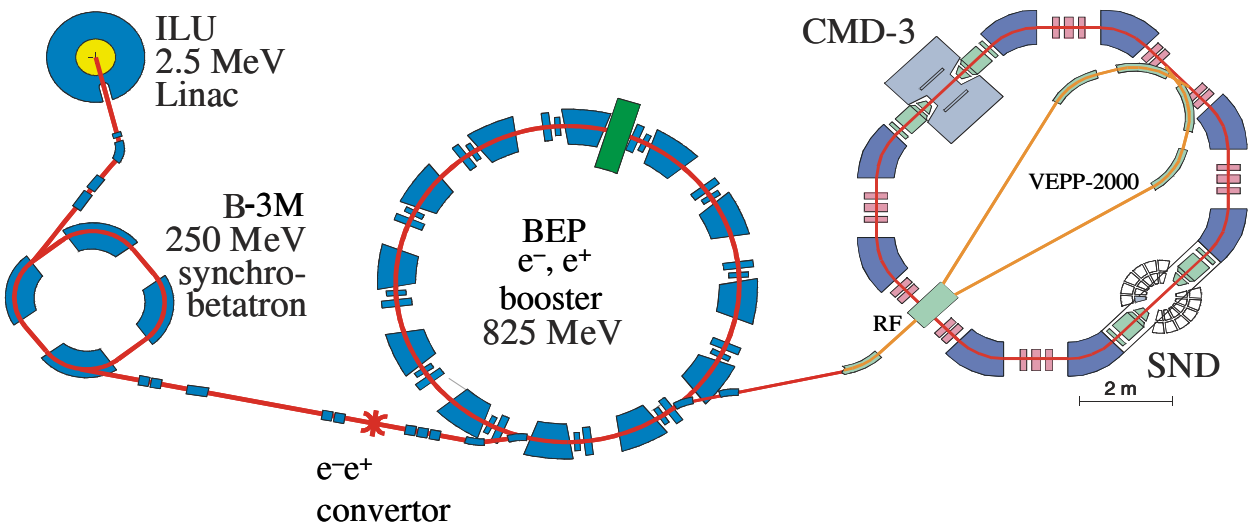

Figure 1: VEPP-2000 complex layout

* Work supported by Russian Ministry of Education and Science, basic project of BINP SB RAS 13.3.1, Physics branch of RAS project OFN.1.1.2, Scientific school NS-5207.2912.2 and Grant of the Novosibirsk region Government 2012
# Yu.M.Shatunov@inp.nsk.su

ISBN 978-3-95450-125-0

e^+e^- COLLIDER VEPP-4M: STATUS AND PROSPECTS

E.Levichev for the VEPP-4 team [1]
BINP, Novosibirsk 630090, Russia

Abstract

VEPP-4M is an electron-positron collider operating in the wide beam energy range from 0.9 GeV to 5.5 GeV. Since 2002 experiments on HEP are conducted at the collider with detector KEDR. Besides HEP, there are other scientific programs at the VEPP-4 accelerator complex including SR experiments, nuclear physics studies with internal gas target, CPT-theorem verification, accelerator physics experiments, etc. The paper discusses the recent results, present status and prospective plans of the facility.

INTRODUCTION

Starting from 2002 experiments are carried out with the universal magnetic detector KEDR [2] at the electron-positron collider VEPP-4M [3]. The VEPP-4M collider consists of the booster ring VEPP-3 with energy from 350 MeV to 2000 MeV and the main ring operating in the beam energy range from 0.9 GeV to 5.5 GeV. The physics program of the detector is focused on the study of ψ-, Υ-mesons and $\gamma\gamma$-physics. Precise mass measurements of J/ψ, $\psi(2s)$, $\psi(3770)$, D mesons and τ lepton were the goal of the first series of the experiments. Also electron partial width for J/ψ and ψ'-mesons were measured.

Table 1: Main Parameters of VEPP-4M.

Parameters	Values	Units
Circumference	366	m
Bending radius	34.5	m
Tunes Q_H/Q_V	8.54/7.58	
Mom. compaction	0.017	
Max. energy	5.5	GeV
Nat. chromaticity C_H/C_V	-13/-20	
RF-frequency	181.8	MHz
Harmonic number	222	
RF power	0.3	MW
RF voltage	5	MV
No.of bunches per beam	2	

The resonant depolarization (RD) technique [4] was used for precise instantaneous energy calibration. Continuous energy measurements were performed by determination of the utmost energy of the γ-quanta obtained from the Compton backscattering of laser photons against the electron beam [5, 6]. Main parameters of VEPP-4M are given in Table 1. The layout of the complex is shown in Fig.1.

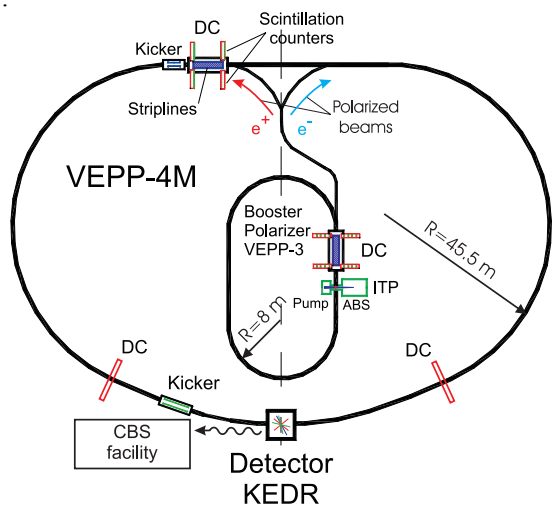

Fig.1: The VEPP-4 layout with main HEP experimental set-up: detector KEDR, Compton backscattering (CBS) system, gas internal target (ITP), counters (DC) and kickers for precise polarization experiments.

Besides the particles physics, there are other various experimental programs at VEPP-4 including studies with the synchrotron light, nuclear physics with polarized/unpolarized internal gas target, extracted test beam of e^- or γ for methodical goals, etc.

As the scientific program initially planned at 2000 for the decade is close to completion, it is good time for discussion of the results obtained and future plans.

HEP PROGRAM

In spite of rather moderate luminosity of the collider we were able to conduct experiments providing interesting and actual results due to the following factors:

- Wide beam energy span available for experiments that extends from 0.9 GeV to 5.5 GeV;
- The record-breaking accuracy (~10^{-6}) beam energy calibration that was developed at VEPP-4M with the help of the RD technique invented at BINP in the past;
- On-line monitoring of the beam energy during the luminosity run by Compton backscattering of the laser photons (accuracy is ~$3\cdot10^{-5}$);
- Universal magnetic detector KEDR with *LKr* calorimeter and Cherenkov aerogel counters with characteristics comparable with the best detectors in the world.

ISBN 978-3-95450-125-0

TECHNOLOGY DEVELOPMENTS FOR CLIC

H. Schmickler, CERN, Geneva, Switzerland

Abstract

Just after the publication of its Conceptual Design Report (CDR) the CLIC study has made detailed plans for necessary technology developments in the coming years. This program includes the development of fully working prototypes of several technical subsystems as well as first pre-series or industrialization concepts of components needed in large identical quantities. The presentation will explain the development program and show in particular fields for potential collaboration.

INTRODUCTION

CERN's latest and foremost accelerator, the LHC, will probe the "terascale" energy region and provide a rich program of physics at a new high-energy frontier over the coming years. In this energy domain, it will study the validity of the standard model and explore the possibilities for physics beyond the Standard Model, such as super-symmetry, extra dimensions and new gauge bosons. The discovery potential is huge and will set the direction for future high-energy colliders. Particle physicists worldwide supported by ICFA [1] have reached a consensus that the results of the LHC will need to be complemented by experiments at a lepton collider in the Tera-Electron-Volt (TeV) energy range. The required beam collision energy range will be better defined following Physics requirements based on LHC results when substantial integrated luminosity will have been accumulated, tentatively by 2013-15.

The highest energy of lepton collisions so far, 209 GeV, was reached with electron–positron colliding in LEP at CERN. In spite of the 27 km diameter of LEP, beam energy was limited by synchrotron radiation losses just compensated by the most powerful super-conducting RF system built so far and providing up to 3640 MV per revolution. Since synchrotron radiation is inversely proportional to the bending radius and proportional to the fourth power of the particle mass, two alternatives are being explored to overcome this limitation and build a terascale lepton collider:

- use muons with a mass 207 times larger than electrons. The feasibility of Muon Colliders is being studied [2] addressing critical challenges specially the limited muon lifetime and their production in large emittances requiring developments of novel cooling methods,
- mitigate bends of particle trajectories in e+/- linear colliders where two opposing linear accelerators accelerate the particles to their final energy in one pass before focusing and collision in a central interaction point inside a detector.

Following preliminary Physics studies based on an electron-positron collider in the multi-TeV energy range [2,3], the CLIC study is focused on the design of a linear collider with a colliding beam energy of 3 TeV and a luminosity of 2.10^{34} cm-2 s-1 at the extreme of the considered parameter space. A scaled-down design is deduced at a lower energy, arbitrarily set at 500 GeV with the same luminosity for comparison with the alternative ILC technology.

The layouts of a 3 TeV linear collider using the CLIC technology is displayed in Fig 1.

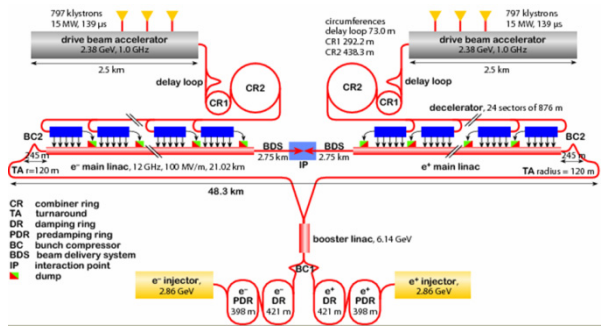

Figure 1: Layout of a 3 TeV cms energy linear collider based on the CLIC specific two-beam acceleration scheme.

WHY TWO-BEAM ACCELERATION?

In order not to confuse the arguments, no explicit references are given in this section. All important
Details including further references can be found in the CLIC Conceptual Design Report [4].

– The main objective is to build at reasonable cost and at a reasonable size a linear collider for the Multi-TeV range. This requires a very high acceleration gradient (100 MV/m), which cannot be achieved with super-conducting technology.

– For a given breakdown rate there is a very steep scaling between gradient and RF pulse length, hence the beam pulse has to be limited to about 150 ns. This short beam pulse is the fundamental design parameter, which has major consequences for the physics analysis of the events, for beam parameters to achieve the required luminosity, and for the RF power generation.

– In a circular accelerator the counter-rotating beams collide with a high repetition frequency, typically in the tens of kHz range. The repetition frequency of a linear collider by contrast is typically only 5–100 Hz. The luminosity necessary for the particle physics experiments has then to be reached with challenging parameters for bunch charge, beam emittance, and strength of the final focusing magnets. In the case of CLIC about 300 bunches

ISBN 978-3-95450-125-0

STORAGE, ACCELERATION AND SHORT BUNCHED BEAM FORMATION OF $^{197}AU^{+79}$ IONS IN THE NICA COLLIDER

A.V. Eliseev, O.S. Kozlov, I.N. Meshkov, A.V. Sidorin, A.V.Smirnov, G.V. Trubnikov,
JINR, Dubna, Moscow Region, Russia
T. Katayama, GSI, Darmstadt, Germany
V.N. Volkov, E.K.Kenzhebulatov, G.Y. Kurkin, V.M. Petrov, BINP SB RAS, Novosibirsk, Russia

Abstract

The regimes of high intensity beam of $^{197}Au^{+79}$ ions in NICA Collider are considered. The first stage – ion storage is proposed to be performed with Barrier Bucket technique at ion energy of 1 – 4.5 GeV/u. Ion accumulation at optimum for cooling energy level accompanied by slow acceleration with the same BB method to the energy of experiment also considered. Formation of bunched beam is fulfilled in two steps – first, at 24th harmonics and then, final formation, at 72th harmonics of the revolution frequency. The possibility of achievement of designed bunch parameters is shown.

INTRODUCTION

The goal of the NICA facility in the heavy ion collision mode is to reach the luminosity level of the order of 10^{27} $cm^{-2}s^{-1}$ in the energy range from 1Gev/u to 4.5 Gev/u. Collider circumference is 503 m and beta-function in IP is supposed to be 0.35m. The beam parameters required to achieve the design luminosity are listed in the Table 1 [1]:

Table 1: $^{197}Au^{+79}$ beam parameters

Number of bunches	24		
Rms bunch length	0.6m		
Ion energy, GeV/u	1	3.0	4.5
Ion number per bunch	$2.75\cdot10^8$	$2.4\cdot10^9$	$2.2\cdot10^9$
Rms dp/p, 10^{-3}	0.62	1.25	1.65
Rms beam emittance, h/v, (unnormalized), π·mm·mrad	1.1/ 1.01	1.1/ 0.89	1.1/ 0.76

Collider RF systems have to provide:

- Accumulation of required numbers of Ions in the energy range 1÷4.5 Gev/u.
- Accumulation at some optimum energy and acceleration up to the energy of experiment
- Formation of necessary number of bunches (24)
- Achievement of designed bunch parameters

This can be done with the help of three RF systems: one broad band type and two narrow-bands. The first one accumulates particles in longitudinal phase space with application of RF barrier bucket (BB) technique. By applying additional voltage meander between barriers it can be used also for acceleration (inductive acceleration). Second RF system works on 24-th harmonics of revolution frequency and is used for formation of proper number of bunches. The third RF system is used for the final bunch formation and maintenance bunch parameters during collision mode.

All stages of bunch formation as well as collision mode are accompanied by cooling process either stochastic or electron. General scheme of beam preparation is represented in the Fig. 1.

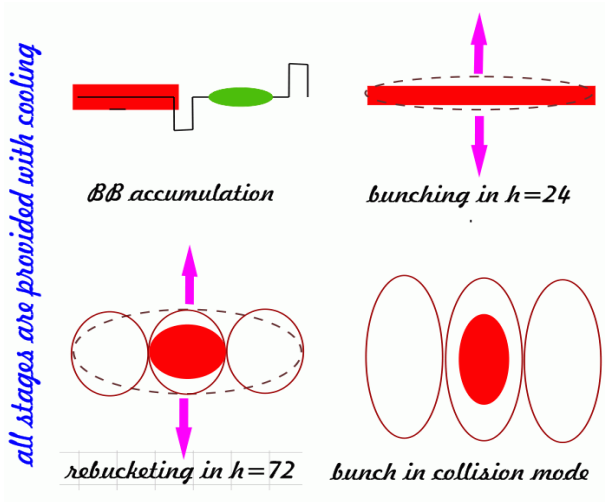

Figure 1: Scheme of RF cycle in Collider.

SHORT BUNCHED BEAM FORMATION

Accumulation of Ions $^{197}Au^{+79}$

Application of RF barrier bucket (BB) technique provides independent optimization of the bunch intensity, bunch number as well as controlling of the beam emittance and momentum spread during the bunch formation. In presence of cooling the number of the injection pulses can be large enough with suitable stacking efficiency. Intensity of the injected portion influences on the stacking process duration only and can vary widely.

Collider rings receive bunch every 4-5 seconds from Nuclotron. Bunch contains $1\div2\cdot10^9$ particles. Its total length and momentum spread are about 10 m and 10^{-3} accordingly. The BB pulses divide the ring circumference by two zones of equal length: the injection zone (where the synchrotron motion is unstable) and that one for the stack (with stable synchrotron motion). Barrier pulse phase width – π/6 rad and voltage amplitude – 2kV.

Numerical simulations of ion stacking with barrier bucket method have been performed independently by T.

ISBN 978-3-95450-125-0

BEAM INSTABILITY PHENOMENA OBSERVED AT HIRFL-CSR IN THE PRESENCE OF ELECTRON COOLER*

Xiaodong Yang#, Jie Li, Lijun Mao, Guohong Li, Xiaoming Ma, Tailai Yan, Ruishi Mao, Tiecheng Zhao, Junxia Wu, Youjin Yuan, Jiancheng Yang, Peng Li
Institute of Modern Physics, CAS, Lanzhou, 730000, P. R. China

Abstract

Some signal samples acquired from Schottky probes and beam position monitor during operation were presented in this paper, and they were observed in the different operation stages such as during injection, after cooling and cooling force measurement. These signals were considered related with the ion beam instability. The central frequency of ion beam varied with the time. Some were caused by the ripple of hardware, the other were created by ion beam itself. The reasons which caused these phenomena were analyzed. The possible solutions were suggested, and some necessary upgrade and improvements were expected. These results were helpful to attempt the Schottky Mass Spectrometry measurement in the CSR.

INTRODUCTION

The Cooler Storage Ring of Heavy Ion Research Facility at Lanzhou (HIRFL-CSR) has been operating since 2007. The heavy ion beams in the energy range of few MeV/u to few GeV/u can be produced and delivered for the mass spectrometry experiments, the cancer therapy and atomic experiments and so on [1]. The latest results were reported in many papers and conferences [2-5].

In several machine runs the beam instability phenomena has been observed in the different operation stages such as during injection, after cooling and cooling force measurement. Besides this, the beam loss was also happened and investigated for electron cooling force measurements.

The instability resulted in beam loss and emittance growth, thus the achievable beam intensity and experimental precision is however limited. The instability of electron cooled beam has been studied in the different accelerators and reported by several laboratories in the world [6-9]. In this paper, the instability phenomena of electron cooled beam observed at HIRFL-CSR was described, and the Schottky spectra were analyzed.

The Schottky Mass Spectrometry (SMS) [10-12]is one of the high precision mass spectrometers based on storage ring with 10^{-6} or higher precision [13,14]. At HIRFL-CSR, the ultimate relative frequency spread $\Delta f/f$ of about 5×10^{-7} and about 1000s long-term beam stability are necessary for high precision mass measurements.

In order to improve the stable increasing beam intensity at HIRFL-CSR, and prepare the condition for SMS experiments, the mechanisms of instability have to be investigated and different cures methods should be tested.

BEAM ACCUMULATION IN CSRM

The main goal of the electron cooler application at HIRFL-CSR main ring is to increase the beam intensity with the help of stacking-electron cooling procedure at the injection energy [15,16]. A typical longitudinal Schottky signal during stacking-cooling procedure was shown in Fig. 1.

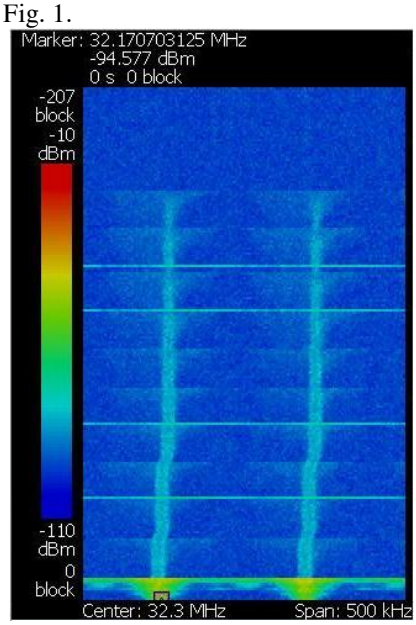

Figure 1: A typical Schottky spectrum of ion beam accumulation in CSRm under electron cooling.

For an effective electron cooling, the ion beam and electron beam have to overlap coaxially, and in principle the relative velocity of the ion beam and electron beam should be zero in the particle reference frame. It's obviously in Fig. 1 that the ion beam was symmetrically cooled down to the central frequency, which means that the injected ion energy, the electron beam energy, the magnetic field of dipole and the RF frequency were matched well. In addition, the deep colour of Schottky signal means the beam intensity increased step by step.

The cooling time obtained from Fig. 1 is corresponding to the simulation result, and there is no obvious sideband signal between the neighbour harmonic. It demonstrated that the HIRFL-CSRm was operated at reasonable work-point settings. The average velocities of electron and ion were almost equal. Further more, the central frequency shifted to left at the end of stacking procedure because of the changing of beam orbit at injection point.

*Work supported by The National Natural Science Foundation of China, NSFC(Grant No. 10975166, 10905083)
#yangxd@impcas.ac.cn

ISBN 978-3-95450-125-0

HIGH VOLTAGE ELECTRON COOLER*

M. Bryzgunov, A. Bubley, A. Goncharov, V. Panasyuk, V. Parkhomchuk, V. Reva,
D. Skorobogatov, BINP SB RAS, Novosibirsk, Russia
J. Dietrich, TU Dortmund and Helmholtz Instituit Mainz, Germany
V. Kamerdzhiev, FZJ, Jülich, Germany

Abstract

Discussions on physical requirements and technical design of the 2 MeV electron cooler for the synchrotron COSY began in 2002.

In 2009 contract for cooler production was signed. In this report results of cooler commissioning with electron beam at BINP are discussed.

INTRODUCTION

The new generation of particle accelerators operating in the energy range of 1-8 GeV/u for nuclear physics experiments requires very powerful beam cooling to obtain high luminosity. For example the investigation of meson resonances with PANDA detector requires momentum spread in antiproton beam, which must be better than 10^{-4}. To obtain such a momentum spread cooling time in the range of 0.1- 10 s is needed. The 4 MeV electron cooler at the RECYCLER ring (FNAL) [1] achieves cooling time about 30 min. The new cooler for COSY should provide a few orders of magnitude more powerful longitudinal and transverse cooling that requires new technical solutions. [2] The basic idea of this cooler is to use high magnetic field along the orbit of the electron beam from the electron gun to the electron collector. In this case high enough electron beam density at low effective temperature can be achieved in the cooling section [3].

The basic parameters of the COSY cooler are listed in Table 1. The length of the cooling section is given by the space available in the COSY ring.

Table 1: Basic Parameters of the 2 MeV electron cooler.

Energy Range	0.025 ... 2 MeV
High Voltage Stability	$< 10^{-4}$
Electron Current	0.1 ... 3 A
Electron Beam Diameter	10 ... 30 mm
Length of Cooling Section	2.69 m
Toroid Radius	1.00 m
Magnetic Field (cooling section)	0.5 ... 2 kG
Vacuum at Cooler	10^{-9} ... 10^{-10} mbar

The calculation of cooling of a 2GeV proton beam with high density electron beam is shown in fig.1 The beam on each turn passes hydrogen target with density 10^{15} 1/cm^^{2}. Magnetic field in the cooling section was taken as B=2 kGs.

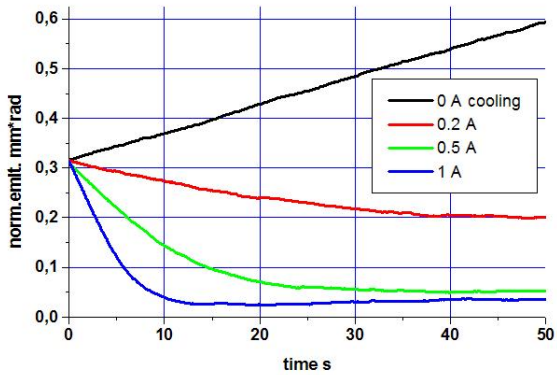

Figure 1: Cooling of 2 GeV proton beam .

From fig.1 one can clearly see that cooling shrinks the proton beam to small emitance and just 0.2 A suppressed the scattering on target. The equilibrium emittance decreases with increasing electron current by the more powerful cooling.

MAIN COMPONENTS OF COOLER

. The main features of the cooler are [2]:

1. The design of the cooling section solenoid is similar to the ones of CSR (IMP) and LEIR (CERN) coolers designed by BINP [3]. However, for the 2 MeV cooler the requirement on straightness of magnetic field lines is so high ($\triangle\theta < 10^{-5}$) that a system for control of magnetic field lines in vacuum becomes necessary.
2. For suppression of high energy electron beam losses at IMP and LEIR coolers electrostatic bending was used [4]. The shape of the 2 MeV transport lines, however, dictates a different approach. The collector (inside the HV terminal) is complemented by a Wien filter to suppress return electron flux.
3. Both acceleration and deceleration tubes are placed in the common high voltage tank.
4. The high power cascade transformer is installed around high voltage column for powering solenoids for generation of magnetic field along electron beam trajectory(Fig.2).

*Work supported by the Ministry of Education and Science of the Russian Federation

ISBN 978-3-95450-125-0

NEW DEVELOPMENTS IN HIGH ENERGY ELECTRON COOLING

J. Dietrich#, TU Dortmund and Helmholtz Institut Mainz, Germany

Abstract

Electron cooling of hadron beams is a powerful technique by which accelerator facilities achieve the necessary beam brightness for their physics research. An overview on the latest developments in high energy electron cooling (electron beam energy higher than 500 keV) is given. Technical feasibility for electron beam energy up to 8 MeV is discussed.

INTRODUCTION

The use of electron coolers in the range of electron beam energy lower 400 keV is well established and state of the art. For higher electron energies there exists up to now only one machine – the Recycler Electron Cooler (REC) of Fermilab with a terminal voltage of 4.4. MV [1]. The cooler was successful installed into the Recycler during the summer of 2005 and was operating until end of 2011 when the Tevatron was shut off. The cooling opened the possibility for several times higher, record luminosities. The REC overcame not only the great challenge of operating 4.4 MV pelletron accelerator in the recirculation mode with up to 1A beams, but also resolved the hard issue of high quality magnetised beam transport through non-continuous magnetic focusing beamline [2]. The next unique high energy electron cooler -the 2 MV COSY electron cooler- is now under commissioning in the Budker Institut in Novosibirsk and will be installed in the Cooler Synchrotron COSY in spring of next year [3]. Development of high energy electron coolers is a technical challenge due to the engineering problems like high voltage generation, power transmission to the gun and collector in the accelerator "head" and the power transmission to the magnetic coils at the accel/decel tubes for magnetised electron beam transport. Today there is a need for further development. In the high energy storage ring HESR for antiprotons in the FAIR facility in Darmstadt a 4.5 MV electron cooler is planed [4]. The proposed concept of a polarized Electron-Nucleon Collider (ENC) integrates the 15 GeV/c HESR of the FAIR project for protons/deuterons and an additional 3.3 GeV electron ring [5]. A new 8.2 MV electron cooler is an essential part in this concept. In the NICA collider project of the JINR Dubna a 2.5 MV electron cooler is foreseen with one electron beam per each ring of the collider [6]. There are some special features of high energy cooling. The cooling rate decreases with γ^{-2}. To obtain a maximum friction force the "waveiness" of the magnetic force line should be as small as possible to get a smaller contribution to the effective electron velocity [7]. To get a high cooling rate magnetised electron cooling is necessary. All low-energy (3-400 keV) electron coolers are based on magnetised cooling. The electron beam transport and alignment of electron and ion beam is done with continuous magnetic field. Strong magnetic field completely suppresses transverse temperature of electron beam, so that effectiveness of cooling is determined by a very low longitudinal temperature of electrons. Non-magnetised cooling relies on the fact that rms velocity spread of electrons is comparable or smaller than the one of ions which need to be cooled. For the REC (non-magnetised case) cooling times of about one hour was sufficient. The new coolers for COSY and the new future projects should provide a few orders of magnitude more powerful longitudinal and transverse cooling. This requires new technical solutions. The basic idea of the new COSY cooler and for the future HESR and NICA collider coolers is to use a high magnetic field along the orbit of the electron beam from the electron gun to the collector. Faster cooling times are essential for the future projects. The technical problems for electrostatic accelerator at 8-10 MV and needed electron beam currents up to 3 A look too hard. An alternative can be a low frequency linac with bunched electron beam. Today this system achieved electron peak currents of about 10 A [8].

juergen.dietrich@tu-dortmund.de

ENGINEERING PROBLEMS OF HIGH ENERGY ELECTRON COOLERS

The engineering problems are listed in the following:

- High voltage generators (< 10 MV).
- High voltage performance.
- Limiting performance of accelerator tubes.
- Power transmission to the accelerator "head" (gun, collector).
- Power transmission to the magnetic coils (at accel/decel tubes).
- Electron current and high voltage stability (1-3 A, 10^{-5}).
- Electron beam formation, transportation and recovering.
- Magnetic field measurement system in the cooling section.
- Magnetic field straightness in the cooling section (< 10^{-5}).
- Electron beam diagnostics.

Power transmission in commercial available pelletrons is realised by isolated rotating shafts combined with generators located on high voltage level. In case of magnetised coolers, where additional power is needed for the magnetic coils around the accel/decel tubes this method seems to be too complicated. Another solution is cascaded resonant transformers and proposed turbines on high voltage level or combinations of both. The technical solution is strongly influenced by the location of the magnetic coils at the accelerator/ decelerator tubes. Due to the difficulties the magnetic coils (superconducting) in

ISBN 978-3-95450-125-0

APPROACH TO THE LOW TEMPERATURE STATE ORIENTED FOR CRYSTALLINE BEAM*

Akira Noda#, , Masao Nakao, Hikaru Souda, Hiromu Tongu, ICR, Kyoto University, Uji-city, Japan
Kouichi Jimbo, IAE, Kyoto University, Uji-city, Japan
Hiromi Okamoto, Kazuya Osaki, AdSM, Hiroshima University, Higashi Hiroshima-city, Japan
Yosuke Yuri, Takasaki Advanced Radiation Research Institute, JAEA, Takasaki-city, Japan
Igor Nikolai Meshkov, Alexander V. Smirnov, JINR, Dubna, Moscow Region, Russia
Manfred Grieser, MPIK, 69029 Heidelberg, Postfach 103980, Germany,
Koji Noda, Toshiyuki Shirai, National Institute of Radiological Sciences, Chiba-city, Japan
Zhengqi He, Tsinghua University, 1 Qinqhuayuan, Beijing, China.

Abstract

With the use of S-LSR, an ion storage and cooler ring at ICR, the approach to attain a low temperature beam has been continued. With electron cooling one dimensional ordered state has been realized for 7 MeV proton beam, resulting in an abrupt longitudinal temperature jump from 2K to 0.3 K at a particle number ≈2000. A transverse temperature at a particle number of 4000 at the observation point with a beta-function of ≈1.7 m is estimated to be 12 K. Laser cooling has also been applied to $^{24}Mg^{+}$ ion beam with a kinetic energy of 40 keV. The lowest longitudinal temperature of a coasting beam was limited at 3.6 K for a beam intensity of 4 x 10^4 due to intra-beam scattering (IBS) and residual gas scattering, while a transverse temperature is reduced to ≈500 K by IBS for a beam intensity of 2 x10^7, which is accompanied by the increase of the longitudinal temperature to 11K. In order to actively cool down the transverse temperature, synchro-betatron resonance coupling (SBRC) has been applied to a bunched beam. By reduction of the beam intensity with scraping, the average transverse beam temperature has been cooled down to <15-50 K and 7-15 K for the horizontal and vertical directions, respectively, by SBRC for the beam intensity of 1 x 10^4.

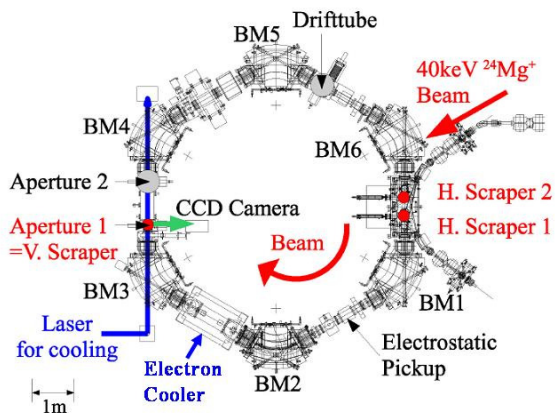

Fig.1 Layout of S-LSR and its beam monitoring and scraping apparatuses.

*Work supported by Advanced Compact Accelerator Development project by MEXT of Japanese government. It is al so supported by GCOE project at Kyoto University, "The next generation of Physics-Spun from Universality and Emergency.
#noda@kyticr.kuicr.kyoto-u.ac.jp

Table 1 Main Parameters of S-LSR

Ion species (energy)	H^{+} (7 MeV), $^{24}Mg^{+}$ (40 keV)
Cooling Methods	Electron beam cooling, Laser cooling
Circumference	22.557 m
Average radius	3.59 m
Length of straight section	2.66 m (including Q mag. parts)
Number of superperiods	6
Betatron tune (ν_x, ν_y)	
Electron cooling	(1.64,1.21)
Laser cooling	(2.07,1.12)
Bending magnet	H-type
Maximum field	0.95 T
Curvature radius	1.05 m
Gap height	70 mm
Pole end cut	Rogowskii cut + field clamp
Deflection angle	60°
Weight	4.5tons
Quadrupole magnet	
Core length	0.20 m
Bore radius	70 mm

INTRODUCTION

A lot of efforts to approach to the low temperature states of a beam have been continued in these two decades so as to improve the beam characteristics which is usually in a gaseous state. At ICR, Kyoto University, an ion accumulation and cooler ring, S-LSR had been constructed and it became in operation in 2005. In Fig.1 and table 1, its layout and main parameters are shown. Originally it was oriented for the realization of compact ion accelerator for cancer therapy by combination of RF accelerator technology and laser plasma interaction [1]. After the successful demonstration of effective electron cooling of a hot ion beam with a relative velocity sweep between the ion and electron beams [2] utilizing TSR at MPIK [3] and S-LSR, the main experimental researches are oriented for the realization of lower beam temperature by application of beam cooling utilizing such a special characteristics of S-LSR lattice satisfying the so-called maintenance condition given by the following relations [4,5],

$$\gamma < \gamma_T \quad (\gamma_T : \text{the transition gamma}) \qquad (1)$$

ISBN 978-3-95450-125-0

BEAM COOLING AT NICA COLLIDER

T. Katayama, GSI, Darmstadt, Germany
I. Meshkov, A. Sidorin and G. Trubnikov, JINR, Dubna, Russia.

Abstract

At the heavy ion collider NICA presently promoted at the JINR, the beam cooling will play the crucial roles to attain the designed performance. The primary goal of the collider is to achieve the high luminosity ~1e27 /cm^2/sec, preventing the IBS diffusion effects by beam cooling to keep the luminosity during the experimental period. The other purpose of the cooling is to accumulate the required beam intensity up to several times 1e10 from the injector Nuclotron with use of the barrier bucket method. After the BB accumulation the coasting beam is adiabatically bunched with the help of RF field and the beam cooling. In the present paper the detailed simulation results are presented for the above process mainly in the longitudinal freedom.

INTRODUCTION

The heavy ion collider proposed at the JINR aims to achieve the head-on collision of 1-4.5 GeV/u, $^{197}Au^{79+}$ ion beam with the luminosity of ~1e27/cm^2/sec. [1] The number of bunches in the collider is 24 and each bunch contains the ion number of ~1e9, depending upon the operation energy. Thus totally around ~2.4e10 ions should be accumulated in the collider ring. The injector for the collider is the existing superconducting synchrotron, Nuclotron, which could provide the beam of 1-4.5 GeV/u with the intensity of 1e8-1e9/cycle of the cycle time 5 sec. The bunch length of the beam from the Nuclotron is around 1/3 of the circumference, 300 nsec. [2, 3]

In the present scenario, the bunch is transferred to the collider without any manipulation for the short bunch formation in the Nuclotron which allows us much easier operation of the Nuclotron. The long bunch is transferred in the longitudinal injection area which is provided by the barrier voltages, and is accumulated with the assistance of stochastic cooling for the high energy and the electron cooling for the low energy, say below 2 GeV/u.

Thus accumulated heavy ion beam is the coasting beam condition, and then the large RF voltage is applied adiabatically as well as the beam cooling. The beam is gradually bunched to the required rms bunch length for the collision experiment ~2ns (rms). The bunch length is the equilibrium state of RF field, beam cooling, Intra Beam Scattering (IBS) and space charge repulsion. Especialy at low energy, the IBS diffusion and space charge force could affect the beam motion at the short bunch condition.

The detailed analysis of the beam dynamics for the stochastic cooling application was reported elsewhere [4] and here the main emsphasis is given on the electron cooling and space charge problem.

STOCHASTIC COOLING

The operation energy of the collider is from 1 GeV/u to 4.5 GeV/u where the ring slipping factor is drastically changed. In Table 1 the ring slipping factor, transition gamma being fixed as 7.09 and the local slipping factor from the stochastic cooling PU to Kicker are tabulated. The distance from PU to kicker is assumed as 170 m. The coasting equivalent particle number is given as the product of bunch number/ring, number of ions /bunch and the bunching factor. Thus obtained coasting equivalent particle number is corresponding to the condition that the peak intensity of the bunched beam are populated as the coasting beam in the ring.

Table 1. Beam parameters for various energies

Energy (GeV/u)	1.5	2.5	3.0	4.5
Ring slipping factor	0.1268	0.0537	0.0350	0.00949
Local slipping factor	0.1173	0.0442	0.02546	-5.4e-5
Particle number/bunch	3.0e8	1.50e9	2.50e9	6.0e9
Coasting equivalent particle number	7.26e10	3.63e11	6.05e11	1.45e12

The bandwidth of the stochastic cooling system is preferably as wide as possible because the cooling time is inversely proportional to the bandwidth. On the other hand the momentum acceptance of the cooling system is, in general, becomes narrower for the wider bandwidth. Also the momentum acceptance is closely related with the ring slipping factor as well as the local slipping factor. In the present scenario the Palmer cooling method is envisaged where only the local slipping factor limits the momentum acceptance. Presently two bandwidth, 2-4 GHz and 3-6GHz are candidates.

Barrier Bucket Accumulation with Stochastic Cooling

The beam accumulation is designed to use the fixed barrier bucket method whose concept was experimentally verified at the POP (Proof Of Principle) experiment at the ESR GSI.[5] It should be noted that the POP experimental results are in well agreement with the simulation results. [6] The parameters of the barrier voltage as well as the stochastic cooling in the collider are tabulated in Table 2.

In the present simulation, the PU and kicker structure is assumed as the classical $\lambda/4$ electrode structure. In the meanwhile the new structure is being developed [7] which has the larger sensitivity and then the small number of electrode could be enough. Then the parameters of stochastic cooling system could be slightly changed in the construction phase.

ISBN 978-3-95450-125-0

STATUS OF THE HIGH VOLTAGE ELECTRON COOLER PROJECT FOR NICA COLLIDER

E.V.Ahmanova, I.N.Meshkov, R.V.Pivin, A.U.Rudakov, A.V.Shabunov, A.V. Smirnov, N.D.Topilin, Yu.A.Tumanova, S.L.Yakovenko#, JINR, Dubna
A.G.Kobets, Institute of Electrophysics and Radiation Technologies, NAS of Ukraine
A.V.Ivanov, Budker Institute of Nuclear Physics SB RAS, Novosibirsk
A.A.Filippov, M.P.Kokurkin, N.Yu.Lysov, M.M.Pashin, AREI, Moscow

Abstract

The 2.5 MeV electron cooler for the NICA collider is being designed at JINR [1]. The conceptual design of the electron cooling system has been developed and working design has been started. The 250 kV prototypes of the high voltage (HV) generator of the cooler has assembled and being tested.

DESIGN OF THE COOLER

The electron cooler (Fig. 1) consists of three tanks filled with SF6 gas under pressure of 8 at. The tanks 1 and 3 contain acceleration tube and electron gun for one of the electron beam and deceleration tube and electron collector for opposite direction electron beam. HV generator is placed in the tank 2.

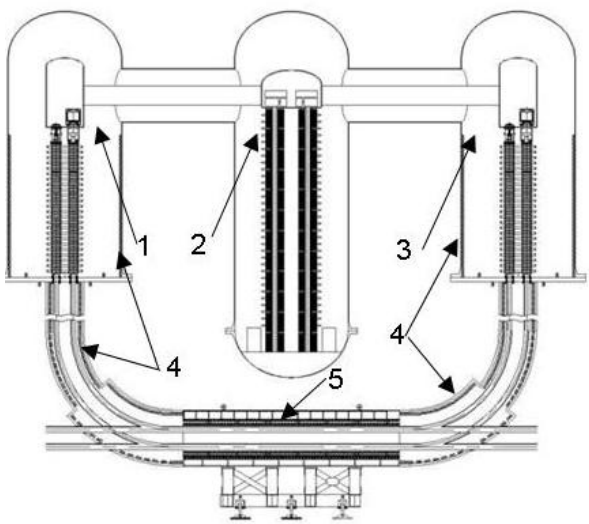

Fig.1. General view of the electron cooler (working design). 1, 3 – tanks with electron gun and acceleration tube and deceleration tube + collector for electron beam of opposite direction, 2 – tank with HV generator, 4 – beam transportation solenoids, 5 - electron cooling section.

MAGNETIC SYSTEM

The magnetic field is formed by a set of straight and toroidal solenoids (Fig.1). The solenoids forming the magnetic field in the region of acceleration/deceleration tubes are placed outside the tanks that resolve the problem of the high voltage insulation (Fig.2).

Table 1. Cooler parameters

Electron energy, MeV	0.5 ÷ 2.5
Electron beam current , A	0.1 ÷ 1,0
Beam diameter, cm	1,0
solenoid magnetic field, T	0.1 ÷ 0.2
HV PS current, mA	1
Collector PS, kW	2×2
HV PS stability, ΔU/U	1×10^{-4}
SF_6 gas pressure, at	5 ÷ 8

To form 2 kG magnetic field the solenoids have to have the next parameters: linear current density of 1.6 kA/cm; height of 2500 mm; diameter of 2100 mm. Comparing warm and superconducting solenoid parameters (cost, weight, power consumption, a.e.t), we have chosen the last one for tanks region (Table 2).

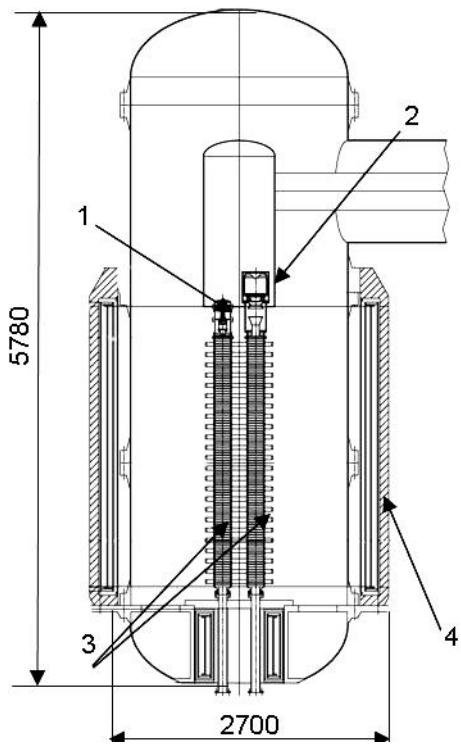

Fig.2. 1 - electron gun, 2 - electron collector, 3- acceleration/deceleration tubes, 4 - the SC solenoid in cryostats with iron shields.

yakoven@jinr.ru

ISBN 978-3-95450-125-0

LONG TERM BEAM DYNAMICS SIMULATION WITH THE BETACOOL CODE

A.O.Siodrin, A.V.Smirnov#, JINR, Dubna, 141980, Russia

Abstract

General goal of the BETACOOL program is to simulate long term processes (in comparison with the ion revolution period) in the ion storage ring leading to variation of the ion distribution function in 6 dimensional phase space. The ion beam motion inside a storage ring is supposed to be stable and it is treated in linear approximation. Results of the numerical simulation of the beam dynamics for new project NICA (JINR, Russia) are presented.

APPLICATIONS OF BETACOOL CODE OVER THE WORLD

The idea of the BETACOOL code was appeared about 18 years ago for the simulation of the beam dynamics under action of the electron cooling. BETACOOL means that simulations take into account the beta function in the cooling section.

In the present time the BETACOOL code includes different models of a few physical process which are usually exist in the storage rings [1]: electron, stochastic and laser cooling, intrabeam scattering, scattering on atoms of the residual gas and different types of internal target, colliding regime and particle losses, etc.

The BETACOOL code was elaborated in the collaboration with different scientific centres in the world where was benchmarked on the existing experiments and used for the simulation of new accelerator projects:

- Benchmarking of IBS and electron cooling models: CELSIUS (TSL) [2], ESR (GSI), TechX (Colorado), RHIC (BNL) [3], Recycler (FNAL), COSY (FZJ) [4], S-LSR (Kyoto Univ.) [5];
- Luminosity preservation in colliders: MUSES (RIKEN) [6], RHIC-II (BNL) [7], PAX (FAIR) [8], NICA (JINR) [9];
- Simulations of experiments with internal target: PANDA@HESR (FAIR) [10], WASA@COSY (FZJ) [11], ESR (GSI) [12];
- Beam ordering (crystalline beams): S-LSR (Kyoto University) [13], NAP-M (BINP), COSY (FZJ) [14], ESR (GSI) [15];
- Simulations of cooling-stacking process: LEIR (CERN), HIRFL-CSR (Lanzhou), NICA Booster (JINR) [16];
- Low energy electron cooling: TSR [17] and USR (MPI) [18], ELENA (CERN);
- RF burrier bucket system: Recycler (FNAL) [19], ESR (GSI), NESR and HESR (FAIR) [20], NICA Collider (JINR).

#smirnov@jinr.ru

Basic algorithms and software structure are described in details in BETACOOL guide [21]. The possibilities of the BETACOOL application for optimization of a storage ring operational regimes are illustrated in this report on example of the heavy ion mode of the NICA collider operation mainly. The beam cooling (both – electron and stochastic) at the NICA collider has two relatively independent goals: beam stacking using barrier bucket technique and luminosity preservation during collisions.

PARTICLE ACCUMULATION WITH RF BARRIER BUCKET SYSTEM

RF barrier bucket system was proposed for the particle accumulation in the NICA collider in order to provide required beam intensity independently on intensity of the bunch at single injection [22]. In the ion energy range from 1 to about 3 GeV/u the beam stacking is planned to be realized using stationary burrier pulses with the electron cooling of the injected beam.

RF barriers divide a ring circumference on two parts: one of them corresponds to unstable synchrotron motion, in the second one the motion is stable. After injection into the unstable region the particles are cooled down with the electron cooling and accumulated between barriers in the part opposite to the injection region. At the next injection all the particles located in the injection region are killed by the injection kicker pulse. The NICA collider RF barrier bucket system is designed to provide the barriers of rectangular shape. Example of the stacking process simulation with BETACOOL is presented in the Fig.1.

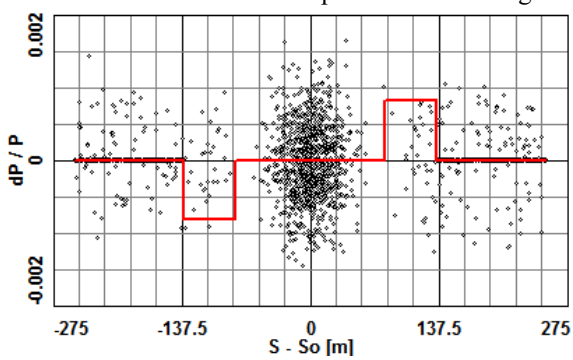

Figure 1: Longitudinal phase space after second injection for the ion energy 1.5 GeV/u: dots – model particles, red line – barrier bucket potential distribution in the momentum deviation units.

The stacking efficiency is determined by the ratio between the injection repetition period and the cooling time. The working cycle of the NICA injection chain is equal to about 5 seconds and it provides single bunch of about 10^9 Gold nuclei. Even accelerated bunch is injected into the first collider ring the odd – into the second ring. It

ISBN 978-3-95450-125-0

CURRENT PLANS FOR BEAM COOLING AT FAIR

M. Steck, C. Dimopoulou, A. Dolinskii, O. Gorda, T. Katayama, S.A. Litvinov, Yu.A. Litvinov, F. Nolden, C. Peschke, Th. Stöhlker, GSI Darmstadt, Germany,
J. Dietrich, R. Maier, D. Prasuhn, R. Stassen, H. Stockhorst, FZ Jülich, Germany

Abstract

The improvement of the quality of secondary beams by beam cooling is an essential component in the scenario of the Facility for Antiproton and Ion Research (FAIR). Beam Cooling is applied to match the secondary beams, antiprotons and rare isotopes, which are produced in thick solid targets, to the needs of experiments. Pre-cooling in the Collector Ring, accumulation and preparation for experiments in the High Energy Storage Ring are the main tasks of the Cooling Systems. Many of the beam cooling concepts for FAIR are studied experimentally in the existing Experimental Storage Ring ESR which has been operated at GSI over more than two decades and which will also be available for beam physics experiments in the coming years.

INTRODUCTION

The construction of the international Facility for Antiproton and Ion Research (FAIR) [1] is presently focussed on the Modularized Start Version (MSV). The funding of this first stage of the project is secured and the goal is to provide beams for all major experimental programs. The scientific programs cover research with high energy antiprotons in the PANDA experiment, Compressed Baryonic Matter (CBM), nuclear structure and related astrophysics, and atomic and plasma physics and applications. Already in the MSV, all the various types of experiments expect unprecedented possibilities for their research field. The programs with secondary beams are largely based on beam cooling which will be used for phase space reduction of antiprotons, rare isotope beams and highly charged ions.

The MSV of the FAIR project comprises various existing, but even more new accelerator systems. The program with heavy ion beams requires the existing UNILAC linear accelerator and the heavy ion synchrotron SIS18 as injector chain. By the addition of the synchrotron SIS100 [2] the heavy ion beam energy can be increased according to the higher rigidity of 100 Tm, alternatively lower charge states can be accelerated gaining in beam intensity by abandoning intermediate stripping with associated intensity reduction. With a new 70 MeV proton linac a source of intense proton beams is under construction which serves as injector into the chain with SIS18 and SIS100 which will result in 29 GeV protons for the production of antiprotons.

The high energy, high intensity beams after SIS100 will produce either highly charged ions, rare isotope beams by projectile fragmentation, or antiprotons from a primary proton beam. The antiprotons exit from a nickel production target where antiprotons at 3 GeV are selected in a magnetic separator for injection into the new Collector Ring (CR) [3]. For Rare Isotope Beams (RIBs) the new large acceptance superconducting fragment separator SuperFRS [4] will conduce to the production of high intensity secondary beams which can be used for fixed target experiments or for injection into the CR in order to apply phase space compression.

With respect to beam cooling the CR will be the key accelerator to improve the quality of secondary beams, both antiprotons and RIBs. For both species the primary beams in SIS100 will be compressed into a short single bunch with a length of 50 ns. The secondary particles after production in the target basically retain this time structure, however, with an increased momentum spread. Immediately after injection of the short bunch a bunch rotation system reduces the momentum spread and subsequent stochastic cooling will allow a fast reduction of the momentum spread providing a high quality secondary beam for transport to a subsequent storage ring where it is stored and prepared for the experiment. In the MSV the High Energy Storage Ring (HESR) [5] will be the exclusive user of pre-cooled CR beams. It is mainly designed for the storage of antiprotons and experiments using the PANDA set-up. Recently plans for the operation of the HESR with ion and rare isotope beams were discussed and are being worked out in detail.

As a continuation of ongoing GSI activities and in view of the delay of the RESR and NESR storage rings which are postponed within the FAIR project, the operation of the existing ESR storage ring [6] will be continued. Since it is equipped with a stochastic and an electron cooling system, it can be used as a test bed for FAIR developments. The option to decelerate heavy ions to 4 MeV/u opens already now the field of low energy beams foreseen in the FAIR project. Further deceleration with the HITRAP [7] decelerator and the plan to install the CRYRING [8], which is a contribution to the FAIR program with low energy antiprotons and ions, will allow accelerator and experimental developments for a low energy physics program at FAIR.

PRE-COOLING IN THE COLLECTOR RING CR

The Collector Ring CR is a large acceptance storage ring for the storage of secondary particles. The production of the secondary beams in a thick solid target results in a large emittance increase, both transversely and longitudinally. The large transverse acceptance of the CR allows efficient use in the capturing of secondary beams emerging from the target. Different optical modes will be used for antiprotons and ions. This is a consequence of the requirements of stochastic cooling for proper mixing

ISBN 978-3-95450-125-0

MA THEMATICAL MODELING AND OPTIMIZATION OF BEAM DYNAMICS IN ACCELERATORS

D. A. Ovsyannikov, SPbSU, Saint-Petersburg, Russia

Abstract

In this paper we treat the problem of beam dynamics optimization as a control theory problem. We consider different mathematical models of optimization. The approach to solving optimization problem for charged particle dynamics in accelerators includes: construction of mathematical model of controlled dynamical process; choice of control functions or parameters of optimization; construction of quality functionals, which allow efficient evaluation of various characteristics of examined controlled motion; analytical representation of the functional variations, which allow to construct various methods of optimization for quality functionals; construction of methods and algorithms of optimization. Problem of statement is considered on the pattern of RFQ channel.

INTRODUCTION

Mathematical methods of modeling and optimization are extensively used in many fields of science and technology. Development of specialized software for various applications is of more and more importance. A special class of tasks attracting attention of numerous researches includes the problems associated with the beam dynamics optimization in accelerator [1–13]. There are not the general methods of accelerating and focusing structures optimization. However as the demand to output beam parameters are progressively increasing it is needed to develop a new approaches and methods to solve these problems. In the paper the different mathematical control models describing beam dynamics are presented. Especially we consider the problems related to charged particles interaction. In this case we investigate the controlled dynamic process described by a system of integro-differential equations. The optimization methods are developed for the different functionals concerned with the quality of beam [3–12]. They are used for solution of various beam dynamics problems in. In particular, we investigate the optimization problem of a radial matching section in RFQ channel. We consider the problem of construction self-consistent distribution for charged particle beam in magnetic field too [14–19].

MATHEMATICAL OPTIMIZATION MODELS

The problem of beam control of interacting particles, which dynamics is described by integro-differential equations, is considered. Let us assume that evolution of particle beam is described by equations

$$dx/dt = f(t,x,u) \tag{1}$$

$$f(t,x,u) = f_1(t,x,u) + \int_{M_{t,u}} f_2(t,x,y_t)\rho(t,y_t)dy_t, \tag{2}$$

$$\frac{\partial\rho}{\partial t} + \frac{\partial\rho}{\partial x} f(t,x,u) + \rho\,\mathrm{div}_x f(t,x,u) = 0, \tag{3}$$

$$x(0) = x_0 \in M_0, \quad \rho(0,x) = \rho_0(x). \tag{4}$$

Here t is is the time; x is n-vector of phase coordinates; $u = u(t) \in D$ is r-dimensional control vector-function; D is the set of admissible control functions; $\rho = \rho(t,x)$ is the particle distribution density in the phase space; f_1 is n-dimensional vector-function determined by external electromagnetic fields; f_2 is n-dimensional vector-function associated with the particle interactions; the set $M_{t,u}$ is the cross-section of the trajectory set. It is obtained by time shift of the initial set M_0 through solutions of equation (1) with given control $u = u(t)$. The set M_0 is a given set in the phase space, which describes the set of initial states for a charged particle beam at the initial time moment. The function $\rho_0(x)$ is a given function describing the particle distribution density at the moment $t = 0$. The equations (1)-(2) can be considered as Vlasov equations. We meet with these equations if interaction between particles, for example the Coulomb repulsion, is taken into account. Let us introduce a functional

$$I(u) = \int_0^T \int_{M_{t,u}} \varphi(t,x_t,\rho(t,x_t),u)dx_t dt + \int_{M_{T,u}} g(x_T,\rho_T(T,x_T))dx_T \to \min_{u\in D}, \tag{5}$$

characterizing the dynamics of the process. Here φ and g are given non-negative functions, T is fixed. Consider the minimization problem of functional (5). Analizing various systems which are designed for acceleration, focusing and transporting of charged particle beams, it should be noticed that electrical and magnetic fields can be treated in a certain structural and parametric form. Thus certain components and parameters of electromagnetic fields and geometric systems of accelerating or focusing can be taken as control variables. The developed approach can be applied to another kind of functionals:

$$I(u) = \Phi(\mu_{ks}^{(1,1)},\ldots,\mu_{ks}^{(i,j)},\ldots,\mu_{ks}^{(n,n)}), \tag{6}$$

ISBN 978-3-95450-125-0

TRANSIENT BEAM RESPONSE IN SYNCHROTRONS WITH A DIGITAL TRANSVERSE FEEDBACK SYSTEM

V. M. Zhabitsky, JINR, Dubna, Russia

Abstract

The transient beam response to an externally applied impulse force in synchrotrons with a digital transverse feedback system is studied. Experimental data from the LHC on damping of coherent transverse oscillations excited by the discrete-time unit impulse are analysed. Good agreement on the measured and theoretically predicted decrements has been obtained. A method of feedback fine tuning, based on measurements of the bunch response to the harmonic excitation impulse, is discussed.

INTRODUCTION

Transverse feedback systems (TFS) in synchrotrons (see Fig. 1) are used for damping coherent transverse oscillations caused by injection errors and for suppression of coherent transverse instabilities [1]. The transverse momentum of a bunch is corrected by the damper kicker (DK) in proportion to the bunch displacement from the reference orbit at the location of the beam position monitor (BPM). The digital signal processor (DSP) module allows to obtain optimum damping by adjustment of the TFS parameters in agreement with the beam time of flight from BPM to DK and the corresponding betatron phase advance.

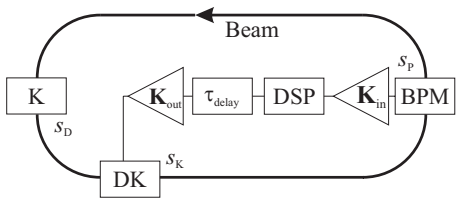

Figure 1: TFS Layout

Coherent oscillations can be originated by DK or a specialised driving kicker K (see Fig. 1). For example, the kicker can be fed with the discrete-time unit impulse or the harmonic excitation impulse. The beam response observed by BPM in this case can be used for tuning the TFS.

The transient beam response to a driving force is analyzed below in framework of the discrete transformation approach developed in [2, 3] for describing transverse beam dynamics in synchrotrons with a digital TFS.

BASIC NOTIONS

Let the column matrix $\widehat{X}[n,s]$ describe the bunch state at the n–th turn and in point s on the reference orbit (see Fig. 1). Its first element $x[n,s]$ is the bunch deviation from the orbit and the second one $x'[n,s]$ is the angle of the bunch trajectory. Let the driving kicker K located in point $s_{\rm D}$ change the angle of the bunch trajectory on $\Delta x'_{\rm D}[n]$. For the bunch states at two consecutive turns after passing the damper kicker DK located in point $s_{\rm K}$ one can write [2, 3]:

$$\widehat{X}[n+1,s] \equiv \widehat{X}[n,s+C] = \widehat{M}(s)\widehat{X}[n,s] + \Delta x'[n,s_{\rm K}]\,\widehat{M}_{\rm K}\widehat{E} + \Delta x'_{\rm D}[n]\,\widehat{M}_{\rm D}\widehat{E}\,, \quad (1)$$

where C is the circumference of the reference orbit; elements $E_1 = 0$ and $E_2 = 1$ in the column matrix $\widehat{E}$. Here 2×2 matrix $\widehat{M}(s_2|s_1)$ for passage from s_1 to s_2 is used [4] so that: $\widehat{M}(s) \equiv \widehat{M}(s+C|s)$, $\widehat{M}_{\rm K} \equiv \widehat{M}(s+C|s_{\rm K})$, $\widehat{M}_{\rm D} \equiv \widehat{M}(s+C|s_{\rm D})$.

$\Delta x'[n,s_{\rm K}]$ is proportional to output voltage $V_{\rm out}$ on the amplifier in a feedback chain and linearly depends on input voltage $V_{\rm in}$:

$$\Delta x'[n,s_{\rm K}] = S_{\rm K}\,V_{\rm out}[n] = S_{\rm K}\,{\rm K}_{\rm out}\,{\rm K}_{\rm in}\times \times \sum_{m=0}^{N_{\rm F}} h[m]\,V_{\rm in}[n-\hat{q}-m]\,u[n-\hat{q}-m]\,, \quad (2)$$

where $S_{\rm K}$ is the DK transfer characteristic; ${\rm K}_{\rm in}$ and ${\rm K}_{\rm out}$ are voltage gains of the output and input amplifiers (see Fig. 1); $u[n]$ is the Heaviside step function; $h[m]$ are coefficients of a finite impulse response (FIR) digital filter in DSP; $N_{\rm F}$ is the FIR filter order. The total delay $\tau_{\rm delay}$ in the signal processing of the feedback path from BPM to DK adjusts the timing of the signal to match the bunch arrival time. If $\tau_{\rm PK}$ is the time of flight of the particle from BPM to DK and $T_{\rm rev} = 1/f_{\rm rev}$ is the particle revolution period, then $\tau_{\rm delay} = \tau_{\rm PK} + \hat{q}\,T_{\rm rev}$.

$V_{\rm in}$ voltage linearly depends on $x[n,s_{\rm P}]$ displacement:

$$V_{\rm in}[n] = (x[n,s_{\rm P}] + \delta x_{\rm P})\,S_{\rm P}\,u[n]\,, \quad (3)$$

where $\delta x_{\rm P}$ is a deviation of the BPM electrical centre from the reference orbit, $S_{\rm P}$ is the BPM transfer characteristic.

Let the driving force be the discrete-time unit impulse with amplitude $a_{\rm D}$ at the $n_{\rm D}$ turn so that

$$\Delta x'_{\rm D}[n]\sqrt{\hat{\beta}_{\rm D}\hat{\beta}_{\rm P}} \equiv V_{\rm D} = a_{\rm D}\,\delta[n-n_{\rm D}]\,, \quad (4)$$

where $\hat{\beta}_i \equiv \hat{\beta}(s_i)$ is the Twiss beta function [4]. In the case of harmonic excitation impulse of $Q_{\rm D}f_{\rm rev}$ frequency, $N_{\rm D}T_{\rm rev}$ duration and $\phi_{\rm D}$ phase one can write: $V_{\rm D} = a_{\rm D}\sin\big(2\pi(n-n_{\rm D})Q_{\rm D}+\phi_{\rm D}\big)\big(u[n-n_{\rm D}]-u[n-n_{\rm D}-N_{\rm D}]\big)$.

The system of linear difference equations (1), (2), (3) and (4) can be solved using unilateral $\mathcal{Z}$–transform [6]:

$$\mathbf{y}(z,s) = \mathcal{Z}\{y[n,s]\} \equiv \sum_{n=0}^{\infty} y[n,s]\,z^{-n}\,, \quad (5)$$

$$y[n,s] = \mathcal{Z}^{-1}\{\mathbf{y}(z,s)\} = \sum_k {\rm Res}\left[\mathbf{y}(z,s)\,z^{n-1};\,z_k\right].$$

ISBN 978-3-95450-125-0

SIMULATION OF BEAM DYNAMICS IN THE EXTRACTION SYSTEM OF THE JINR PHASOTRON

S. Kostromin, L. Onischenko, A. Chesnov, S. Shirkov, JINR, Dubna, Russia

Abstract

Beam dynamics is studied in the extraction by the regenerative method from the JINR Phasotron (657 MeV, 3μA protons) using special complex of computer programs. Parameters of the beam at the deflector entrance are calculated. The beam extraction efficiency is found to be ~40%. The mean movement in the extraction channel is investigated. Calculated beam transverse parameters agree with the experimental ones to accuracy of~20%.

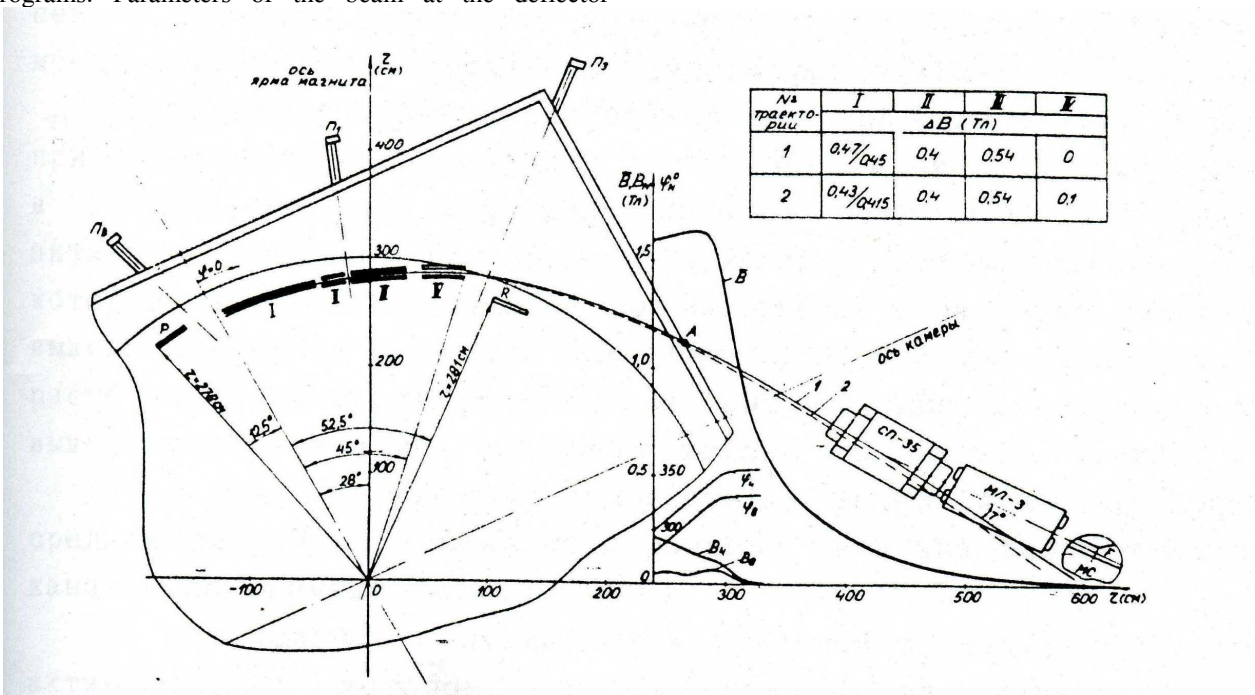

Figure 1: Layout of the Phasotron extraction system P is the peeler, R-regenerator, I, II, III, IV are the sections of the extraction channel.

EXTRACTION SYSTEM OF THE JINR PHASOTRON

The calculation of the beam acceleration in the JINR Phasotron ("F") and its throe to the extraction channel entrance is performed [1] with e special computer code for the beam dynamics simulation in the cyclotron-type accelerators. The regenerative method [2] is used for the beam extraction from "F". The extraction efficiency is ~40% and mainly depends on the beam losses at the entrance to the extraction system.

The position of the beam extraction system inside "F" vacuum chamber is shown in Fig. 1. System consists of peeler, regenerator and four channels. Each element has adjustable radial position. First of four channels is a current supplied channel with the thickness of the septum of 4mm. Other three sections are passive magnetic channels.

Figures 2-5 show portraits end energy distribution of the accelerated beam (2000-proton bunch) at the entrance to the extraction channel.

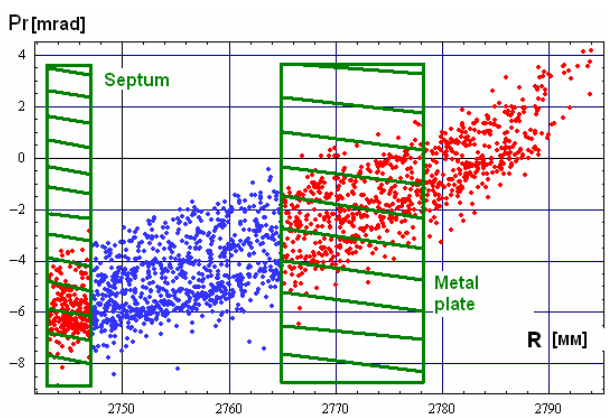

Fig 2: Position of the beam particles on the radial phase plane at the extraction channel entrance

ISBN 978-3-95450-125-0

NEW IDEAS FOR CRYSTAL COLLIMATION*

V.V. Tikhomirov, A.I. Sytov, INP, BSU, Minsk, Belarus

Abstract

Both channeling and volume reflection (VR) effects are used for proton beam deflection by bent crystal. We propose the modifications of both these two effects to drastically improve the deflection efficiency. For the channeling it is a narrow plane cut [1] increasing the fraction of channeled particles up to 98-99%. In order to simplify the fabrication technology we suggest to use a buried amorphous layer instead of a crystal cut [2]. We also suggest to use the multiple volume reflection in one crystal (MVROC) [3], instead of single one because the MVROC increases the deflection angle in 5 times in comparison with VR.

The cut method can be applied with high efficiency for the extraction of high intensity proton beam from the Recycler Ring (FNAL) [5] as well as the MVROC will provide very good deflection parameters for the future LHC crystal-based collimation system. We also argue that the channeling effect is not efficient in the LHC case because of large angular divergence of halo beam particles caused by the elastic nuclear scattering on residual gas.

INTRODUCTION

Bent crystals possess wide capabilities for accelerator physics. Very strong intracrystal electric fields applied with accuracy of Angstrom provide high deflection efficiency. The main advantages of crystals are very compact size, low price of production and simplicity of installation and exploitation. Additionally, they can efficiently deflect the beams of different types of charged particles, of very different energies (from hundreds MeV up to tens TeV and higher) and of different beam angular divergence. The latter parameter is critical for the proper effect choice.

For small beam angular divergence the channeling effect provides rather high performance. For the best case the deflection efficiency exceeds 80%. For multiturn case it can exceed 95%. If the angular divergence is large, the volume reflection will be efficient. It provides less deflection efficiency than the channeling but the angular acceptance of it is much higher.

The efficiency of the channeling can also decrease because of the miscut angle characterizing nonparallelity of the channeling planes and crystal surface. It is shown in [4] that for UA9 experiment [6] the nuclear reactions rate in crystal increases by a factor of 4.5. So, we should consider both the beam impact parameter and angular divergence for effect choice. If the beam impact parameter is rather large for most of particles not to enter in the miscut influence zone and the beam angular divergence is less than the critical angle for the channeling, the latter will provide good deflection efficiency. Otherwise the VR must be chosen.

In this paper we will consider bent crystal application for two opposite cases relevant to two different machines: the future LHC crystal-based collimation system and the 8GeV proton beam extraction from the Recycler Ring at Fermi National Accelerator Laboratory (FNAL) [5]. As we will show below the volume reflection should be chosen in the LHC case while the channeling in the case of the Recycler Ring. Also we suggest for both cases some modifications: a narrow plane cut increasing the channeling efficiency up to 98-99% [1] for channeling and multiple volume reflection in one crystal (MVROC) instead of "single" one.

MVROC FOR LHC COLLIMATION

In order to solve the future LHC collimation problem it is very important to understand the main source of halo formation. Knowing the latter we can calculate the beam profile as well as both the impact parameter and angular divergence distributions in the beam collimation zone (6σ). Then we can exactly choose the proper deflection effect. The main mechanisms of beam loss are inelastic, diffractive and elastic scattering in interaction points (IP) and on residual gas. We can exclude as halo particle production reasons the inelastic and diffractive scattering on gas and in IP because of large scattering angles and energy losses. So, only elastic scattering on residual gas and in interaction points should be considered.

It is known that β-function of interaction points is 2-3 orders less than the average value. That's why the scattering at the same angle increases the amplitude of betatron oscillations for gas 10 times more than for IP:

$$X = \sqrt{\beta_{avr}\epsilon} = \sqrt{\beta_{avr}\beta\theta^2}, \quad (1)$$

where X is an amplitude of betatron oscillations, β_{avr} is average beta function, ϵ is emittance after scattering, β is β-function in a scattering point, θ is a scattering angle. According to (1) the multiple Coulomb scattering on residual gas gives emittance increase of less than initial LHC beam emittance. So, we can exclude the multiple coulomb scattering. The single coulomb scattering at large angles can be excluded because of very small probability and scattering angle of such events insufficient to achieve 6σ. Thus, only elastic nuclear scattering stands for examination.

One obtains that for sufficient scattering angle (at IP) the probability is 5 orders less than for the distribution maximum. More accurate estimates give that about 10^4 particles enter the collimation zone per second. It is at least two or-

* Work supported by Belarusian State Program of Scientific Research "Convergence".

ISBN 978-3-95450-125-0

BEAM DYNAMICS INVESTIGATIONS FOR 433 MHZ RFQ ACCELERATOR

Yuri Svistunov, NIIEFA, St. Petersburg, Russia
Alexander Durkin, MRTI RAS, Moscow, Russia
Alexander D. Ovsyannikov#, St. Petersburg State University, St. Petersburg, Russia

Abstract

Modeling results for deuteron dynamics in RFQ structure with operational frequency 433 MHz and 1 MeV output energy are presented. The results are compared with experimental data. The purpose of investigation is to find optimal input RFQ emittance parameters for off-nominal values of input current and vane voltage.

INTRODUCTION

There are presented theoretical and experimental results of researches short length 1 MeV, 433 MHz RFQ which is part of RF neutron generator (NG). Description of this RFQ was given in article [1] where were discussed problems design and tolerances under manufacturing of such resonator. In [1] installation was considered with ECR deuteron (D^+) source and forming beam system including electrostatic preacceleration, focusing solenoid, electromagnetic correctors and electrostatic focusing lens before RFQ entrance. Later injection system was changed because D^+ source don't permit to obtain required beam emittance on RFQ input. The new injection system have multicusp D^- ion source and it is shown on fig.2 together with RFQ and foil monitor which was used for energy measuring during NG testing.

RFQ DESIGN

RFQ design was based on following main parameters presented in table 1.

Table 1: Initial parameters for RFQ design

Frequency	433 MHz
Ions	$D^{\pm}$
Output beam energy	1 MeV
Output pulsed current	10 mA
Output average current	10 mkA
Input beam energy	25-30 keV
Input beam current	≥10 mA
Maximal surface gradient	≤2xKP

Items 2-5 are determined by use of NG for its proper purposes; item 6 is determined by requirement of small gabarits of feed system; item 7 take into account possible loss of beam; item 8 is determined by requirement of absence of electrical break-down. Calculated RFQ parameters are given in table 2.

Table 2: Calculated RFQ parameters

Beam injection energy	25 keV
Beam output energy	1 MeV
Input pulsed current	13 mA
Output pulsed current	10 mA
Input phase length of bunches	360°
Output phase length of bunches	36°
Input beam synchronous phase	-90°
Output beam synchronous phase	-23.4°
Average channel radius	1.8 mm
Minimal radius	1.18 mm
Intervane voltage	50 kV
Vane length	1090 mm

Data of tables 1, 2 may be added experimental results, obtained during tests and working of NG.

Assembling of four-vanes RFQ was made with high accuracy. Difference of distances between adjacent vanes not more 10 mkm (see fig. 1). Vane modulation was roduced with an accuracy of 2…5 mkm Measured quality factor is 6800. It value was provided by good uality of machining of four-cavity RFQ surfaces. Maximal measured vane voltage without breakdown under testing is 70 kV. Deviation of electrical field tensity from average value along RFQ length is ±5%.

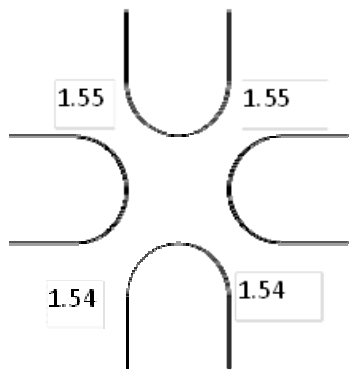

Figure 1: Distances are given in mm between vanes.

#ovs74@mail.ru

ISBN 978-3-95450-125-0

ACCELERATOR COMPLEX U70 OF IHEP: STATUS AND UPGRADES

S. Ivanov, on behalf of the U70 staff#
Institute for High Energy Physics (IHEP), Protvino, Moscow Region, 142281, Russia

Abstract

The report overviews present status of the Accelerator Complex U70 of IHEP-Protvino comprising four machines (2 linear accelerators and 2 synchrotrons). Particular emphasis is put on the recent upgrades implemented since the previous conference RuPAC-2010.

GENERALITIES

Layout and technical specification of the entire Accelerator Complex U70 of IHEP-Protvino were specified in the status report of 2008, Ref. [1]. Since October 2007, the complex comprises four facilities — 2 linear (I100, URAL30) and 2 circular (U1.5, U70), Fig. 1.

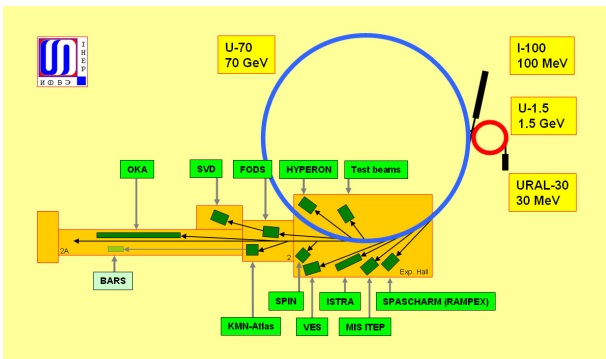

Figure 1: Accelerator Complex U70, beam transfer line network and fixed-target experimental facilities included. Proton mode (default) — cascade of URAL30–U1.5–U70, light-ion mode — I100–U1.5–U70.

Due to recent advances of the light-ion acceleration program, refer to Table 1, former proton synchrotrons U1.5 and U70 can be attributed to the (light-) ion synchrotron category as well.

Table 1: Light-ion program milestones

	Deuterons $^{2}H^{1+}$	Carbon $^{12}C^{6+}$
U1.5	16.7–448.6 MeV/u March 30, 2008	16.7–455.4 MeV/u December 08, 2010
U70	23.6 GeV/u April 27, 2010	34.1 GeV/u April 24, 2011

In the mid-April 2012, IHEP was reorganised into Federal State Budgetary Enterprise and moved under the auspices of the National Research Centre (NRC) “Kurchatov Institute”, which implies a revision of funding schemes to perform R&D and maintain special and general-purpose engineering infrastructure of the IHEP facilities.

ROUTINE OPERATION

Since RuPAC-2010, the U70 complex operated for four runs in total. Table 2 lists their calendar data. The first run of a year is shorter and solves, mainly, R&D and methodological tasks.

Figure 2 shows beam availability data during machine development (MD) and fixed-target experimental physics program (XPh) with averages over 2002–12. The extracted beam is delivered to experimental facilities with 82.8% availability, on average.

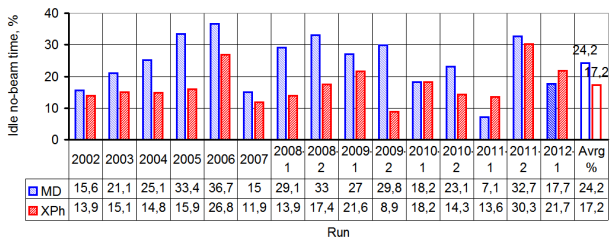

	2002	2003	2004	2005	2006	2007	2008-1	2008-2	2009-1	2009-2	2010-1	2010-2	2011-1	2011-2	2012-1	Avrg %
MD	15,6	21,1	25,1	33,4	36,7	15	29,1	33	27	29,8	18,2	23,1	7,1	32,7	17,7	24,2
XPh	13,9	15,1	14,8	15,9	26,8	11,9	13,9	17,4	21,6	8,9	18,2	14,3	13,6	30,3	21,7	17,2

Figure 2: Beam availability statistics.

Figure 3 is a screenshot of the on-line statistics monitor that is an example (December 2011) of a long-term sustained operation of the complex. The large ring (i.e., the U70 PS itself) delivers $0.98 \cdot 10^{13}$ ppp. Beam losses through a cycle amount to 4%. Slow stochastic extraction spills some $6.7 \cdot 10^{12}$ ppp, while internal targets and Si-crystal deflectors consume the allowed $2.5 \cdot 10^{12}$ ppp.

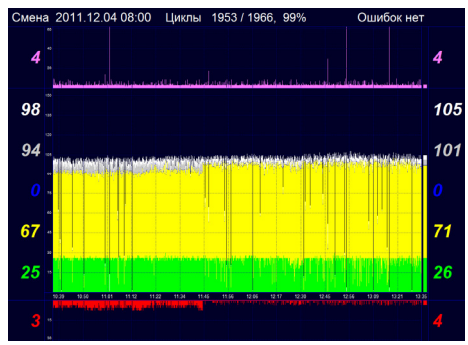

Figure 3: Screenshot of the on-line monitoring over the U70 operation. Time interval (abscissa) extends over 3 hr, or 1000 ramping cycles. Yellow trace slows intensity of slow stochastic extraction, green trace — operation of internal targets and crystal deflectors. Red (inverted) trace indicates spent beam remains dumped onto internal absorber.

Fixed-target experimental setups (from 6 to 10 per a run) acquire the beam via sequential and parallel sharing of the U70 magnetic field flattop (about 3.2 s at 50 GeV).

N. Tyurin, Yu. Fedotov, O. Zyatkov, A. Minchenko, A. Afonin, E. Ludmirsky, O. Lebedev, D. Demihovskiy, V. Lapygin, A. Ermolaev, Yu. Milichenko, I. Tsygankov, I. Sulygin, N. Ignashin, S. Sytov, V. Zenin, Yu. Antipov, D. Khmaruk, and G. Kuznetsov.

ISBN 978-3-95450-125-0

MULTIPURPOSE RESEARCH COMPLEX BASED ON THE INR HIGH INTENSITY PROTON LINAC

A.Feschenko, M.Grachev, L.V. Kravchuk, V.L.Serov,
Institute For Nuclear Research, Moscow 117312, Russia

Abstract

Scientific Complex based on 600 MeV Proton Linac is in operation at the Institute for Nuclear Research, Troitsk, Moscow and provides the beam for both basic and applied research. At present proton beam with the energy up to 209 MeV and with the average current up to 130 μA is used for three Neutron Sources and Beam Therapy Complex, located in the Experimental Area, as well as for Isotope Production Facility. The status of the Linac and the Experimental Area is presented. Accelerator tuning procedures providing minimization of beam loss are described as well.

INTRODUCTION

INR Accelerator Complex is located in science city Troitsk (Moscow) 20 kilometers to the south-west from Moscow circular road. It includes the high-intensity proton Linac, Experimental Area with three neutron sources and Beam Therapy Complex as well as Isotope Production Facility (IPF). Though the initial name of the Complex was Moscow Meson Factory in the recent years the main activity has been shifted towards neutron studies, isotope production and other researches connected with the above mentioned experimental facilities.

In nineties INR accelerator was the second large high intensity and medium energy linac after LANSCE (former LAMPF) at LANL, Los Alamos, USA. In the last decade two new linacs of this type with improved parameters have been put in operation (SNS and J-PARC) and several more ones are being constructed or designed now. This activity shows the urgency of the researches made at the accelerators of this type and confirms extreme topicality of the INR multi-purposes complex.

LINEAR ACCELERATOR

General Description and Parameters

The detail description of the INR proton Linac is given in [1, 2]. The simplified diagram of the accelerator is shown in Fig. 1. The accelerator consists of proton and H-minus injectors, low energy beam transport lines, 750 keV booster RFQ, 100 MeV drift tube linac (DTL) and 600 MeV coupled cavity linac (CCL, Disk and Washer accelerating structure). There are seven 198.2 MHz RF channels for five DTL tanks and RFQ (including one spare channel) as well as thirty two 991 MHz RF channels for 27 CCL accelerating cavities and one matching cavity (including three spare channels and one channel for equipment tests). Design, obtained and currently available operational Linac parameters are summarized in Table 1.

Table 1: Main accelerator parameters.

Parameter	Design	Obtained	September 2012
Particles	p, H-minus	p, H-minus	p
Energy, MeV	600	502	209
Pulse current, mA	50	16	15
Repetition rate, Hz	100	50	50
Pulse duration, μs	100	200	0.3÷200
Average current, μA	500	150	130

The accelerator is in regular operation since 1993. 102 accelerator runs with total duration of more than 38000 hours have been carried out so far including 63 runs of total duration of 18000 hours within the last decade. The availability of the beam for the users is 80÷90 % of the total beam time.

Main Current Goals

The main goal for the nearest future is improvement of accelerator efficiency. To attain this goal two problems have to be solved. The first one is increasing the beam pulse repetition rate from the current 50 Hz to 100 Hz. The second one is distribution of the beam between IPF and Experimental Facility. To double the beam pulse repetition rate the repetition rate of RF system pulses as well as that of proton injector must be doubled.

The activity on increasing RF pulses repetition rate is in progress for several years, but has been intensified recently [3]. The studies with the aim of increasing proton injector repetition rate are also being conducted. Completion of building of H-minus injector enabled a task to be formulated on simultaneous acceleration of proton and H-minus beams. It is supposed that two beams will be accelerated pulse by pulse each with the rate of 50 Hz.

With the aim of distributing the beam between IPF and Experimental Facility the intermediate beam extraction area (160 MeV) has been upgraded [4]. Instead of the first DC bending magnet (Fig.1) the pulse magnet along with the power supply developed and fabricated in D.V.Efremov Institute (St. Petersburg) [5] has been installed. The tests of the system including the tests with the beam have been done [4]. The maximum frequency of the magnet pulses is 50 Hz so the possibility to direct up to half of the beam pulses to IPF will be implemented.

ISBN 978-3-95450-125-0

USE OF BENT-CRYSTAL DEFLECTORS TO STEER BEAM IN U-70 ACCELERATOR OF IHEP- STATUS AND PROSPECTS

A.G.Afonin, V.T.Baranov, Yu.A.Chesnokov, V.A. Maisheev,
V.I.Terekhov, I.A.Yazynin, IHEP Protvino, Russia

Abstract

The report presents an overview the results of IHEP activity in the field of study and using bent crystals to steer high-energy proton and ion beam obtained during 2010-2012. The hardware installed to study crystal collimation and extraction is described. A new dedicated beam transfer line was arranged to study the performance of crystals. It has been shown that the crystal deflections developed are capable of sustaining long-term operation to deliver high-energy extracted beams for fixed-target physics. Experience with practical applications of bent crystals are outlined. First results on the extraction

24.1 GeV nucleon carbon ions are also presented.

BEAM EXTRACTION FROM U-70

The method to use bent crystals to extract protons has found the widest practical application on U-70 accelerator of IHEP during more than 20 years.

Different types of extraction schemes with bent crystals and technical equipment are realized now as for extraction so as for experiments to test new crystal devices and to study beam collimation processes.

The location of the stations with bent crystals in U-70 is presented on Table 1.

Table1:Crystal location in U-70.

Crystal station	Si-19 Si-22 Si-106	Si-24	Si - 27	Si-30	Si-84 Si-86
Beam line	8,22,23	2,14	4	8,22.23	absorber

The subscript means the straight section index or the index of a magnet in which the crystal or internal target is installed..

On U-70 three different possibilities to use bent crystals for physics are realized.

1. One way to use bent crystals is to extract proton by crystal directly. In this case we use long crystals which gives the possibility to receive big angles of deflection. We have two station of this type Si-24 and Si-27.

They extract the beams of protons to experimental facilities, which usually work with secondary particle from internal targets. The angles of bending for such deflectors (80-90) mrad and efficiency ~ 10^{-5}.

2. Second way is to use short crystals with small deflection angle.

The small deflection angle (in our case 0.5-2 mrad, it depends on scheme) is sufficient to put the beam into aperture of septum-magnet, which then provide the larger deflection angle need for the extraction

For this purposes we have crystal stations Si-106, Si-19, Si-22 . The length of deflectors 2-5 mm and the efficiency in this case was achieved 85% [1,2].

3. Third way is to split extracted beam by crystal for two directions. For this regime we use Si-30, which is intended to remove a small fraction of a beam (it can be ~ 10^7 protons per cycle) to beam line 8 or 22.

Beam extraction using bent crystals allows simultaneous operation with internal targets. The diagrams of the beam extractions using bent crystals is shown on Fig 1.

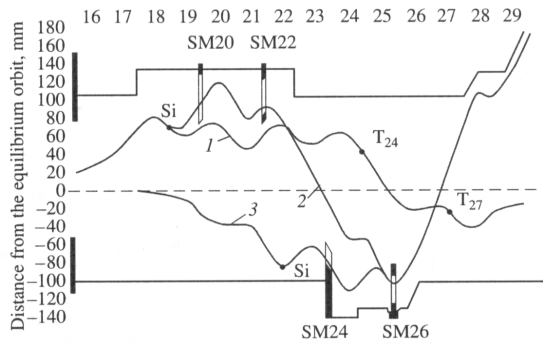

Figure 1. Schematic diagrams of proton beam extraction using bent crystals: (1) the trajectory of circulating beam during its simultaneous guidance onto the crystal in straight section no.19 (Si) and internal target T24 and T27, (2) the trajectory of beam extraction from crystal SS-19 (Si), and (3) the trajectory of beam extraction from crystal Unit 22 (Si).

Since RuPAC-2010, the U-70 complex has been working for four runs in total. Table 2 presents the results of bent crystal extraction during this period.

Table2: The use of slow extraction by bent crystals on U-70 in 2010-2012.

Run of U-70	2-2010	1-2011	2-2011	1-2012
Duration of a run (hours)	744	240	744	288
Crystal extraction (hours)	846	636	672	240

A crystal can extract from 10^6 up to (5-6)* 10^{11} ppp without special cooling technique during hundreds hours without degradation seen. This extraction is a good addition to the slow extraction existing at the U-70 IHEP accelerator, which provided proton beam with intensities of $5*10^{11}$ – 10^{13} particle per pulse. It shows reliable, reproducible and predictable work.

During the runs, all the beam extraction system available in the U-70 were engaged- fast single- turn, slow resonant

ISBN 978-3-95450-125-0

NEW DEVELOPMENTS AND A REVIEW OF THE ACCELERATOR FACILITIES AT ITHEMBA LABS

J.L. Conradie, R. Bark, A.H. Botha, J.C. Cornell, M.A. Crombie, J.G. De Villiers, J.L.G. Delsink, H. Du Plessis, J.S. Du Toit, W.D. Duckitt, D.T. Fourie, M.E. Hogan, I.H. Kohler, R.H. McAlister, H.W. Mostert, J.V. Pilcher, P.F. Rohwer, M. Sakildien, R.W. Thomae, M.J. Van Niekerk, P. Van Schalkwyk, J.P. Slabbert, N.P. Stodart, iThemba LABS, Somerset West 7130, South Africa
J. Dietrich, Technische Universitaet Dortmund, Germany
M. Poggi, INFN Laboratori Nazionali di Legnaro, Viale dell'Universita' 2, 35020, Legnaro, Padova, Italy

Abstract

iThemba LABS is a multi-disciplinary research facility that provides accelerator-based facilities for physical, biomedical and material sciences, treatment of cancer patients with neutrons and protons and the production of radioisotopes and radiopharmaceuticals. The successful utilization of beam diagnostic equipment is critical and essential for the effective running of such a facility and will be discussed in more detail. The current status of the facility and future projects, which entail a radioactive-ion beam project as well as a dedicated facility for proton therapy, will also be discussed.

INTRODUCTION

At iThemba LABS proton beams are accelerated with a K=8 injector cyclotron (SPC1) for injection into a K=200 separated sector cyclotron (SSC) [1]. Production of radioisotopes and neutron therapy is done at 66 MeV and a 200-MeV beam is used for proton therapy. For radioisotope production a beam current varying from 80 to 300 μA is used depending on the target material. Low intensity beams of light and heavy ions and polarized protons, pre-accelerated in a second injector cyclotron (SPC2) with K=11, are available for nuclear physics research.

During the past several years extensive development work has been done on the accelerators to increase the beam intensity for radioisotope production. Flat-top acceleration systems were installed in both the injector SPC1 and the SSC which led to a threefold increase in beam intensity for radioisotope production [2]. The increase in beam intensity also necessitated the development of beam diagnostics that can handle the high beam intensity.

OPERATING STATISTICS

The performance of the iThemba LABS facility was outstanding during the 2011 calendar year. The unscheduled interruptions to operations amounted to a meagre 4.8% of the scheduled beam time, down from 7.3% the year before.

Fig. 1 shows the beam outages per failure category for the calendar year 2011. The bulk of the beam outages in 2011 were caused by RF interruptions, amounting to 25%. Despite this, the beam time loss to the user communities as a result of RF interruptions shows a very encouraging decline. In 2010, the beam outages as a result of the RF systems amounted to 224 hours and in 2011 this figure decreased to only 98 hours. This significant drop in interruptions can largely be ascribed to a pro-active approach to maintenance. As part of this approach, a number of water-cooled components in both the 150-kW amplifiers were replaced and ICs on various PCB boards in the amplifiers were resoldered to remove dry joints after 28 years of operation. These steps greatly contributed to the reduced beam time loss as a result of RF interruptions.

Another major interruption that plagued the operations at the facility in 2011 was power failures. In 2011, power failures resulted in a beam time loss of 40 hours, which was significantly lower than the 60 hours of beam time loss it caused the previous year. This beam time loss is mostly caused by power dips, which are brief interruptions of power to the facility. To lessen the impact of such power dips, iThemba LABS has invested in a 4-MW Uninterrupted Power Supply (UPS). The UPS sustains power when the externally supplied power falls away. However for certain beam energies, power cannot be delivered to all equipment by the UPS. Developments are underway to improve this situation.

Other contributions to operational interruptions were caused by water leaks interrupting the vacuum, servicing and tuning of the ion sources, and problems with cooling water and power supplies.

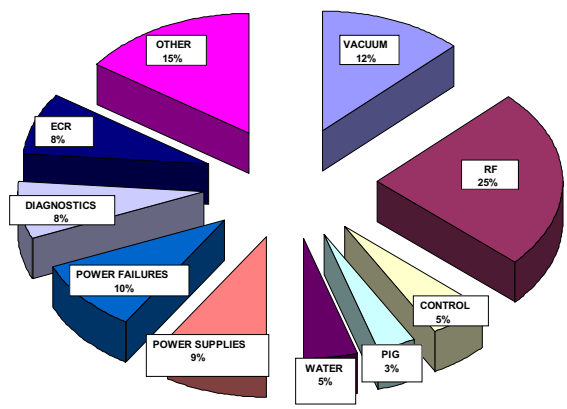

Figure 1: Beam outages per failure category in 2011.

ISBN 978-3-95450-125-0

THE STATUS OF THE SARAF PHASE-I LINAC

L. Weissman*, D. Berkovits, A. Arenshtam, Y. Ben-Aliz, Y. Buzaglo, O. Dudovitch, Y. Eisen, I. Eliahu, G. Feinberg, I. Fishman, I. Gavish, I. Gertz, A. Grin, S. Halfon, D. Har-Even, Y. F. Haruvy, D. Hirschmann, T. Hirsh, Z. Horovitz, B. Keizer, D. Kijel, A. Kreisel, G. Lempert, Y. Luner, I. Mardor, A. Perry, E. Reinfeld, J. Rodnizki, G. Shimel, A. Shor, I. Silverman, E. Zemach, Soreq NRC, Yavne 81800 Israel

Abstract

Phase I of the Soreq Applied Research Accelerator Facility - SARAF is under operation at the Soreq Nuclear Research Center. The status of Phase I main components is reported as well as the beam operation experience accumulated in the recent months. The latter include acceleration of a 1 mA CW protons beam up to 3.9 MeV and 1 mA pulsed, duty cycle of few %, deuterons beam up to 4.7 MeV. Recent and future improvements in the current facility are discussed.

INTRODUCTION

Phase I of SARAF [1] consists of a 20 keV/u ECR Ion Source (EIS), a Low Energy Beam Transport (LEBT) section, a 4-rod Radio Frequency Quadrupole (RFQ) injector, a Medium Energy (1.5 MeV/u) Beam Transport (MEBT) section, a Prototype Superconducting Module (PSM), a Diagnostic plate (D-plate), beam dumps (BD) and temporary beam line (Fig. 1).

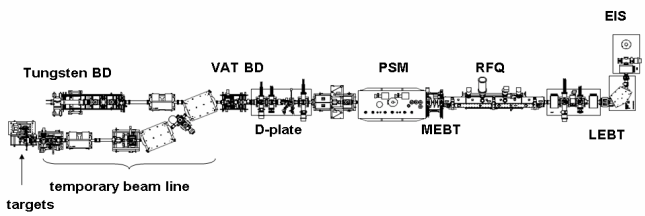

Figure 1. Layout of SARAF Phase I and the temporary beam line.

According to Phase I design specifications; SARAF superconducting linear RF accelerator should yield 2 mA CW beams of protons and deuterons, at energies up to 4 and 5 MeV, respectively. These specifications have not been achieved yet. Nonetheless, during the last two years, alongside with continuous development of the facility, the accelerator has been operated extensively at each opportunity and significant new experience in beam operations has been accumulated.

In the current proceeding we report the accelerator status, improvements of the accelerator subsystems, as well as experience in beam operations that has been accumulated since the last reports [1,2].

* Corresponding author: weissman@soreq.gov.il

STATUS OF MAIN COMPONENTS

EIS/LEBT

The SARAF ECR ion source has been in operation during six years effectively without any maintenance. We experienced two failures connected to the magnetron supply which were promptly resolved. The source could provide up to 6 mA beams of proton or deuteron, in DC or pulsed mode, at the RFQ entrance. The latter mode is used for tuning the accelerator and for beam line optics. The performance of the EIS/LEBT system has been previously reported in detail ([2] and references therein).

First experience with the slow LEBT chopper and plans regarding the fast LEBT chopper are discussed in [3]. Introduction of the chopper would allow for more flexible working range of the beam duty cycle and also allow abandoning pulsed operation of the ion source magnetron.

Reduction of the beam transmission through RFQ at higher LEBT current [2] is still one of the important unresolved issues. It is difficult to explain this reduction without an assumption that the emittance at the RFQ entrance is significantly larger than the value measured upstream the RFQ. . Alternatively, it might be possible that emittance measurements performed with a slit/wire apparatus are dominated by systematic errors which are not yet fully understood. We have performed several measurements aiming at understanding the correlation between the beam emittance in the LEBT and the transmission through the RFQ, as well as attempts to understand the degree of beam neutralization in the LEBT region [4,5]. Further studies are currently in progress.

An additional new water cooled beam-blocker/ collimator has been installed recently in the LEBT, just in front of the RFQ entrance. Installation of this element allows for separate operation of the EIS/LEBT system regardless of the status of the downstream elements.

Increase of hydrogen partial pressure in the RFQ and MEBT was observed when the ion source was operated. To resolve the problem of hydrogen diffusion along the accelerator, hydrogen pumping in the EIS and LEBT sections will be upgraded in the near future.

RFQ/MEBT

The SARAF RFQ is a 176 MHz ~3.8 meter four-rod CW RFQ. The details on the RFQ can be found in [6].

ISBN 978-3-95450-125-0

THE C-80 CYCLOTRON SYSTEM. TECHNICAL CHARACTERISTICS, CURRENT STATUS, PROGRESS AND PROSPECTS.

Yu.N. Gavrish#, P.V. Bogdanov, I.N. Vasilchenko, A.V. Galchuck, S.V. Grigorenko, V.I. Grigoriev, L.E. Korolev, A.N. Kuzhlev, Yu.D. Menshov, V.G. Mudrolyubov, V.I. Ponomarenko, Yu.I. Stogov A.P.Strokach S.S.Tsygankov,
D.V. Efremov Scientific Research Institute of Electrophysical Apparatus, Saint Petersburg, Russia,
S.A. Artamonov, G.I. Gorkin, V.P. Gres, E.M. Ivanov, Yu.T. Mironov, G.F. Mikheev, I.A. Petrov, G.A. Ryabov, B.B. Tokarev,
The B.P. Konstantinov Petersburg Nuclear Physics Institute, Gatchina, Leningrad district, Russia

Abstract

A C-80 cyclotron system is intended to produce proton beams with an energy ranging from 40 up to 80 MeV and current up to 200 μA.

Over a number of years, works on the designing a cyclotron for the acceleration of H^- ions up to 80 MeV were carried out in the PNPI in cooperation with NIIEFA specialists [1-4]. Since September 2010, NIIEFA and PNPI have been carrying out works on building the C-80 cyclotron system intended for production of isotopes, proton therapy of eye diseases and superficial oncologic diseases as well as for fundamental and applied research. In addition, the cyclotron is supposed to be used as an injector of the C-230 synchrotron to ensure an additional acceleration of the extracted proton beam up to approximately 230 MeV. This will allow the Bragg's peak-based procedures to be applied in the proton therapy of oncologic patients.

Rapid advancement of modern methods of the nuclear medicine resulted in higher demand for the radioisotopic products used both in diagnostics and therapy. A rapid upgrowth of the PET diagnostics is observed, which uses radiopharmaceuticals based on radioisotopes with a half-life from several seconds up to several minutes. It is clearly enough that PET diagnostics can be done only in the direct vicinity of functioning cyclotron systems, that is, in large regional centers. The situation can be changed by using Sr-Rb generators, which can be produced on 70-90 MeV cyclotrons under irradiation of a Rb-85 target with protons. The parent isotope, Sr-82 with a half-life of 25.3 days decays and produces a daughter positron emitter Rb-82 used in the production of radiopharmaceuticals for PET. Thus, if Sr-82 is available, a PET center can function in hospitals located sufficiently far from the cyclotron system.

In view of the above, the most evident and cost-effective is the use of the C-80 cyclotron for commercial production of Sr-82. At the 200 μA design current of the extracted proton beam, 40-50 mCi of Sr-82 will be produced for one hour; the price of 1 mCi is not less than 250$. However, this fact does not exclude the possibility to produce commercially the whole assortment of isotopes for medicine as well.

#gavrish@luts.niiefa.spb.su

Parameters of the C-80 cyclotron (Table 1) make possible the realization of the proton radiation therapy of eye diseases and superficial oncologic diseases as well as the implementation of a research program aimed at the development of innovative methods of the proton therapy and promising radionuclides for diagnostics and therapy. Long-term fruitful cooperation of specialists from the PNPI and medical specialists from the Research center for Radiology and Surgical Technology, St.Petersburg in the treatment of patients using the TS-1000 accelerator is of great importance in this matter.

Table 1: Major characteristics of the C-80 cyclotron

Systems/Parameters	Characteristics
Accelerated particles	H^-
Extracted particles	H^+
Beam energy, variable, MeV	40...80
Beam current, μA	2000
Electromagnet - type - pole diameter, cm - mass, t	 E-shaped 2050 245
Resonance system - operating frequency, MHz - RF voltage amplitude, kV	 41.2 60
RF-generator power, kW	80
Ion source	external
Operating mode	continuous/pulse
Total power consumption, no more, kW - with the beam on - in the stand-by mode	 500 200

The major unit of the cyclotron, the electromagnet, has been designed using the magnet of the synchrocyclotron functioning in the PNPI. The main electromagnet has a traditional design with an E-shaped magnet yoke. The system to move upward the magnet upper part (the half-yoke) is worn-out and outdated. It was decided to replace it for 4 pairs of ball bearings and screws equipped with servomechanisms and position sensors The height of the half-yoke lifting is not less than 600 mm, the setting accuracy is not worse than 50 μm. Figure 1 shows the

ISBN 978-3-95450-125-0

SOME DESIGN FEATURES OF THE 80 MEV H⁻ ISOCHRONOUS CYCLOTRON IN GATCHINA

G.Riabov, S.Artamonov, E.Ivanov, G.Mikheev, B.Tokarev, Yu.Mironov, Petersburg Nuclear Physics Institute, S-Petersburg, Russia
P.Bogdanov, V.Mudrolubov, NIIEFA, S-Petersburg, Russia

Abstract

The history of the design and costruction of the 80 MeV H⁻ isochronous cyclotron as well as some design features are discribed.

INTRODUCTION

The cyclotron complex is designed for fundamental and applied researches – production of medical isotopes, beam therapy of eye melanoma and surface types of cancer. Besides the cyclotron is to be used as injector for C-230 synchrotron which is planed to be built for proton therapy of cancer diseases of human internal organs utilizing the Bragg peak.

To minimize the expenditures while designing the cyclotron an attempt was made to use at most the existing synchrocyclotron infrastructure, i.e. building, the bridge crane for 30 ton, electric power, water cooling, ventilation system etc. The iron yoke of the existing synchrocyclotron magnet model is used for the magnet system.

Acceleration of H⁻ ions has obvious advantages: possibility for 100% extraction of the beam with high intensity and variable energy. On the other hand it requires special source of H⁻ ions, high vacuum and what is most important magnetic field strength in the magnet sector should not exceed in our case 17 kGs to prevent H⁻ electromagnetic dissociation.

Design and construction of H⁻ isochronous cyclotron have been in progress for many years and by the year 2010 design and drawings for the main accelerator subsystems had been completed [1,2,3]. The cyclotron magnet was designed, produced, commissioned and put into operation, full scale magnetic measurements were begun. The main problem by that time became purchase of industrially and commercially produced equipment that was realized in the frame of the nuclear medicine program of National Research Centre Kurchatov Institute. Starting from September of 2010 the cyclotron and beam transport line equipment is mounted in experimental hall.

GENERAL DESCRIBTION

Main parameters of the cyclotron are presented in Table 1. The detailed information about cyclotron equipment is presented in the report on this conference.

FEATURES OF THE MAGNETIC SYSTEM

In addition to the standard cyclotron for H⁻ machine there is an additional and essential requirement - to keep H⁻ losses on dissociation below than 5%.

H⁻ Losses and the Magnetic Structure

Two alternative versions of the magnetic structures have been examined. The first one (1) have flutter F = 0.04, spiral angle γ =55°, harmonic amplitude A4 = 4.15 kGs and the second one (2) have F = 0.025, γ = 65°, A4 = 3.28 kGs on the final radius. Here γ is an angle between the radius vector at radius r and tangent to the median line of sectors at the same radius. Both modifications provide about the same net axial focusing and differ by the field in the hill region. Fig. l. presents the beam losses due to electromagnetic dissociation for two versions of the magnetic structures. The second version - with low flutter and high spiral angle was selected for Gatchina cyclotron since it provides beam losses below than 5%.

Table 1: Main parameters of the cyclotron

MAGNET	
Pole diameter	2.05 m
Valley gap	386 mm
Hill gap (min)	164 mm
Number of sectors	4
Spiral angle (max)	65 degrees
Isochronous filed in the center	1.352 T
Flatter (max)	0.025
Ampere- turns	3.4×10^5
Power	120 kW
Weight	250 t
HF. SYSTEM	
Frequency	41.2 MHz
Potential	60 kV
Harmonics	2
HF power	2×40 kW
VACUUM	
Pressure	10^{-7} tor
2 cryogenic pumps	2×3500 l/s
1 turmomolecular	(H_2)
H⁻ source	
Multipole	1.5 mA
Injection energy	26 kV
AXIAL INJECTION	
Transport system: solenoid lens, solenoid, inflector	
EXTRACTION SYSTEM	
Stripping method	
Energy range	40-80 MeV

Magnetic Structure with High Spiral Angle

Parameters of the C-80 magnetic structure are presented in table 1. Fig.2 presents top view of the pole tips of the magnetic system

ISBN 978-3-95450-125-0

ITEP-TWAC RENEWAL AND UPGRADING PROGRAM

N.N.Alexeev, P.N.Alekseev,V.A.Andreev, A.N.Balabaev, A.I.Balabin, V.N.Balanutsa, A.A.Golubev, M.M.Kats, V.I.Nikolaev, A.S.Ryabtsev, Yu.A.Satov, V.S.Stolbunov,V.A.Schegolev, B.Yu.Sharkov, A.V.Shumshurov, V.P.Zavodov, ITEP, Moscow, Russia

Abstract

The ITEP-TWAC facility has been put out of operation this year as a result of some equipment damage by the fire, so the program of machine renewal and its equipment upgrading for accelerated beams parameters improvement and experimental area expansion is now under processing and development. Main items of this program and status of machine restoration activity are presented.

INTRODUCTION

ITEP Ring Accelerator Facility has celebrated last year 50-th anniversary of first 7 GeV accelerated proton beam, so substantial part of the ITEP-TWAC components has been in keeping with its age requiring some additional efforts for rejuvenation of obsolete equipment, communications and structural components and the problem of machine upgrade has been discussed last few years [1]. The main directions of the ITEP-TWAC upgrade were considered for realisation in parallel with machine operation with proton and heavy ion beams in different applications on a base of new accelerator technologies development. The laser ion source technology development was oriented to getting of high current and high charge state ion beam of Z/A up to 0.4 for elements with A ~ 60 to be effectively stacked in the accumulator ring with multiple charge exchange injection technique at the beam energy of up to 700 MeV/u. The new high current heavy ion linac was under construction. Design of proton injection and beam slow extraction for UK ring was performed for its utilizing as self-depending synchrotron in medical application and for imitation of cosmic radiation.

Decommissioning of accelerator facility in this year and destruction of some part of its equipment forced to reconsider the program of machine upgrade on the basis of achieved results in development of ITEP-TWAC project and substantial refinery of the ultimate aim, purpose and main tasks of the proposed reconstruction.

STATUS OF ITEP-TWAC IN 2011

The ITEP-TWAC facility (Fig.1) consisting of main synchrotron-accumulator U-10 with 25 MeV proton injector I-2 and linked to U-10 Ring booster synchrotron UK with 4 MV ion injector I-3 has been in several operation modes accelerating protons in the energy range of 0.1-9.3 GeV, accelerating ions in the energy range of 0.1-4 GeV/u and accumulating nuclei up to Cu at the energy of 200-300 MeV/u. Accelerated beams were used in following modes: secondary beams generated in internal targets of U-10 Ring transferred for experiments to Big experimental hall (BEH); beams extracted from U10 Ring in one turn transferred to Target hall (TH); and proton beam bunch extracted from U-10 ring was transferred to Biological research hall (BRH). Some of secondary beam lines were used for transferring of slow extracted beams from U-10 Ring.

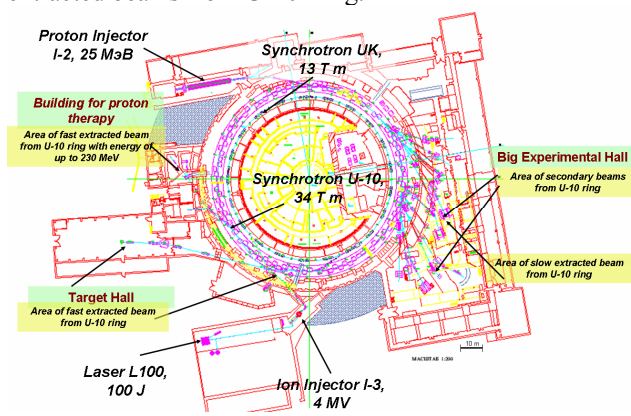

Figure 1: Layout of ITEP-TWAC Facility.

Statistic of machine operation time is shown on Fig.2. The total beam time of near 4000 hours per year was divided between three operation modes: acceleration of protons (~50%), acceleration of ions to intermediate and relativistic energy (~30%) and nuclei stacking (~20%).

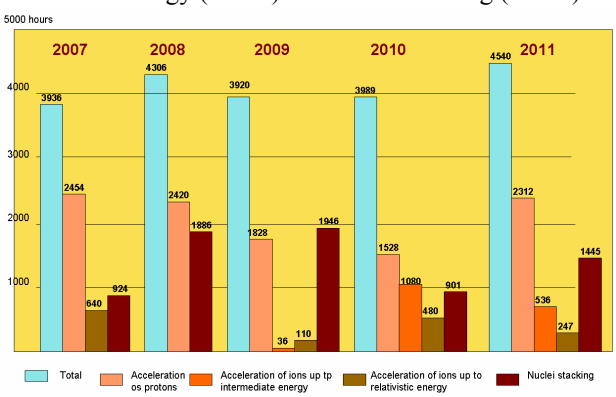

Figure 2: Statistic of ITEP-TWAC operation time.

Statistic of machine using for different research fields (Fig.3) shown the tendency of beam time increase for applications such as biology, medicine, protonography and testing of heavy ion radiation steadiness of electronics destined for cosmic apparatus. The demand for beam time exceeded the offering one by factor of two. This discrepancy was supposed to be cardinally reduced in a result of machine infrastructure improvement.

One of a challenge technologies implemented in ITEP-TWAC is laser ion source (LIS) with high power CO_2-laser. Charge states of ions generated in the LIS are shown in Fig.4.

ISBN 978-3-95450-125-0

STATUS OF THE NUCLOTRON

A. Sidorin, N. Agapov, A. Alfeev, V. Andreev, V. Batin, O. Brovko, A. Butenko, D. E. Donets, E. D. Donets, E.E. Donets, A. Eliseev, V.Fimushkin, A. Galimov, E. Gorbachev, A. Govorov, E. Ivanov, V.Karpinsky, V.Kekelidze, H. Khodzhibagiyan, A. Kirichenko, A. Kobets, A. Kovalenko, O. Kozlov, N.Lebedev, I.Meshkov, V. Mikhailov, V. Monchinsky, A. Philippov, S. Romanov, T. Rukoyatkina, N. Shurkhno, I. Slepnev, V.Slepnev, A. Smirnov, A.Sorin, G. Trubnikov, A. Tuzikov, B. Vasilishin, V. Volkov,
JINR, Dubna, Moscow Region

Abstract

The Nuclotron upgrade – the Nuclotron-M project, was successfully completed in 2010. Following the project goals, Xe ions were accelerated to about 1.5 GeV/u in March 2010. In December 2010, the stable and safe operation of the power supply and energy evacuation system was achieved with a field in the lattice magnets of 2 T. In 2011 - 2012 three runs of the Nuclotron operation were carried out. The facility development is aimed to the performance increase for current physical program realization and to test equipment and operational modes of the NICA collider.

INTRODUCTION

The "Nuclotron-M" project, started in 2007 was considered as a key part of the first stage of the JINR general project NICA/MPD [1]. The extension of JINR basic facility capabilities for generation of intense heavy ion and high intensity light polarized nuclear beams, including design and construction of heavy ion collider aimed at reaching the collision energy of $\sqrt{s_{NN}}$ = 4÷11 GeV and averaged luminosity of $1 \cdot 10^{27}$ $cm^{-2}s^{-1}$ is necessary for realization of the NICA/MPD.

During the Nuclotron-M project realization course almost all the Nuclotron systems were modernized and six runs at total duration of about 3200 hours were carried out. To the end of 2010 all general goals of the project were reached : the Xenon ($^{42+}Xe^{124}$) beam was accelerated up to 1.5 GeV/u and reliable work of the Nuclotron magnetic system at 2 T was provided [2].

Presently the creation of the NICA general elements is realizing in the frame of three officially approved JINR projects: "Nuclotron-NICA" (accelerator part), MPD (the project oriented to creation of one of the collider detectors) and BM@N (Baryonic Matter at Nuclotron – the new fixed target experiment with heavy ions, the detector is under construction in the existing experimental building). The Nuclotron is the key element of all three projects: as the ion source for MPD element testing and for experimental program BM@N realization, as the main synchrotron in the injection chain of the future collider and as the basic facility for testing of new equipment of the booster and collider rings.

The results of the Nuclotron upgrade and development of the accelerator complex during last two years are briefly described in this report.

RESULTS OF THE NUCLOTRON UPGRADE PROGRAM

The "Nuclotron-M" program was oriented to the development of the existing Nuclotron accelerator complex to the facility for generation of relativistic ion beams over atomic mass range from protons to gold ions at the energies corresponding to the maximum design magnetic field (2 T) in the lattice dipole magnets. Another important goal of the project was to reach new level of the beam parameters and to improve substantially reliability and efficiency of the accelerator operation, renovate or replace some part of the equipment that have been under operation since 1992-93.

As an element of the NICA collider injection chain, the Nuclotron has to accelerate single bunch of fully stripped heavy ions (as a reference Au^{79+} is considered) from 0.6 to about 4.5 GeV/u. The required bunch intensity is about $1 \div 1.5 \cdot 10^{9}$ ions. The particle losses during acceleration have to be minimized and do not exceed 10%. The magnetic field ramp rate has to be 1 T/s and more. To demonstrate the ability of the Nuclotron complex to satisfy these requirements, the general milestones of the Nuclotron-M project were specified as an acceleration of heavy ions (at atomic number larger than 100) and stable and safety operation at 2 T of the dipole magnet field.

In the frames of the "Nuclotron-M" project the following works on the LHEP accelerator complex development were performed.

1. Full scale modernization of the cryogenic system was carried out. As result the cooling power at 4,5 K was increased up to 4 kW, the reliable work at maximum magnetic field and at prolonged magnetic cycle duration was provided. The operation term was sufficiently increased; today the new equipment can be used for the NICA/MPD purposes already.

2. The vacuum system modernization permitted to decrease the residual gas pressure in the Nuclotron beam pipe by two orders of magnitude and to provide a possibility of heavy ion acceleration. The obtained result allows solving general task of the Nuclotron as a part of

ISBN 978-3-95450-125-0

ADVANCES OF LIGHT-ION ACCELERATION PROGRAM IN THE U70

S. Ivanov, on behalf of the U70 light-ion task team#
Institute for High Energy Physics (IHEP), Protvino, Moscow Region, 142281, Russia

Abstract

The paper reports on the recent progress in implementing the program of accelerating light ions in the Accelerator Complex U70 of IHEP-Protvino. The list of milestones achieved since RuPAC-2010 includes: (1) Proof-of-principle acceleration of carbon-12 to the top available 34.1 GeV/u (specific kinetic energy). (2) Circulation and slow extraction from the U70 of the carbon beam at flat-bottom 453–455 MeV/u. (3) The first ever successful extraction of carbon nuclei at 24.1 GeV/u to the existing beam transfer line #22 followed by feeding the FODS experimental facility with carbon beam for fixed-target high-energy nuclear physics start-up.

INTRODUCTION

The program to accelerate light ions (deuterons, carbon nuclei) with a charge-to-mass ratio q/A = 0.4–0.5 in the Accelerator Complex U70 of IHEP-Protvino aims at diversification and development of the accelerator facilities. The ion mode of operation involves a sequence of Alvarez DTL I100 (2 tanks of 3, 4π mode), rapid cycled synchrotron U1.5, and the main synchrotron U70 itself.

This program is fulfilled incrementally, each recent machine run constituting a noticeable step in accomplishing the task.

This report overviews chronologically the progress achieved since the previous conference RuPAC-2010.

The starting point is acceleration in the U70 of deuterons to the specific kinetic energy 23.6 GeV/u (flattop 8441 Gs) with $5{\cdot}10^{10}$ dpp, see Ref. [1], RuPAC-2010.

Since then, the cascade of I100, U1.5, and U70 involved was switched to the **carbon-beam mode.** The procedure implies re-assembly of the solid-state laser (CO_2, 5 J) ion source, acceleration of ions $^{12}C^{5+}$ in the I100, thin-foil (Mylar, 4 μm) stripping to bare ions (nuclei) $^{12}C^{6+}$, and their subsequent acceleration in the synchrotrons U1.5 (6.9 T·m) and U70 (233 T·m).

RUN 2010-2

During this run, on Dec 8, 2010, the fully stripped carbon ions $^{12}C^{6+}$ were **first accelerated** to 455.4 MeV/u (kinetic**) in the U1.5**. Beam intensity varied between 5.3–$3.5{\cdot}10^{9}$ ipp through 26 ms ramp (once in 8 s), Fig. 1.

There were, at least, two prerequisites for this success:

1. Operational experience gained earlier with the more intensive deuteron beam.
2. Abundance of ions delivered by the I100, Fig. 2.

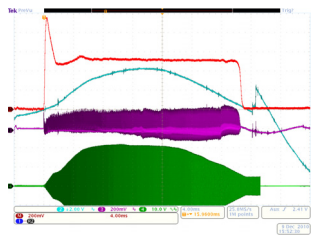

Figure 1: Carbon ($^{12}C^{6+}$) beam intensity monitored with a DCCT (upper (red) trace) and ramping rate of the U1.5 guide field (lower (blue) trace). In-out transfer is 65%.

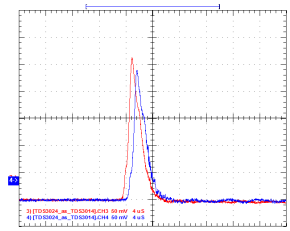

Figure 2: Beam at exits from the I100 (red) and BTL I100–U1.5 (blue). Pulsed current 21 mA, max. Pulse length 5 μs. In-out transfer through the BTL is 90%.

The first turns of carbon beam **in the U70** at flat-bottom 353.1 Gs were committed on Dec 10, 2010, Fig. 3. Bunch length is 80 ns FW at base. The lattice behaves as a magnetic ion separator, and 149.70 kHz beam rotation frequency is a signature of the particular $^{12}C^{6+}$ ion species due to mass defect in a bound system of nucleons (Table 1).

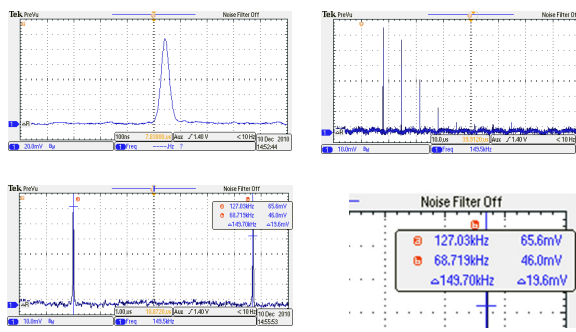

Figure 3: The first turns of carbon beam in the U70.

Table 1: Rotation frequency at 353.1 Gs flattop in the U70

Ion species	Rotation frequency, kHz
Carbon $^{12}C^{6+}$	149.70
Deuterons $^{2}H^{1+}$	149.24
Protons $^{1}H^{1+}$ (*p*)	183.80

RUN 2011-1

During this run, on Apr 24, 2011, carbon beam (single bunch) was **first accelerated in the U70 to the ultimate** available **energy** of 34.1 GeV/u (flattop 12 kGs) with max $5{\cdot}10^{9}$ ipp (8 s), design figure being $3{\cdot}10^{9}$ ipp.

Organizationally, the ion-mode MD was very challenging with the use of a low-intensity pilot proton beam and

N. Tyurin, A. Zaitsev, A. Soldatov, A. Afonin, Yu. Antipov, G. Britvich, A. Bulychev, A. Ermolaev, V. Garkusha, G. Hitev, N. Ignashin, D. Khmaruk, V. Kryshkin, V. Lapygin, O. Lebedev, V. Ledenev, E. Ludmirsky, A. Maximov, Yu. Milichenko, A. Minchenko, V. Seleznev, V. Stolpovsky, I. Sulygin, S. Sytov, and G. Kuznetsov.

ISBN 978-3-95450-125-0

MARS: FOURTH GENERATION X-RAY LIGHT SOURCE BASED ON MULTITURN ENERGY-RECOVERY LINAC

G. N. Kulipanov, Ya. V. Getmanov, O. A. Shevchenko, A. N. Skrinsky, Budker INP SB RAS, Novosibirsk, Russia
N. A. Vinokurov*, Budker INP SB RAS, Novosibirsk, Russia and KAERI, Daejeon, S. Korea
M. V. Kovalchuk and V. N. Korchuganov, NRC "Kurchatov Institute", Moscow, Russia

Abstract

In the recent years, Russian government and scientific society have been coming gradually to an understanding the way of development science in Russia. Government have accepted a program of building six mega-science projects, and one of them can be a new fourth generation x-ray light source based on accelerator-recuperator. Multiturn energy recovery linacs (ERL) looks very promising for making modern synchrotron radiation sources, being less expensive and more flexible. At this time only one multiturn ERL exists. This Novosibirsk ERL operates with two orbits and two free electron lasers based on one linac now. The conception of Multiturn Accelerator-recuperator Radiation Source (MARS) was proposed in 1997 by G.N. Kulipanov, A.N. Skrinsky and N.A. Vinokurov. The use of the ERL with two separated accelerating structures allows to exclude main disadvantages of scheme with one linac, such as the pass of electron bunches with different energies through the same magnetic arcs. The feasibility study for such ERL-based high brightness x-ray source is presented.

INTRODUCTION

In the recent years, Russian government and scientific society have been coming gradually to an understanding the way of development science in Russia. Government has accepted a program of building one of the six mega-science projects, and one of them can be a new fourth generation x-ray light source. At the last 30 years the development of the synchrotron radiation (SR) sources has been aiming to different purposes. The main ones are the increase of spectral brightness and energy of generated quanta, using specific properties of SR radiation (coherence, polarization, time structure, etc.). Also, it is very important that each SR source is used by a large number of research groups (up to 60) from different areas of science and is worked for 7000 hours a year. Today, the SR sources of the third generation became the efficient factories for generating new knowledge, new technologies and new materials.

REQUIREMENTS TO FOURTH GENERATION SYNCHROTRON RADIATION SOURCES

For the last two decades, the development of SR sources of the fourth generation has been actively discussed. The world's physical community has worked out the following requirements to these sources. Full spatial coherence; the highest temporal coherence ($\Delta\lambda/\lambda<10^{-4}$) without additional monochromatization; the averaged brightness of the sources has to exceed 10^{23}-10^{24} photon$\cdot$ s^{-1}mm^{-2}mrad^{-2}(0.1% bandwidth)$^{-1}$; the full photon flux for the fourth generation sources must be at the level of the third generation SR sources; high peak brightness of the order of 10^{33} photon$\cdot$s^{-1}mm^{-2}mrad^{-2}(0.1% bandwidth)$^{-1}$ is important for some experiments; electron bunch length shorter, than 1 ps; high long-term stability; generation of linear and circular polarized radiation with fast switching of the polarization type and sign; constant heat load on chambers and optics, etc.; servicing the multi-user community [1].

During the last 30 years, the brightness of the x-ray SR sources based on storage rings has been increased by a factor of 10^9. Nevertheless, on the modern sources, the flux of coherent quanta is only 10^{-3} of the total flux. Therefore, in spite of successful demonstrating x-ray holography, it has not become an efficient technique for structural studies of real objects of mostly non-crystalline structure. Even for crystalline structures it is very important to use the speckle spectroscopy, which is accessible only in coherent light. Accordingly, the most important from all the requirements are: - the obtaining a fully spatially coherent flux of quanta with full photon flux at the level of the third generation SR sources, - a possibility of obtaining undulator radiation with a monochromaticity of 10^{-3} - 10^{-4} without using monochromators, which as a rule spoil the beam spatial coherence.

It is impossible to satisfy all requirements for the fourth generation SR sources using only one type of sources. High peak brightness and femtosecond length of light pulses can be achieved by using x-ray free electron lasers based on linacs with high (more than 1 kA) peak current.

Other requirements can be implemented easier and cheaper by using radiation from long undulators installed on the accelerator-recuperator.

ACCELERATOR SCHEME

A concept of accelerators-recuperators with one accelerating structure was proposed for realization a fully spatially coherent x-ray source in 1997 [2, 3]. Today, there is only one multiturn ERL in the world. It is

*vinokurov@inp.nsk.su

ISBN 978-3-95450-125-0

THE DEVELOPMENT OF SYNCHROTRON RADIATION SOURCE OF NRC "KURCHATOV INSTITUTE"

V. Korchuganov, A.Belkov, Y.Fomin, E.Kaportsev, G.Kovachev, M.Kovalchuk, Yu.Krylov, K.Kuznetsov, V.Kvardakov, V.Leonov, V.Moiseev, V.Moryakov, K.Moseev, N.Moseiko, D.Odintsov, S. Pesterev, Yu.Tarasov, S.Tomin, V.Ushkov, A.Valentinov, A.Vernov, Yu.Yupinov, A.Zabelin, NRC Kurchatov Institute, pl. Akademika Kurchatova 1, Moscow,123182 Russia

Abstract

Russia`s first dedicated SR source based on electron storage ring Siberia-2 entered service in late 1999, Kurchatov Institute, Moscow. The report focuses on the consumer parameters of an electron beam and the further development of actual SR source, SR beam lines and experimental stations in 2012.

INTRODUCTION

The accelerating complex of the Kurchatov SR source includes: a for-injector - the linear accelerator of electrons on energy of 80 MeV, the small electron storage ring SIBERIA-1 with energy of electrons of 450 MeV, the big electron storage ring SIBERIA-2 with energy of electrons of 2.5 GeV and two electron-optical channels – EOC-1 and EOC-2 [1]. The accelerator complex parameters are specified in Table 1. Official opening of the Kurchatov SR source took place 1.09.1999.

Table 1: Parameters of KSRS facilities

Linac	**SIBERIA-1**	**SIBERIA-2**
E = 80 MeV	E = 80÷450 MeV	E = 0.45÷2.5 GeV
I = 0.2 A	I = 0.2÷0.3 A (singlebunch)	I = 0.1÷0.3 A (multibunch)
L = 6 m	C = 8.68 m	C = 124.13 m
DE/E = 0.005	B = 1.5 T	B = 1.7 T
ε_0 300 nm·rad	ε_{x0} 800 nm·rad	ε_{x0} 78÷100 nm·rad
τ_{pulse} = 18 ns	T_0 = 29 ns	T_0 = 414 ns
f_{rep} = 1 Hz	T_{rep} = 25 s	τ =10÷25 hrs
	λ_c=61 Å , BMs	λ_c=1.75 Å, BMs λ_c=0.40 Å, SCW
For-injector	Booster, VUV and soft X-ray source	Dedicated SR source 0.1-2000Å [1]

KSRS FACILITIES WORK

Before 2012 the work of SIBERIA-2 on experiments is carried out with use of SR from bending magnets in energy range фотонов 4-40 keV и спектральных потоках (10^{13}-10^{11}) ph/s/mrad/0.1%BW of photons 4-40 keV and spectral flux (10^{13}-10^{11}) ph/s/mrad/0.1%BW during week runs in a round-the-clock mode. Within one week 9 working 12-hour shifts are presented.

But, a regular work of X-Ray structure analysis station (RSA) with SR of 7.5T wiggler`s is planned (beamline 1.4-3, 17 mrad) starting from October 2012.

Diagram in Fig.1 shows the integral time devoted for SR experimental work at Siberia-2 in 2000 – 2011 years. Table 2 presents statistic of SR source Siberia-2 work at experiment in the first half of 2012. Note that in 2012 the SR source spent relatively much time in standby and adjustment mode due to stops for the firms which work according contracts (opening shielding walls, new beam lines installation, etc).

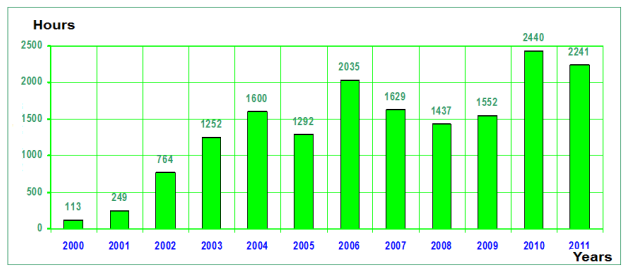

Figure 1: Experimental time at Siberia-2 in 2000-2011.

Table 2. Statistics of Siberia-2 on July 2012.

Parameter	**SIBERIA-1**	**SIBERIA-2**
Total working time, hrs : min	2371:18	2371:24
Experiment mode		
Duration, hrs	43	1074
% of total working time	2%	45%
Maximum current, mA	300	130
Average current, mA	116.6	46.0
Full integral, A-hrs	348.3	1046
One half of year 2012, A-hrs	5.0	49.3
Lifetime, hrs (100 mA)	1:56	38.5
Lifetime, hrs (50 mA)	1:11	51
Injection	10%	5%
Adjustment	34%	24%
Mode on duty	54%	25%

DEVELOPMENT OF KSRS ON 2010-2012

The works on modernization of systems of actually accelerating complex during 2008-2010 were in detail reported at conference RUPAC 2010 [2].

The purpose of works on 2010-2012 is both modernization of the existing equipment of a SR complex, and introduction in a system of new development.

ISBN 978-3-95450-125-0

CURRENT FEL PHYSICS RESEARCH AT SLAC*

G. Stupakov, SLAC National Accelerator Laboratory, Menlo Park, CA, USA

Abstract

In this paper we review several techniques being pursued at SLAC National Accelerator Laboratory with the goal of improving the longitudinal coherence and increasing the output power of x-ray FELs. They include echo enabled harmonic generation (EEHG), hard x-ray self-seeding, using undulator tapering to increase the FEL power, and noise suppression in the electron beam.

INTRODUCTION

Free electron lasers (FELs) can provide tunable high-power coherent radiation which is enabling forefront science in various areas. At x-ray wavelengths, most of the FELs operate in the self-amplified spontaneous emission (SASE) mode [1, 2]. The Linac Coherent Light Source (LCLS) at SLAC working in the SASE mode at hard x-ray wavelengths [3] marked the beginning of a new era of x-ray science [4–6]. However, since SASE FEL radiation starts from beam shot noise, the FEL output has limited temporal coherence (i.e. noisy in both temporal profile and spectrum). FELs with improved temporal coherence (i.e. a well-controlled pulse shape and a bandwidth close to transform limit) should benefit many applications and enable new capabilities in many disciplines.

Various techniques [7–13] have been proposed to improve the FEL temporal coherence. In the self-seeding scheme, a monochromator is used to purify the spectrum of a SASE FEL and an additional undulator is employed to amplify the quasi-monochromatic radiation to GW level. Alternatively, seeding with an external source generated from an external laser may provide a fully coherent output having well-defined timing with respect to the laser. One way to directly seed an FEL is to use the high harmonic generation (HHG) source generated when a high power laser is injected to a noble gas.

EEHG SEEDING

To circumvent the need for a high power laser at short wavelength, frequency up-conversion techniques [10–14] have been envisioned to convert the external seed to shorter wavelengths. In the classic high-gain harmonic generation (HGHG), a single modulator-chicane system is used to bunch the beam at a harmonic frequency of the seed laser [10].

* Work supported by the U.S. Department of Energy under contract DE-AC02-76SF00515.

The frequency multiplication efficiency can be greatly improved with the recently proposed echo-enabled harmonic generation (EEHG) technique [12, 13]. In this scheme, an electron beam is first energy modulated by a laser with wave number k_1 and then sent through a chicane with strong momentum compaction after which the modulation is macroscopically smeared. Simultaneously, separated energy bands with a spread much smaller than the initial energy spread are introduced into the beam phase space. It turns out that if a second laser with wave number k_2 (k_2 can equal k_1) is further used to modulate the beam, after passing through a second chicane, density modulation at the wave number

$$k_E = nk_1 + mk_2 \tag{1}$$

can be generated (n and m are integers). The key advantage of EEHG is that by trading the large energy modulation from a laser with a large momentum compaction from a chicane, high harmonics can be generated from those separated energy bands with a relatively small energy modulation. Thus it promises both bunching and gain at very high harmonics, allowing the generation of coherent soft x-rays directly from a UV seed laser in a single stage.

The advanced frequency up-conversion efficiency has stimulated a broad interest in using the EEHG scheme to seed x-ray FELs [15–18]. In recent proof-of-principle experiments performed at SLAC's Next Linear Collider Test Accelerator (NLCTA) [14] and the SDUV-FEL at SINAP [19], the 4th and 3rd harmonics from EEHG have been observed. They demonstrated that a long-term memory of the beam phase space correlations could be properly controlled and preserved in the experiment. The latest results from the NLCTA presented the first evidence of 7th harmonics from the EEHG technique [20].

The novelty of the experiment [20] is that an rf transverse cavity (TCAV) was used to increase the slice energy spread by one order of magnitude such that the ratio of energy modulation to energy spread is similar to that in real seeded x-ray FELs. In this experiment, the 7th harmonic of the second laser at 227 nm was generated when the energy modulation is approximately $2 \sim 3$ times the slice energy spread.

The parameters of the experiment [20] are listed in Table 1.

Representative spectra of beam radiation after the seeding for various TCAV voltage are shown in Fig. 1. Fig. 1(a) through Fig. 1(d) show the HGHG spectra obtained with only the 1590 nm laser on, and Fig. 1(e) was obtained with

ISBN 978-3-95450-125-0

BUDKER INP FREE ELECTRON LASER FACILITY – CURRENT STATUS AND FUTURE PROSPECTS *

O.A.Shevchenko#, V.S.Arbuzov, K.N.Chernov, E.N.Dementyev, B.A.Dovzhenko, Ya.V.Getmanov, E.I.Gorniker, B.A.Knyazev, E.I.Kolobanov, A.A.Kondakov, V.R.Kozak, E.V.Kozyrev, V.V.Kubarev, G.N.Kulipanov, E.A.Kuper, I.V.Kuptsov, G.Ya.Kurkin, L.E.Medvedev, L.A.Mironenko, V.K.Ovchar, B.Z.Persov, A.M.Pilan, V.M.Popik, V.V.Repkov, T.V.Salikova, M.A.Scheglov, I.K.Sedlyarov, G.V.Serdobintsev, S.S.Serednyakov, A.N.Skrinsky, S.V.Tararyshkin, V.G.Tcheskidov, N.A.Vinokurov, M.G.Vlasenko, P.D.Vobly, V.N.Volkov, BINP, Novosibirsk, Russia

Abstract

The free electron laser (FEL) facility at Budker INP is being developed for more than 15 years. It is based on the normal conducting CW energy recovery linac (ERL) with rather complicated magnetic system lattice. Up to now it is the only one in the world multiorbit ERL. It can operate in three different regimes providing electron beam for three different FELs. Its commissioning was naturally divided in three stages.

The first stage ERL includes only one orbit placed in vertical plane. It serves as electron beam source for terahertz FEL which started working for users in 2003. Radiation of this FEL is used by several groups of scientists including biologists, chemists and physicists. Its high peak and average powers are utilized in experiments on material ablation and biological objects modification. The second stage ERL is composed of two orbits located in horizontal plane. The second stage FEL is installed on the bypass of the second orbit. The first lasing of this FEL was achieved in 2009. The last stage ERL will include four orbits. Its commissioning is in progress now.

In this paper we report the latest results obtained from the operating FELs as well as our progress with the commissioning of the two remaining ERL beamlines. We also discuss possible options for the future upgrade.

ACCELERATOR DESIGN

The Novosibirsk FEL facility is based on the multiturn energy recovery linac (ERL) which scheme is shown in Fig. 1. In this scheme the beam goes through the linac several times before it enters undulator. As the result one can increase the final electron energy.

Multiturn ERLs look very promising for making ERLs less expensive and more flexible, but they have some serious intrinsic problems. Particularly in the simplest scheme shown in Fig.1 one has to use the same tracks for accelerating and decelerating beams which essentially complicates adjustment of the magnetic system. This problem can be solved by using more sophisticated scheme based on two linacs [1].

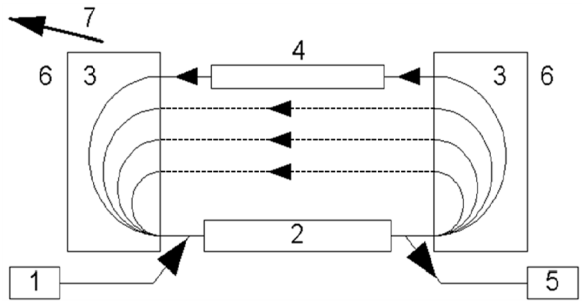

Figure 1: Simplest multiturn ERL scheme: 1 – injector, 2 – linac, 3 – bending magnets, 4 – undulator, 5 – dump.

At present the Novosibirsk ERL is the only one multiturn ERL in the world. It has rather complicated lattice as it can be seen from Fig. 2. The ERL can operate in three modes providing electron beam for three different FELs. The whole facility can be treated as three different ERLs (one-turn, two-turn and four-turn) which use the same injector and the same linac. The one-turn ERL is placed in vertical plane. It works for the THz FEL which undulators are installed at the floor. This part of the facility is called the first stage. It was commissioned in 2003 [2].

The other two ERL orbits are placed in horizontal plane at the ceiling. At the common track there are two round magnets. By switching these magnets on and off one can direct the beam either to horizontal or to vertical beamlines. The 180-degree bending arcs also include small bending magnets with parallel edges and quadrupoles. To reduce sensitivity to the power supply ripples, all magnets on each side are connected in series. The quadrupole gradients are chosen so that all bends are achromatic. The vacuum chambers are made from aluminium. They have water-cooling channels inside.

The second horizontal track has bypass with the second FEL undulator. The bypass provides about 0.7 m lengthening of the second orbit. Therefore when the beam goes through the bypass it returns back to the linac in decelerating phase and after two decelerations it finaly comes to the dump. This part (the second stage) was commissioned in 2009. The final third stage will include full-scale four-turn ERL and FEL installed on the last track.

The basic beam and linac parameters common for all three ERLs are listed in Table 1.

*Work supported by the Ministry of Education and Science of the Russian Federation; RFBR grant 11-02-91320
#O.A.Shevchenko@inp.nsk.su

ISBN 978-3-95450-125-0

INDIRECT COOLED SUPERCONDUCTIVE WIGGLER MAGNET

A.V. Bragin, S.V. Khruschev, N.A. Mezentsev, E.G. Miginskya, I.V. Poletaev, V.A. Shkaruba, V.M. Syrovatin, V.M. Tsukanov, A.A. Volkov, K.V. Zolotarev*,
Budker Institute of Nuclear Physics, Lavrentiev ave. 11, 630090 Novosibirsk, Russia

Abstract

Superconducting wigglers are very popular devices for generation of the synchrotron radiation in the hard X-ray spectral range. The one direction of the future progress in wigglers development is reducing of the technical complexity wigglers design as well as technical service for cryogenic system. The BINP wigglers without liquid helium consumption were a noticeable milestone of these efforts. The next significant step toward additional simplification wiggler design and service is indirect cooling of the wiggler magnet. In this case the wiggler magnet not immersed into the liquid helium, but cooled by thermal connection link with the head of cryogenic cooler.

This approach is used for design of the indirect cooled wiggler for IMAGE beamline on the ANKA light source (KIT, Germany). This wiggler also will be tested as a prototype for damping wiggler for the damping rings in the project of the Compact Linear Collider (CLIC) for CERN.

This report summarizes some details of the wiggler design as well as a result of the short prototype testing.

INTRODUCTION

Budker Institute of Nuclear Physics produced more than twenty superconductive insertion devices which are working now in many SR centres over whole world [1-5].

During thirty years history the number of goals for design has been established and fulfilled. Among different goals, the simplicity of the regular service and cryogenic requirement is a very important.

From this point of view the wigglers development history can be divided by few period. The fist devises used a external storage for liquid helium, and operation procedure included regular refilling, Later the using of the commercial available Gifford-McMahon cryocoolers permits reduced difficulties of regular cryogenic operations, essentially reduce LHe consumptions and increase the refilling time.

Cryocoolers and common progress in the cryostat design permits achieve the real zero consumption of the liquid helium, and since 2005 all manufactured devises have this feature.

A currently developed wiggler can be the next step in the cryogenic design. Here magnetic coils connected with LHe volume by the number of cupper links and thermosiphons. This approach permits to have relatively simple access to the magnet and to the beam vacuum chamber. Principally it's possible to change whole magnetic system inside cryostat during relatively short time period (about two weeks) without complicated operation (machining, welding).

This approach had been selected for prototype of the damping wiggler for CLIC damping ring [6]. The huge number of wiggler on the damping ring requires extremely high reliability for every wiggler, so traditional approach for magnet isolation in the LHe tank is not suitable for this task. Moreover final selection of the CLIC damping wiggler design requires testing different technologies for coils wiring and the beam vacuum chamber coatings. It is possible test different options inside single cryostat.

The currently developed wiggler is dedicated for such research work as well as for regular work for SR user on the IMAGE beam line at ANKA storage ring. In according to agreement between CERN, KIT and Budker INP this wiggler should be installed on the ring in the middle of the 2013.

PARAMETERS OF THE WIGGLER

The main parameters of the wiggler are presented in the Table 1. These parameters are the subject of the compromise between CERN and KIT requirement.

Table 1: Main parameters of the wiggler with indirect cooling

Parameter	Value
Period	51 mm
Peak fiels	3 T
Magnet structure	1/4,-3/4,1,-1,…,-1,3/4,-1/4
Number of the full field poles	68×2
Full number of the poles	72×2
Magnetic gap	18 mm
Vacuum chamber vertical aperture	13 mm
Beam heat load	50 W
Maximum ramping time	< 5 min
Period for LHe refill with beam	> 6 months
LHe boil off @ quench	< 15
Field stability for two weeks	$\pm 10^{-4}$

*Zolotarev@inp.nsk.su

ISBN 978-3-95450-125-0

SUPERCONDUCTING QUADRUPOLE MODULE SYSTEM FOR THE SIS100 SYNCHROTRON

E. Fischer*, P. Schnizer, K. Sugita, J. Meier, A. Mierau,
P. Spiller, O. Kester, GSI, Darmstadt, Germany
H. Khodzhibagiyan, G. Trubnikov, JINR, Dubna, Russia

Abstract

The SIS100 heavy ion synchrotron, the core machine of the FAIR complex, uses fast ramped superconducting magnets. As for its ancestor, the Nuclotron operational at JINR Dubna since 1993, its superconducting magnets are based on iron dominated design and coils made of Nuclotron type cables. The SIS100 magnets differ from the Nuclotron magnets in the following points: they are longer, the beam aperture was enlarged and the field quality improved, its AC losses reduced. The coils have a lower hydraulic resistance and the operation current is doubled. These achievements were obtained in a R&D collaboration between JINR and GSI. Now in the realisation phase GSI will procure and test the SIS100 dipole magnets, while JINR together with GSI will finalise the design of the quadrupoles units (consisting of one quadrupole and one corrector), procure, test and assemble them into doublets. We report on the status of the project, the scheme of the JINR-GSI collaboration for developing and manufacturing the SIS100 quadrupole modules and the steps required to achieve the start of the series production.

INTRODUCTION

SIS100 is following the design of the Nuclotron, but its circumference was increased by a factor of about 4 that had several implications: the dipole magnet length was increased by a factor of about 2, the aperture was increased and a continuous triangular cycle demanded. Even though the AC losses occurring in the magnet were reduced by making a smaller end coil loop, replacing the ferritic brackets with a stainless steel version, which acted as a flux short path and thus created large losses, while the former two parts reduced the eddy currents and thus the AC losses due to the longitudinal B_z field component matching the original set target of 30% total loss reduction, the cable had to be redesigned to adjust the hydraulic resistance for the larger magnet, which now will provide ample cooling margin for the SIS100 magnets [1, 2]. This approach was then picked up for the NICA Booster and collider magnets [3] based on the common R&D conducted from 2002 until now. Further the field quality of the magnets was improved [4, 5, 6].

All that common interactions just naturally lead that GSI is now producing the SIS100 dipoles and JINR the quadrupole units of the SIS100 machine.

* e.fischer@gsi.de

THE SIS100 MAIN MAGNETS

The redesigned Nuclotron cable, necessitated by the cryogenic losses of the SIS100 dipole, is now also used for the quadrupole (see Fig. 1), which allows introducing the

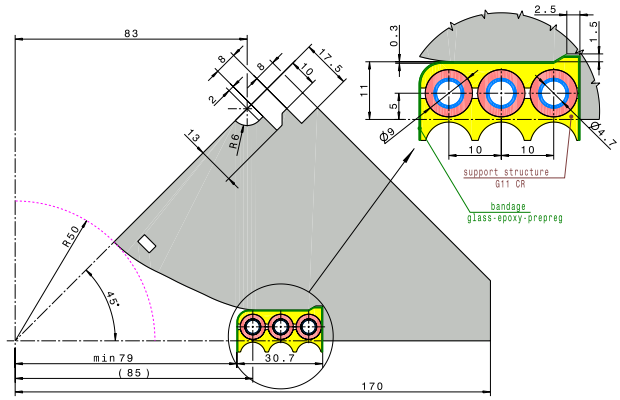

Figure 1: The 3-turn quadrupole magnet lamination design.

reinforcement coil support structure similar to the dipole and reusing the same components for the cable itself, the bus bars, the voltage breakers, soldering joints and current leads. Further low current quadrupoles are required for the extraction and injection section, which now can be produced using the same magnet yoke but using an adjusted low current Nuclotron type cable; the same as foreseen for the correctors. The 3 turn quadrupole design reduces further the types of various utilities as only one type of HTS current leads is required and only one type of bus bars and voltage breakers in the dipoles, quadrupole doublets, bypass lines, feed in lines, superconducting links, current lead boxes. Quench measurements of the dipole can be directly used for the quadrupole and only one single type of high current superconducting joints is needed.

QUADRUPOLE UNITS

The quadrupole units consist of a quadrupole on which one or two corrector magnets or a beam position monitor are mounted.

The corrector magnets are requested to be operated with low current (< 300 A) in order to reduce the heat leak from the copper current lead pair as each magnet is powered individually. Taking into account the advantage of Nuclotron type cables for fast ramped magnets, this design was adopted with individually insulated superconducting

ISBN 978-3-95450-125-0

PRODUCTION OF SUPERCONDUCTING MAGNETS AND CRYOGENIC SYSTEMS AT IHEP*

S. Kozub, A. Ageyev, A. Bakay, I. Bogdanov, E. Kashtanov, A. Orlov,
V. Pokrovsky, P. Slabodchikov, P. Shcherbakov, L. Shirshov, M. Stolyarov,
V. Sytnik, L. Tkachenko, S. Zinchenko, IHEP, Protvino, Russia

Abstract

Results of the development of fast-cycling superconducting magnets for the FAIR project (European Research Centre of Ions and Antiprotons, Germany) are presented. Largest in Russia cryogenic system of 280 W refrigeration capacity at 1.8 K temperature for cooling with superfluid helium of superconducting RF separator for the OKA experimental complex to produce a separated Kaon beam from U-70 proton accelerator was developed and commissioned at Institute for High Energy Physics (IHEP). Experience of the cryogenic system operation is discussed.

RESULTS OF ACTIVITY

New generation of high energy proton accelerators is based on fast cycling superconducting (SC) magnets [1]. From 2002 IHEP collaborated with GSI, Darmstadt, Germany. SC high field fast cycling dipole model was developed and produced for SIS300 accelerator of FAIR project (European Research Centre of Ions and Antiprotons). The dipole is shown in Fig. 1 and its parameters are presented in Table 1 [2].

Figure 1: SIS300 SC high field fast cycling dipole model.

Figure 2 presents the magnet training curve. The dipole reached its operating current at third quench. The quench current continued to increase and finally reached 7738 A (about 6.8 T magnetic field). The ratio between maximum current on the load line and nominal current is 7738/6720 = 1.15. During the training, quenches occurred alternately in the upper and lower poles. This shows that the two poles have the same quality as well as the same level of stress.

*Work supported by ROSATOM

Table 1: Parameters of the SIS300 SC dipole

Magnetic field, T	6
Operating current, kA	6.72
Field ramp rate, T/s	1
Number of layers	2
Strand number in cable	36
Stored energy, kJ	260
Inductance, mH	11.7
Coil inner diameter, mm	100
Length of SC coil, m	1
Mass of magnet, ton	1.8

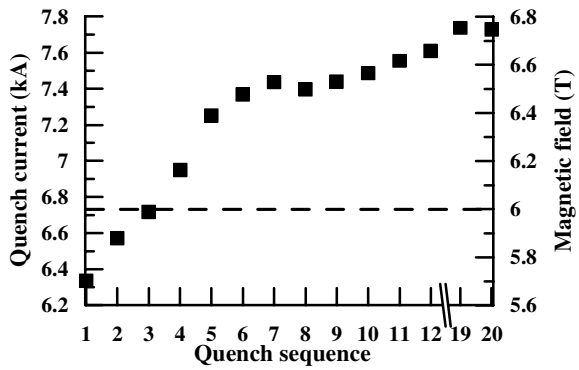

Figure 2: Training curve of the SIS300 dipole model.

Figure 3 presents quench currents for different ramp rates. One can see that the quench current did not decrease up to 1300 A/s (1.2 T/s).

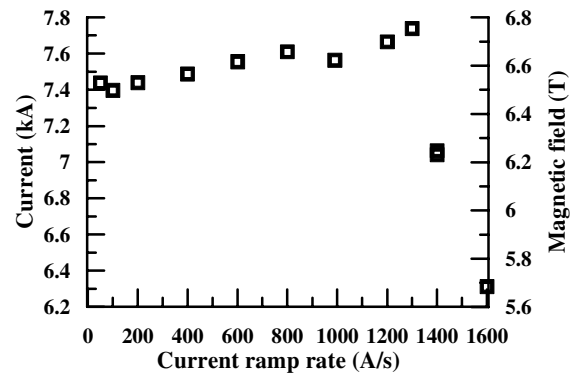

Figure 3: Ramp rate dependence of the SIS300 dipole model.

Special design of SC wire and cable with stainless steel core was developed for this dipole to decrease AC losses. Measured AC losses exceeds computed values at currents more than 3 kA because of eddy current losses in the iron

ISBN 978-3-95450-125-0

STATUS OF THE DESIGN AND TEST OF SUPERCONDUCTING MAGNETS FOR THE NICA PROJECT

H. Khodzhibagiyan, P. Akishin, A. Bychkov, A. Donyagin, A. Galimov, O. Kozlov, G. Kuznetsov, I. Meshkov, V. Mikhaylov, E. Muravieva, P. Nikitaev, A. Shabunov, A. Smirnov, A. Starikov, and G. Trubnikov, JINR, Dubna, Russia

Abstract

NICA is a new accelerator complex being under design and construction at the Joint Institute for Nuclear Research in Dubna. The actual design and the main characteristics of superconducting magnets for the NICA booster and collider are given. The magnets are based on a cold window frame iron yoke and a single-layered superconducting winding made from a hollow NbTi composite superconductor cable cooled with the forced two-phase helium flow. The first results of cryogenic tests of the magnets for the NICA project are presented.

INTRODUCTION

The NICA/MPD project [1] started at the Joint Institute for Nuclear Research (JINR) in Dubna in 2007. The goal of the project is to carry out experimental studies of the hot and dense strongly interacting quantum chromodynamics matter and light polarized ions. The NICA accelerator complex will consist of two injector chains, a new 600 MeV/u superconducting booster synchrotron, the existing superconducting synchrotron – Nuclotron [2], and the new superconducting collider having two rings each of about 503 m in circumference.

DESIGN AND MANUFACTURING OF THE PROTOTYPE MAGNETS

The Nuclotron-type design [3-5] based on a cold iron yoke and a saddle-shaped superconducting (SC) winding has been chosen for the booster and the collider magnet. The magnet includes a cold (4.5K) window frame iron yoke and a SC winding made of a hollow NbTi composite SC cable cooled with a two-phase helium flow. Lorentz forces in the winding are supported by the yoke. The main characteristics of the cable for the NICA magnets are given in Table 1. A cross-section view of the booster dipole and quadrupole magnets is shown in Figures 1 and 2, correspondingly. The main characteristics of the NICA booster and collider magnets are summarized in Tables 2 and 3, respectively. A full-scale curved model dipole magnet for the NICA booster was manufactured at the Laboratory of High Energy Physics (LHEP) JINR in April 2011. The magnet is 2.2 m long and has a radius of the curvature of 14 m.

The full-scale model quadrupole magnet for the NICA booster was manufactured by LHEP at the end of 2011.

Table 1: Main characteristics of the cable for the NICA booster and collider magnets

Characteristic	Booster	Collider
Channel diameter	3 mm	3 mm
Number of strands	18	16
SC strand diameter	0.78 mm	0.9 mm
Superconductor	50% Nb – 50% Ti	
Diameter of filaments	7 μm	8 μm
Cable outer diameter	6.6 mm	7.0 mm
Operating current (1.8T, 4.65K)	9.68 kA	10.4 kA
Critical current (2.5T, 4.7K)	14.2 kA	16.8 kA

The Nuclotron-type design was chosen for the NICA collider. Two identical single-layer windings are located in the common straight iron yoke one over the other (see Fig. 3). Lorentz forces in the windings are supported by the yoke. The yoke consists of three parts made of laminated electrical steel. They are held together by longitudinal steel plates welded with laminations and frontal sheets. The magnets are cooled with the two-phase helium flow which in series passes from the supply header through the cooling channels of the bus bars, lower and upper windings, iron yoke and then - enters the return header. Each twin bore dipole or quadrupole magnet is connected in parallel to the supply and return helium headers.

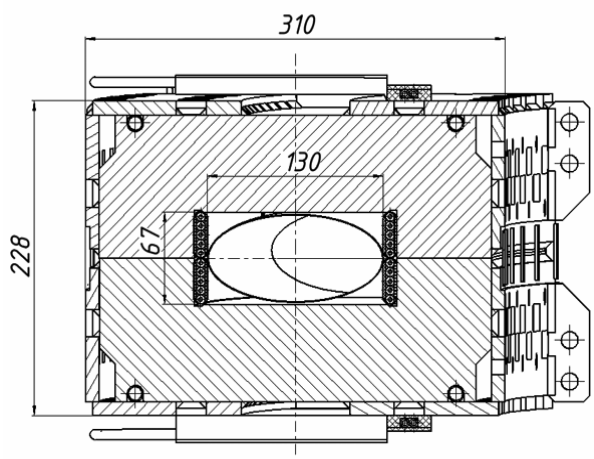

Figure 1: Cross-section view of the bent dipole magnet for the NICA booster.

ISBN 978-3-95450-125-0

UPDATE ON SCRF DEVELOPMENT AT TRIUMF

V. Zvyagintsev, R.E. Laxdal, B. Amini, K. Fong, P. Harmer, D. Kishi, P. Kolb, A. Koveshnikov, D. Lang, A.K. Mitra, N. Muller, C. Schaub, R.W. Shanks, B. Waraich, Q. Zheng,
TRIUMF, Vancouver, Canada
M. Gusarova, I. Petrushina, N. Sobenin, D. Tikhonov, MEPhI, Moscow, Russia
R. Edinger, PAVAC, Richmond, B.C., Canada
A. Vrielink, UBC, Vancouver, B.C., Canada
S.H. Abidi, R.S. Orr,University of Toronto, Toronto, Ontario, Canada

Abstract

Since 2007 TRIUMF started development of e-LINAC which is a 50 MeV 10 mA CW electron superconducting linear accelerator to be used as a driver to produce radioactive ion beams through photofission. The accelerator is based on five 1.3 GHz TTF/ILC elliptical bulk Nb cavities technology to be mounted in three cryomodules; an injector cryomodule with one cavity and two accelerating modules with two cavities each. The ISAC-II project superconducting heavy ion linear accelerator was successfully completed in 2010 and we now have in operation 40 superconducting bulk Nb QWR cavities assembled in eight cryomodules. Results and plans of the SCRF program and experience of ISAC-II operation at TRIUMF will be discussed.

INTRODUCTION

SCRF development at TRIUMF started with the ISAC-II project in 2000 [1]. In 2010 this project was completed with commissioning of a 40 MV superconducting linac for heavy ions. SCRF technology is now being used in a second `in house' linear accelerator, the e-LINAC, to produce 50 MeV electrons with intensities to 10 mA, which will be used as a photo-fission driver for the ARIEL rare isotope program at TRIUMF.

SCRF DEVELOPMENT FOR E-LINAC

E-LINAC [2] will consist of a 300 keV thermionic DC electron gun with RF modulated cathode grid and five elliptical 9-cell cavities, operating at 2^0K, in three cryomodules [3]. The layout and staging of the project are presented in Fig.1.

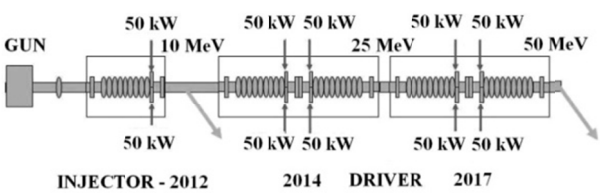

Figure 1: E-LINAC layout

Cavity Design

The e-LINAC cavity design draws from the 1.3 GHz elliptical TESLA-type cavity. Each cavity operates at an effective acceleration voltage of 10 MV with a design goal of Qo=1e10. Operating at 2^0K, the cavity dissipates 10 W in the liquid He system. Operation with 10 mA beam current requires 100 kW CW RF power into the cavity. To deliver RF power into the cavity two symmetrically opposed 65 kW CPI couplers are employed, providing the appropriate beam-loaded power while avoiding asymmetric coupler kicks. In result the e-LINAC 9-cell cavity differs from the TESLA cavity in the end cells, which are customized to adapt to the power couplers on the one end and also to mitigate HOMs and to flatten the field profile for the accelerating mode [4]. The main RF parameters of the cavity are very close to TESLA (Table 1). Simulations [5] show that multipacting occurs in the equatorial region of the cavity. Stable multipacting trajectories (over 40 RF periods) of order 2-4 were obtained in the range of 1.32 … 3.08 MV/m of the accelerating gradient and 1-2 order trajectories are obtained in a range of 3.08…17.16 MV/m.

Table 1: RF parameters of TRIUMF cavity in comparison with TESLA (DESY) cavity

	TRIUMF	DESY	TRIUMF/DESY
Frequency [MHz]	1300	1300	-
R_{sh}/Q [Ohm]	1000	1030	3% less
Geometric factor G [Ohm]	290	270	7% more
E_p/E_a	2.1	2.0	5% more
B_p/E_a [mT/(MV/m)]	4.4	4.2	5% more
Cell coupling [%]	2.0	1.9	-

HOM Dampers

HOM damper design concept is described in [4, 6]. A stainless steel damper ring is used for the coupler end while a CESIC ring is used for the opposite end. The rings are connected to a liquid Nitrogen heat sink. The conductivity of CESIC is measured by using the Q perturbation method in the elliptical cavity at 100^0K [7]. The result lies in the range 600…6200 S/m measured at 1.3 GHz and 660…3400 S/m at 2.4 GHz. The conductivity value is significantly below the rated value for CESIC, which is 15000 S/m.

ISBN 978-3-95450-125-0

A POSSIBILITY OF HIGH-ENERGY BREMSSTRAHLUNG DOSIMETRY BY INDIUM ACTIVATION

A.N. Dovbnya, V.V. Mytrochenko, V.I. Nikiforov, S.A. Perezhogin, Yu.V. Rogov, V.A. Shevchenko, I.N. Shlyakhov, B.I. Shramenko, A.Eh. Tenishev, V.L. Uvarov#, NSC KIPT, Kharkov, 61108, Ukraine

Abstract

Development of a number of promising photonuclear technologies is connected with the use bremsstrahlung (X-ray) sources having end-point energy up to 100 MeV and average power of tens kW. Commonly, such radiation sources are created on the basis of electron linacs. A possibility of dosimetry of high-energy bremsstrahlung by means of activation of a target from indium of natural composition and establishment of absorbed dose on the specific activity of the ^{115m}In isomer is reported. Preliminary study of isomer activation as well as yield of reference reactions from natural molybdenum in the energy range 8…70 MeV was conducted by simulation technique. Joint measurement of ^{115m}In, ^{90}Mo, ^{99m}Mo activity as well as absorbed dose in the PMMA standard dosimeters were carried out at LU-10 and LU-40 electron linacs of NSC KIPT.

INTRODUCTION

It is known that photoactivation of isomeric states in some nuclei is characterized by low energy threshold values. For example, the threshold of the ^{115}In(γ,γ′)^{115m}In reaction equals 1078 keV [1]. The ^{115m}In isomer goes into the ground state with the half-life $T_{1/2}$=4.48 h, emitting in the process the gamma-quantum of energy 336.2 keV, which is convenient for detection. Owing to a low reaction threshold, the natural indium (the ^{115}In abundance makes 95.8%) can be activated by practically all photons of the bremsstrahlung spectrum. This circumstance allows suggest the presence of a relationship between the specific activity of ^{115m}In and the bremsstrahlung absorbed dose.

In a number of studies, the ^{115}In(γ,γ′)^{115m}In reaction has been used for dosimetry in γ-facilities having ^{60}Co sources [2, 3]. In that case the activation of indium was realized with the photons of energy near the reaction threshold. The present communication deals with the conditions of the method applicability for high-energy bremsstrahlung.

MATERIALS AND TECHNIQUES

Experimental studies on indium activation processes were performed at NSC KIPT linear accelerators LU-10 (electron energy E_0=8…12 MeV) and LU-40 (E_0=35…95 MeV). For absorbed dose measurements, Harwell Red 4034 (HR) detectors were used. They represent 30x11x3 mm plates made from dyed PMMA, commonly used as a standard dosimetry material [4].

To investigate the relationship between the specific activity of ^{115m}In and the dose absorbed in the PMMA, it was suggested that the natural indium detectors together with the HRs should be exposed to X-ray under conditions of electron equilibrium. Besides, each target incorporates a natural molybdenum foil to check the activation conditions against the yields of the reference reactions ^{92}Mo(14.84%)(γ,2n)^{90}Mo and ^{100}Mo(9.63%)(γ,n)^{99}Mo.

The bremsstrahlung-induced γ-spectra of indium and molybdenum were measured with the HPGe detector, which provided FWHM of 1.3 keV at 1332 keV.

For independent analysis of the photoactivation processes and absorption of radiation energy in the detectors, we have used the simulation method based on a modified transport code PENELOPE-2008 [5]. The cross sections for the reference reactions on the ^{92}Mo and ^{100}Mo isotopes (see Figs. 1 and 2) were taken from the database [6]. In the case of the ^{115}In(γ,γ′)^{115m}In reaction the situation has turned out to be more complicated. Namely, the data on its cross section, reported in different works, have shown considerable variations (see Fig. 3).

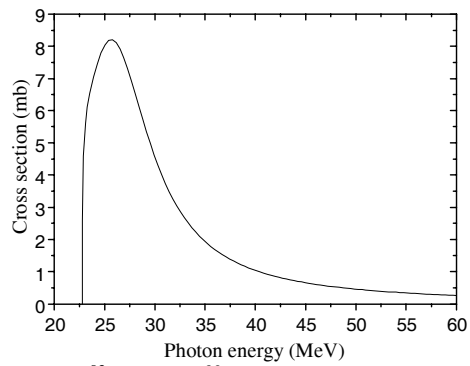

Figure 1: ^{92}Mo(γ,2n)^{90}Mo reaction cross section.

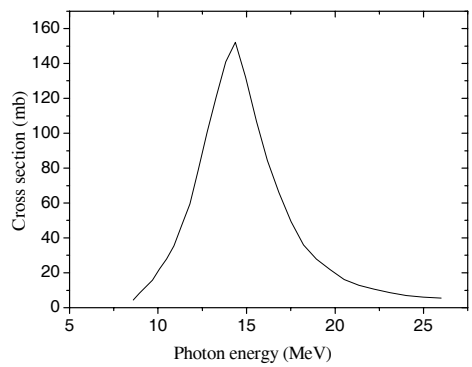

Figure 2: ^{100}Mo(γ,n)^{99}Mo reaction cross section.

uvarov@kipt.kharkov.ua

ISBN 978-3-95450-125-0

HIGH PRECISION POWER SUPPLY FOR ACCELERATOR MAGNETS

Ajoy Sankar Banerjee, Variable Energy Cyclotron Centre, Kolkata 700064, India

Abstract

High precision power supplies used in accelerator systems have stability of the order of 5ppm to 100ppm depending on the functional requirement of the magnet to be excited. The paper highlights the various design considerations, aspects and important features for obtaining high current stability of such high precision power supplies.

INTRODUCTION

The stability of the high precision power supplies used in an accelerator system is an important factor for obtaining highly stable beam output required for various experimental studies. Line, load and temperature variations are the three important factors against which these power supplies have to combat to maintain high stability.

MAIN FEATURE OF THE POWER SUPPLY

Stability is the main important feature of these power supplies which lies between ±5ppm to ±100ppm i.e. the output current will have to remain in the error band of ±5ppm to ±100 ppm under various environmental perturbations such as

1. The input AC lines may ramp or step by ±10%
2. The magnet resistance may vary by 20%.
3. The ambient temperature could change from 15°C to 45°C.
4. There are AC line harmonics and notches generated by other power supplies.
5. The power supplies themselves generate a fundamental 600Hz rectifier ripple and some harmonics of 50Hz due to line imbalances.
6. There are R.F. interferences.

The table 1 shows stability requirement of high precision power supplies used for VECC room temperature accelerator system.

Table 1. Stability Table

High precision Power Supply	*Stability*
Main Magnet P.S. 3000A/150V Analyzing Magnet P.S. 500A/150V	5 ppm.
Trim coil P.S. 2500A/30V, 300A/25V Switching magnet P.S. 300A/150V	10 ppm.
Quadrupole magnet P.S. 300A/30V Steering magnet P.S. 10A/100V Valley coil P.S. 300A/30V	100 ppm.

ACTION TO ACHIEVE HIGH STABILITY

- Proper selection of rectifier circuit configuration for high ripple frequency to reduce ripple voltage
- Using both passive and active filter circuit for fine reduction of ripple voltage
- Adoption of proper regulating loops for good voltage and load regulation
- Using DCCT, working on zero flux principle, for sensing load current with 0.001% accuracy for high current regulation and stability
- Proper thermal management to control temperature of the heat dissipating devices and critical components of the power supply to minimize drift in characteristics
- Attenuation of R.F. pick-up and noise
- Taking proper action to reduce line disturbances

BLOCK DIAGRAM OF A HIGH PRECISION POWER SUPPLY

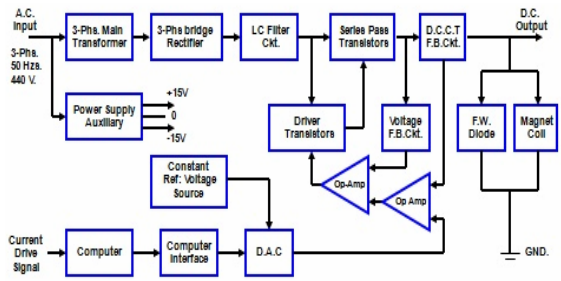

Figure 1: Block diagram of power supply

Series pass transistor controlled linear mode circuit configuration is generally adopted for simplicity in design and control.

Rectifier Circuit

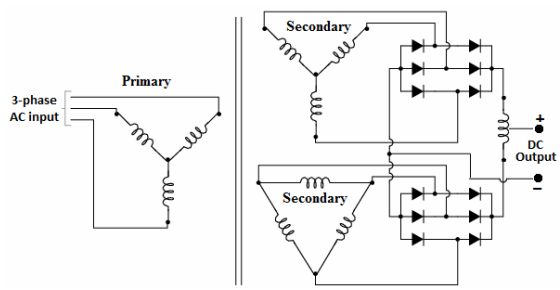

Figure 2: Rectifier circuit

Considering the optimum rectification condition twelve pulse bridge rectifier circuit as shown in the Fig.2 is adopted. This connection provides a low ripple voltage of 1.02%

LC Filter Circuit

The LC filter has almost constant ripple characteristics at all load currents above I_b where the diode conduction angle reaches 180° and the current becomes continuous.

ajoy_banerjee2000@yahoo.com

ISBN 978-3-95450-125-0

BEAM EXTRACTION SYSTEM FOR INDUSTRIAL ELECTRON ACCELERATOR ILU-14

V. Bezuglov, A. Bryazgin, B. Faktorovich, E. Kokin, V. Radchenko, E. Shtarklev, A. Vlasov,
BINP SB RAS, Novosibirsk

Abstract

This paper describes beam extraction system for pulse linear electron accelerator ILU-14 with energy range 7.5-10 MeV and beam power up to 100 kW. The main aim of this work was to achieve the uniform dose field in radiation zone. Admissible dose nonuniformity is of no more than ± 5% along the scanning length up to 1m (if necessary, the scanning length may be reduced). Geometrical and electron-optical characteristics of all the beam channel elements were optimized after computer simulation of electron trajectories. To achieve the required nonuniformity of dose field additional electromagnets were installed. These magnets realize beam focusing and centering of the beam endwise of the channel, as well as correction of the scanning field. Control system of magnets power supply allows the online correction of electron beam.

INTRODUCTION

Radiating technologies reached now such wide application in the industry that became its separate branch. And improvement of generators of electron beams occurs at the same time to high-quality improvements of extraction devices. Questions of efficiency of radiation, i.e. efficiency of process of radiation became the main requirements at radiation of production. The nomenclature of irradiated objects considerably increased and diversified. Rigid modern requirements to uniformity of dose fields of electronic accelerators demand detailed consideration of the questions connected with operation of extraction devices. To improve radiation quality (dose uniformity) and obtain competitive advantages the new system of the beam output for the industrial accelerators of the ILU series is developed. The main requirements to this system are nonuniformity of the dose field not worse ±5 %, and also width of the beam scanning of 1 m (at energy of an electron beam up to 10 MEV). In industrial accelerators of ILU type an electron beam with duration 0.5 ms is scanned along the output window from a titanic foil (thickness of 50 microns). Uniformity or the set nonuniformity of distribution of the beam intensity along a foil is one of the most important parameters of radiating and technological complexes on ILU base. The general block diagram of the output path of the accelerator is provided on fig. 1. After accelerating structure 1 beam gets to the electron-optical channel. For control of the beam position of rather central axis of the channel input of the directing magnet 2, representing the two-coordinate corrector of electron trajectories in the range ±5sm is supposed see. For formation of the cross-section size of a beam (at initial adjustment of system without beam scanning) the quadrupole doublet 3 is provided. For control of beam parameters the graphite diaphragm 4 from which the signal will be taken off further will be located. Necessary uniformity of the output current density is offered to be reached by installation before the main beam scanning system 6 of the correction system of the scanning magnetic field 5. Also in extraction system possibility of so-called horizontal beam scanning 7 across the bell is provided. For receiving on the bell foil of a beam with identical angular characteristics, especially at big angles of scanning, it is necessary to install the additional turning devices 8 (Panovsky lenses) which transform trajectories of electrons so that a beam falls on a foil everywhere on its length at right angle. After an exit of an electron beam from a bell possibility of its transformation to bremsstrahlung by means of the converter 9 is provided.

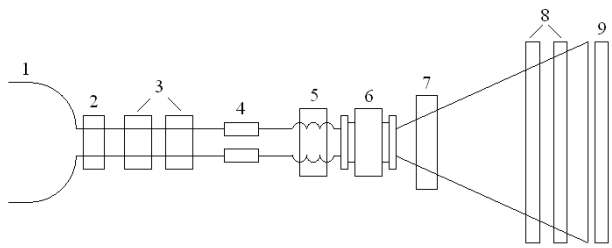

Figure 1: 1 – accelerating structure, 2 – control magnet, 3 – quadrupole doublet, 4 – diaphragm, 5 – bellows unit with correction system of scanning field, 6 – scanning chamber with scanning electromagnet, 7 – transverse beam scanning system, 8 – Panovsky lenses, 9 – converter.

BEAM SCANNING SYSTEM

It is necessary to give special attention to formation of a demanded dose field on an exit from the accelerator. First of all, it is necessary to consider influence on a form of a scanning field of the processes occurring in metal walls of the vacuum chamber of beam scanning (a bell filler).

When giving a pulse magnetic field in a metal not magnetic shield (screen) of scanning system which divides on vacuum space of a beam deviation and the scanning electromagnet which was outside, there is a reaction of the induced currents which distorts a scanning field. From [1] follows that the field inside the screen H0(t) is superposition of the influencing field H1(t) and the field H2(t) raised by currents, induced in the shield thickness by pulse of H1(t). In the same place it is deduced that the field in the screen H0(t) raised by pulse H1 (t), satisfies to the ordinary differential equation:

ISBN 978-3-95450-125-0

CHARACTERISTICS OF THE MODEL OF LINEAR ACCELERATOR BASED ON PARALLEL COUPLED ACCELERATING STRUCTURE WITH BEAM LOADING

Yu. Chernousov, V. Ivannikov, I. Shebolaev, ICKC, Novosibirsk, Russia
E. Levichev, V. Pavlov, BINP, Novosibirsk, Russia

Abstract

The 5-cavity model of linear accelerator based on parallel coupled accelerating structure (LAPCAS) with periodic permanent magnet focusing system (PPMFS) and RF-controlled three-electrode electron gun is under study. The work of the accelerator with electron beam is demonstrated. Parameters of short pulses mode are the following: electron energy – 4 MeV, pulse current – 0.3A, pulse duration - 2.5 ns; parameters of long pulses mode are the following: energy – 2.5 MeV, pulse current – 0.1A, pulse duration – (0.1 - 4) μs. Working frequency of the accelerator – 2.45 GHz. In RF-controlled mode the capture about 100 % has been demonstrated. Beam loading effect in the LAPCAS takes place. Data of observation of this effect and compensation of energy spread of accelerated electrons by delaying the moment of injection in the LAPCAS are demonstrated. The equations describing the transient process in the accelerating cavity which is powered by an external RF generator and excited by electron bunches are presented in a simplified form.

INTRODUCTION

Parallel coupled accelerating structure (PCAS) is a new type of the structures and consists of separate accelerating cavities feeding from common exiting cavity in parallel [1]. The structure is equipped with an inside installed reverse periodic permanent magnet focusing system (PPMFS). The possibility to use the PCAS in the accelerator technique demands experimental studies. Accelerating cavities of PCAS work in standing wave regime and beam loading effect – dependence of average energy of accelerated electrons on time during the pulse takes place in this structure. The methods of compensation the energy spread of accelerated electrons in the standing wave and traveling wave structures have been discussed for a long time [2-5]. Now in some installations the issue came into practical implementation [1,6,7]. One of the methods to reduce this negative effect – injection the electron pulse with delay relatively to pulse of feeding RF power, so called ∇T-method. In this paper the equations describing the transient process in the accelerating cavity which is powered by an external RF generator and at the same time excited by electron bunches in a simplified form are obtained and data of experimental observation of the beam loading characteristics, beam loading effect and compensation of energy spread in the LAPCAS by ∇T-method are represented. For experimental observation of the beam loading effect we used energy spread measurements by method of absorption in retarding metallic plates [8].

THEORY

Beam loading is defined as the energy reduction of charged particles due to their interaction with an accelerating structure [2]. Charged bunches, when passing through the structure, generate RF oscillations that decelerate the subsequent bunches. As a result average energy of accelerated beam depends on time during the pulse. To evaluate the energy spread due to the transients, it is necessary to take into account that acceleration voltage on the accelerating cavity is excited by two independent sources: the external RF generator and modulated electron beam. In the theoretical description we assume that the electron beam consists of a train of short bunches, RF pulse is an ideal step-function and that all charged particles travel with the speed of light, the difference between the frequencies of generator, cavities and moving bunches is zero.

Evaluation of complex magnitude of equivalent acceleration voltage U in the standing wave accelerating cavity, which is powered by an external RF generator and at the same time excited by electron bunches can be described, as may be shown from [5], by the following equations:

$$\tau\frac{dU}{dt}+U=U_G-U_{B0},$$

$$\tau=\frac{2Q_0}{\omega_0(1+k)},\ U_G=U_{G0}\exp(i\theta),$$

$$U_{G0}=\frac{2(kZLP_G)^{1/2}}{(1+k)},\quad U_{B0}=\frac{IZL}{(1+k)} \qquad (1)$$

where τ is the filling time constant of these evaluations; U_G is complex amplitude of equivalent acceleration voltage on the cavity, excited by the generator; U_{G0} and U_{B0} are steady-state values of amplitudes of equivalent acceleration voltage on the cavity, excited by the generator (U_{G0}) and beam (U_{B0}) correspondently, real positive quantities; ω_0 is cavities eigenfrequency; k is the coupling coefficient between the cavity and feeder line; Q_0 is the cavities unloaded Q - factor; Z is effective shunt impedance per unit length; L is the length of the accelerating cavity; P_G is the RF power which excites the cavity; $\theta-\pi$ is the phase of generator-induced oscillations relatively to beam-induced

ISBN 978-3-95450-125-0

NIIEFA ACCELERATORS FOR INDUSTRY AND MEDICINE

M.F. Vorogushin#,
D.V. Efremov Scientific Research Institute of Electrophysical Apparatus, Saint Petersburg, Russia

Abstract

The D.V. Efremov Institute (NIIEFA) is a leading enterprise in Russia involved in designing and manufacturing of applied and medical charged particle accelerators, as well as electrophysical systems based on these accelerators. Since the foundation of the Institute, we have designed, manufactured and delivered to Russian customers and abroad more than three hundred accelerators of different types, in particular, cyclotrons, high-frequency linear electron accelerators, high-voltage accelerators and neutron generators. The activities of the Institute in the field of accelerating engineering encompasses all the stages of an accelerator manufacturing, starting from R & D works to manufacturing, installation, adjustment and maintenance of the equipment delivered.

NUCLEAR MEDICINE

Among the present-day methods of medical examination, the radionuclide diagnostics presents the most complete information on available pathologies. The method is characterized with a high sensitivity, the shortest possible time needed for analysis and reliability of the data obtained. A single-photon emission computer tomograph (SPECT) is an apparatus the most widely used for examination of great masses of population. This apparatus uses radiopharmaceuticals labeled with short-lived isotopes with the half-life period from several hours up to 2-3 days. The clinical experience gained over a number of years demonstrates that in about 20% of cases more accurate positron-emission diagnostics is needed, which applies ultra-short-lived isotopes with the half-life from two up to one hundred and ten minutes. Radio-isotopic examinations allow cardio-vascular and oncologic diseases, the death rate from which is the main factor determining the age of a human life, to be detected at very early stages. Cyclotron is the most proper accelerator allowing necessary ultra and short-lived isotopes to be produced in the most cost-effective way.

NIIEFA has been involved in designing and production of cyclotrons since the day of its foundation. More than forty different models of cyclotrons have been delivered to Russian customers and abroad, and the majority of these machines have been operated until now. Recently, a series of compact cyclotrons has been designed specially for production of medical isotopes [1]. The main parameters of these cyclotrons are given in Table 1.

Specific features of these cyclotrons are: the external injection of hydrogen negative ions, beam extraction by stripping negative ions on carbon foils, the main electromagnet of shielding-type with the vertical median plane, the same principle of construction of the RF-power supply system, vacuum system and automatic control system.

Table 1: Main Parameters of Cyclotrons for Medicine

Parameters	CC-12	CC-18/9	MCC-30/15
Accelerated ions	H^-	H^- / D^-	H^- / D^-
Ion energy, MeV	12	18/9	18…30 / 9…15
Extracted beam current, μA	50	100/50	200/70
Electromagnet:			
- pole diameter, cm	90	115	140
- supply power, kW	5	7	12
- mass,t	10	20	41
Frequency of RF oscillations, MHz	76.4	38.2	40.68
RF generator power, kW	15	20	25
Energy consumption, kW	30	70	100

To give an access to in-chamber components, the iron core is made as a fixed part and a movable part. The movable part is fixed on a support and can be moved apart for a distance up to 800 mm.

The CC-12 compact cyclotron is intended for production of ultra short-lived isotopes directly in medical diagnostic centers. The CC-18/9 cyclotron (Fig. 1) allows both ultra short-lived isotopes and short-lived isotopes to be produced. The CC-18/9 machines are successfully operated in PET centers in Turku (Finland), Saint-Petersburg and Snezhinsk (Tchelyabinsk district), Russia.

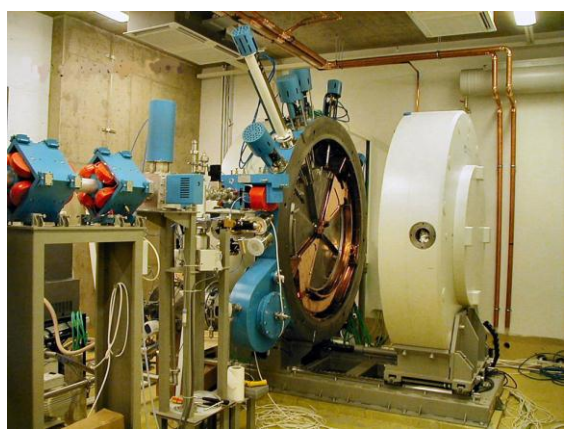

Figure 1: The CC-18/9 cyclotron installed in Turku (Finland).

#vorogushin@luts.niiefa.spb.su

ISBN 978-3-95450-125-0

FLNR HEAVY ION CYCLOTRONS FOR INVESTIGATION IN THE FIELD OF CONDENSED MATTER PHYSICS INDUSTRIAL APPLICATIONS

B. N. Gikal, Joint Institute for Nuclear Research, Dubna, Russia

Abstract

Applied research on heavy ion beams are carried out in many scientific centres of the world. Some of the developed technologies are successfully used in industry, for example, a well-known method of track membranes production using heavy ion beams, which as a rule have an energy from 1 to 3.5 MeV/nucleon. At FLNR several specialized accelerators have been created for this purpose.

Since 1983 a complex based on the IC-100 cyclotron for industrial manufacturing of track membranes operates at the JINR Flerov Laboratory of Nuclear Reactions (Dubna, Russia). The modernization in 2003 equipped the cyclotron with a superconducting ECR ion source as well as with an axial injection system. High intensity heavy ion beams of Ne, Ar, Fe, Kr, Xe, I, W have been accelerated to an energy of 1.2 MeV/nucleon.

The DC-60 cyclotron with smooth ion energy variation was designed by FLNR for the research center at L.N. Gumilev Euroasian State University in Astana (Kazakhstan). The cyclotron equipped with an ECR ion source accelerates ions from Carbon to Xenon. The energy of the extracted beams can be varied from 0.35 up to 1.7 MeV/nucleon.

In 2009-2010 a cyclotron complex for a wide spectrum of applied research in the field of nanotechnologies (template technologies, track membranes, surface modification, etc.) was designed at the Flerov Laboratory of Nuclear Reactions. This complex includes a specialized DC-110 cyclotron, which produces high intensity beams of accelerated Ar, Kr, and Xe ions with a fixed energy of 2.5MeV/nucleon. The DC-110 cyclotron is at the commissioning stage now.

The accelerated ion beams of U400 and U400M cyclotrons (FLNR) have been used for several years already by the Russian Space Agency (Roscosmos) for investigation of radiation resistance of electronic devices. For these experiments ions with atomic masses of 4÷209 and an energy of 3÷6 MeV/nucleon are used. Now a specialized channel and a facility for carrying out these investigations on the beams of ions with energies of 25-55 MeV/nucleon is being mounted.

IC-100 CYCLOTRON

In 1985, at the Laboratory of Nuclear Reactions of Joint Institute for Nuclear Research, the IC-100 cyclic implanter of heavy ions was developed [1, 2]. The cyclotron was designated for acceleration of ions from $^{12}C^{2+}$ to $^{40}Ar^{7+}$ with a fixed energy of ~1.2 MeV/nucleon at acceleration at the fourth harmonic of the high voltage system and ~0.6 MeV/nucleon for acceleration at the sixth harmonic. A PIG type internal ion source was used at this accelerator; the mentioned source determined the mass range of accelerated ions. For more efficient application of the complex and for industrial production of track membranes, it was proposed to switch to irradiation of films with heavier ions [2].

In the course of the upgrade performed in 2003–2005, the IC-100 implantation complex was equipped with a system of beam axial injection from an external superconducting ECR ion source (Fig. 1). This provided a possibility of obtaining intense beams of highly charged ions of Xenon, Iodine, Krypton, Argon, and other heavy elements of the Periodic Table [4]. The launching and the adjustment of systems of the IC-100 cyclotron were performed using $^{86}Kr^{15+}$ and $^{132}Xe^{23+}$ beams. The intensity of accelerated and extracted beams is ~2μA. $^{40}Ar^{7+}$ beams with a current of more than 2μA, $^{56}Fe^{10+}$ beams with a current of 0.3μA, $^{127}I^{22+}$ beams with a current of up to 0.25μA, $^{132}Xe^{24+}$ beams with a current of ~0.6μA, $^{182}W^{32+}$ beams with a current of ~0.015μA, and so on were also accelerated.

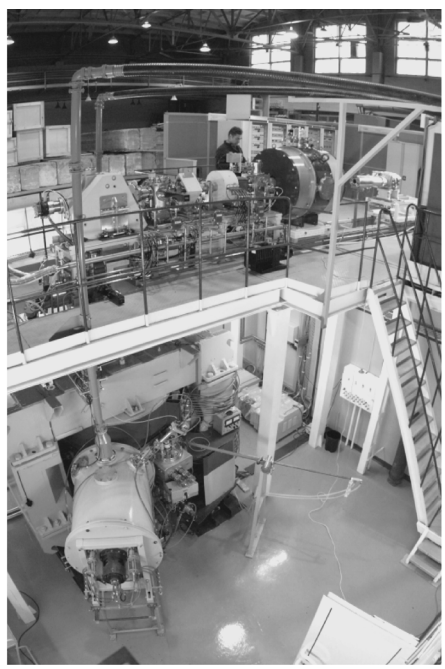

Figure 1: General view of the IC-100 cyclotron.

DC-60 CYCLOTRON

A specialized accelerating facility based on the DC-60 cyclotron was built by the Flerov Laboratory of Nuclear Reactions in collaboration with the Institute of Nuclear Physics (Almaty, Kazakhstan) for the Interdisciplinary Scientific Research Center of the Gumilev Eurasian

ISBN 978-3-95450-125-0

IRRADIATION FACILITIES AND COMPLEXES OF INRP RFNC-VNIIEF

V.F.Basmanov, S.V.Vorontsov, V.S.Gordeev, S.A.Gornostaj-Pol'ski, A.V.Grishin, A.V.Grunin, A.A.Devyatkin, N.V.Zavyalov, V.F.Kolesov, G.A.Myskov, S.T.Nazarenko, V.T.Punin, V.A.Savchenko, I.G.Smirnov, A.V.Tel'nov, FSUE RFNC-VNIIEF, Sarov, Russia

Abstract

There are presented in the review the facilities and complexes that were created and are applied in the Institute of Nuclear and Radiation Physics (INRP) RFNC-VNIIEF to simulate under laboratory conditions the effect of NM penetrating radiation on the special-purpose objects. There is given a brief description of the design and characteristics of different-type electron accelerators, pulsed nuclear reactors (PNR) as well as two irradiation complexes PUL'SAR and LIU-10M-GIR2 that are located in the adjacent halls.

INTRODUCTION

Within several decades there was being created in INRP RFNC-VNIIEF a specialized stock of irradiation facilities on the base of electron accelerators, PNR and complexes aimed at carrying out - under laboratory conditions - system researches of radiation resistance of armament and defense technology (A and DT) standard objects against the effect of NM penetrating radiation.

According to state standards there is performed certification of experimental facilities as test equipment – simulating facilities for B and BT testing as to radiation effect of NM, power generating systems and space.

IRRADIATION COMPLEX PUL'SAR

The multi-purpose irradiation complex PUL'SAR [1,2] that has been under operation since 1991, possess widest test potentialities in factor-by-factor and joint loadings for laboratory elaboration and resistance tests of B and BT against NM penetrating radiation.

The leading facility of the complex is a high-power pulsed linear induction accelerator of electrons LIU-30 [3-5]. Into the complex structure there is also included a booster reactor BR-1M [6] aimed at generation of gamma-neutron radiation - both independently and jointly with accelerator LIU-30 [7]. In order to provide more precise simulation of penetrating radiation effect, into the complex there are included: pulsed electron accelerators STRAUS-2 and ARSA and generator of X-radiation pulses ILTI-1. The typical chart of PUL'SAR facilities arrangement is given in Fig.1 while the basic characteristics of the facilities are available in Table 1.

Fig.2 gives the chart of LIU-30 accelerating system of which is evident that it is produced of 36 sequentially connected modules with self-contained supply and independent control of each module. Into accelerator structure there are also incorporated a transportation channel and output device with a target ensuring the required characteristics of electron beam and bremsstrahlung field.

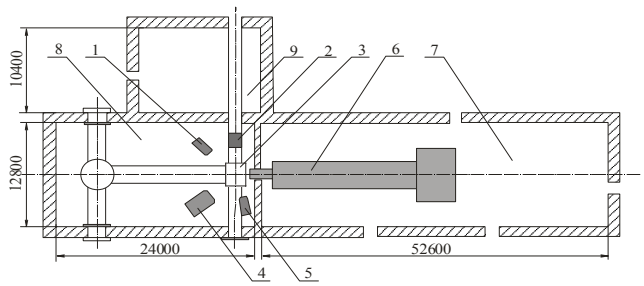

Fig. 1. Chart of PUL'SAR irradiation complex facilities arrangement. 1 – accelerator ILTI-1; 2 – booster-reactor BR-1M; 3 – object under irradiation; 4 – accelerator STRAUS-2; 5 – accelerator ARSA; 6 – accelerator LIU; 7 – accelerator hall; 8 – irradiation hall; 9 – reactor hall.

Table 1. Irradiation complex PUL'SAR

Facility	Radiation characteristics
LIU-30	$P_{bs}^{max} = 1{,}5\cdot10^{13}$ R/s in ∅ 11 cm, $P_{bs}^{1M} = 5\cdot10^{11}$ R/s in ∅ 60 cm, $E_{bound.}$ = 4, 15, 25, 40 MeV, $\tau_{ти}$ = (5-25) ns
BR-1M	$\Phi_n^{max} = 10^{15}$ n/cm^2 in ∅ 10 cm, $\Phi_n^{1M} = 5\cdot10^{12}$ n/cm^2, D_γ^{max} = 160 kR, D_γ^{1m} = 1,1 kR, W_0 = 11 MJ, $\tau \geq 55$ μs
STRAUS-2	$P_{bs}^{max} = 10^{12}$ R/s in ∅ 5 cm, $P_{bs}^{1m} = 10^{9}$ R/s in ∅ 80 cm, $E_{bound.}$ =3 MeV, τ_{bs} = (18-25) ns
ILTI-1	$P_{uhr}^{max} = 3\cdot10^{10}$ R/s in ∅ 5 cm, $P_{uhr}^{1m} = 5\cdot10^{7}$ R/s, $E_{bound.} \leq 700$ keV, τ_{bs} = 40 ns
ARSA	$P_{bs}=3\cdot10^{10R}$P/s in ∅10 mm, $E_{bound.} \leq 1$ MeV, τ=10 ns

where $P_\gamma^{1m}(P_{bs}^{1m})$, $D_\gamma^{1m}(D_{bs}^{1m})$, Φ_n^{1m} – dose rate, dose of gamma-radiation, bremsstrahlung and neutron fluence at a distance of 1m from facility at the area with diameter ∅.

Each module of the accelerator channel contains one block of four inductors on radial lines (RL) with water insulation possessing common accelerating tube 2 (see Fig. 2). Each inductor has two radial lines formed by a central disc electrode and grounded toroidal screen disconnected on the internal diameter. The energy in the radial line is stored at their electric capacitance charging ~ 850 ns from five-cascade pulse voltage generators (PVG) produced using Arkadiev-Marx circuit. Into the accelerator structure there are included 72 PVGs, their total energy store being ~1,5 MJ. At closing the RL gap by controlled switches of trigatron type 3, located uniformly by azimuth, there are formed at the inductors output the pulses of accelerating voltage of alternate polarity. The acceleration of high-current electron beam takes place within the first voltage pulse ~ 0.8 MV/block amplitude and 30 ns duration at

ISBN 978-3-95450-125-0

TECHNIQUE AND INSTRUMENTATION FOR BUNCH SHAPE MEASUREMENTS

A.V. Feschenko, Institute For Nuclear Research, Moscow 117312, Russia

Abstract

Bunch shape is one of the most important, interesting but difficult to observe characteristics of a beam in ion linear accelerators. Different possibilities of bunch shape measurements are considered but the emphasis is put on the Bunch Shape Monitors (BSM) developed in INR RAS. The operation of BSM is based on coherent transformation of a longitudinal structure of a beam under study into a transverse distribution of a secondary electron beam through rf scanning. BSM characteristics found both by simulations and experimentally are presented. Modifications of BSM are described. Some experimental results of bunch observations are demonstrated.

INTRODUCTION

A longitudinal distribution of intensity in bunches $I(\varphi)$ or $I(z)$ as well as more complicated functions additionally dependent on transverse coordinates and time are meant by a bunch shape. The main requirement for bunch shape measurements is phase resolution. In ion linacs for typical bunch phase durations ranging from several degrees to several tens of degrees the resolution of 1° looks adequate. The corresponding temporal resolution, for example for 400 MHz, equals to 7 picoseconds. Small dimensions along the beam line, small beam distortion, wide range of measurements in beam intensity and sufficient one in phase, small power consumption and sufficient lifetime are of importance as well.

In ion beams, as opposite to electron ones, an attempt to extract information on bunch shape through beam electromagnetic field results in aggravation of phase resolution due to large longitudinal extent of the particle field to say nothing of the frequency response range of a beam monitor. The problem can be overcome if one localizes a longitudinal space passing through which the bunch transmits information on its shape. This approach can be implemented if a longitudinally small target is inserted into the beam and some kind of radiation due to interaction of the beam with this target is detected.

Different kinds of radiation are used or proposed to be used: Cherenkov radiation [1], detached electrons in case of H-, including photo-detachment by a laser beam [2-4], high energy electrons (δ-electrons) [5], X-rays [6]. Electrons obtained due to residual gas ionization are also used [7,8], the space of their generation being localized by electron collimation and separation in energy.

However low energy secondary electrons are used most extensively. The distinctive feature of these electrons is a weak dependence of their properties both on the type of primary particles and on their energy. Due to this features the detectors can be used for almost any ion beam. Among the characteristics of low energy secondary emission, influencing the parameters of the bunch shape monitor, one can mark out initial energy and angular distributions as well as time dispersion or delay of the emission. Time dispersion establishes a fundamental limitation on the resolution of the detector. The value of time dispersion for metals is estimated theoretically to be about $10^{-15} \div 10^{-14}$ s [9], which is negligible from the point of view of bunch shape measurements. The experimental results of time dispersion measurements give not exact value but its upper limit. It was shown that the upper limit does not exceed $(4\pm2)\cdot10^{-12}$ s [10].

Operation of bunch shape monitors with low energy secondary electrons is based on coherent transformation of a time structure of the analyzed beam into a spatial distribution of secondary electrons through rf modulation. The first real detector is described in [11]. In this detector the electrons emitted from the thin strip target are accelerated by electrostatic field and simultaneously modulated in energy by rf electric field. Further energy analysis in a magnetic field enables to spatially separate the electrons with different energies, each point of the spatial distribution corresponding to a particular point of the longitudinal distribution of the analyzed beam. The detector described in [12] uses the same principle except for the feature that the processes of electrostatic acceleration and rf modulation are separated in space. Both the above detectors use rf modulation in energy or in other words a longitudinal modulation. Another possibility is using a transverse scanning. The electrons are modulated in transverse direction and deflected depending on their phase. Spatial separation is obtained after a drift space. In the first proposal of the bunch shape detector with transverse modulation of low energy secondary electrons, made in the early sixties [13], a circular scan with the help of two rf deflectors is foreseen. The circular scan provides a band of measurements equal to a full period of the rf deflecting field. However the bunches in linear accelerators are normally much shorter than the period and instead of a circular scan one can use a linear one thus twice loosing the phase range of measurements but essentially simplifying the detector.

BSM WITH TRANSVERSE SCANNING

Principle of Operation

The BSM operation principle has been described in detail earlier [14÷16]. Briefly it can be repeated with the reference to fig. 1. The series of bunches of the beam under study crosses the wire target 1 which is at a high negative potential ($U_{t\,\mathrm{arg}}$ about -10 kV). The target represents a tungsten wire of 0.1 mm diameter. Interaction of the beam with the target results in emission of low energy secondary electrons. The electrons are

ISBN 978-3-95450-125-0

BEAM DIAGNOSTIC INSTRUMENTATION FOR THE NSLS-II BOOSTER *

O.I. Meshkov, BINP, Novosibirsk, Russia; NSU, Novosibirsk, Russia
V.V. Smaluk, BINP, Novosibirsk, Russia

Abstract

For a successful commissioning and for effective operation of the NSLS-II Booster a number of beam parameters should be measured in real-time mode. The main parameters and features of the diagnostics of the NSLS-II booster are briefly described. The diagnostics will be applied as well as during booster commissioning as well as during routine operations.

List of diagnostics

Six fluorescent screens (beam flags) are used for Booster commissioning and troubleshooting. The beam closed orbit is measured using electrostatic BPMs with turn-by-turn capability. The circulating current and beam lifetime are measured with DCCT. The fill pattern is monitored with FCT. The betatron tunes are measured with a set of two pairs of striplines, the first pair is for excitation and the second one – for beam response measurement. Visible synchrotron radiation is used for observation of the beam image during ramp and for emittance measurement. (Fig.1)

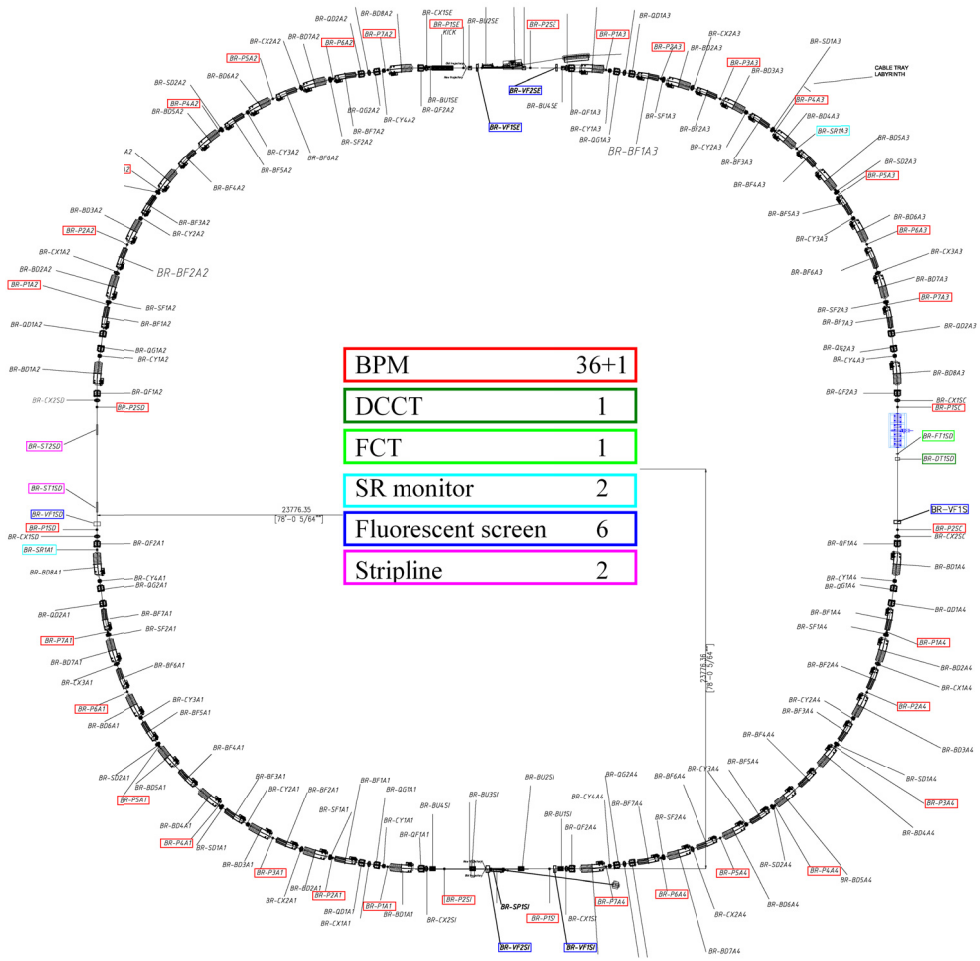

Figure 1. Layout of Booster beam diagnostic

The supplied equipment and subsystem components are durable and capable of operating in the accelerator environment (with the presence of EMI, radiation, vibration, etc.). The schematic layout of the Booster is shown in Fig. 1, the beam diagnostic instruments are marked. The beam diagnostic instruments are listed in

ISBN 978-3-95450-125-0

HIGH-VOLTAGE ACCELERATORS INTENDED TO PRODUCE CONTINUOUS AND PULSE NEUTRON FLUXES

D.A. Solnyshkov#, G.G. Voronin, A.V. Morozov, N.P. Mikulinas, A.N. Kuzhlev, V.D. Shiltsev, D.V. Efremov Scientific Research Institute of Electrophysical Apparatus, Saint Petersburg, Russia

Abstract

Recently, in NIIEFA a series of high-voltage accelerators intended to produce continuous and pulse neutron fluxes with a yield of 10^{10}-10^{12} n/s has been designed. The facilities designed can be used for operation in the continuous, microsecond and nanosecond modes, in any combination. In the pulse microsecond mode, ion currents of up to 100 mA with pulse lengths ranging from 2 up to 100 μs can be obtained on target. In the nanosecond mode, the accelerator produces an ion beam current of up to 5 mA with a pulse length in the range of 2-30 ns.

Over the last years the interest towards pulse neutron generators is growing due to continuation of research in the field of nuclear physics using time-of-flight methods. One more reason of such interest is that the development of high-effective systems for the detection of fissionable substances, explosives, drugs and poisons is a currently central issue. R & D works have been carried out in NIIEFA to design and build neutron generators, which produce neutron fluxes of high-intensity in the continuous operating mode and, in addition, will be capable of producing neutron fluxes in a wide range of the pulse repetition rate and pulse length.

The NG-12-2 neutron generator [1] is a high-voltage accelerator of deuterium ions with an acceleration voltage of 300 kV and a beam current of deuterium atomic ions of up to 15 mA.

The general view of the NG-12-2 neutron generator is shown in figure 1.

Figure 1: The NG-12-2 Neutron Generator Installed in the Institute of Nuclear Physics and Chemistry, CAEP, China.

#d-soln@luts.niiefa.spb.su

The ion injector is installed in a high-voltage terminal of the accelerator and consists of an ion source with initial beam forming system, analyzing 90^0 electromagnet, autonomous vacuum system, electric power supply and control systems. The ion source is of an ECR type with a four-electrode ion beam forming system [2]. Spatial and angular characteristics of the beam at the accelerating tube input are controlled with a double-focusing analyzing electromagnet and electromagnetic solenoid lens.

The ion optical system of the accelerator was designed so that to obtain at the accelerator output in the switching magnet plane a deuterium ion beam with a current of up to 20 mA, an emittance and regular divergence values required for its further transport towards the target. A 45^0 electromagnet serves for the beam switching to two beamlines. The first of them is intended for the operation in the continuous and pulsed microsecond modes. An ion beam with a pulse length of 10-100 μs and pulse repetition rate up to several kHz is produced by the microwave discharge modulation in the ion source. The second is designed for the production of ion pulses with the 1-2 ns length on a stationary target. Such pulses are produced in a beamline, which consists of a beam chopper, klystron particle buncher, target device and beam focusing and measuring system. The system of nanosecond pulse forming is described in detail in [3]. The length of the beamline is about 6 m.

Thus, the neutron generator described in the paper allows a beam of atomic ions with a current of up to 15 mA and beam diameter of 20 mm to be obtained on a rotating target of 230 mm diameter. In the pulsed mode, a pulse length can be 10-100 μs and current amplitude of up to 20 mA. In the second beamline, a peak ion current of 10 mA with a pulse length of 1.7 ns was obtained. The pulse repetition rate can be set to 1, 2, 4 MHz; a mode is provided when it can be smoothly varied in the 1-100 kHz range.

The generators of the NH-12-2 model can be successfully operated at large research centers. However, there exists a demand for less expensive generators with lower neutron yield but also equipped with auxiliary systems to widen the fields of possible applications.

The NG-11I neutron generator is designed for a neutron yield of 5×10^{11}n/s in the continuous operating mode. It is equipped with a system for production of pulse neutron fluxes in the microsecond range by modulating the ion source discharge. The generator is a deuterium ion accelerator with an acceleration voltage of 180 kV and atomic ion beam current on target up to 5 mA. An ECR ion source is also used in the accelerator. An electromagnetic analyzer mounted behind the accelerating

ISBN 978-3-95450-125-0

THE CC1-3 CYCLOTRON SYSTEM

V.G. Mudrolyubov#, I.N. Vasilchenko, Yu.N. Gavrish, A.V. Galchuck, S.V. Grigorenko, V.I. Grigoriev, M.T. Kozienko, L.E. Korolev, A.N. Kuzhlev, Yu.I. Stogov, V.I. Ponomarenko, A.P. Strokach, S.S. Tsygankov, V.D. Shiltsev,
D.V. Efremov Scientific Research Institute of Electrophysical Apparatus, Saint Petersburg, Russia
Nebojsa Neskovic, Petar Belicev, Aleksandar Dobrosavljevic, Velibor Vujovic,
The Vinca Institute of Nuclear Sciences, Belgrade, Serbia

Abstract

A CC1-3 cyclotron system has been designed to be installed in the Vinca Institute of Nuclear Sciences, Belgrade, Serbia. This system will be operated in the laboratory of nuclear-physical methods of the elemental analysis. The system includes a compact cyclotron and a system for beam shaping with specified energy characteristics. The cyclotron ensures the acceleration of negative hydrogen ions up to energy in the range from 1 to 3 MeV and a beam of protons is extracted by stripping on a thin carbon foil. The beam-shaping system ensures the beam of protons with a spectrum width not more than 0.1%. The main unit of the beam-shaping system is a magnetic analyzer with a bending angle of 270º. To date, the equipment of the cyclotron system has been manufactured and tests have been carried out on test facilities in the D.V. Efremov Institute. Installation will be performed in 2012.

The CC1-3 cyclotron system has been designed at the D.V. Efremov Scientific Research Institute of Electrophysical Apparatus (NIIEFA), St. Petersburg with an active participation of specialists from the Vinca Institute of Nuclear Sciences, Belgrade, Serbia. The system will ensure effective technological facilities necessary to carry out analytical research in the Vinca Institute, in particular RBS, PES, NRA и PIXE spectroscopies. Strict requirements are imposed for parameters of accelerated proton beams: the energy range should be from 1 to 3 MeV, spectrum width no more than 0.1%, accuracy of energy setting not worse than 1 keV and current ranging from 10 to 100 nA.

To attain the aforementioned parameters, we have chosen the version of the system consisting of a compact cyclotron with a beam-forming system (Fig. 1) and systems of power supply, automatic control, vacuum pumping and water cooling.

The compact cyclotron is intended to accelerate negative hydrogen ions. An extraction by stripping on a thin carbon foil allows a proton beam with a final energy up to 1-3 MeV to be delivered. The current of the extracted beam of protons is 20 μA. The cyclotron comprises the following units and elements: an electromagnet with a vacuum chamber, resonance system, probes and stripping device, external injection system and high-frequency generator.

#Mudrolubov_VG@luts.niiefa.spb.su

The beam-forming system is designed to ensure beam parameters, which are not typical for cyclotrons. The beam-forming system includes a matching magnet and switching magnets, doublet of quadrupole lenses, correcting electromagnets and magnetic analyzer.

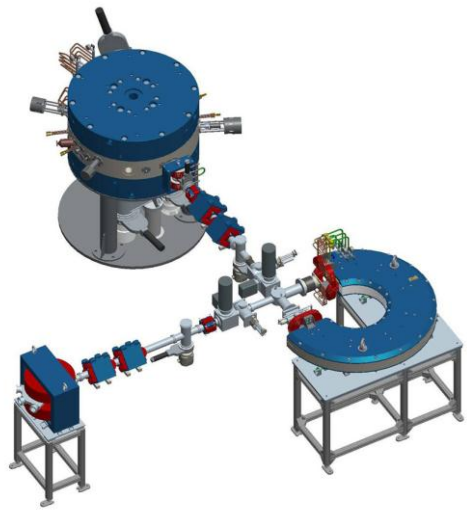

Figure 1: The compact cyclotron CC1-3 with a beam-forming system.

The major part of the cyclotron is a four-sector shielding-type electromagnet (Fig. 2). The electromagnet is 1400 mm in dia, pole diameter is 600 mm and average induction is 0.98 T. Gap hills/values are 50/100 mm. The maximum acceleration radius for the 3 MeV energy is 250 mm. The power consumption of the magnet is 5.2 kW; its mass is 6.5 tons. The upper beam of the magnet can be moved upward up to 500 mm.

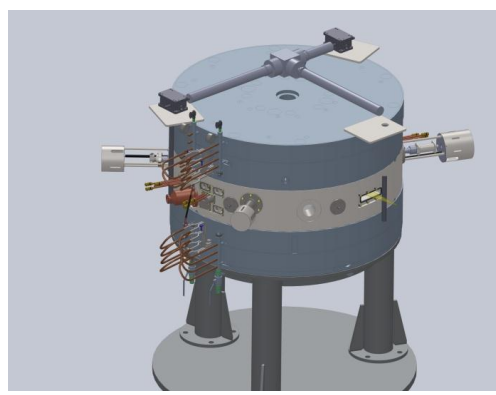

Figure 2: The magnet of the cyclotron.

ISBN 978-3-95450-125-0

ACCELERATION TECHNIQUE DEVELOPED AT JINR FOR HADRON THERAPY

E.M. Syresin, Joint Institute for Nuclear Research, Dubna, Russia

Abstract

The JINR activities are aimed on the construction of accelerators for proton and carbon ion therapy. JINR-IBA have developed and constructed the proton cyclotron C235-V3. The cyclotron will be delivered in the first Russian hospital center of the proton therapy in Dimitrovgrad in 2012.

The project of the medical carbon synchrotron was developed in JINR. The project goal is accumulation of the superconducting Nuclotron technology at construction of the medical carbon synchrotron. Accelerated ^{12}C ion beams are effectively used for cancer treatment.

The PET is the most effective way of tumor diagnostics. The intensive radioactive ^{11}C ion beam could allow both these advantages to be combined. JINR-NIRS collaboration develops formation of a primary radioactive ion beam at intensity on the tumor target of 10^8 pps for the scanning radiation.

A superconducting cyclotron C400 has been designed by the IBA-JINR collaboration. This cyclotron will be used for radiotherapy with proton, helium and carbon ions. Its construction was started in 2010 within the framework of the Archarde project (France).

The interaction between delta electrons and DNA molecules is one of the important processes in the hadron therapy. The formation of low energy electrons and DNA ions are presented for the KEK electrostatic storage ring with the electron target developed by JINR-NIRS collaboration.

PROTON CYCLOTRON C235-V3

The JINR-IBA collaboration has developed and constructed the C 235-V3 proton cyclotron for Dimitrovgrad hospital proton center. The C235–V3 cyclotron, superior in its parameters to the IBA C235 medical proton cyclotron, has been designed and manufactured by the JINR-IBA collaboration. This cyclotron is a substantially modified version of the IBA C235 cyclotron.

Modification of the extraction system is the main aim of the new C235-V3 cyclotron [1-2]. The main feature of the cyclotron extraction system is a rather small gap (9 mm) between the sectors in this area. The septum surface consists of several parts of circumferences of different radii. The septum thickness is linearly increased from 0.1 mm at the entrance to 3 mm at the exit. The proton extraction losses considerably depend on the septum geometry. In the septum geometry proposed by JINR, where the minimum of the septum thickness is placed at a distance of 10 cm from the entrance, the losses were reduced from 25% to 8%. Together with the optimization of the deflector entrance and exit positions it leads to an increase in the extraction efficiency to 80%. The new extraction system was constructed and tested at the IBA C235 cyclotron. The experimentally measured extraction efficiency was improved from 60% for the old system to 77% for the new one.

One of the nearest goals is to modify the sector spiral angle at R>80 cm for improving the cyclotron working diagram and reducing of coherent beam losses at acceleration. The coherent beam displacement z from the median plane is defined by the vertical betatron tune Q_z: $z \propto Q_z^{-2}$. At $Q_z \cong 0.2$ the coherent beam displacement corresponds to 7 mm and at the free axial oscillation amplitude of 2-3 mm can cause beam losses due to reduction of the sector gap in the C235 cyclotron. An increase of the vertical betatron tune from $Q_z \cong 0.2$-0.25 to $Q_z \cong 0.4$ in C235-V3 permits the coherent losses at proton acceleration to be reduced by a factor of 3-4.

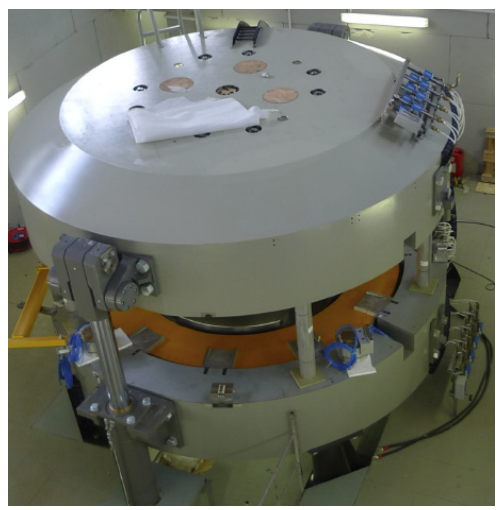

Figure 1: Cyclotron C235-V3 in JINR engineering center.

SUPERCONDUCTING SYNCHROTRON FOR CARBON THERAPY

A project of the medical superconducting synchrotron (Fig. 2) dedicated for the carbon therapy has been designed in JINR [3]. The basis of this medical accelerator is the superconducting JINR synchrotron – Nuclotron [4]. The Nuclotron type straight dipole magnets [4] were adopted for the optic of the medical synchrotron and beam delivery system. The

ISBN 978-3-95450-125-0

PROSPECTS FOR INTRODUCTION OF HOME-MADE EQUIPMENT FOR RADIONUCLIDE DIAGNOSTICS

A.P. Strokach#, M.F. Vorogushin, A.V. Stepanov, O.G. Filatov
D.V. Efremov Scientific Research Institute of Electrophysical Apparatus, Saint Petersburg, Russia

Abstract

The radionuclide diagnostics allows the most of diseases to be diagnosed at a very early stage and therefore it has received much attention over the last years. The current concept of the radionuclide diagnostics advancement takes into account Russia geographic and demographic features, and supports the introduction of the home-made equipment into practice. As a basis, the concept assumes the establishment of regional diagnostic centers at large hospitals in each Russian Federal district. Each such a center should be equipped with a cyclotron of the CC-18/9 model, modules for radiopharmaceuticals' synthesis, single-photon emission (SPECT) and positron (PET) scanners. The yield of radiopharmaceuticals' production will satisfy the needs of such a center and of 30-35 SPECT-"satellites" located in diagnostic departments of hospitals situated up to 1000 km from the center. In future, autonomous PET- centers, each equipped with specialized CC-12 cyclotrons, modules for radiopharmaceuticals' synthesis and with 3-4 PET scanners can be established on the basis of these diagnostic departments. The implementation of the Federal Targeted Program on the serial production of cyclotrons and SPECT will require 5-6 years to increase the number of the people examined per year up to 1.0-1.2 million.

Nowadays in Russia the radionuclide diagnostics based on the use of radioactive isotopes is beyond the reach of the majority of people. In accordance with the program of the Ministry of Health and Social Development of the Russian Federation in force at present, three large federal medical high-technology centers are to be built in Dimitrovograd, Obninsk and Tomsk; PET-centers and radionuclide therapy departments are to be built in Krasnoyarsk, Nizhniy Novgorod and Novorossisk. The higher yield of radioisotopic products should be provided in Moscow, Obninsk and Tomsk.

The suggested construction of federal high-tech medical centers in the vicinity of the nuclear-power industry facilities offer definite advantages due to the location of the sources of radioactive products close to consumers. However, there are serious disadvantages connected with necessary staffing these federal centers with a qualified medical and technical personnel and a large volume of capital construction. It is sufficient to note that thousands of patients and accompanying persons from all regions of the Russian Federation will come to these center,s and all these people will need a place to live in. For example, Dimitrovgrad or Obninsk, towns with a population of 100-120 thousand people, will have to accommodate tens of thousands of people per year who need diagnostics and treatment. In this context, a developed infrastructure is needed including hospitals with medical and auxiliary personnel, hotels, public catering, transport, etc. The total number of tomographs functioning in three federal centers will be much lower than it is required for Russia in compliance with the world standards.

So, this program does not take into account geographic and demographic features of our country and in view of large volumes of necessary capital construction, including residential housing, and serious staff problems, the delivery of modern therapies to the majority of people will be postponed for an indefinite period of time. There are grounds to suppose that an expensive import equipment will be purchased to equip these centers, and interests of the national manufactures will be completely ignored.

NIIEFA in cooperation with other organizations can manage to completely equip radionuclide diagnostic centers mostly with home-made equipment by analogy with the operating PET center in the Russian Research Center for Radiology and Surgical Technologies, Pesochnyi, St. Petersburg [1].

In NIIEFA the designing of a new series of cyclotrons, the CC-12, CC-18/9 and MCC-30/15, has been finished and prototypes of these machines have been manufactured (digits here denote the design energy of proton/ deuterium ion beams). When designing these machines, the following innovations were realized: the acceleration of negative hydrogen ions generated by an external source and extraction of beams of accelerated protons and deuterons by recharging on thin carbon foils. Three CC-18/9 and one MCC-30/15 cyclotrons have been manufactured and put into operation. These machines are used for production of a wide set of ultra short-lived and short-lived radionuclides used in medicine for PET and SPECT diagnostics. The CC-18/9 and MCC-30/15 cyclotrons also produce short-lived radionuclides for the contact radiation therapy. The CC-12 cyclotron specialized only in production of ultra short-lived radionuclides is nowadays under tests at a test facility in NIIEFA.

A prototype of the double-detector single-photon emission computerized tomograph "EFATOM" has been designed and manufactured [1]. After successful technical and clinical tests, the "EFATOM" was put on the list of the medical equipment allowed to be produced in Russia.

So, prototypes of the major equipment, cyclotrons and tomographs, to be used in the present-day radionuclide diagnostics have been designed and manufactured in

#strokach@luts.niiefa.spb.su

ISBN 978-3-95450-125-0

METHOD OF STATE AND ALIGNMENT MONITORING FOR CRYSTAL DEFLECTORS OF RELATIVISTIC IONS*

A. Gogolev#, S. Uglov, TPU, Tomsk, Russia
A. Taratin, JINR, Dubna, Russia

Abstract

The calculations of the parametric X-ray radiation (PXR) characteristics produced by 158 GeV/u Pb nuclei in silicon crystal deflectors were carried out. The PXR intensity at the maximum angular distribution was about 4 ph/Pb/sr, which should allow to monitor the state and the orientation of the deflector by means of the observation of the PXR spectrum characteristics.

INTRODUCTION

Systems of relativistic particle beam steering based on the use of channeling effect are widely applied in leading research centers of Russia and foreign countries. It was experimentally shown that with use of short crystals one can obtain extracted beams with intensity of ~ 10^{12} protons/cycle with efficiency of ~ 85% [1].

The radiation resistance of crystals is one of important characteristic in the applications of crystals for beam control of accelerator. Estimation of the limit value of the particle flux through the crystal before its destruction has been obtained in the experiments carried out at CERN (Switzerland) and BNL (USA) and is equal to ~ $2 \cdot 10^{20}$ protons/cm^2. Silicon crystals with efficiency $80 \div 85\%$ reliably provide the extraction up to 10^{12} particles per cycle duration of $1 \div 2$ seconds. When intensity of beam is about 10^{13} protons the crystal loses the capability to deflect the particles [2].

An operative control is required in the case of using crystal deflectors for the accelerator intensive beam collimation. The control should allow to conclude about the state and alignment of the crystal collimator relative to the beam halo.

In paper [3] we were proposed concept a method of exploiting parametric PXR as a monitor of deflector quality and orientation. PXR is emitted in directions satisfying the Bragg condition when relativistic charge particles are incident on a crystal and its properties strongly depend on kinematics of process [4-6]. Since its first observation [7] one studied using electron beams of different energies [8, 9]. The first experiment with the aim of PXR observation from heavy charged particles was carried out on the 70 GeV proton beam at IHEP [10]. After that PXR has been successfully observed from 5 GeV protons and 2.2 GeV/u carbon nuclei in a silicon crystal on the external beams of the Nuclotron at LHE JINR [11, 12]. Recently, PXR produced by 400 GeV/c protons in silicon deflector has been observed [13].

*Work supported by Russian Foundation for Basic Research grant 12-02-16130 and the GK #14.B37.21.0912
#gogolev@tpu.ru

The aim of this paper is to calculate the spectral and angular characteristics of the PXR from silicon deflectors when relativistic Pb nuclei are passing through them.

SIMULATION

The layout of numerical experiment is similar to work [13]. Fig. 1 shows the layout in the horizontal plane for the experiments with quasi-mosaic (QM) and strip (ST) silicon crystals. A beam of Pb nuclei with energy 158 GeV/u entered a crystal in the collimation geometry so that it is parallel to the deflecting planes, which are the (111) and (110) crystallographic planes for the QM and ST crystals, respectively.

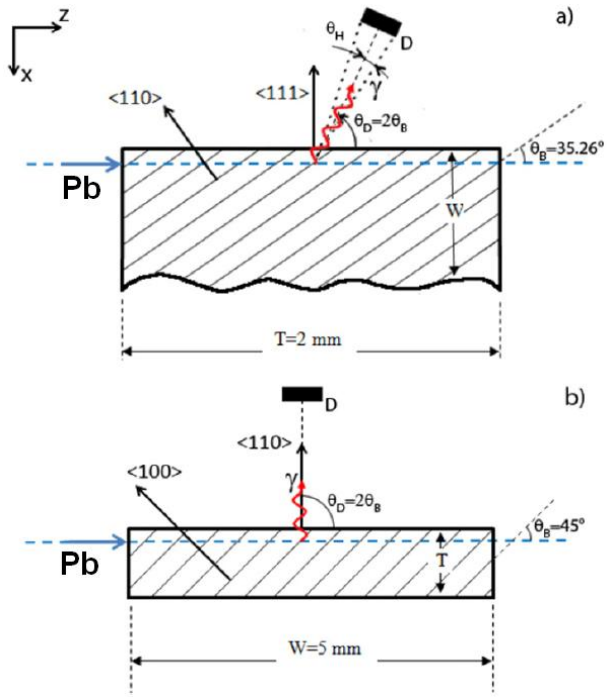

Figure 1: The simulation scheme details: (a) for quasi-mosaic crystal, (b) for strip crystal.

Simulation was carried out for a Gaussian incident beam with the cross-section σ = 1,0x0,7 mm^2 and σ = 10,7x7,8 μrad^2 divergence. A beam of Pb nuclei crossed the crystal with an offset of 0,7 mm depth in the QM case and in the centre in the ST case.

PXR is generated by particle field when it crossing a set of the crystallographic planes. PXR reflexes (110) and (100) in the case of (a) and (b) shown in Fig. 1, respectively, was calculated.

The energy of PXR photons is determined in the following way:

ISBN 978-3-95450-125-0

RECENT DEVELOPMENT IN ECR ION SOURCES AT FLNR JINR

S.Bogomolov, V.Bekhterev, A.Efremov, B.Gikal, G.Gulbekian, Yu.Kostukhov, A.Lebedev, V.Loginov, N.Yazvitsky, JINR, Dubna, Russia

Abstract

In the Flerov Laboratory of Nuclear Reactions (JINR) the development of ion sources based on the plasma electrons heating at the frequency of electron cyclotron resonance (ECR) is stimulated by the necessity of the accelerator complex (U-400, U-400M and CI-100 cyclotrons) upgrading as well as by creation of the new high current cyclotrons for basic and applied research.

Several ECR ion sources have been operated in the Flerov Laboratory of Nuclear Reactions (JINR) supplying various ion species for the U400 and U400M cyclotrons correspondingly for experiments on the synthesis of heavy and exotic nuclei, using ion beams of stable and radioactive isotopes, for solid state physics experiments and polymer membrane fabrication. In this paper the new development concerned with modernization of ECR4M ion source, development of the new superconducting source DECRIS-SC2 and creation of the DECRIS-5 ion source for the DC-110 cyclotron complex will be presented.

INTRODUCTION

Main theme of FLNR JINR is super heavy elements research. From 2000 up to 2010 more then 40 isotopes of elements 112, 113, 114, 115, 116, 117, 118 were synthesized in the laboratory.

At present four isochronous cyclotrons: U-400, U-400M, U-200 and IC-100 are under operation at the JINR FLNR. Three of them are equipped with ECR ion sources. In the DRIBs project for production of accelerated exotic nuclides as ^{6}He, ^{8}He etc. the U-400M is used as radioactive beam generator and U-400 is used as a post-accelerator. Layout of FLNR accelerators complex is presented in Fig.1 [1]. Red stars indicate the location of the ECR ion sources.

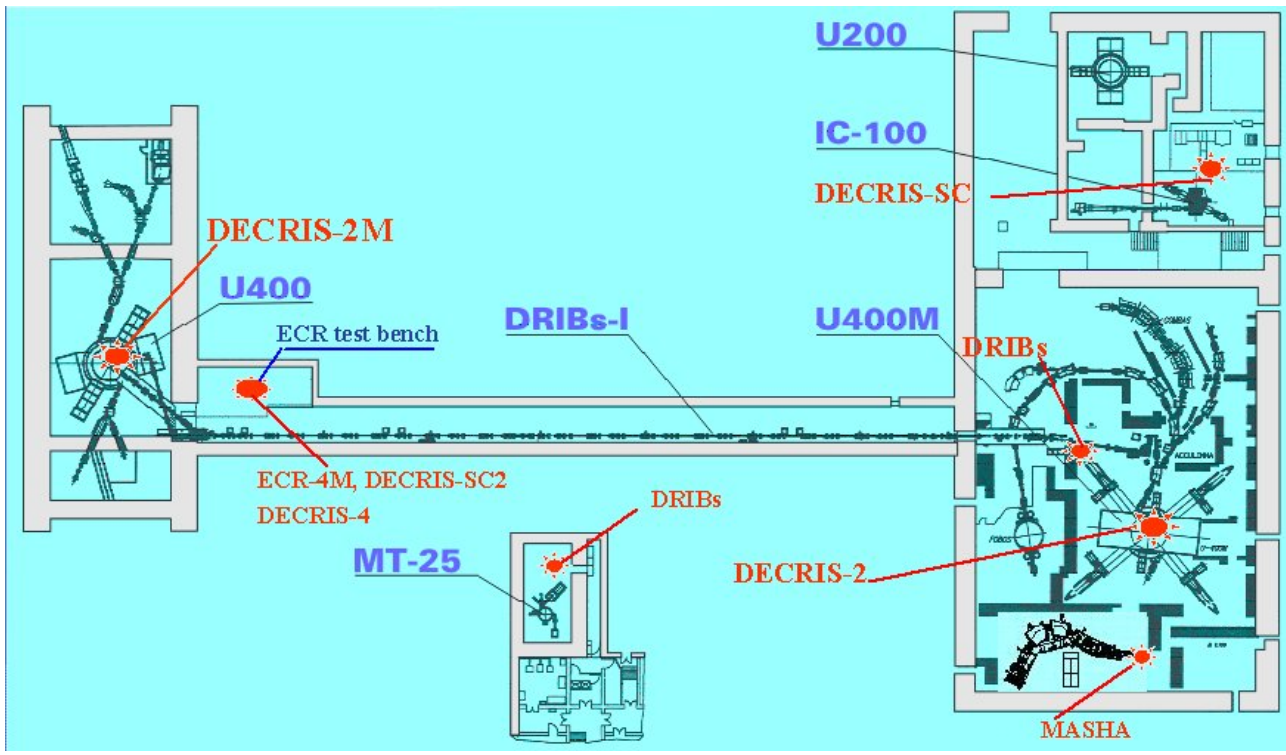

Figure 1: Layout of FLNR JINR accelerator complex. Red stars indicate the location of the ECR ion sources.

ECR4M ION SOURCE

The ECR4M source and the axial injection system were assembled and commissioned in 1996. First accelerated Ar beam was produced in November 1996 [2]. The main goal was to provide the intense beam of the ^{48}Ca ion beam for the experiments on synthesis of super heavy elements at a minimal consumption of this enriched and expensive isotope. First experiment on the synthesis of superheavy elements with the beam of ^{48}Ca was performed in November 1997. Since that about 66% of total operation time was used for acceleration $^{48}Ca^{5+,6+}$ ions for research

ISBN 978-3-95450-125-0

STATUS REPOTR ON PHYSICS RESEARCH AND TECHNOLOGY DEVELOPMENTS OF ELECTRON STRING ION SOURCES OF MULTICHARGED IONS

A.Yu. Boytsov, S.V. Gudkov, D.E. Donets, E.D. Donets, E.E. Donets, A.Yu. Ramsdorf, V.V. Salnikov and V.B. Shutov, Laboratory of High Energy Physics, Joint Institute for Nuclear Research, Dubna, 141980, Russia

Abstract

Electron String Ion Source (ESIS) "Krion-2" (JINR) is the first and now only ion source of such type in the world. ESIS is a sophisticated modification of Electron Beam Ion Source (EBIS) working in a reflex mode of operation under very specific conditions. Using the results of the research and the technology development the following main results were achieved in JINR with Krion-2 ESIS during recent years: Au^{54+} ion beams with intensity $5x10^7$ particle per pulse were first produced and ion-ion cooling technology was demonstrated to prove its efficiency for a thermal ion loss reduction; Krion-2 was used for production and injection of Xe^{42+} ion beam into LINAC injector of JINR synchrotron Nuclotron, where the beam was first accelerated to relativistic energy in March 2010 [1-3].

At the present time an essential progress was achieved in construction of the new 6 Tesla ESIS, which is expected to be the full scale prototype of a highly charged ion source for NICA - the new JINR accelerator complex. It is foreseen in the NICA project that new ESIS will provide Au^{32+} beams with the ion yield about $2x10^9$ ppp. However, a project parameters of new Krion-6T(esla) ion source allow to expect production of even more highly charged states of heavy elements, up to Au^{69+} in terms of gold. In this case the new Krion-6T ESIS may be used on operating JINR "Nuclotron" facility in near future for experiments with an extracted accelerated gold ion beams on a fixed target.

INTRODUCTION

Electron string phenomenon occurs during the reflex mode of EBIS operation. The interest in the studies of reflex mode operation was motivated by an attractive possibility to decrease the power of the electron beam by a hundred times while simultaneously preserving the same ion yield. Indeed, the power of the electron beam in a direct mode can reach many hundreds of KW that provides serious technical obstacles for a successful realization.

The study of the reflex mode of EBIS operation was initiated in JINR in 1994. These research were performed with use of JINR EBIS Krion-2. The reflex mode of EBIS operation is realized by using the specially designed electron gun and electron reflector that allows multiple use of beam electrons. The electrons do not reach electron collector after one pass through the drift space of the source (1.2 m long). Usually emitter has a negative voltage of few KV, anodes and drift tube structure are at ground potential, and the reflector has negative voltage few KV lower than the emitter. As a result, the emitted electrons after one path are reflected back towards the emitter side and then are reflected again in a vicinity of the emitter and so on. The emitter and reflector are placed in a fringe magnetic field (in a region of about 1/20 of a maximal magnetic field) hence each electron reflection is accompanied by some transformation of the longitudinal electron velocity to the radial/azimuthal velocity. As a result, the electrons are accumulated in a drift tube space of the source. The stored multiply reflected electrons can be used for highly charged ions production similarly to the beam electrons.

An unknown phenomenon was unexpectedly observed in JINR in 1994, which became a key physics ingredient of the proposed EBIS development in the reflex mode of operation. It was found that under certain conditions one component pure electron plasma, which consists of the multiply reflected electrons, confined in a strong solenoid magnetic field, exhibits a stepwise increase of the confined electron plasma density in a new steady state called "electron string". The transition usually goes via an unstable pre-string state in which the electron energy spectrum expands, which further suppresses the instability.

The electron string can arise if a definite number of electrons which exceeds some threshold value is stored in the source drift tube space. This threshold value depends on various parameters such as the electron injection energy, the applied magnetic field strength, the magnetic compression of the injected electron beam and so on. Electron strings are occurred to be stable in a certain frames that allows to use them for an effective production of highly charged ions in Electron String Ion Sources (ESIS), similarly to electron beams in EBIS.

An interesting observed feature of electron strings is a high energy tail in a total electron energy distribution. For example, for electrons with injection energy 3 KeV, this tail extends up to 5 KeV , see [1] and refs therein.

HIGHLY CHARGED ION BEAMS PRODUCED WITH KRION-2

Kr and Xe Highly Charged Ions

Production of highly charged Kr and Xe ion beams has been done in a framework of preparing Krion-2 ESIS for the Nuclotron run. Nuclotron – superconducting synchrotron which includes Linac LU-20 as a part of its injection complex. LU-20 accepts highly charged ions

ISBN 978-3-95450-125-0

PROGRESS IN THE NEGATIVE ION SOURCES DEVELOPMENT

Vadim Dudnikov#, Muons, Inc., 552 N. Batavia Ave., Batavia, IL 60510 USA

Abstract

Recent progress in development of advanced negative ion sources was connected with optimization of cesiation in surface plasma sources (SPS). The cesiation effect, a significant enhancement of negative ion emission from gas discharges with decrease of co-extracted electron current below negative ion current, was observed for the first time in 1971 by placing into the discharge a compound with one milligram of cesium. Subsequent developments of SPS for highly efficient negative ion production caused by the interaction of plasma particles with electrodes on which the adsorbed cesium reduced the surface work-function are described. In the last 40 years, the intensity of negative ion beams has increased by cesiation up to 10^4 times from three milliamp to tens of Amperes.

INTRODUCTION

One practical result of the development of high brightness surface plasma negative ion sources with cesiation (SPS) [1-4] is the wide use of charge-exchange injection in circular accelerators for routine operation[5,6]. Now SPS are "working horses" for large accelerator complexes at ORNL (SNS Spallation Neutron Source, Oak Ridge National Laboratory), FNAL (Fermi National Accelerator Laboratory), LANSCE (Los Alamos Neutron Science Center), BNL (Brookhaven National Laboratory), RAL (ISIS proton synchrotron at the Rutherford Appleton Laboratory), DESY (Deutsches Elektronen-Synchrotron), KEK/J-PARC (Japan Proton Accelerator Research Complex), and other accelerators.

The efficiency and operational reliability of these sources have determined the productivity of these laboratories and their big machines. Many results of high energy physics were discovered using negative ion sources. The development of high brightness H^- sources was first stimulated by successful high current proton beam accumulation using charge-exchange injection [4] and further supported by the interest in particle beam weapons as part of the "Star Wars"[3,4] program. The testing of H^- beam acceleration and neutralization in space (The Beam Experiment Aboard Rocket (BEAR)) considered in [3]. Military uses and classified work caused long delays of first publications, but nonofficial communication was relatively fast. Until 1971, the main attention was concentrated on charge-exchange ion sources because there was no hope to extract more than 5 mA of H^- directly from plasma.

The cesiation effect, a significant enhancement of negative ion emission from a gas discharge with decrease of co-extracted electron current below negative ion current, was observed for the first time in 1971 by placing into the discharge a compound with one milligram of cesium at the Institute of Nuclear Physics (INP), Novosibirsk, Russia [1].

This observation, considered in review [4], was further developed and understood as on principle new surface plasma method of negative ion production. In the patent application [1] it was stated: "a method of negative ion production in gas discharges, comprising adding into the discharge an admixture of substance with a low ionization potential such as cesium, for example, for enhancement of negative ion formation".

In subsequent experiments it was demonstrated that cesium adsorption decreases the surface work function from 4-5 eV to ~1.5 eV, which enhances secondary emission of negative ions caused by the interaction of the plasma with the electrode surface and thereby enhances surface plasma generation (SPG) of negative ions. Ion sources based on this process have been named Surface-Plasma Sources (SPS). The theoretical explanation of this enhancement of negative ion emission by cesiation was presented by Kishinevsky [4]. A small admixture of cesium or other impurity with low ionization potential (ILIP) in the gas discharge significantly improves H^- production. When done correctly, a cesiated SPS works very well [1-4] . However, improper cesiation can complicate ion source operation. For example, injection of too much cesium can cause the discharge to become unstable and sparking occurs in the extractor with loss of stable ion source operation. With low cesium concentration the efficiency of negative ion production is too low. With "proper" cesiation the efficiency of negative ion production is high and extended ion source operation is stable.

Further development of SPS was conducted by collaboration of Belchenko, Dimov, and Dudnikov . The development of the first high brightness SPS for accelerators was presented in[4]. The Semiplanatron SPS with efficient geometrical focusing has been developed by the author [3]. The development and adaptation of SPS started soon after in many USA laboratories, in Europe, and in Japan. A very active program of SPS development was established in BNL by Sluyters and Prelec. BNL Symposiums for Production and Neutralization of Negative Ions and the European Workshops on Production and application of Light Negative Ions Beams were established. Physical principles of SPS operation were presented in [2-4] and were reproduced in many reviews and books. Good reviews of SPS for accelerators were presented in reports of Peters. The development of high brightness SPS by Allison's group in LANL is considered in[3]. The development of high current SPS (tens of Amperes) for thermonuclear plasma heating was conducted by teams at LBNL and in Japan which is still in progress and is used in large tokamaks and stellarators[4]. Production of polarized negative ions by

#vadim@muonsinc.com

ISBN 978-3-95450-125-0

CREATING STRONGER ACCELERATOR BEAMS

Richard M. Kriske, University of Minnesota, Minneapolis, Minnesota, USA

INTRODUCTION

Many new designs for Particle Accelerators have been proposed including the ILC (The International Linear Collider and the CLIC (The Compact Linear Collider). Both the ILC and the CLIC are high energy electron-positron colliders. The CLIC seems somewhat more impressive in its ability to operate up to 3TeV, but the ILC uses the more normal means of operation as a superconducting machine. The CLIC has a more ambitious output but with a more experimental approach. Prototypes of many of the subsystems of CLIC have been constructed at CERN and around the world, but the ILC has in general been subject to a more larger review in this authors view. Of course the ILD and SiD detectors where originally designed for the ILC, but have now become appendages of the CLIC design, showing that no good idea goes to waste. There has been some debate as to the physics obtainable using e+e- colliders, but the consensus is that this is a useful idea, but as always a greater beam strength would be better. Of course the LHC (the large Hadron Collider) has a potential range from 8 TeV to 14TeV . The demand for a stronger beam can be seen from the differences and trade-offs between the ILC and the CLIC. This paper is not meant to be comprehensive in the comparison between these designs.

CLIC DESIGN

The CLIC has a broad center-of-mass range from 500Mev to 3TeV, which may be crucial for some experiments. The discovery of a particle in the 125 GeV range at the LHC may warrant a collider that can “scope” this energy range out in greater detail. The CLIC design is currently in the 500 GeV range and the 3 TeV range. In the CLIC there are drive beam accelerators. The drive beam energy is transferred to the colliding beam through RF power through waveguides. The bunch spacing is 60cm. The major design difference between the 500 GeV range and the 3 TeV range is a greater number of Klystrons, which has a greater number due to the larger beam current. A larger bunch charge and more bunches per pulse gives the 500 GeV design more luminosity. The designs are about the same length, but the 3 TeV design has a larger gradient.

ILC DESIGN

The ILC has a narrower center-of-mass range from about 500 GeV to 1 TeV, and uses superconducting klystron tubes as its construction. A large number of Tubes have to be used and this like the CLIC is a linear device.

TRADE-OFFS

The major difference between CLIC and ILC seems to be the amount of current in the beam. The CLIC claims to be able to produce 100 Amps (Is this true?) and do this because it is not technically a superconducting device (klystrons?). The ILC produces about 7milliamps, which is large compared to the average current at Fermilab.

NEW PHYSICAL IDEAS

From both designs, there could be an advantage to supplying more electons and positrons. It may be possible to use very fine nanotubes as conduits to supply the these particles. There is some evidence that the Quantum Field Theory allows for the tubes to act as springs in the Quantum Field that exists inside the klystron tubes of the Particle Accelerators. Experiments could be done to see if this is the case, and fine tubes could be attached to the klystrons. A mathematical model of this is available. It may be that it is not possible to generate and use such large currents with existing technology even if the large number of klystrons can be produced. Larger currents need to be produced, but it is this authors opinion that this can not be done without having larger sources and means for storing particles for creating larger bunch charges. Although this is without experimental evidence it may be possible to use nanotubes to store positrons, at least in very short time periods, but within the times allowed to create bunches. It is this authors opinion that the limits on these machines is going to be the storage of these particles and that research into nanotubes as storage devices may be more important than any other parameter in their construction.

CONCLUSION

Both systems seem to be designed for the same range, but neither seems to have enough klystrons available, in order to produce such large amounts of klystrons, a Japanese company has agreed to produce more sheet niobium which is needed in the production of these tubes. Both designs seem to be a little grand in their expectations of current and for that matter damage by using larger currents. Both designs lack for testing of their components, although both reports seem encouraging in their outlook. Of course both lack for funding.

REFERENCES

[1] M. Aicheler et al. (editors), A Multi-Tev Linear Collider based on CLIC Technology: CLIC Conceptual Design Report, JAI-2012-001, KEK Report 2012-1, PSI012-01, SLAC-R-985, https://edms.cern.ch/document/1234244/

[2] I., Linssen et al. (editors), Physics and Detectors at CLIC: CLIC Conceptual Design Report, 2012, ANL-HEP-TR-12-01, CERN-2012-003, DESY 12-008, KEK Report 2011-7, arXiv:1202.5940

ISBN 978-3-95450-125-0

NON-GATED FIELD EMISSION ARRAY AS LOW-ENERGY ELECTRON SOURCE: EXPERIMENT AND SIMULATION

K.A. Nikiforov*, L.I. Antonova, N.V. Egorov, V.V. Trofimov,
St. Petersburg State University, St. Petersburg, Russia
V.V. Makeev, O.F. Ogurtsov, Molecular Electronics Research Institute, Zelenograd, Russia

Abstract

A non-gated NbN on Si wafer field emission arrays are studied. The I-V measurements and emission characteristics of edge-shaped cathodes in atmosphere low-voltage regime are considered. Mathematical and computer models are presented. The current density obtained from experiment was up to 384 Ampere per square centimeter in emission area 9 mm^2. Low-voltage regime (20 V) for near ($\sim$1 μm) interelectrode distance in diode configuration is discussed. High-voltage operation in high vacuum was experimentaly studied and preliminary results are discussed.

BACKGROUND

The standard emission mechanisms of the cathodes used in the accelerator electron guns are photoemission and thermionic emission. One alternative technology is field-emitter arrays (FEA) where electrons are emitted with energies close to the Fermi level. Such cathodes have potentially a lower mean transverse kinetic energy of the produced electron beam, which is mainly determined by the geometry of the electric field lines. We present first measurements on commercial field-emitter arrays in atmosphere pulsed low-voltage operation and DC high-vacuum high-voltage regime as well as numerical simulations of the electric field near the cathode surface.

There are 2 main architectures of field-emission cathodes: (i) the needle cathode, i.e. one single sharpened tip and (ii) FEA which are arrangements of field emitters on a periodically spaced lattice.

In these proceedings we consider FEA with axial-symmetric emitters of sharp edge type. The photo and SEM image in Figure 1 represent 1×1 cm cathode in pincers with NbN thin-film emitters on heavy As-doped Si wafer from JSC Mikron.

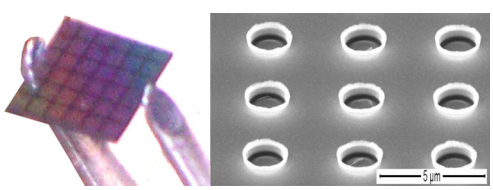

Figure 1: FEA 1×1 cm (left) with $\sim$4000000 NbN emitters (right).

* nikiforov_k@mail.ru

PULSED LOW-VOLTAGE OPERATION IN ATMOSPHERE

Experiment

An ungated NbN field-emitter array was placed at atmospheric pressure in a close-diode configuration with a planar anode with area 9 mm^2. The anode-cathode gap was set 1 μm using precision dielectric spacers shown in Figure 2.

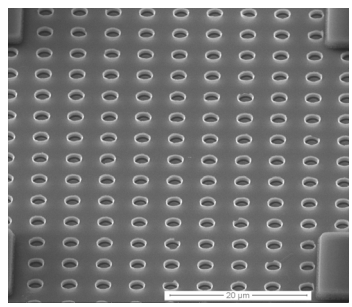

Figure 2: SEM picture of 1 μm height spacers on cathode surface.

The anode was heavy As-doped Si plate electrically isolated from ground and pressed close to cathode by probe tungsten tip of micromanipulator, 300 μs voltage pulses at low frequency was applied. A 100 Ω resistor was placed in series with the cathode and attached to a sensitive voltage meter. A schematic of the experimental configuration is shown in Figure 3.

Results

The field emission characteristics of the system are shown in Figure 3, as a function of bias voltage.

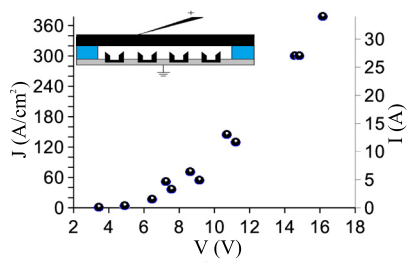

Figure 3: Field emission current and current density vs. cathode voltage. Insert: a schematic of the FEA cathode, emitters, spacers and anode used to collect the field emission.

ISBN 978-3-95450-125-0

DEVELOPMENT OF THE IBA-JINR CYCLOTRON C235-V3 FOR DIMITROVGRAD HOSPITAL CENTER OF THE PROTON THERAPY

S. Kostromin, S. Gursky, G. Karamysheva, M. Kazarinov, S. Korovkin, S. Mokrenko, N. Morozov, A. Olshevsky, V. Romanov, E. Samsonov, N. Shakun, G. Shirkov, S. Shirkov, E. Syresin, JINR, Dubna, Russia
P. Cahay, Y. Jongen, H. Nkongolo, Y. Paradis, Ion Beam Application, Louvain-la-Neuve, Belgium

Abstract

The Dimitrovgrad project, the first Russian hospital center of the proton therapy, was approved in 2010. The JINR-IBA collaboration developed and constructed the C235-V3 proton cyclotron for this center. The assembly and the beam tests of the machine were done in 2011-2012 in special experimental hall in JINR.

This cyclotron is a substantially modified version C235-V3 of the IBA C235 serial cyclotron. C235-V3 has the improved extraction system which was constructed and tested. This system allows raise the extraction efficiency up to 77% from 50% in comparison with serial C235.

Special mapping system (for B_r-component) of the magnetic field was developed and constructed by JINR for the shimming of the B_r-field in the middle plane of the cyclotron.

Tests with accelerated and extracted beam were performed in August 2012 in JINR. Beam vertical motion in the cyclotron is in the acceptable limits ($\Delta Z_{beam} \leq 3$ mm). Transmission from r=300mm to 1030 is 72% without beam cutting diaphragms. This allows reduce irradiation dose of the machine elements in comparison with serial C235. Extraction efficiency is 62%. Total efficiency of the machine is 45%. Further improvement of the parameters expected after final tuning of the cyclotron in Dimitrovgrad.

Recommendations are formulated to modify the magnetic system and reduce sensitivity of the machine to the magnetic field imperfections. Most of changes concerned with the increasing of the vertical focusing at the final radii where the aperture equals two vertical size of the beam.

PROTON THERAPY AT JINR

Dubna is one of the leading proton therapy research centers in Russia [1-2]. The synchrocyclotron (JINR Phasotron) with the proton energy of 660 MeV and current of 3 μA has been used for medical applications since 1967. The modern technique of 3D conformal proton radiotherapy was first effectuated in Russia at this center, and now it is effectively used in regular treatment sessions [1-2]. The irradiated dose distribution in 3D conformal proton therapy coincides with the tumor target shape with an accuracy of 1 mm. About 100 patients undergo a course of fractionated treatment here every year. About 880 patients were treated by proton beams during the last 12 years.

C235-V3 PROTON CYCLOTRON

Federal Medico-Biological Agency in collaboration with JINR developed the Dimitrovgrad project of the first hospital proton center in Russia. The center (Fig.1) consists of two gantry systems, a medical treatment room with a fixed beam used at the treatment angles of 0° & 60°, an eye treatment room and a PATLOG system of preliminary patient positioning. The JINR-IBA collaboration has developed and constructed the C235-V3 proton cyclotron for this center.

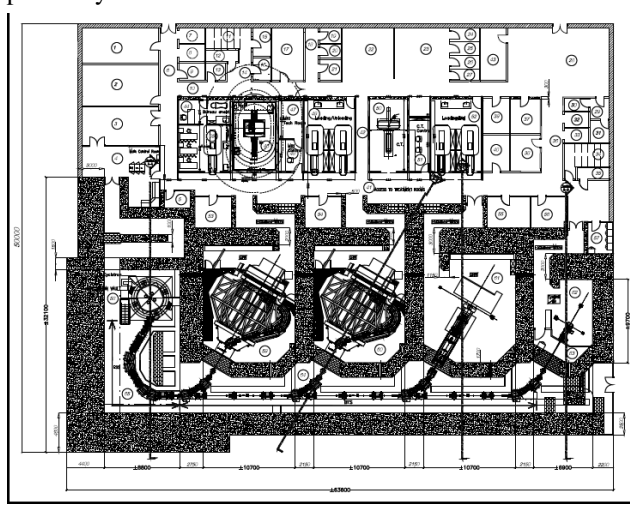

Figure 1: Layout of Dimitrovgrad proton therapy hospital center.

The C235–V3 cyclotron is superior in its parameters to the IBA C235 medical proton cyclotron. It has been designed and manufactured by the JINR-IBA collaboration. This machine is a substantially modified version of the IBA C235 cyclotron.

C235-V3 has modified extraction system [3-4]. After complete study of the beam dynamics in C235 it is clear that the beam extraction losses considerably depend on the septum of electrostatic deflector geometry. In the septum geometry proposed by JINR, where the minimum of the septum thickness is placed at a distance of 10 cm from the entrance, the beam losses on outer surface of the septum were reduced from 25% to 8%. Together with the optimization of the deflector entrance and exit positions it leads to an increase in the extraction efficiency to 80%. The new extraction system was constructed and tested at the IBA C235 cyclotron for Orsay (France). The experimentally measured extraction efficiency was

ISBN 978-3-95450-125-0

PROJECT OF LOW-ENERGY ACCELERATOR DRIVEN POWER PLANT

I.V. Kudinovich, A.A. Bogdanov, V.P Struev,
Krylov Shipbuilding Research Institute, St.Petersburg, Russia
A.G. Golovkina, D.A. Ovsyannikov, Yu.A. Svistunov,
SPbSU, St.Petersburg, Russia

Abstract

Project of low-energy accelerated driven nuclear power plant is considered. It is proposed the accelerated driven system (ads) with subcritical fast reactor, proton linac and fissile target. The main performance data of the ads: proton beam energy 300-400 MeV, accelerator average current 5ma, reactor thermal power 200mw, core effective multiplication factor k_{eff}= 0.98. The principal design features of the power plant is represented.

INTRODUCTION

The accelerator driven system – subcritical reactor driven by high power proton accelerators through a spallation target which is neutronically coupled to the core – have been proposed for addressing certain missions in advanced nuclear fuel cycles [1]. The interest is induced by a number of ADS applications in field of nuclear technologies:

- Transmuting actinides and fission products;
- Producing fissile materials;
- Power generation.

LINEAR ACCELERATOR

For transmuting and large power ADS there are needed high energy proton beams obtained in unique expensive accelerators. For ADS with reactor power 200-400 MW accelerator requirements are much less and traditional proton linac without superconductivity may be used [2].

In Fig. 1 it is shown layout of proton linac with output energy 300 MeV which can be suitable for ADS. Linac consists of multicusp ion source, 4 vane spatially homogeneous strong focusing structure (RFQ), six resonators with alternating phase focusing structure (APF DTL) and working frequency in diapason 424-433 MHz, coupled cavity linac structure (CCL). Injector, RFQ and six APF DTL resonators are LEBT system, eight resonators of CCL with working frequency in diapason 800-861 MHz are MEBT system. APF DTL structure is IH-cavity which have many cells with thick holders turned on right angle in each following cell and magnetic lenses in the drift tubes [3].

Accelerating gradients, collateral disposition of LEBT and MEBT connected by isochronous turning with help of magnetic system (270° bending magnet and focusing lenses).

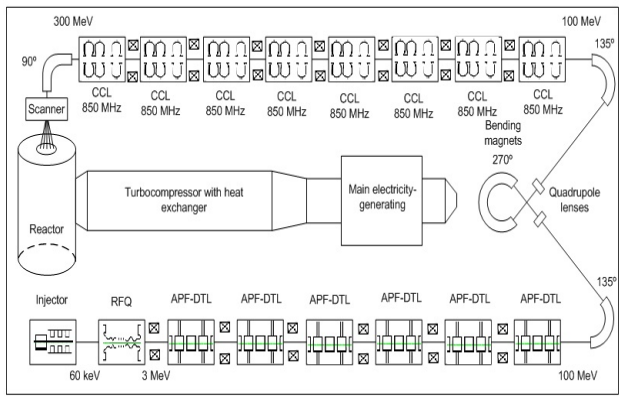

Figure.1: Layout of ADS Power Plant with proton linac.

According to results achieved at SNS accelerator in Oak-Ridge laboratory one can suppose accelerating gradients for LEBT and MEBT 4 MeV/m and 10 MeV/m accordingly [4]. Linac current adjustment can be realized by varying of pulse current repetition frequency. Main parameters of proton linac are given in Table 1.

Table.1: Main parameters of linac.

Output energy	300 MeV
Average current	up to 5 mA
Duty factor	10%
Frequency range of RFQ and DTL	424 - 433 MHz
Beam power	1,5 MW
Working frequency of CCL	805-861 MHZ
Number of RFQ	1
Number of APL-DTL resonators	6
Number of CCL modules	8

TARGET

Neutron yield from the target irradiated by charge particles depends on parameters of particle beam, target composition and it dimensions.

Characteristics of targets were defined with code Geant 4.9.5.

In case of non-fissile target materials spallation neutrons aren't multiplicated inside target and neutron source intensity is specified by leakage from target surface. In target with fissile materials spallation neutrons are multiplicated in target due to fissile processes and neutron source intensity is specified by yield of spallation neutrons inside target.

Calculated values of optimal dimensions of cylindrical non-fission targets are presented in Fig. 2, it also represents neutron yields for them.

ISBN 978-3-95450-125-0

HIGH VOLTAGE ELV ACCELERATORS FOR INDUSTRIAL APPLICATION (FAMILY OF ACCELERATORS AND TENDENCY OF DEVELOPMENT)

N.K. Kuksanov, Y.I. Golubenko, P.I. Nemytov, R.A. Salimov,S.N. Fadeev, A.V. Lavruhkin, A.I. Korchagin, D.S. Kogut, A.V. Semenov, BINP SB RAS, Novosibirsk, Russia

Abstract

Budker Institute of Nuclear Physics Siberian Branch of Russian Academy of Science (SB RAS) continue its activity in the development and manufacturing of electron accelerators of the ELV-type for their use in the industrial and research radiation-technological installations. The ELV-type accelerators were designed with use of the unified systems and units enabling thus to adapt them to the specific requirements of the customer by the main parameters such as the energy range, beam power, length of extraction window, etc.. INP proposes a series of electron accelerators of the ELV-type covering the energy range from 0.3 to 2.5 MeV with a beam of accelerated electrons of up to 400 mA and maximum power of up to 400 kW. The design and schematic solutions provide the long term and round-the -clock operation of accelerators under the conditions of industrial production processes. The ELV accelerators are especially popular accelerators not only in Russia, but in China, Korea, and etc.

INTRODUCTION

Radiochemical technologies with the use of electron accelerators as ionizing radiation sources were generally developed in the early sixties. By recent, they had strongly consolidated in world industrial production and, thereby, confirmed their efficiency as well as their uniqueness. The technological processes with the use of electron beams for polymer radiation modification, stimulation or initiation of chemical reactions, smoke purification, waste waters treatment, grain disinfection, etc., are widely used in modern industry. A lot of accelerators are installed and operated in different science and research centers and applied-research laboratories. That leads to growth of radiation-modified goods production and development of new matters and technologies, where electron beams are used to obtain new and, sometimes, unique properties.

Budker Institute of Nuclear Physics (BINP) of Siberian Branch of Russian Academy of Sciences is one of the world leaders in the development, design, manufacture and application of electron accelerators of different series (such as DC accelerators of continuous action based on high-voltage rectifier, high-frequency accelerators, pulsed accelerators), the accelerated electron energy and power of which are much more. ELV-series accelerators are some of them. Their compact size and high functional quality allowed BINP to stand as a leading institution at industrial accelerators market as in Russia and abroad.

DESIGN OF ACCELERATOR

ELV high voltage power source is cascade generator with parallel inductive coupling. The rectifier column is installed inside the primary winding. The primary winding is supplied with frequency converter on IGBT transistors. The operation frequency is near 400 Hz. The coil of secondary winding has maximum induced voltage

Figure 1. ELV-8 accelerator.

on its ends 20 kV. This voltage is rectified with the voltage doubling circuit. Thus, the output voltage of the rectifying section is 40 kV. The rectifying sections are connected either in series. The rectifier section column is terminated with the high voltage electrode inside of which there is the injector control unit. The accelerating tube are located inside the column of high voltage rectifier.

All these elements are installed inside of pressure tank filled with SF6. Due to these circumstances ELV-accelerators are the most compact among the devices of this class. Accelerator is equipped with gas system that allow to recovery SF6 during service and maintenance. The vacuum system components and extraction device are fixed to the bottom of the tank. Electrons emitted by the cathode, placed on the upper end of the accelerating tube, have the total energy eU0 on the output of the

ISBN 978-3-95450-125-0

VITA BASED NEUTRON SOURCE - STATUS AND PROSPECTS *

S. Taskaev#, V. Aleynik, B. Bayanov, A. Kuznetsov, A. Makarov, I. Sorokin, M. Tiunov,
BINP SB RAS, Novosibirsk, Russia,
A. Bashkirtsev, I. Schudlo, Novosibirsk State Tehnical University, Russia,
M. Kamkin, D. Kasatov, Novosibirsk State University, Russia

Abstract

At the BINP, a pilot epithermal neutron source is now in use. It is based on a compact Vacuum Insulation Tandem Accelerator (VITA) and uses neutron generation from the reaction ^{7}Li(p,n)^{7}Be. Generation of neutrons was established and *in vitro* experiments were held. Most recent investigations on the facility are related with: i) studying of the dark currents and breakdowns, ii) analyzing and suppressing the high intensity dark currents, iii) measuring the intensity and the spectra of the X-ray radiation, iv) optimization of the H^- beam injection into the accelerator, v) placing and calibrating the new charge-exchange target. The results of these studies are discussed in the present work. Investigations resulted in increasing of mean current of the proton beam in stable mode (from 0.1 – 0.7 to 1.5 – 2 mA). In the nearest future new experiments are planned, including *in vitro* tests, blistering investigation, spectrum and flux measuring for neutrons and gamma, calculating the dose absorbed by phantom. Different ways of providing additional stability to the accelerator, of increasing the current of the proton beam are discussed in this work, as well as the ways of creating the therapeutic beam and strategies of applying the facility for clinical use.

INTRODUCION

Presently, Boron Neutron Capture Therapy (BNCT) [1] is considered to be a promising method for the selective treatment of malignant tumours. The results of clinical trials, which were carried out using nuclear reactors as neutron sources, showed the possibility of treating brain glioblastoma and metastasizing melanoma incurable by other methods [2, 3]. The broad implementation of the BNCT in clinics requires compact inexpensive sources of epithermal neutrons. At the BINP the source of epithermal neutrons based on 2 MeV Vacuum Insulation Tandem Accelerator (VITA) and neutron generation through ^{7}Li(p,n)^{7}Be reaction was proposed [4] and realized. Although the accelerator is designed to obtain a 5 mA proton beam, but in the experiments carried out in 2008-10 we usually got the proton beam currents of hundreds of microamperes, and occasionally for a short time – a few milliamps. Such a current was enough to demonstrate the generation of neutrons [5] and monochromatic gamma-rays [6], to carry out initial *in vitro* investigations [7], but it is clearly not sufficient for the thorough BNCT research and other applications. This paper presents the results of experiments carried out after the IPAC-2011 [8], aimed at increasing the current of the proton beam and improving the stability of the accelerator. We also discuss plans of works and strategies of applying the facility for clinical use.

VITA

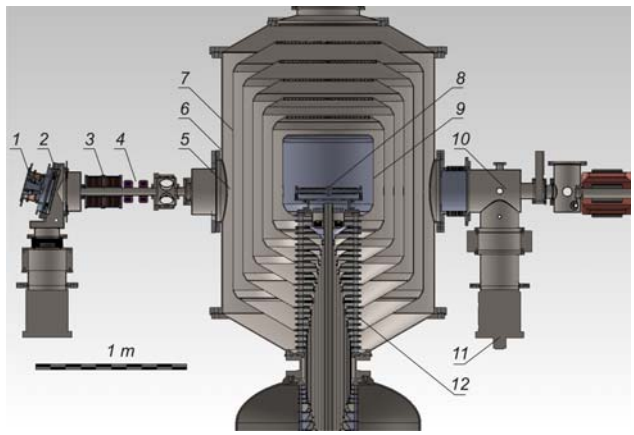

Figure 1: High-current vacuum insulation tandem accelerator. 1 – H^- ion source, 2 – diaphragm, 3 – magnetic lenses, 4 – corrector, 5 – a temporary location of the beam detector, 6 – accelerator, 7 – electrodes, 8 – high voltage electrode, 9 – stripper, 10 – high energy beam transport, 11 – turbo molecular pumps, 12 – insulator.

General view of the accelerator is shown in Fig. 1. Negative hydrogen ions are injected and accelerated up to 1 MeV by potential applied to the electrodes, then H^- turn into protons in the stripping target and at last the protons are accelerated up to 2 MeV by the same potential. Pumping of the gaseous stripping target is carried out by cryogenic and turbomolecular pumps through the jalousies. The potential of the high-voltage and five intermediate electrodes is supplied by a high-voltage source through the insulator which has a resistive divider.

DARK CURRENTS

The accelerator has a high electric field in the electrode gap – about 25 kV/cm, and a large total area of the electrodes – tens of square meters. In such a system in the electrode gap dark currents of different nature must inevitably occur, which may have a significant impact on the potential distribution along the accelerating channel.

When training the accelerator, at the time of voltage increasing, a dark current is recorded. It is associated with the appearance of micro-discharges, accompanied by

*Work is supported by Ministry of Education and Science of RF
taskaev@inp.nsk.su

ISBN 978-3-95450-125-0

APPLICATION OF SMALL-SIZED VACUUM ACCELERATING TUBES FOR NEUTRON CONTROL OF INCREASING DEBIT OF OIL WELLS BY ACOUSTIC INFLUENCE OF THE FORMATION*

A. E. Shikanov, B.Yu. Bogdanovich, A.V Ilyinsky, D. R. Khasaya#, A. Nesterovich, D.D. Ponomarev, E. Shikanov, MEPhI, Moscow, Russia

Abstract

The report presents experimental studies results of the possibility using the technique of neutron "labeled" reagent (NaCl) for monitoring of the acoustic effect (AE) results in the oil reservoir to increase oil production debits. These obtained data allow us to estimate the effectiveness of acoustic influence the method on managed oil reservoirs in conjunction with the equipment which pulsed neutron-neutron ray logging based on vacuum accelerator tubes that implements the method of neutron "labeled" reagent. The proposed instrumental set ensures reliable process control stimulation of oil from the reservoir and the allocation of layers to abnormal filtration and capacitive properties and their subsequent development.

MANUSCRIPT

One of the most effective methods of cleaning fluid productive zone recovery in oil well is AE at her longitudinal ultrasonic pressure wave. In the pores of the reservoir fluid-filled productive, there are transient oscillatory micro streams. With sufficient intensity ultrasonic wave cleaning these areas contribute microstreams productive fluid extraction from the above contaminants. [1]

The effectiveness of the AE direction in oil reservoirs can be improved by controlling the parameters of the processes occurring before and after AE in oil reservoirs and selecting intervals stimulation oil. Measurements of changes in the formation of these processes are made remotely through a metal pipe casing, which requires the use of transparent methods of control.

The most effective is the pulsed neutron-reagent method. It allows the monitoring of changes in the formations chlorine containing fluid during its displacement pumped reagent containing solution. The specified control is pulsed neutron method based on the measurement of the lifetime of thermal neutrons in the formation, depending on the composition of the substance contained in the pores. This structure defines the process of formation in the reservoir and the well resulting deceleration,thermalization and diffusion of the field of thermal neutrons, falling in time exponentially.

The time variation of the decrement recession thermal neutron density characterizes the content of chlorine in the reservoir due to its abnormally high radiative capture cross section. This solves the problem of determining water contact due to shortage of chlorine in the oil-rich part of the formation and the presence of excess reagent in a solution in water due to its mineralization. Lack of formation water or hydrocarbons in the reservoir also affects the damping rate of the neutron density decline, which is proportional to the total cross section of neutron absorption.

In implementing the method of pulsed neutron-neutron logging (PNNL) with the reagent before and after AE in the reservoir in the study area creates a pulsed periodic field of fast neutrons emitted by the accelerating tube (AT), the result of passing on its target nuclear reaction T(d, n) ^{4}He. After slowing down neutrons to thermal velocities begins the process of decay of the neutron density. In this case, the decline of the spatial density of neutrons occurs exponentially with a decrement proportional to the total neutron absorption cross-section [2]. Measuring the density of a neutron decay detector is filled with 3He, which proceeds in the amount of nuclear reaction ^{3}He (n, p) T, followed by analysis of the time spectrum known methods used in experimental nuclear physics. [3]

The measurements were carried out using hardware methods complex AIOC-43 (development VNIIA named by N.L.Duhov) [4] on the basis of compact pulsed neutron generator [5] and multi-channel time analyzer [3].

Upon command from the ground control unit through the correctional system is launched neutron emitter in a repetitively pulsed mode. As a result of the interaction of fast neutrons generated in the target vacuum accelerating tube, in the study of the geophysical environment shapes the field of thermal neutrons.

The detection system converts this field into analog electrical signals that are in well telemetry system are converted into digital information that is sent in geophysical well logging cable telemetry unit to the ground. In this unit, this information is decoded and formatted as a series of files, coming to a computer. The computer is processing the information on the two-component processing algorithms logging signal [3,6]. The result depends decrement Depreciation thermal neutron density λ of the depth of the test bed.

If the acoustic impact inflow of hydrocarbon fluid, it will be recorded a significant decrease in the decrement recession thermal neutron density, since this reduces the concentration of nuclides detected. In the case of failure of the process of acoustic impact or fill water reservoir effect of changing the decrement will be less significant.

Equipment complex consists of ground control unit (geophysical station), which controls the change of geophysical instruments (instrument pulsed neutron

*Work supported by Shikanov A.E. and Khasaya D.R.

#damir_hasaya@rambler.ru

ISBN 978-3-95450-125-0

PROJECT OF THE RADIOISOTOPE FACILITY RIC-80 (RADIOACTIVE ISOTOPES AT CYCLOTRON C-80) IN PNPI

V.N. Panteleev, A.E. Barzakh, L.Kh. Batist, D.V. Fedorov, A.M. Filatova, V.S. Ivanov, K.A. Mezilev, F.V. Moroz, P.L. Molkanov, S.Yu. Orlov, Yu. M. Volkov, PNPI, NRC Kurchatov Institute, Gatchina, 188300, Russia
E.K. Dyakov, I.B. Savvatimova, RISPA "LUCH", Podolsk, 142100, Russia

INTRODUCTION

It is well known that the main sources for production of the radioactive nuclides are thermal neutrons reactors and accelerators of charged particles. Since in the last years new reactors were not constructed (in Russia the only reactor which construction has been finished in 2011 was the PIK reactor at PNPI in Gatchina) on the front place go the accelerators of the charged particles - cyclotrons, as the most safe and reliable technological installations. The list of cyclotron radio nuclides is much longer and more varied, than ones got on reactors. Cyclotron radio nuclides can be used both for diagnostics and for therapy. As to cyclotrons used in Russia for radioisotope production, mostly they have the energy of bombarding particles lower than 30 MeV, therefore the variety of nuclides produced with these installations is limited. The cyclotron of NRC "Kurchatov institute" is at present time the only working cyclotron with the energy of external proton beams of 30 MeV. As a result only there the isotope ^{123}I can be produced with the high radionuclide purity from a xenon target.

At INR of RAS (Troitsk) the powerful linear accelerator is in operation - Moscow meson factory. At 160 MeV proton beam branch the laboratory, which has the installation for irradiations of targets was created for production of medical radio nuclides [1]. This installation is one of the largest in the world in respect of beam energy accumulated in production of radio nuclides and providing a possibility to produce practically the whole list of accelerator radio nuclides. The essential disadvantage of this method is that the usage of the accelerators of such kind is very expensive and the production cost of medical radio nuclides by that method is considerably higher than by means of cyclotron with the proton energy up to 80 MeV.

SCHEME OF THE DESIGNED INSTALLATION RIC-80 (RADIOACTIVE ISOTOPES ON CYCLOTRON C-80)

In PNPI NRC KI (Gatchina) the project of the radioisotope facility RIC-80 (Radioactive Isotopes at cyclotron C-80) is being developed [2]. In fig. 1 the layout of RIC-80 installation is presented. The proton beam energy at the target will be of 40-80 MeV and the intensity up to 200 μA. This cyclotron is intended for production of a wide spectrum of medical radio nuclides for diagnostics and therapy and also for a treatment of ophthalmologic diseases by irradiations of a malignant eye formation. The cyclotron is located in the right side of experimental hall (ground floor) of the PNPI synchrocyclotron.

The outgoing proton beam is directed down to the underground floor and traced in the horizontal direction. After that the beam can be directed to one of target stations: a) the isotope mass-separator target by the 37 degrees clockwise deflection from "zero" beam direction; b) the target station by "zero" deflection and c) the target station by the 34 degrees counterclockwise deflection. The mass-separator with its target as the first target station will allow getting the separated isotopes of a high purity, which are implanted into a corresponding collector from which they can be easily extracted. Target stations will be equipped with special devices to download highly radioactive targets into protection containers to transport them safely to special storage places or to hot cells for the after-treatment and production of corresponding pharmaceutics.

ESTIMATED YIELDS OF RADIO NUCLIDES EXPECTED TO BE PRODUCED AT RIC-80 FACILITY

RIC-80 facility is unique being the largest in Russia cyclotron facility in respect of beam energy accumulated in production of radio nuclides and providing enough high energy of bombarding particles (proton energy of 80 MeV). It gives an opportunity to produce sources of a high activity within practically the whole list of radio nuclides produced at accelerators. In table 1 calculated activities of radio nuclides are shown, which are planned to be obtained at RIC-80 facility.

It is necessary to emphasize that the activities of radioisotopes are shown for production in the target. The actual activities extracted out of target material can be less because of incomplete extraction of produced radioisotopes.

ISBN 978-3-95450-125-0

TRANSFORMATION OF BEAMS IN THE PLASMA LENS AND INVESTIGATION OF Z-PINCH DYNAMICS*

A.Drozdowskiy, N.Alexeev, S.Drozdowskiy, A.Golubev,
Yu.Novozhilov, P.Sasorov, S.Savin, V.Yanenko. ITEP, Moscow, Russia

Abstract

The plasma lens can carry out sharp focusing of ion beam with considerable reduction sizes of focal spot. At those stages of the plasma discharge at which the magnetic field is nonlinear, formation of other interesting configurations of beams is possible. The report presents the results of studies transformation the Gaussian beam into hollow one and into beam with homogeneous spatial distribution. The discharge current distributions obtained by numerical calculation ensure the experimental beam transformations. Thus possibility of the research of the plasma discharge dynamics by means of relativistic ions beams is shown. The plasma lens represents the universal device for scientific and technical applications in particular for irradiation of medical objects.

INTRODUCTION

The ion beam focusing in the plasma lens is carried out as shown in Fig.1. The discharge current produces an azimuthal magnetic field. The ions are injected along the lens axis, and the radial Lorentz force focuses the ion beam [1].

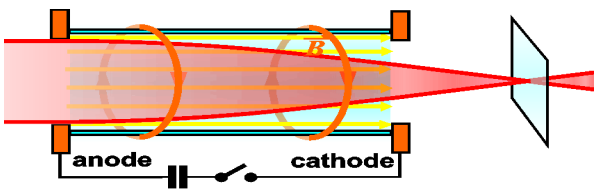

Figure 1: Ion focusing in a plasma lens.

The focusing properties of plasma lenses depend on the current density distribution along the radius of the plasma discharge. The current distribution across the tube changes significantly during the discharge. Therefore, plasma lens, in general, is nonlinear. Uniform current distribution exists for a limited time, so the plasma lens, as a device for sharp focusing, operates for about 1 μs or less. As a non-linear focusing device, the plasma lens can be used to produce beams of special shape.

The studies of possibility of use of a plasma lens were carried out at ITEP both for sharp focusing, and for formation of tubular beams and beams with homogeneous distribution of density [3,4]. Researches were carried out of ion beams of carbon and iron with energy 200-300 Mev/a.e.m.. Duration of an impulse of a current of the plasma was 5 and 20 μs, and the duration of an impulse of a current of an ion beam – 0.3 μs . Sizes of a discharge tube: length – 10 cm, diameter – 2 cm. Pressure of gas (argon) before a discharge impulse was of 0.5-10 mbar.

Z-PINCHS DYNAMIC RESEARCH

Research of that implosion of plasma and mechanisms of penetration into it a magnetic field - is a fundamental scientific problem. The understanding of the mechanisms defining distribution of a current in plasma is absolutely necessary for thermonuclear synthesis, lasers in the field of XUV and a soft X-ray, transportation of powerful laser beams, focusing of powerful beams of ions, etc.

Active corpuscular diagnostics, based on application of special beams of fast atoms and ions, have considerable development. The main problems of use of that technique - limited transparency of plasma for beams. Therefore the beams of relativistic energy is necessary for plasma researches. The systematic researches z-pinchs by means of relativistic ion beams weren't carried out yet. Meanwhile in a plasma lens Z-pinches creation in a wide interval of parameters is possible: with a current to 0.5 MA at duration of impulses of 1-30 microsec.

We developed a numerical technique of receiving distribution of currents and self magnetic fields in the plasma lens, adequate to the configurations of an ion beams received experimentally. Some results of this work are presented in [4].

The results of experimental researches of influence of a plasma lens on a beam of ions with gauss distribution of density at various stages of development of the plasma discharge are shown on fig. 2. The each column of the figure corresponds to a certain moment of time after the beginning of the plasma discharge: 0.5, 1.7 and 8.5 μs. On the first line of the figure the distributions of ion beam density are shown. On the second line of the figure the experimental distributions self magnetic field in lens z-pinch are shown. On the third line of the figure the modeling distributions self magnetic field in lens z-pinch are shown.

* Work supported by the *Russian Federal Ministry of Education and Science*, and by the Russian Foundation for Basic Research

ISBN 978-3-95450-125-0

EXCITATION OF THE FOCUSING WAKEFIELDS BY A RELATIVISTIC BUNCH IN ISOTROPIC CAPILLARY DISCHARGE PLASMA*

R.R. Kniaziev#, KhNU them. V.N. Karazin, Kharkov, Ukraine
G.V. Sotnikov, NSC Kharkov Institute of Physics and Technology, Kharkov, Ukraine

Abstract

The present paper offers research of wake waves by the relativistic electron bunch in the capillary tube filled with plasma. Analytical expressions for the electromagnetic field component with approaching "hard" bunches have been obtained. Numerical calculations of the appearing fields for capillary tubes samples have been made. The transversal and axial structure of wake fields in the slowing structure with plasma in the transport channel has been researched in detail. The regimes in which focusing of the accelerated bunch is clearly seen have been studied. The results of numeric PIC modeling of fields in the structure under consideration have been provided.

INTRODUCTION

One of the promising ways of accelerating by wake fields excited by relativistic electron bunches uses plasma, created by the same bunches [2] or by external sources, as the slowing medium [1]. The capillary discharge can be used as an external source [3, 4]. The capillary tube is the slowing structure, therefore eigen waves of dielectric structure, modified by the presence of plasma in the transport channel, as well as plasma waves are excited in the tube channel when electron bunches are travelling in it. Below we research the influence of electrodynamic properties of the capillary tubes material on wake waves excitation.

NUMERICAL CALCULATIONS

For the cylinder all-over bunch having the radius r_b and the length L_b, and with homogeneously distributed density of particles:

$$n(r_0, t_0) = \frac{Q/e}{\pi L_b r_b^2}\left[\Theta(t_0) - \Theta(t_0 - L_b/v_0)\right]\Theta(r_b - r) \ , \quad (1)$$

where Q is bunch charge, -e is electron charge.

Final expressions for the wake field components were presented in the paper [5]. Here are the results of the wake field calculations. For our calculations we choose the dielectric waveguide with dimensions presented in the Table 1, with the dielectric tube made of fused silica. In the same table electron bunch parameters are given. Plasma parameters are given in Table 2. The results of calculations for plasma with such parameters are shown in Figures 1-2.

Table 1: Dielectric structure (Fused silica).

Parameter	Value
Outer radius of dielectric tube	0.6 mm
Inner radius of dielectric tube	0.5 mm
Relative dielectric constant, ε	3.75
Bunch energy	5 GeV
Bunch charge	3 nC
Bunch length L_b (box charge distribution)	0.2 mm
Bunch radius r_b (box charge distribution)	0.45 mm
Density of drive bunch electrons, n_b	$1.47\cdot10^{14}$ cm^{-3}
Vacuum wavelength of 1st radial mode of the vacuum DWA	~1 mm
Vacuum wavelength of 2nd radial mode	~0.3 mm
Vacuum wavelength of 3rd radial mode	~0.16 mm

Table 2: Parameters of the plasma

Plasma density	$4.41\cdot10^{14}$ cm^{-3}
Plasma wavelength	1.59 mm
Radius of plasma	0.5 mm

Fig.1 shows axial distribution of the axial force, acting on the probing particle. It follows from the dependence, given in Fig. 1, that we can ensure acceleration of charged particles with their simultaneous radial focusing by placing the testing bunch at some distance from the drive bunch head. As it can be seen in the Figure, the radial force almost harmoniously depends on the axial coordinate with the period of approximately 0.16 cm, i.e. the Langmuir wave makes the greatest contribution into the radial force. At the same time, its contribution into the axial force, accelerating test particles, is predominantly small. The axial force is predominantly determined by the eigen modes of the dielectric waveguide; its complex behavior from the axial coordinate is caused by excitation several radial modes of the dielectric waveguide. For the used in analytical calculations parameters of the dielectric waveguide, bunch and plasma, the focusing force amplitude is approx. 300MeV/m, which equals the focusing magnetic field induction ~1T.

* The research is supported in part by STCU, project №. P522.
# RKniaziev@gmail.com

ISBN 978-3-95450-125-0

NONLINEAR THEORY OF EXCITATION OF AN AXIALLY ASYMMETRIC WAKEFIELD IN DIELECTRIC RESONATOR*

K. V. Galaydych#, G. V. Sotnikov
Kharkov Institute of Physics and Technology, Kharkov, Ukraine
I. L. Sheynman, LETI (ETU), Saint-Petersburg, Russia

Abstract

A nonlinear self-consistent theory of excitation of an axially asymmetric wakefield by relativistic electron bunches in cylindrical dielectric resonator with a vacuum channel for the charged particles transportation through the resonator is constructed. The formulated nonlinear theory allows investigating numerically the nonlinear effects such as increasing of the transverse bunch size, and head-tail beam breakup instability, which occurs if an electron bunch in the structure is misaligned.

INTRODUCTION

The dielectric wakefield accelerator is one of the modern trends of acceleration schemes, which can provide high-accelerating gradient for future colliders. But besides for high output energy of an accelerated bunches high demands are made on their quality, the same, for example, as low emittance. No loss of current under acceleration of the bunch are also desirable. This information about the bunch can not be obtained using assumption of the absence of reverse influence the excited field on the dynamics of electron bunches. In this paper we present nonlinear self-consistent theory of wakefield excitation in a dielectric–lined resonator by an electron bunches. The previous theoretical investigations on wakefield excitation in dielectric–lined structures, have been done for longitudinally unbounded structures [1]–[4]. In cited papers was noted, that it is necessary to taking into account the contribution of higher multipole modes to the total transverse field. A presented complete bunch–excited electromagnetic field includes all azimuthal modes, which allows calculating transverse wakefield in order to investigate bunch deflection problems.

STATEMENT OF THE PROBLEM

Consider cylindrical metallic resonator with inner radius b, partially filled with isotropic material with dielectric constant ε, containing on-axis vacuum channel of radius a which allows charged particles to pass through. We suppose that the end walls of the resonator are closed by metal grids transparent for charged particles and nontransparent for an excited electromagnetic field. Consider an electron bunch, injected into the resonator and moving along a line parallel to the axis of the resonator.

The electron bunches will be described in terms of macroparticles, therefore the charge density ρ and the current density $\mathbf{j}$ will be written as:

$$\rho = \sum_{p\in V_R} q_p \delta\left(\mathbf{r}-\mathbf{r}_p(t)\right),\ \mathbf{j} = \sum_{p\in V_R} q_p \mathbf{v}_p(t)\delta\left(\mathbf{r}-\mathbf{r}_p(t)\right), \qquad (1)$$

where q_p is the charge of the macroparticle, $\mathbf{r}_p$ and $\mathbf{v}_p$ are its time-dependent coordinates and velocity, respectively. The summation in Eq. (1) is carried out over the particles being in the resonator volume V_R.

FIELD SOLUTION

We introduce the solenoidal $\mathbf{E}^t$ $\mathbf{H}^t$ and the potential $\mathbf{E}^l = -\nabla\Phi$ fields defined as

$$\mathrm{div}(\varepsilon\mathbf{E}^t) = 0,\ \mathrm{div}(\mu\mathbf{H}^t) = 0,\ rot\mathbf{E}^l = 0, \qquad (2)$$

which are given by Maxwell's and Poisson equations:

$$rot\mathbf{E}^t = -\frac{\mu}{c}\frac{\partial\mathbf{H}^t}{\partial t},\ rot\mathbf{H}^t = \frac{\varepsilon}{c}\frac{\partial\mathbf{E}^t}{\partial t} + \frac{4\pi}{c}\mathbf{j}, \qquad (3)$$

$$\Delta(\varepsilon\Phi) = -4\pi\rho \qquad (4)$$

The solenoidal $\mathbf{E}^t$ and potential $\mathbf{E}^l$ electric fields are mutually orthogonal [5] and satisfy the boundary conditions, making their tangential components vanish on the metal walls of the resonator.

First we solve the equation (4) for the potential in the vacuum channel and dielectric. In cylindrical coordinate Eq.(4) rewrites as:

$$\frac{1}{\varepsilon r}\frac{\partial}{\partial r}\left(r\varepsilon\frac{\partial\Phi}{\partial r}\right) + \frac{1}{r^2}\frac{\partial^2\Phi}{\partial\varphi^2} + \frac{\partial^2\Phi}{\partial z^2} = -\frac{4\pi}{\varepsilon}\rho \qquad (5)$$

Eq.(5) should be complemented by boundary conditions consisting in that the potential Φ on the resonator metal walls becomes zero

$$\Phi(z=0) = \Phi(z=L) = \Phi(r=b) = 0, \qquad (6)$$

*The research is supported in part by STCU, project №. P522.
#kgalaydych@gmail.com

ISBN 978-3-95450-125-0

A COAXIAL TWO-CHANNEL DIELECTRIC WAKEFIELD STRUCTURE FOR TWO-BEAM ACCELERATION EXPERIMENTS AT SLAC*

G.V.Sotnikov[1,2#], T.C. Marshall[3,2], J.L. Hirshfield[2,4], , S.V. Shchelkunov[4]

[1]NSC Kharkov Institute of Physics and Technology, Kharkov, Ukraine
[2]Omega-P, Inc., New Haven Connecticut, USA
[3]Columbia University, New York City, USA
[4]Yale University, New Haven, Connecticut, USA

Abstract

Results of analytical and numerical investigations of a coaxial dielectric wakefield accelerator structure (CDWA) for experiments at FACET (SLAC) on two-beam acceleration are presented. For these experiments it is proposed to use ~1THz structure with two nested silica cylindrical shells having these diameters: outer shell, OD = 2mm, ID = 1mm; inner shell OD = 360μm, ID = 100μm. A conventional CDWA structure is energized by an annular drive bunch travelling in the annular vacuum channel. Our analytical studies prove clearly that an annular drive bunch can be substituted by a solid bunch having the same charge. For the simulation we used the SLAC drive bunch parameters: energy is 23 GeV, charge is 3nC, axial RMS size is 20μm, transverse RMS size is 10 μm. This bunch sets up at the central channel axis an accelerating gradient of ~1 GeV/m.

INTRODUCTION

The use of wakefields produced by a relativistic "drive bunch" charge moving inside a dielectric-lined channel to accelerate a following "witness" bunch has promise for making a linear Collider with gradient ~ 1-3GeV/m [1,2], and has received modest attention for the past 25 years [3-5]. More recently, there is experimental evidence [6], consistent with theoretical expectation [7], that certain dielectric materials can withstand the brief (nsec) pulses of high intensity radiation associated with passage of a drive bunch through the dielectric structure. Drive bunches having relativistic energy and charge of several nC can produce a train of THz wakefields having intensity > 1GeV/m in a hollow coaxial dielectric structure of mm-scale transverse dimension [8]. This, together with the use of a smooth-bore structure (DWA) that can accelerate positrons or electrons, has recommended the concept for further study as an "advanced" linear Collider accelerator module. The simplest structure, a hollow cylindrical dielectric tube with an outer metallic surface, in which the drive and witness bunches travel the same path, is unfortunately afflicted with stability problems, and its transformer ratio (**TR**) is no larger than 2. In order to avoid these problems, other structures, such as a wide rectangular channel lined with dielectrics [9] that is excited by a sheet beam, or a coaxial two-channel structure that is excited by an annular bunch, have been proposed and studied [8,10,11] computationally and analytically.

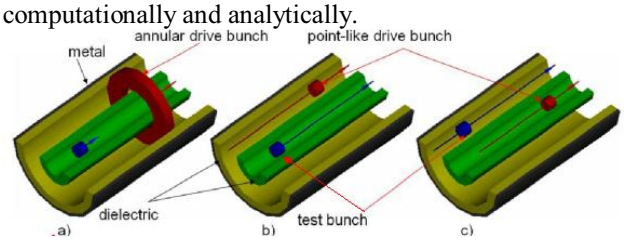

Figure 1: The CDWA structure excited in three different ways by a drive bunch (red), to accelerate a witness bunch.

We have planned at FACET (SLAC) proof-of-principle experiments E-207 to test a mm-scale THz CDWA. Because SLAC cannot provide at present a drive bunch of annular shape we propose to substitute such a bunch by a solid bunch having the same charge. In what follows, we shall show that a solid drive bunch will establish the same wake fields we wish to study. Furthermore, we shall show how we may obtain information from this study whereby the data can be compared with theoretical simulations obtained with the CST STUDIO code. This is possible because of the reciprocity principle [12].

We will consider three regimes of operation of the CDWA (see Fig.1): a) conventional CDWA; b) the CDWA with a point-like drive bunch that moves in the annular channel while the witness bunch accelerates along the central channel axis, c) "inverse" CDWA when the structure excited by a solid drive bunch that moves along the central channel axis while the witness bunch samples its wakefield as it moves along the annular channel. Certain of these field components are simply related, as we shall establish in the next section. This allows us to study regimes b) and c) at FACET, and relate the measurements made there to the desired operation with an annular drive bunch, conventional regime a).

CDWA UNIT FOR E-207 EXPERIMENTS

Parameters of CDWA structure under investigation are listed in Table 1. The CDWA structure with similar parameters will be tested at SLAC.

Table 1: Parameters used for THz CDWA

Frequency of dominant mode (E_{04})	473 GHz
External diameter of outer coaxial cylinder	2.0 μm
Inner diameter of outer coaxial cylinder	1.0 μm
External diameter of inner coaxial cylinder	0.36 mm

* Supported by the US Department of Energy, Office of High Energy Physics, Advanced Accelerator R & D.
#sotnikov@kipt.kharkov.ua

ISBN 978-3-95450-125-0

ENERGY SPREAD DECREASING IN LINEAR MODE OPERATING LASER PLASMA WAKEFIELD ACCELERATOR

S.M. Polozov
National Research Nuclear University - Moscow Engineering Physics Institute, Moscow, Russia

Abstract

Laser plasma wakefield acceleration (LPWA) [1] is one of most popular novel methods of acceleration. The LPWA is very perceptively because the accelerating gradient in plasma channel can be a number of orders larger than in metal structures. But the LPWA has two serous disadvantages as very high energy spread and low part of electrons trapped into acceleration. The energy spectrum better than 10 % does not observed anyone in simulations or experiments. Bunching before injection into plasma channel will discuss to decrease the energy spread and to enlarge the electron trapping efficiency.

INTRODUCTION

A number of ideas for increasing the rate of the energy gain have been discussed in the last few decades. Among others, the acceleration of electrons in a modulated plasma channel was proposed by Ya.B. Feinberg in the 1950's [2]. Possible schemes for the plasma wakefield acceleration (PWA) differing in ways of modulating the plasma channel were developed later. The first one uses a high energy (tens of GeV) beam of particles to form a plasma wave and accelerate a fraction of the injected particles or a probe beam [3]. Another method is the laser plasma wakefield acceleration (LPWA) [1], in which a laser pulse is used to create a plasma wave. The modulation period of the accelerating field (the wakefield) is $L_w=\lambda_w/2=\pi c/\omega_p$, were c is the speed of light in vacuum, $\omega_p=(4\pi e n_0/m)^{1/2}$ is the plasma frequency, e end m are the elementary charge and mass, and n_0 is the electron density in plasma. Using two lasers with close frequencies ($\Delta\omega \sim \omega_p$) was also suggested for enhancing the accelerating gradient even further. The advantage of the PWA technique vs. conventional accelerators is obvious: the accelerating gradient in a plasma channel can reach hundreds of GeV/m and hence the accelerator can be very compact. This statement does not at present include high power lasers with powers up to 10^{22} W/cm^2, which are necessary for LPWA, although significant progress is happening in this area with the introduction of fiber lasers. The idea is very popular at present and a number of international collaborations are working on analytical and experimental demonstration of PWA. Large scale projects based on PWA are being discussed now. These include electron-positron colliders, X-FELs and medical facilities. However, the step from a novel acceleration technique to routinely operating facilities has not been made yet. LPWA has two serious disadvantages: a very high energy spread of the accelerated electrons and only a small fraction of electrons is captured into the process of acceleration. An energy spectrum better than 10 % has not yet been demonstrated either in simulations or experimentally. A beam with such a wide energy spread can not be used for the majority of applications including medical and particle physics as the beam can not be transported efficiently.

BEAM DYNAMICS IN LPWA

Considering LPWA, two regimes are distinguished: the underdense plasma, in which $\pi^2 r_l^2/\lambda_p >> a_0^2/2\gamma_l$, (quasi linear regime) and the non-linear regime with $\pi^2 r_l^2/\lambda_p << a_0^2/2\gamma_l$. Here r_l is the laser spot size, $a_0=eA/W_0$ normalized laser intensity, $\gamma_l=(1+a_0^2/2)^{1/2}$. The electron beam dynamics is different in the two regimes. Both regimes, however, experience the high energy spread and low capturing. Conventional accelerators experienced similar problems in the past, where they were solved by bunching the beams using klystron or waveguide type bunchers, and later by producing short bunches with photocathodes. Making a bunch shorter than the accelerating field modulation period L_w in a plasma channel does not seem to be viable. However, pre-modulation (bunching) of the electron beam can still be used as discussed below.

A few methods for improving the energy spread in the non-linear regime have been proposed. The first is to use two plasma stages with constant but not equal plasma densities and a transient stage with exponentially varying plasma density between them for the beam modulation [4, 5]. The second is so-called ponderomotive injection using two synchronized laser pulses [6]. Two lasers can also excite a beat wave in the plasma, which is then used for bunching in the third method [7]. These methods improve the energy spread to about 3 % for a 1 GeV beam. Still, this number is too high for many applications. The electron capturing efficiency also remains problematic. All the methods described above apply to the non-linear regime. However, the linear LPWA mode is also interesting for practical use. The rate of the energy gain can still be very high, while the laser power requirements are comparatively moderate, meaning that compact, laboratory scale facilities could be designed for accelerating electron beams to hundreds of MeV. Studies of the linear LPWA regime have been conducted at LBNL and INFN LNF and showed that electrons can be accelerated to 1 GeV with an energy spread of 6-10 %. Below two possible bunching schemes can be proposed to decrease the energy spread and improving the number of electrons captured by the plasma wave in the linear LPWA mode.

ISBN 978-3-95450-125-0

LASER-WAKEFIELD ACCELERATION WITH EXTERNAL BUNCH INJECTION AT REGAE*

J. Grebenyuk† and K. Floettmann, DESY, Hamburg, Germany
T. Mehrling and J. Osterhoff, University of Hamburg, Germany

Abstract

We present particle-in-cell simulations with the code OSIRIS [1] for future laser-plasma wakefield experiments with external bunch injection at the REGAE accelerator at DESY. The topics of particular interest are: emittance evolution of electron bunches and longitudinal bunch compression inside the wakefield. Results show significant transverse emittance growth during the injection process, if the electron bunch is not matched to its intrinsic betatron motion inside the wakefield. In addition, when externally injected at the zero-field crossing of the laser-driven wake, the electron bunch may undergo significant compression in longitudinal direction and simultaneously be accelerated due to the gradient in the accelerating field. This mechanism would allow for production of high-energy, ultra-short (on the order of one femtosecond) bunches at REGAE.

EXTERNAL BUNCH INJECTION AT REGAE

Laser-plasma acceleration (LPA) is a technology which exploits large electric wakefields created by high-intensity laser pulses in plasma. Such wakes support field gradients which are many orders of magnitude larger than in conventional accelerators and can be used to accelerate particle bunches over short distances. Experiments demonstrated GeV energy gain in centimeter distances [2, 3]. Nevertheless, the energy increase in a single LPA module is limited by energy depletion of the laser pulse. Further energy gain is thus possible by placing LPA modules one after another, i.e. by staging [4], or by using a stronger laser for wakefield generation. LPA might potentially develop into a technology to be used for driving compact and brilliant X-ray sources, and possibly particle colliders. Thus achieving a beam quality sufficient for these demanding applications is of crucial importance.

The injection process of electrons into a plasma wake in the wave-breaking regime is sensitive to fluctuations in laser and plasma parameters, and difficult to manipulate. Our aim is to inject externally accelerated and phase-space tailored beams from a conventional accelerator into a laser-driven wake for full control over the electron-trapping process. These experiments will open numerous opportunities for probing wakefields and exploring fundamental properties of laser-plasma interaction and electron acceleration. Moreover, external injection experiments are of crucial importance for exploring the concept of staging. The aim of external injection is to place electron bunches with a length much shorter than the plasma wavelength, λ_p, and a transverse extent much smaller than the laser spot size in the phase-region of the wake which is both focusing and accelerating.

The Relativistic Electron Gun for Atomic Exploration (REGAE) is a linear accelerator at DESY which produces 2 to 5 MeV velocity-grouped electron bunches of 10-15 fs RMS length, ∼1 pC charge, 3-5 μm RMS width, and 0.3 mm mrad emittance. Originally designed for femtosecond electron diffraction experiments, the REGAE injector will be used together with a high-intensity laser and a plasma target for LPA external injection experiments.

EMITTANCE EVOLUTION

External controlled injection is a direct way to study bunch emittance evolution in LPA. Minimising emittance growth during the acceleration process is crucial for most applications. Emittance growth in LPA was earlier investigated in [5, 6, 7]. The transverse trace-space emittance, $\epsilon = \sqrt{\langle x^2\rangle \langle x'^2\rangle - \langle xx'\rangle^2}$ [8], is a figure of merit for the transverse beam quality, where x is the transverse particle position, $x' = p_x/p_z$ is the ratio of transverse and longitudinal particle momenta and $\langle Y^k\rangle = \sum_i^N (Y_i - \overline{Y})^k/N$ the k-th central moment of a discrete variable Y. We consider an electron bunch with transverse properties defined by the emittance ϵ and the Courant-Snyder parameters (CSP)[9] :

$$\beta = \frac{\langle x^2\rangle}{\epsilon}, \qquad \gamma = \frac{\langle x'^2\rangle}{\epsilon}, \qquad \alpha = -\frac{\langle xx'\rangle}{\epsilon}. \quad (1)$$

Combining emittance definition and (1) yields the relation between these parameters, $\beta\gamma = 1 + \alpha^2$.

While being accelerated, the individual particles perform transverse betatron oscillations with a betatron frequency ω_β. Due to the particle oscillations, the ellipse with area $\pi\epsilon$, defined by the CSP (1), $\gamma x^2 + 2\alpha xx' + \beta x'^2 = \epsilon$, rotates according to the single particle trajectories in trace space. Since the transverse field and ω_β are ξ-dependent ($\xi = z - ct$ is a co-moving variable, where z is the longitudinal coordinate, c is the speed of light and t is time), the individual longitudinal slices of the bunch oscillate at different frequencies which leads to a betatron-oscillation phase mixing during the acceleration process, as illustrated in Fig. 1. Slice ellipses develop a tilt with respect to each other which increases the projected area and hence causes emittance growth. Emittance growth due to this mechanism can be suppressed by matching the transverse properties of the electron beam to the intrinsic electron betatron motion in the plasma wake [10, 5]. Expressing the matching con-

* Work supported by the Helmholtz Alliance "Physics at the Terascale" and a grant of computing time by the Juelich Supercomputing Centre on JUGENE under project id HHH09.
† julia.grebenyuk@desy.de

ISBN 978-3-95450-125-0

WAKEFIELD PRODUCED BY A SMALL BUNCH MOVING IN COLD MAGNETIZED PLASMA ALONG THE EXTERNAL MAGNETIC FIELD*

S.N. Galyamin#, D.Ya. Kapshtan, A.V. Tyukhtin,
Saint Petersburg State University, Saint Peterburg, Russia

Abstract

Plasma wakefield acceleration (PWFA) is a promising tool for acceleration of charged particles to high energies at relatively small lengths. Knowledge about the structure of the electromagnetic field produced by the driver bunch in plasma plays the essential role for the realization of this accelerating scheme. Constant external magnetic field which can be used for focusing the driver bunch affects the field structure essentially because plasma acquires both anisotropy and gyrotropy. However, the field in the latter case has not been practically investigated until present. Here we study the field produced by point charge and small bunch moving in cold magnetized plasma along the external magnetic field. We note the singular behavior of some components of the wave field produced by point charge near the charge trajectory. We also analyze the influence of the external magnetic field and bunch size on the field components.

INTRODUCTION

Cherenkov radiation in a cold magnetized plasma has been investigated for the first time in the early fifties [1], but the detailed analysis of the electromagnetic field structure in this situation has not been performed until present. However, this question is of essential interest in the context of wakefield acceleration method [2] and especially plasma wakefield acceleration (PWFA) method [3], which has achieved a 40 GeV/m gradient for now [4]. Outcomes of the present paper concerning the peculiarities of the electromagnetic field of small bunch moving in the considered medium can be used for further development of PWFA technique.

We consider cold electron plasma under the external magnetic field H_{ext} described by permittivity tensor [5]

$$\hat{\varepsilon} = \begin{pmatrix} \varepsilon_1 & -i\varepsilon_2 & 0 \\ i\varepsilon_2 & \varepsilon_1 & 0 \\ 0 & 0 & \varepsilon_3 \end{pmatrix}, \qquad (1)$$

$$\varepsilon_1 = 1 - \frac{\omega_p^2}{\omega^2 - \omega_h^2},\ \varepsilon_2 = \frac{-\omega_p^2 \omega_h}{\omega(\omega^2 - \omega_h^2)},\ \varepsilon_3(\omega) = 1 - \frac{\omega_p^2}{\omega^2}, \qquad (2)$$

where $\omega_p^2 = 4\pi N e^2/m$ is a plasma frequency (N is an electron density, e and m are an electron charge and a mass respectively), $\omega_h = |e|H_{ext}/(mc)$ is a "gyrofrequency" and c is the light speed in vacuum.

*Work is supported by Saint Petersburg State University, the Dmitry Zimin "Dynasty" Foundation and Russian Foundation for Basic Research (Grant No. 12-02-31258).

galiaminsn@yandex.ru

FIELD OF POINT CHARGE

The electromagnetic field generated by point charge q moving with constant velocity $\upsilon = \beta c$ along H_{ext} in (1) is given in the ultrarelativistic case $\gamma >> 1$ (γ is Lorentz factor) for $\zeta < 0$ ($\zeta = z - \upsilon t$) and $|\zeta| >> c/(\gamma\omega_p)$ by the following formula

$$H_\varphi = \int_{\omega_p}^{\omega_\Sigma} h_\varphi(\omega) J_1(\rho s_e) \sin(\omega\zeta/\upsilon) d\omega \qquad (3)$$

for the azimuthal magnetic component (the cylindrical frame with z axis coinciding with H_{ext} is used) and by similar ones for the rest of components [1, 6]. Here

$$h_\varphi = \frac{qc\beta}{\omega_p^2 \omega_h} \frac{\omega_h^2 - \omega^2}{\sqrt{\omega^2 - \omega_c^2}} \left[\frac{\omega^2}{c^2} \left(\varepsilon_2^2 - \varepsilon_1^2 + \frac{\varepsilon_1}{\beta^2} \right) + \varepsilon_1 s_e^2 \right] s_e, \qquad (4)$$

$$s_e^2 = \frac{(\beta^2 - 1)(u - u_1)(u - u_3)(u - u_4)}{\beta^2 c^2 (u - u_2)},\ u = \sqrt{\omega^2 - \omega_c^2}, \qquad (5)$$

$$\omega_c^2 = \omega_p^2 - \omega_h^2 [1 - \beta^2]^2/(4\beta^2),\quad \omega_\Sigma = \sqrt{\omega_p^2 + \omega_h^2}, \qquad (6)$$

$$u_{1,2} = \frac{\omega_h(1 \mp \beta^2)}{2\beta},\ u_{3,4} = \frac{\omega_h \beta}{2} \mp \frac{1}{2\beta} \sqrt{\frac{\omega_h^2}{4} - \frac{\omega_p^2 \beta^2}{1 - \beta^2}}. \qquad (7)$$

Two analytical approaches have been applied to calculation of (3). First one gives the field representation in the far-field zone within the Cherenkov cone $\rho s_{e1,2} >> 1$, $|\zeta| > \zeta_{\min}(\rho)$:

$$H_\varphi \approx \left[-h_\varphi(\omega_{s1}) \sin(\rho s_{e1} - \omega_{s1}|\zeta|/\upsilon) / \sqrt{s_{e1}|s''_{e1}|} + h_\varphi(\omega_{s2}) \cos(\rho s_{e2} - \omega_{s2}|\zeta|/\upsilon) / \sqrt{s_{e2}|s''_{e2}|} \right] / \rho, \qquad (8)$$

where $s_{e1,2} = s_e(\omega_{s1,2})$, $\omega_{s1,2}$ are solutions of $ds_e/d\omega = |\zeta|/(\rho\upsilon)$, $\zeta_{\min}(\rho) = \rho\upsilon s'_{e\min}$, $s'_{e\min} = ds_e(\omega_{s0})/d\omega$, ω_{s0} is solution of $d^2 s_e/d\omega^2 = 0$. In the special case of $\gamma >> 1$ and $\omega_h << \omega_p$ one obtains:

$$\omega_{s0} \approx \omega_p \left[1 + \omega_h^2/(8\omega_p^2) \right],\quad s'_{e\min} \approx 4\omega_p^2/\omega_h^2. \qquad (9)$$

For $|\zeta| >> \zeta_{\min}$ we have

$$\omega_{s1}^2 \approx \omega_p^2 + \left[\rho\omega_p^2/(2|\zeta|\sqrt{\omega_h}) \right]^{4/3}, \qquad (10)$$

$$\omega_{s2}^2 \approx \omega_p^2 + \left[\omega_h - \left[\rho\omega_p\omega_\Sigma/(2|\zeta|\sqrt{\omega_h}) \right]^{2/3} \right]^2. \qquad (11)$$

Formula (8) predicts the beating behavior of the field.

Another approach describes the field in the vicinity of the charge motion line behind the charge [6]:

ISBN 978-3-95450-125-0

PARAMETER OPTIMIZATION OF A RECTANGULAR DIELECTRIC BASED WAKEFIELD ACCELERATING STRUCTURE

S. Baturin, A. Altmark, I.L. Sheynman, St.Petersburg Electrotechnical University "LETI", Saint-Petersburg, Russia
A. Kanareykin, St.Petersburg Electrotechnical University "LETI", Saint-Petersburg, Russia and Euclid Techlabs LLC, Gaithersburg, MD USA

Abstract

In this talk, we present the algorithm and simulation results of a single mode wakefield parametric study of the rectangular dielectric based wakefield accelerating structure. Analytical solutions of wakefield generation in rectangular dielectric structures have been studied in order to achieve optimal relations between the geometrical parameters and dielectric constant of the structure, and the drive beam parameters like bunch charge and bunch length. Optimization has been carried out for maximization of the accelerating gradient in the single LSM_{11} mode approximation.

INTRODUCTION

In this paper we consider dielectric based wakefield acceleration technology [1-4] as one of the most promising for the development of the high gradient accelerating structures to be used for the next generation of linear colliders [5] and future X-ray FELs [6].

It is assumed that dielectric lined structures will be excited by a high intensity electron beam (e.g., the CLIC collider project [7,8]) for generating high power X-band, mm-wave or THz radiation. This type of electromagnetic wave generation is essential for avoiding the need to develop high power upper GHz/THz sources and coupling components that are able to sustain and transmit into the structure GW-level power in the same frequency ranges [2-4].

An accelerating structure with dielectric loading is a dielectric waveguide with an axial vacuum channel for beam propagation. The dielectric is surrounded by a conducting metal wall [1-4]. Recent experiments have proved that the dielectric based structures can sustain accelerating gradients in excess of 100's of MV/m [8,9] and GV/m [3] in the upper GHz and THz frequency ranges respectively.

For example, a high current (up to 100 nC) short (1–2 mm) relatively low energy (15–100 MeV) electron bunch in this type of a structure can generate Cerenkov wakefields with a longitudinal field magnitude up to 100-300 MV/m in the X - Ka band frequency ranges [9]. A 3 nC charge and 30 μm long bunch from the 23 GeV FACET/SLAC accelerator generates 1-10 GV/m wakefields in the THz range [3,10]. These wakefields are used for accelerating a less intense but high energy electron bunch propagating behind the drive bunch at a distance corresponding to the accelerating phase of the E_z field [11]. Dielectric based structures provide in addition to a high accelerating gradient the control over the frequency spectrum of the structure by introducing additional ferroelectric layers [12,13] as well as the possibility of using new promising microwave/THz materials (such as diamond and sapphire) with unique breakdown strength and thermoconductive properties [14]. Cerenkov radiation generated by a relativistic electron bunch in a rectangular waveguide with a transverse, inhomogeneous dielectric layers has been analyzed in [15], where a modification of the transverse operator method was used. In [15], the Sturm–Liouville second order operator with an alternating sign weight function was considered. This approach makes it possible to obtain a complete analytic solution for eigenmodes and to solve the problem of Cerenkov wakefield generation in a rectangular accelerating structure with a composite dielectric loading in the most general form [15].

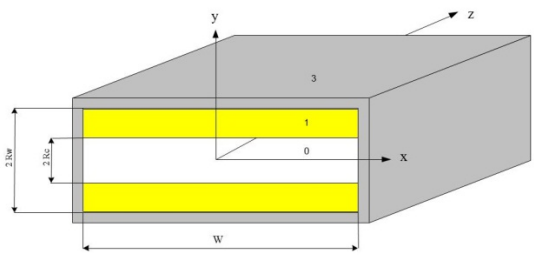

Figure 1: A rectangular dielectric based accelerating structure.

Below, we present the analytical solution for wakefield generation in the rectangular dielectric structure to optimize relations between both the geometrical parameters and dielectric constant of the structure, and the beam parameters for two specific user facilities, the Argonne Wakefield Accelerator (AWA) and the FACET facility at SLAC.

ANALYTICAL APPROXIMATION

We consider an ultrarelativistic Gaussian electron bunch passing along the central axis of a rectangular DLA (dielectric loaded accelerating) structure presented in Fig.1.

Let us take into account first the symmetric accelerating LSM mode ($H_y = 0$), which corresponds to the first asymmetric eigenfunction of the transverse $\hat{T}_E$-operator of the wave equation [15]. We introduce dimensionless parameters as follows:

ISBN 978-3-95450-125-0

AN ANALYTICAL APPROACH TO SOLUTION OF SELF-COORDINATED BEAM DYNAMICS IN DIELECTRIC WAKEFIELD ACCELERATING STRUCTURES*

I. Sheynman#, LETI (ETU), Saint-Petersburg, Russia

Abstract

Self-coordinated transverse dynamics of the high current relativistic electronic bunches used for generation of wake fields in wakefield accelerating structures with dielectric filling is investigated. An analytical approach to solution of self-coordinated beam dynamics is developed.

INTRODUCTION

Wakefield acceleration in a dielectric wakefield waveguide structures is one of the most intensively developed direction among new methods of particle acceleration. Linear accelerators are considered also as sources of sequence of electronic bunches for the free electron laser, which is considered now the major candidate for creation of ultra short impulses (of attosecond range) X-ray radiation. Waveguide structures with dielectric filling excited by a high current electronic bunch were investigated intensively for the last years [1] – [5]. The main purpose is of prospects of their use as high gradient linear accelerators.

One of the main problems in realization of the wakefield method is keeping of an intensive electronic bunch in the channel of a wave guide and prevention of subsidence of particles on its wall. In this regard, a key task in the wakefield method of acceleration is modeling of the self-coordinated movement of a relativistic electronic bunch passing through dielectric structure in fields of Vavilov-Cherenkov created by it.

In recent years in tasks of the analysis of self-coordinated dynamics of relativistic electronic bunches in wakefield accelerating structures methods of direct numerical modeling where developed. These methods are «particle – particle» and «particle – grid». These methods allow on the set parameters of accelerating structure and an initial condition of a bunch to simulate process of its movement. The results of calculations are determination of flight range of the bunch to a contact to them accelerating structure walls, emittance of the bunch, and also transferred or received by bunch energy of particles.

Shortcomings of these methods are considerable duration of calculations for ensuring accuracy of calculations, insistence to volume of random access memory and productivity of computer system. Let us note also that at change of parameters of the bunch and of accelerating structure complete recalculation of a problem of the bunch movement is necessary.

For design of accelerating structures, solutions of problems of optimization in which the structure and bunch parameters maximizing efficiency of accelerating process are determined are necessary. The solution of similar tasks based on direct numerical modeling of dynamics demands repeated carrying out numerical calculations. Creation of the analytical description of self-coordinated dynamics of the bunch allowing direct parametrical research of process in this regard is of interest.

BEAM DYNAMICS EQUATIONS

The description of movement of the electronic bunch was carried out on the basis of the equations of relativistic dynamics [3]:

$$F_r = d\left(m_e V_r \gamma\right)/dt ,$$

where

$$F_r = F_{focus} - eq\sum_{n,m}\Big[\psi_{F_r\,n,m} I_n'\left(k_{r\,n,m} r(\zeta,t)\right)\cdot$$

$$\cdot\int_0^{\zeta} f(\zeta_0)\sin\left(k_{z\,n,m}\left(\zeta-\zeta_0\right)\right) I_n(k_{r\,n,m} r(\zeta_0,t))d\zeta_0\Big],$$

$r(\zeta,t)$ is a bunch deflection from waveguide axes, $\zeta = z - vt$ is a distance behind the bunch, F_f is a focusing force, e and m_e are charge and mass of electron, q and γ are charge and relativistic factor of the bunch, $k_{z\,i,j}$ and $k_{r\,i,j}$ are longitudinal and radial components of wave vector, $\psi_{E_z\,i,j}$ and $\psi_{F_r\,i,j}$ are coefficients of series, depending of geometry and wave guide filling permittivity, $f(\zeta_0)$ is a function describing longitudinal charge distribution, $I_n(x)$ are modified Bessel function of n-th order.

The task of the description of macroparticle movement is self-coordinated: the mutual provision of particles in ensemble influences a field created by particles which, in turn, leads to change of their position. Let's consider an analytical method of the solution of the integro-differential equation of self-coordinated dynamics at the following simplifying assumptions:

1. Let's consider that the charge of the bunch is distributed evenly in the longitudinal direction, thus $f(\zeta_0) = 1/l$, where l is a length of the bunch.

*Work supported by the Russian Foundation for Basic Research and the Ministry of Education and Science of the Russian Federation in the framework of the Federal Program "Human Capital for Science and Education in Innovative Russia" for 2009–2013.

#ishejnman@gmail.com

ISBN 978-3-95450-125-0

NUMERICAL AND ANALYTICAL METHODS OF MODELLING OF BUNCH DYNAMICS IN DIELECTRIC FILLED ACCELERATING STRUCTURES*

I. Sheynman#, LETI (ETU), Saint-Petersburg, Russia,
A. Kanareykin, Euclid TechLabs, LLC, Solon, Ohio, USA
G. Sotnikov, NSC/KIPT, Kharkov; Omega-P, Inc., New Haven

Abstract

RF waveguide structures are a basis for development of new generation of accelerators on the basis of a wakefield method of the charged particle acceleration, and also free electron lasers. Numerical and analytical calculation methods of Vavilov-Cherenkov radiation generated by relativistic electronic bunches in wave guides with dielectric filling, and also self-coordinated bunch dynamics in own and external fields are considered.

INTRODUCTION

The modern accelerating technique is in search of new methods for ensuring progress in the field of experimental physics of high energy. The developed technologies of dielectric wakefield acceleration of electrons on Vavilov-Cherenkov effect are one of the most perspective directions of creation of high gradient structures of modern linear accelerators for high energy physics [1].

Linear accelerators are considered also as sources of sequence of electronic bunches for the free electron laser which is considered now the major candidate for creation of ultra short impulses (of attosecond range) X-ray radiation. Waveguide structures with dielectric filling (Fig. 1) excited by a high current electronic bunch were investigated intensively for the last years [1] – [5]. The main purpose is of prospects of their use as high gradient linear accelerators.

For linear accelerator the achievement of high accelerating fields in structure where the electronic bunch gained energy ~GeV at extremely short distances is necessary. Increase of wake fields is reached on the basis of increase in a charge of generating bunch creating a wakefield wave, and also optimization of the geometrical sizes and a material of filling of accelerating structure. However along with accelerating fields the high current bunch generates the considerable rejecting fields leading to a bend of the bunch and its deviation from an axis of wave guide structure. In this regard one of the main problems in realization of the wakefield method is control of an intensive electronic bunch in the channel of the wave guide and prevention of subsidence of particles on its wall.

*Work is supported by the Russian Foundation for Basic Research and the Ministry of Education and Science of the Russian Federation in the framework of the Federal Program "Human Capital for Science and Education in Innovative Russia" for 2009–2013.
#ishejnman@gmail.com

Key task in the wakefield acceleration method is modelling of the self-coordinated movement of a relativistic electronic bunch passing through dielectric structure in Vavilov-Cherenkov fields created by it.

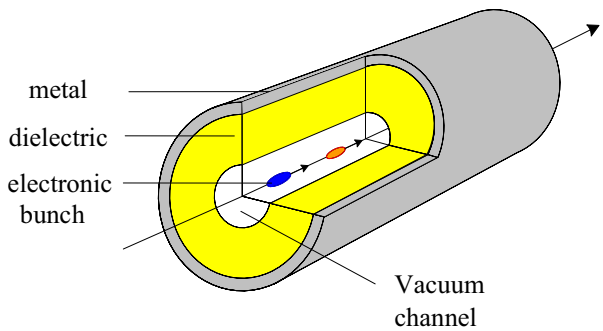

Figure 1: Wakefield waveguide structure.

To research of bunch dynamics the numerical approaches based on modelling of electronic bunches by a method of macroparticles are applied. The method of macroparticles is based on splitting of phase volume of a bunch into a large number of not being crossed elementary volumes; movement of each is identified with movement of one macroparticle with a total charge and mass of particles entered into this volume.

BEAM DYNAMICS EQUATIONS

The description of movement of an electronic bunch was carried out on the basis of the equations of relativistic dynamics [3]:

$$F_z = -eE_z = m_e\, d\left(V_z\gamma\right)/dt\,, \qquad F_r = d\left(m_e V_r\gamma\right)/dt\,,$$

where

$$E_z = q\sum_{n,m}\Big[\psi_{E_{z\,n,m}} I_n\left(k_{r\,n,m} r(\zeta,t)\right)\cdot$$

$$\cdot\int_0^{\zeta} f(\zeta_0)\cos\left(k_{z\,n,m}\left(\zeta-\zeta_0\right)\right) I_n(k_{r\,n,m} r(\zeta_0,t))\,d\zeta_0\Big],$$

ISBN 978-3-95450-125-0

OPTIMIZATION OF LASER RADIATION PRESSURE ACCELERATOR FOR ION GENERATION

G. Dudnikova#, ICT SB RAS, Novosibirsk, Russia
D. Gorpinchenko, ICM&MG SB RAS, Novosibirsk, Russia
C.S. Liu, T.C. Liu, R. Z. Sagdeev, X. Shao, J.J. Su, UMD, College Park, MD, USA

Abstract

Compact laser-driven accelerators are an attractive alternative for monoenergetic proton and ion generation in conventional RF accelerator because the particle acceleration electric fields can reach tens GV/cm, which allows reduction of the system size. The scheme for generating quasi-monoenergetic proton with Radiation Pressure Acceleration (RPA) has the potential of leading to table-top accelerators as sources for producing 50-250 MeV protons. Theoretical and computational studies of ion energy scaling of RPA are presented. 2D and 3D PIC simulations are performed to study limitations of energy gain due to Rayleigh-Taylor instability and how is the Rayleigh-Taylor instability suppressed by density fluctuations or inhomogeneities of targets. Energy transfer efficiencies and qualities of accelerated proton beams are discussed.

INTRODUCTION

One of the most attractive applications of ultra-short superintense laser pulses is connected with the development of new methods of accelerating charged particles. The generation of high energy particles, both electrons and ions, when strong electromagnetic radiation interacts with a plasma is a well known phenomenon. However it is necessary to find the plasma and radiation parameters that optimize this process. Thick targets with thicknesses ranging from a few to tens of laser wavelengths were employed in early studies of ion acceleration. and the target normal sheath acceleration (TNSA) was the predominant mechanism leading to the production of multi-tens MeV ion beams but with wide energy spectra [1, 2]. Recently, the scheme of laser radiation pressure acceleration (RPA) of ultra-thin target shows promising aspect of efficient quasi-monoenergetic proton generation [3-5]. In the RPA scheme, a circularly polarized, high power, short pulse laser is focused on a suitable ultra-thin foil, which leads to the acceleration of the whole foil. The RPA focuses on increasing the efficiency of acceleration and producing monoenergetic protons. The scheme for generating quasi-monoenergetic proton with RPA has the potential of leading to table-top accelerators as sources for producing monoenergetic 50 - 250 MeV protons suitable for widespread dissemination for cancer therapy and other applications such as fast ignition in laser fusion. In comparison to the conventional TNSA-scheme, the conversion efficiency with the RPA scheme is estimated to be more than 40 times higher. During the RPA of a ultra-thin foil, the laser ponderomotive force sweeps all electrons in the foil forward until the electrostatic force on the electrons due to the ions left behind balances the ponderomotive force on electrons at a distance D. These electrons form a charged layer and their electrostatic force now accelerates the ions left behind. When the thickness of the target, Δ, is equal to this distance of maximum charge separation, we obtain optimal thickness $D = \Delta$, at which the electrons are pushed to the rear end of the target and the space charge force balances the ponderomotive force $eE = F_P(\Delta)$ on the electrons. In the limit of the normalized laser amplitude $a_0 = e|E|/(m\omega c) >> 1$, we obtain the thickness as

$$\Delta \cong \frac{4\pi}{\lambda_L}\left(\frac{c}{\omega_p}\right)^2 a_0 = \frac{\lambda_L}{\pi}\left(\frac{\omega}{\omega_p}\right)^2 a_0 \qquad (1)$$

where m and e are the electron mass and charge, λ and ω are the laser wavelength and angular frequency, ω_p is the electron plasma frequency, E is the electric field amplitude, a_0 is the dimensionless laser amplitude. To minimize the wave tunneling through the target, $\Delta > c/\omega_p$ should be satisfied.

In RPA, high intensity circularly polarized laser light with a high contrast ratio accelerates the ultra-thin foil with radiation pressure, and the foil has a definite, optimal thickness. It must be sufficiently thin so that

- The ponderomotive force of the laser radiation accelerating the electrons in the foil is balanced by the electric force due to ions at the outer edge of the thin foil.
- The mass of the thin foil must be sufficiently light so that the whole foil is accelerated by the laser radiation pressure in the short duration of the order of ion plasma period. In this case, protons are subject to both the electric force of the electron layer accelerating them forward, and the inertial force pulling them back in an accelerated frame. The balance of these two opposing forces forms a trap for the ions in real and phase spaces.
- These stably trapped protons and electron layers form a self-organized double layer. The laser radiation pressure accelerates this double layer as a whole, with protons trapped in it.

#gdudnikova@gmail.com

ISBN 978-3-95450-125-0

PROPOSAL OF LASER ION BEAM ACCELERATOR FOR INERTIAL FUSION

F. Scarlat, Valahia University of Targoviste, Targoviste, Romania
A. Scarisoreanu, INFLPR, Bucharest-Magurele, Romania

Abstract

The inertial nuclear fusion with laser beams, relativistic electron beams, ion beams, micro-particle beams and superconducting projectiles has been analytically investigated and numerically calculated by various authors along years and nowadays. Starting from the record laser peak power of 1.25 PW and radiation peak intensity of 100 EW per square centimeter produced at LLNR using the chirped pulse amplification (CPA) laser technology as well as from ELI Nuclear Physics - laser system, 3 APPOLON 10 PW (150 J / 15 fs) (http://www.eli-np.ro/) proposed to be realized, this paper presents the principle and the configuration of a compact ion accelerator operated by an optical laser in an ultra-relativistic regime, for the inertial confinement fusion. Ions acceleration is based on the acceleration mechanism named "Radiation Pressure Acceleration". By the application of this mechanism the calculations for the physical parameters of an ion accelerator operated by laser were made. Calculation results are also presented in this paper.

INTRODUCTION

Fusion by inertial confinement (ICF) represents an alternative energy source to the nuclear fission energy, hydraulic energy, wind energy, etc. That can be achieved by means of a thermonuclear target (TN) consisting of a capsule housing the fusion fuel located in the centre of a spherical cavity surrounded by a pusher and an ablator.

The fusion fuel may be deuterium (D) and tritium (T) since the nuclear fusion reaction of the two has the most probable efficient section.

The fusion with inertial confinement of D-T is developing on the irradiation of the TN target with particle beams of a certain energy followed by the ablation of the surface material outside the target, the acceleration and compression of the capsule for igniting the fuel core and burning which is spread fast through the compressed fuel.

The fusion of both light nucleus to high temperature and density generates the 17.6 MeV thermonuclear energy by the reaction: D + T → n (14.1 MeV) + α (3.5 MeV). This energy is absorbed by the reactor blanket and converted in thermal energy that is transformed in electric energy by classic methods and techniques.

The TN target containing 1 g D-T produce TN energy of 340 GJ. A fusion reactor with inertial confinement can produce 1.25 GW (electric) with 40 % thermal efficiency with a consumption of 10 mg of DT per second. From the produced electric energy, 1 GW goes to consumer and 36 GW is used for the driver supply.

At present, worldwide, there are more powerful facilities under construction, such as "The National Ignition Facility (NIF) at LLNL [1] and "The Laser Megajoule" (LMJ) in France [2].

There are also programs for light ion accelerators, e.g.: p, ^{12}C and heavy ion accelerators e.g.: $^{55}Fe \rightarrow U$, as drivers for inertial confinement fusion. This drivers are by types: induction accelerator, linear accelerator, synchrotron [3, 4, 5].

The construction of a 10 PW (150 J / 15 fs) laser system in Bucharest – Magurele led to the elaboration of some programs for the application of the laser beam generated by the laser [6].

One of such applications proposed in the paper, is the use of the laser radioation beam generated by APPOLON 10 PW system to accelerate the ions for to be used as drivers for the conventional ICF or hot-spot ignition with spherical configuration [7].

LASER ION ACCELERATOR

Requirements for ICF

One of the requirements for ICF is represented by the DT fuel capsule compression. Since the fuel mass depends on fuel density square inverse, one may chose a smaller mass capable to generate a managing energy output. Choose the inertial fusion parameter $\rho R = 2.8$ g/cm^2 for the burn-up efficiency $\Phi = \rho R / (\rho R + 6\ \text{g/cm}^2) = 0.32$, where ρ is the fuel density and R is the target radius [8].

For the fuel mass $M = 10^{-3}$ g, the density of the compressed fuel is $\rho = ((4\pi / 3)(\rho R)^3 / M)^{1/2} = 300$ g/cm^3. The required specific energy to compress this mass is given by the Fermi-Dirac internal specific energy $\varepsilon_{FD} = 3 \times 10^5 \rho^{2/3}$ J/g $= 1.35 \times 10^7$ J/g. The compression energy for $\alpha_C = 2$ is $E_C = \alpha_{cf}\ \varepsilon_{FD} M = 0.027$ MJ [9].

The energy per gram required to heat a DT plasma at 8.6 keV, which is twice the ideal ignite temperature, is $E_H = 1$ MJ. If 2% of the fuel mass is kept for central hot spot, the energy required to heat this mass would be about 0.02 MJ.

The total energy required for compression and ignition would be about 0.05 MJ. The driver energy required to assemble energy for the plasma efficiency with $\eta_P = 10$ % is equal with 0.5 MJ, resulting in G = 200.

The fusion energy for 1 mg DT with burning efficiency by 32 % is equal with $E_{DT} = \varepsilon_{DT} \Phi M = 3{,}4 \times 10^{11}$ J/g $\times 0.32 \times 10^{-3}$ g = 100 MJ, where $\varepsilon_{DT} = 17.6$ MeV/5amu is the energy specific to DT fuel per reaction. A nominal 100 MW fusion power plant would consume 1 mg / s of DT.

ISBN 978-3-95450-125-0

DYNAMICS OF $^{197}AU^{+78}$ IONS GENERATED IN RECOMBINATION WITH COOLING ELECTRONS IN THE NICA COLLIDER

A.V. Eliseev, O.S. Kozlov, A.B.Kuztnetsov, I.N. Meshkov, A.O. Sidorin, A.V. Tuzikov, A.V. Philippov, JINR/VBLHEP, Dubna, Russia

Abstract

In the NICA Collider [1], recombination of original $^{197}Au^{+79}$ ions with cooling electrons in the electron cooler will lead to generation of $^{197}Au^{+78}$ ions. Dynamics of these ions in the energy range 1 – 4.5 GeV/u when the ion beam is bunched with RF voltage (collision mode operation) is considered in this report. It is shown that some part of 78+ ions can be involved into synchrotron motion when other part suffers a chaotic motion regime. Most of these ions circulate in vacuum chamber until further recombination into the charge state of $^{197}Au^{+77}$ and then leave the Collider acceptance very fast. The evolution in time of the ion distribution over the Collider aperture is presented

INTRODUCTION

Longitudinal motion of a multi-component ion beam can be in synchronism with an accelerating field when the revolution period T does not depend on the charge and mass of the ion in any moment of time. In differential form this condition is:

$$\frac{\Delta T}{T} = \frac{\Delta R}{R_0} - \frac{\Delta \beta}{\beta} = 0 \qquad (1)$$

Variation of the average radius R can be expressed as follows:

$$\frac{\Delta R}{R_0} = \alpha \left[\gamma_0^2 \frac{\Delta \beta}{\beta_0} - \frac{\Delta\left(Z/W_r\right)}{Z_0/W_{r0}} \right] , \qquad (2)$$

The relative velocity and momentum deviations of the beam components are:

$$\frac{\Delta \beta}{\beta_0} = -\frac{\alpha}{1-\alpha\gamma^2} \frac{\Delta\left(Z/W_r\right)}{Z_0/W_{r0}}, \quad \frac{\Delta p}{p_0} = \frac{\alpha\gamma^2}{1-\alpha\gamma^2} \frac{\Delta\left(Z/W_r\right)}{Z_0/W_{r0}} \quad (3, 4)$$

Where α is the ring compaction factor, β, γ – relativistic parameters, Z – particle charge, W_r – rest energy, index zero corresponds to the main component of the beam.

All the particles can be accelerated if aperture allows. As for collider operating at constant energy the particles not involved in synchrotron regime circulate in vacuum chamber as well.

In electron cooler of the NICA collider the ions of Au^{+79} after successive recombination with electrons will transfer into Au^{+78}, Au^{+77} and so on. The ions in different charge states, involved into synchrotron motion will arrive to the detector sites simultaneously. This may contort physical experiments and hamper the feedback steering of the main beam. The ions forming coasting beam will create an unwanted noise.

PHASE SPACE MOTION OF IONS WITH DIFFERENT CHARGE STATE

RF Bucket Parameters

The bunch length in the NICA collider is chosen to be 0.6 m (rms) independently on the energy. The relative momentum spread (σ_p) is linearly proportional to relativistic gamma and varies from $6 \cdot 10^{-4}$ at 1 GeV/u to $1.7 \cdot 10^{-3}$ at 4.5 GeV/u [2]. The bucket height keeps ~3.7 σ_p regardless energy. Shift of the synchronous energy between Au^{+79}, and Au^{+78} (centres of corresponding buckets) and the bucket height are represented in the Fig.1 as functions of the particle energy.

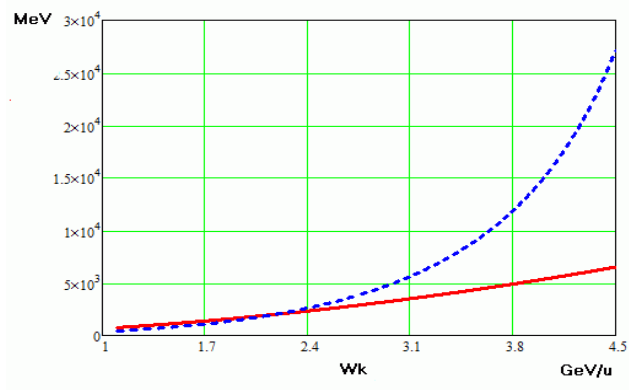

Figure 1: Bucket height (red) and energy shift between synchronous Au^{+79} and Au^{+78} (blue) vs. particle energy.

The buckets of the different charge states are moving apart in the phase plane with the energy increase. Graphically the situation is illustrated by the Fig. 2.

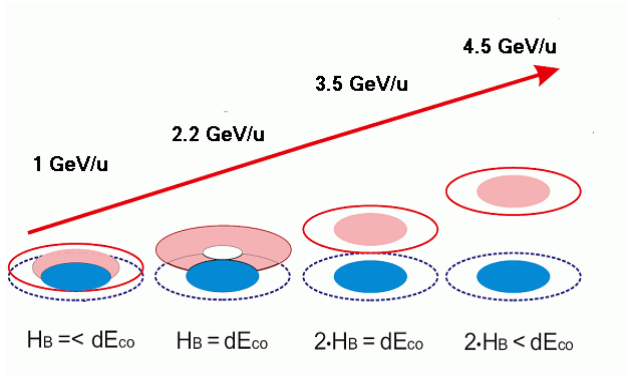

Figure 2: General scheme of buckets Au^{+79} (blue) and Au^{+79} (red) allocations in longitudinal phase space.

Thus new formed ions of Au^{+78} can find themselves either inside or outside the bucket in the energy range from 1 to 3.5 GeV/u and outside the bucket only in the range 3.5 ÷ 4.5 GeV/u. Particles inside the bucket are

ISBN 978-3-95450-125-0

COLLIDER OF THE NICA ACCELERATOR COMPLEX: OPTICAL STRUCTURE AND BEAM DYNAMICS

O.Kozlov, A.Eliseev, H.Khodzhibagiyan, S.Kostromin, I.Meshkov, A.Sidorin, G.Trubnikov,
JINR, Dubna, Russia

Abstract

The Nuclotron-based Ion Collider fAcility (NICA) [1] is a new accelerator complex being constructed at JINR. It is aimed to collider experiments with ions and protons and has to provide the ion-ion (Au^{+79}) and ion-proton collision in the energy range of 1÷4.5 GeV/u and also polarized proton-proton (5÷12.6 GeV) and deuteron-deuteron (2÷5.8 GeV/u) collisions. Two collider rings are designed and optimized to achieve the required luminosity at two interaction points (IP). Providing the intense ion beam life time the space charge effects were considered. Beam accumulation scheme and scenario of collider operation in collision mode with application of electron beam or stochastic cooling methods were proposed.

INTRODUCTION

The goal of the NICA project is construction at JINR of the new accelerator facility that consist of [1]: cryogenic heavy ion source of Electron String type (ESIS), source of polarized protons and deuterons, the existing linac LU-20 of Alvaretz type, a new heavy ion linear accelerators RFQ-DTL, a new superconducting Booster-synchrotron placed inside the decommissioned Synchrophasotron yoke, the existing proton and heavy ion synchrotron Nuclotron, the new system of beam transfer channels, and two new superconducting storage rings of the collider. NICA collider lattice development [2] has many necessary aspects of the design. The collider should operate in the energy range for Au-ions of 1÷4.5 GeV/u, with the average luminosity about $1\cdot10^{27}$ cm^{-2} s^{-1}. The ring should work with the different particle species (Au^{+79}, protons and deuterons). Collider must fit into JINR infrastructure and has a certain circumference limitation. The collider lattice is based on the technology of super-ferric magnets developed in VBLHE, JINR [3]. Such a dipole magnet with up to 2 T bending field operates with hollow composite NbTi cable at 4.5 K. The collider optics optimization includes the certain effects which set some constraints on the lattice parameters: luminosity lifetime limitation by intrabeam scattering in a bunch (IBS); space charge tune shift, threshold of microwave instability; slippage factor optimization for efficient stochastic cooling; maximum required RF voltage amplitude.

Collider operation at fixed energy without acceleration of the injected from the Nuclotron beam is considered. Beam storage at some optimum energy and slow acceleration in the collider (at field ramp rate < 1 T/s) is presumed as a reserve option. The maximum energy of the experiment is determined by the Nuclotron maximum magnetic rigidity of 45 T·m. In this paper we discuss only the most developed heavy ion mode of facility operation and the $^{197}Au^{+79}$ ions as the reference particles.

LATTICE STRUCTURE

Together with the physical effects the another technical constraints were taken into account in lattice optimization: ring circumference, number of the dipole magnets in arc, convenience of the beam injection into the ring. The FODO optics with 12 periods is a principal choise for arc structure. Two arcs and two long straight section form the collider racetrack shape and correspond exactly to two Nuclotron circumferences. The rings are vertically separated (32 cm between axes) and use "twin aperture" superconducting magnets (dipole and quadrupoles) [2]. This lattice has a large efficiency of stochastic cooling at 4.5 GeV/amu. But the luminosity of 10^{27} cm^{-2} s^{-1} could be reached in the wide energy range. The convenient injection scheme could be realized through the arc dipole-empty cell.

Table 1: Collider Ring and Beam Parameters

Ring circumference, m	503.04		
Gamma-transition, γ_{tr}	7.091		
Betatron tunes, Q_x/Q_y	9.44/9.44		
Chromatisity, $\xi_{x,0}/\xi_{y,0}$	-33/-28		
Max. number of bunches	23		
Rms bunch length, m	0.6		
β-function in the IP, m	0.35		
FF lenses acceptance	40π mm mrad		
Long. acceptance, Δp/p	±0.010		
Ion energy, GeV/u	1.0	3.0	4.5
Ion number per bunch	2.75e8	2.4e9	2.2e9
Rms Δp/p, 10^{-3}	0.62	1.25	1.65
Rms emittance, hor/vert, (unnorm), π·mm·mrad	1.1/ 1.01	1.1/ 0.89	1.1/ 0.76
Luminosity, $cm^{-2}s^{-1}$	1.1e25	1e27	1e27
IBS growth time, s	190	700	2500

FODO-cell geometry is set up with the fixed lengths of magnetic elements and spaces. In Fig. 1 the scheme of 11.96 m cell is shown. There are four rectangular dipole magnets per cell (80 magnets per ring), two quadrupoles [3], multipole correctors and BPMs. The maximum field in dipoles of 1.8 T and gradient in quadrupoles of 23 T/m are chosen to possibly avoid the saturation effects in iron yokes at higher energies. Multipole corrector includes the several types of windings – dipole (orbit correction),

ISBN 978-3-95450-125-0

LOCALISATION OF THE RF BREAKDOWN IN THE PARALLEL COUPLED ACCELERATING STRUCTURE

Yu. Chernousov, V. Ivannikov, I. Shebolaev, ICKC, Novosibirsk, Russia
A.Barnyakov, A. Levichev, V. Pavlov, BINP, Novosibirsk, Russia

Abstract

Parallel coupled accelerating structures (PCAS) [1,2] with parallel RF power feeding of accelerating cavities have some features and advantages vs. conventional TW - traveling wave and SW - standing wave structures with sequential (serial) RF power feeding. Parallel feeding of accelerating units - individual cells or accelerating substructures provides normal regime acceleration of the beam by all cells and minimizes the RF power flows via coupling slots and determines individual behavior of each cell in the regime of RF breakdown. These features can be used for developing low energy linear accelerators as well as high gradient accelerating structures. The experimental data of the breakdown regimes in the PCAS are presented in this paper.

INTRODUCTION

The main idea of the PCAS is the feeding of accelerating cells in parallel from the rectangular waveguide [1,2]. Parallel feeding of accelerating units – individual cells or accelerating substructures, provides normal regime of acceleration of the beam by all cells [1], minimizes RF power flows via coupling slots, and as shown in this paper, determines individual behavior of each cell in the regime of breakdown and minimizes absorbed RF energy in each accelerating cavity. These inherent characteristics and features of the PCAS are helpful for developing of low energy linear accelerators [1-3] and as noted in the papers [1,2,4] can be used to overcome difficulties when elaborating a high gradient accelerating structures.

A breakdown violates normal work of the accelerator, destructs the surface of the cells. The damage accumulates and as a result the RF property of separate cells and accelerating structure changes. Numerous investigations are devoted to study of this phenomenon [5-9]. The phenomenon is rather complicated and the processes involved are not clear yet. Nevertheless in recent years some evidence has been found that the RF power flow in particular determines the maximum sustainable gradient in an accelerating structure [6,7]. Using a parallel feeding in the PSAC handles and solves the issue of high level of RF flows in the structure.

Feeding line delivers electromagnetic energy to accelerating sells of the PCAS, it works on TW [1,2,4] or SW [2,3] mode. In the case of TW-mode it is difficult to provide the necessary amplitude and phase distributions of microwaves along the accelerating structure. For these goals it is necessary to employ variable coupling coefficient of cells with feeding line [1,2,4] which reduces advantages of the PCAS. The most straightforward means to solve this problem seems to be the use of SW-mode in the feeding RF line. This mode gives π-phase shift between the accelerating cavities as well as provides required amplitude distribution of an accelerating field along the structure [2,3]. The experimental data of the breakdown in the PCAS [3] which consists of an individual accelerating sells feeding via common exciting cavity – segment of rectangular waveguide working in the SW regime are given below.

EXPERIMENTAL SETUP

A conceptual scheme of PCAS is shown in Fig.1. The Accelerating (Accel.) Cavities are fed in parallel by common Exciting Cavity connected to feeding RF Power line thru Input Diaphragm. Exciting Cavity is shorted at

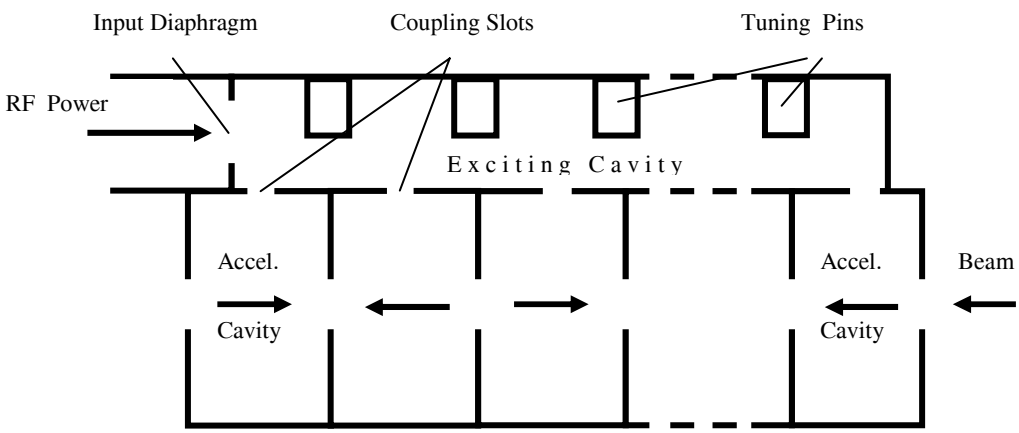

Figure.1: Conceptual scheme of the PCAS

ISBN 978-3-95450-125-0

RF ANTENNA LEAD

A.Barnyakov, A.Levichev, V.Pavlov, BINP SB RAS, Novosibirsk, Russia
Yu.Chernousov, V. Ivannikov, I. Shebolaev, ICKC SB RAS, Novosibirsk, Russia

Abstract

RF antenna lead is described. This lead is used for RF power input to high voltage electrodes. The device consists of receiving and transmitting antennas realized as symmetrical parts of coaxial cavity with dielectric disk between the parts. Main operating characteristics are the following: high voltage is over 60 kV, coefficient of transmission S_{21} at the operating frequency is over 0.97, bandpass is over 70% (at the level of S_{21} = -3dB). The scheme of device, the principles of operation and measured results are presented in the paper.

INTRODUCTION

Antenna leads for the supply of RF signals into isolated high-voltage electrodes are used in the microwave and accelerator technology [1-3].

RF antenna lead was developed for current management of high voltage gun for electron accelerator. The operating frequency is 2450 MHz. The lead must have both high breakdown strength and low microwave losses.

The requirements for the device are following:

1) the transmission coefficient at the operating frequency of 2450 MHz must be more than 0.85;
2) the reflection coefficient at the operating frequency must be less than 0.1;
3) the breakdown voltage must be not less than 60 kV;
4) the leakage currents must be less than 10 μA;
5) the bandwidth of the transmission coefficient on the level -3 dB should be not less than 30 MHz;
6) the power flux density at 1 m from the lead should not exceed 10 μW/cm^2.

DESIGN AND PRINCIPLE OF OPERATION

Figure 1 shows the scheme of the lead. The lead presented consists of two symmetrical parts of coaxial half-wave resonator. The resonator is spitted along the perpendicular to the longitudinal axis plane of symmetry and solid dielectric disk is located between the halves.

The operating scheme is following. Microwave signal from a generator feeds the resonator by coaxial line. The excited mode of electromagnetic field is *TEM*-type. Taking into account the dielectric disk, the cavity length is chosen so that the resonator length fits a half of wavelength.

According to the structure of the *TEM* mode standing wave, the radial electric field has maximum at the location of the dielectric disc; angular components of the magnetic field, longitudinal currents on the inner and outer conductors of the coaxial line have minimum.

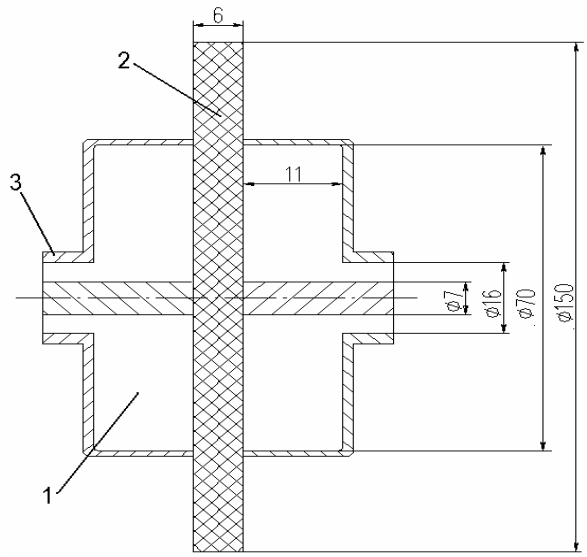

Figure 1: RF antenna lead design: 1 – half of coaxial resonator, 2 – dielectric disk, 3 – coaxial feed line.

The gap of coaxial line, which is set between the dielectric insulating discs, does not rupture the longitudinal currents and does not violate the cavity field structure. For these reasons, the reflected and radiated waves are not formed and the microwave signal passes the cavity without losses.

The breakdown strength of the device is determined by the breakdown voltage of the insulating dielectric. In our case, the dielectric material is formed from ceramics VG-4. The ceramic parameters at the operating frequency of 2450 MHz are following: the relative dielectric constant is 9.6, dielectric loss tangent is $<5\cdot10^{-4}$, the breakdown voltage is >150 kV/cm.

NUMERICAL SIMULATION

Ansoft HFSS [4] was used to calculate the basic characteristics of the device. Sizes of the resonator and thickness of dielectric disk were varied. The purpose of the calculations was to minimize the transfer attenuation and the amplitude of the reflected wave at the operating bandwidth in terms of the transmission coefficient S_{21} = -3dB. Also, the internal losses and radiation losses into the environment at the operating frequency were minimized.

Figure 2 shows the near field at a distance of 1 m from the lead (Y-axis coordinate is directed along the resonator axis). To calculate the characteristics of the device, the following parameters of the microwave signal were used: pulse duration – 5 μs, duty cycle – 1000, pulse power – 1 kW and frequency – 2450 MHz.

ISBN 978-3-95450-125-0

MULTIPACTOR DISCHARGE IN THE ELINAC ACCELERATOR

M.A.Gusarova, I.I.Petrushina, National Research Nuclear University "MEPhI", Moscow, Russia
V.L. Zvyagintsev, TRIUMF, Vancouver BC, Canada

Abstract

This paper concerns numerical simulations and experimental investigation of multipactior discharge in accelerating cavities and the feeding waveguide section of the eLINAC accelerator. The threshold values of the accelerating gradient and of the input power, at which the discharge may occur in these structures, have been obtained experimentally and compared to predictions of numerical simulations. The issues of the influence of secondary emission yield on a discharge growth were also considered.

INTRODUCTION

TRIUMF has recently embarked on the construction of ARIEL, the Advanced Rare Isotope Laboratory [1]. The superconducting electron linear accelerator (eLINAC) was developed under this project. It will be used as a photo-fission driver for the production of short-living rare isotopes. The TRIUMF eLINAC layout with the construction phases is shown in Fig. 1. The elliptic 9-cell accelerating cavities were developed in the TRIUMF laboratory [2] based on the well-known TESLA cavities [3]. The cavity will accelerate 10 mA current up to energy of 10 MeV. Two input CPI couplers [4] with an average operating power of about 60 kW are used for each cavity.

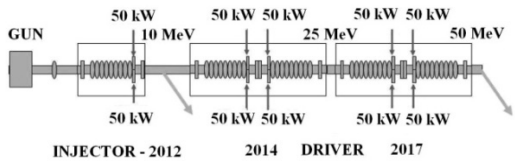

Figure 1: TRIUMF eLINAC layout

Each 9-cell cavity will operate with an acceleration gradient of E_a = 10 MV/m. It is quite safe goal for production. This class of cavities achieved operation gradients of 25-30 MV/m. However, it is necessary to study this structure with respect to the probability of multipactor discharge.

Multipactor discharge (secondary electron discharge) is the undesirable resonant particle number growth in the vacuum space of the RF structure. It may lead to a series of negative effects. The electron avalanche could consume RF power and limit level of the accelerating field. The electron bombardment may cause an overheating of the structure and a quench effect, when the material becomes normal conducting. Therefore, multipacting investigations are important for the RF structure development.

MULTIPACTING SIMULATIONS FOR THE 1-CELL ELLIPTIC TEST CAVITY

The Simulation Results

The investigations were carried out for the elliptic 1-cell superconducting Niobium TESLA cavity. The cavity model and main geometry parameters are shown in Fig. 2 and Table 1.

The special code for multipacting simulations Multp-M has been used [5]. The dependence of secondary particle count vs. accelerating gradient (considering the transit-time factor TTF = 0.52) was obtained for different secondary electron yields (SEY) which correspond to the various methods of the surface treatment (Fig. 3).

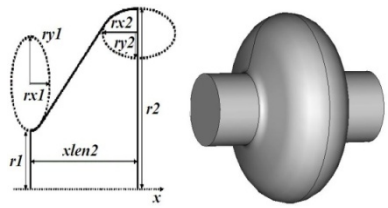

Figure 2: The 1-cell cavity geometry.

Table 1: Main geometry parameters of the 1-cell cavity

xlen2, mm	r1, mm	r2, mm	rx1, mm	ry1, mm	rx2, mm	ry2, mm
56.7	39	103.3	9	12.8	42	42

The generalized plot for the accelerating gradient in the range of 0-30 MV/m is shown in Fig. 4. The main peak of particle growth is obtained at low levels of the accelerating field. The influence of the SEY is insignificant for this kind of calculations; the dependence is the same and the difference is only in the height of the main peaks.

Stable multipacting trajectories of order 2-4 were obtained in the range of 2.6 - 6.3 MV/m and 27.9-35.5 MV/m of the accelerating gradient for over 40 RF periods. The stable 1-2 order multipacting trajectories are obtained in a range of 6.3 – 27.9 MV/m of the accelerating gradient. The latter are the most dangerous.

The direct multipacting simulations were performed in order to find the structure areas which undergo multipacting.

ISBN 978-3-95450-125-0

176 MHZ SOLID STATE MICROWAVE GENERATOR DESIGN

A. Smirnov, A. Krasnov, K. Nikolskiy, N. Tikhomirova, E. Ivanov, S. Polikhov
Siemens Research Center, Moscow, Russia
O. Heid, T.Hughes, Siemens AG, Erlangen, Germany

Abstract

This paper concerns the R&D work upon design of a compact RF amplifier to be used for linear accelerators. The machine under development will operate at 176 MHz with output power of 25 kW in continuous wave regime. It consists of 50 push-pull PCB modules (approx. 500W output power each), connected in parallel to several radial filter rings, which both allow class-F operation and combine the power from the modules, delivering it to a single 50 Ohm coax cable. The CST simulations and the design of 324 MHz test prototype are presented.

INTRODUCTION

High power RF sources are important elements for most of linear accelerators that have found growing number of applications in physics and medicine.

The main benefits of the generator under development will be its smaller size, perspective of lower cost, better reliability and higher efficiency, achieved with class-F operation, compared to conventional RF power sources like klystrons. The solid-state microwave power modules based on SiC vJFET transistors arranged in parallel push-pull circuits, will be designed on PCB boards.

All modules will be connected to a power combiner with common output 50 Ohm coaxial cable.

This generator is planned to be a predecessor to the 'big' 324 MHz machine with pulsed RF output power of 3 MW.

RF POWER MODULES

We have designed and manufactured compact RF power modules with one pair of SiC transistors arranged in circlotron topology [1] as shown on Fig.1.

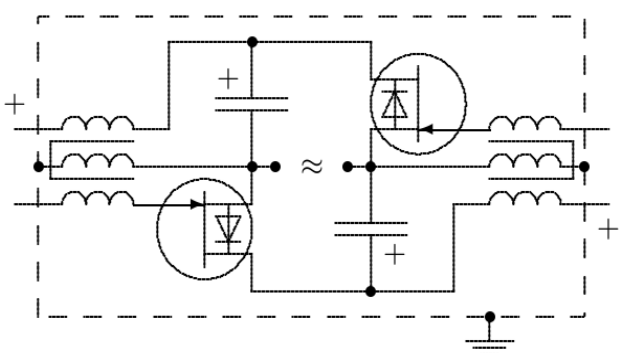

Figure 1: Parallel push-pull circuit

The manufactured module layout is presented on Fig.2. We used Rogers 4003C with ε=3.55 as a substrate material. The transistors are fed with 180^0 phaseshift, provided with external balun. The module provides maximum available gain of 18.9 dB at output power of 2.0 kW and with supply voltage of 150 V.

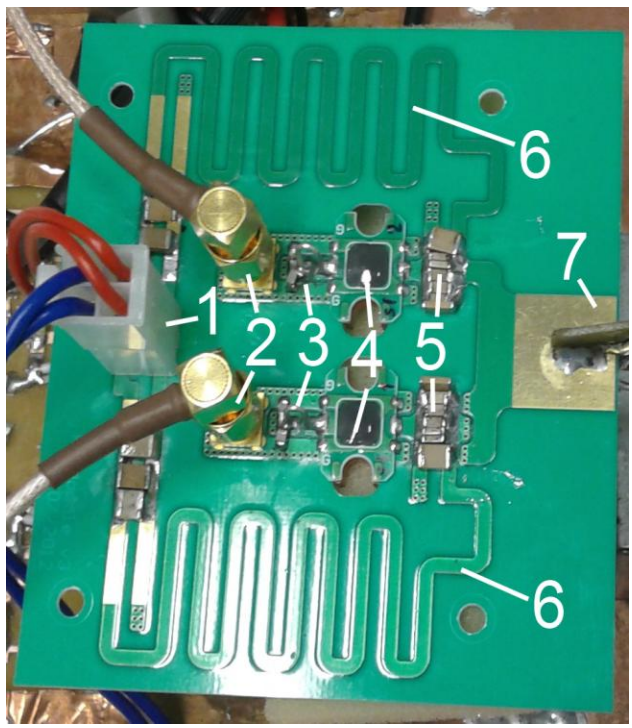

Figure 2: RF power module (heat sink is not shown):
1 – DC supply voltage; 2 – RF inputs; 3 – input matching circuit; 4 – SiC transistors; 5 – DC-blocking capacitors; 6 – quarter-wavelength lines; 7 – symmetric output stripline

Each transistor will be mounted on a water-cooled heat-sink with a sinter paste, as shown on Fig. 3, which can dissipate up to 300 W average thermal power.

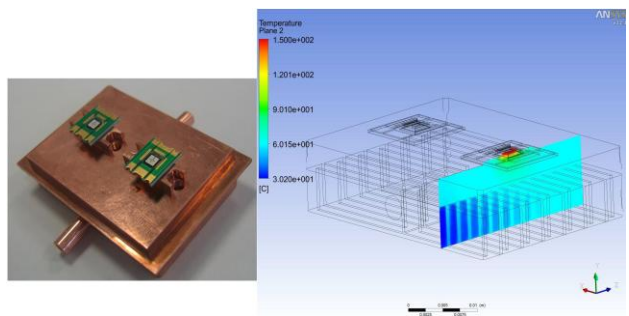

Figure 3: Transistor package mounted on a water-cooling module with temperature distribution

ISBN 978-3-95450-125-0

STATUS OF INR DTL RF SYSTEM

A.V.Feschenko, A.I Kvasha, V.L.Serov, INR RAS, Moscow

Abstract

INR Linac is in regular operation since 1993. The accelerator incorporates DTL and DAW structures operating at 198.2 MHz and 991 MHz correspondingly. Initially two types of high power vacuum tubes specially designed for INR DTL (GI-54A for final amplifier and GI-51A for intermediate amplifier) were used in the RF power system. However production of these tubes has been stopped resulting in a need of DTL RF system upgrade. The main goal of the last upgrades is replacement of the old tubes by modern ones as well as development and implementation of series crowbar system. Replacement of the tubes is not an easy task, because new tubes have to be installed in the old structures. The results and the experience of INR DTL RF system upgrade are presented.

INTRODUCTION

Last time information on the status of INR DTL RF system has been presented eight years ago [1]. Since then several significant upgrades have been done in the DTL RF system including the series crowbar system implementation [2,3] and replacement of powerful grid tubes in both intermediate power amplifier (IPA) and final power amplifier (FPA). Since 1993 up to now grid tubes GI-51A and GI-54A have been in operation in IPA and FPA, correspondingly. However, at the beginning of the nineties manufacture of the above tubes at CSC "SED.-SPb" (former name – Electron Device Mfg. Corp. "Svetlana") has ceased and INR DTL RF system operation continued only due to the earlier plentiful supplies. At the same time the new grid tube GI-71A ("Katran") [4] was developed and designed in the CSC "SED-SPb" as the alternative to GI-54A. The requirement for GI-71A was to keep the dimensions and the anode-grid capacity C_{ag} about the same as for GI-54A in order to avoid essential reworking of the anode-grid cavity.

GI-71A tubes have been tested in the final power amplifiers of INR DTL RF system for ten years. Now they are installed in four of five FPA, including the most powerful amplifier for the third drift tube cavity.

Replacement of GI-51A (tetrode) by GI-57A (triode) appeared to be more complicated task and additional investigations were required.

RESULTS OF THE SERIES CROWBAR SYSTEM LONG TERM OPERATION

The series crowbar system (SCS) has been described earlier [2, 3]. At that time the system was in operation for 700 hours only. By now it is in operation for more than 5000 hours. The system cuts off anode HV pulse in case of discharges or sparking in IPA or FPA. One should note that the SCS can be realized only for vacuum tube modulators, which is the case in INR DTL RF system. Now the modulator is intended for three purposes:

1. Generation of the anode high voltage pulses for IPA and FPA tubes.
2. Control of the anode voltage with the aim of stabilization of the accelerating field amplitude.
3. Protection of IPA and FPA grid tubes in case of sparking or discharges inside of the tubes.

There are two main reasons of crowbar system activation.

The first one is due to HV breakdowns in the anode-grid cavity. Neither in IPA nor in FPA blocking capacitors are used for separation of HV and RF circuits. HV is applied to the central conductor of the coaxial cavity at the node of RF electric field. The voltage between the central conductor and the ground is a superposition of the anode pulse voltage and the cavity RF one. RF voltage is an order of magnitude higher than the anode voltage and the probability of RF breakdown is not negligible. The RF breakdown initiates HV breakdown, and, as a result, the full discharge of modulator storage device capacitors. The activated series crowbar system cuts off the modulator pulse thus preventing discharge of the capacitors and excessive local energy dissipation.

The second reason is breakdown or sparking in the grid tube directly. We have no possibility to preliminary age new tubes so there are numerous breakdowns for several days after installing new grid tubes in RF amplifiers. Earlier each sparking inside the tube resulted in interruption of accelerator operation for 10-15 minutes. New series crowbar system enables to diminish the interruptions to a few sec only. As a result we have got a possibility to age tubes during accelerator operation and have essentially decreased beam interruptions.

INTERMEDIATE POWER AMPLIFIER

Utilization of new grid tube GI-57A in IPA instead of GI-51A was not a trivial task not only due to different sizes of the tubes but also due to different modes of operation: GI-51A has operated with common cathode and GI-57A is foreseen for common grid operation.

Changing of the tube resulted in a need of additional calculation of the anode-grid cavity electrodynamics. Eigen mode frequencies as well as field distributions have been calculated and analysed. Special attention was paid to field distribution in the loop area as well as to higher modes that could be excited.

The model of the anode-grid cavity is shown in Fig.1.

ISBN 978-3-95450-125-0

INVESTIGATION OF INR DTL RF SYSTEM OPERATION AT 100 HZ REPETITION RATE

A.N.Drugakov, A.V.Feschenko, A.I.Kvasha, A.N.Naboka,V.L.Serov, Institute For Nuclear Research, Moscow 117312, Russia

Abstract

INR Linac has been operating with 50 Hz beam repetition rate so far. Increasing the repetition rate up to 100 Hz is of importance as it results in doubling of the beam intensity. To solve the task several accelerator systems have to be modernized but the most critical one is DTL RF system (up to 100 MeV). The problems related to DTL RF system repetition rate increasing are described. One of the problems is a 50 Hz modulation of a 100 Hz RF pulse sequence. Though the instabilities of accelerating field due to the modulation are reduced by the feedback systems, nevertheless investigation of the effect and its minimizing is of importance. The analysis of the effect is given and the results of experimental studies are presented. Other problems to be overcome to increase the repetition rate are mentioned as well.

INTRODUCTION

Operation with the repetition rate of 100 Hz was foreseen by initial design of INR linac [1]. However since commissioning for more than twenty years accelerator operated with 50 Hz repetition rate satisfying requirements of beam users. Recently the goal of doubling of the repetition rate has been formulated with the aim of increasing the beam intensity and efficiency of the accelerator. Several problems have to be solved: increasing of the repetition rate of HV proton injector, commissioning of beam pulse separation system [2] etc. However the most complicated task is related to RF system of the accelerator. The accelerator consists of low energy part (100 MeV, DTL, 198.2 MHz) and high energy part (600 MeV, Disk and Washer structure, 991 MHz). Initial tests of RF equipment with 100 Hz repetition rate revealed modulation of rf field pulses with 50 Hz frequency. One of the origins of the effect was found to be biperiodic triggering of rf equipment. Accelerator clocking pulses are coupled to one of the mains phases and a 100 Hz sequence is generated at zeroes of 50 Hz voltage. Due to distortions of sinusoidal waveform the clocking pulses were not equidistant thus resulting in a different levels of charging of pulse forming lines used to generate HV pulsed for klystrons (high energy part) and power grid tubes (low energy part). Special measures taken to provide exact periodicity of 100 Hz series enabled to eliminate the effect for high energy part but appeared to be ineffective for low energy part. Further study showed that the main reason of the effect in low energy part is using of AC current for directly heated cathodes of power grid tubes.

DTL RF SYSTEM

DTL RF system includes seven RF channels: one for RFQ and six for five accelerating cavities, one of them being a spare channel. A simplified block diagram of one RF channel is shown in fig. 1. The channel represents a four stage amplifier (K1÷K4) with two anode pulse modulators MB and M1.

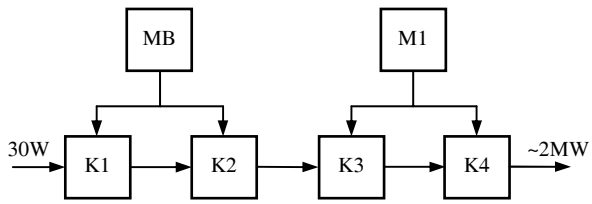

Figure 1: Block diagram of DTL RF channel.

Both amplifier stages and pulse modulators use power grid tubes. The upgrade of DTL RF system with replacement of grid tubes is under way now [3]. The type of grid tubes used in RF channels at present is given in table 1.

It will be shown that the mode of cathode heating (direct or indirect) is essential for 100 Hz operation. It is listed in table 2 for all the types of tubes used in DTL RF system.

Table 1: Type of grid tubes

Unit	RF channel						
	RFQ	1	2	3	4	5	6
K1,K2	GS-31B	GS-31B	GS-31B	GS-31B	GS-31B	GS-31B	GS-31B
K3	GI-51A	GI-51A	GI-51A	GI-57A	GI-57A	GI-51A	GI-51A
K4	GI-54A	GI-71A	GI-54A	GI-71A	GI-71A	GI-71A	GI-54A
MB	GMI-34A	GMI-34A	GMI-34A	GMI-34A	GMI-34A	GMI-34A	GMI-34A
M1	GMI-44A	GMI-44A	GMI-44A	GMI-44A	GMI-44A	GMI-44A	GMI-44A

Table 2: Mode of cathode heating

Tube	GS-31B	GI-51A	GI-57A	GI-54A	GI-71A	GMI-34A	GMI-44A
Directly heated cathode		*	*	*	*		*
Indirectly heated cathode	*					*	

50 HZ MODULATION OF 100 HZ RF PULSE SEQUENCE

After switching the RF channels from 50 Hz mode to 100 Hz mode of operation a 50 Hz modulation of RF channel output power and hence of the envelopes of RF fields in DTL cavities was immediately revealed. As an example Fig. 2 demonstrates a screen view of oscilloscope with the envelopes of RF field in DTL cavity

ISBN 978-3-95450-125-0

X-RAY RADIATION HIGH-VOLTAGE ELEMENTS OF THE TANDEM ACCELERATOR WITH VACUUM INSULATION

I. Sorokin #, A. Bashkirtsev, A. Ivanov, D. Kasatov V., A. Kuznetsov, S. Taskaev, V. Chudaev,
BINP SB RAS, Novosibirsk, Russia

Abstract

In Institute of Nuclear Physics SB RAS the epithermal neutron source is entered into operation based on the tandem – accelerator with vacuum isolation. There was evaluated the accelerating installation components of a x-ray field causing dark current and breakdowns in accelerating gaps. The estimated account of equivalent doze capacity on different distances from the accelerator in the protected hall and behind its limits is made.

The experimental measurements were carried out and the study results of the doze capacity dynamics are submitted, depending on change of a dark current in tandem accelerating gaps at a complete working voltage 1 MV without a beam. The spectrum of x-ray radiation is experimentally measured. It is experimentally revealed and the occurrence of powerful X-ray radiation is investigated at substantial growth of the aperture of the accelerating channel. The design changes of installation for prevention of occurrence of powerful X-ray radiation are offered and realized.

The carried research allows setting necessary parameters for designing medical installation on the basis of an accelerator - tandem with vacuum isolation with the purpose of realization in oncological clinics neutron-capture therapy of malignant tumors.

INTRODUCION

In the BINP, the prototype of epithermal neutrons source in an innovative high-current tandem accelerator with vacuum insulation has been proposed [1] and constructed [2]. It is attractive to be accommodated in oncological clinics for carrying out boron neutron capture therapy of malignant tumors.

In the high-voltage vacuum components of the installation, electrons of auto emission and discharge origin, which are the basic elements of the parasitic "dark" current [3] and are accelerated in a vacuum gaps, emit X-rays after braking at the electrodes, which is the main source of radiation hazard in operation without the accelerated charged particles beam. The study of the unused X-ray field of the installation and the method to reduce its radiation hazard to an acceptable level is an urgent task, as the accelerator is being developed for medical purposes.

EXPERIMENTAL MEASUREMENT OF X-RAYS LEVELS ON THE INSTALATION

For operational monitoring of X-ray radiation levels around the experimental installation and for its biological defense, tandem is equipped with automatic radiation monitoring system (provided services) [4], developed in BINP.

Dose rate measurements of photon radiation in the system are carried out by four detecting units (Fig. 1),

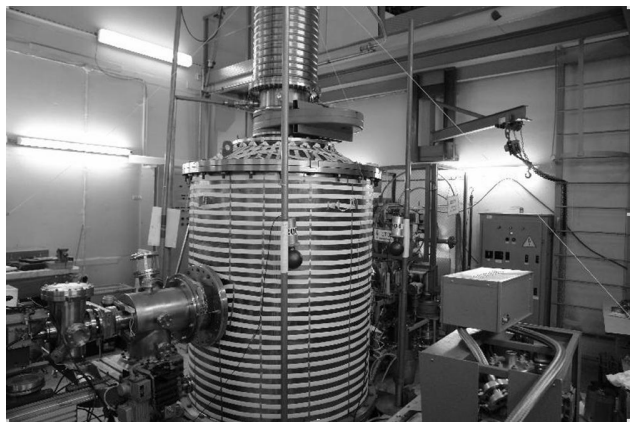

Fig. 1. Placement detection units around the accelerator.

Fig.2. Detection unit dose power of photon radiation.

based on the spherical ionization chambers (Fig. 2) with an air-filling 0.85 liter volume and with a thickness of polyamide wall about 1.1 mm, coated with a thin layer colloidal graphite.

Using the organic dielectric, as a wall material, can reduce overall dimensions and weight of the detector and can help to avoid significant deterioration in the camera's sensitivity to low-energy radiation. The dynamic range of the detector is - 1 ÷ 12 000 mcSv/h.

To determine the uniformity level of X-ray radiation in the azimuth plane, around the accelerator at a distance of

ISBN 978-3-95450-125-0

RESIDUAL ACTIVITY IN HEAVY-ION ACCELERATORS AS BEAM-LOSS LIMITING FACTOR

V. Chetvertkova, E. Mustafin, I. Strasik, GSI, Planckstrasse 1, 64291 Darmstadt, Germany

Abstract

Residual activity is one of the main beam-loss limiting factor in high-energy proton accelerators. In order to ensure 'hands-on' maintenance 4 h after the shutdown, the losses of proton beam should be kept below 1 W/m. It has been shown in our previous publications that the beam-loss criteria for heavy-ion machines may be established by rescaling the '1 W/m criterion' for protons into a similar 'n W/m' criteria for different heavy ions. For protons the scaling factor is obviously 1. Scaling factors for other ions depend on the charge number of the ion and on the beam energy. For example, for U ions with energy E = 200 MeV/u the scaling factor is 60, i.e. 60 W/m losses of U beam are tolerable from the 'hands-on' maintenance point of view, whereas for U ions with E=1 GeV/u the scaling factor is just 5. In the present paper we show that this scaling factor concept has natural limits of applicability. In the case of very low beam energies or in the case of long-term accumulation of the residual activity, the tolerable beam-loss criteria cannot be obtained by simple rescaling of the '1 W/m criterion' with one single number.

INTRODUCTION

An energetic heavy ion penetrating into a bulky target typically destroys several target nuclei. Therefore the total residual activity of the target is usually dominated by the radioactive fragments of the target nuclei and has negligible contribution from the projectile fragments. As it was shown in [1] the relative number of produced radioisotopes in this case does not depend on the type of bombarding heavy ion projectile at the energy range from 200 AMeV to 1 AGeV, and the evolution of the induced radioactivity has the same time dependence for protons and all heavy ion beams. This allows rescaling the whole radioactivity evolution curve from proton induced activity to any heavy ion beam induced activity just by one number. For example, this number is 1/60 in the case of rescaling the 1-GeV-proton induced activity into the activity induced by 200 MeV/u U beam [1]. This means that the well known 1 W/m tolerable beam loss limit for proton accelerators can be rescaled to 60 W/m tolerable loss limit for a 200 MeV/u U beam machine.

This rescaling concept works only for the case when the number of created target fragments considerably exceeds the number of projectile fragments stopped in the bulky target. One could expect a violation of this concept for example in the case of low-energy heavy ion machines. Indeed, low energy heavy ions have very short ranges in a bulky target and do not develop any considerable shower of projectile fragments. Therefore, the interactions with primary projectiles play more important role compared to the production of isotopes via the secondary particles.

The other limit of the simple rescaling concept to be checked is the accumulation of the long-lived isotopes: the long-lived isotope inventory may be different than the short-lived isotope inventory studied in [1].

COMPARISON OF TOTAL ACTIVITIES INDUCED BY PROTON AND URANIUM BEAMS

To study the extremes, let's compare the total activity induced by 1 W beams of protons and U ions lost into a bulky target (a cylinder 20 cm in diameter and 60 cm long, like in [1]) made of Cu.

In order to study the long-term accumulation of isotopes and their following decay, the irradiation time and the consecutive 'cooling-down' time were chosen to be 20 years each. All calculation of the activity were done using FLUKA code [2].

As it is shown in Table 1 the evolution of the total activity has the same time dependence for both p and U beams in the case of high energy beams E=500 and 1000 MeV/u. Indeed, the ratio of the normalised activities (shown in the columns denoted as U/p in Table 1) is within about 30% spread. The normalisation of the activity is done to the end of irradiation (i.e. to the activity at time point 20 years).

Table 1: Time evolution of the total activity for 500 and 1000 MeV/u p and U beams

year	Activity, Bq, 500 MeV/u			Activity, Bq, 1 GeV/u		
	p	U	U/p	p	U	U/p
1	8.2E+9	7.2E+8	0.99	9.3E+9	1.8E+9	0.97
2	8.7E+9	7.6E+8	0.99	9.9E+9	1.9E+9	0.96
5	9.2E+9	8.1E+8	0.99	11E+9	2.0E+9	0.91
10	9.8E+9	8.7E+8	1.00	11E+9	2.2E+9	1.00
20	9.9E+9	8.8E+8	1.00	11E+9	2.2E+9	1.00
21	1.7E+9	1.5E+8	0.99	2.1E+9	3.9E+8	0.93
22	1.2E+9	1.2E+8	1.13	1.6E+9	3.0E+8	0.94
25	7.5E+8	7.6E+7	1.14	1.1E+9	1.9E+8	0.86
30	4.7E+8	4.8E+7	1.15	7.0E+8	1.3E+8	0.93
40	2.6E+8	2.7E+7	1.17	3.9E+8	7.4E+7	0.95

The same shape of the time evolution of the activities for both p and U beams indicates in the case of high-energy beams that the total activity is dominated by the same isotopes, i.e. by the isotopes produced from the target nuclei by the secondary projectiles.

The time evolution of the total activity has a different behaviour in the case of low energy p and U beams. As it is shown in Table 2 only the accumulation of the activity

ISBN 978-3-95450-125-0

STUDY OF DYNAMICAL APERTURE OF NICA COLLIDER WITH ACCOUNT OF MAGNETIC FIELD ERRORS AND COULOMB EFFECTS

A.Ye. Bolshakov, P. R. Zenkevich, ITEP, Moscow, Russia

Abstract

By use of MADX code beam dynamics in NICA collider has been studied. NICA collider has comparatively small kinetic ion energies (1.5-4.5 *GeV/u*) that results in essential one beam Coulomb effects. These effects are simulated by set of "BEAM-BEAM" elements with appropriate chosen strength and location. Moreover it was taken into account beam-beam interaction, system of chromaticity correction and influence of systematic and random errors of the magnetic field. The simulation results are given and discussed.

Coulomb Forces

In collider Coulomb forces result in effect of "beam-beam" interaction. In linear approximation shift of the betatron tune because of the effect is defined of so named "beam-beam parameter", which for symmetrical Gaussian beams is defined by

$$\xi = -r_i \frac{N_b}{4\pi\beta^2\gamma\varepsilon}\frac{1+\beta^2}{2} \qquad (1)$$

Here the classical ion radius $r_i = \frac{Z^2 r_p}{A}$ (r_p - classical proton radius, A and Z are atomic and charge ion numbers), β, γ – relativistic, N_b is the number of ions per bunch, ε is r.m.s beam emittance. Non-linear kick in the interaction point results in appearance of a set of non-linear resonances (see, for example, [1]). Let us use model of "frozen beam", which is assumed that this effect does not influence on a particle distribution in a phase space. In MADX code [2] this effect is described by special element (Beam-Beam element) located in the interaction point. NICA collider has comparatively small kinetic energy (1.5-4.5 GeV) and therefore there are essential "one beam" Coulomb forces, which result in shift of the betatron tune (Laslett tune shift)

$$\Delta Q = -\frac{r_i N_b}{4\pi\beta^2\gamma^3\varepsilon}F_b \qquad (2)$$

Here we assume that the beams have Gaussian distribution. The bunching factor $F_b = \frac{C_{ring}}{\sqrt{2\pi}\sigma_s}$, where C_{ring} is the ring circumference, σ_s is r.m.s. longitudinal size of a bunch. Dependence of the tune shift with longitudinal coordinate z tune shift

$$\Delta Q(z) = \Delta Q \cdot \exp\left(-\frac{z^2}{2{\sigma_s}^2}\right) \qquad (3)$$

Periodical oscillations of the tune shift because of the synchrotron oscillations result in crossing of high order betatron resonances. Coulomb shift due to simultaneous action of both effects (for two interaction points) $\Delta Q_c = \Delta Q + 2\xi = -\frac{N_b r_i}{4\pi\beta^2\gamma\varepsilon}\left[\frac{F_b}{\gamma^2} + (1+\beta^2)\right]$. In choice of machine parameters we assumed that $|\Delta Q_c| \le 0.05$. Then maximal beam intensity

$$N_b^{max} = 4\pi\beta^2\gamma\frac{|\Delta Q_c|}{\frac{F_b}{\gamma^2}+(1+\beta^2)}\frac{\varepsilon}{r_i} \qquad (4)$$

In high energy region (3-4.5 *GeV*) in NICA collider the intensity is limited by IBS and $N_b^{max} = 2.4 \cdot 10^9$ ions [3]. Let us mark that for equal tune shifts Coulomb effect due to the beam-beam interaction is more dangerous than one-beam one. Thus for given intensity the most dangerous point in high energy region corresponds to $E = 3\ GeV$. In low energy region (1.5-3 *GeV*) the intensity is defined by Eq. (3) and the most dangerous point corresponds to the lowest energy ($E = 1.5\ GeV$). In this report we choose for simulations point $E = 3\ GeV$.

Code for numerical simulations

Simulations are made using MAD-X code with account of the following factors:

1) Chromaticity correction system, which is corrected machine chromaticity and chromaticity due to sextupole errors in the collider magnets.
2) Systematic errors and random errors in the collider magnets. Systematic errors are accepted same as in paper [4] (these errors are given at Table 1). Random errors correspond r.m.s. value equal to 1/3 from systematic errors. For simplification we take into account only one set of random errors.
3) Beam-beam Coulomb forces with two similar interaction points.
4) One-beam Coulomb forces.

Table 1: Systematic errors in the magnets

$\frac{1}{BR}\left(\frac{d^2B_y}{dx^2}\right)$ m^{-3}	$\frac{1}{BR}\left(\frac{d^4B_y}{dx^4}\right)$ m^{-5}	$\frac{1}{BR}\left(\frac{d^6B_y}{dx^6}\right)$ m^{-7}
-0.027	76.312	-1.489E5
$\frac{1}{BR}\left(\frac{d^8B_y}{dx^8}\right)$ m^{-9}	$\frac{1}{BR}\left(\frac{d^{10}B_y}{dx^{10}}\right)$ m^{-11}	$\frac{1}{BR}\left(\frac{d^{12}B_y}{dx^{12}}\right)$ m^{-13}
-2.669E10	-7.507E14	-6.616E18

Calculations are made in "thin lens approximation" in order to provide a simplecticity [5]. The synchrotron motion is simulated by inclusion in lattice the cavity with voltage 1 *MV*. Initial distribution in phase space is assumed to be Gaussian one, number of macro particles is 20000-300000, number of turns 1000-5000. Influence of "one beam" Coulomb forces is taken into account by use of "beam-beam" non-linear lenses located in the centers of all lattice elements (such method was used earlier in [6]). Beams in the "beam-beam" elements are assumed to be in one direction, which allows us to describe correctly Lorentz force. Dependence of space charge force on

ISBN 978-3-95450-125-0

EFFECT OF GOLD NUCLEI RECOMBINATION IN ELECTRON COOLING SYSTEM ON BEAM LIFETIME IN THE NICA COLLIDER

O.S. Kozlov, A.B. Kuznetsov, A.V. Tuzikov, A.V. Philippov#
Veksler and Baldin Laboratory of High Energy Physics, JINR, Dubna, Russia
I.N. Meshkov, Dzhelepov Laboratory of Nuclear Problems, JINR, Dubna, Russia

Abstract

On the basis of experimental data the production of the ions Au^{78+} and Au^{77+} as a result of step-by-step radiative recombination of bare nuclei on free electrons in the NICA Collider electron cooling system is presented. The influence of Au^{78+} ions on the luminosity lifetime is discussed. The optimum working cycle of the NICA Collider is described.

LUMINOSITY LIFETIME

The NICA Collider working cycle will consist of the following modes: collision mode during time T and reloading mode during time ΔT. The average luminosity $\langle L(T)\rangle$ can be estimated using the following formula:

$$\left\langle L(T)\right\rangle = \frac{\int_0^T L(t)\,dt}{T+\Delta T}. \qquad (1)$$

For the round beams the peak luminosity L_{max} can be calculated in accordance with the formula:

$$L_{max} = \frac{N^2}{4\pi\varepsilon_\perp \beta^*} F_{coll} f_{HG}\left(\frac{\sigma_s}{\beta^*}\right). \qquad (2)$$

Where N is the bunch intensity; $\varepsilon_\perp$ is the transverse unnormalized rms emittance; β^* is the beta function in the interaction point; σ_s is the rms value of the longitudinal beam size; F_{coll} is the collision repetition frequency and factor f_{HG} is define the hour glass effect. When the emittance and bunch length are stabilized by electron cooling (we assume that the cooling power is adjusted for exact compensation of the beam heating due to intrabeam scattering process) the luminosity lifetime is determined by the bunch intensity variation only:

$$\frac{1}{L}\frac{dL}{dt} = 2\frac{1}{N}\frac{dN}{dt}.$$

During the collision mode the ion losses lead to decrease of the total beam intensity by the value ΔN (in each ring of the NICA Collider). Thereafter one needs to provide debunching of the beam, injection of a few portions of the ions from the Nuclotron and beam bunching to prolong the collisions. The time ΔT required for these procedures can be estimated approximately to $\Delta T = 250$ s [3]. In this estimation the beam preparation time that describes the full period of time required for the beam debunching and adiabatic capturing in the NICA Collider (in the estimations below we used rather optimistic value of 10 s).

Maximizing the average luminosity (1) we can obtain optimum duration for the collision mode of the NICA Collider operation.

More powerful process leading to the ion losses during the collisions is the radiative recombination (RR) of gold ions on free electrons in the NICA Collider electron cooling system i.e.:

$$\frac{1}{L}\frac{dL}{dt} \propto -\frac{2}{\tau^{RR}}. \qquad (3)$$

Here τ^{RR} is the characteristic time of the bunch intensity variation due to RR process.

In this case the average luminosity (1) can be written as follows:

$$\left\langle L(T)\right\rangle = \frac{\tau^{RR}}{T+\Delta T(T)}\cdot\frac{1-e^{-2T/\tau^{RR}}}{2}\cdot L_{max}. \qquad (4)$$

Resume all that was said above the information about beam intensity kinetics is needed.

BEAM INTENSITY KINETICS DUE TO RR PROCESS

The analysis of Au^{79+} bare nuclei and Au^{78+}, Au^{77+} ions beam formed in the NICA Collider electron cooling system in energy range of 1÷4.5 GeV/u has shown (Fig. 1) that most of the Au^{77+} ions will be lost at the vacuum chamber aperture $r_x = 60$ mm during approximately 1.8 μs (one revolution period). The amount of surviving Au^{77+} ions increases with beam energy but does not exceed 5% at 4.5 GeV/u. In this case for our goal it is sufficient to consider RR process of Au^{79+} bare nuclei into Au^{78+} ions. The ions of lower charge states can be neglected because they lost on vacuum chamber aperture at the first turn in the NICA Collider ring after their generation.

Therefore the set of kinetic equations describing formation of Au^{78+} ions owing to RR process of Au^{79+} bare nuclei on free electrons in the NICA Collider cooling system can be written as follows:

#philippov@jinr.ru

ISBN 978-3-95450-125-0

PROGRESS IN NICA BOOSTER DESIGN

A.Butenko, H.Khodzhibagiyan, V.Mikhaylov, I.Meshkov, G.Trubnikov, A.Tuzikov, A.Valkovich, A.Sidorin, JINR, Dubna, Russia

Abstract

NICA is a new accelerator complex being under design and construction at Joint Institute for Nuclear Research in Dubna. A few changes in NICA booster ring design took place over the last half a year.The most significant one is making use of DFO doublet optical structure instead FODO lattice studied previously. Based upon this new optics the injection and extraction systems were proposed. Both "One time, many turn" and "Many times, one turn" schemes of injection are presented here. Fast extraction system (to inject beam to Nuclotron) is mentioned too. Optimal arrangement of the closed orbit correction system (correctors,BPMs) was found. Chromaticity correction system with relatively small reduction in dynamical acceptance is paid attention to.

INTRODUCTION

The NICA/MPD project [1] started at the Joint Institute for Nuclear Research (JINR) in Dubna in 2007. The goal of the project is to carry out experimental studies of the hot and dense strongly interacting quantum chromodynamics matter and light polarized ions. The NICA accelerator complex will consist of two injector chains, a new 600MeV/u superconducting booster synchrotron, the existing superconducting synchrotron – Nuclotron [2], and the new superconducting collider consisting of two rings each of about 503 m in circumference. The report presented is to describe the latest results of the R&D efforts in NICA booster ring design.

OPTICAL STRUCTURE OF THE BOOSTER RING

One of the most significant developments in the overall design of the booster ring is the choice of DFO-doublet-based lattice. In previous reports FODO lattice was considered as the most possible solution for the ring.

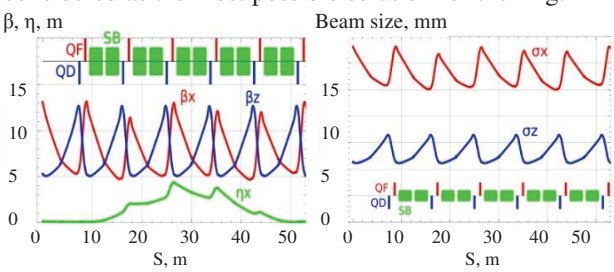

Figure 1: Optical functions and envelopes in the ring.

Optical structure of the booster ring has periodicity and has four super periods. Each of them has 5 regular DFO periods and one period having no bended magnets in it. Regular period includes couple of lenses (defocusing and focusing ones) and couple of bended dipole magnets. Schemes of both regular DFO period and straight section are presented at the Fig.1.

Table 1: Main parameters of the Booster ring

1. Main Parameters		
Energy of injection, MeV		6.2
Maximum energy of the Au+32 ions,MeV/amu		600
Magnetic rigidity, T·m	at injection	2.2
	maximum	600
Circumference, m		211.2
Coulomb intensity limit, part/cycle		5×10e9
Transition energy, GeV/amu		4.5
2. Lattice and Magnetic Elements		
Number of superperiods		4
DFO-type periods		24
Dipole magnets		40
Quadrupole lenses		48
Magnetic field in dipole magnets, T		1.8
Gradient in F/D-lenses, T/m		24.7/-24.2

Lattice functions in one super period are presented at Fig.1 Envelope functions of the beam corresponding to the physical acceptance of the vacuum chamber (Ex=123π mm mrad, Ey=66 π mm mrad) and energy spread (estimated to be ~5×10e-3) are shown at the Fig.1. Main parameters of the optical structure of the booster ring are given at the Table 1.

INJECTION AND EXTRACTION SCHEMES

njection system for the booster ring with new DFO optics was developed. By now, three major injection schemes are at the table: “one time, many turns”, “many times, one turn” and “one time, one turn”.

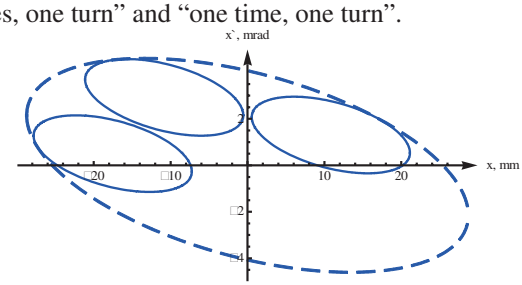

Figure 2: “One time, many turns” injection scheme in phase space.

ISBN 978-3-95450-125-0

DEVELOPMENT OF STOCHASTIC COOLING TECHNIQUE FOR NICA PROJECT

N. Shurkhno#, A. Kobets, I. Meshkov, V. Seleznev, A. Sidorin, G. Trubnikov, JINR, Dubna, Moscow region
R. Stassen, IKP, FZ Juelich, Germany

Abstract

Joint Institute for Nuclear Research (JINR) initiated the creation of a new and unique heavy-ion collider – Nuclotron-based Ion Collider Facility (NICA), which is planned for commissioning in 2016. The luminosity in the colliding beams of gold ions is expected to reach 10^{27} $cm^{-2}s^{-1}$. By estimations the luminosity will be mainly determined by the intra-beam scattering effect. To suppress this, a cooling system should be used. For the medium and high-energy heavy ions such as at NICA collider, stochastic cooling will be more efficient than electron cooling, so that system will be used in the collider. It was decided to construct a prototype stochastic cooling system, which can be tested at the Nuclotron in an early stage of the NICA project. A longitudinal stochastic cooling system was constructed in 2011. The report presents first experimental measurements and further developments of the stochastic cooling system.

INTRODUCTION

JINR is in the initial phase of constructing the NICA collider [1] for which both longitudinal and transverse stochastic cooling systems are obligatory. We are developing the stochastic-cooling system of NICA at the existing Nuclotron superconducting synchrotron at JINR. So, we gain experience of stochastic cooling in a NICA-specific environment [2]. The prototypes has been designed and tested during the years 2010 and 2011. The experiment with this constructed stochastic cooling system was carried out in November 2011. In the course of the experiment, longitudinal Schottky noise and beam transfer function were measured and the optical notch-filter was tested. Since experiment the scheme of the system was significantly developed and improved. The results of the experiment as well as new system design will be discussed below.

EXPERIMENT SETUP AND RESULTS

Main parameters of the accelerator and the cooling system are summarized in Table 1.

Table 1: Parameters of cooling system

Circumference, m	251.5
Ions	Deuterons, C6+
Energy, GeV/u	0.5-4
Rev.frequency, MHz	1.13
Number of particles	10^9
Momentum spread, Δp/p	10^{-3}
Ring slip factor	0.0322
System bandwidth, GHz	2 - 4

The first step of the realization of the stochastic cooling experiment was longitudinal cooling of coasting beam. The dispersion value is too small in the section, where the pick-up is placed, so Palmer method cannot be implemented. Instead a scheme with a notch filter was installed. The octave band of 2-4 GHz was chosen for that system. The scheme of the system is shown in Fig. 1.

Slot ring couplers, developed and produced at FZ Juelich [3], were used for pick-up as well as for kicker. Both structures have identical design – an assembly of 16 rings with 8 electrodes each. Longitudinal coupling impedance of each ring is 9 Ohms. The pick-up is placed in a cryostat at 10 K, while the kicker is placed at room temperature. Each output of pick-up has a 34 dB low-noise pre-amplifier. The outputs are then combined together. The optical notch-filter [4, 2] was adjusted for 2 GeV deuteron beam; the notch depth was not less than 35 dB.

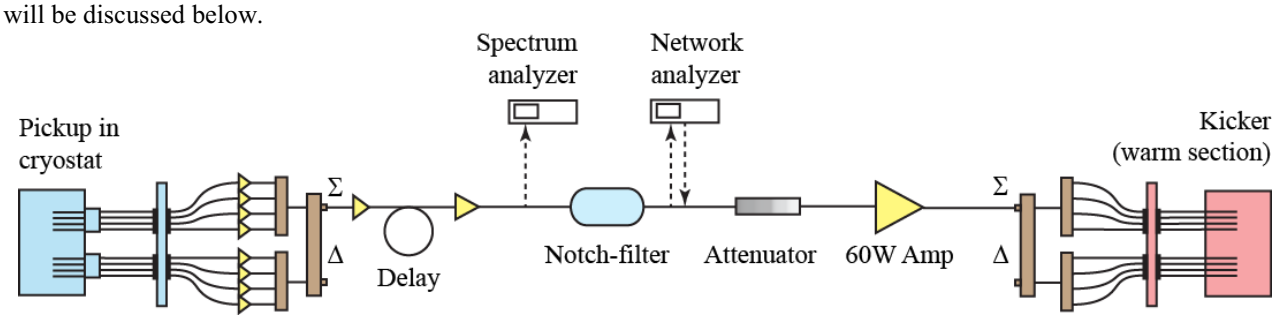

Figure 1: The scheme of stochastic cooling system in experiment.

#shurkhno@physics.msu.ru

ISBN 978-3-95450-125-0

LEPTA PROJECT: TOWARDS POSITRONIUM

E.Ahmanova, V.Kaplin, V.Karpinsky, V.Lokhmatov, I.Meshkov, V.Pavlov, A.Rudakov, A.A.Sidorin, S.Yakovenko, JINR, Dubna
A.Kobets#, JINR, Dubna and Institute of Electrophysics and Radiation Technologies, NAS of Ukraine
M.Eseev, JINR, Dubna and M.V.Lomonosov Pomor State University, Russia

Abstract

The project of the Low Energy Positron Toroidal Accumulator (LEPTA) is under development at JINR. The LEPTA facility is a small positron storage ring equipped with the electron coolin system. The project positron energy is of 2 – 10 keV. The main goal of the facility is to generate an intense flux of positronium atoms – the bound state of electron and positron.

Storage ring of LEPTA facility was commissioned in September 2004 and was under development up to now. The positron injector has been constructed in 2005 ÷ 2010, and beam transfer channel – in 2011. By the end of August 2011 experiments on electron and positron injection into the ring have been started. The recent results are presented here.

LEPTA RING DEVELOPMENT

The Low Energy Particle Toroidal Accumulator (LEPTA) is designed for studies of particle beam dynamics in a storage ring with longitudinal magnetic field focusing (so called "stellatron"), application of circulating electron beam to electron cooling of antiprotons and ions in adjoining storage electron cooling of positrons and positronium in-flight generation.

For the first time a circulating electron beam was obtained in the LEPTA ring in September 2004 [1]. First experience of the LEPTA operation demonstrated main advantage of the focusing system with longitudinal magnetic field: long life-time of the circulating beam of low energy electrons. At average pressure in the ring of 10^{-8} Torr the life-time of 4 keV electron beam of about 20 ms was achieved that is by 2 orders of magnitude longer than in usual strong focusing system. However, experiments showed a decrease of the beam life-time at increase of electron energy. So, at the beam energy of 10 keV the life time was not longer than 0.1 ms. The possible reasons of this effect are the magnetic inhomogeneity and resonant behaviors of the focusing system.

Positron Transfer Channel

The channel is aimed to transport positrons extracted from the trap of the injector (see below) and accelerate them up to 10 keV (maximum) in electrostatic field in the gap between the trap and the channel entrance. The designing and manufacturing of the channel elements was completed in 2010(Fig. 1).

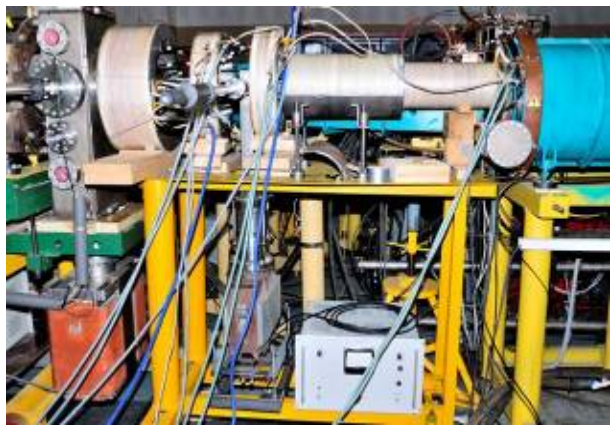

Figure 1. The transfer channel.

Circulating e+ Beam Detector

For fine tuning of the trajectory and control of circulating positron beam aperture probe based on semiconductor gamma detector has been designed (Fig.2). Fabrication of the probe is in progress.

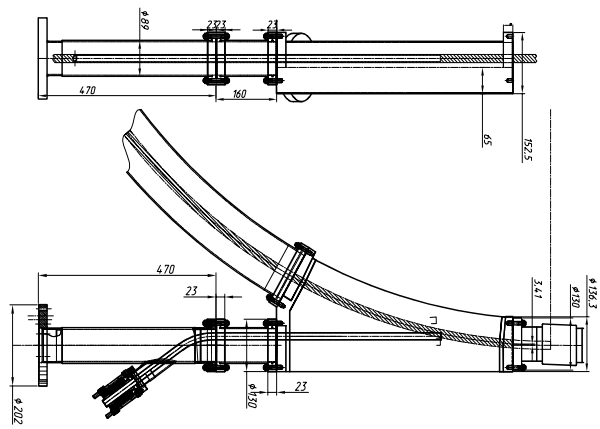

Figure 2. The circulating e^+ beam detector.

THE POSITRON INJECTOR

In summer 2010 the slow positron source and the trap have been assembled. The first attempts of slow positron storage were performed (Fig.3) and stored positrons were extracted to the collector.

kobets@jinr.ru

ISBN 978-3-95450-125-0

COMPRESSION AND CONFINEMENT OF POSITRON CLOUDS IN THE SURKO TRAP OF LEPTA FACILITY*

E. Ahmanova, A. Kobets, I. Meshkov, A. Rudakov, S. Yakovenko, JINR, Dubna, Russia
M. Eseev#, A. Vititnev, NAFU, Arkhangelsk, Russia

Abstract

A bunch of positrons confined in a cylindrical Penning-Malmberg trap can be compressed radially by applying a rotating asymmetric dipolar electric field. An explanation of this effect presented in the report is based on the solutions of particle 3D dynamics equations in the fields of the trap taking into account the positron collisions with a neutral buffer gas. The result agrees well with experimental data obtained at the positron injector of LEPTA facility at JINR. Essential feature of the compression process is resonant character of applied rotating field and coincidence its frequency with the frequency of longitudinal positron bouncing in the trap.

INTRODUCTION

The LEPTA facility consists of the source of positrons, the trap and storage ring for generating positronium stream [1]. The Penning-Malmberg trap operates in pulsed mode, accumulating positrons from the source. At accumulation is important to increase the number of the storage particles and clouds in the lifetime of the trap and optimized parameters for this accumulation. It is important to ensure the uniformity of the longitudinal, in relation to the axis of the trap, the magnetic field required pressure of the buffer gas (nitrogen), the distribution of confining potential (see Fig. 1).

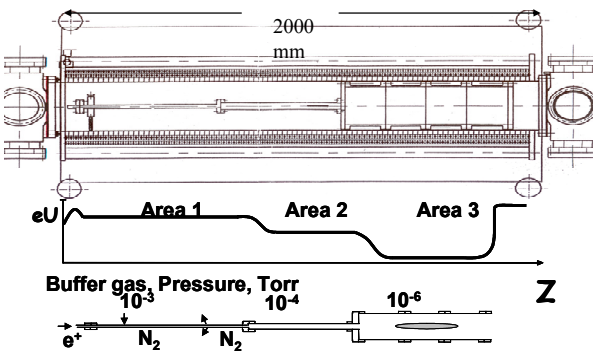

Figure 1: The scheme of the trap. Longitudinal section. Injector accumulated particles to the left in Figure.

In the Surko trap the rotating electric field (the RW-field) created by the electrodes of discontinuous (see Fig. 2). This can significantly improve the accumulation of particles [2,3]. The trap scheme is shown in Figure 1. Previously presented the optimal parameters of accumulation of particles in the trap [4]. Mechanism of action of the rotating field on the accumulation of particles has been discussed. There are different approaches to explain this effect [3,5,6]. For further consideration is the formulation of hypotheses about the need to consider context of longitudinal and transverse motion of the particles in the trap to explain the effect of the rotating field. Will also present experimental verification of the hypothesis.

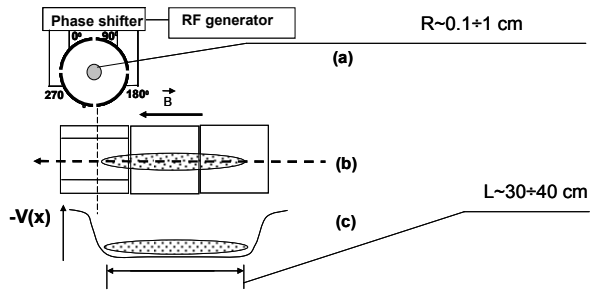

Figure 2: "Rotating wall" (RW) technique: rotating electric field at the trap entrance.

3D-DYNAMICS OF PARTICLE

What is the mechanism for increasing the lifetime confinement and focus particle clouds the use of RW field?

3D-hypothesis

Consider the field and the forces acting in the transverse and longitudinal section of the trap on the particle (see Fig. 3). This is **B** – the longitudinal magnetic field (axis z), $\mathbf{E}_R$ – the field of the space charge of the particle cloud, $\mathbf{E}_\omega$ – the rotating wall field, $\mathbf{E}_{b,r}$, $\mathbf{E}_{b,z}$ – transverse and longitudinal component of the field locking electrode traps.

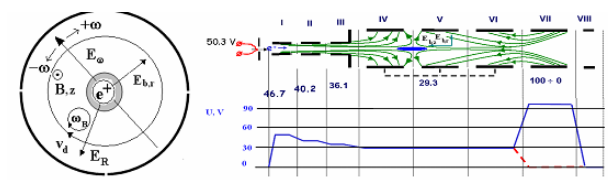

Figure 3: Field distribution in the trap in the longitudinal and transverse section.

Previously, we and other authors have noted the good agreement of the resonance frequency of the RW field f with the drift frequency in the transverse direction $f_{drift} = cE/B$. Some studies indicated agreement with the longitudinal bounce frequency f. This allowed us to assume that the effect of compression and increase the lifetime of clouds stored particles is observed in agreement longitudinal and transverse 3D-motion of the

*Work supported by grants RFBR №09-02-00084, FCP№14.A18.21.1302.
#m.eseev@narfu.ru

ISBN 978-3-95450-125-0

TRANSFER CHANNEL FROM BOOSTER TO NUCLOTRON AT THE NICA FACILITY

G. Filatov#, I. Meshkov, V. Mikhaylov, A. Sidorin, N. Topilin, G. Trubnikov, A. Tuzikov,
JINR, Dubna, 141980, Russia

Abstract

In the last years the Nuclotron-based Ion Collider fAcility (NICA) project is developed at Joint Institute for Nuclear Research (JINR), Dubna, Russia. Important elements of the NICA are two synchrotrons: Booster and Nuclotron. Connection between these synchrotrons is provided with the transfer channel for heavy ions at energy of 600 MeV/u. The transfer channel includes a stripping station and charge separation system. General goal of the optic design is to minimize emittance at the exit of the channel. Magnetic system of the channel will be constructed using magnets of the Nuclotron type.

INTRODUCTION

The NICA project [1] aims to construct the new accelerator facility for colliding beam experiments. The first stage of the project is experiments on heavy ion beams particularly gold ions. Goals of the transfer channel between Booster synchrotron and existing Nuclotron are the following: the beam transport with minimum ion losses and minimum increase of the beam emittance; ion stripping to a maximum charge state (the goal charge of the beam) and the separation of parasitic charge states. The design parameters of the ion beam are given in Table 1.

Table 1: Design parameters of the beam

Sort of ions	
before stripping station	Au^{31+}, Au^{52+}, Au^{65+}
after stripping station	Au^{79+}
Maximum energy of ions, MeV/u	685
Maximum magnetic rigidity of ions, T m:	
before stripping station	25
after stripping station	11
Ion number	$2 \cdot 10^9$

The channel has some features considered in the physical design of the channel:

- complex 3D geometry which proposes the installation of tilt bending magnets;
- presence of the striping station and the necessity of the separation of parasitic charge states;
- different magnetic rigidities of ions before and after the striping station;
- wide ranges of momentum spread values, horizontal and vertical emittances at the entry of the channel;
- increase of the beam emittance in the channel because of ion stripping and betatron coupling;
- mismatch of the beam parameters with lattice functions of Nuclotron.

Old version of physical design of the channel has been presented in early works [2, 3]. New schemes of the beam extraction from Booster and the beam injection into Nuclotron are applied that impact on the channel geometry. Also, the new lattice of the channel is designed considering minimization of transverse emittances after the beam injection into Nuclotron.

LATTICE OF THE TRANSFER CHANNEL

The geometry and the magnetic system of the channel are mainly defined by the mutual position of Booster and Nuclotron. These synchrotrons have different radii and vertical positions of their median planes. The vertical distance between median planes of the synchrotrons is 3.76 m. The beam is extracted from Booster in both directions. The horizontal extraction angle is 120 mrad, the vertical extraction angle is 30 mrad. The beam is injected into Nuclotron in the vertical plane at an angle of 350 mrad. The beam in the channel is transported in the horizontal and vertical directions simultaneously. The total length of the channel is 23.2 m. Its azimuthal size is 45°, which corresponds to the beam injection through one Nuclotron octant from the point of extraction from Booster.

The channel consists of 5°tilt sector bending magnets and 7°quadrupoles, 2 of which are tilt ones. Magnetic elements of the beam are superconductive with an iron yoke. One quadrupole has the opportunity to reverse a polarity. Vacuum chamber of the channel has a circle cross section with a diameter of 60 mm.

The stripper station is situated inside the Booster yoke. Parasitic charge states after stripping is separated by the optical system of the channel and then a superconductive Lambertson magnet.

General view of the Booster-Nuclotron channel and a view from above are given in Fig. 1, 2. Vertical profile of the channel is shown in Fig. 3 (the profile means a side view of the linearized channel so it differs from any lateral view of the channel itself). Lattice of the channel is presented in Fig. 4, where BM1-BM5 — bending magnets, Q1-Q7 — quadrupoles, LM — Lambertson magnet, Str — stripping station. Main parameters of the magnetic elements are given in Table 2.

#filatov.jinr@mail.ru

ISBN 978-3-95450-125-0

SNOP – BEAM DYNAMICS ANALYSIS CODE FOR COMPACT CYCLOTRONS

V.L. Smirnov, S.B. Vorozhtsov, JINR, Dubna, Russia

Abstract

The SNOP program complex intended for particle dynamics simulations in a compact cyclotron from the injection line to the extraction system is described. The main features of the SNOP are usage of 3D electric and magnetic field maps, beam space charge effect calculation, and analysis of the beam losses on the structure elements of the facility under consideration. The optimal usage of modern computer capabilities and graphic libraries for visualization is a key issue in the SNOP development. The beam dynamics modeling results for various cyclotrons are presented.

INTRODUCTION

Recently, compact cyclotrons are widely used for solution of fundamental and applied problems. Noticeable expenses that are needed for the design and operation of the cyclotrons impose stringent requirements on the accuracy of the simulations conducted to select the facility parameters and to assess the beam dynamics peculiarities. There are a number of available codes such as TRANSPORT [1], MAD [2], TRACE3D [3], and COSY [4] based on the matrix formalism for the design and study of beam-optics systems. Some of them include detailed beam space charge calculations. However, none of these codes provides a full description of the peculiarities of beam dynamics in a compact cyclotron. The other group of the programs is prepared for special accelerating facilities [5, 6]. It is problematic to use these codes for the beam dynamics analysis in the cyclotron as a complete setup, from the injection line to the extraction system. This situation appeals to preparation of programs that can be easily applied to any cyclotron facility, operate with 3D (spatial) electric and magnetic field maps, take into account the beam space charge effects, and most effectively use resources of modern computers. The program complex SNOP that is produced at JINR and intended for simulation of beam dynamics in a compact cyclotron complies with all the above-mentioned requirements. The SNOP is a qualitative extension of the CBDA code described in [7].

PROGRAM COMPLEX DESCRIPTION

The main features of the SNOP are usage of 3D electric and magnetic field maps, beam space charge effect calculation, and analysis of the beam losses on the structure elements of the facility under consideration. The optimal usage of the modern computer capabilities is a key issue in the SNOP development.

Complex Structure

The program complex is convenient to use due to its user-friendly interface (see Fig. 1). The SNOP is structured in such a way that there are dedicated blocks responsible for real units in the beam transport line and accelerator itself. There are also separate menus to control parameters of acceleration particles and setting parameters for the equation of particle motion including beam space charge effects.

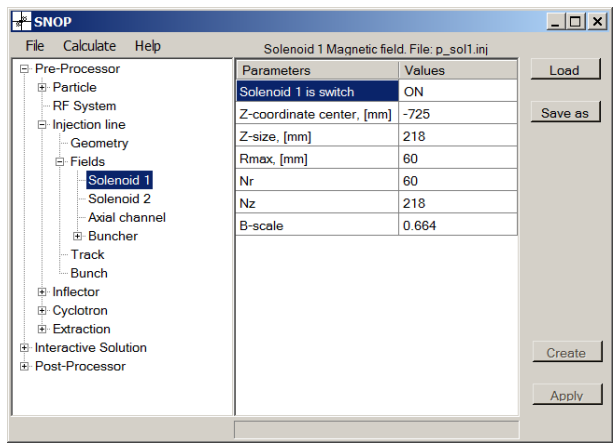

Figure 1: SNOP main window.

The program complex shell permits one to control parameters of the electromagnetic devices for the beam acceleration and focusing, such as the dee electrode, solenoid, electrostatic inflector, magnetic and electrostatic quadrupole, magnetic channel, electrostatic deflector, and main, trim and harmonic coils.

The SNOP shell is prepared in such a way that it is possible to modify available parameters without editing any files manually.

The tooling for the magnetic field analysis permits full-size calculations of the magnetic field characteristics. The mean magnetic field, flutter, betatron tunes, amplitudes of radial oscillations, etc can be calculated using analytical formulas and closed equilibrium orbit computation.

There is a possibility of using such systems as MathCAD and AutoCAD, with which data exchange can be carried out. MathCAD is applied at the initial data generation and for analysis of the results. AutoCAD permits one to specify geometry of the objects when calculating particle losses and to depict the positions of the accelerated and lost particles against the background of the real geometry of the facility (see Fig. 2).

ISBN 978-3-95450-125-0

RF SELF–CONSISTENT ELECTRON BEAM DYNAMICS SIMULATION IN THZ GENERATOR BASED ON PHOTOINJECTOR AND CHERENKOV DECELERATING SYSTEM

T.V. Bondarenko, S.M. Polozov, O.A. Tatsyuk,
National Research Nuclear University Moscow Engineering Physics Insitute, Moscow, Russia

Abstract

The generator of high intensity monochromatic radiation in sub-mm range is currently under R&D at the Department of Electrophysical Facilities of MEPhI. This generator is based on photoinjector and irradiating Cherenkov capillary. It is necessary to have high brightness electron beam for generation of monochromatic radiation in this type of structure. Such beam can be produced by photocathode and accelerated to energy of several MeV using short structure with high acceleration efficiency. Irradiating capillary represents as metal tube with inner radius of the radiation wavelength order and covered with dielectric layer or made of corrugated waveguide. It is important to study the self-consistent dynamics of the beam during the acceleration as the current pulse is equal to several A, i.e. the beam dynamics should be studied considering both RF (radiation) and Coulomb components of self-field of beam. Another problem is to study the electron beam dynamics and fields irradiated by it in decelerating structure in the absence of external fields. The scheme of irradiating facility, its operation mode and high-current beam dynamics simulation results in accelerating structures are presented.

INTRODUCTION

The generators of high intensity monochromatic radiation in sub-mm range are highly demanded nowadays and developed for a number of research centers and applied tasks. One of the applications is cargo inspection system that demands high power THz radiation and working mode with repetition rate about tens of Hz.

High radiation power can be generated using large accelerator (linear or synchrotron) and free electron laser (FEL) but such facilities are not compact. Traditional vacuum (e.g. traveling wave tubes) and solid state (OLED, resonant tunnel diodes) generators doesn't provide the power level higher than 1 W.

THz radiation generation can be obtained using Cherenkov or Smith-Purcell radiation capillary channels and photoinjector accelerating system [1].

The important problem is investigation of self-consistent beam dynamics, mathematical model development and high current relativistic beam dynamics simulation during the acceleration and going through the irradiating structure.

In common case it is necessary to solve the motion equation together with Maxwell's equations. But sometimes we can replace the solution of Maxwell's equations (this is a quite complicated task) by the solution of Poisson's equation (for example, if we are looking for the solution of motion equation for intensive non-relativistic ion beams) or excitation equation (in case of ultrarelativistic beams, when we can neglect the Coulomb component of self-field of the beam). But for some tasks we have to consider both quasi static Coulomb component of self-field and RF radiation field of the beam.

The developed model considers full self-consistent field (both Coulomb component and radiation field), induced by beam in structure.

The key feature of the model is external field absence in irradiating structure.

FACILITY SCHEME

The coherent Cherenkov radiation can be generated using short and well collimated electron bunches with ps or sub-ps duration and 100-200 μm transverse size. Such bunch can be formed using a photocathode and compact accelerating system providing high accelerating gradient. The laser system in photogun is proposed to generate a series of short laser pulses which irradiate photocathode placed in the sidewall of an accelerating system. It was proposed to separate the accelerating structure into two sections (Fig. 1).

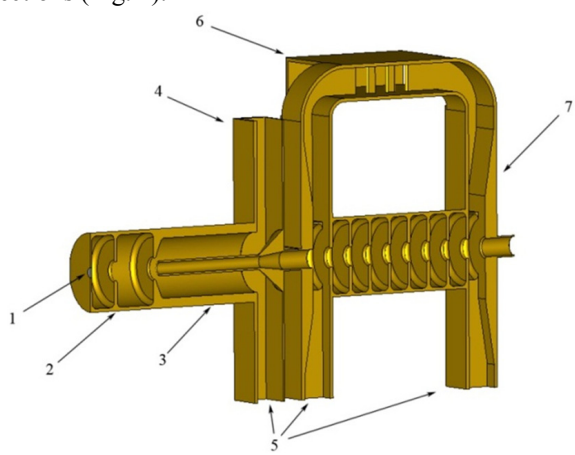

Figure 1: Accelerating system: 1 – photocathode, 2 – 1.6 cell structure, 3 – coaxial wavetype transformer, 4 – power input, 5 – vacuum ports, 6 – directional coupler, 7 – travelling wave resonator structure.

The first accelerating system is based on 1.6-cell disk loaded waveguide (DLW) and provides maximum accelerating fields on the cathode surface. After that the bunch (or bunch packet) should be accelerated in the

ISBN 978-3-95450-125-0

RF QUADRUPOLE FOCUSING LATTICES

A.S. Plastun, T.V. Bondarenko,
NRNU MEPhI, Moscow, Russia

Abstract

Spatial homogeneity of a conventional RFQ allows estimating parameters of the lattice easily. Hybrid-RFQ structures with spatially periodic RFQ lenses are more complicated in respect of beam dynamics. Transverse stability of beam motion is defined by lattice parameters. Basically parameters of RF focusing lattices are influenced by longitudinal emittance of a bunch in contrast to static focusing lattices. The paper presents a method which allows evaluating parameters of a very wide class of RF and static quadrupole lattices. Transverse acceptance and acceleration rate could be determined. The method is useful to compare Hybrid-RFQ structures with a conventional RFQ.

INTRODUCTION

The main parameter of periodical focusing lattices is acceptance. It is extremely important for high intensity beams. It is known from the Hill`s equation theory that the acceptance A of any periodical lattice can be defined as [1]:

$$A = \frac{\gamma}{c}\omega_{r\,\min}a^2 , \qquad (1)$$

γ –Lorentz factor, c – the speed of light, $\omega_{r\,min}$- minimum frequency of transverse oscillations of a particle, a – aperture radius of a focusing channel. Another lattice parameter, which describes transverse motion of particle, is a phase advance μ.

$$-1 < \cos\mu < 1 \qquad (2)$$

should be performed to provide stability of transverse motion. The phase advance can be represented as

$$\mu = \int_{t}^{t+T_f} \omega_r(t)dt , \qquad (3)$$

where $\omega_r(t)$ – frequency of transverse oscillations of a particle, t – time, T_f – the period of time for which a particle passes one period of focusing lattice. Thus phase advance μ means the averaged frequency of transverse oscillations for one period.

The accelerating structure of ion linac can be studied with quasi-static approach usually. Estimations for transverse motion of particles in static periodical lattices are generally performed by matrix method or smooth approximation. However range of application of these methods for RF focusing lattices is limited. There is an experience of application of these methods for a conventional RFQ and spatially periodic quadrupole focusing [1]. The limitation consists of low phase advance $\mu << 2\pi$, thin lens approximation and simplicity mainly for FODO lattices [1]. Unfortunately transverse motion of particles in a Hybrid-RFQ is too complicated to be considered by these methods [2].

The focusing lens of a Hybrid-RFQ is too long to use thin lens approximation in the scale of focusing period. Strength of RF focusing lens dependent on time and long focus length don't allow us to use smooth approximation easily.

The paper presents a method which allows studying a very wide class of RF and static quadrupole lattices.

HYBRID-RFQ

A Hybrid-RFQ structure is combined from accelerating gaps and RF quadrupole lenses [3]. Simplified scheme of the structure and its placement with respect to the first RFQ section are shown in Figure 1.

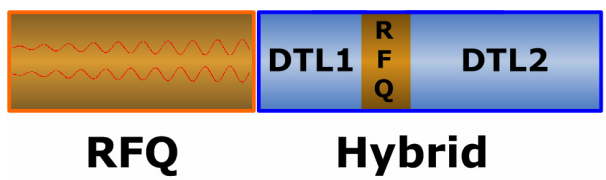

Figure 1: Scheme of Hybrid-RFQ structure.

Focusing regions are formed by vanes with quadrupole symmetry - RFQ-lenses [4]. This part of Hybrid-RFQ structure acts as a conventional triplet of quadrupole lenses. Required focusing strength of RFQ-lenses is defined by distance from axis to vanes.

THE METHOD

The method proposed in this paper is based on several stages:

1. RFQ lens is approximated by electrostatic thin lens with effective gradient $G_{ef} = G_{ef}(\psi, \beta_z)$ dependent on arriving phase ψ and particle velocity β_z. Arriving phase ψ is phase of RF field when a particle arrives at an entrance of RF lens.
2. Effective gradient of the lens and RF defocusing effects of accelerating gaps forms a lattice gradient function $G_{lat} = G_{lat}(z, \psi, \beta_z)$ as a "rectangular" function.
3. Smooth approximation [5] is used to describe the transverse motion of a particle in the gradient G_{lat}. An effective potential function U_{eff} is defined.
4. Study of effective potential function U_{eff} is carried out.

ISBN 978-3-95450-125-0

ANALYTICAL APPROACH FOR BEAM MATCHING

V.S. Dyubkov*, S.M. Polozov, NRNU MEPhI, Moscow, Russian Federation

Abstract

Charge particle beams transportation with small cross-sections and low energies is an actual problem for a gantry. That beams are used actively for isotope therapy. Beam emittance is its quality factor, and it should be matched with a facility channel acceptance. The method for beam dynamics analysis in lattice is developed in terms of non-coherent particle oscillation study. Nonlinear beam dynamics is investigated by using this method. It is shown that this technique allows one to realize effective beam emittance control. Analytical results obtained are verified by means of numerical simulation.

INTRODUCTION

One of the most interesting problems of accelerator engineering to date are the design and development of high-performance high-current compact systems for an injection and acceleration of low-velocity heavy-ion beams. This problem as well as others cannot be solved without taking into account problem solution on beam emittance matching with an acceptance of an accelerator channel. Effective acceptance evaluation for the resonance accelerator channel depends on a mathematical model used for describing a beam dynamics. Effective acceptance evaluation of the resonance accelerator channel was performed previously on basis of charged particle beam oscillation as a whole [1] – [4], that is under the assumption of coherent oscillations of individual particles. It is of particular interest to consider a model, which is taking into account non-coherent particle oscillations in the beam, and analyse results based on it.

BEAM DYNAMICS

It is difficult to analyse a beam dynamics in a high frequency polyharmonic field. Therefore, we will use one of methods of an averaging over a rapid oscillations period, following the formalism presented in [1] – [4]. One first expresses RF field in an axisymmetric periodic resonant structure as Fouriers representation by spatial harmonics of a standing wave assuming that the structure period is a slowly varying function of a longitudinal coordinate z

$$E_z = \sum_{n=0}^{\infty} E_n I_0\left(k_n r\right) \cos\left(\int k_n\, dz\right) \cos\omega t,$$

$$E_r = \sum_{n=0}^{\infty} E_n I_1\left(k_n r\right) \sin\left(\int k_n\, dz\right) \cos\omega t,$$

where E_n is the nth harmonic amplitude of RF field on the axis; $k_n = (1+2n)\pi/D$ is the propagation wave number for the nth RF field spatial harmonic; D is the resonant structure geometric period; ω is the RF frequency; I_0, I_1 are modified Bessel functions of the first kind.

As it was stated above, we will take into account non-coherent particle oscillations in the beam being accelerated. To this end, one introduces a notion of a reference particle, i.e. a particle moving on the channel axis. A magnetic force can be neglected for low-energy ions. We will assume that $dr/dz \ll 1$. Then, one passes into the reference particle rest frame. There is a differentiation over longitudinal coordinate in the beam motion equation. Thus, the motion equation together with an equation of particle phase variation can be presented in a view of a system of the first order differential equations as follows

$$\begin{cases} \dfrac{d\Gamma}{d\xi} = e_z(\xi, 0, \tau^*) - e_z(\xi, \rho, \tau), \\ \dfrac{d\beta_r}{d\xi} = \beta_z^{-1} e_r(\xi, \rho, \tau). \end{cases} \tag{1}$$

Here we introduced the following dimensionless variables: $\Gamma = \gamma^* - \gamma$; γ^* and γ are the Lorentzs factors for the reference and given particles respectively; $\xi = 2\pi z/\lambda$ is dimensionless longitudinal coordinate; $e_{z,r} = eE_{z,r}Z\lambda/2\pi m_0 c^2$; e is the elementary charge; Z is a charge state of an ion; λ is a wave length of RF field; m_0 is an ion rest mass; c is the light velocity in free space; $\beta_{z,r}$ is normalized velocity component.

Let us introduce a new dynamical variable $\psi = \tau - \tau^*$ ($\tau = \omega t$, τ^* is a normalized motion time of the reference particle at the laboratory coordinate system). Note, that

$$\frac{d\psi}{d\xi} = \beta_s^{-3}\Gamma, \tag{2}$$

β_s is normalized synchronous particle velocity, s is the field harmonic number.

Suppose that $|\beta_z - \beta_s| \ll 1$ one can obtain

$$\frac{d^2\psi}{d\xi^2} + 3\varkappa\frac{d\psi}{d\xi} = \frac{1}{\beta_s^3}\frac{d\Gamma}{d\xi} \tag{3}$$

upon differentiation of Eq. 2. The second equation of Eq. 1 can be rewritten as

$$\frac{d^2\delta}{d\xi^2} + \varkappa\frac{d\delta}{d\xi} = \frac{e_r}{\beta_s^3}, \tag{4}$$

where $\delta = \rho/\beta_s$, $\rho = 2\pi r/\lambda$, $\varkappa = \ln'_\xi \beta_s$.

* vsdyubkov@mephi.ru

ISBN 978-3-95450-125-0

SEARCH OF THE MOTION INTEGRAL AT LINAC WITH RF FOCUSING

V.S. Dyubkov*, S.M. Polozov, NRNU MEPhI, Moscow, Russian Federation

Abstract

The problem of the effective linac design is of interest to many fields of science, industry and medicine. It is well known that nonsynchronous harmonics of RF field (RF undulator) are focusing the low-energy particles. Analytical beam dynamics investigation can be carried out by means of the averaging method over the rapid oscillations period (the so-called smooth approximation) in the oscillating fields. Motion equation is presented in the form of the Hamilton's equations. Motion integrals are sought by means of Poincare mapping.

INTRODUCTION

The problem of the effective low-energy linac design is of interest to many fields of science, industry and medicine (e.g. nuclear physics, surface hardening, ion implantation, hadron therapy). There are a few problems that lead to beam instabilities at linacs. Nonlinear effects are the most important among it. Certain nonlinear problems of accelerator physics are both important for successful operation of accelerator and interesting as problems in their own right. In this paper we consider nonlinear interaction between beam particles and a field of accelerator structure. In order to accelerate the low-energy ion beams one of the following fruitful rf focusing types can be used: alternating phase focusing (APF), radio frequency quadrupoles (RFQ), focusing by means of the nonsynchronous wave field as well as the undulator rf focusing. Each of mentioned focusing types has its advantages as well as disadvantages. For example, we consider axially symmetric Wideröe type structure with the rf focusing by the nonsynchronous harmonics [1], [2].

BEAM DYNAMICS

It is difficult to analyse a beam dynamics in a high frequency polyharmonic field. Therefore, we will use one of methods of an averaging over a rapid oscillations period, following the formalism presented in [1] – [3]. One first expresses RF field in an axisymmetric periodic resonant structure as Fouriers representation by spatial harmonics of a standing wave assuming that the structure period is a slowly varying function of a longitudinal coordinate z

$$\begin{aligned} E_z &= \sum_{n=0}^{\infty} E_n I_0\left(k_n r\right) \cos\left(\int k_n\, dz\right) \cos\omega t, \\ E_r &= \sum_{n=0}^{\infty} E_n I_1\left(k_n r\right) \sin\left(\int k_n\, dz\right) \cos\omega t, \end{aligned} \tag{1}$$

where E_n is the nth harmonic amplitude of RF field on the axis; $k_n = (1+2n)\pi/D$ is the propagation wave number for the nth RF field spatial harmonic; D is the resonant structure geometric period (depends on z implicitly); ω is the RF frequency; I_0, I_1 are modified Bessel functions of the first kind.

We shall assume the beam velocity (the one-particle approximation) differs from one of the field harmonic phase-velocities strongly except the synchronous harmonic of rf field, the gap-to-gap spacing of rf structure along the beam axis being defined as $D = \beta_s \lambda\,(s+0.5)$, where s denotes the synchronous harmonic number, β_s is the normalized velocity of the synchronous (equilibrium) particle.

It is convenient to introduce the nondimensional variables $\widehat{\mathbf{\Omega}} = (\xi;\varrho)$ and τ as

$$\widehat{\mathbf{\Omega}} = 2\pi\mathbf{R}/\lambda, \quad \mathbf{R} = \big(z;r\big), \quad \tau = \omega t, \tag{2}$$

then one can write the second Newton's law

$$\frac{d^2\widehat{\mathbf{\Omega}}}{d\,\tau^2} = \widehat{\mathbf{e}}\Big(\tau, \widehat{\mathbf{\Omega}}\Big), \tag{3}$$

where $\widehat{\mathbf{e}} = q\mathbf{E}\lambda/2\pi mc^2$, q and m are charge and mass of a particle.

The particle path in the rapidly oscillating field (1) we search as a certain sum of a some slowly varying term and a rapidly oscillating one. We assume that the amplitude of the rapid velocity oscillations is much smaller than the slowly varying velocity component for the smooth approximation to be employed.

On averaging Eq. 3 over rapid oscillation period one can present the motion equation in the smooth approximation with the restrictions mentioned above in the following form of the Hamilton's equations

$$\frac{d\,\mathbf{\Omega}}{d\,\tau} = \frac{\partial\,\mathcal{H}}{\partial\,\mathbf{\mathcal{P}}}; \qquad \frac{d\,\mathbf{\mathcal{P}}}{d\,\tau} = -\frac{\partial\,\mathcal{H}}{\partial\,\mathbf{\Omega}}, \tag{4}$$

where $\mathbf{\mathcal{P}}$ and $\mathbf{\Omega}$ are the canonically conjugate variables, the canonical coordinates being selected in such a way that the origin in a phase space is an equlibrium point, i.e. $\mathbf{\Omega} = (\overline{\widehat{\mathbf{\Omega}}} - \widehat{\mathbf{\Omega}}_s)/\beta_s$ and the beam-wave system Hamiltonian is

$$\mathcal{H}\left(\mathbf{\mathcal{P}}, \mathbf{\Omega}\right) = \frac{1}{2}\mathbf{\mathcal{P}}^2 + U_{\text{ef}}(\mathbf{\Omega})\,. \tag{5}$$

Here $U_{\text{ef}}(\mathbf{\Omega})$ is the Effective Potential Function which describes the low-energy beam interaction with the polyharmonical field of the system. The EPF depends solely on the averaged variable $\mathbf{\Omega} = (\zeta;\eta)$.

* vsdyubkov@mephi.ru

ISBN 978-3-95450-125-0

DEPENDENCE ON BETATRON OSCILLATIONS OF THE ANGULAR VELOCITY

O.E. Shishanin, Moscow State Industrial University

Abstract

Study of the topic, along with other factors necessary to understand the role of electron oscillations in the formation of the synchrotron radiation. The above-mentioned problem is considered by the author in various periodic magnetic fields. Emergence of the correction terms to the angular velocity of storage rings is also discussed.

At first let us take an axially-symmetric magnetic field as the most extensively studied. In the neighborhood of equilibrium orbit the magnetic field is chosen as

$$H_x = H_y = 0, H_z = br^{-n},$$

where b is the constant, $r = \sqrt{x^2 + y^2}$, n is the field gradient $(0 < n < 1)$. If $rot\bar{H} = 0$ one can concede that the potentials in cylindrical coordinates take the form

$$\Phi = 0, \quad A_r = A_z = 0,$$

$$A_\varphi = \frac{b}{r^{n-1}(2-n)}[1 + \frac{n(2-n)}{2r^2}z^2],$$

where φ is the azimuth angle. The relevant Hamiltonian $\mathcal{H}$ for electron can be written as

$$\sqrt{m^2c^4 + c^2p_z^2 + c^2p_r^2 + \frac{1}{r^2}c^2p_\varphi^2 + e^2A_\varphi^2 + 2ec\frac{A_\varphi}{r}p_\varphi}.$$

One of the Hamilton equations is

$$\dot{\varphi} = \frac{\partial\mathcal{H}}{\partial p_\varphi} = \frac{1}{\mathcal{H}}(\frac{c^2}{r^2}p_\varphi + \frac{ec}{r}A_\varphi),$$

where p_φ is the integral of motion.

Let us denote a small variable by $\rho = r - R$, where the equilibrium radius R can be deduced on condition that linear in ρ terms for Hamiltonian are absent (parabolic approximation). This gives

$$R = (\frac{2-n}{1-n}\frac{cp_\varphi}{eb})^{\frac{1}{2-n}}.$$

Restricting our selves to terms $\rho^2/R^2, z^2/R^2$, we can obtain the angular velocity as

$$\dot{\varphi} = \omega_0(1 - \frac{\rho}{R} + \frac{3-n}{2}\frac{\rho^2}{R^2} + \frac{n}{2}\frac{z^2}{R^2}), \qquad (1)$$

where $\omega_0 = ceH_0/E$ is the frequency, energy E is the constant, $H_0 = b/R^n$. The well-known asymptotics for oscillations have the form

$$\rho = A\cos(\sqrt{1-n}\omega_0 t + \chi), z = B\cos(\sqrt{n}\omega_0 t + \psi), \quad (2)$$

where A and$B$ are, respectively, the amplitudes of radial and axial vibrations, χ and ψ are the initial phases. Total velocity $v = \beta c$ is also constant and

$$v = R\omega_0\sqrt{1 + (1-n)\frac{A^2}{R^2} + n\frac{B^2}{R^2}}.$$

Expressions (1) and (2) made it possible to solve the synchrotron radiation problem [1] for given magnetic field. In such a case it has been found an essential influence of vertical oscillations on the spectral and angular properties of radiation in agreement with experiment. Here we can take only the linear terms and the accuracy was limited by decision (2).

Taking into account for oscillations the quadratic terms one can obtain nonlinear equations

$$\ddot{\rho} + (1-n)\omega_0^2\rho = \frac{\omega_0^2}{2R}[(1-n)(3+n)\rho^2 + n(1+n)z^2],$$

$$\ddot{z} + n\omega_0^2 z = n(1+n)\omega_0^2 z\frac{\rho}{R}.$$

Resolving them by the iterated method we can find, for example, an expression for radiation intensity [2] in a given approximation

$$W = W_0[(1 - \frac{n^2}{2})\frac{A^2}{R^2} - n\frac{3 - 2n + n^2}{2(1-n)}\frac{B^2}{R^2}],$$

where intensity for homogeneous magnetic field

$$W_0 = \frac{2}{3}\frac{ce^2}{R^2}\frac{\beta^4}{(1-\beta^2)^2}.$$

Clearly formula (1) may be also derived from equation

$$\frac{d}{dt}(r^2\dot{\varphi}) = -\frac{e_0}{mc}r(\dot{z}H_r - \dot{\rho}H_z),$$

where the constant of integration is defined as $\omega_0 R^2$.

In studies of radiation in the straight section accelerators we expanded in a power series the transverse components of magnetic field or gradient. Here an electron revolves on orbit consisting of N periods, where one element of the system includes a bending magnet of length $a = 2\pi R/N$ and free gap of length l. The length of entire orbit will be

$$2\pi R + Nl = 2\pi R_0,$$

where $R_0 = (1+k)R$ is the averaged radius, $k = l/a$. After expansion in a series we can put $n(\tau) = f(\tau)n$, where $\tau = N\varphi$ and the discrete function

$$f(\tau) = \frac{1}{1+k}[1 + \frac{2(1+k)}{\pi}\sum_{\nu=1}^{\infty}\frac{\sin\nu\tau_1}{\nu}\cos\nu(\tau - \tau_1)]$$

ISBN 978-3-95450-125-0

COOLING OF ELECTRON BEAMS

V. Khoruzhiy, Kharkov Institute of Physics and Technology, Kharkov, Ukraine

Abstract

We considered cooling of electron beams in synchrotrons (storage rings) using gyro-oscillator by the example of gyromonotron as part of cyclic accelerator at straight-line portion. Gyromonotron is a simplest gyro-oscillator for converting energy of transversal beam energy to oscillation of electromagnetic energy. Cooling of electron beams due to synchrotron radiation (radiative "cooling") is ineffective not only for energy W<50 MeV (low level of synchrotron radiation), but for high relativistic energies too, when positive radiative losses for cooling of a beam were prevailed by another increasing negative force named as Ternov-Sokolov effect (beam radius and emittance growth take place as result of quantum fluctuations of electron trajectories in accelerators). Hence, under high energies (starting from some hundreds MeV) synchrotron radiation is source not only focusing radiative cooling force, but defocusing force too due to recoil effect of electrons under radiation high energy quantum. Using gyromonotrons give possibility to increase maximal beam energy in synchrotrons through cooling of electron beam for prevention beam particles losses due to Ternov-Sokolov effect.

INTRODUCTION

We proposed cooling of electron beams in synchrotrons [1-3] (storage rings [4, 5]) using gyromonotron [6-12] for converting energy of transversal beam energy to oscillation of electromagnetic energy. A gyromonotron is a simplest gyro-device from possible variants (gyrotron, gyromonotron, gyro_BWO) for this purpose. A gyromonotron is cylindrical resonator placed into solenoid's longitudinal magnetic field. We suggest effective cooling of electron beam for energy of one less 50MeV (low level of synchrotron radiation [13, 14]) and especially for energy W of electron beam more than some hundreds MeV, when starts action quantum fluctuations of macroscopic electron trajectories in accelerators (Ternov-Sokolov effect[15-17]). Analytical expression for Ternov-Sokolov effect is

$$W_0 > mc^2 (2\pi mcR / h)^{1/5}$$

where $h / 2\pi$ is reduced Planck constant, R is synchrotron's radius.

Expression for W_0 can be rewritten in a more convenient form for electrons

$$W_0(MeV) > 151.82(R)^{1/5}$$

where radius dimension is [R]=meter.

Quantum fluctuations (recoil of electrons) lead to growth of emittance through additional particles divergence, hence, as result, growth beam dimensions. As result, high energy electron beams have upper limit for synchrotrons energy despite all efforts for focusing one. For former LEP collider maximal beam energy was achieved approximately 100GeV for each beam (electron and positron). We proposed cooling of electron (positron) beams in synchrotrons by gyromonotron as part of cyclic accelerator (storage ring) at straight-line portion for multiple passing the same bunches. Gyromonotron converts energy of transversal movement electrons (positrons) into RF oscillation under corresponding longitudinal magnetic field for constancy of cyclotron frequency. Relativistic cyclotron frequency approximately has to equal RF frequency in synchrotron during accelerating process.

BASIC EXPRESSIONS

The gyromonotron is a HF oscillator for cm and mm band of wavelength. Electron (positron) beams with nonzero transversal velocities are used for excitation electromagnetic wave in resonator nearly cut off frequency. No transversal velocities mean no exciting of electromagnetic waves at all (in gyromonotron). Energy of transversal motion of electron beam converts into energy of electromagnetic wave during multiple passing the same bunches with synchrotron's RF frequency f_0 through gyromonotron nearly cut off frequency $f_{cut\ off.}$ (f_0 - $f_{cut\ off.}$>0). Output window is absent. We choose frequency $f_{cut\ off.}$ (and corresponding wavelength λ) as minimal frequency (H_{111} mode) for gyromonotron's resonator with length L. As well known [18], frequency $f_{cut\ off.}$ of H_{111} mode provides possibility to determine radius of the resonator

$$R = 1.841 / \sqrt{(2*\pi / \lambda)^2 - (\pi / L)^2};$$

$$R \approx \lambda / (2*1.71) \quad for \quad L^2 >> (\lambda / 2)^2$$

We assumed above that resonator's length is

$$L / (2*R) > 1$$

for exciting of H_{111} mode.

Then it is possible for gyromonotron's solenoid to determine longitudinal magnetic field

$$H_{Z0}(kOe) \simeq 10.7 * f_0 / c$$

for low relativistic beam's energy (dimension $[c / f_0] = cm$).

For gyromonotron's operation at given frequency f_0 its needed realization of condition for relativistic cyclotron frequency

$$n * \Omega_{c.rel} / (2*\pi) \approx f_0;\ n = 1, 2...$$

ISBN 978-3-95450-125-0

THE PARAMETERS EXTRACTED BEAMS IN RECIRCULATOR SALO

I.S. Guk, S.G. Kononenko, F.A. Peev, A.S. Tarasenko National Science Centre "Kharkov Institute of Physics and Technology", Kharkov, 61108, Ukraine

Abstract

Optimization of recirculator SALO magnetic structure has allowed to refine essentially beam parameters in points of a leading-out of particles. Beam parameters on an inlet and an exit of the basic channels of an extraction of particles from recirculator are given in article. Calculations are spent taking into account nonlinear field components of dipole and quadrupole magnets of the accelerator.

INTRODUCTION

The recirculator SALO project envisages an extraction of electrons in several experimental halls [1]. As it has been shown in paper [2], nonlinear field component of dipole and quadrupole magnets can exert on recirculator beam parameters appreciable influence. Channels of beam transportation contain enough large number of dipoles and quadrupoles. Therefore beam characteristics can change on these channels under the influence of the same causes. By means of program code MAD X [3] lateral dimensions of beam in extraction points from recirculator and on an exit of beam transportation channels have been counted. Magnitudes sextupole component field of dipole magnets of the injection channel and the first ring of recirculation were are taken from papers [4, 5]. They have been measured in these publications on prototypes of magnets which will be used in recirculator SALO. Dipole magnets of the second recirculation ring and output channels were not produced yet. Because these magnets window type it is natural to assume that the sextupole component of the field of the magnets will not exceed the values measured for the first ring magnets [4]. Octupole component of the value of the quadrupole lenses was calculated based on data from the literature [2].

These data were used for the numerical simulation of the particle dynamics in the recirculator. Sextupole component is taken into account in the description of the dipole. Octupole field component simulated thin lens on the entrance and exit of the quadrupole. The figures present the results of modeling the movement of 3000 electrons through the recirculator magnetic structure.

BEAM PARAMETERS

Location of the main beam channels on the recirculator shown in Fig. 1.

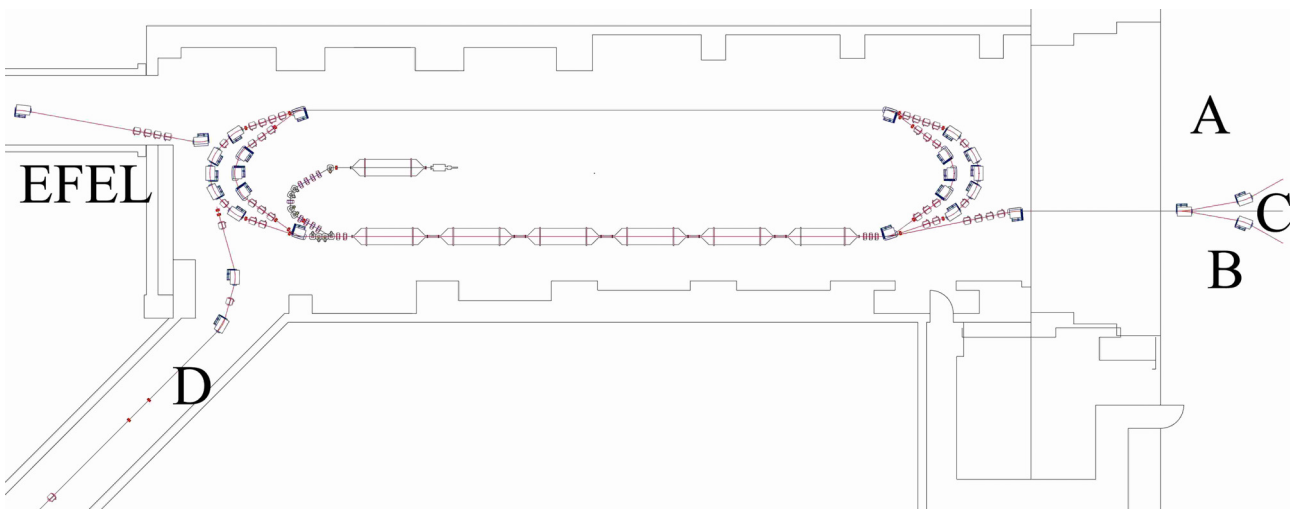

Figure 1: Beam output channels on SALO recirculator.

In channels A, B and C the beam with energy from 60 to 750 MeV [1, 6] can be extracted. For beam formation on channels A and B four quadrupole and two dipole magnets are used (one dipole magnet on the channel C). The electrons with energy to 270 MeV can be received in these halls with use of injection magnetic system and the magnets which are a part of channel magnetic system [3]. To produce a beam with energy of up to 490 MeV it is necessary to use magnetic system of the first ring of recirculation. For obtaining the maximum energy also magnetic system of the second ring of recirculation is used. Thus the bunch will pass accelerating structure three times. The cross-section of a bunch on an entrance to the transportation canal at the maximum energy of 730 MeV is presented on fig. 2. On fig. 3 distribution of particles on an exit from the channel B at distance of 26 m from input point for the same energy is presented.

ISBN 978-3-95450-125-0

INVESTIGATION OF PHASE TRAJECTORIES OF PARTICLE MOTION IN A SYNCHROTRON NEAR THE NONLINEAR RESONANCE OF THIRD ORDER

Yu.A.Bashmakov
P.N.Lebedev Physical Institute, Leninsky Prospect 53, 119991 Moscow, Russia

Abstract

The nonlinear resonance of third order plays an important role in the particle dynamics in circular accelerators, colliders and storage rings and is widely used for slow extraction of particles from synchrotrons. Consideration is carried out in the canonical variables X, Y which at a given accelerator azimuth are simply related to the angle and the deviation of the circulating particles relative to the equilibrium orbit. The problem is reduced to the construction of the phase trajectories, which are the curves of the third or fourth order and determine the type of the motion near the resonance under consideration. The construction of the phase trajectories is performed by the Klein's perturbation method. The influence on the particles dynamics of octupole component of the magnetic fields is investigated.

INTRODUCTION

The problems of nonlinear dynamics play an important role in different fields of modern physics such as elementary particle physics, nuclear physics, plasma physics, quantum electronics and, certanly, in the particle accelerators physics [1]. The nonlinear resonance excitation is wiedly used for particle extraction from circular accelerators [2], the nonlinear resonances action determines dynamical aperture of large circular accelerators and storage rings. One of the most important problems in nonlinear oscillations study is construction of the trajectories of representive points on phase plane and stable motion regions finding.

BASIC THEORETICAL STATEMEMTS

When considering a particle motion in a circular accelerators it is convenient to replace longitudinal coordinate s by so called generalized azimuth ϕ

$$\phi = 2\pi\frac{s}{R_0},$$

where $R_0 = \Pi/2\pi$, and Π - accelerator perimeter.

The equation of one-dimensional particle motion in an accelerator in the presence of a perturbation has the form

$$\frac{d^2x}{d\phi^2} + \nu_x^2 x = \epsilon F\left(\phi, x, \frac{dx}{d\phi}\right), \qquad (1)$$

where x is the transverse displacement of the circulating particle with respect to the equilubrium orbit, ν_x is the betatron oscillation frequency, ϵ is small positive parameter, $\phi = \int \frac{ds}{\nu_x \beta(s)}$, $\beta(s)$ is the betatron function. The function $F\left(\phi, x, \frac{dx}{d\phi}\right)$ is periodic with respect to ϕ function with period equal to 2π. Taking the smallness of the perturbation into acount the solution of the equation (1) can represented in the form, that it has for the homogeneous equation, but now with the amplitude a and the phase ψ depending on the azimuth ϕ [3].

$$x = a(\phi)\cos(\nu_x\phi + \psi(\phi)). \qquad (2)$$

The amplitude a and phase ψ are subjected to the following equations

$$\begin{aligned}\frac{da}{d\phi} &= A(a,\psi),\\ \frac{d\psi}{d\phi} &= \Psi(a,\psi).\end{aligned} \qquad (3)$$

Canonical variables

For further analysis it is convenient to move to the new variables X and Y [4]

$$X = a\cos\psi, \qquad Y = -a\sin\psi. \qquad (4)$$

At a given accelerator azimuth variables X, Y are connected in a simple way with the angle and the displacement of the circulating particle with respect to equilibrium orbit. In these variables equations (3) take the canonical form

$$\begin{aligned}\frac{dX}{d\phi} &= \frac{\partial H}{\partial Y},\\ \frac{dY}{d\phi} &= -\frac{\partial H}{\partial X},\end{aligned} \qquad (5)$$

where $H(X,Y)$ is the Hamiltonian. Such change of the variables and use of the Hamiltonian allow to make a descriptive analysis of the particles motion on the phase plane (X,Y). Curves on which the particles move are determined by the equation $H(X,Y) = const$. From the conditions

$$\begin{aligned}\frac{dX}{d\phi} &= \frac{\partial H}{\partial Y} = 0,\\ \frac{dY}{d\phi} &= -\frac{\partial H}{\partial X} = 0,\end{aligned} \qquad (6)$$

the postions of the specific points on the phase plane are determined.

ISBN 978-3-95450-125-0

MULTY FREQUNCY STORED ENERGY RF LINAC

V.G.Kurakin, P.V.Kurakin, Lebedev Physical Institute, Moscow, Russia

Abstract

Due to beam loading, accelerating gradient in rf linac is reduced in time if the energy acquired by charged bunches is not compensated by external generator that feeds the linac. Since the bunch energy gain in this mode of operation correlates strongly with bunch number, the energy spectrum of total bunch train might be corrected in order to suppress this additional spectrum widening. This spectrum control might be achieved with the rf cavity that operates at frequency shifted relative the main one in such a way, that any new bunch sees the cavity field in the appropriate phase correlated with bunch number. The first bunch traverses correcting cavity in field node while the last one in the phase, where the energy acquired by this bunch is equal to resulting bunch train energy spread arising from beam loading effect. Measures for suppression of non coherent bunches spectrum widening are suggested leading to insertion additional cavity excited at frequency shifted relative the main and adjacent frequencies.

INTRODUCTION

In RF linac, that might be represented as RF cavity and a train of charged bunches traversing the cavity, the bunches increase their energy due to the work of electric force of electromagnetic field inside the cavity. If the energy being carried out of cavity is compensated by external RF generator one has steady state acceleration. In this case, any new bunch from the bunch train acquires the same energy while traversing the cavity. In stored energy mode, external rf generator is used to excite cavity – to produce definite level of rf field before acceleration takes place while charged bunches get energy from the power stored in the cavity. Any new bunch carries away some portion of stored electromagnetic energy thus resulting in reduction of this energy and hence in corresponding reduction of the field level. The total bunch train is found to have energy spread after acceleration, its width being the function of the train charge accelerated. This seems to be the main shortcoming of stored energy mode of linac operation that limits this method for many applications.

In this paper, we discuss the possibility to avoid or compensate partially this spectrum widening for coherent motion.

QUALITATIVE ESTIMATIONS AND THE MAIN IDEA

The energy W stored inside rf cavity

$$W = QP/\omega \tag{1}$$

where Q is the cavity quality factor and ω stands for cavity eigen frequency, while P is the power dissipated in cavity walls. Any bunch from bunch train carries out of cavity the portion of energy

$$\Delta w = qU = ITU = IT\sqrt{PR}\,. \tag{2}$$

Here q, U, I, T denote bunch charge, accelerating voltage, average beam current and RF field period respectively, R is real part of cavity shunt impedance. After acceleration bunch train consisting of N bunches, reduction of accelerating gradient can be estimated as

$$\Delta U = \frac{\Delta E}{e} = \pi N I \frac{R}{Q} \tag{3}$$

Depending on relation between cavity time constant $\tau = 2Q/\omega$ and beam pulse duration t bunch energy drops down as linear function of time for the case $t << \tau$. This linear energy fall down might be eliminated by the accelerating gap with linear dependence of gap voltage on the number of the bunch entering the gap, the difference between the energy gain of the last bunch and the first one being equal to the energy spread defined by the formula above. A cavity on the beam path that is excited at frequency that differs from the main one by the value defined below provides necessary spectrum correction, and fig,1 serves to illustrate such a correction.

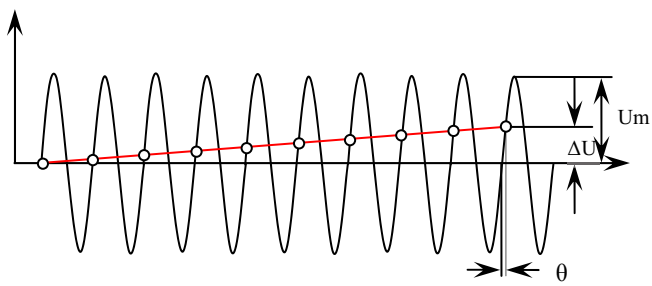

Fig.1 Spectrum correction

It can be calculated from fig.1 that $\theta = \Delta E / eU_m$. From the other hand

$$\theta = \omega(N-1)(T_1 - T_2) = 2\pi(N-1)\frac{\Delta\omega}{\omega}. \tag{4}$$

It follows from these two expressions that

$$\frac{\Delta\omega}{\omega} = \frac{\Delta E}{2\pi e U_m (N-1)}. \tag{5}$$

Taking into account formula (3)for cavity voltage reduction after all bunches acceleration one arrives at the next formula for the frequency of correcting cavity

$$\frac{\Delta\omega}{\omega} = \frac{I}{2U_m}\frac{R}{Q} \tag{6}$$

While deriving this expression, we supposed that $\Delta U << U_m$.

ISBN 978-3-95450-125-0

SIMULATION OF HOLLOW ION BEAM FORMATION LINE

H. Barminova, N. Alexeev, A. Golubev, T. Kulevoy, A. Sitnikov, T. Tretyakova
ITEP, Moscow, Russia

Abstract

Heavy ion beam may be used for the matter extreme state creation [1], a forming line must satisfy to certain requirements on beam brightness, spot size and focus position. The original method of hollow ion beam formation - wobbler system - was proposed to deposit the beam energy at cylindrical target [2]. To verify wobbler parameters the beam dynamics simulation was carried out by means of two codes – "Transit", that is a modified code "DINAMION" [3], and G4Beamline [4]. The results obtained are discussed.

INTRODUCTION

Intense heavy ion beam is an effective tool to create matter extreme states in laboratory conditions. The advanced experiments in high energy density physics require the cylindrical target irradiated by the hollow beam [1]. The wobbler system [2] allows to shape such a hollow beam. Preliminary system simulation has illustrated the feasibility of the method [5]. In paper presented the beam dynamics simulation is carried out in order to consider some nonlinear effects that may influence on the beam spot size and focus position.

ITEP WOBBLER SYSTEM DESCRIPTION

A layout of the wobbler system for hollow beam formation line in ITEP (ITEP TWAC project) is based on the system layout for GSI FAIR project [2]. The ITEP wobbler system consists of two four-cell RF-cavities and focusing triplet of quadrupole magnetic lenses. RF-cavities deflect the beam in x- and y-directions. The phase shift between RF-fields in first and second cavities is chosen so that the particle with zero deflection in the first, x-cavity, gains the maximum deflection in the second, y-cavity, and vice versa.

The general requirements for layout were the target size satisfaction and the beamline length limitation in case of the real initial parameters of ITEP beam. In Fig.1 designed layout of the ITEP wobbler system is shown.

The asymmetric quadrupole magnetic triplet follows by the second cavity, the triplet focusing the beam on the target. In this project the target assume to be irradiated from one side.

The whole length of the system is about 8 m, and it is sufficient length under conditions of the ITEP experimental area limitation.

The structure of the channel as well as preliminary parameters of beamline elements are shown in Table 1.

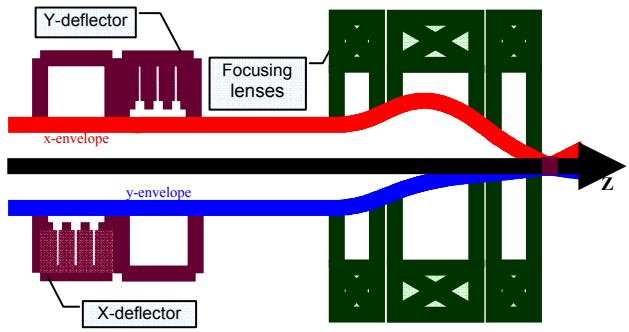

Figure 1: A principal layout of ITEP wobbler system.

Table 1: System structure.

Element	Field value	Element length, mm	Aperture radius, mm
Drift	-	800	100
Wobbler X	1.5 MV/m	4*368	100
Drift	-	184	100
Wobbler Y	2.5 MV/m	4*368	100
Drift	-	800	100
1st magnetic quadrupole lense	15.3 T/m	400	100
Drift	-	160	100
2nd magnetic quadrupole lense	-16.3 T/m	800	100
Drift	-	160	100
3rd magnetic quadrupole lense	18.8 T/m	400	100
Drift	-	~ 900	100

PARTICLE DYNAMICS SIMULATION

The first simulation was carried out for ions Co^{27+}_{59} by means of "Transit-DINAMION" code, developed in ITEP [3]. The beam parameters taken for simulation are close to the real beam parameters in ITEP project. For cobalt ions the beam energy was taken 450 MeV, the pulse duration – 120 ns. Energy spread was varied between 1% and 0.1%. Maximum beam intensity per pulse – $2*10^{12}$ particles. Normalized effective x-emittance (4 rms) was 8 π mm mrad, and normalized effective y-emittance was the same. Initial radius of the beam (at the entrance to the first cavity) was 40 mm.

ISBN 978-3-95450-125-0

MATHEMATICAL MODEL OF BEAM DYNAMICS OPTIMIZATION IN TRAVELING WAVE

A.D. Ovsyannikov, A.Y. Shirokolobov, SPbSU, Saint-Petersburg, Russia

Abstract

In works by B.I. Bondarev, A.P. Durkin, A.D. Ovsyannikov mathematical model of optimization of charged particles dynamics in RFQ accelerators was proposed. In this paper a new mathematical model of optimization of particle dynamics in traveling wave is considered. Joint optimization model of program and disturbed motions is investigated.

INTRODUCTION

In works [1] mathematical model for optimization of RFQ structure was suggested. Transverse and longitudinal motions were investigated separately. But characteristics of transverse motion were considered and analyzed at the stage of longitudinal motion optimization. In particular restrictions were imposed on defocusing factor.

In this paper other model of longitudinal motion based on the selection of program motion (synchronous particle motion) and beam of charged particles (movements in deviations from program motion). This model has been tested for RFQ structure.

Phase of synchronous particle and intensity of accelerating field are considered as control parameters (functions). It should be noted that in paper [1] those parameters also were considered as controls, but mathematical model of optimization was different from the model proposed in this paper.

PROBLEM STATEMENT

Let us investigate the problem of control of longitudinal dynamics of beam in waveguide accelerator as a problem of joint optimization of synchronous particle motion and ensemble of trajectories [3]. As control functions let us choose the laws of changing of dimensionless parameter of the amplitude of the accelerating wave $\alpha(\xi)$ [5] and synchronous phase $\varphi_s(\xi)$ along the structure.

Adopt the following notation $u_1 = \alpha(\xi), u_2 = \varphi_s(\xi)$, where functions $u_1(\xi),\ u_2(\xi)$ are *controls*.

Let the phase of the particle is given by [1]

$$\varphi = \omega \int_0^z \frac{dz}{v(z)} - \omega t + \varphi_s. \tag{1}$$

Under *program motion* (synchronous particle motion) we mean a solution of the system

$$\frac{d\gamma_s}{d\xi} = -\alpha(\xi)\sin\varphi_s,$$
$$\varphi_s = u_2(\xi)$$

with initial condition

$$\gamma_s(0) = \gamma_{s0}.$$

Here γ_s — reduced energy of synchronous particle.

Phase of the beam particles, according to (1) will be considered in the deviation of the phase of the synchronous particle:

$$\widehat{\varphi} = \varphi - \varphi_s.$$

Considering that the longitudinal velocity of the synchronous particle coincides with the phase velocity of the wave, i. e.

$$\beta = \beta_s = \frac{\sqrt{{\gamma_s}^2 - 1}}{\gamma_s}, \tag{2}$$

obtain controlled dynamical system described by the system of ordinary differential equations

$$\frac{d\gamma_s}{d\xi} = -u_1(\xi)\sin(u_2(\xi)), \tag{3}$$
$$\frac{d\gamma}{d\xi} = -u_1(\xi)\sin(\widehat{\varphi} + u_2(\xi)), \tag{4}$$
$$\frac{d\widehat{\varphi}}{d\xi} = 2\pi\left(\frac{\gamma_s}{\sqrt{\gamma_s^2 - 1}} - \frac{\gamma}{\sqrt{\gamma^2 - 1}}\right) \tag{5}$$

with initial conditions

$$\gamma_s(0) = \gamma_{s0}, \tag{6}$$
$$\gamma(0) = \gamma_0, \quad \widehat{\varphi}(0) = \widehat{\varphi}_0. \tag{7}$$

Here $\xi \in T_0 = [0, L]$ — independent variable; $(\gamma_0, \widehat{\varphi}_0)^T \in M_0, \gamma_s \in \Omega_x \subseteq R^1$; $(\gamma, \widehat{\varphi})^T \in \Omega_y \subseteq R^2$ — vector of system variables; $(u_1, u_2)^T \in U \subseteq R^2$ — 2-dimensional vector-function of control; L — constant value.

It is assumed that the sets of Ω_x and Ω_y — are open, set U and set of positive measure $M_0 \subset \Omega_y$ — are compact.

We also assume that the admissible controls $u = u(\xi)$, $\xi \in T_0$, constitute a class of piecewise smooth on the interval $[0, L]$ functions with values in a compact set U. By piecewise smooth functions we mean functions, which derivatives have only a finite number of discontinuities of the first kind.

Equations (3)–(5), where $\widehat{\varphi}$ — phase in deviations from the synchronous phase, and γ — complete reduced energy, convenient when considering optimization problems. But in the future equations in deviation of energy of the synchronous particle will be considered.

ISBN 978-3-95450-125-0

CALCULATION OF TOLERANCES AND STATISTICAL TEST

Y. Yelaev, SPbSU, Saint-Petersburg, Russia

Abstract

In the paper mathematical methods of tolerance determination of different parameters of accelerating and focusing structures are considered. The determination of tolerances is based on the analytical representation of variation of functional characterizing the beam dynamics. Method of statistical analysis of calculated tolerance values is represented. The purpose of the work is to determine the maximum possible deviations of the real (actual) parameters from nominal, when the qualitative structure function satisfies to the required modes.

INTRODUCTION

In the design of any kind of system, whether is it a linear accelerator or some other system, the nominal (rated) values of parameters are determined. The system must satisfy the specified criterion of the quality according to these parameteres. But accelerator of any type is a very difficult complex structure. It is almost impossible, and sometimes not economical to provide in accelerator the equality of actual parameters values with their nominal values. Deviations from the rated values influence on the quality of the system functioning and cause deviations from the specified quality criterion. These deviations can have a negative impact.

In this work the analytical and statistical method of tolerance determination is considered on the example of the longitudinal motion of charged particles in an accelerator with drift tubes. Thus, the maximum possible deviations of the real (actual) parameters from nominal are found when the qualitative structure function satisfies to the required modes. The statistical analysis of the getting results is carried out.

PROBLEM STATEMENT

In the paper we consider the problem of tolerances calculation for the dynamics of longitudinal motion of charged particles in an accelerator with drift tubes. The equations describing this process have the following form [1], [2]

$$\begin{aligned} \frac{d\varphi}{d\xi} &= \frac{2\pi\gamma}{\sqrt{\gamma^2-1}}, \\ \frac{d\gamma}{d\xi} &= \alpha(\xi)\cos(\varphi), \end{aligned} \tag{1}$$

where $\alpha(\xi)$ — the stepwise function defined on the interval [0, L],

$$\alpha(\xi) = \alpha^i, \quad \xi \in [\mu_{i-1}, \mu_i], \quad i = \overline{1,m}.$$

Here $0 = \mu_0 < \mu_1 < \ldots < \mu_m = L$, m — fixed non-negative integer. Further, we consider tolerances determination only of parameters μ_i, which are coordinates of the drift tubes. We introduce into consideration the functional characterizing the quality of the system functioning according to the μ_i parameters

$$I(\mu) = \int_{M_{L,\mu}} \left(a(\frac{\gamma_L}{\bar{\gamma}} - 1)^2 + b(\varphi_L - \bar{\varphi})^2 \right) d\varphi_L d\gamma_L. \tag{2}$$

Here $\bar{\varphi}$, $\bar{\gamma}$ — average energy and phase, $M_{L,\mu}$ — beam cross-section of paths depending on μ parameters.

The nominal values of the parameters are known, and they are $\mu_0 = (\mu_{01}, \ldots, \mu_{0m})$. It is necessary, according to the given value of $\triangle > 0$, to determinate the tolerances $\triangle_i > 0$, $i = \overline{1,m}$, such that

$$|\triangle I| = |I(\mu_0 + \triangle\mu) - I(\mu)| \leq \triangle,$$

where $|\triangle\mu_i| \leq \triangle_i$, $\triangle\mu = (\triangle\mu_1, \ldots, \triangle\mu_m)$, and realize statistical analysis of the tollerances value.

ALGORITHM OF THE TOLERENCE ESTIMATE

We assume that the deviations from the nominal values of the parameters are small and that the changes within the tolerances bands are linear. So the total increment of the functional I can be changed by its variation [3]

$$\delta I \approx \sum_{i=1}^{m} \left(\frac{\partial I(\mu_0)}{\partial \mu_i} \right) \triangle\mu_i. \tag{3}$$

There are two basic principles for the determination of the tolerances: the principle of equal influences and the principle of equal tolerances [4]. The sense of principle of equal influences is that the change of each input parameter affects the same way on the output value. So we obtain the formula for the calculation of tolerance:

$$\triangle_i = \triangle(m^{-\frac{1}{2}}) \left| \frac{\partial I(\mu_0)}{\partial \mu_{i0}} \right|^{-1}, \quad i = \overline{1,m}. \tag{4}$$

The sense of principle of equal tolerances is that the all tolerances are equal, i. e. $\triangle_i = \bar{\triangle}, i = \overline{1,m}$. So we

ISBN 978-3-95450-125-0

MATHEMATICAL MODEL OF BEAM DYNAMIC OPTIMIZATION

V.V. Altsybeyev, SPbSU, Saint-Petersburg, Russia

Abstract

We treat here the process of simulation of charged particle dynamics using so called hybrid system. Hybrid system is a system with continuous and discrete parts, described by differential and difference equations, respectively. In this case new mathematical model of beam dynamics optimization is suggested. The main parameters of optimization are: coefficient of particle capture in the acceleration mode, phase and energy spectra of particles at the exit of the accelerator, the transverse beam characteristics, etc. Optimization was carried out for the drift tubes accelerator.

INTRODUCTION

At present time design of accelerators with accelerating field focusing become important [1–6]. Such a focusing in RFQ accelerators being established, but APF focusing still requires development. For various problems of accelerator physics it is necessary to use a different mathematical models [4, 6–10]. Often it is necessary to build several models, taking into account their hierarchy. For example, it is interesting to consider the model "square wave" approximation of the accelerating field in DTL [5] to optimize its parameters. Such a model allows us to construct a well implemented on a computer optimization algorithm. In this paper, an attempt to optimize APF accelerator of deuterons was considered. Similar problems are discussed, especially in [6]. APF structure considered, as well, in the papers [1, 2], where the selection of the parameters of accelerators was made by using stability diagramm.

MATHEMATICAL MODEL OF OPTIMIZATION

"Square wave" approximation of the accelerating field in DTL allows to accept the following mathematical model of optimization, in which the dynamics of the beam is described by the so-called hybrid system of equations having a continuous (1) and discrete part (2) whith initial conditios (3).

$$\dot{x} = f_1(t, x, u), \quad t \in [\mu_{i-1}, \mu_i), \tag{1}$$

$$x(\mu_{i+1}) = f_2(\mu_i, x(\mu_i), v_i), \quad t \in [\mu_i, \mu_{i+1}), \tag{2}$$

$$x(0) = x_0 \in \overline{M}_0, \tag{3}$$

$$i = 2k + 1, \quad k = 0, \ldots, N - 1.$$

Let us consider beam quality functional. We consider the problem of its minimizing for the admissible controls.

$$I = \sum_{i=0}^{2N} \int_{M_{\mu_i,u}} \varphi(x(\mu_i), \mu_i) dx_{\mu_i} + \int_{M_{T,u}} g(x_T) dx_T \to min. \tag{4}$$

The variations of functional (4) can be written as

$$\delta I = -\sum_{k=0}^{N-1} \Bigg(\int_{\mu_{2k}}^{\mu_{2k+1}} \int_{M_{t,u}} \big(\psi(t)^T \Delta_u f_1(t, x, u) + \lambda(t, x) \Delta_u \mathrm{div}_x f_1(t, x, u)\big) dx_t dt + \int_{M_{\mu_{2k+2},u}} \big(\psi(\mu_{2k+2})^T \Delta_u f_2(\mu_{2k+1}, x(\mu_{2k+1}), v_{2k+1}) + \lambda(\mu_{2k+2}, x(\mu_{2k+2})) \Delta_u J(\mu_{2k+1})\big) dx_t \Bigg). \tag{5}$$

Where ψ and λ are satisfying the following equations

$$\psi(\mu_{i+1} + 0) = \psi(\mu_{i+1} - 0) + \frac{\partial \varphi(x(\mu_{i+1}), \mu_{i+1})}{\partial x}, \tag{6}$$

$$\psi(\mu_i) = J(\mu_i) \Big(\frac{\partial}{\partial x} f_2(\mu_i, x(\mu_i), v_i) \Big)^T \psi(\mu_{i+1}) + \lambda(\mu_{i+1}) \left(\frac{\partial J(\mu_i)}{\partial x} \right)^T + \frac{\partial \varphi(x(\mu_i), \mu_i)}{\partial x}, \quad t \in [\mu_{i+1}, \mu_i), \tag{7}$$

$$\frac{d\psi}{dt} = -\Big(\frac{\partial}{\partial x} f_1(t, x, u) + E \mathrm{div}_x f_1(t, x, u) \Big)^T \psi - \lambda \left(\frac{\partial \mathrm{div}_x f_1(t, x, u}{\partial x} \right), \quad t \in [\mu_i, \mu_{i+1}). \tag{8}$$

$$\lambda(\mu_{i+1} + 0) = \lambda(\mu_{i+1} - 0) + \varphi(x(\mu_{i+1})), \tag{9}$$

$$\lambda(\mu_i) = J(\mu_i) \lambda(\mu_{i+1}) + \varphi(x(\mu_i)), \quad t \in [\mu_{i+1}, \mu_i), \tag{10}$$

$$\frac{d\lambda}{dt} = -\lambda \mathrm{div}_x f_1(t, x, u), \quad t \in [\mu_i, \mu_{i+1}). \tag{11}$$

$$\lambda(T, x(T)) = -g(x_T), \tag{12}$$

$$\psi(T, x(T)) = -\left(\frac{\partial g(x_T)}{\partial x} \right)^T. \tag{13}$$

So, analitical representation of variation of functional (4) was obtained.

ISBN 978-3-95450-125-0

DEVELOPMENT OF THE OBJECT-ORIENTED PROGRAM IN C ++ FOR SIMULATION OF BEAM DYNAMICS IN ACCELERATOR INJECTION SYSTEMS

S.A. Kozynchenko *, Saint-Petersburg State University, Saint-Petersburg, Russia

Abstract

In this paper the program for simulation and optimization of beam dynamics in injection systems is considered, which at the same time allows the choice of parameters of the accelerating-focusing system. This permits designing the injection system during optimization process, taking into account the required output characteristics of the beam. The given program is based on Win 32 API dialog boxes and is developed in standard C++, using parallel programming tools based on the MPI-1.

INTRODUCTION

At present both in Russia and abroad, more attention is paid to design and creation of the accelerator complexes which provide generating the high-precision ion beams. When developing an accelerator complex, the injection system design is of importance, because it largely determines the output characteristics of the beam. For the design of such systems it is necessary to carry out numerical simulation and optimization of beam dynamics in the electro-magnetic fields. To reduce the calculation time for beam dynamics, the external fields in each step of optimization are usually approximated by analytical expressions, obtained for the simplified model of the real system under consideration. In order to design the accelerating structures providing high- precision ion beams, it is necessary to optimize the beam dynamics in the fields to be closed to real ones. In this paper, the program for simulation and optimization of beam dynamics in injection systems is considered, which at the same time allows the choice of parameters of the accelerating-focusing system. This permits designing the injection system during optimization process, taking into account the required output characteristics of the beam. Examples of such problems will be considered in the next section. The given program is based on Win 32 API dialog boxes and is developed in standard C++, using parallel programming tools based on the MPI-1.

SOME PROBLEMS OF MODELING AND OPTIMIZATION OF BEAM DYNAMICS IN THE INJECTION SYSTEMS OF ACCELERATORS.

Following D.A. Ovsyannikov [1], the dynamics of the beam in the external field, taking into account the beam space charge, is described by integro-differential equaions:

$$\begin{cases} \frac{dX}{dt} = V, \\ \frac{dV}{dt} = \frac{1}{m_p} f_1\left(t, X, \varphi\left(X, u\right)\right) + \\ \qquad \frac{1}{m_p} \int\limits_{M_{t,u}} f_2\left(t, X, V, \xi\right) \rho\left(t, \xi\right) d\xi = f_3\left(t, X, V, u\right), \\ X\left(t_0\right) = X_0, \quad V\left(t_0\right) = V_0, \quad \left(X_0, V_0\right) \in M_0, \end{cases} \tag{1}$$

$$\frac{\partial \rho\left(t,\eta\right)}{\partial t} + \frac{\partial \rho(t,\eta)}{\partial \eta} f\left(t,\eta,u\right) + \rho\left(t,\eta\right)\, div_{\eta} f\left(t,\eta,u\right) = 0 \tag{2}$$

$$\rho\left(t_0,\eta\right) = \rho_0\left(\eta\right). \tag{3}$$

Here $t \in [t_0, T]$ — the independent variable (time); parameters t_0, T are fixed; m_p, — the mass, $X(t) \in R^3$ — the position, $V(t) \in R^3$ — the velocity of a charged particle, respectively; $u = (u_1, u_2, ..., u_p) \in D$ — vector of control parameters, where $D \subset R^p$ — limited and a closed set; $\eta = (X, V) \in R^6$ — the position of the charged particle in the phase space; $\varphi = \varphi(X, u) \in C^2(G)$ — potential of the external field, where $G \subset R^3$ — limited and open set; function $f_1\left(t, X, \varphi\left(X, u\right)\right)$ describes the force, defined by external field; the choice of the function $f_2\left(t, X, V, \xi\right)$ defines the vay of modeling of the Coulomb interaction of charged particles; vector-function $f\left(t, \eta, u\right) = \left(V\left(t\right), f_3\left(t, \eta, u\right)\right)$; $\rho(t, \eta)$ — density distribution of particles due to the system (1); $\rho_0\left(\eta\right)$ — given charge density in the space M_0 at the moment t_0, where $M_0 \subset R^6$ — bounded closed set of measure zero; $M_{t,u} = \{X = X\left(t, X_0, u\right), V = V\left(t, V_0, u\right) : \left(X_0, V_0\right) \in M_0\}$ — image of the set M_0, due to system (1) under the vector u a the moment t.

For a given vector u the potential of the external electrostatic field φ, defined and continuous in $\bar{G}$, is a solution of the Dirichlet problem for the Laplace equation:

$$\begin{cases} \Delta\, \varphi\left(x, u\right) = 0, \quad x \in \mathrm{G}, \\ \varphi\left(x, u\right)|_{\Gamma_G(u)} = \varphi_0\left(x\right), \end{cases} \tag{4}$$

where $\Gamma_G\left(u\right)$ — piecewise smooth boundary of G, $\varphi_0\left(x\right)$ – known function.

On the cross-sections of the beam trajectories, the functional characterizing the beam dynamics is introduced. We consider the problem of finding the vector of controls $u^0 \in D$, delivering an extremum to the functional under the restrictions on the beam output energy, the particle losses, the max- imum radius of the beam, the potentials of the electrodes, the value of the functional, and some others.

* Sergey_Kozyntchenko@hotmail.com

ISBN 978-3-95450-125-0

INVESTIGATION OF PROGRAM AND PERTURBED MOTIONS OF PARTICLES IN LINEAR ACCELERATOR

Irina D. Rubtsova#, Elena N. Suddenko, SPbSU, Saint-Petersburg, Russia

Abstract

Beam control model for program and perturbed motions with interaction account is realized. Quality functional gradient is obtained.

BEAM DYNAMICS EQUATIONS

The problem under study is longitudinal beam dynamics control in linear waveguide electron accelerator. Let coordinate axis Oz be aligned the waveguide symmetry axis. Accelerating wave fundamental mode in device axis neighborhood is described by the expression [1, 2]:

$$E_z(z,t) = E_0(z)\sin\left(\omega\int_0^z \frac{d\eta}{v_{ph}(\eta)} - \omega t + \varphi_0\right).$$

Here z is longitudinal coordinate, t is the time, $\omega = \frac{2\pi c}{\lambda}$, c is velocity of light; λ, $E_0(z)$, $v_{ph}(z)$ and φ_0 are correspondingly wavelength, intensity amplitude, phase velocity value and initial phase of accelerating wave fundamental mode.

Longitudinal beam dynamics equations are as follows [2]:

$$\frac{d\xi}{d\tau} = \frac{p}{\sqrt{1+p^2}},$$
$$\frac{dp}{d\tau} = -\alpha(\xi)\sin\varphi - \frac{e\lambda}{m_0c^2}E_z^{(\rho)}(\xi\lambda),. \qquad (1)$$
$$\varphi(\tau) = 2\pi\int_0^{\xi(\tau)}\frac{d\eta}{\beta_{ph}(\eta)} - 2\pi\tau + \varphi_0.$$

Independent variable $\tau = \frac{ct}{\lambda}$ is introduced to be analogue of time to provide convenient Coulomb field account; $\xi = \frac{z}{\lambda}$; $p = \frac{mv_z}{m_0c}$; m_0 and m are correspondingly rest mass and relativistic mass of electron, v_z is particle velocity longitudinal component; $\alpha(\xi) = \frac{e\lambda E_0(\xi\lambda)}{m_0c^2}$; e is absolute value of electron charge; φ is particle phase; $E_z^{(\rho)}(\xi\lambda)$ is longitudinal component of Coulomb field intensity (integral representation of this field is given hereinafter in Eq. 5); $\beta_{ph}(\xi) = \frac{v_{ph}(\lambda\xi)}{c}$.

The problem of beam control in such a system was treated by Dmitry Ovsyannikov [2] as trajectory ensemble control problem; $\alpha(\xi)$ and $\beta_{ph}(\xi)$ were assumed to be control functions.

PROGRAM AND PERTURBED MOTIONS CONTROL

To continue the research, let us describe beam evolution in terms of program motion and the ensemble of perturbed motions. This approach was suggested by Alexander Ovsyannikov and successfully applied for beam control in RFQ structures [3, 4, 5, 6, 7]. The same approach was used for longitudinal beam dynamics investigation in traveling-wave linear accelerator [8] without Coulomb field account. The idea is to describe the controlled process as a combination of program motion (i.e. the motion of assigned particle) and perturbed motions ensemble (with respect to program motion). Assigned particle is the object with special dynamics equations; its initial position coincides with bunch centre and its velocity coincides with accelerating wave phase velocity $v_{ph}(z)$. Parametrized function $\varphi_a(\xi,\boldsymbol{\theta})$ (where $\boldsymbol{\theta}$ is control parameters vector) characterize the phase of assigned particle; $\varphi_a(\xi,\boldsymbol{\theta})$ is assumed to be control function instead of $\beta_{ph}(\xi)$, which is expressed in terms of assigned particle impulse. Consequently, initial control may be constructed with due account of requirements on program motion and provide rather high quality of controlled process even at optimization start. In particular, $\varphi_a(\xi,\boldsymbol{\theta})$ mathematical form may be chosen to follow synchronous phase variation tendency observed for "good" beam dynamics. Besides, different mathematical descriptions and simultaneous optimization of program motion and the ensemble of perturbed motions provide additional possibilities of beam dynamics optimization by means of control action upon assigned particle and upon beam particles.

In this paper simultaneous optimization approach is applied to time-dependent beam dynamics model with particle interaction account. This model is derived on the base of Eq. 1.

Let coordinates and characteristics of assigned particle have index "a". Program motion is described by the equations:

#rubtsova05@mail.ru

ISBN 978-3-95450-125-0

COMPARISON OF MATRIX FORMALISM AND STEP-BY-STEP INTEGRATION FOR THE LONG-TERM DYNAMICS SIMULATION IN ELECTROSTATIC FIELDS*

A. Ivanov†, Saint-Petersburg State University, Russia

Abstract

An approach based on matrix formalism for solving differential equations is described. Effective in sense of performance matrix formalism can be tested with less efficient, but accurate traditional algorithm of numerical simulation based on the Runge-Kutta scheme. In both cases the symplectic version of the algorithms are used. The results coincide to analytical calculations, but some disagreements have been identified. The approach implementation is demonstrated in the problem of long-term spin dynamics in electrostatic fields.

INTRODUCTION

Particles dynamics in electromagnetic fields is described by Newton-Lorentz equation. This system of ordinary differential equations can be solve by appropriate numerical methods. In this research two approaches are developed. Firstly, for step-by-step integration a symplectic Runge-Kutta scheme is used. As second approach a mapping algorithm based on matrix formalism [1] is implemented.

In the EDM search COSY Infinity [2] is also used. COSY Infinity is known as a very powerful instrument for particle tracking in electromagnetic fields. The key idea of this research is to develop another high-performnce approach for simulation of spin-orbital dynamics. Both Matrix Formalism and COSY Infinity allow to simulate spin-orbital motion of millions of particles. So these methods can be verified by each other. At present, in the EDM search the MPI (Message Passing Interface) version of the COSY Infinity program is installed on a supercomputer with 310^5 processors. For matrix formalism code we can use OpenMP or OpenCL for running tasks on clasters in St.Petersburg State University (e.g. GPU accelerators).

Due to the fact that one of the tasks in JEDI is examination of spin dynamics in electrostatic fields [3], in this paper magnetic fields are not considered. But all described techniques can be used in common case of electromagnetic fields without modifications.

In the article particle dynamics is considered in 9-dimensional space. A state of dynamic system is described as $(x,\ x',\ y,\ y',\ S_x,\ S_y,\ S_s,\ dv,\ t)$ vector, where x, x' and y, y' are transverse and vertical displacement and velocity respectively; $S_x,\ S_y,\ S_s$ are components of spin vector in curvilinear coordinate system (see Fig. 1); $dv = \Delta v/v_0$ is deviation of the initial particle velocity; t is time variable. Note, that a state vector depends on arc length s, which is chosen as an independent variable.

* Work performed under JEDI collaboration (Juelich Electric Dipole Moment Invenstigations)

† 05x.andrey@gmail.com

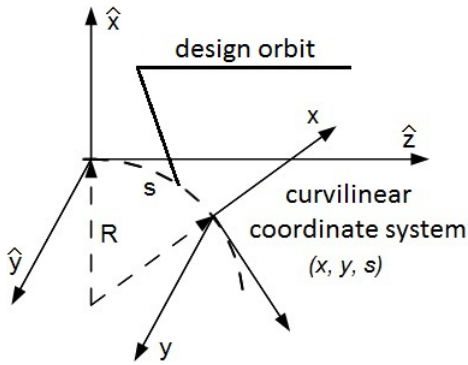

Figure 1: Curvilinear coordinate system.

The mathematical models that used for description of partical motion and spin dynamics are presented in [4]. In this article only numerical approaches are considered.

STEP-BY-STEP INTEGRATION

The Newton-Loretz (particle motion) and BMT (spin dynamics) equations can be written as following system

$$\begin{aligned} \frac{d}{ds}X &= F(s, X), \\ \frac{d}{ds}v_0 &= 0, \end{aligned} \tag{1}$$

where $X = (x, x', y, y', S_x, S_y, S_s, dv, t)$.

This allows us to use classical step-by-step integration methods to solve this system. Article [5] provide both symplectic Runge-Kutta integration schemes, and the algorithm for it derivation up to the 12 order. For the current research a symplectic 2-stage Runge-Kutta scheme of 4 order was implemented.

Table 1: 2-stage 4-order implicit Runge-Kutta scheme

$b_1 + \tilde{c_1}$	$b_1/2$	$b_1/2 + \tilde{c_1}$
$b_1 - \tilde{c_1}$	$b_1/2 - \tilde{c_1}$	$b_1/2$

$$b_1 = 1/2,\ 2b_1\tilde{c_1}^2 = 1/12$$

According to this scheme (Table 1), the solution of the equations (1) can be presented in iterative form

$$\begin{aligned} \mathbf{X}_{n+1} &= \mathbf{X}_n + h\textstyle\sum_{j=1}^{2} b_j \mathbf{F}(s + hc_j, \mathbf{X}^{(i)}), \\ \mathbf{X}^{(i)} &= \mathbf{X}_n + h\textstyle\sum_{j=1}^{2} a_{ij} \mathbf{F}(s + hc_j, \mathbf{X}^{(i)}). \end{aligned}$$

This integration method provide a symplectic solution by choosing of the corredponded coefficients a_{ij}, b_j, c_j.

ISBN 978-3-95450-125-0

SOME PROBLEMS OF BEAM SLOW EXTRACTION*

S. Andrianov†, SPbSU, SPb, Russia

Abstract

In this paper we discuss some problems of modeling of beam slow extraction systems. It is known that similar type of beam extraction is used for different kind of circular accelerators. Among the most important requirements for such systems is necessary to mention the time uniformity of the extracted beam. There exist the following two key causes. The first of them is induced by time discontinuity of the corresponding steering electrical currents, and the second cause is induced by an beam inertia which usually connected with beam feedback mechanism, which is usually used for temporal smoothing of the corresponding magnetic (and electrical) fields. In the base of our approach we put the matrix formalism for Lie algebraic tools, which allows us to analyze different kind of the time discontinuity cause.

INTRODUCTION

The objectives of modeling long-term (multi-turn) evolution of particles in circular accelerators various purposes to make demands not only the adequacy of mathematical tools and related software, but taking into account the possibility of control actions necessary for the implementation of corresponding scenarios. For example, in the problems of beam particles extraction from the accelerator it is necessary not only to ensure particles extraction satisfying to some certain criteria are met but also to provide quality control for extraction system. Consideration of real (not ideal) conditions should provide an existence of instability of control systems on one side and not the "ideal" in the extraction system itself. As to the quality of the beam in modern accelerators makes more and more demanding, it is very important to develop adequate mathematical models, effective software products. Besides it is very important also to develop an uniform data-processing system, which provides support for a given extraction mode. Obviously, a required step for the creation of such a complex must be provided a predictive modeling of possible deviations as control beam and the beam characteristics from the program scenario. Under the program characteristics we mean a set of control parameters (characterized, first of all, the beam transport system itself and provides stability of the beam during an extraction process) and the extraction system, which provide the required extraction characteristics.

It is well known that the energy and intensity rise of modern accelerators also requires increasing of the slow extraction duration. Just this increasing demands much of hard requirements on the uniformity of the temporal structure of the extracted beam. These demands are caused by, first of all, a beam inertia (see further), and the feedback systems limitations. That is why the methods are needed that allow to realize effective numerical experiments to determine the degree of influence of various factors on the temporal structure of the extracted beam, and propose suppression mechanisms for unwanted effects using global optimization methods and symbolic computation that allow for parametric optimization of beam systems.

A THEORETICAL MODEL

To track the dynamics commonly used the well-known Poincaré sections method. In the case of periodic motion the one turn map generates a discrete map – a Poincaré map. This generated map can be written in the form of an operator equation for k-th turn – $\mathcal{M}_k$:

$$\mathfrak{X}_{k+1} = \mathcal{M}_k \circ \mathfrak{X}_k, \qquad (1)$$

where $\mathfrak{X}_k$ is a phase set occupied by beam particles on the k-th turn. In the case of $\mathcal{M}_k = \mathcal{M}_{k+1}, \forall\, k \geq 1$ we will speak about a periodical map. We should note that the support of periodic motion is a standard problem for most circular accelerators. In the case of the slow or fast beam extraction this periodic evolution is disturbed by introducing an additional magnetic (or electric) field, which is a time-varying field and provide the required extraction process. In this paper, the operator equations (1) is replaced by the matrix equations according to the matrix formalism [1]

$$\mathbb{X}_{k+1} = \sum_{i=1}^{\infty} \mathbb{M}_k^{1i} \mathbb{X}_k^j,$$

where $\mathbb{M}_k^{1i}$ are matrices corresponding to aberrations of i-th order, and $\mathbb{X}_k^j$ is a matrix constructed from all Kronecker degrees of all phase vectors $\mathbf{X}_k$ of j-th order ($k = \overline{1, N}$, where N is particles number). It should be noted that in the case of an infinite series equation preserves the very important properties of symplectic and energy conservation law (for stationary fields).

However, these are two very important properties violated in termination of the series, which leads to disruption qualitative and quantitative behavior of the beam. Therefore, in this paper we use the process of symplectification matrices [1] until the desired order of nonlinearity and the law energy conservation [3]. It should be noted that the property of symplecticity is universal, which is satisfied for all Hamiltonian systems, while the law energy conservation is connected with the Hamiltonian function, which is

*Work supported by Federal Targeted Program "Scientific and Scientific-Pedagogical Personnel of the Innovative Russia in 2009-2013" (Governmental Contract no. p 793)

† sandrianov@yandex.ru

ISBN 978-3-95450-125-0

DEGENERATE SOLUTIONS OF THE VLASOV EQUATION

O.I. Drivotin, St.-Petersburg State University, St.Petersburg, Russia

Abstract

The present report deals with degenerate solutions of the Vlasov equation. By degenerate solution we mean a distribution which has a support of dimension smaller than dimension of the phase space. Well known example is the Kapchinsky-Vladimirsky (KV) distribution, when particles are distributed on the 3-dimensional surface in the 4-dimensional phase space.

We use covariant formulation of the Vlasov equation developed previously [1]. In traditional approach, the Vlasov equation is considered as integro-differential equation with partial derivatives on phase coordinates. For the covariant formulation of the Vlasov equation, we use such tensor object as the Lie derivative. According to the covariant approach, a degenerate solution is described by differential form which degree is equal to the dimension of its support.

Main attention is paid to the KV distribution, which is described by the differential form of the third degree. It is demonstrated that the KV distribution satisfies to the Vlasov equation in covariant formulation.

This work has theoretical as well as practical significance. Presented results can be applied for description and simulation of high-intensity beam.

PHASE SPACE AND PARTICLE DISTRIBUTION DENSITY

Consider a domain D in 4-dimensional space-time and a system of smooth spacelike 3-dimensional surfaces filling the domain D. Introduce a continuous parameterization of that surfaces and system of continuously differentiable one-to-one mappings of those surfaces to some selected surface. Let as call the selected surface a configuration space associated with this foliation of the space-time.

If we specify some reference frame, then we can take the layers of simultaneous events for this reference frame as that surfaces, and the time t a parameter. In this case, the configuration space is the configuration space associated with the reference frame.

When time passes, particles move from one layer to another, but we can examine dynamics of particle ensemble in 3-dimensional configuration space. Let us consider tangent bundle of the configuration space as the phase space. Denote by q a position in the phase space.

If there exists some kind of symmetry, we can pass to a phase space of dimension less than 6. Denote the dimension of the phase space by K.

We shall consider various types of distributions. In the simplest case, consider continuous charged media occupying a domain G_0 in the phase space instead of set of discrete particles. Take a family of subdomains $\{G\}$, $G \subset G_0$, with smooth boundaries for which their characteristic functions are defined:

$$\chi_G(q) = \begin{cases} 1, & q \in G, \\ 0, & q \notin G. \end{cases}$$

Let us call differential form of $K-$th degree

$$n = n_{1\ldots K}(q) dq^1 \wedge \ldots \wedge dq^K \tag{1}$$

the particle distribution density in the phase space (or phase density), if for each subdomain G

$$\int_{G_0} \chi_G(q) n(q) = N_G. \tag{2}$$

Here N_G is the number of particles in G, which in this model may be not integer.

Consider the space of functions $f(q)$ for which $\int_{G_0} f(q)\omega(q)$ exists for any form of $K-$th degree $\omega(q)$ from given class. Let us call such functions integrable and denote by $\mathcal{F}$ their space. For some form $\omega(q)$, define a linear functional on $\mathcal{F}$ by the rule

$$< \omega, f >= \int_{G_0} f(q)\omega(q), \quad f \in \mathcal{F}. \tag{3}$$

Then definition (2) can be written as

$$< n, \chi_G >= N_G. \tag{4}$$

Let us consider now the discrete model of point-like particles. In the frames of this model each particle is represented by a point in the phase space. Let us introduce the linear functional $\delta(q)$ on $\mathcal{F}$:

$$< \delta(q), f >= f(q), \quad f \in \mathcal{F}. \tag{5}$$

The measure $\mu_D =< \delta(q), \chi_D >$ is usually called the Dirac measure. Therefore, let us call the functional (5) the density of the Dirac measure. Let us call a linear combination of functionals (5)

$$< \sum_i \alpha_i \delta(q_{(i)}), f >= \sum_i \alpha_i f(q_{(i)})$$

such that for each subdomain G the equality (4) holds the phase density. It is easy to see that in this case $\alpha_i = 1$, and $q_{(i)}$ are particle positions in the phase space, $i = \overline{1, N}$ where N is the total number of particles:

$$n(q) = \sum_{i=1}^{N} \delta(q_{(i)}). \tag{6}$$

ISBN 978-3-95450-125-0

TRANSVERSE DYNAMICS OF A RING BEAM IN A COAXIAL TWO-CHANNEL DIELECTRIC WAVEGUIDE

A. Altmark, Electrotechnical University, Saint-Petersburg, Russia
A. Kanareykin, Electrotechnical University, Saint-Petersburg, Russia and EuclidTechlabs LLC, Gaithersburg, MD,USA

Abstract

The most critical issue of wakefield accelerating schemes is transformer ratio (maximum energy gain of the witness bunch/maximum energy loss of the drive bunch) which cannot exceed 2 in collinear wakefield accelerator with use of Gaussian bunches. We observe new scheme of wakefield acceleration in collinear two-channel waveguide, where accelerating field created by electron bunch with annular charge distribution passing in vacuum layer. This radiation is used for acceleration of witness beam which passing through central vacuum channel. These vacuum areas separated by dielectric tube. Transformer ratio for this scheme can be much greater than 2.

The main problem of wakefield accelerators is transverse beam dynamics of the driver bunch, because of high value of its charge and low energy of the particles. We present results of the beam dynamics calculation of the annular drive beam by "macroparticle" method based on analytical expressions for Cerenkov radiation. The upgraded BBU-3000 code has been used for calculation of the beam dynamics in coaxial dielectric wakefield accelerating structures. It is shown that dynamics depends on radial and azimuthally structures of HEM modes excited by the drive beam there. Initial beam imperfections to the beam dynamics was carried out.

INTRODUCTION

A new application of microwave and THz Cherenkov radiation has been proposed and studied in the last decade to be used for high energy physics colliders and X-ray FELs, the Dielectric Wakefield Accelerator, or DWA [1-3].

In a general sense, a high gradient is desirable for a TeV level linear collider design because it can reduce the total linac length and hence the cost. Recently a high energy linear collider based on a short rf pulse (~22 ns flat top), high gradient (~267 MV/m loaded gradient), high frequency (26 GHz) dielectric two beam accelerator scheme has been proposed. The major parameters of a conceptual 3-TeV linear collider based on a DWA have been developed and are presented in reference [4].

X-ray free-electron lasers (FELs) are expensive instruments and the accelerator contributes the largest portion of the cost of the entire facility. Using a high-energy gain dielectric wakefield accelerator instead of a conventional accelerator may facilitate reduction of the facility size and significant cost savings. It has been shown that a collinear dielectric wake-field accelerator can accelerate low charge and high peak current electron bunches to a few GeV energy with up to 100 kHz bunch repetition rate [5].

Dielectric loaded accelerator (DLA) structures using various dielectric materials [6] and excited by a high current electron beam or an external high frequency high power RF source have been under extensive study recently [1-3]. The basic wakefield RF structure is very simple - a cylindrical, dielectric loaded waveguide with an axial vacuum channel is inserted into a conductive sleeve. Following at a delay adjusted to catch the accelerating phase of the wakefield is a second electron (witness) beam. The witness beam is accelerated to high energy by the wakefield produced by the drive beam [1].

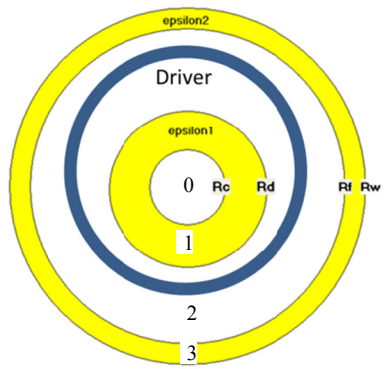

Figure1. Wakefield acceleration by ring driver beam in coaxial cylindrical waveguide

A series of proof of principle experiments have been successfully performed at Argonne's Advanced Accelerator providing accelerating gradient in the range exceeding 100 MV/m at X-band [1-3,6]. THz wakefields of ~ GV/m magnitude range have been successfully generated by the UCLA-SLAC collaboration as well [7].

Energy transfer efficiency from the drive to witness bunches is a critical issue for wakefield acceleration techniques. The transformer ratio R is defined as the ratio of the maximum energy gain of the witness bunch to the maximum energy loss of the drive bunch. There are two major classes of wakefield accelerator geometries, collinear and two beam. For a collinear wakefield accelerator, R is less than 2 under very general conditions: linear media; a relativistic, longitudinally symmetric drive bunch; and identical paths through the system of both drive and witness beams [8-9]. A number of techniques have been proposed to overcome the transformer ratio limitation. Some of the methods that can be employed to obtain R>2 for the dielectric based accelerator include: a triangular longitudinal drive bunch profile [8]; a train of Gaussian drive bunches of progressively increasing

ISBN 978-3-95450-125-0

COMPUTER SIMULATION OF THE ELECTRON BEAM ENERGY SPECTRUM MEASUREMENT BY THE MAGNETIC ANALYZER METHOD BASED ON SCANNING SYSTEM OF THE STERILIZATION INSTALLATION

P. A. Bystrov, M. A. Alekseev, N. E. Rozanov, MRTI RAS, Moscow, Russia

INTRODUCTION

Currently, there is a demand for the sterilization of medical products using radiation technology, including the use of accelerated electron beams. To meet this demand sterilizing devices are being developed. Such a device, with a compact local radiation shielding, was created in the Moscow Radiotechnical Institute [1]. This installation is based on a linear high-frequency accelerator working on a standing wave, with the focusing of electron beam by the radial component of the electric microwave field [2].

Energy spectrum of accelerated electron beam is one of the important characteristics that define the efficiency of sterilizing installation. The task to create the electron beam with the optimal spectrum for the accelerator with relatively short grouping part has not been yet stated. So the form of the spectrum is defined by physical mechanisms of the beam accelerating process, and it is still, in general, has satisfied the basic requirements.

While working on increasing the efficiency of sterilizing installation, there is a need for a physical-mathematical model of processes in systems of output the beam into the atmosphere and scanning system for the sterilization of the objects. Such model that uses the information about the electron beam from the calculations of acceleration process of the beam [3] was created [4]. Perfection of this model requires the establishment of correspondence between calculated energy spectrum and real spectrum of the beam.

This paper describes a method for measuring the characteristic, which allows restoring the energy spectrum of the beam in one of the regimes of operation of the accelerator of the sterilization installation. It is based on the method of magnetic analyzer, implemented on the basis of scanning system of the electron beam of the installation. This method does not require the use of additional equipment, and this fact is important one for installation with local radiation shielding. Result of measurement is the dependence of the beam current, deflected by a transverse magnetic field, which falls in the region of the induction current sensor, on the value of deflecting magnetic field. With the computer code "BEAM SCANNING" [4], specially modified for this purpose [5], the simulation of processes in the scanning system in the regime of measuring of this characteristic was performed. It is shown that the important factors which influence the form of curve of the measured characteristic are the reflections of the beam electrons from the walls of the funnel of the scanning system and the non uniform distribution of the magnetic field in the direction of the scanning. In this case, the calculated dependence of the current in the induction sensor on deflecting magnetic field is consistent with the experimental dependence, and the restored form of the energy spectrum corresponds to the calculated beam spectrum in a particular regime of operation of the accelerator.

THE SCHEME OF MEASURMENT THE CHARACTERISTICS FOR RESTORING THE ELECTRON BEAM ENERGY SPECTRUM

Fig. 1 shows the measurement scheme, which in its time was conventionally called "scheme of spectrum measurement at the edge of the funnel".

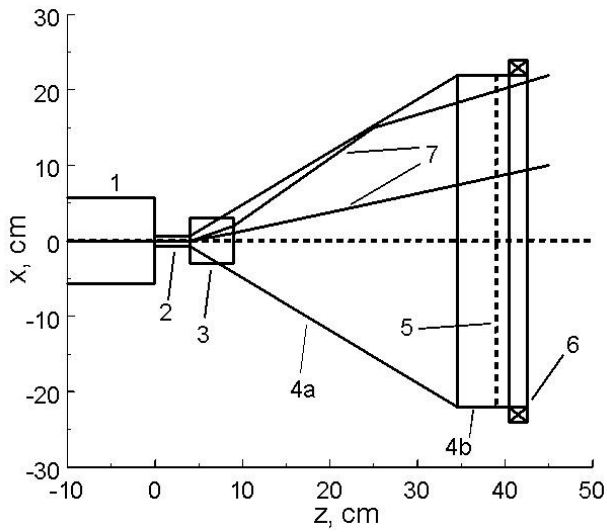

Figure 1: The scheme for measurement the characteristics for restoring the electron beam energy spectrum. 1 - end of the accelerating structure, 2 - drift tube, 3 - the area of the transverse deflecting magnetic field of scanning system, 4 - the funnel of the scanning system (a - cone part, b - rectangular part), 5 - titanium foil, 6 - inductive sensor for measure the beam current, 7 - some electron trajectories.

The electron beam emerging from accelerating structure passes the short length drift tube and appears in the location of an electromagnet that is creating a transverse magnetic field of the beam scanning system of the sterilization installation. Passing region of the

ISBN 978-3-95450-125-0

MEASUREMENT OF BEAM PARAMETERS IN THE VEPP-5 DAMPING RING USING BETATRON OSCILLATIONS DECOHERENCE*

K. Astrelina†, A. Petrenko, Budker INP SB RAS, Novosibirsk

Abstract

The measurement of beam parameters during the commissioning of VEPP-5 Damping Ring is presented. Coherent betatron oscillations of the 380-MeV electron beam were induced by a fast kick. Electrostatic beam position monitors were used to obtain the turn-by-turn transverse beam position data. The form and behavior of the envelope of oscillations are determined by the beam parameters, chromaticity and nonlinear detuning. The values of beam emittance $\epsilon = 1.5 \cdot 10^{-8}$ m·rad, energy spread $\delta = 3.6 \cdot 10^{-4}$ and beam length $\sigma_l = 1.5$ cm have been obtained from the analysis of the beam envelope, nonlinear detuning and chromaticity measurements. The results are in a good agreement with theoretical predictions which were made for calibrated model of the Damping Ring.

INTRODUCTION

VEPP-5 Injection Complex is designed for the production of intense high-quality electron and positron beams [1]. Damping Ring stores the electron and positron beams of 510 MeV which are injected from the Linac. These beams are to be used at the electron-positron colliders at BINP and plasma wake field acceleration (PWFA) facility [2]. The necessary requirements to the produced beams are of $2 \cdot 10^{10}$ particles in the bunch, emittance of ($\epsilon_x = 2 \cdot 10^{-8}$ m·rad, $\epsilon_y = 0.5 \cdot 10^{-8}$ m·rad with the rate of the beam accumulation 10^{10} positrons per second.

At the present moment Injection Complex and its Damping ring are under commissioning. Currently the electron beam with energy 380 MeV has been stored in the Damping Ring; the experiments with positron beam injection and storage are planned for October 2012.

There are 17 electrostatic beam position monitors (BPMs) in the Damping Ring. Each monitor can record the transverse coordinates of beam centroid over 32000 turns or less. Turn-by-turn measurements from BPMs can be used for the storage ring optics measurements as well as indirect beam parameters measurements. The envelope of coherent betatron oscillations is influenced by the energy spread, transverse and longitudinal beam sizes and emittances. Therefore, the analysis of oscillation envelopes [3] or synchrotron spectra [4] can yield these beam parameters.

This simple technique was used during the Damping Ring commissioning with electron beams and will be used for positron beams.

* Work supported by the Ministry of Education and Science of the Russian Federation, RFBR (grant N 09-02-00594)

† K.V.Astrelina@inp.nsk.su

BETATRON OSCILLATION ENVELOPE

Transverse betatron beam oscillations induced by fast inflector kick. For low enough beam intensity betatron particle motion is independent for the all particles in the beam. Single particle turn-by-turn transverse position may be written as

$$x(t) = \sqrt{2I\beta}\cos(2\pi \int_0^t \nu(t)dt + \psi_0), \qquad (1)$$

where β – beta-function at the point of BPM location, ψ, I – action-angle coordinates [3].

Initially kicked beam behaves like a single particle (coherent oscillations) but because of betatron tune spread the decoherence is developed in several thousands of turns and the beam centroid oscillations amplitude decreases due to detuning of betatron oscillations.

There are two main sources of tune spread: chromaticity and amplitude-dependent tuneshift

$$\nu = \nu_0 + \delta\xi + aI, \qquad (2)$$

where $\delta = \Delta p/p_0$, ξ – chromaticity, a is the constant describing amplitude-dependent tuneshift. Assuming that the initial beam distribution is Gaussian in longitudinal and transverse planes one can express the position of beam centroid as:

$$< x(t) >= \sqrt{2\beta I(t)}\cos(\psi(t) + \psi_0) \qquad (3)$$

where

$$I(t) = \frac{1}{1+\theta^2}\exp\left(-\frac{Z^2}{2}\cdot\frac{\theta^2}{1+\theta^2}\right)\cdot \cdot\exp\left(-2\left(\frac{\xi\delta}{\nu_s}\right)^2\sin^2(\pi\nu_s t)\right) \qquad (4)$$

$$\psi(t) = 2\pi\nu_0 t + \frac{Z^2}{2}\cdot\frac{\theta}{1+\theta^2} + 2\arctan\theta.$$

Here $Z = \sqrt{2I_{max}/\epsilon}$ – kick strength, $\theta = 2\pi a\epsilon t$, ν_s - synchrotron frequency. One can see that the form of the oscillation envelope depends on two values $\xi\delta$ and $a\epsilon$. Amplitude-tune dependence contributes as the main damping of the oscillations amplitude; chromaticity modulates the envelope with synchrotron frequency. Given the values of ξ and a from preliminary measurements, one can deduce energy spread and beam emittance by fitting the formula (Eq. 4) to the envelope by varying ϵ and δ.

ISBN 978-3-95450-125-0

SIMPLIFIED BEAM LINE WITH SPACE CHARGE COMPENSATION OF LOW ENERGY ION BEAM

A. Dudnikov#, Budker Institute of Nuclear Physics, SB RAS, Novosibirsk, Russia

Abstract

Simplified beam line for low energy Ion implantation is considered. Compensation of the space charge of high perveance, low energy ion beam in beam lines for ion implantation and isotope separation has been investigated. Different mechanisms of the compensating particle formation such as ionization by the beam, secondary emission of electrons and negative ions, electronegative gas admixture, and external plasma sources are discussed. Advanced space charge compensation increases an intensity of low energy ion beam after analyzer magnet up to 3–4 times. Space charge compensation of positive ion beam by admixture of electronegative gases and damping of the beam instability are discussed. Up to 6 mA of $^{11}B^{+}$ ions with energy 3 keV, 11 mA with 5 keV, and 18 mA with 10 keV have been transported through an analyzer magnet of a high current implanter with space charge compensation by electronegative gases

INTRODUCTION

Ion implantation is the largest commercial application for particle accelerators. Several thousand ion implanters are used for semiconductor circuits fabrication. Most difficult task of ion implantation is high dose implantation of ion with lowest energy. Now for the high-current implanters are used the beam-line (BL) shown in Fig. 1 [1]. Implanters energy is up to 40 or 80 kV, but they have been optimized for sub-1 keV implants, where space charge forces have a dominant effect. The beam line uses a couple of deceleration stages that allow the beam to be transported mainly at higher energies. It is also designed to produce a broad beam at the wafer to maximize the cross section and to minimize the space charge forces at the final implant energy. The wafer is scanned across the ribbon beam in one direction. This beam line is very long, complex and expansive. Due to the complex interactions between the ion beam and the magnetic field applied for beam expansion, this approach creates severe technical, practical, and process related problems that increase the total production cost of such equipment and lead to more complicated operation procedures for carrying out the ion implantation. In particular, the beam path through this system is relatively long, and at low energies and high beam currents it becomes increasingly difficult to control the uniformity of the ion beam and the angular variation within the beam with the precision required by certain commercial processes. Recently were proposed some simplified beam lines for production the same broad ribbon beam as in [1] directly after analyzing magnet [2-4].

Schematic of these BL is shown in Fig. 2. Main feature of this BL is very large magnet aperture along magnetic field for production of ribbon beam with width up to 300 mm .

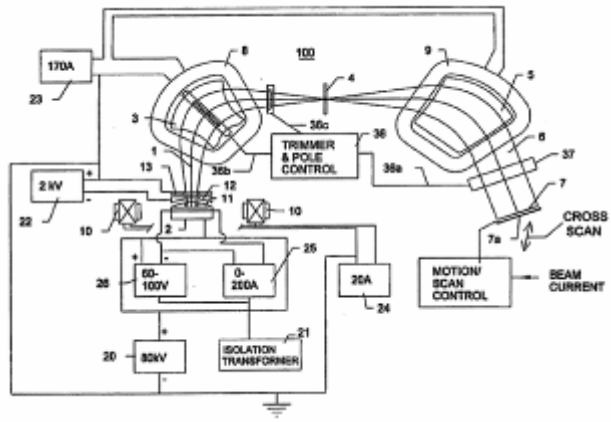

Figure 1: Schematic of high current low energy implanter from [1].

For transportation of low energy heavy ion beam through analyzer magnet is important to have a very good space charge neutralization (SCN) to avoid a beam divergency and particle loss. The space charge compensation energy of low energy ion beam was tested in the simplified beam lines described below.

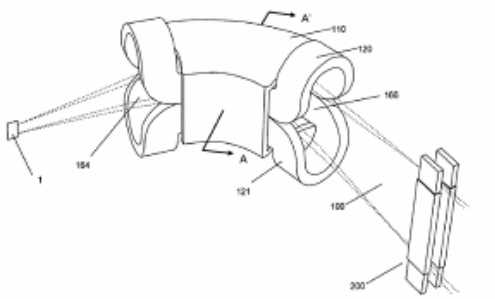

Figure 2: Beam line of implanter with a large vertical aperture. 1-ion source; 100-extended robbon iom beam; 110 magnet; 12, 1210-saddle type coils; 200-multipole beam corrector.

EXPERIMENTAL IMPLANTERS

In first experiments was used the high current ion implanted VESUVII-8M with modified Bernars type ion sources adopted for separation of Rubidium isotopes from RbCl salt. Schematic of the experimental device is shown in Fig. 3. A gas delivery systems (9-14) and plasma sources (16) were used for improved space charge compensation of ion beam generated by ion source (2) and analyzed by magnet (1) with uniform field and vertical edge field focusing.

#Andreidud@gmail.com

ISBN 978-3-95450-125-0

LOW ENERGY COOLER FOR NICA BOOSTER

M. Bryzgunov, A. Bubley*, V. Panasyuk, V. Parkhomchuk, V. Polukhin, V. Reva,
BINP SB RAS, Novosibirsk, Russia

Abstract

Low energy cooler for NICA project is being currently designed at BINP in collaboration with JINR. From the point of view of its features it is similar to previous low energy coolers manufactured at BINP, i.e. equipped with variable electron beam, electrostatic bending, high precision solenoid etc. The article describes some technical solutions applied to the cooler design.

INTRODUCTION

NICA is abbreviation of one of the most challenging recent Russian project in high energy physics [1]. It is going to be largest heavy ion collider ever been built in Russia. It contains a number of complicated systems and subsystems. One of them is heavy ion booster which is located at the existing hall of former synchrophasotron, and new magnetic elements sit inside old giant iron yokes [2]. Low energy cooler is quite important element of the booster which provides sufficient improvement of the ion beam quality.

Main specifications of the cooler are listed below:

ions type	p+ up to $^{197}Au^{31+}$
electron energy, E	1,5 ÷ 50 keV
electron beam current, I	0,2 ÷ 1,0 Amp.
energy stability, $\Delta E/E$	$\leq 1\times10^{-5}$
electron current stability, $\Delta I/I$	$\leq 1\times10^{-4}$
electron current losses, $\delta I/I$	less than 3×10^{-5}
longitudinal magnetic field	0,1 ÷ 0,2 T
inhomogeneity of the field, $\Delta B/B$	$\leq 3\times10^{-5}$
transverse electron temperature	≤ 0,3 eV
ion orbit correction:	
displacement	≤ 1,0 mm
angular deviation	≤ 1,0 mrad
cooling section length (effective),	1940 mm

The requirement for vacuum condition in not very strict (10^{-11} mbar), on the other hand the cooler is the only 'warm' element, since all magnets of the booster are superconductive. This leads to some difficulties in design of junctions of different types of elements.

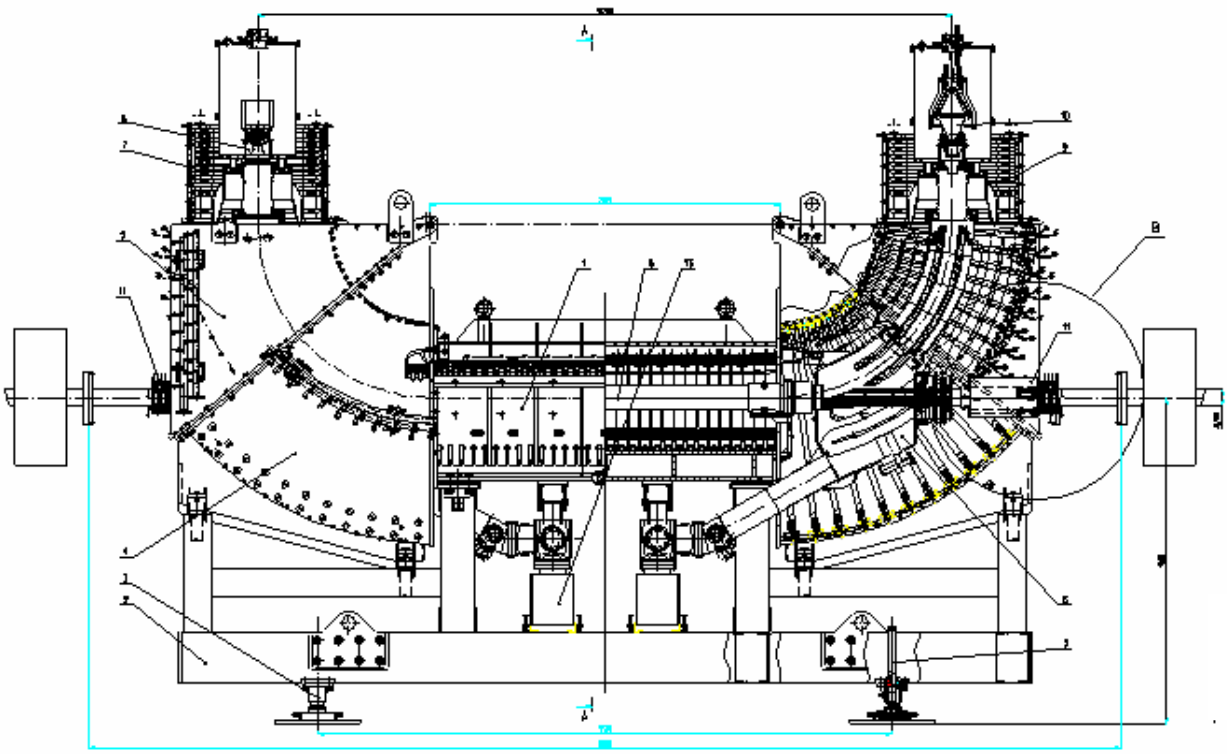

Fig.1 The general layout of the cooler.

ISBN 978-3-95450-125-0

THE KICKER PARAMETERS ESTIMATION FOR LONGITUDINAL INSTABILITY DAMPING OF THE BEAM AT SR STORAGE RING "SIBERIA-2"

A. Smygacheva, A. Vernov, V. Korchuganov
NRC Kurchatov Institute, Moscow, Russia

Abstract

The coupled-bunch instabilities can limit a maximum beam current and lead to a beam loss in some cases at the storage ring "Siberia-2". To cure this problem we have to develop a longitudinal feedback (LFB) system based on a high impedance kicker. In the article a result of the high order mode (HOM) spectrum measurements and the main kicker parameters are presented. Besides, an interaction of the beam with three cavities is considered theoretically.

INTRODUCTION

The RF system of the Kurchatov Institute Synchrotron Radiation storage ring "Siberia-2" consists of three cavities (181 MHz). Each of them has two HOM tuners. The fundamental mode in the cavities is tuned by feedback loops in accordance with a beam loading and temperature changes. The HOM frequencies are not controlled automatically.

Due to a shunt impedance and a quality factor of HOMs are high, the beam-cavity interaction leads to the instability and the beam loss as the result. It is not possible to reduce the HOM influence on the beam motion due to unavailability of the HOM automatic controller and an additional waveguide load for the HOM-damping. To suppress coupled-bunch instabilities we'll plane to establish the longitudinal feedback system at the storage ring. For example of the longitudinal kicker, a model of the DUKE kicker cavity will be taken.

LONGITUDINAL MOTION

For estimation of the HOM influence on the beam motion it is convenient to consider a circulating electron beam. Each bunch of the beam, represented as macroparticle, performs the small dipole synchrotron oscillations

$$\ddot{\varphi} + 2\alpha\dot{\varphi} + \omega_s^2\varphi = 0,$$

where ω_s is the synchrotron frequency, α is the growth rate. The stability synchrotron motion is determined by a sign of the growth rate, which consist of

$$\alpha = \alpha_{rad.} + \alpha_{rf} + \alpha_{kick.},$$

$\alpha_{rad.}$ is the synchrotron radiation growth rate, α_{rf} is the instability growth rate due to HOMs, $\alpha_{kick.}$ is the growth rate of the LFB system. If the growth rate, α, is positive, the longitudinal motion is stable. The sign of α_{rf} is depend on whether the Robinson stability condition is satisfied [1].

The radiation damping is small to compensate the harmful HOM influence. The necessary damping is set by the LFB system. The coefficients of α_{rf} and $\alpha_{kick.}$ [2] are expressed as

$$\alpha_{rf} = -\frac{e}{2T_0E_0}\alpha_c \sum_{p=1}^{+\infty} \frac{2I_p^2}{I_0}\frac{p\omega_0}{2\omega_s}(Z_r^+ - Z_r^-),$$

$$\alpha_{kick} = \frac{1}{2} f_0 \frac{V_{kick}}{\Delta E},$$

where f_0 - the revolution frequency, E_0 - the beam energy, α_c - the momentum compaction factor, I_0 - the average beam current, I_p - the harmonic beam current, V_{kick} - the kicker voltage, ΔE - the maximum energy oscillation amplitude, $Z_r^+ \, u \, Z_r^-$ - the real parts of the HOM impedance at $p\omega_0 + \omega_s$, $p\omega_0 - \omega_s$ frequencies, respectively.

In our case at the storage ring there are three cavities, then α_{rf} has additional terms under the sum

$$\alpha_{rf} = -\frac{e}{2T_0E_0}\alpha_c \sum_{p=1}^{+\infty} \frac{2I_p^2}{I_0}\frac{p\omega_0}{2\omega_s}[(Z_r^+ - Z_r^-)\cdot (1 + \cos\omega_s\tau_{12} + \cos\omega_s\tau_{13}) + (-2Z_i^0 + Z_i^+ + Z_i^-)\cdot (\sin\omega_s\tau_{13} + \sin\omega_s\tau_{12})].$$

where τ_{12} and τ_{13} - the time of the bunch passage from the first cavity to the second and the third, respectively. If to take into account the parameters of the high order mode of all cavities are the same and the passage time is small, then the HOM influence on the beam motion is increased in three.

To damp the instabilities, the energy kick should be applied to each bunch of the beam. The necessary output kicker voltage is limited by the amplifier power [3]

$$V_{kick} = \sqrt{2P_{out}R_{sh}},$$

where P_{out} - the maximum output power of the amplifier, R_{sh} - the effective shunt impedance of the kicker cavity.

We should take into account a RF power loss between the amplifier and the LFB kicker, a group delay, a nonlinearity of the phase and gain of the LFB system, to calculate the kicker voltage. Hence, the estimated amplifier power should be taken larger, then it is necessary in practice [4].

ISBN 978-3-95450-125-0

STUDY OF PROTON INJECTOR BEAM TRANSVERSE PHASE SPACE VARIATIONS DURING ACCELERATING VOLTAGE PULSE

A.S.Belov, O.T.Frolov, E.S.Nikulin, V.P.Yakushev, and V.N.Zubets,
Institute for Nuclear Research of RAS, Moscow, 117312, Russia

Abstract

The proton injector of INR RAS linac provides a pulsed beam with the following parameters: current – 100÷120mA; duration – 200 μs; pulse repetition rate – 50 Hz; energy of ions – 400 keV. The results of numerical calculations and experimental studies of beam phase space variations during injector high voltage pulse are presented. It is shown that these variations are caused by instabilities of both beam current and accelerating tube intermediate electrode potential. Instability of beam current has been minimized by using of noiseless mode of operation for the pulsed duoplasmatron and by stabilization of ion source discharge current. The high voltage pulse stability has been improved and is now better than ±0.1%. For the most part of beam pulse duration a transverse normalized emittance for 90% of beam current has been measured to be of 0.09π cm·mrad and variations of the emittance are in limits of ±4% value.

INTRODUCTION

INR RAS linear accelerator proton injector is operated regularly from the end of 80-ies. And the work on its improvement is in progress all the recent years. The basic conditions of beam loss minimization in linac are as more as possible smaller transverse emittance and stability of beam phase portrait position. After installing a new expander cup isolated from duoplasmatron the beam transverse normalized emittance of 0.076π cm•mrad for 63% of central part of the 115 mA beam has been measured at the injector output in noiseless mode and 0.2π cm•mrad for 90% of the beam, respectively [1].

A number of measurements and numerical simulation of injector ion beam formation and transport to the linac LEBT input have been performed. Significant changes in the beam phase portrait position/shape have been found as a result of calculations and beam emittance measurements. In the past two years the injector structure has undergone further modifications which have improved qualitative characteristics of the beam.

NUMERICAL SIMULATION

Numerical simulation using Trak and TriComp SpaceCharge package developed Field Precision LLC has been conducted. Schematic drawing of the proton injector is shown in Fig.1. A beam of hydrogen ions is generated in duoplasmatron type ion source. The beam is accelerated and focused in two-gap accelerating tube by the electric fields between the ion source focusing electrode, intermediate and output (grounded) accelerating tube electrodes.

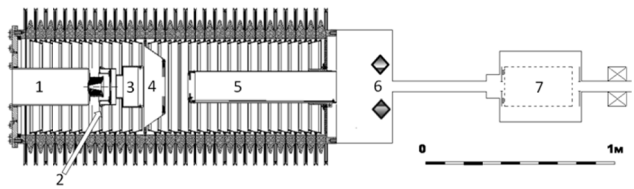

Figure 1. Schematic drawing of the proton injector:
1 - ion source, 2 – extracting electrode, 3 - focusing electrode,4 - intermediate electrode, 5 - grounded electrode, 6 – steering magnet, 7 – diagnostics box.

Simulation have shown that changing of the intermediate electrode potential by a value less than 1% already leads to significant changes in beam properties at the injector output. The example of calculations result is shown in Fig. 2.

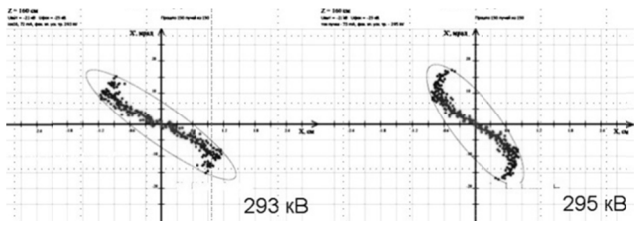

Figure 2. The influence of intermediate electrode potential value on position/shape of the injector output beam phase portrait. Intermediate electrode potential equals 293 kV and 295 kV.

Agreement between simulation and measurement is particularly evident when considering the various aberrations of beam. One of the aberration types studied is shown Fig.3.

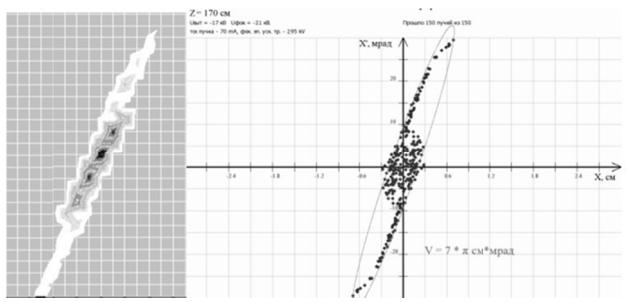

Figure 3. One of the phase portrait aberration types studied when transporting hydrogen ions beam
(left - measurement, right - simulation)

ISBN 978-3-95450-125-0

SECOND-ORDER CORRECTION IN THE ISOCHRONOUS MODE OF THE COLLECTOR RING (CR) AT FAIR

S. Litvinov, C. Dimopoulou, A. Dolinskii, O. Gorda, F. Nolden, M. Steck, H.Weick
GSI, Darmstadt, Germany

Abstract

A challenge for nuclear physics is to measure masses of exotic nuclei up to the limits of nuclear existence which are characterized by low production cross-sections and short half-lives. The large acceptance Collector Ring (CR) [1] at FAIR [2] tuned in the isochronous ion-optical mode offers unique possibilities for such measurements. However, the mass-measurement resolution is inversely proportional to the transverse emittance. In order to reach a resolving power of 10^5 the transverse beam emittance would have to be limited up to 10 mm mrad in both planes, which drastically reduces the transmission of the exotic nuclei. We demonstrate here that the negative influence of the transverse emittance on the mass resolution can be significantly reduced by a proper second-order correction.

Isochronous Mode of the CR

The Collector Ring of the FAIR project is a symmetric, achromatic ring with two arcs, two straight sections and a total circumference of 221.5 meters. It is designed for operation at a maximum magnetic rigidity of 13 Tm. The CR will be operated in three ion-optical modes, two of them providing fast pre-cooling of either antiprotons or radioactive ion beams [1]. In the third mode (isochronous optics) the CR will be operated as a Time-Of-Flight (TOF) spectrometer for the mass measurement of exotic very short-lived nuclei ($T_{1/2} > 20\mu s$) produced and selected in flight with the Super-FRS fragment separator [3]. This technique for mass measurements has been developed at the ESR at GSI [4]. An advantage of this method is that a large number of nuclei can be measured in one experimental run.

The relative change of revolution time T due to different mass-to-charge ratio m/q and velocity v of the stored ions circulating in the ring is [5]:

$$\frac{\Delta T}{T} = \frac{1}{\gamma_t^2} \cdot \frac{\Delta(m/q)}{(m/q)} + \left(\frac{\gamma^2}{\gamma_t^2} - 1\right)\frac{\Delta v}{v} - \frac{dT}{T}, \quad (1)$$

where γ is the relativistic Lorentz factor and γ_t is the transition energy of the ring. The isochronous condition is reached when $\gamma = \gamma_t$. It means, the second term in Eq. (1) vanishes and T defines the m/q. The resolution depends on the width of the time dT. Effects of nonlinear field errors, fringe fields of magnets, closed orbit distortion and transverse emittance negatively act on dT. Their influence has been investigated in [5].

Ions with different m/q are separated in time if their mean time separation ΔT is larger than the full time width of the beam.

$$\Delta T > dT. \quad (2)$$

Influence of Transverse Emittance

For good adjustment of γ_t the largest contribution to dT comes from the second-order geometric aberrations. In order to distinguish their influence, we consider a beam of one species in the ideal isochronous ring without higher-order field errors, fringe fields and closed orbit distortions. Only pure betatron motion exists. For such a ring the time spread is directly related to the transverse emittance ($\varepsilon_{x,y}$) [5]:

$$\left(\frac{dT}{T}\right)_{Emitt.} \approx \frac{1}{4}\left(\varepsilon_x <\gamma_x^{\text{Twiss}}> + \varepsilon_y <\gamma_y^{\text{Twiss}}>\right), \quad (3)$$

where $<\gamma_{x,y}^{\text{Twiss}}>$ are the Twiss parameters averaged over the whole circumference of the ring.

Thus, from Eqs. (1, 3) one can derive the mass resolving power depending on the beam emittance [5]. For the CR, where acceptance is 100 mm mrad in both planes, the limit of the mass resolving power is about 10^4, which is insufficient for precise mass measurements. Therefore, in order to reach the necessary resolving power of 10^5 the transverse emittance would have to be limited to 10 mm mrad in both planes. As a result, the transmission of the ions into the ring would be reduced drastically.

Revolution Time in Second-Order

However, the mass resolving power can be improved using second-order corrections and keeping the transverse emittance large. Let us assume a beam of one species circulating in the ring turn by turn. We observe it in the symmetry plane of the ring where the phase-space ellipse is upright ($\alpha^{\text{Twiss}} = 0$) and this condition is restored after each turn.

Statistical uncertainty gets reduced with increasing number of revolutions, and for accurate mass measurements it is essential to measure the revolution time of the particle over many turns. Therefore, the relative revolution time deviation between an arbitrary and the reference particle can be expressed in terms of the initial coordinates as a Taylor

ISBN 978-3-95450-125-0

THE MOTION OF IONIC FLUX IN AN ELECTRON LAYER

A.S.Chikhachev, Yu.A. Kovalenko
All-Russian Electrotechnical Institute,
111250, Moscow, Russia

Abstract

An acceleration of ion flux in an electronic layer is studied beam in electron layer are studied. The layer is created by electrons that move in transverse electric field and are confined by self-generating magnetic field. It is shown that from such one can extract heavy ions with the velocities up to ion-sound velocity.

INTRODUCTION

The process of extraction of ions from plasma is very important in terms of experiment. A great number of theoretical studies are dedicated to this process. The paper [1] shows that ions leave plasma at velocities which are in excess of ionic sound velocities.Under conditions close to be actual environment when the temperature of electrons is above that of ions ($T_e >> T_i$), the number of ions being accelerated turns out to be exponentially small. The paper [2] deals with the process of accelerating ions in a non-stationary problem. The paper [3] discloses that a transition layer in the plasma-vacuum system appears out to be infinitely large. The paper [4] considers equilibrium conditions with the presence of an electron flow that is directed in line of an ionic flux. This paper deals with equilibrium states when a non-zero flow of electrons is perpendicular to across an ionic flux.

IONIC FLUX STATES IN AN ELECTRON LAYER

Let us assume that at $x = 0$ there is given an ionic flux with a negligible ($\sim v_{Ti}$) initial velocity v_0. We consider 1-D problem where physical quantities are independent of coordinates y and z. The magnetic field has only one component $B_z = -\frac{dA_y}{dx}$, where A_y is a component of a $4-D$ potential. This a magnetic field is induced by the electron flow along the y axes. The electrons move in the x, y plane under the action of electric end magnetic fields with $v_z^{(e)} \equiv 0$. We describe ensemble of electrons by means of a collisionless kinetic equation. A solution of this equation may be form of an arbitrary function of motion integrals: energy H and generalized momenta $P_y = p_y - \frac{e}{c}A_y(x)$ and $P_z = p_z$. Here p_y, p_z - are components of an electron momentum. We take a distribution function in following form:

$$f(\vec{p},\vec{r}) = \Psi(H, P_y, p_z) = \kappa\frac{\sigma(H_0 - H)}{\sqrt{H_0 - H}}\delta(P_y - p_0)\delta(p_z), \quad (1)$$

where $\sigma(x)$- is Heaviside function: $\sigma(x) = 1, x > 0; \sigma = 0, x < 0$. The Hamiltonian $H = \frac{p_x^2}{2m} + \frac{p_y^2}{2m} + \frac{p_z^2}{2m} - e\Phi$, m - is the mass of an electron,$-e$ - is a charge, $\Phi(x)$ -is a potential of electric field. The distribution of type (1) leads to a compact description of the complicated physical situation.

The calculated density of electrons is as follows:

$$n_e = \kappa\int\frac{dH}{\sqrt{H_0 - H}}\frac{1}{\sqrt{H + e\Phi - \frac{1}{2m}(p_0 + \frac{e}{c}A_y(x))^2}}. \quad (2)$$

One can get:

$$n_e = n_0\sigma(H_0 + e\Phi - \frac{1}{2m}(p_0 + \frac{e}{c}A_y)^2), \quad (3)$$

where $n_0 = \pi\kappa\sqrt{H_0}$ and the current density j_y takes the following form:

$$j_y = -\frac{e}{m}\int p_y f d\vec{p} = -\frac{e}{m}(p_0 + \frac{e}{c}A_y(x))n_e. \quad (4)$$

Let us introduce dimensionless variables:

$$\frac{e\Phi}{H_0} = \phi, \xi = \frac{x}{l_0}, l_0 = \sqrt{\frac{H_0}{4\pi n_0 e^2}}, a(x) = \frac{e}{p_0 c}A_y(x).$$

The density of ions specified by hydrodynamical equations: $n_i = \frac{\Gamma_i}{v_i}$ where Γ is density of ionic flux, v_i is velocity of ions.If M -is the mass of ions, v_0- initial velocity then $n_i = \frac{\Gamma_i}{\sqrt{v_0^2 - \frac{2e\Phi}{M}}}$.

The equation for components of $4-D$ potential will transform to the following form:

$$\frac{d^2\phi}{d\xi^2} = \sigma\left(1 + \phi(\xi) - \frac{p_0^2}{2mH_0}(1 + a(\xi))^2\right) - \frac{\nu_i}{\sqrt{u_0^2 - 2\phi(\xi)}}, \quad (5)$$

where $\nu_i = \Gamma_i/(n_0 v_s), v_s = \sqrt{H_0/M}, u_0 = v_0/v_s,$

$$\frac{d^2a(\xi)}{d\xi^2} = \frac{H_0}{mc^2}(1+a(\xi)) = \varrho^2(1+a(\xi)), \varrho = \sqrt{H_0/mc^2}. \quad (6)$$

Let us examine the condition $1 + \phi - \frac{p_0^2}{2mH_0}(1 + a)^2$, that defines boundaries of the electron layer. Assume that $\phi(0) = 0$, then

$1 + \phi - \frac{p_0^2}{2mH_0}(1 + a)^2 < 0$ with $\xi < 0$. Let us have $\frac{p_0^2}{2mH_0} = 1$ and write a general solution of the equation (6) can be written in the following form: $a = -1 + \alpha\sinh(\varrho\xi) + \beta\cosh(\varrho\xi)$, where constants α and β are defined by physical conditions. If $\beta = 1$, the it turns out that electrons may be localized only at $\xi > 0$, i.e. $\xi = 0$ is a boundary of the layer. The value of H_0 fulfils a role of temperature of the electron ensemble.For a characteristic quantity of this temperature, $50eV$ may be taken. Then

ISBN 978-3-95450-125-0

ANGIOGRAPHY X-RAY MONOCHROMATIC SOURCE BASED ON RADIATION FROM CRYSTALS

Yu.A. Bashmakov, Lebedev Physical Institute of RAS (LPI), Moscow, Russia and National Research Nuclear University (MEPhI), Moscow, Russia
T.V. Bondarenko, Siemens LLC, Moscow, Russia and National Research Nuclear University (MEPhI), Moscow, Russia
S.M. Polozov, National Research Nuclear University (MEPhI), Moscow, Russia
G.B. Sharkov, Siemens LLC, Moscow, Russia

Abstract

Nowadays angiography has become one of the most commonly used medical procedures. However the X-ray tubes are mostly used in angiography imaging systems. The problem that encounters in using X-ray tubes is low monochromaticity due to bremsstrahlung while angiography imaging requires quasimonochromatic energy spectrum for better image quality and lower dose rate obtained by the patient. The use of the monocrystaline target at the medical electron LINAC can be one of the possible ways to obtain the monochromatic X-ray radiation. This type of X-ray generator will provide monochromatic radiation with photon energy dependent on the electron beam energy. The X-ray generation mechanism, possibilities of monocrystal usage as an X-ray source for angiography and requirements for beam parameters are discussed.

INTRODUCTION

Angiography nowadays is the state of the art medical imaging technique used to visualize the inside, or lumen, of blood vessels and organs of the body, with particular interest in the arteries, veins and the heart chambers. This method is traditionally done by injecting a radio-opaque contrast agent into the blood vessel and imaging using X-ray based techniques.

X-ray sources in angiography applications are based on X-ray tubes. These sources are well explored and provide high rates of radiation intensity. In X-ray tubes the source of the radiation is tungsten rotating anode that is irradiated by the electron beam from the thermal cathode. The main drawback of the tube is wide bandwidth of the generated radiation spectrum provided by two principles: fluorescence and bremsstrahlung. The low energetic part of the X-ray is cut-away by the alumina or beryllium filter.

Angiography principle lies in using a contrast medium that allows to clearly identify the agent in the patient body. A medical contrast medium is a substance used to enhance the contrast of structures because of the high rates of mass attenuation coefficient for X-ray radiation in specific narrowband peak e.g.: at 33.1 keV for iodine contrasts, 37.4 keV for barium and 50.2 keV for gadolinium. All bands of radiation spectrum from X-ray tube that differs from the agent attenuation energy peak penetrating patient is less attenuated by the contrast agent and therefore will degrade the clearness of the contrasted part of the image and leads to the unnecessary high dose rate delivered to the patient.

There are several methods of eliminating undesirable spectrum parts of the radiation. The most widespread is usage of X-ray tubes with filters like beryllium windows to suppress the low energy spectrum part that is absorbed in the skin and is the most harmful for the patient. Another method lies in the utilization of X-ray fluorescence method: radiation obtained from the X-ray tube illuminates the fluorescent target and irradiates the characteristic lines. The disadvantage of this method is low level of radiation intensity [1].

Another idea is based on using of the inversed Compton scattering principle. The light beam from the laser is counter-propagated against an electron beam produced by a linear accelerator. X-ray photons are generated by inverse Compton scattering that occurs as a consequence of the "collision" that occurs between the electron beam and IR photons generated by the laser. The disadvantage of this method is concerned in necessity for terawatt laser pulses with ps duration [2].

CHANNELLING RADIATION

The method of obtaining of the narrow-band X-rays lies in utilizing the principle of so called channeling radiation from crystals [3].

Channeling radiation is emitted by relativistic electrons passing through single crystals along a direction of high symmetry. The radiation is forward directed into a narrow cone with an angle of emission $\Theta \sim \gamma^{-1}$.

There are two different types of channeling dependent on the electron track – axis channeling and planar channeling. In the first case electron captured in the channel is moving along the crystal axis and experience the influence of the axially-symmetrical coulomb field of the crystal axis. In the planar channeling the particle is forced by the fields of the atoms situated on the crystalline plane.

The mechanism of channeling radiation can be described in two principal ways: classical physics model and quantum mechanics.

Electrical field formed between the crystallographic planes forming the channel can be characterized with an averaged potential $U(x)$ where x is transversal offset from the channel central plane. As a rule $U(x)$ is smooth,

ISBN 978-3-95450-125-0

PROGRAM COMPLEX FOR VACUUM NANOELECTRONICS FINITE ELEMENT SIMULATIONS

K.A. Nikiforov*, N.V. Egorov,
St. Petersburg State University, St. Petersburg, Russia

Abstract

The program complex in MATLAB intended for vacuum nanoelectronics simulations is described. Physical and mathematical models, computational methods and algorithms of program complex are presented. Electrostatic simulation of electron transport processes is discussed under electron massless approximation; current function method and Matlab PDE Toolbox finite element solutions are used. Developed program complex is able to simulate diode and triode structures with complicated submicron geometry, current-voltage characteristics, calculate electric field distribution, estimate electric line interaction. The modelling results by the example of two different triode structures are presented. Matlab stand-alone application with graphical user interface for demonstration purposes is presented.

INTRODUCTION

The development of a new accelerator electron gun with the lowest possible emittance is actual important problem. Due to the recent advances in nanotechnologies and vacuum nanoelectronics, a field-emitter array (FEA) based gun is a promising alternative for thermionic or photocathode technologies. Indeed, several thousands of microscopic tips can be deposited on a 1 mm diameter area. Electrons are then extracted by a grid layer close to the tip apex and maybe focused by a second grid layer or anode several micrometer above the tip apex. Although simple diode system is sufficiently to start electron emission, triode configuration with field emitter as cathode, extractor electrode as gate and distant anode as collector is used for many applications. It is necessary to perform computer simulations for design and development of various types FEAs. First of all we'll say a few words about emission nanostructures by the example of wich we'll demonstrate wide possibilities of programmes writen in Matlab. The first one is FEA Spindt-type nanotriode from the company SRI Inc. A schematic of triode cell from is shown in Figure 1.

The second one is the FEA cathode with NbN sharp-edged cylindrical emitters from JSC Mikron. The SEM image in Figure 2 represents NbN thin-film emitters on heavy As-doped Si wafer.

PROGRAM COMPLEX

The device modeling is broken traditionally into two different projects. The first is to model the fields and particle motions within the device to verify the design parameters and to locate design possible problems before fabrication. The second project is to model the operation of the device and its electrical interaction with an external circuit.

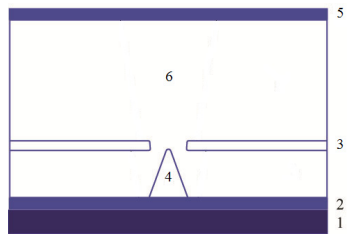

Figure 1: Vacuum nanotriode cell: 1 – wafer, 2– cathode layer, 3 – gate layer electrode, 4 – Mo emitter tip, 5 – anode, 6 – vacuum channel.

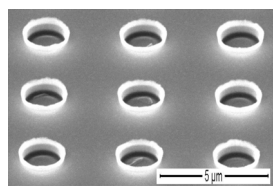

Figure 2: SEM picture of FEA cathode with NbN sharp-edged cylindrical emitters (diode/triode operation is possible).

Electron trajectories

In zero order approximation emitted electron trajectories are supposed to coincide with electric field force lines. This approach is known as electron massless approximation and used for electrostatic simulation of vacuum emission micro/nanoelectronic devices. In vacuum micro/nanoelectronics due to strong dependency of emission current density upon electric field strength the main part of electron current is formed on areas with maximum surface field. On the other hand due to potentiality of electrostatic field the larger field strength is, the smaller force lines curvature will be and the more adequate electron massless approximation will be. Figure 3 represents visualization example of trajectories simulation for Spindt triode nanostructure.

Electric field distribution

Due to axial symmetry of considered FEAs cells we use Matlab two-dimensional static field finite element analysis code (functions from Partial Differential Equations Tool-

* nikiforov_k@mail.ru

ISBN 978-3-95450-125-0

THE KNIFE-EDGED FIELD EMITTER MATHEMATICAL MODELING

E.M. Vinogradova, M.G. Fomenko, SPbSU, Saint Peterburg, Russia

Abstract

Numerous nano-scale electronic devices are based on the field emitters such as carbon nanotubes. The field emitters are extensively applied in the various domains of an instrument engineering. In the present work the problem of a field emission cathode as the knife-edged field emitter mathematical modeling is solved. The supposed shapes of the emission diode system with the field emitter are the lune's type (as a cathode) and the infinitely thin spherical segment (as an anode). The effect of the space charge is neglected. The boundary – value problem for the Laplace equation in the toroidal coordinate system is presented. To solve the electrostatic problem the variable separation method is used. The potential distribution is represented as the series with respect to Legendre functions. The boundary conditions and the normal derivative continuity conditions lead to the linear algebraic equations system relative to the series coefficients. In this way the distribution of the potentials for the whole region of the considered electro-optical systems was obtained.

INTRODUCTION

Field emitters (FE) have unique parameters for industrial applications in the domain of vacuum micro- and nano-electronics — scanning electron microscopy, x-ray sources, emission displays, parallel e-beam lithography, etc. FE are manufactured of various materials with different morphologies [1–4].

In the present work the rotationally symmetric knife-edged field emitter mathematical modeling is under investigation (see Fig.1).

PROBLEM BACKGROUND

It is presented the solution to Laplace's equation for the axisymmetric diode systems: cathode is simulated by two spherical segments with the toroidal top (lune's type), an anode modeled by thin spherical segment (see Fig.2).

To solve the rotationally symmetric electrostatic problem the variable separation method is employed. The toroidal coordinate system (α, β, φ) is used.

The parameters of the problem are as follows:

$\beta = \beta_1$ $(0 \le \alpha \le \alpha_1)$ — the surface of anode;

$\beta = -\beta_2$, $\beta = 2\pi - \beta_3$ $(0 \le \alpha \le \alpha_0)$ and

$\alpha = \alpha_0$, $(\beta_2 \le \beta \le 2\pi - \beta_3)$ — the surface of tip;

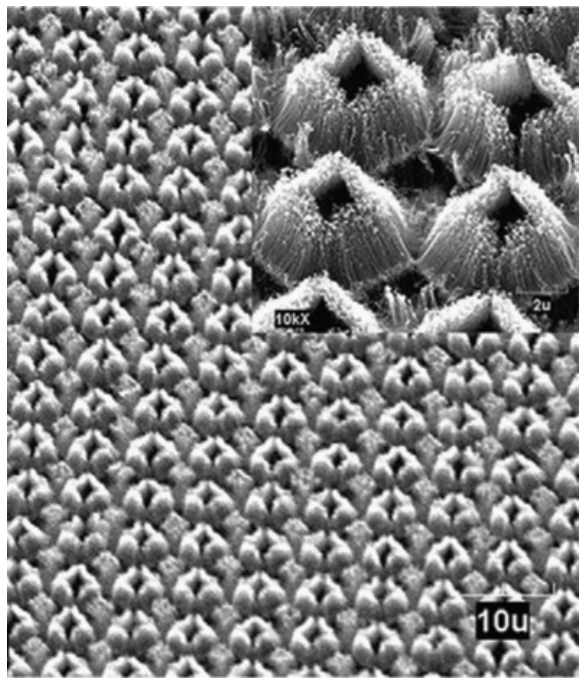

Figure 1: SEM images for aligned and patterned carbon nanotube emitters [1].

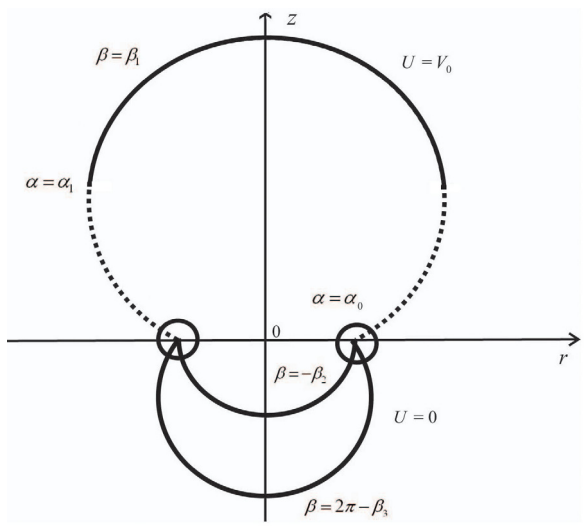

Figure 2: Schematic diagram of the diode systems based on a knife-edged field emitter.

$U(\alpha, \beta_1) = V_0$ $(0 \le \alpha \le \alpha_1)$ — the boundary condition on anode.

ISBN 978-3-95450-125-0

THE FIELD CATHODES WITH THE EFFECT OF SPACE CHARGE MODELING

M. Makarova, E. M. Vinogradova, Saint-Petersburg State University, Saint-Petersburg, Russia

Abstract

This work is devoted to the question of the effect of space charge on the field electron emission. The electrostatic potential distributions for the diode emission systems are calculated. The diode systems, which can be readily constructed, are generally used for the characterization of field emission properties of novel materials. They have some effective applications in vacuum nano- and microelectronics. In this work the plane diode emission system and cylindrical diode emission system are investigated. The solutions of Poisson's equation for the electrostatic potential distribution are received for the boundary-value problems. The right side of Poisson's equation is assumed to be the piecewise constant function. The charge conservation law and the energy conservation law are used. One and two dimensional cases are investigated.

INTRODUCTION

Currently there are great interest in research and practical applications of the field electron emitters, where emission occurs from a nanoscale inclusions of conducting material, carbon nanotubes and fibers, protrusions of nanometer size. Microfabricated field emission arrays (FEAs) have been studied extensively both theoretically and experimentally. FEAs are considered as excellent candidates for use as electron sources operating with high efficiency, high currents for vacuum electronic applications.Much effort has been directed towards the commercial applications of FEAs, including their use as electron sources in various types of visualization equipment, including lithography, x-ray sources, microscopes, high-power microwave amplifiers, transistors and especially for generation high-brightness flat panel displays [1, 2, 3].Field emission diodes and triodes are the most commonly used device architectures for FEAs. The diode structure, which can be readily constructed, is generally used in laboratories for the characterization of field emission properties of novel materials [1].

Electron field emission from a single emitter is a barrier tunneling, quantum mechanical process that can be described by the Fowler-Nordheim equation. At high emission current densities, however, the space charge caused by the cathode may affect the current densityvoltage characteristics predicted by the Fowler-Nordheim theory [1, 4, 5]. This work is devoted to the investigation of the effect of space charge on the field electron emission. Plane diode emission system and cylindrical diode emission system are considered.

MATHEMATICAL MODELING AND CALCULATION

Plane Diode Emission System

The problem is to calculate electrostatic potential distribution in the region between the electrodes of the plane diode emission system. This is a simple case of the electrode configuration of diode system [6]. At first a one-dimensional case was studied. Potential distribution is described by the Poisson's equation

$$\triangle \bar{U}_p(z) = -\bar{\rho}_p(z) \tag{1}$$

with following boundary conditions:

$$\bar{U}_p(z_1) = 0, \quad \bar{U}_p(z_2) = V. \tag{2}$$

Function $\bar{U}_p(z)$ is the potential distribution; $\bar{\rho}_p(z) = \frac{\bar{\rho}_d^*(z)}{\varepsilon_0}$, where $\bar{\rho}_d^*(z)$, is the space charge density, ε_0 is the vacuum dielectric constant. Function $\bar{\rho}_p(z)$ is unknown. In our work we assumed that these function is a piece-wise constant function

$$\bar{\rho}_p(z) = \begin{cases} \widetilde{\rho}_1^1, & z \in [R_1 = z_1, R_2), \\ \widetilde{\rho}_2^1, & z \in [R_2, R_3), \\ \dots & \\ \widetilde{\rho}_N^1, & z \in [R_N, R_{N+1} = z_2]. \end{cases}$$

where N is the number of parts for which the region between the electrodes is divided. Solution of (1) with boundary conditions (2) is

$$\bar{U}_p(x,z) = \sum_{s=1}^{k-1} \widetilde{\rho}_s^1 \bar{P}_{s_1}(x,z) + \sum_{s=k+1}^{N} \widetilde{\rho}_s^1 \bar{P}_{s_2}(x,z) + \\ + \widetilde{\rho}_k^1 \bar{P}_k(x,z) + \bar{L}_p(z),$$

where $\bar{P}_{s_1}, \bar{P}_{s_2}, \bar{P}_k, \bar{L}_p$ is a several known functions, $\widetilde{\rho}_i^1$ is unknown values. To find these values we considered the equations

$$\mathrm{div}\vec{j_p} = 0, \tag{3}$$

$$\frac{1}{2} m \vec{V_p}^2 = -e\bar{U}_p(z), \tag{4}$$

where $\vec{j_p}$ is a current density, $\vec{V_p}$ is a speed of the electrons, e is the electron charge. Eq. 3 is the current continuity equation, Eq. 4 is the energy conservation law. Combining these equation gave

$$\bar{\rho}_p(z)\sqrt{\bar{U}_p(z)} = A = \mathrm{const},$$

ISBN 978-3-95450-125-0

THE TRIODE-TYPE SYSTEM ON THE BASIS OF THE FIELD EMITTER MODELING

Televnyi D. S, Vinogradova E. M., Saint Petersburg State University, Russia

Abstract

The mathematical model of a cylindrical triode-type system on the basis of the field emitter is under consideration. The internal area of the system is filled of two different dielectrics. Effect of space charge is not considered. The field emitter is modeled by a charged filament of finite length, which located on the system's axis. The modulator has a form of a circular diaphragm. The Poisson equation with the given values of potentials at the electrodes is solved. The variable separation method is used to determine distribution of electrostatic potential. An unknown function of the charge density is approximated by a piecewise constant linear function. The problem of finding unknown coefficients in the potential eigenfunction expansion is reduced to the linear algebraic equations system. Numerical calculations emitter's forms are represented.

INTRODUCTION

Vacuum electronic devices based on the field emission are used in many areas of scientific research. Particularly in the development of new high-precision devices as an electron microscopes, flat panel displays, systems of surface diagnostics, devices of micro- and nano-electronics [1]. The main characteristics of these devices are small dimensions and low consumption of power for efficient operation. The field cathode makes it possible to generate emission of electrons at low values of the potentials in the system. The high current density provided by the small radius of curvature of the tip and does not require in consumption energy for heat the emission region. To improve the emission characteristics into the system usually include an additional electrode called as a modulator. This modulator allows to change the field close by the emitter within a wide range, with a low value of the potential [2].

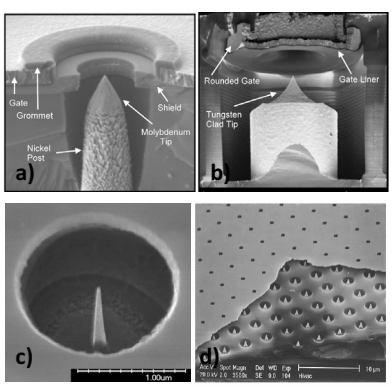

Figure 1: Pictures of cells triode-type systems based on field-emitter.

FORMULATION OF THE PHYSICAL PROBLEM

Consider a cylindrical triode-type system which consists of a substrate on which the field cathode is situated, the modulator in the form of a flat diaphragm and an anode (Fig. 2). The internal part of the system is filled by two different dielectrics with dielectric constants ε_1 and ε_2. One of them serves as a casing of dielectric shell. There is a tip on the axis of the system. This tip is modeled by charged filament which length is z_0. It is assumed that the cross geometrical dimensions of the field cathode are much smaller than the cross dimensions of the system. Cathode has a zero potential, the modulator's potential is V_1 ,the anode's potential is V_2. The main task consists in finding of potential distribution in the triode-type system with a field tip. (System's section with the axial symmetry)

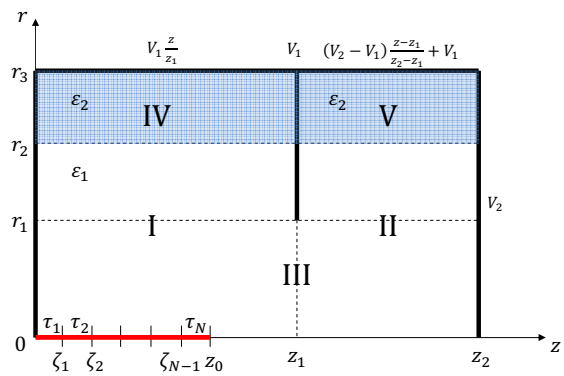

Figure 2: System's section with the axial symmetry.

FORMULATION OF THE MATHEMATICAL PROBLEM

The function of potential distribution must satisfy the Poisson's equation with considering an axial symmetry of the system

$$\triangle U(r,z) = -\frac{\rho(r,z)}{\varepsilon_0}, \tag{1}$$

with boundary conditions

$$\begin{aligned} &U(r,0) = 0, \quad r \in [0, r_3], \\ &U(r,z_1) = V_1, \quad r \in [r_1, r_3], \\ &U(r,z_2) = V_2, \quad r \in [0, r_3], \\ &U(r_3,z) = V_1\frac{z}{z_1}, \quad z \in [0, z_1], \\ &U(r_3,z) = \frac{V_2 - V_1}{z_2 - z_1}(z - z_1) + V_1, \quad z \in [z_1, z_2], \end{aligned} \tag{2}$$

ISBN 978-3-95450-125-0

THE MULTI-TIP FIELD EMISSION CATHODE MATHEMATICAL MODELING

N.V. Egorov*, E.M. Vinogradova, SPbSU, Saint Peterburg, Russia

Abstract

The multi-tip field cathode as the field emission cathode arrays for rectangular lattice is considered. The field emission cathodes are of interest for vacuum nano-scale electronic devices. The electrostatic potential distribution is presented for the periodic system of free-number thin tips on a plane substrate as a field emission cathode and a plane substrate as an anode. The tips shape may be various. The potential of the substrate and cathode is equal the zero, the anode's potential is equal a constant. The effect of space charge is neglected. The each tip is represented as a system of the point charges. The point charges are determined to the zero equipotential coincides with the cathode's shape. The potential distribution is found for whole region of the field emission cathode arrays. The exact three-dimensional solution to the Laplace/Poisson equation has been obtained in the Cartesian coordinate system. This solution has direct applications in three-dimensional calculations of electron trajectories in micron- and submicron-sized field-emitter arrays.

INTRODUCTION

Field emission is of great commercial interest in electronic devices. Over the last decade, carbon-based and several others nanomaterials, such as carbon nanotubes, nanotips, various zinc oxide nanostructures, have attracted considerable attention due to their unique physical, chemical, and mechanical properties [1–3]. These nanostructures as the field cathodes are applied for surface diagnostics, low-energy electron diffraction, Auger-spectroscopy, scanning tunneling microscopy and others potential applications in the areas of electron field emission [4–6].

In this work the multi-tip field cathode as the field emission cathode arrays for rectangular lattice is under investigation.

PROBLEM BACKGROUND

The solution of Laplace's equation for the electrostatic potential distribution is presented for the diode systems: the multi-tip emitter as a field emission cathode of the on a flat metal substrate (base) and a plane as an anode. Each thin tip is placed in the rectangular lattice point (see Fig.1). The tip's shape may be various. The effect of the space charge is neglected.

* egorov@apmath.spbu.ru

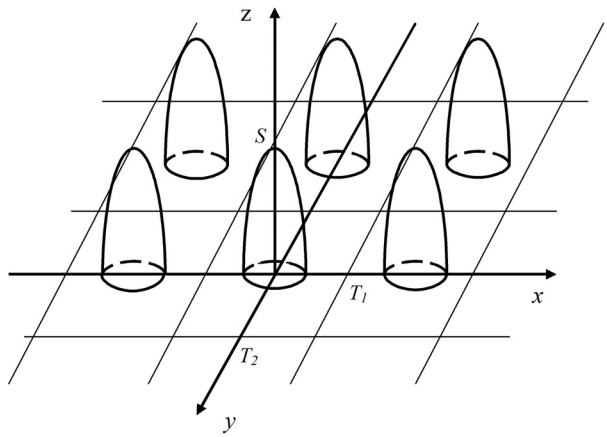

Figure 1: Illustration of a field emission cathode arrays for rectangular lattice.

To solve the electrostatic problem the variable separation method is employed. The cartesian coordinate system (x, y, z) is used.

The parameters of the problem are as follows:

$z = Z_{N+1}$ — the surface of anode;

$z = 0$ — the surface of substrate;

S — the length of tip;

$z_0(x, y)$ — the surface of tip;

T_1 — x-direction half-period;

T_2 — y-direction half-period;

$V(x, y, Z_{N+1}) = V_0$ — the boundary condition on anode;

$V(x, y, 0) = 0$ — the boundary condition on substrate.

The potential of the tip is assumed to be zero without the loss of general character of the problem.

Let us to interchange each tip influence for periodic lattice cell with a charge system q_i $(i = \overline{1, N})$ effect so that the tip surface is matched with the zero's equipotential as the virtual cathode (see Fig.2).

The parameters of the charge system are as follows:

N — the number of charges;

q_i — the values of charges;

$(0, 0, Z_i)$ — the coordinates of charges.

ISBN 978-3-95450-125-0

FIRST TEST RESULTS OF RF GUN FOR THE RACE-TRACK MICROTRON RECUPERATOR OF BINP SB RAS*

V.N. Volkov#, V.S. Arbuzov, E.I. Gorniker, E.I. Kolobanov, C.A. Krutikhin, I.V. Kuptsov, G.Ya.Kurkin, V.N. Osipov, V.M. Petrov, A.M. Pilan, I.K. Sedlyarov, V.A. Scheglov, N.A.Vinokurov, BINP SB RAS, Novosibirsk, Russia

Abstract

A new electron source for the Race-Track Microtron Recuperator is being developed by BINP SB RAS. It will increase average beam current and brightness of synchrotron radiation.

Instead of the static 300kV electron gun operated now we are developing RF gun with the same energy of electrons. This RF gun consists of RF cavity with a gridded thermo cathode mounted on the back wall. RF cavity is driven by a 60 kW generator with last stage equipped by GU101A tetrode tube. Operational frequency of the cavity is 90.2 MHz. It is equal to the second subharmonic of the Microtron RF system frequency. A set of low power electronics controls amplitude of the cavity voltage and its tuner.

This system, including a diagnostics beam line, has been installed to serve as a test bench to test the RF cavity and for beam dynamics studies. In continuous regime the designed 300 kV voltages at the acceleration gap is obtained. This paper summarizes the first test results of the cavity in this configuration.

INTRODUCTION

The RF electron gun for the Race-Track Microtron Recuperator [1] operated in BINP SB RAS (Novosibirsk) is described in [2]. RF cavity of the electron gun is made on base of the Microtron accelerating cavity [3]. The layout of the RF cavity is shown in Fig.1. Only the insertion assembly (3, 5, 11) and the conic nose (4) were designed and build anew. The other parts of the existing cavity were modified to the electron gun design requirements. This cavity is manufactured at the BINP workshop where novel technologies were used widely in the manufacture process such as electron beam welding and turner's work by diamond cutting tool.

CAVITY MANUFACTURE

The cavity cylindrical wall and side walls are made of copper-stainless steel bimetal. We have selected two side walls by ultrasonic scanner for checking the quality of bonding between copper and stainless steel layers.

Assembling of the cavity was made as follows. Firstly, the conic nose (4) was welded to the left side wall (2) (see Fig. 1). Then the left side wall was welded to the cylindrical wall (1), the insertion was welded to the right wall and finally the assembly was welded to the cylindrical wall.

*Work supported by the Ministry of Education and Science of the Russian Federation; RFBR grant 11-02-91320

#V.N.Volkov@inp.nsk.su

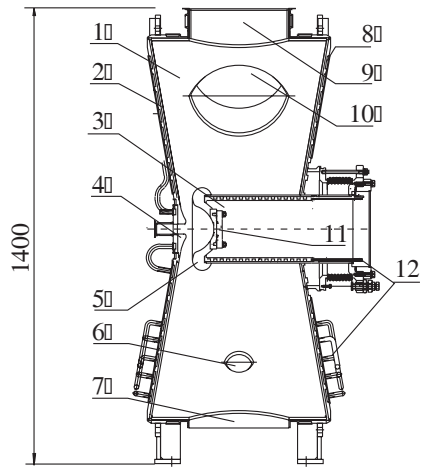

Figure 1: RF gun cavity layout. 1- cylindrical wall, 2-left side wall, 3-insertion, 4-conic nose, 5-electrode, 6-port for sampling loop, 7-vacuum pumping port, 8-right side wall, 9-RF power input port, 10-port for frequency tuning plunger, 11-vacuum cap, 12-water cooling tubes.

Conic Nose Welding

The maximum surface electric field with E_{peak}=10 MV/m is concentrated on the conic nose and on the electrode. To prevent an electric breakdown in the gap these parts were machined by diamond cutting tool using numerically controlled lathe. All other surfaces were mechanically polished by a tangle of thin nichrome wire. Then the conic nose was welded to the left wall in vacuum chamber of BINP electron beam welding installation (see Fig.2).

Welding of the Cavity

Before welding to the right wall the position of the insertion was set so that the resonance frequency of RF cavity under vacuum will be 90.2 MHz. To guarantee this the axial deformation of both discs after welding and deformation of disks under atmospheric pressure of both were accounted for. (see Fig.4). Measurement of the deformations was made only for the left disk. The other side of the cylindrical wall and all other ports were closed vacuum tight during measurements. It was presumed that deformation of the right side wall will be the same. The deformation under atmospheric pressure was measured to be 0.64 mm, welding deformation was 5.5÷7μm.

It is possible to correct the inaccuracy of the resonance frequency and cathode radial position by deformation of thin copper membrane close to the welding contact within ±0.5 mm. The cathode position is controlled by a rough tuning mechanism installed on the right side wall.

ISBN 978-3-95450-125-0

THE SYSTEM OF POWER SUPPLIES, CONTROL AND MODULATION OF ELECTRON GUN FOR FREE ELECTRON LASER

E.A. Kuper, V.R., Kozak V.R.Mamkin, V.K. Ovchar, V.V. Repkov, S.S.Serednyakov,
S. V. Tararyshkin, D.A. Zverev, BINP, Novosibirsk, Russia

Abstract

The system of power supplies, control and modulation based on triode cathode-grid unit was designed for producing of pulsed electron beam for free electron laser FEL [1]. The main part of the system located inside the tank filled with SF6 gas and has -300kV potential. It's supplied through the isolated transformer and controlled through the fiber optic link with CAN interface. The GaN RF transistor in the output stage of modulator composed of hybrid assembly on the BeO ceramic plate. Pulsed output voltage of modulator can be regulated 0-120V on the load 25Ω. Time duration is <1ns. Repetition rate is 20kHz-20MHz (90MHz). Start of modulator from timer performed through the 1GHz fiber optic link.

The inverter is supplying of isolated transformer and timer for start of modulator with synchronization to RF voltage for grouping and accelerating are located in the control room. The timer ensured the compensation of the slow time shift of the electron beam relatively to RF voltage phase.

The control code was wrote on C++ language under Windows operating system using QT framework, and provide all algorithm of steering in real time with others operating programs for FEL with remote control Channel Access server from EPICS.

INTRODUCTION

For effective work of electron accelerator for Free Electron Laser (FEL) the system of power, control and modulation of triode cathode-grid unit was designed. It was designed with the high end components: GaN JFET transistors, 1GHz fiber optic link and RF micro strip transformers. The pulses on the output of modulator have very high parameters.

- Time width of pulses 1ns
- Pulse amplitude 0-120V
- Repetition rate 20kHz-90MHz
- Load 25Ω
- Part 2 of the system works at -300kV potential

SYSTEM DESCRIPTION

The system can be divided on two parts as depicted in Figure 1. The part 1 is under ground potential and provide power, control and start pulses (St) for part 2. It consists of power inverter, timer and two fiber optic converters. Power inverter has 220V input line with 50 or 60Hz. The output of power inverter is connected to input coil of isolated power transformer (300kV). Timer generates start pulses (St) with phase attached to RF voltage on the grouping resonator. The first fiber optic converter works as galvanic isolation for start pulses (St) and has 1GHz bandwidth. The second fiber optic converter works as galvanic isolation for CAN interface and has 1MHz bandwidth. The part 2 works under -300kV accelerating potential in the tank filled pressed SF6 gas (1.5 excessive bars). Figure 2 shows the total view of part 2. It consists of a cathode-grid unit, modulator, power supplies, isolated transformer, control unit CEAC124 and fiber optic converters.

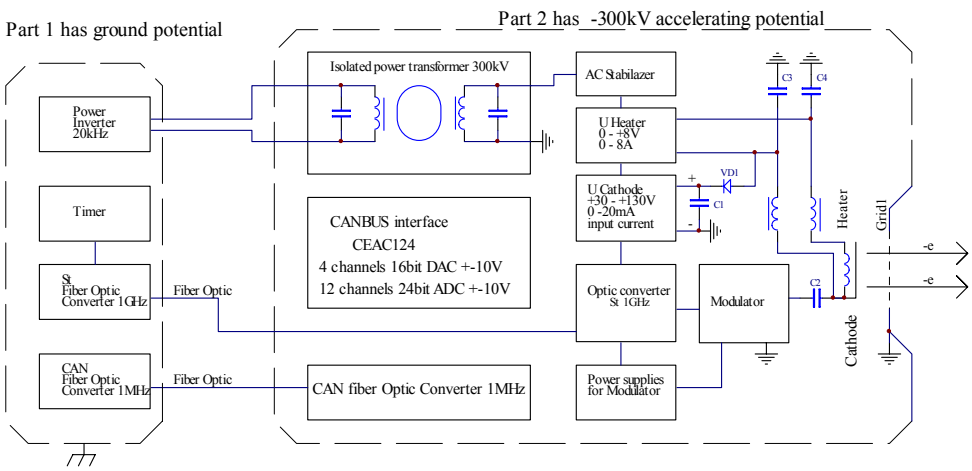

Figure 1: Block diagram of the system.

ISBN 978-3-95450-125-0

A PS-PULSED E-GUN ADVANCED TO A T-WAVE SOURCE OF MW-LEVEL PEAK POWER

A.V. Smirnov, RadiaBeam Technologies Inc., Santa Monica, CA 90404, USA

Abstract

A coherent source based on an electron gun is considered to deliver high instantaneous power comparable to that available from a few most powerful sources operating at mm-sub-mm wavelengths. A DC or RF E-gun is integrated with a robust, compact, efficient, dismountable radiator inside the vacuum envelope. Resonant Cherenkov radiation is driven by a low-energy photoinjector operated in a custom mode combining strong over-focusing, robust slow-wave structure, and pulse sub-ps photoinjectior employing on-cathode beam modulation. Single pulse mode operation is enhanced with filed compression effect at high group velocity. The performance is analyzed analytically and numerically.

INTRODUCTION

A huge variety of applications in biology, medicine, chemistry, solid state physics, radio astronomy, homeland security, environment monitoring, spintronics, advanced spectroscopy, and plasma diagnostics need several orders higher THz peak power than it is available today for universities, middle-sized and small labs and businesses. Many of these applications are related to fast processes, emerging time-domain spectroscopy (TDS), and imaging that require short THz pulses of high intensity.

So far only a few FELs are dedicated to operate at THz frequencies. Typically such an FEL is driven by tens of MeV electron accelerator and contains an undulator and an optical cavity. The first FEL facility to provide THz radiation to users has been the UCSB-FEL (0.3-0.8mm wavelength, ~10kW power in 1-20μs pulse length). The world-largest FEL Facility at JLAB produces a broadband THz radiation [1] with 100W average and about 1MW peak power. To date the Novosibirsk FEL [2] is the most powerful coherent THz source operating at 0.12-0.24mm wavelengths and 0.3% line width to deliver 0.4kW average power and up to ~MW peak power. It comprises 20m long optical cavity, 4m long undulator driven by a 40-50 MeV e-beam accelerated in RF linac with energy recovery. The ENEA-Frascati FEL-CATS source operates in the 0.4-0.7 THz range with about 10% FWHM line width [3] in a super-radiant mode without long optical cavity. A ~1.5 kW power is measured in 5-μs macropulse at 0.4 THz (corresponding to up to 8kW peak in each 3-10 ps micropulse).

More compact, but still powerful, undulator-free, sub-mm wavelength source is considered here. The beam is microbunched on the photocathode with laser using beatwave or multiplexing technique. Important property exploited in the concept is capability of natural focusing of the intense electron beam down to sub-wavelength spot size in a conventional RF high-brightness photoinjector. These two remarkable features allow effective THz radiation resulted from interaction between high-impedance, slow-wave structure and very high-density, microbunched electron beam.

DESIGN FEATURES

The design concept of the radiator integrated into the E-gun driver is illustarted in Figure 1. The radiator can be based on periodic stricture (gratings) or dielectric (PECVD diamond). It may be circular (capillary), rectangular, or planar. The source can operate in two modes: single microbunch and train of microbunches with corresponding laser system.

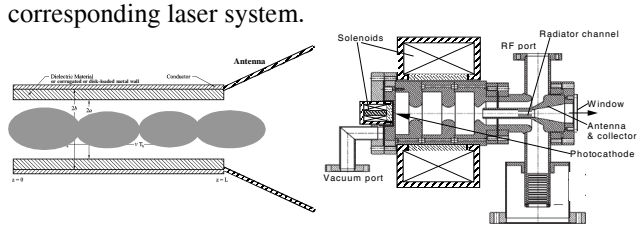

Figure 1: LEFT: THz extractor scheme (radiator). RIGHT: Schematic layout of sub-mm source based on 2-cell, pulse RF or DC-RF electron gun.

Different schemes of THz and exhaust electron beams separation and utilization are exemplified in Figure 2. Simple tapering of the radiator channel turns it into a broader spectrum source for powerful time domain spectroscopy or active "colorful" imaging for inspection and security applications.

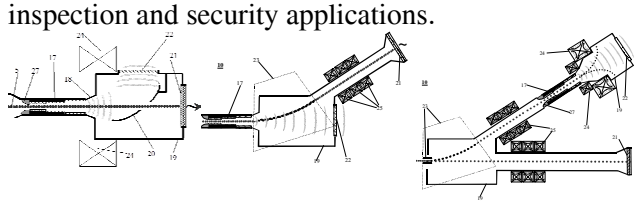

Figure 2: Schematic configurations of a combined T-X-ray source. LEFT: straight electron beam and bended THz beam. MIDDLE: bended electron beam and straight THz beam; RIGHT: alternating electron beam deflected on X-ray target or THz radiator with e-beam scattering and dumping.

A capillary channel has already been used in a number of wakefield research setups (see, e.g., [4]). It is exemplified in Figure 3, left. Radiation directivity can be enhanced with optimized shaping of the dielectric (see Figure 3, right). By sacrificing shunt impedance (see Table 1) one can make the radiator much more robust to sustain THz-field-induced stress and heat as well as beam halo

ISBN 978-3-95450-125-0

HIGH DUTY CYCLE ION SOURCES AT GSI AND FAIR

J. Pfister*, A. Adonin, R. Hollinger and K. Tinschert
GSI - Helmholtz Center for Heavy Ion Research, Darmstadt, Germany

Abstract

Future heavy ion experiments at GSI and FAIR demand for high current as well as highly brillant ion beams of various metallic and gaseous ions produced by the GSI accelerator facility. Therefore GSI's Ion Source Group is continously developing and operating various types of ion sources feeding the UNIversal Linear ACcelerator (UNILAC). In this contribution a status overview of operated high duty cycle ion sources including important ion source data as beam current and beam spectrum as well as future perspectives for the ion source operation for FAIR is presented.

INTRODUCTION

GSI Helmholtz Center for Heavy Ion Research is providing beams of almost every chemical element up to the heaviest stable ions like Uranium to users of the worldwide scientific community. Among others [1] two types of ion sources are dedicated for operation in the high duty cycle regime, namely the Penning Ionisation Gauge (PIG) placed at the high current injector and the Caprice-type Electron Cyclotron Resonance Ion Source (ECRIS) placed at the high charge state injector.

STATUS OF ION SOURCES

During the last years, apart from regular continuous operation of GSI's injectors, the performance of the high duty cycle ion sources has been improved. The operational results and improvements are shown in the following subsections.

Penning Ionisation Gauge - PIG

The PIG is in use for more than 30 years at GSI [2]. This type of source is the working horse especially for experiments carried out at the experimental hall of the UNILAC. Therefore the main feature is the 50 Hz operation with duty factors up to 25%. For the PIG a combination of extraction and post-acceleration is used in order to deliver the injection energy of 2.2 keV/u to the beam injected into the radio-frequency quadrupole (RFQ) for all available elements. The low energy beam transport line (LEBT) from post-acceleration towards the RFQ is about 10 m long and consist of several magnetic focussing quadrupole doublets and triplets, steerers, beam diagnostic stations (profile grids, faraday cups, beam transformators) as well as an analysing magnet for mass separation of multi-isotopic elements. Finally the beam is bend to the axis of the UNILAC via a 12.5 degrees magnetic switchyard, where also the high current beam is inclined to the linac.

The PIG is used for producing beams of gaseous as well as for metallic elements. Depending on experimentalists request development of new elements and isotopes has been done in the recent years. Most common and recent elements from the PIG source are shown in Tab. 1.

It is obvious that for metallic ions using a sputter electrode the lifetime of the source is normally not longer than a day with 25% duty cycle and reasonable currents whereas the sources with gaseous elements have lifetimes of more than just a few days. For the sputter as well as sources for gaseous elements a general refurbishment campaign is ongoing which is almost a general setup of a new source. 90% of the parts are replaced and only about 10% are carefully cleaned.

Table 1: Selections of ion beam species with corresponding beam currents in front of the RFQ.

Ion species	Intensity (eμA)	Ion species	Intensity (eμA)
$^{12}C^{+}$	300	$^{74}Ge^{4+}$	20
$^{12}C^{2+}$	60	$^{84}Kr^{3+}$	40
$^{12}C^{3+}$	73	$^{86}Kr^{2+}$	26
$^{20}Ne^{+}$	150	$^{86}Kr^{3+}$	200
$^{20}Ne^{3+}$	35	$^{92}Mo^{4+}$	5
$^{22}Ne^{+}$	200	$^{97}Mo^{4+}$	6
$^{40}Ar^{+}$	22	$^{98}Mo^{4+}$	3
$^{40}Ar^{2+}$	250	$^{124}Sn^{5+}$	8
$^{40}Ca^{+}$	80	$^{132}Xe^{5+}$	60
$^{40}Ca^{2+}$	100	$^{132}Xe^{6+}$	30
$^{40}Ca^{3+}$	50	$^{136}Xe^{3+}$	250
$^{46}Ti^{2+}$	20	$^{136}Xe^{4+}$	6
$^{50}Ti^{2+}$	70	$^{152}Sm^{3+}$	60
$^{51}V^{2+}$	55	$^{197}Au^{4+}$	500
$^{52}Cr^{2+}$	70	$^{197}Au^{7+}$	200
$^{56}Fe^{2+}$	200	$^{197}Au^{8+}$	20
$^{56}Fe^{3+}$	60	$^{208}Pb^{4+}$	100
$^{58}Ni^{2+}$	100	$^{208}Pb^{5+}$	10
$^{58}Ni^{3+}$	200	$^{208}Pb^{9+}$	20
$^{58}Ni^{4+}$	50	$^{209}Bi^{4+}$	200
$^{60}Ni^{2+}$	18	$^{209}Bi^{5+}$	300

* j.pfister@gsi.de

ISBN 978-3-95450-125-0

HIGH CURRENT ION SOURCES FOR THE FAIR ACCELERATOR FACILITY

R. Hollinger*, A. Adonin, J. Pfister, GSI, Darmstadt, Germany

Abstract

Vacuum arc ion sources and filament driven multi cusp ion sources are used for the production of high current ion beams of a variety of metallic and gaseous ions at the GSI accelerator facility.

For the future project FAIR (Facility of Antiproton and Ion Research) it is foreseen to provide in addition to the existing ion beams a high current proton beam from a separate linear accelerator (plinac) and an exclusive high current uranium beam from a new ion source injector.

The contribution gives an overview of the performance of the existing high current injector and presents the challenges for the future injectors for proton and uranium production.

INTRODUCTION

The GSI facility is known as an accelerator with a variety of ion species within a wide range of energy at the end of the accelerator. Two ion source platforms arranged as a "Y" deliver ion beams for the universal linear accelerator UNILAC [1] (the high charge state injector HLI equipped with an ECR is not topic of this paper). One of it is equipped with a Penning ion source the other allows the operation with MUCIS, MUCIS2010, CHORDIS, MEVVA and VARIS ion sources.

For low energy experiments (3.6-11.4 MeV/u) with high duty factor the ion source Penning [2] is used generally. With this working horse we are able to offer a multiplicity of ion species with a large range of mass over charge ratio (A/ζ) [3]. For injection into the synchrotron SIS18 for high energy experiments (up to 4 GeV/u) the ion sources MUCIS, MUCIS2010, CHORDIS, MEVVA, and VARIS are used generally at low duty factor.

The specific injection energy for the RFQ is 2.2 keV/u with its space charge limit of 0.25×A/ζ [mA]. The acceptance of the RFQ is 138π mm mrad within a maximum mass over charge ratio of 65.

The article gives an overview of ion source data and injection parameter of most important ion species generated from the high current injector. Due to the fact that experiments at GSI request a wide range of beam intensity (single particle up to 10^{11} per spill) the reached ion source intensities do not assign the physical limit, even when the ion source operates with non-enriched material.

LOW ENERGY BEAM LINE

Fig. 1 shows the low energy beam transport section (LEBT) from the high current terminal (terminal north) to the radial matching section of the RFQ [4]. The Penning terminal (terminal south) with its LEBT section is not shown here, because it is equipped with the same components.

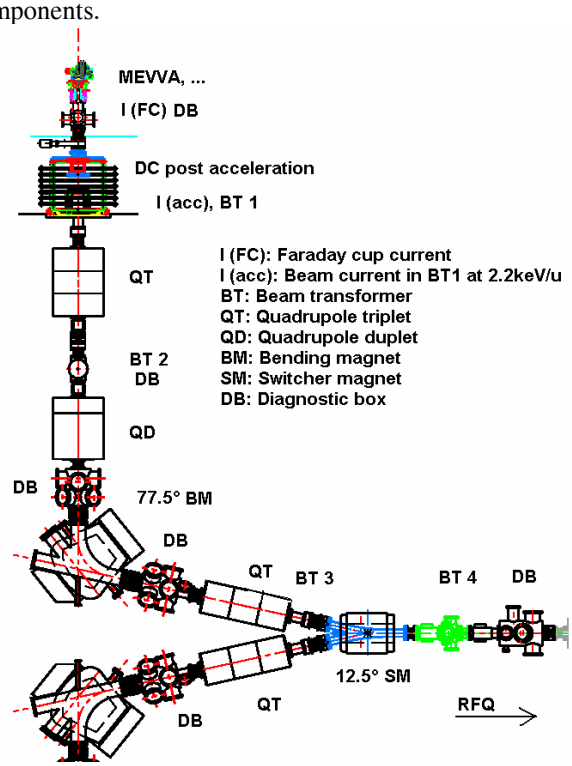

Figure 1: High current LEBT section of the UNILAC.

Close behind the ion source the LEBT section consists of a dc-post acceleration system to meet the right specific injection energy of 2.2 keV/u. In combination with the extraction system of the ion source it allows to accelerate the lightest ion species $^{1}H_{3}^{+}$ with an acceleration voltage of 6.6 kV up to $^{124}Xe^{2+}$ with 136.4 kV. A quadrupole triplet and doublet belong to the first transport section, followed by a 77.5° bending magnet for separation of the desired ion specie and charge state. The 12.5° switching magnet operates in a 50 Hz switching mode to allow the injection into the RFQ simultaneously from terminal north (max 5 Hz) and south (max 50 Hz) with two different ion species. Faraday cups, beam transformers, diagnostic grids and horizontal and vertical slits are installed to analyze the ion beam. A quadrupole quadruplet finally matches the ion beam into the RFQ.

HIGH CURRENT ION SOURCES

The ion sources MUCIS, CHORDIS, MEVVA, and VARIS are well described in the references [5-8]. All these ion sources are equipped with the same multi aperture 13-hole triode extraction system. The aspect ratio

* R.Hollinger@gsi.de

ISBN 978-3-95450-125-0

IMPROVING EFFICIENCY OF PLASMA GENERATION IN H- ION SOURCE WITH SADDLE ANTENNA*

V. Dudnikov#, R. P. Johnson, Muons, Inc., Batavia, IL 60510, USA
S. Murray, T. Pennisi, C. Piller, M. Santana, M. Stockli, R. Welton, ORNL, Oak Ridge, TN 37831

Abstract

Improving efficiency of plasma generation in RF H- surface plasma source (SPS) with saddle (SA) RF antenna is considered. Several versions of new plasma generators with different antennas and magnetic field configurations were tested in the SNS small Test Stand. The efficiency of positive ion plasma generation has been improved ~4x times up to 0.18 A/cm^2 per 1 kW of RF power 13.56 MHz. A first prototype SA SPS with AlN chamber was installed in the SNS Test that achieved current of H- ions up to 67 mA with an apparent efficiency of up to 1.6 mA/kW at RF frequency 2 MHz. A new version of the RF assisted triggering plasma source (TPS) has been designed, fabricated and tested. A Saddle antenna SPS with water cooling is being fabricated for high duty factor have been tested.

INTRODUCTION

Development of a high current Surface Plasma H- ion Source (SPS) with plasma generation by RF discharge with Saddle antenna in magnetic fields is described in Refs. 1,2. A prototype of RF H- surface plasma source (SPS) with saddle (SA) RF antenna is developed. Several versions of new plasma generators with a small AlN test chamber and different antennas and magnetic field configurations were tested in the Test Stand. A prototype SA SPS was installed in the Test Stand with a larger, normal sized SNS AlN chamber that achieved peak currents of up to 67 mA with an apparent efficiency up to 1.6 mA/kW at 2 MHz RF frequency. Control experiments with H- beam produced by SNS SPS with internal and external antennas were conducted in similar conditions.

In this period main effort was concentrated on development:

1- more reliable version of the triggering plasma source (TPS);

2- improved efficiency of the plasma generators;

3- saddle antenna SPS with water cooling for high duty factor testing.

RF TRIGGERING PLASMA SOURCE

For fast igniting a powerful pulsed RF discharge at low gas density is used a separate triggering plasma gun (TPG). The hollow-anode dc glow discharge plasma gun (discharge voltage: ~600 V and current ~5 mA), designed at ORNL, has been described previously [3]. It used for injecting H_2 gas and ~20 μA of electrons into the AlN 30-70 kW discharge. It was observed that guns configured with Mo cathodes often failed to ignite after several days. In response to this issue, it was designed and developed a chamber, which is sufficient to ignite the main 2 MHz, of stable operation due to decrease a secondary electron emission.

RF assisted TPG utilizing the existing 13 MHz system. Figure 1 shows a cross-sectional view of the SA SPS with RF TPG which employs a water-cooled Al_2O_3 (Φ = 1.3 × length 10 cm) plasma chamber surrounded by a 10-turn Cu antenna. The plasma chamber integrity has been tested up to 1.2 kW of RF power with plasma. Under normal conditions (RF power: 300 W; cathode bias: −250 V; >10 SCCM H_2 flow) about 2 mA of discharge current is supplied to the cathode fabricated from W. This current is then compressed through a circular 2 mm diameter opening in the ceramic plasma chamber to a hollow anode (also fabricated from W). This gun configuration has been found to reliably ignite the main ion source plasma and has been tested coupled to an ion source over several multi-day runs on the test stand. Comparing performance to the Mo, Cu gun, the RF gun produces ~10× electron flux to the ion source with sputtering estimates suggesting ~10^3 less cathode sputtering.

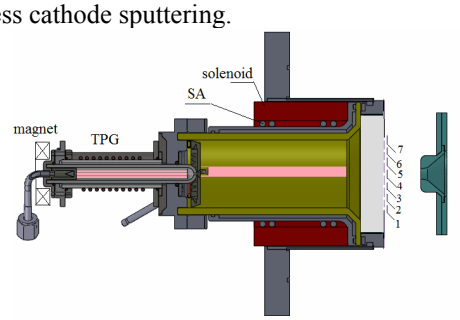

Figure 1: Drawing of the SA Plasma generator with RF TPG and plasma plate with 7 collectors opposite 7 emission apertures of 2 mm diameter (S=3.2 mm^2). Magnetic accelerator electrode is attached for producing of correct magnetic field distribution.

With attached ring permanent magnet the plasma flux from TPG was increased and the minimal gas density, necessary for TPG and pulsed discharge triggering was decreased.

IMPROVING EFFICIENCY OF PLASMA GENERATION

An external antenna source employing solenoidal antenna is under development at the SNS, which was recently described in Ref. 3. The high RF power required for the sources as well as triggering of the pulsed discharge can create problems for very long term operation.

*Work supported by Contract DE-AC05-00OR22725 and by STTR grant DE-SC0002690.
#Vadim@muonsinc.com

ISBN 978-3-95450-125-0

LOW ENERGY CHANNEL FOR MODERNIZED LU-20

V. Alexandrov #, A. Govorov, V. Monchinsky, G. Trubnikov
JINR, Dubna, Moscow Region

Abstract

The modernization of LU-20 accelerator expects change existing electrostatic for-injector on RFQ type pre-accelerator. Low energy channel of transportation of beams is offered from three sources of ions: ESIS, LIS and SPIon - to RFQ. Parameters of channel and results of numerical modeling on fitting beams parameters with acceptance of RFQ are presented.

INTRODUCTION

The modernization of LU-20 accelerator expects change existing electrostatic for-injector on RFQ type pre-accelerator. Under this acceleration modes in the Alvarez linac must be preserved. Since at RFQ exit different energy of particles with Z/A =1 and Z/A ≤ 0.5 are required, it is expected use two separate RFQ. Modernization is conducted in 2 stages, first stage – RFQ for particles with 0.3 ≤ Z/A ≤ 0.5. A variant of low energy channel for beam transportation (LEBT) common for 3 ion sources: ESIS, LIS and SPIon – is offered.

ELEMENTS OF CHANNEL

Each source is situated on high-tension (before 150 kV) platform. The channel (Fig.1) begins from electrode with potential U0, after which a vacuum valve is fixed. In initial part of channel (IPC) the focusing electrodes with potentials U1 and U2 are located. IPC ends the tube with potential, falling off from U3 up to 0. Two solenoids, stated after initial part, form beams at the input of RFQ.

PARAMETERS OF BEAMS AND RFQ

Parameters of beams at the input in channel are given in Table 1, the input parameters of RFQ are specified in Table 2.

Table 1: Beam Parameters at IPC entrance

source, ions	Z/A	current mA	ε_n(4rms) π cm mrad	∅ beam mm	energy keV/Z
LIS, $^{27}Al^{+8}$	0.3	20	0.2	19	1
ESIS, $^{197}Au^{+60}$	0.3	10	0.15	10	19.7
SPIon, $^{2}D^{+}$	0.5	10	0.2	15	20

Table 2: RFQ Entrance Parameters

Z/A	I_{inj} mA	4rms $\varepsilon_{n\,x,y}$ π mm mrad	$\alpha_{x,y}$ rad	$\beta_{x,y}$ mm/mrad	U_{inj} kV
0.3	0	1.5	0.8818	0.0680	103
	10		0.9472	0.0721	
0.5	0	2.0	0.8818	0.0680	61.8
	20		0.9906	0.07545	

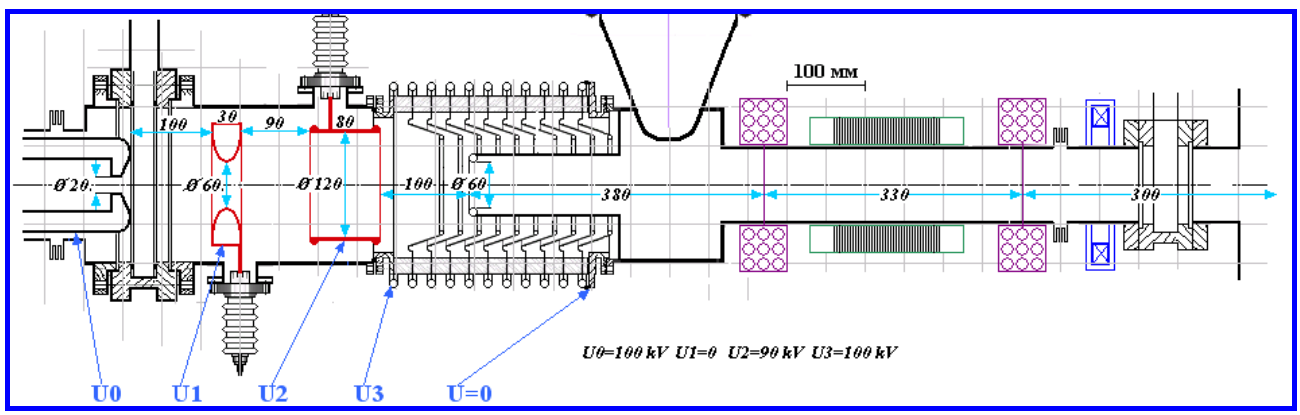

Figure 1: Schematic view of LEBT.

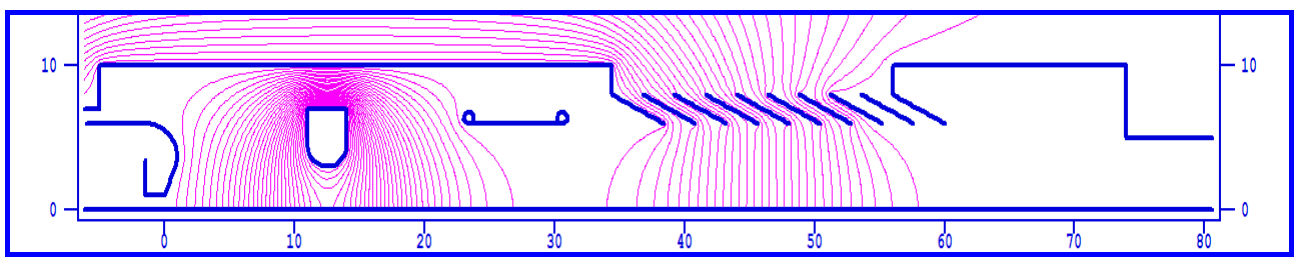

Figure 2: View of initial part of LEBT at POISSON code interface.

#aleks@jinr.ru

ISBN 978-3-95450-125-0

A SIMULATION STUDY ON ACCELERATOR CAVITIES FOR A SW LINAC

N. Khosravi, University of Zanjan, Zanjan
S. A. H. Feghhi, E. Ebrahimibasabi, Department of Radiation Application,
Shahid Beheshti University, Tehran, Iran

Abstract

An on axis-coupled cavity structure has been studied using S-band microwaves at 2856MHz, suitable for industrial and research applications. It uses a bi-periodic SW structure with constant impedance that operates at π/2 mode. This structure consists of Bean-like shaped slots, placed symmetrically with respect to the accelerating axis. We compared different shapes, places and sizes of slots with respect to coupling coefficient, resonance frequency and some of cavity parameters. Sensitivity analyses of accelerating cavity on details of structure have been done and their behaviour, with respect to the resonance frequency has been investigated. According to the simulation results using SUPERFISH and CST Studio package, each accelerating cavity is capable to deliver 0.56 MeV to electrons in a 50μA beam.

INTRODUCTION

In designing of accelerator cavities for SW linacs, we should consider some figures of merit such as quality factor, effective shunt impedance and also transit time factor of cavity. This linac is intended to deliver an electron beam up to 10MeV with a Klystron power of 2MW having a pulse width of 5 μsec and a waveguide operating in the TE01 mode. And our cavity will be operated in the TM010 mode.

DESIGN CONCEPTS

Designing the cavity can be started with a simple pillbox cavity with beam holes on the end plates, adding nose cones to create a region of more concentrated axial electric field that it reduces the gap and raises the transit-time factor [1]. The optimization procedures depend on the constraints of our equipments. The nose cone, septum thickness and lower wall radius might be constrained by the technology of cavity machining. So they are known before starting our work. We should mention that Borehole radius R_b is determined from beam dynamics considerations.

Some relations can help us to find other parameters. For example, Upper wall radius, R_{co}, is determined for each cavity by[2].

$$R_{co} = L/2 - S - \Delta x \qquad (1)$$

In which L and S refer to length and septum thickness of a cavity, respectively. A small straight section Δx on the circumference of the wall cavity might be required to increase effective shunt impedance (ZT^2) slightly. This effect is more evident for larger β values than for small ones. The best value of Δx is about 10% of half-cavity length. The two remaining parameters, D and g have the strongest effect on ZT^2 and frequency [2]. Thus the Sketch of the cavity had been done. In following by sensitivity analyzing the optimization of our cavity has been performed to maximize the efficiency. using diagrams of frequency, ZT^2, Z, Quality factor etc. respect to cavity geometrical parameters[2].

Some of electromagnetic codes have been used to solve Maxwell's equation with the specified boundary conditions. In this paper SUPERFISH[3] and CST suit studio package[4] have been used for simulation of our designs.

Sensitivity analysis and benchmarking for all cavity parameters have been done. But two diagrams which are more determinative have been shown in Fig (1) and (2). Fig (1) Shows Resonant Frequency vs. Gap Length. As it is clear, there is a good agreement between CST and SUPERFISH results. The SUPERFISH results are more accurate than CST results. This discrepancy is due to different normalization coefficients, although the behavior of results in is the same in both. It can be seen in Fig (2) that these results can be coincident by varying Effective Shunt Impedance in vertical Axis. Effective Shunt Impedance is a very significant parameter in SW cavity, since it can be set to achieve a maximum value by sweeping this parameter in gap length and optimization demanded cavity [2].

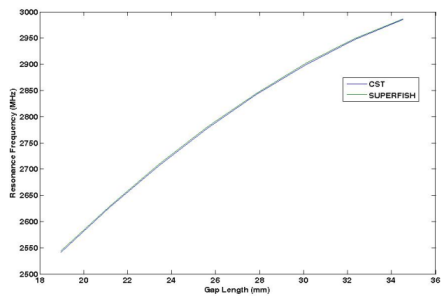

Figure 1: Resonant Frequency vs. Gap Length

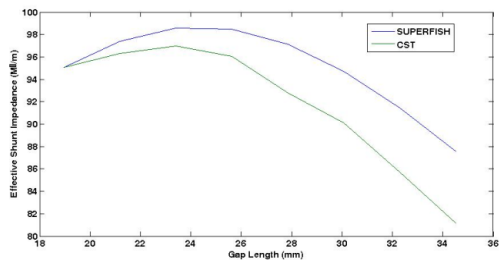

Figure 2: Effective Shunt Impedance vs. Gap Length

ISBN 978-3-95450-125-0

RF DESIGN AND TUNING OF LINAC4 RFQ

A.C. France, M. Desmons, O. Piquet, CEA Saclay, France
C. Rossi, CERN, Geneva, Switzerland

Abstract

Linac4 is scheduled to deliver 160 MeV H^- beam to LHC injection chain by year 2015. The first stage of Linac4 is a 352 MHz, 3-meter long Radio Frequency Quadrupole (RFQ) accelerator [1]. It will accelerate the 70 mA, 45 keV H^- beam from the RF source up to 3 MeV energy. Fabrication of RFQ, which started in 2009, is completed [2] and tuning operations are in progress. RF controls performed at each fabrication step have shown that RFQ electrical parameters are well within bounds specified after envelope of fabrication tolerances. Tuning operations have started with adjustment of so-called quadrupole rods inserted in end plates, in order to achieve adequate voltage boundary conditions at both RFQ ends. A preliminary slug tuning test demonstrates voltage percent accuracy after a few slug tuning iterations.

RF DESIGN

Linac4 RFQ is a 3-meter long, single segment RFQ. Cross-section is kept constant over full RFQ length, in order to simplify mechanical fabrication (refer to [3] for detailed RF design). Specified voltage is constant over full RFQ length, and boundary conditions are tuned with quadrupole rods (QR) inserted in end plates, close to vane tips. Electrical parameters of RFQ however vary slightly vs. abscissa, as a consequence of vane modulations. Resulting voltage error is 10% at most, and will be easily suppressed with the 36 tuners (8 slugs and 1 RF port per quadrant). Tuners are also designed to compensate for construction errors. Envelope of fabrication tolerances may yield inter-vane capacitance errors of 2.3% (quadrupole-like errors) and/or 3.5% (dipole-like errors). The resulting tuner position range is about 34 mm, and is centered mostly "inside cavity", where tuner are efficient. To this purpose resonance frequency is set to 345.3 MHz when tuners are in flush position.

THEORETICAL BACKGROUND

A general statement is that RFQ tuning requires some bridge to be made between the 3D field maps of the desired object, and measurable quantities which are field profiles along bead-pull lines and spectra. This bridge is the 4-wire transmission line model (TLM) described in [4]. Field maps in the axial region of a 4-vane RFQ may be approximated by transverse electric-magnetic (TEM) field maps, since there the axial component of magnetic field is close to zero. These TEM field maps are assumed to be supported by a 4-wire system, whose voltage 3-vector U verifies

$$\frac{\partial}{\partial z}\left(C_Q \frac{\partial U}{\partial z}\right) + \frac{1}{c^2} L_Q U = \frac{\omega^2}{c^2} C_Q U \,, \qquad (1)$$

where z is abscissa, C_Q, L_Q are the capacitance (F/m) and inductance (H.m) matrixes, ω is the radian frequency, c is the speed of light. Quadrupole (U_Q) and dipole (U_S,U_T) components of U are related to inter-electrode voltages by $U_Q = (u_1 - u_2 + u_3 - u_4)/4$, $U_S = (u_1 - u_3)/2$, $U_T = (u_2 - u_4)/2$. Note that (1) is diagonal for a perfectly symmetric RFQ. Boundary conditions at RFQ ends in z = a,b are

$$\partial U(a)/\partial z = -s_a U(a) \,, \quad \partial U(b)/\partial z = +s_b U(b) \,, \qquad (2)$$

where s_a, s_b are 3 × 3 matrixes. The vector Sturm-Liouville (SL) operator defined after (1) and (2) is self-adjoint if and only if $(C_Q)^{-1}s_{a,b}$ are Hermitian, which is always the case since $s_{a,b} = -j(\omega/c^2)C_Q^{-1}y_{a,b}$, where $y_{a,b}$ are end-circuit admittance matrixes, and are imaginary symmetric for lossless reciprocal circuits. All TLM electrical parameters are deduced from exact 3D simulations [3], in such a way TLM is able to accurately mimic RFQ eigen-modes and eigen-functions. On the other hand, magnetic field measured along bead-pull lines are easily transformed into inter-vane voltage (eventually using simulated field maps), eigen-values $(\omega/c)^2$ are directly given by spectrum analysis, and our "bridge" is established. First-order perturbation analysis of the SL eigen-problem leads to orthogonal bases for C_Q and L_Q perturbations, which are duals of voltage eigen-basis. This important property will be applied for RF controls and for slug tuning.

RF CONTROLS

RF controls are performed at each fabrication step of each 1-meter long section: copper pieces assembly, first braze of electrodes, second braze of stainless flanges and vacuum ports. The most desirable goal would be to obtain a diagnosis of electrical properties vs. abscissa along the RFQ. This is a typical inverse problem: given voltage vector function U(z), find originating $C_Q(z)$ matrix pencil. The hard point is that U may be deduced from measured magnetic field only in small intervals, far enough from local field perturbations induced by tuners and vacuum ports. Applying sampling theory to our SL problem, a linear filter bank may be built which uses valid field samples to deliver a few spectral amplitudes estimates (6 first in present case). First-order perturbation analysis is then used to reconstruct originating perturbations. This method is of course unable to reveal strongly localized defaults; however the same procedure will be used for tuning, and these estimated perturbations are exactly the ones that will have to be cancelled by tuners. Results are displayed in Fig. 1, where successive fabrication steps are identified with color code. Typical precision of the method is ±0.003, after processing typically 5 or 6 bead-pulls. A digital "roofing" filter is also used to reduce high-frequency noise. Black traces apply to the full-length

ISBN 978-3-95450-125-0

BEAM PULSE SEPARATION SYSTEM OF INR LINAC

N.I. Brusova, A. Feschenko, O. Grekhov, Yu. Kalinin, V. Mikhailov, V.L. Serov, A.A. Stepanov,
INR RAS, Moscow, Russia
B.O. Bolshakov, A.V. Pozhensky, NIIEFA, St. Petersburg, Russia

Abstract

The activity for beam intensity increasing and beam use efficiency improvement is under progress in INR linac. An important stage is the development and implementation of the Beam Pulse Separation System in the accelerator intermediate extraction area (160 MeV). The system is intended for distribution the beam pulses between Isotope Production Facility (up to 160 MeV) and the Experimental Facility located downstream of the accelerator exit. The report describes the upgrade of intermediate extraction area as well as the first results of experiments with the beam.

INTRODUCTION

INR linac is a medium energy high intensity linac [1]. The accelerator includes an intermediate extraction area where the beam with the energy up to 160 MeV is extracted from the main line and is directed to isotope production facility (IPF). To extract the beam a series of two 13° bending magnets are used. The magnets are of DC type so the total beam only can be extracted. Meanwhile the intensity of the beam is sufficient to be used simultaneously for both IPF and experimental facility located downstream of the accelerator exit. Moreover, the activity of doubling the beam intensity by increasing beam pulse repetition rate from 50 Hz to 100 Hz is in progress [1,2]. That is why implementation of the mode of simultaneous operation of the accelerator for IPF and for experimental facility is of importance. A decision to develop and build a beam pulse separation system for beam distribution has been made. The system including a pulse bending magnet and a power supply has been designed and manufactured in NIIEFA [3]. The pulse magnet replaces the first DC magnet. The system can operate with the frequency up to 50 Hz providing distribution of the beam pulses between IPF and experimental facility in different ratios. In case of 100 Hz mode of accelerator operation up to 50% of the beam pulses can be directed to IPF. A DC mode of the magnet is also foreseen thus providing a full beam direction to IPF.

INTERMEDIATE EXTRACTION AREA UPGRADE

The simplified schematic of the intermediate extraction area is shown in Fig. 1. The length of the area along the main beam line is near 14 m. Besides beam extraction the purpose of the area is to match both longitudinally and transversally the beam with the subsequent structure.

In order to implement beam separation the DC bending magnet #1 was replaced by the pulsed one. To avoid distortions of the magnetic field and heating of the vacuum chamber inside the magnet the latter was replaced by the chamber made of electron-tube glass (Fig.2). Vacuum sealing of the chamber is made with the telescopic joints. For mechanical load relief the bellows are used at each of three chamber ports. To have sufficient space for chamber mounting the distance between the magnets was increased: magnet #1 was translated by 50 mm upstream of the beam and magnet #2 - towards IPF target by the same distance. After installation the flanges of the bellows were fixed with special stays to avoid load transfer to the chamber when pumping and venting the system.

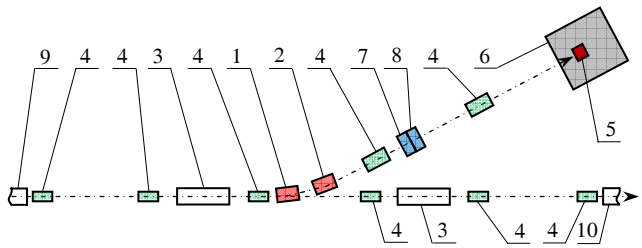

Figure 1: Intermediate extraction area (1 - bending magnet #1, 2 – bending magnet #2, 3 – two-section matching cavity, 4 – quadrupole doublets, 5 – IPF target, 6 – shield, 7 – horizontal beam corrector, 8 – vertical beam corrector, 9 – accelerating cavity #9, 10 - accelerating cavity #10).

Figure 2: Glass vacuum chamber

For beam separation the magnet #1 operates in a pulse mode meanwhile magnet #2 is turned on in DC mode. It was found that the fringe fields of magnet #2 influence the beam moving directly and result in excessive beam loss. The measurements showed that the value of B-field at the beam axis exceeds several hundred gauss and ranges along the beam line for about 40 cm. To eliminate the effect a 60 cm section of stainless steel beam pipe in the vicinity of magnet #2 was replaced by the one made of magnetic steel with the wall thickness of 6 mm. B-field decreased to the level of several gauss thus resulting in no observable influence on the beam. The view of the magnets in the extraction area is given in Fig. 3.

When operating in the beam pulse separation mode the beam matching must be done for both deflected and non deflected beams. For this purpose a separate powering of

ISBN 978-3-95450-125-0

MAXIMUM VALUE OF THE STANDING WAVE AND TRAVELLING WAVE ACCELERATING STRUCTURES ELECTRONIC EFFICIENCY

S. S. Proskin, A. P. Kulago, I. S. Shchedrin, National Research Nuclear University – Moscow Engineering Physics Institute, Moscow, Russia

Abstract

A new theoretical approach to a calculation of the standing wave and travelling wave structures electronic efficiency is described. As a result the electronic efficiency of DLWG and biperiodic structure is evaluated regarding a new definition.

INTRODUCTION

Conventional theory of linear accelerators is based on the power balance equation applied to the chosen accelerating structure: disk loaded waveguide (DLWG, working on travelling wave) or biperiodic structure.

Consider the different physically justified approaches to the issue of electron current loading in the accelerating structure. The idea of accelerating field definition forcing on accelerating electrons as algebraic sum of power source accelerating field and total decelerating field emitting by accelerating electrons [1] in chosen accelerating structure is put within this approach basis. A detailed description is reviewed in [2]. According to the ideas of electronic efficiency of DLWG and biperiodic structure are defined below.

EVALUATION OF ELECTRONIC EFFICIENCY

Consider the accelerating section of electron linac based on DLWG with relative phase velocity $\beta_{ph} = 1$. Working modes are as a rule $\theta = \pi/2$ and $\theta = 2\pi/3$. An electromagnetic field is generated by two sources. A microwave generator which supplies accelerating section produces following electromagnetic field on DLWG axis [4, 5]:

$$E_S = E_{S0}e^{-\alpha z}.$$

Where E_{S0} is the accelerating field at the input of accelerating section.

The second source which generates the electrical field is an accelerated electron beam. A summary field radiated by a series train of pointed bunches with charge q after completion of the transient processes is equal to:

$$E_S = \frac{qvR_S}{1-e^{\frac{-\pi}{Q_L}}}.$$

Where R_S – series impedance and Q_L – loaded Q factor. It should be noted that the ideal case is considered when every bunch is placed in the maximum of the total decelerating field of all bunches and in the maximum of the generator accelerating field:

$$E = E_{S0}e^{-\alpha z} - \frac{E_q}{\left(1-e^{\frac{-\pi}{Q_L}}\right)}$$

The energy obtained by every electron bunch at the exit of the accelerating section with length l equals (in terms of voltage):

$$U = E_{S0}l\frac{1-e^{-\alpha l}}{\alpha l} - \frac{E_q l}{1-e^{\frac{-\pi}{Q_L}}}.$$

Since the beam pulsed current is equal to $I_0 = q/T$ it can be written as:

$$I_0 = qc/\lambda.$$

And the expression for E_q takes the following form:

$$E_q = I_0 R_S \lambda.$$

The power of the accelerated electrons beam equals:

$$P = I_0 E_{S0} l\frac{1-e^{-\alpha l}}{\alpha l} - \frac{I_0^2 R_S \lambda l}{1-e^{\frac{-\pi}{Q_L}}}. \quad (1)$$

The electronic efficiency of the accelerating section correspondingly equals:

$$\eta = \frac{1}{P_0}\left[I_0 E_{S0} l\frac{1-e^{-\alpha l}}{\alpha l} - I_0^2\frac{R_S\lambda l}{1-e^{\frac{-\pi}{Q_L}}}\right].$$

Consider the case when the beam power is maximal and the electronic efficiency of DLWG reaches the maximal value correspondingly. Determine the accelerated beam value when $P = P_{max}$. It is necessary derivative dP/dI_0 to be equaled 0. Then using (1) get current value I_0 when $P = P_{max}$:

$$I_0 = \frac{1}{2}\frac{E_{S0}}{R_S\lambda}\frac{1-e^{-\alpha l}}{\alpha l}\left(1-e^{\frac{-\pi}{Q_L}}\right).$$

$$P_{max} = \frac{1}{2}P_0\frac{l}{\lambda}\left(\frac{1-e^{-\alpha l}}{\alpha l}\right)^2\left(1-e^{\frac{-\pi}{Q_L}}\right).$$

ISBN 978-3-95450-125-0

EXTREME DENSITY CHARGE ELECTRON BUNCHES

S. S. Proskin, A. P. Kulago, I. S. Shchedrin, National Research Nuclear University – Moscow Engineering Physics Institute, Moscow, Russia

Abstract

This paper presents untraditional approach of obtaining the DLWG limited bunch charge (LBC). The maximum energy of accelerated bunch is considered. As a result the bremsstrahlung maximum dose rate evaluation is obtained.

INTRODUCTION

Conventional theory of linear accelerators is based on the power balance equation applied to the chosen accelerating structure: disk loaded waveguide (DLWG, working on travelling wave, or biperiodic decelerating structure).

Consider the different physically justified approaches to the issue of electron current loading in the accelerating structure. The idea of accelerating field definition forcing on accelerating electrons as an algebraic sum of power source accelerating field and total decelerating field emitting by accelerating electrons [1] in chosen accelerating structure is put within this approach basis. Detailed description is reviewed in [2]. According to this idea, the maximum dose rate of bremsstrahlung from target at the exit of linear accelerator is defined within this research.

MAXIMUM DOSE RATE OF BREMSSTRAHLUNG

Consider a specific data of obtaining charges density in DLWG in order to solve an issue of designing an electron linac with output energy of 4 MeV and a bunch charge of 50 pC to obtain powerful bremsstrahlung.

According to methodic described in [2] perform a calculation of bunch charges density with modern power sources made by Mitsubishi Electric Corporation. The company produces klystrons for high energy scientific accelerators, small and middle energy accelerators with application in medicine, for airports in landing control locators.

It is important to note that a choice of power source for different accelerators should be made focusing on a serial model and a production company that has enough orders. It is desirable that the power source has a demand in different sectors of economy, for instance, in aviation, in military sector, in national security.

Back to the charge density calculation and describing main equations from [2].

The field accelerating the bunch with charge q equals:

$$E = E_{S0}e^{-\alpha z} - qcR_S \ .$$

Energy of the accelerated bunch in terms of voltage:

$$U = E_{S0}l\frac{1-e^{-\alpha l}}{\alpha l} - qcR_S l.$$

LBC value, when energy gain in terms of voltage equals 0:

$$q_{lim} = \frac{E_{S0}}{cR_S}\frac{1-e^{-\alpha l}}{\alpha l}.$$

Where E_{S0} – power source field, l – accelerating structure length, α – attenuation factor, R_S – series impedance.

The maximum dose rate absorbed in the air P_D from bremsstrahlung of accelerated electrons with bunch current equaled 1 mA and obtained on the distance of 1 m from the target with atom number Z could be defined with less than 4% tolerance by equation [3]:

$$P_D = P_{0Z}(Z) \times W^{d(Z)}.$$

Where P_D units are $Gy/(min \times mA)$, W units are MeV and a coefficient and a degree are defined by following expressions:

$$P_{0Z}(Z) = 0.144 + 7.38 \times 10^{-3} \times Z,$$

$$d(Z) = 3.19 - 6.9 \times 10^{-3} \times Z.$$

Consider a case of copper target (Z=29). $p_{0Z}(29) = 0.35802$, $d(29) = 2.9899$, $P_D = 0.358 \times W^3$.

Copper target is chosen due to simplicity of further calculations, since conversion is easy when $P_D \sim W^3$, i. e. in a degree of a whole number 3.

If consider a value of accelerated bunch pulse current I_0 (mA) then full dose rate at the exit of linear accelerator and copper target equals:

$$P_{fD} = 0.358 \times W^3 \times I_0. \quad (1)$$

Expression (1) could be written with pulse current $I_0 = qc/\lambda$:

$$P_{fD} = 0.358 \times W^3 \times q \times c/\lambda.$$

Energy in voltage term is expressed through pulse current I_0 [2]:

$$U = E_{S0}l\frac{1-e^{-\alpha l}}{\alpha l} - I_0 R_S \lambda l. \quad (2)$$

By adding expression (2) in (1) the expression for full dose rate becomes:

ISBN 978-3-95450-125-0

BIPERIODIC ACCELERATING STRUCTURE WITH INNER COUPLING CELLS WITH AN INCREASED COUPLING COEFFICIENT

M.A. Gusarova, I.I. Petrushina, E.A. Savin, N.P. Sobenin, National Research Nuclear University «MEPhI», Moscow, Russia

Abstract

In this article the research results of advanced biperiodic accelerating structure (BAS) re presented. This structure features increased coupling coefficient together with keeping of effective shunt impedance high value and another electrodynamics parameters.

ELECTRODYNAMICS CHARACTERISTICS

In order to characterize of accelerating cavity efficiency for low current case the effective shunt impedance per unit length is commonly used:

$$r_{\text{sh.ef}} = \left| \int_0^l E_z(z) \exp(ik_z z) dz \right|^2 \Big/ (P_{\text{loss}} l). \quad (1)$$

where $\dot{E}_z(z)$ – accelerating field electric complex amplitude; l– cavity length; P_{loss} – power losses, k_z – wave number in the z direction.

One of the most important electrodynamics characteristics for accelerating cavities is Q-factor

$$Q = 2\pi \frac{W_{stor}}{(W_{scat.res})_{T_0}} = \omega_0 \frac{W_{stor}}{P_{scat.res}}. \quad (2)$$

where W_{stor} – stored energy in magnetic end electric fields in cavity

$(W_{scat.res})_{T_0} = P_{scat.res} \cdot T_0$ – scattered energy in cavity during oscillations period, $P_{scat.res}$ – scattered power in active resistance at resonance.

Last parameter worth to be mentioned is coupling coefficient. It is defined by ratio of frequencies of π, π/2 and 0 modes

$$k = \frac{|f_\pi - f_0|}{f_{\pi/2}}. \quad (3)$$

SIMULATION MODEL

Model used for numeric simulation consists of two accelerating cells and one coupling cell between them. On Fig.1 illustrates this model with geometry parameters shown.

CALCULATION PROCESS

Each type of BAS design has been optimized on π/2 mode operating frequency both for accelerating and coupling cells.

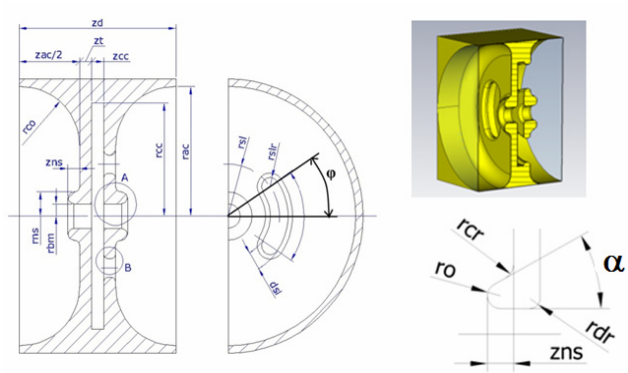

Figure 1: Structure geometry.

During researching in order to increase coupling for BAS design with inner coupling cells dual LINAC geometry was used [2]. Accelerating structure of this LINAC is designed to operate at 2856 MHz. Maximum value of coupling coefficient in accelerating section of this LINAC (with wave phase velocity equal to the 0.999c) became 10.3% instead of original 5% [1].

During the cavity optimization the following parameters remained invariable: beam pipe radius rbm, structure period zd, coupling gap thickness zt, coupling cell length zcc. The electrodynamic characteristics dependence of coupling gap radial position rsl, coupling gap width dsl, accelerating cell equator rounding rco were studied.

SWEEPING OF ACCELERATING CELL EQUATOR RADIUS

With increasing of accelerating cell equator rounding (rco) values of shunt impedance and Q-factor are increased. But this geometry change leads to coupling slots displacement – they are no longer in the maximum magnetic field region in accelerating cells and coupling cell. This results in coupling coefficient drop.

SWEEPING INNER COUPLING CELLS THICKNESS

With increasing of coupling gap thickness dsl from 9 to 13 mm angular size of coupling gap φ must be reduced from 30^0 to 25^0 to avoid coupling gaps overlapping.

In the same way radius of coupling gap middle line rsl must be reduced from 21.4 mm to 19.82 mm to place coupling gap as close to accelerating cell blend edge that leads to coupling coefficient

ISBN 978-3-95450-125-0

USING GENETIC ALGORITHMS FOR ELECTRODE SHAPE OPTIMIZATION IN ACCELERATORS WITH RF FOCUSING

K.A. Aliev, S.M. Polozov, A.V. Samoshin#
National Research Nuclear University "MEPhI", Moscow, Russian Federation

Abstract

The drift tubes shape choice which provides the necessary distribution of the spatial RF field harmonic amplitudes is an important problem in the design of RF focusing accelerators. It is necessary to have various relationships of the main (accelerating) and the first (as main focusing) harmonics of RF field for different types of accelerators. High order harmonics should be negligible for accelerators with an external focusing, and this ratio should be E_1/E_0 = 3-5 for the efficient operation of the axially symmetric RF focusing accelerator. Thus, the distribution and harmonic amplitude's ratios at the accelerator axis which provides stable beam dynamics are always known. The drift tubes shape study problem cannot be solved directly by ordinary methods because of unknown boundary conditions belongs to a class of incorrectly defined problem. At present, this problem can be solved by using genetic algorithms (GA). For this purpose, we will define electrode's shape, and then solve the Laplace equation with boundary conditions of Dirichlet and Neumann. The necessary electrodes shape can be quickly and easily simulated using the adaptive search.

INTRODUCTION

The acceleration of high intensity low beta ion beams is one of the priority tasks of applied accelerating technology. But conventional RF low energy linacs are needed to use any external focusing elements as solenoids or quadrupole lenses to provide the beam transverse focusing. Any type of radiofrequency focusing is an alternative. It's necessary to control the spatial RF field harmonics spectrum to provide focusing condition. As an example, in axi-symmetrical RF focusing linac (ARF) [1] the base (zero order) spatial harmonic is the accelerating and high order harmonics are uses for focusing. The ratio of focusing and accelerating harmonics should be equal E_1/E_0 = 3-5 for effective beam focusing. In the other hand in RF linear undulator accelerator (UNDULAC, [2]) the acceleration is realized without synchronism with anyone of RF harmonics (beat-wave acceleration) and this ration should be equal E_1/E_0 = 0.25-0.3 for the stable beam motion. Note than in the second case the channel period can be simplest in contrast to ARF linac.

The problem of drift tubes geometry definition providing the necessary spatial RF field harmonics spectrum is not an easy task because it is an incorrectly defined problem. An other way to define the necessary electrodes geometry is to solve the analysis-syntheses problem with numerical optimization.

#avsamoshin@mephi.ru

SIMULATION MODEL

Let we consider the structure with the drift tubes (Figure 1).

Figure 1: Layout of periodic structure.

It is necessary to solve electromagnetic problems for accelerating facilities designing. In this case, it is possible to use a quasi-static approach and necessary to solve the Poisson equation in a system with a complex geometry. As stated above, the problem of electrode shapes definition for a specified field on the axis is an incorrectly defined problem. In the other hand, the problem of the field distribution simulation over the electrodes is simple, and there are many numerical methods for this simulation. For the specified field distribution we must choose the correct shape and dimensions of the electrodes, which in some cases can be a difficult problem, since changing several parameters may take a long time to find the optimal one. Therefore to solve this problem, we propose to use genetic algorithms (GA), and using one is discussed in this article.

tubeOpt console code was developed to solve this problem, which allows optimizing the accelerating structure geometry and carrying out the field calculation. tubeOpt code consists of two parts: the first electrostatic solver to find the field distribution in the cavity by numerical simulation the Laplace equation with boundary conditions of Dirichlet and Neumann, the second - a genetic algorithm which optimizes the drift tubes geometric parameters. The chosen accelerating structure has axially symmetric geometry and we can consider a quarter one (Figure 2). In this case, the following parameters will be optimized: the bore radius of the drift tube R_{in}, the external radius of the drift tube R_{out}, the bending radii R_{b1} and R_{b2} and the half-length of the tube L_{tube} (see Fig. 2).

ISBN 978-3-95450-125-0

H-CAVITY BASED ACCELERATING STRUCTURE FOR PROTON ACCELERATOR

M.V. Lalayan, A.A. Kalashnikova, S.E. Toporkov, National Research Nuclear University "MEPhI",Moscow, Russia

Abstract

Nowadays there is a growing interest in high intensive proton sources for different types of applications: neutron sources, Accelerator-Driven Subcritical Reactors (ADSR), nuclear waste transmutation, neutron factory, etc. Different types of accelerating structures for different beam energies are developed in leading centers all over the word [2]. This paper presents the results of numerical modeling accelerating structure for low (0.01-0.04) beta range. Two operating frequencies 144 MHz and 433 MHz were analyzed in detail. The influence of geometrical sizes to the main electrodynamic characteristics was investigated to find out the optimal configuration.

CAVITY DESIGN

Today there are many projects of high current accelerator complexes one of which is BWLAP (Backward Wave Linear Accelerator of Particles). The R&D work was dedicated to the front-end part of this complex. For this purposes inter-digital H - mode (IH) resonators (see Fig. 1) consist of drift tubes, stems and pilons were chosen [3].

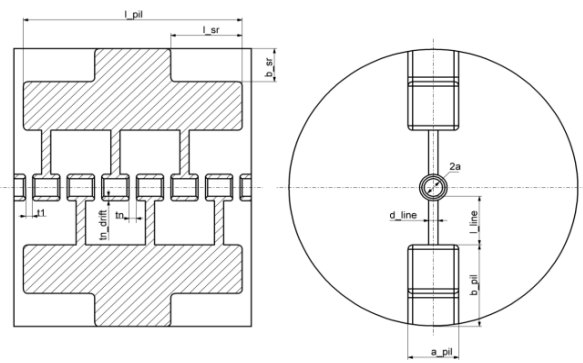

Figure 1. IH - Tank layout.

Period D of the structure is constant and it is equal to:

$$D = \frac{\beta\lambda}{2} \qquad (1)$$

as for all IH-structures working in π - mode regime.

Operating frequencies (144 MHz and 433 MHz) of front - end part were chosen according to the frequency of the main accelerator (1300 MHz). It is third (433 MHz) and ninth (144 MHz) harmonics.

Simulation Process

Since the IH - structure is periodical the first step of research process was performed on one geometric period (see Fig.2) which includes two electric periods.

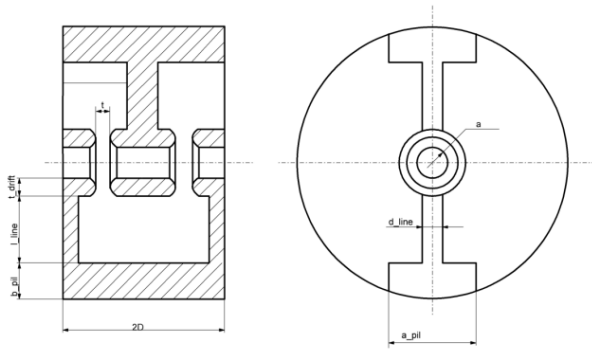

Figure 2. One period layout.

Two magnetic boundary planes were used at the opposite sides of the model to create correct field distribution. In such type of cavities electric field concentrates between drift tubes in opposite directions in neighboring gaps. Magnetic field also directed along the beam axis but it is suited at the opposite sides of the stems.

At the center of drift tubes there is a lack of electric field and presence of the longitudinal component of magnetic field. It would be the best place to locate magnetic boundary plane. Also one magnetic symmetry plane (belonging to the axis of the stems) was used to increase the accuracy.

At this stage IH - resonator demonstrated high values of shunt impedance: from 300 MOhm/m to 800 MOhm/m for different frequencies, aperture radii, accelerating gaps and geometric sizes of the stems and pilons. It should be noted that for this beam velocity range better to use lower frequency since it's got higher wavelength and higher period value. For example in case of the 433 MHz and $\beta = 0.01$ period D is equal to 3.5 mm. Such design couldn't be practically realized and they were not taken into further consideration.

Full Structure Modelling

After structure adjusting at one geometric period full tank (see fig.1) was simulated. But the field inside whole resonator isn't the same as inside one period. There is a difference of the magnetic field distribution at the central part of the resonator and at the end part of resonator. At the central part magnetic field has longitudinal component as in case with one period. At the end parts magnetic field turns around the pilon. It leads to the different field

ISBN 978-3-95450-125-0

MODERNISATION OF AN INITIAL PART THE MILAC HEAVY ION LINEAR ACCELERATOR

V.O.Bomko, A.P.Kobets, V.V.Panov, K.V.Pavlii, G.V.Sotnikov, B.V.Zajtsev, National Science Center "Kharkov Institute of Physics and Technology", Kharkov, Ukraine.

Abstract

New pre-stripping section (PSS-20) the MILAC heavy ion linear accelerator with the relation of their mass to charge A/q=20 is developed. That will allow to extend considerably a range accelerating ions and to increase intensity of beams. On an initial part of acceleration of ions from 6 keV/u up to 150 keV/u high capture in process of acceleration of the injected ions is provided interdigital (IH) accelerating structure with Radio-Frequency Quadrupole (RFQ) focusing. On the second part of acceleration of ions from 150 keV/u up to 1 MeV/u the highest rate of acceleration is created interdigital (IH) accelerating structure with drift tubes. Mathematical modeling geometrical and dynamic characteristics of accelerating structures pre-stripping section PSS-20 is executed. Dynamics of heavy ions in the course of acceleration is optimized.

INTRODUCTION

Main objective of investigations is development a complex on the basis of the Kharkov heavy ion linear accelerator MILAC for modeling of radioactive processes in nuclear reactor core, and also use of the accelerated heavy ions beams for investigations in the field of a nuclear physics and in the applied purposes.

Now MILAC accelerates ions from He^{+} to Ar_{40}^{3+}, i.e. ions of those elements which can be gained in ion source with mass to charge ration of A/q≤15. After the system of injection energy of ions makes 30 keV/nucleon and after acceleration in prestripping section PSS-15 - 0,975 MeV/nucleon. At such energy ions are exposed stripping, i.e. transit through a thin carbon film where their charge is incremented within and, after acceleration in the main section MS-5(DTL with quadrupole focusing) energy of ions makes 8,5 MeV/nucleon. Intensity of the accelerated beam to such energy makes 10^{9}-10^{10} particles/s and essentially decreases for ions with a mass number above 40. Such quantity of a current of the accelerated ions is caused by an out-of-date method of radio-frequency focusing on all extent prestripping section PSS-15.

The procurement problem on new prestripping section PSS-20 of the accelerated heavy ions beams with mass to charge ration of A/q≤20 with energy 1MeV/nucleon and the average beam intensity of 10^{12}-10^{13} particles/s is put.

In a Fig.1 the perspective plan of linac MILAC on which two new sites prestripping section PSS-20 is given, on first of which the accelerating structure with radiofrequency quadrupole focusing RFQ, and on second - accelerating structure with drift tubes DTL is used. On all sections of linac MILAC the interdigital H-type IH accelerating structure is used.

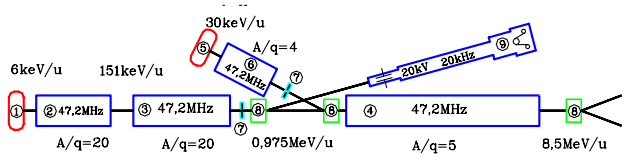

Fig. 1 Perspective plan of linac MILAC.

ACCELERATING STRUCTURE WITH RADIOFREQUENCY QUADRUPOLE FOCUSING RFQ

The accelerating structure with the radiofrequency quadrupole focusing RFQ, the offered I.M.Kapchinsky and V.A.Teplyakov [1,2], is used now almost in all existing heavy ions linacs. The basic design features and methodical workings out have been executed in many accelerating laboratories, studying of such accelerating structure in Los Alamose where all basic backgrounds for structure RFQ construction on sites of formation and an initial acceleration of high-current beams [3,4] have been created was especially intensively conducted. According to these workings out all section RFQ is divided into 4 sites: radial matcher, the phase shaper, a site of the adiabatic grouping (gentle buncher) and an acceleration site (accelerating section). However in case of acceleration of heavy ions (major A/q) the site of the adiabatic grouping demands a considerable quantity of the cells which had on major length. The problem of cutting of total length created prestripping sections PSS-20 together with injection system costs is very sharp. Besides, in a linac of heavy ions intensity of a current of a beam much more low, than in proton accelerators.

Therefore forces of a space charge are small and other plan of grouping providing higher of acceleration rate without deterioration of radially-phase characteristics of a beam can be used. Such plan of acceleration has been offered S.Yamada in which the grouping site is divided into two: prebuncher and buncher. [5]. On a site prebuncher the prompt phase compression proceeding on half of a period of phase oscillations is made. On a site buncher aspire to create high acceleration rate, without worsening thus radial and phase characteristics beam. The site booster where the peak acceleration rate is reached is entered also.

Such variant of build-up of sites prestripping section PSS-20 is developed with reference to acceleration of heavy ions with A/q=20. Thus for each of 6 sites programs of calculation of parameters of structure and characteristics beam of ions are created. Results of optimizing calculations of structure are given in [6]. In Table 1 parameters of accelerating structure and the characteristics beam on an exit of sites of section RFQ for PSS-20 accelerator MILAC are given.

ISBN 978-3-95450-125-0

NOVEL DTL SECTION FOR ITEP-TWAC HEAVY ION INJECTOR

V. Andreev, N.N. Alexeev, A.Kolomiets, V. Koshelev, ITEP, B. Cheremushkinskaya 25, 117218, Moscow, Russia
A. Plastun, NRNU MEPhI, Moscow , Russia

Abstract

A novel 81.5 MHz H-type drift tube (DTL) accelerating structure with RF quadrupoles following RFQ in the new injector I-4 for acceleration ions up to energy about 5 MeV/u for ITEP TWAC facility has been proposed. It is based on a combination of a DTL structure and the resonator with magnetic coupling windows. Computer simulations show that it can provide some advantages in comparison with conventional IH-DTL structure. Results of both electrodynamics and beam dynamics computer simulations of the structure as well as a new approach for beam matching RFQ and the section are presented.

INTRODUCTION

The new high current ion injector I-4 for ITEP TWAC facility is under construction [1]. The facility consists of main synchrotron accumulator U-10 with 25 MeV proton injector I-2 and booster synchrotron UK with 4 MeV ion injector I-3. It runs presently in several operation modes accelerating protons in the energy range of 0.1-9.3 GeV, ions in the energy range of 0.1-4 GeV/u and accumulating nuclei up to Cu at the energy of 200-400 MeV/u [2].

The injector I-4 have to accelerate ions with charge-to-mass ratio Z/A = 1/3 up to the energy of W = 7 MeV/u with beam current up to I = 30 mA. These parameters are required to increase the intensity of the ion beam in UK ring to reach the terawatt level of stacked beam power in storage ring U-10.

The 81.5 MHz RFQ with output energy of 1.57 MeV/u as initial part of I-4 has been successfully commissioned in 2011 [3]. The initial design of the second section (IH-DTL) was completely revised and a new design of the section has been proposed. The main goal of the new design is to provide compact, efficient and relatively inexpensive part of the injector.

The design of the accelerating channel is based on a hybrid scheme [4, 5]. A new resonant structure based on four vanes with displaced magnetic coupling windows (MCW) [6] similar to existing RFQ was proposed for second section.

The paper presents results of both electrodynamics and beam dynamics computer simulations of the new structure.

HYBRID STRUCTURE

General Injector Layout

Hybrid structure combines accelerating gaps and RF quadrupole focusing. A simplified scheme of the structure and its placement with respect to the first RFQ section is shown in Figure 1. Focusing part is formed by vanes with quadrupole symmetry. Its length is $L_q = 3\beta\lambda/2$, so focusing gradient changes its sign three times while particle passes this length. It means that this part of the hybrid structure acts as a conventional triplet of quadrupole lenses. Required focusing strength of each cell is defined by distance from axis to vanes.

TWAC injector RFQ output beam parameters allow direct injection into DTL part of the hybrid structure without any additional focusing or RF elements for matching of transverse and longitudinal beam parameters. So the design doesn't assume use any MEBT between RFQ and second accelerating section.

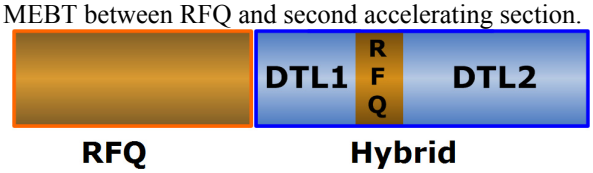

Figure 1: Simplified scheme of the hybrid structure.

Choice of the Resonator

Conventional IH and CH structures have twice lowered accelerating electric field in the space between the flanges and the tubes. In order to equalize the field distribution along the accelerating channel a new design of the resonator, using four-vane structure with displaced MCW like that was used for TWAC RFQ has been proposed. The displaced MCW structure has longitudinal electric field on the axis between the flanges and the vanes due to coaxial component of the operational mode. It allows equalizing electric field in end gaps of the CH and IH structures. Figure 2a and Figure 2b depict two 11- gap structures which have been simulated to evaluate RF parameters and choose most suitable design for second section. Varying the windows displacement and their dimensions allows very easy tuning both resonant frequency and field distribution along the structure. Normalized electric field distribution (E_{zn}) on the axis shown in Figure 3 is the same for IH and CH structures with displaced MCW.

Parameters of CH and IH structures with MCW simulated by OPERA-3d code are shown in Table 1.

Table 1: Structure parameters

Parameter	IH	CH
Inner diameter of the cavity, mm	760	880
Length of the resonator	1520	
Resonant frequency, MHz	81.5	
Frequency of nearest mode, MHz	105.1	106.2
Quality factor	17000	

ISBN 978-3-95450-125-0

PERFORMANCE OF THE MAGNETIC SYSTEM OF A 12 MEV UPC RACE-TRACK MICROTRON*

Yu. A. Kubyshin, J. P. Rigla, Technical Univ. of Catalonia, Barcelona, Spain
I.Yu. Vladimirov#, N.I. Pakhomov, V. I. Shvedunov, SINP, Moscow State University, Russia,
V.V. Zakharov, I.V. Chernov, Elmat-PM, Kaluga, Russia

Abstract

The design and characteristics of the end magnet of a 12 MeV electron race-track microtron (RTM) which is under construction at the Technical University of Catalonia is described. The RTM end magnet consists of four dipoles with the main field level about 0.8 T. As a source of the magnetic field a Sa-Co rare earth permanent magnet material (REPM) is used. This helps to get a quite compact design of the RTM and allows to place its magnets in a high vacuum environment of the accelerator vacuum chamber. We discuss results of numerical simulations of the tuning of the end magnets by means of special plungers and describe their engineering design which permits to assemble the magnets and fix the Sa-Co blocks without gluing. Also a method and results of the REPM blocks residual magnetization control are reported.

INTRODUCTION

The Technical University of Catalonia in collaboration with the Skobeltsyn Institute of Nuclear Physics (SINP) of the Moscow State University and CIEMAT (Madrid) is building a race-track microtron (RTM) whose main envisaged application is Intraoperative Radiation Therapy. The design of the accelerator is described in [1], the course of its development was reported in [2].

A schematic view of the RTM main unit is given in Fig. 1. It consists of electron gun (1), accelerating structure (linac) (2) with four accelerating and three coupling cavities, two end magnets (3, 4) and a horizontally focusing quadrupole (5). These elements are precisely fixed on a common rigid platform placed inside a steel box which plays the role of the vacuum chamber. The beam can be extracted from any of the four orbits with extraction magnets (6) and exits the microtron along the output trajectory (7). The main RTM parameters are listed in Table 1.

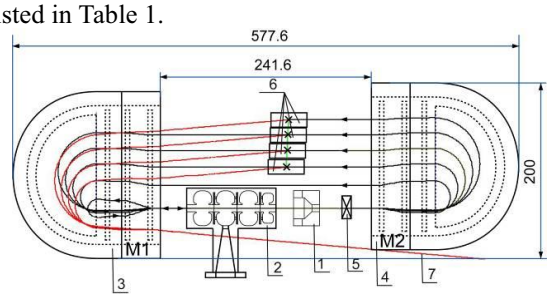

Figure 1: RTM scheme

Table 1: RTM parameters

Parameter	Value
Beam energies	6, 8, 10, 12 MeV
Operating frequency	5712 MHz
Synchronous energy gain	2 MeV
Pulsed beam current at the RTM exit	5 mA
End magnets field	0.8 T
Injection energy	25 keV
RTM head dimensions	670×250×210 mm

In all the RTM magnets as the source of the magnetic field a Rare-Earth Permanent Magnet (REPM) material is used. This allows to achieve rather compact magnetic systems which can be used inside the high-vacuum chamber.

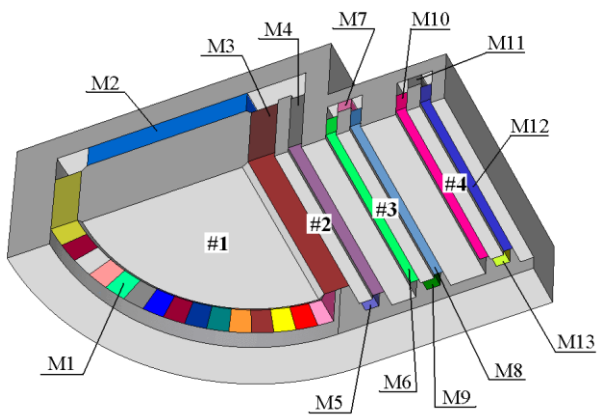

Figure 2: Geometry of the RTM end magnet used in ANSYS 3D simulations.

In the present machine with a low energy injection the end magnets, besides bending the particle trajectories by 180º, have other functions. Namely, end magnet M1 (see Fig. 1) also reflects the beam after the first acceleration back into the accelerating structure thus solving the problem of linac bypass. In addition, the beam vertical defocusing by the fringe field of the 180º bending dipole must be supressed and even converted in vertical beam focusing. All these requirements are implemented in a four-pole magnetic system described in Refs. [1], [3], its 3D geometry is shown in Fig. 2. The end magnets are symmetric with respect to the median plane and the vertical central plane, therefore from a one quarter of the magnet given in Fig. 2 the complete 3D geometry can be determined.

*Work supported by the grants 2009 SGR 1516 of AGAUR (Generalitat of Catalonia) and FPA2010-11911-E of MICINN (Spain).
e-mail: timerke@mail.ru

ISBN 978-3-95450-125-0

HIGHLY ACCURATE 3D MODELING OF THE C-80 ISOCHRONOUS CYCLOTRON MAGNETIC STRUCTURE

S. A. Artamonov, E. M. Ivanov, G. A. Riabov, N. A. Chernov, PNPI, Gatcina, Russia

Abstract

Very complicated magnetic structure with extremely high spiral angle and set of 17 correction shim types in each of 8 sectors is used in the H-minus ion isochronous cyclotron C-80. The 3D Novosibirsk code MERMAID was applied to optimize geometry of the sectors and shims in the hill and value region. A precision finite-element model allows take into account the iron non-linear effects and the detailed magnet geometry. MERMAID makes use about 20.5 millions nodes and provides magnetic field calculation accuracy in 10-20 Gs. The integral magnetic field parameters (isochronism, transversal motion frequency, H-minus ion electromagnetic dissociation) have been optimized by using the trajectory analyses. Program provides the significant reduction the time and efforts for the determination the necessary shims set in comparison with trial-and-error method.

INTRODUCTION

The isochronous cyclotron C-80 constructed at PNPI is planned to use as well for fundamental researches in nuclear physics, the solid state physics and biology, as for applied program - production of medicine isotopes for, therapy of an eye melanoma and surface forms of a cancer. As a first approximation the magnetic system of cyclotron C-80 was designed a few years ago on the basis of 2D calculations by using the POISSON program and measurements on two small models [1, 2]. The final version of C-80 magnetic structure optimized by 3D calculations with the MERMAID program was used for measurements and the field correction on the full scale magnet is presented in this report.

MAIN CALCULATION DIFFICALTIES

One of the central problems for every isochronous cyclotron is forming the radial and azimuthally magnetic field distribution. Another problem is connected with acceleration of H^- ions. To reduce the H^- dissociation losses in C-80 is used magnetic structure with very high spiral angle [3]. It is also necessary to mention the essential mathematical nonlinearity of the problem. It is to note that in isochronous cyclotron C-80 the magnetic structure is used three types of the steels. The main magnet yoke is constructed from a set of two types of the steels: steel 3 – μ_3(B) and steel 10 – μ_1(B). Poles are constructed from steel 10 – μ_1(B). Sectors, 17 correction shim types in each of 8 sectors and valleys shims are constructed from other steel 10 – μ_2(B). In the following figure it is visible that these curves μ(B) very strongly differ in a working range of magnetic fields of a cyclotron: 11000-18000 Gs. It is obvious that this creates additional computing difficulties and problems at creation of 3D model.

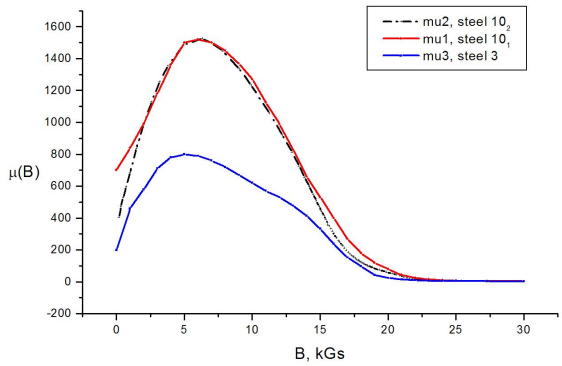

Figure 1: Permeability curves μ(B) in C-80.

PROCEDURE OF A MAGNETIC FIELD FORMATION

Procedure of the necessary magnetic field formation and selection of magnetic structure parameters for C-80 according to the program MERMAID [4] was made step by step method.

As the first step, the key parameters of magnetic system C-80 [5] were fixed. It was supposed that the geometry and height of sectors equals to 90 mm and during the further optimization is not changed. For obtaining the required isochronisms the heights of the correction sector shims have been varied. The initial heights of these shims were selected equal to 20 mm. Besides, in the course of optimization special the constrained condition was used. The amplitude of 4-th harmonic do not exceeded ~3000 Gs and the hill $B_{max} \leq 17000$ Gs near the extraction radius. Under this conditions H^- dissociation are below ≤5 % [3]. For this purpose it was introduced into the magnetic system additional valley shims. Thus formation of a demanded isochronous field is carried out only by changing iron geometry without use of corrector coils.

At the second stage 3D model of the magnetic system C-80 was developed and was constructed. It carefully describes geometry of magnet yoke, sectors (4 pairs), sector shims (17 correcting shims on each sector), and valley shims, the coils current, external boundaries. It also considers nonlinear magnetic properties used electro technical steels μ (B).

Due to high spiral angle sectors we were forced to use in calculations 1/2 magnets with the vertical

ISBN 978-3-95450-125-0

UPDATE OF CLASSICAL CYCLOTRON U-150 MAGNETIC SYSTEM. SIMULATION AND EXPERIMENT

Yu.Alenitsky, N.Azaryan#, A.Chesnov, O.Lepkina, E.Samsonov,
I.Sedych, V.Smirnov, JINR, Dubna, Russia
I.Gulamov, Z.Shukurov, R.Umerov, Y.Uzakov, UAS, Tashkent, Uzbekistan

Abstract

Classical cyclotron U-150 located in the Academy of Sciences of the Republic of Uzbekistan, Tashkent, was developed more than 50 years ago in Efremov's institute for acceleration various particles (p, d, He). For magnetic field re-tuning the current coils are used. Nowadays U-150 is used to accelerate only protons to energy of 15-22 MeV for producing isotopes for medical or industrial applications. In order to save the electrical energy and operating simplification it is proposed to create a decreasing average magnetic field in cyclotron only by means of ferromagnetic parts. To create a negative gradient of the magnetic field steel parts are made and installed in the magnet.

Analysis of measurement results showed the possibility of production of the required isotopes in updated U-150 with power economy of about 15%. Experimental irradiation of the target showed that the created field gradient did not provide an achievement of the required proton energy at radius of 64-65 cm. To achieve required energy one correction coil is kept in operation and measured magnetic field showed a satisfactory result. For estimation of possibility of creating the required magnetic field gradient without correction by coils the simulation of the cyclotron magnetic system were done and the results of calculations and its analysis are presented in this paper.

INTRODUCTION

On Fig.1 you can see a photo of the classical cyclotron U-150 which located in Tashkent in the Academy of Sciences of the Republic of Uzbekistan. Magnetic yoke of classical cyclotron U-150 has an E-type core.

Figure 1: Cyclotron U-150 during the measurements of the magnetic field.

#azaryan@jinr.ru

One sees in Fig. 2, 3 the pole, the vacuum chamber cover and the steel rings located inside the vacuum chamber. In the gap between the poles of magnet and the vacuum chamber of cyclotron (top and bottom), which is 25 mm in height, steel discs having varying thickness along the radius were installed.

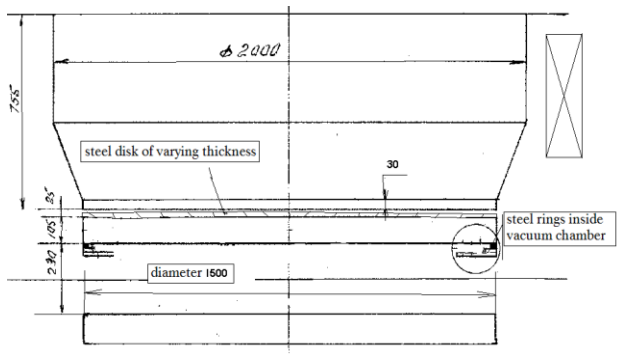

Figure 2: Size and cross section of the magnet SP-72 pole.

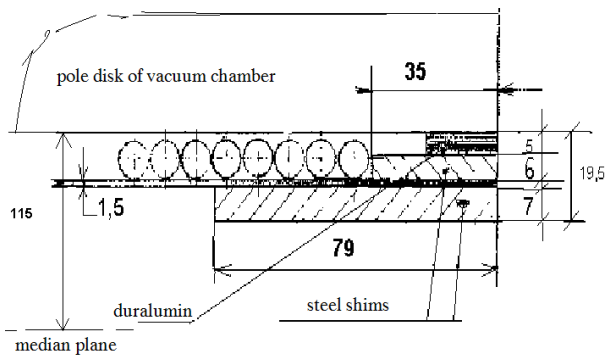

Figure 3: Cross section of the steel shims and coil located inside the vacuum chamber of the cyclotron.

Originally correction coils were included in the design of the cyclotron to provide a possibility of acceleration particles of various types. Nowadays U-150 accelerates only a proton beams and the need for using of the coils for forming of magnetic field is missing. Required profile of the magnetic field is possible to be obtained by the modification of the design of cyclotron's pole using additional iron components without the correction coils which allows saving the electric power for the operation of the cyclotron.

Overview of the modification of the magnetic system and its experimental results is presented in this write-up.

ISBN 978-3-95450-125-0

PULSE GENERATOR FOR THE BEAM INJECTION SYSTEM OF NICA COLLIDER

V.S. Aleksandrov, E.V. Gorbachev, N.I. Lebedev, A.V. Tuzikov, A.A. Fateev
Joint Institute for Nuclear Research, Dubna, 141980, Russia

Abstract

The new scheme of injection kicker elements distribution is described. Parameters of the circuit main elements are estimated. The system allows producing flat top of the injection pulse with high evenness. The suggested design allows building reliable and cost effective injection system satisfying the project parameters.

MAIN CHARACTERISTICS OF BUMP MAGNET

To provide one-turn injection of the ion beam in the collider NICA [1] there are two bump magnets (one piece for each ring). Bump magnet can be composed of several modules. Main requirements for the parameters of bump magnet are shown in table 1.

Table 1:. Kicker Parameters

Effective length , mm	3000
Aperture, mm × mm	55×42
Pulse duration, nsec	<900
Pulse flat top duration , nsec	≥100
Field integral, T·m	0,3
Spatial inhomogeneity of the magnetic field in the beam area,%	<5
Deviation of the field through the bunch length,%	<5

Figure 1 shows the operating aperture of the bump magnet, the envelope of the circulating beam (red), the envelope of the injected beam (blue). Blue area is the required area of "good" field.

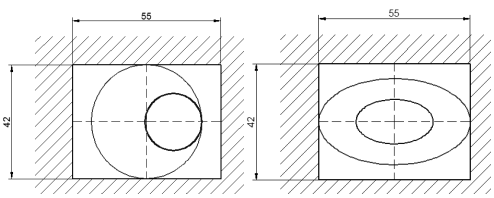

a) the kicker beginning area b) the kicker end area

Figure 1: The bump magnet aperture, the envelope of the circulating beam (outer curve), the envelope of the injected beam (inner curve).

PROJECT OF BUMP MAGNET

Several different types of magnets have been considered. The “iron-free" version of the kicker was chosen. It consists of two forward and two reverse conductors in a relatively wide-aperture vacuum chamber. Figures 2 and 3 show the position of the conductors and the distribution of magnetic fields that are optimized for the design parameters of the beam. It should be noted that the selected option almost as good as traditional ferromagnetic one in terms of energy performance, but it is much easier and cheaper to implement.

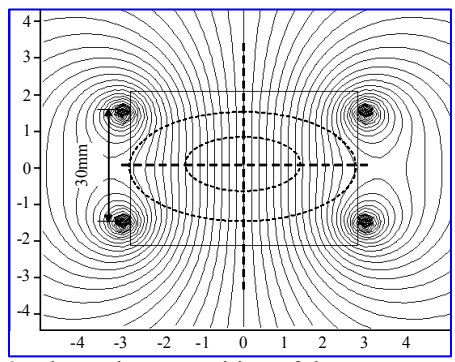

Figure 2: The optimum position of the current-carrying conductors relative to injected and circulating beams at the kicker end area .

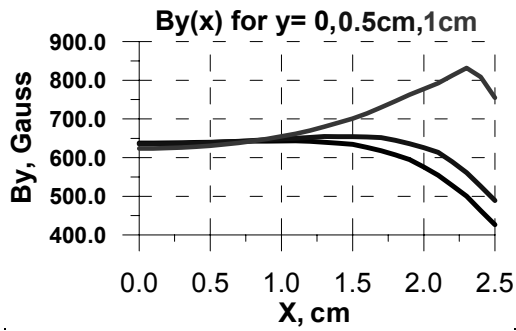

Figure 3: The distribution of the magnetic field.

PULSED POWER SUPPLY SYSTEM

Pulsed power supply is based on an capacity aperiodic discharge with the inductive load. This scheme allows to form a bell-shaped pulse. For forming the flat top of the acting impulse it is proposed to establish in the area of transportation (the best location - in the middle of the main kicker split into modules) the correcting module with a bell-shaped magnetic pulse with shorter duration, less amplitude and with opposite direction of magnetic field. Power supply circuits for main and correction magnets are shown in Figure 4. The total effect a pair of magnets is illustrated in Fig.5. To facilitate visualization the magnetic fields integrals are expressed in the normalized currents. Flatness at the top of the resulting pulse can be achieved very high, but require high precision timing switches. Besides the amplitude of

ISBN 978-3-95450-125-0

FAST KICKER

V. Gambaryan, A. Starostenko, Budker INP SB RAS, Novosibirsk, Russia

Abstract

Pulsed deflecting magnet (kicker) project was worked out in BINP (Budker Institute of Nuclear Physics). The kicker design task is: impulsive force value is 1 mT*m, pulse edge is 5 ns, and impulse duration is about 200 ns. The unconventional approach to kicker design was offered. The possibility for set of wires using instead of plates using is considered. This approach allows us to reduce the effective plate surface. In this case we can decrease effects related to induced charges and currents. In the result of modelling optimal construction was developed. It includes 6 wires (two sets in threes). Wires are 2 mm in cross-section. The magnet aperture is about 5 cm. Integral magnet length is about 1 meter. This length can be obtained by single magnet or by multiplied length of magnets array. Calculated field rise time (about 1.5 ns) satisfies the conditions. Induced current effect reducing idea was confirmed. For configuration with 3 wires pair (with cross section of 2 mm) induced current in one wire is about 10% and in the wall is about 40%. However for design with plates current is about 40% and 20% respectively. Obtained magnet construction allows controlling of high field homogeneity by changing currents magnitudes in wires. In general we demonstrated the method of field optimization. *Summary.* Optimal kicker design was obtained. Wires using idea was substantiated.

THE KICKER CONCEPT DESIGN

The kicker design should accept several requirements. The first one is vacuum chamber and kicker symmetry axis coincidences. The second one is that central angel should be about 90˚. The optimisation parameter is magnetic field homogeneity in centrally located square area (2 cm x 2 cm).

GEOMETRY OPTIMIZATION

Computer simulation was carried out for kicker's parameters optimization. Calculations were realised in FEMM and Maxwell. The central angle, the wires number and diameter was optimized.

The Number of Wires

The initial geometry is shown in Fig. 1a. The wires with fixed diameters were placed in the vacuum chamber (with the radius of 7.5 cm) at a distance of 6 cm from its centre. The wires number arranges from 4 to 20. For comparison, geometry with plates was simulated (Fig. 1b). For simulating magnetic fields, the task formulated in harmonic analysis was solved on a frequency of 200 MHz. In this task wires are parallel connected to a current source. The impressed current in three left wires is +1kA, and in three right wires is –1kA.

Simulation results allow us to obtain the follow geometry characteristic: field homogeneity, mean value of magnetic field in the centre of the magnet, and magnet impedance.

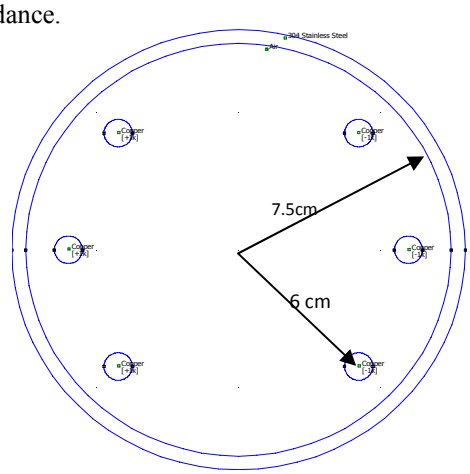

Fig. 1a: Geometry concept.

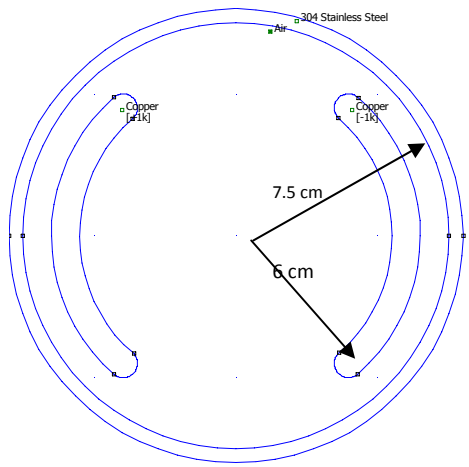

Figure 1b: Geometry with plates.

Field homogeneity is calculated according to Formula (1):

$$\delta B = \frac{B_{\max} - B_{\min}}{B_{\min}} \cdot 100\%, \qquad (1)$$

where B_{max}, B_{min} – magnetic field maximum and minimum values, respectively, determined in centrally located square area (2 cm x 2 cm).

The field homogeneity dependence on the wires number is shown in Fig. 2. Here we can see that homogeneity with using 6 wires is equal 1%, and it does not dramatically change with the wires number increase. However, the increasing number of wires leads to a lot of technical problems associated with the vacuum feedthroughs. Thus we should strive for the minimum number of wires.

ISBN 978-3-95450-125-0

IMPROVEMENT OF QUADRUPOLE MAGNETS FIELD QUALITY IN SERIAL PRODUCTION *

A.A. Starostenko#, P. Burdin, T. Devyataikina, E.S. Kazantseva, T.V. Rybitskaya, B.A. Skarbo, A.S. Tsyganov, Budker Institute of Nuclear Physics, Novosibirsk, Russia

Abstract

Technology of production of quadrupole magnets for NSLSII main ring is presented in the article. Quadrupoles have laminated iron yokes and are manufactured in Budker Institute of Nuclear Physics. The technology includes the method of correction octupole and sextupole harmonics. Field quality measurements of the magnets are presented.

INTRODUCTION

NSLS-II [1], the new 3GeV 3rd generation light source, is presently under construction at Brookhaven National Laboratory. Six types of quadrupole magnets for main ring NSLSII were successfully manufactured in Budker Institute of Nuclear Physics (see fig 1). The magnets had three yoke length and use the same lamination shape. The lamination with thickness of 1 mm had two poles with a common back leg. The magnet aperture was 66 mm. One length magnets had two types of yoke side insertions. One of the types is used to accommodate X-ray extraction. The form of the insertions had no influence on the field quality, so magnet types will be referred to as "short", "middle" and "long" below.

Prescribed specification on field quality of quadrupole magnets are reviewed in the paper [2]. Magnets field quality is specified by harmonics volume. Harmonics are defined as coefficients in the Fourier expansion of the integrated radial or azimuthal component of the magnetic field (see attachment). Harmonics are well below 10^{-4} of the main field (1 "unit") at a radius of 25 mm.

Table1. Parameters

Magnets type	**9801 & 9802 (short)**	**9804 & 9807 (long)**	**9810 & 9813 (middle)**
Quantity	60	60	7
Yoke length	217 mm	415 mm	250 mm
Maximum field gradient	10.6 T/m	19.2 T/m	19.2 T/m
Ampere-turns	4.7 kA	8.6 kA	8.6 kA

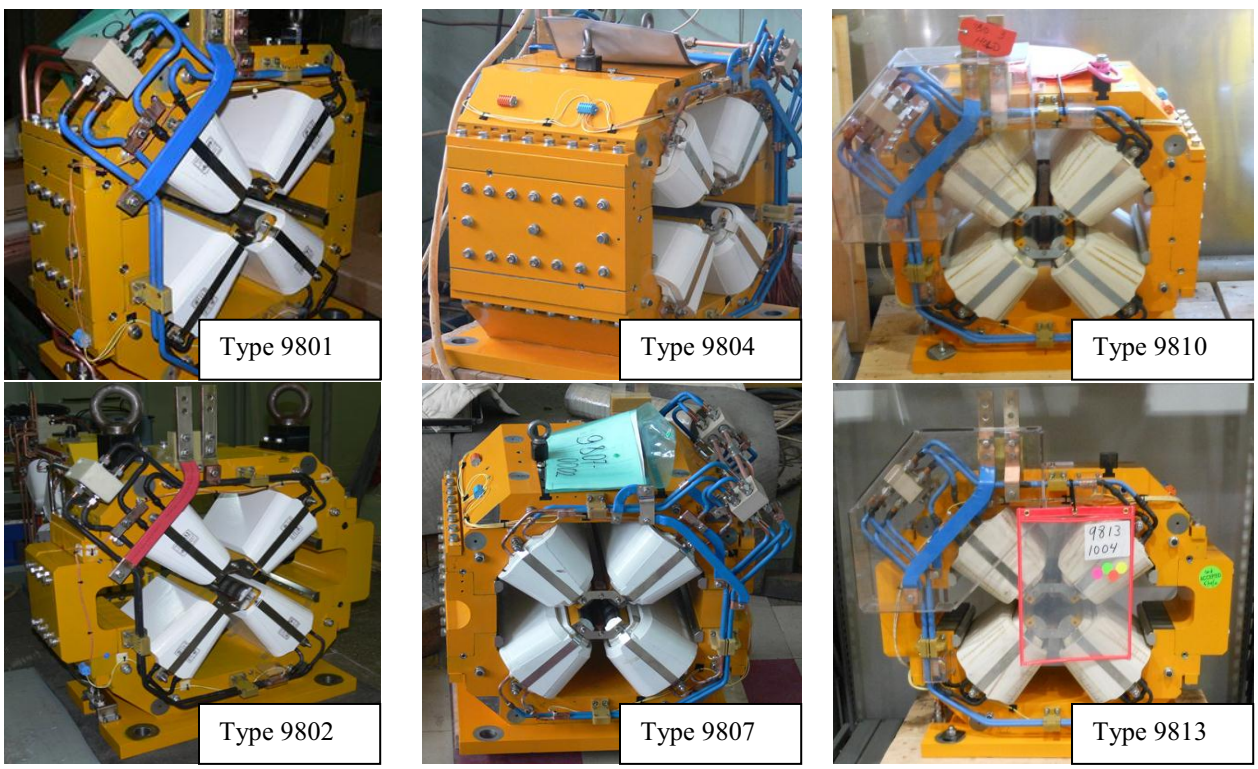

Figure 1: Quadrupole magnet types.

*Work supported by the Ministry of Education and Science of the Russian Federation (grant 14.B37.21.0784), Federal Target Program "Scientific Manpower of Innovative Russian Federation" 2009 - 2013.
#A.A.Starostenko@inp.nsk.su

ISBN 978-3-95450-125-0

QUADRUPOLE HARMONICS TUNING BY NOSE PIECES*

T.V. Rybitskaya#, E.S. Kazantseva, B.A. Skarbo, A.A. Starostenko, A.S. Tsyganov, Budker Institute of Nuclear Physics, Novosibirsk, Russia

Abstract

Six types of quadrupole magnets for NSLS-II main ring have been manufactured at the Budker Institute of Nuclear Physics. Some types of magnets have nose pieces on poles. Nose pieces permit the correcting of magnetic field harmonics. Corrections of octupoles, sextupoles and allowed harmonics have been implemented. Also for some magnets, corrections of amplitude of dependence sextupole harmonic from current have been implemented.

INTRODUCTION

The magnets had three yoke length (see table 1). Yoke of all magnets were glued from the same type of laminations. The lamination had two poles with a common back leg and thickness of 1 mm. The magnet aperture was 66 mm. One length magnets had two types of yoke side insertions. One of the types is used to accommodate X-ray extraction. The form of the insertions had no influence on the field quality, so magnet types will be referred to as "short", "middle" and "long" below.

Table 1. Parameters

Magnets type	**9801 & 9802 (short)**	**9804 & 9807 (long)**	**9810 & 9813 (middle)**
Quantity	60	60	7
Yoke length	217 mm	415 mm	250 mm
Maximum field gradient	10.6 T/m	19.2 T/m	19.2 T/m
Ampere-turns	4.7 kA	8.6 kA	8.6 kA

Magnets field quality is specified by harmonics volume. Harmonics are defined as coefficients in the Fourier expansion of the integrated radial or azimuthal component of the magnetic field (see attachment). Harmonics are well below 10^{-4} of the main field (1 "unit") at a radius of 25 mm.

The great labour has been applied to obtain the required field quality [2].One of the additional elements, which used to improve the field quality, was nose pieces. They were installed on middle and long magnets.

NOSE PIECES

Nose piece is a part of pole with chamfer. Its length and height are 15 mm and 35 mm correspondingly (see fig. 1). Nose piece fasten to yoke with stud. The fastening allow nose pieces be shift on 1 mm along pole face. The shift was used for corrections of sextupole, octupole and sometimes decapole harmonics.

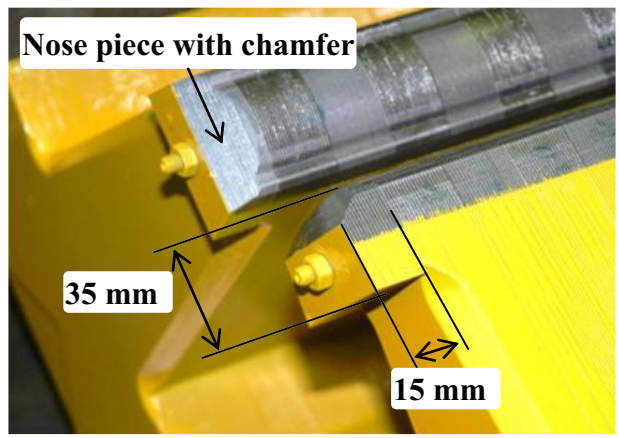

Figure 1: Nose pieces on one halve of magnet yoke.

The corrections demand the continual control of the magnet field quality. So, nose pieces position was tuned on the magnetic measurement stand [3] by iterations of tuning first then measuring the result changes. Usually three-five iteration was enough for tuning the field quality to achieve the desired result. Figure 2 shows measurements of lowest harmonics of magnet before the nose pieces installation and after the tuning. After the tuning, nose pieces got fixed by pins.

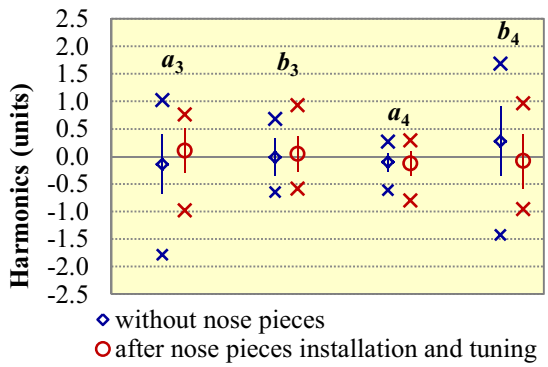

Figure 2: Statistic for 60 long magnets tuning. The circles and diamonds show the mean value of each parameter, the lines give a ±sigma spread, and the x – the maximum and minimum value.

One of the nose pieces well-known advantages is the integral increasing without increasing outer magnet dimensions. For long magnets the field integral was increased by 2.5 % and for middle ones by 5.1 % at design current.

*Work supported by the Ministry of Education and Science of the Russian Federation (grant 14.B37.21.0784), Federal Target Program "Scientific Manpower of Innovative Russian Federation" 2009 - 2013.

#T.V.Rybitskaya@inp.nsk.su

ISBN 978-3-95450-125-0

NONLINEAR SHUNTING AS A METHOD OF MAGNETIC FIELD CORRECTION IN QUADRUPOLE LENSES*

A. Tsyganov#, A. Batrakov, E. Kazantseva, A. Pavlenko, T. Rybitskaya, B. Skarbo, D. Shichkov, A. Starostenko, P. Vobly, Budker INP, Novosibirsk, Russia

Abstract

The quality requirements for magnetic field of elements in modern particle accelerators are high. For example, the harmonic fields quadrupole lenses main ring synchrotron source NSLS-II manufactured in BINP SB RAS must have no more than $1 \div 2 \cdot 10^{-4}$ from the field at 75% of the aperture of the lens. In the production process of magnetic lenses to adjust the fields of various methods of mechanical improvements are used, resulting in the increased time and the cost of production. The report proposes a method for precise non-destructive correction of some of the harmonics of the magnetic field of quadrupole lenses. The correction is performed using an additional element – the non-linear current shunt of coils. The report contains experimental data showing the possibilities of this method.

INTRODUCTION

In the Brookhaven laboratory, USA, synchrotron 3GeV light source NSLSII [1] is currently being constructed. For the main ring in BINP, several types of quadrupole lenses were designed and manufactured [Table1].

The magnets had three yoke length and use the same lamination shape. The lamination with thickness of 1 mm had two poles with a common back leg. The magnet aperture was 66 mm. One length magnets had two types of yoke side insertions. One of the types is used to accommodate X-ray extraction. The form of the insertions had no influence on the field quality, so magnet types will be referred to as "short", "middle" and "long" below.

Prescribed specification on field quality of quadrupole magnets are reviewed in the paper [2]. Magnets field quality is specified by harmonics volume. Harmonics are defined as coefficients in the Fourier expansion of the integrated radial or azimuthal component of the magnetic field (see attachment). Harmonics are well below 10^{-4} of the main field (1 "unit") at a radius of 25 mm.

To obtain the required field quality, many efforts were applied.

There are different tuning techniques of magnetic field during quadrupoles manufacturing. Most of these techniques require mechanical improvements.

The purpose of this article is to propose method of correction sextupole components using nonlinear shunt in power supply circuit of the quadrupole lens.

Table1. Parameters

Magnets type	**9801 & 9802 (short)**	**9804 & 9807 (long)**	**9810 & 9813 (middle)**
Quantity	60	60	7
Yoke length	217 mm	415 mm	250 mm
Maximum field gradient	10.6 T/m	19.2 T/m	19.2 T/m
Ampere-turns	4.7 kA	8.6 kA	8.6 kA

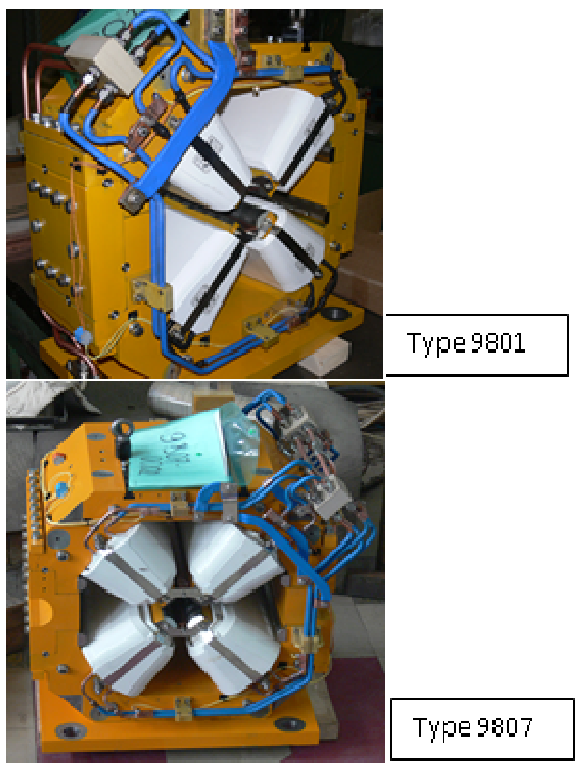

Figure 1. Two types of magnets, the experimental data are used in this article

*The work is supported by the Ministry of Education and Science of the Russian Federation (grant 14.B37.21.0784), Federal Target Program "Scientific Manpower of Innovative Russian Federation" 2009 - 2013.

A.S.Tsyganov@inp.nsk.su

ISBN 978-3-95450-125-0

STAND FOR PRECISE MEASUREMENTS OF MAGNETIC LENSES FIELD QUALITY*

A. Tsyganov, A. Batrakov, E. Kazantseva, A. Pavlenko, T. Rybitskaya, B. Skarbo, D. Shichkov, A. Starostenko, P. Vobly, Budker INP, Novosibirsk, Russia

Abstract

Strict requirements are imposed on the field quality of magnetic elements in today's synchrotron radiation sources. For example, magnetic field harmonics of quadrupole lenses (currently manufactured in BINP) of main ring NSLS-II, should have no more than one or two ten-thousandths parts of main harmonic at the 75% of lens aperture. The stand is designed for precise measurement of the quadrupole lenses. The well-known technique with a rotating coil was used. The design and location of coils used in the measuring shaft and the method of commutation allow to compensate for both quadrupole and dipole components of the magnetic field. This, in turn, minimizes shaft beats effect and power supply noises effect on the accuracy of the results. During measurements, the shaft is rotated without stopping, and the data received from the gauge angle and digital integrators are processed "on the fly" strictly synchronous. The measurement procedure is performed in one and a half turn of the shaft and takes six seconds. The report describes mechanical design of the stand, principle of work, parameters of the equipment, and software. Results of measurements of the quadrupole lenses synchrotron source NSLS-II are given in conclusion. The results demonstrate possibilities of the stand.

INTRODUCTION

Six types of quadrupole magnets for main ring NSLSII [1] were manufactured in Budker INP. The total quantity of magnets was 127. The high quality of magnetic field [2] was achieved by tuning directly on magnetic measurement stand. This stand was developed specially for similar task.

Requirements for MMS:

- Accuracy of magnetic field harmonics measurement is at level 10^{-5} relative to main quadrupole component.
- Short time required for one measurement with obtaining results.
- Automation of carrying out a series of measurements.
- Suitability for usage in mass production.

MECHANICAL CONSTRUCTION

All the construction is set on the girder (see Fig.1 and Fig.2). During the measurements the magnet is installed on the support, which provides the positioning of magnet in 3 coordinates. The rotating coil is installed on special supports. The rotating system is easily removable so that one can set or remove shaft in few minutes. The self-aligning shaft bearings are arranged on special steel bases, which are removable on one side due to the provided removability of shaft. Cable connections are at the both ends of shaft and they are fixed, which means that wires are rotating with the shaft. Lengths of cables were chosen for unobstructed shaft rotation of 3-4 turns in each direction.

Figure 1.Magnetic measurement stand.

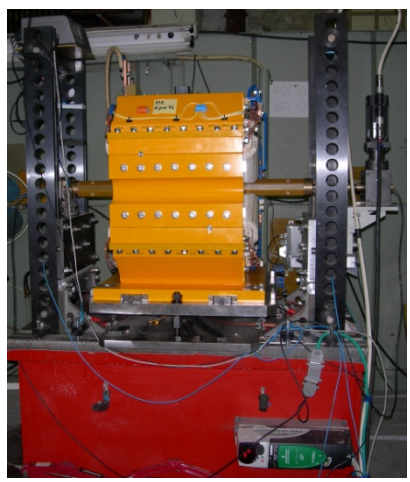

Figure 2. Mechanical construction of MMS.

The scheme of MMS interconnections is shown on Fig. 3. The integrators (VsDC3) were developed in the Budker INP [3].

MEASUREMENT SHAFT

The compensation scheme of rotating coil is shown on Fig. 4. Such connection of coils provides compensation of dipole and quadrupole components of magnetic field, so we get better signal for higher harmonics.

ISBN 978-3-95450-125-0

DESIGN, SIMULATION AND OPTIMIZATION OF A SOLENOID FOR ES-200 ELECTROSTATIC ACCELERATOR

M. Asgarpour, S. A. H.Feghhi, E. Ebrahimibasabi, M. khorsandi, Department of Radiation Application, Shahid Beheshti University, Tehran, Iran
N. Khosravi, University of Zanjan, Zanjan, Iran

Abstract

Solenoids have an important role from the viewpoint of focusing the beam in drift tube of charged particle accelerators. In order to optimize the beam current in ES-200, an electrostatic proton accelerator at Shahid Beheshti University (SBU), design and simulation of a suitable solenoid has been performed. The CST Studio package has been used for simulation and design. Simulation results from the CST have been validated in comparison with theoretical formula and equations. According to the results we optimized the design to have minimum lost beam current on drift tube.

INTRODUCTION

ES-200, an electrostatic proton accelerator at SBU, is a compact and portable electrostatic accelerator, which includes the basic components of a Cockcroft-Walton high voltage terminal, accelerating column, vacuum system, electromagnetic lens, drift tube, control system and etc. In this system a radio frequency ion source has been used to generate positive ions. Extraction voltage (adjustable from 0 to 5 kV) applies to the anode electrode for leading the ions to the entrance of accelerating column. Accelerating column has been composed of thirteen electrodes that can be divided into two main parts. The first part includes four electrodes for extracting, focusing and accelerating the ion beam. The second part includes nine electrodes with uniform shape which provide homogeneous field to accelerate and steer the beam. The maximum beam current on the target is about 500μA with the maximum energy of 200 keV. [1].

In order to optimize the beam current in ES-200, designing and simulation of a focusing system seems to be necessary. Magnetic lenses such as Solenoids, Quadrupoles and electrostatic lenses like Einzel lens are devices that are used as a focusing system in accelerators. In this paper, for minimizing the lost beam current on drift tube and changing the beam diameter on the target, design and simulation of the solenoid has been done by using the CST package.

DESIGN CONCEPTS

As it can be seen in Figure 1, On-axis longitudinal magnetic field for a single solenoid with the internal radii (r_1), external radii (r_2) and length of (l) is given by:

$$B=\frac{\mu_0 in}{2(r_2-r_1)}\left[x_2\ln\frac{\sqrt{r_2^2+x_2^2}+r_2}{\sqrt{r_1^2+x_1^2}+r_1}-x_1\ln\frac{\sqrt{r_2^2+x_1^2}+r_2}{\sqrt{r_1^2+x_1^2}+r_1}\right] \quad (1)$$

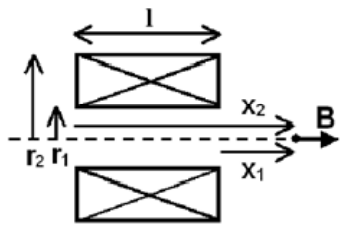

Figure 1. Solenoid in cross section view.

Where B is the magnetic field on the axis, μ_o is the permeability constant, (i) is the wire current , n is the number of turns of wire per unit length of solenoid, and x_1 and x_2 are the distances, on axis, from the ends of the solenoid to the magnetic field measurement point [2].

Some of electromagnetic codes have been used to solve Maxwell's equation with the specified boundary conditions. CST was introduced as software that analyses the structure with Finite Element Method. In this paper, CST PARTICLE STUDIO has been used to simulate charged particles travelling through electromagnetic fields [3]. Figure 2 and 3show an overview of a desired solenoid on the drift tube which was done by CST for a proton beam with energy of 200 keV (after passing through the accelerating column). The length and thickness of solenoid was considered 180 mm and 100 mm, respectively. Solenoid was set at distance of 450 mm from the end of accelerating column. Beam diameter was investigated at distance of 768.5 mm from the solenoid where the target was placed.

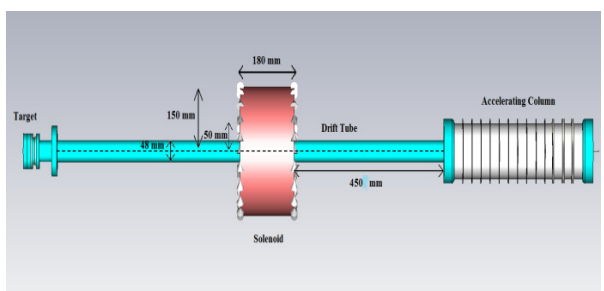

Figure 2. Simple model of a typical ES-200.

ISBN 978-3-95450-125-0

CORRECTING MAGNET POWER SUPPLIES FOR THE NSLS-II BOOSTER

K.R. Yaminov, O.V. Belikov, A.S. Medvedko, V.V. Kolmogorov, A.I. Erokhin, S.R. Singatulin, S.E. Karnaev, P.B. Cheblakov, Budker INP SB RAS, Novosibirsk

Abstract

Budkers Institute of Nuclear physics builds booster for synchrotron light source NSLS-II. Booster should accelerate electrons from energy 200MeV to energy 3GeV, acceleration phase duration is 250msec, repetition rate — up to 2Hz. Booster magnet system includes 16 sextuples and 36 dipole correcting magnets powered separately. Forth-quadratant current sources for sextuples and correcting magnets have maximum output current ±6A, maximum output voltage ±100V, maximum output current ripples and long-term stability are better than 0,1% relative to 6A. In ramping mode with current slew rate up to 200A/sec time lag between setpoint and output current is not more than 1msec and can be compensated by software. Results of power supplies system tests and commissioning will be presented in paper.

INTRODUCTION

The National Synchrotron Light Source II is a third generation light source under construction at Brookhaven National Laboratory. The project includes a highly optimized 3 GeV electron storage ring, linac pre-injector and full-energy booster-synchrotron. Budker Institute of Nuclear Physics builds booster for NSLS-II. The booster should accelerate the electron beam continuously and reliably from minimal 170 MeV injection energy to maximal energy of 3.15 GeV and average beam current of 20 mA. The booster shall be capable of multi-bunch and single bunch operation. A nominal repetition rate of the booster is 1 Hz with possibility to upgrade it up to 2 Hz. Main booster parameters are presented in the Table 1.

Table 1: Main booster parameters

Parameter	Value
Beams Energy: Injection/Ejection	200MeV/3GeV
Number of periods	4
Circumference, m	158.4
Repetition rate, Hz	1(2)
Bunch number	40-150
Revolution Frequency, MHz	1.893
Synchrotron frequency, kHz	35.5/20.3 (0.2/3GeV)
Betatron tunes: $\nu x/\nu y$	9.65/3.41
3D Damping time, sec	16.2s to 7.7s (0.2GeV) 4.8ms to 2.3ms (3GeV)
Energy rise time, sec	0.26

SEXTUPOLES AND CORRECTING DIPOLE MAGNETS

Quadratic nonlinearity of the magnetic field at the quadrupole lenses are proposed to be tuned using 16 sextupole lenses (8 lenses to X direction and 8 – to Y one). All the lenses are identical in design and in electrical parameters. The specified parameters of sextupole lenses are presented in Table 2.

Table 2: Sextupoles parameters

Magnet	I_{max}, A	R, OHm	L, H
BR-SXV	5,6	1,2	0.104
BR-SXH	5,6	1,2	0.104

It is proposed that for the beam orbit correction 36 dipole correcting magnets will be installed in the Booster magnet system. 20 dipole correctors are for X coordinate and 16 – for Y one. The specified parameters of correctors are presented in Table 3.

Table 3: Dipole correctors parameters

Magnet	I_{max}, A	R, OHm	L, H
BR-CX	5	2	0. 4
BR-CY	5	2	0.25

POWER SUPPLIES REQUIREMENTS

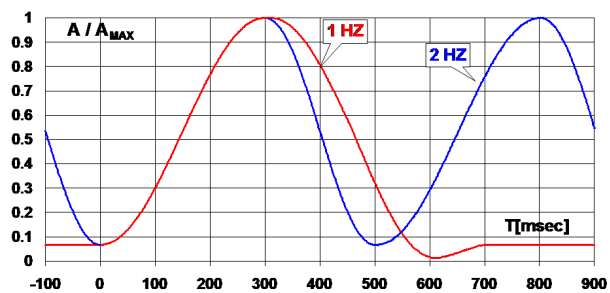

Figure 1: Magnetic field evolution during the ramp.

Cosine approximation of magnetic field evolution during the ramp for 1 and 2Hz modes is shown in Fig. 1. Sextupoles and dipole correctors are used to compensate higher harmonics caused by non-linearity of magnetic system. Therefore, power supplies should provide output voltages enough for necessary current slew rate. Output

ISBN 978-3-95450-125-0

HIGH VOLTAGE TERMINAL IN COSY ELECTRON COOLER

V.A. Chekavinskiy, E.A. Bekhtenev, I.A. Gusev, M.N. Kondaurov, V.R. Kozak, E.A. Kuper, V.R. Mamkin, A.S. Medvedko, D.N. Pureskin, D.V. Skorobogatov, BINP SB RAS, Novosibirsk

Abstract

In Budker INP SBRAS was developed electron cooler with energy up to 2MeV for COSY accelerator (Germany). Due to restricted footprint, cooler's collector and gun parts were combined in a single acceleration system – high voltage terminal. All power and control electronics were placed in a single isolated volume, filled with SF6 gas under 4-6 atm. pressure. Electronics is controlled via wireless CAN, and powered by multistage transformer, capable of 15 kW power at 26 kHz. Wireless control is passed through dedicated optically transparent window, also served for modulated laser beam, used in electron beam diagnostic. By construction, electronics is divided on two standalone units: collector power supply and gun-filter system (SGF). SGF is built on 19" EuroPak chassis, where were placed all power modules, needed for collector and gun pipe electrodes. All power outputs were protected against overvoltage and sparks, available while cooler exploitation. In SGF there were controlled up to 40 parameters altogether. SGF inner power supply provides stable operation in wide range of input voltage, up to +/- 50% from nominal. Also included in SGF are 2 auxiliary systems, used for beam guiding and beam diagnostics.

INTRODUCTION

High Voltage Terminal (HVT) in electron cooler is intended for generating of electron cooling beam and collecting the beam back, producing thus continuous up to 3A electron current. Due to this task, it consists of:

- Gun of electron beam, including cathode, anode and 4 control grid electrodes.
- Collector of electron beam, including collector, suppressor and 2 Wien filter electrodes.

Both grid and collector bodies are encircled with a number of magnetic solenoids intended for shaping a proper magnetic field profile inside. Also measurement of the collector current and the so-called leakage current should be provided. HVT has an outer metal shielding cap with smooth rounded shape, intended for uniform voltage distribution under high voltage circumstances. Powering of HVT electronics is provided by cascade transformer, that is a part of accelerator column, with output voltage varying in wide range of 400 – 800VAC at 26 kHz frequency [2]. Accelerator column itself provides up to 2MV negative acceleration voltage, so HVT chassis ground is under this voltage too.

The electronics needed for providing power supply (P.S.) for HVT electrodes and solenoids is divided on 3 separate units. The most power consuming is collector power supply, with up to 15KW output power, therefore it was designed as standalone unit equipped with an oil force-cooling system. Another unit, housing magnetic solenoids power supplies, is situated at opposed to collector power supply side on HVT chassis. The remaining electrodes power supplies are united in the third unit, named Gun-Filter System (SGF), it is mounted on top of the second unit. Each unit was developed by the different developer; we will focus from now on mainly on SGF unit.

SGF UNIT DEVELOPMENT

SGF power supplies detailed specifications are summarized in Table 1. Besides power supplying, the following additional requirements are imposed for SGF functioning:

- Each of 4 grid electrodes can be modulated individually with 3MHz sinusoidal wave at regulated amplitude from 0 to 8Vrms.
- Computer control of the whole cooler system is based on CAN protocol.
- Collector power supply unit control requires CAN control with optic fibre transport.
- Collector and leakage current should be measured by means of voltage drop on the corresponding resistors given.
- The collector to cathode return current is passed via HVT chassis.

Table 1: SGF Power Supplies Specifications

Name	Uout, Iout	Tolerance
Anode	0…+10kV, 1,5mA	0,1%
Suppressor	-3…+5kV, 3mA	0,1%
Control grid	-3…+5kV, 3mA	0,1%
Filament	+7…+25V, 5A	1,0%
Wien filter x2	0…+30kV, 1mA	0,1%

Connections requirements

The layout of collector and gun on the HVT chassis is illustrated in Fig. 1. Note how the electron return current (shown in red colour) flows on the chassis. Taking into account that the material of chassis is stainless steel, and the current value is up to 3A, care must be taken to eliminate unexpected voltage drops in control paths, because both gun and collector electrodes (shown in blue colour) are powered from a single unit (SGF), which is electrically and mechanically connected to the same chassis. Due to high risk of damage because of high voltage breakdowns and uncontrollable discharges, all electrodes power supply's return paths must be of low impedance, that is achieved by 10kV rated coaxial cable used for all electrodes except Wien filter electrodes. Those are to power with a voltage up to +30kV, so an appropriate shielded cable could not be used. Instead, a

ISBN 978-3-95450-125-0

HIGH-VOLTAGE SOURCE WITH OUTPUT VOLTAGE UP TO 110 kV WITH OUTPUT CURRENT UP TO 100 mA

I.A. Gusev, A.S. Medvedko, A.Yu. Protopopov, D.N. Pureskin, D.V. Senkov,
BINP, Novosibirsk, Russia

Abstract

The presented report contains the description of high-voltage source with output voltage up to 110 kV and output current up to 100 mA. The source consist of the chopper with IGBT switches working with a principle of pulse-width modulation and the full H-bridge converter with IGBT switches, both working on programmed from 15 to 25 kHz frequency, and the high voltage transformer powering the four-stage multiplier with the additional capacity filter at output. The transformer and multiplier both are made in common volume separated on oil tank part with silicon oil for transformer and SF6 part for multiplier. The additional capacity filter provides low ripple and noise level in working range of output currents. A nominal output voltage of the source is 110 kV. The source can operate in normal mode with series of high-voltage breakdown in output voltage. In the high-voltage breakdown the released in load and matching circuit energy is less than 20 J at maximum operating voltage 120kV. The efficiency of system is more than 80% at the nominally output power 11 kW. The controller of the source is developed with DSP and PLM, which allows optimizing operations of the source. For control of the source serial CAN-interface is used. The description of the source and the test results are presented.

DESCRIPTION

The presented source was designed for some different applications at the BINP tasks. That was reason for some specific terms like: strong reliability to high-voltage breakdown, low energy dissipated in high voltage breakdown, low voltage ripple for maximal power operation. The energy is dissipated in components of source and in the load during the high voltage breakdown less than 30J for 110 kV operations. The basic characteristics of high-voltage source are shown in Table1.

Overview

The circuit diagram of power part of high-voltage source is shown in Fig.1. The high-voltage source consists of the 20 kHz power converter with insulated gate bipolar transistors (IGBT) as switches (part A) and high-voltage transformer with the four-stage multiplier (part B). The power converter consists of 3-phase rectifier VD1, electromagnetic (EMI) filter F1, switch SW1, rectifier's filter capacitors C1-C2, 20 kHz chopper with IGBT switch Q1, 20 kHz inverter with IGBT switches Q3-Q6, output filter circuit L2 C5 C6, and isolation transformer T1.

Table 1. Basic characteristics of high-voltage source.

Parameter	**Unit**			
		Min	**Nom**	**Max**
Output voltage	kV	10	110	120
Output current	mA	0.1	100	120
Output power	kW		11	
Voltage ripple	%			0.5
Voltage stability	%			0.2
Transient time	ms		50	
Converter frequency	kHz	15	20	25

Input Rectifier

EMI filter is used to eliminate high-frequency noise to the power line from the source. 3-phase rectifier and filter C1-C2 is used to convert input AC 3-phase voltage 380V 50Hz to DC 550-600V voltage. Contactor SW1 consists of 2 groups of contact: the first is used for soft start of converter and another is used for normal operations. First group of contacts is switched ON and the filter's capacitors C1-C2 are charged with 10A current. When the voltage on filter is up to 450 volts level the second group of contacts is switched ON and the rectifier is connected directly to 3-phase AC line.

Chopper

The chopper switch Q1 is operated with principle of pulse-width modulation on programmed from 15 kHz to 25 kHz frequency. The working frequency of inverter is the same. The operating frequency is selected depending on the characteristics of high-voltage transformer and the requirements to the spectrum of output high voltage ripple. The output voltage of chopper is changed from 10 to 450 volts DC by control circuit to obtain the required output high voltage of source.

Inverter

Full-bridge inverter Q3-Q6 converts DC voltage from chopper's capacitors C3-C4 to AC voltage with programmed from 15 to 25 kHz frequency. When the high voltage breakdown or over current is detected the inverter switches are switched OFF in 10 microseconds to protect power circuit from damage.

ISBN 978-3-95450-125-0

3-CHANNEL CURRENT SOURCE WITH CHANNEL OUTPUT CURRENT UP TO 180 A AND OUTPUT VOLTAGE UP TO 180 V

I.A. Gusev, D.V. Senkov, A.I. Erokhin, V.V. Kolmogorov, A.S. Medvedko, S.I. Potapov, D.N. Pureskin, Budker INP SB RAS, Novosibirsk, Russia

Abstract

The presented report contains the description of 3-channel current source with channel output current up to 180 A and output voltage. Each channel can be operated and controlled independently. The source consists of 2 part. First part is charging source with capacitance bank at output. And the second part is 3 current sources powered by a capacitance bank. The charging source is converter with IGBT switches, working with a principle of pulse-width modulation on programmed from 15 to 25 kHz frequency, with high power rectifier at output. The source output voltage is up to 180 V, peak power is 40 kW and average power is 20 kW. Capacitance bank has 120 kVA storage energy. Second part contains 3 independent current sources with up to 180 A output current each. Each current source consists of H-bridge 2-quadrant convertor with MOSFET switches working on 50 kHz frequency and the output LC filter. The controllers of the sources are developed with DSP and PLM, which allows optimizing operations of the sources. The controllers are connected by internal control network for more flexibility and efficiency. The description of the source and the test results are presented.

DESCRIPTION

The presented current source was designed for supply of quadrupole magnets with 2 Hz ramping 180A current. There are three group of quadrupole magnets is used BF BD BG. That way three current sources are needed. Parameters Current scenario for quadrupole magnets is shown in Figure1. In the beginning there is a few-millisecond injection plateau - the current should be 1/15 from the maximum current and have the stability not worse than 0.05 %. It is followed by a 0.26-second controllable rise of current . The current stabilization accuracy at rising should be better than 0.1 %. Then there is a short flat-top for extraction of the particles with the fixed energy – followed by fall. The repetition period is 1 or 2 Hz.

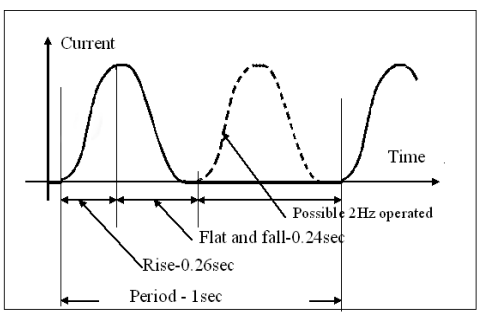

Fig.1. Current scenario.

The load parameters are the same for each channel. Load inductance is 0.14Hn. Load resistance is 0.3Om. At the specified current scenario, the average power of active losses is 2.5 kW for channel, the energy accumulated in inductance is 2 kJ. Time constant of the magnets is approximately 0.5 sec, thus, to provide the current fall during the necessary (<0.2 sec) time, the current source should be two-quadrant and the part of current from inductance at fall should be recuperated to the source buffer capacitor. The capacitance value is 0.1F per channel for 40V over voltage and 200V operating voltage. The selected diagram of power source is shown on Fig.2. The common 30kW bulk power supply with 200V output voltage and common 0.3mF capacitance bank are used. Three separate current sources are powered from capacitance bank. Each of the Output sources has their own channel of computer control via PSC and PSI controllers. Bulk Power supply is controlled current sources by local bus. The circuit with the single bulk PS and the common capacitance allows optimizing the magnet energy recuperation for asynchronous operation or for different values of maximum currents in channels.

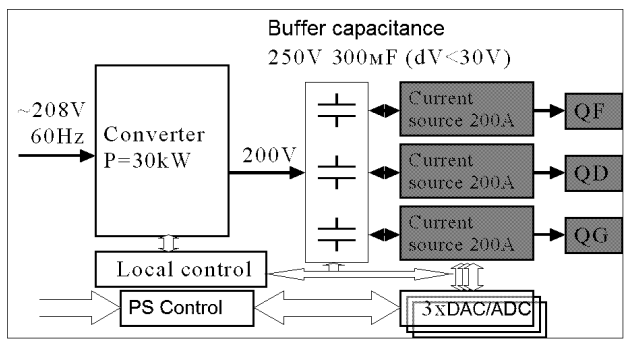

Fig. 2. Power source block diagram.

Overview

The current source circuit diagram is shown in Fig.3. The bulk power supply consists of 3-phase rectifier VD1, electromagnetic (EMI) filter F1, switch SW1, rectifier's filter capacitors C1-C2, 20 kHz inverter with IGBT switches Q1-Q4, isolation transformer T1 output rectifier circuit VD1-VD3, and the capacitance bank C4. The current sources are identical. Current source consists of input capacitance C5, 50 kHz two quadrant H Bridge with MOSFET switches Q5-Q12, filter circuit L1 C6 C7 and DCCT circuit.

ISBN 978-3-95450-125-0

THE POWER SUPPLY SYSTEM FOR THE ACCELERATING COLUMN OF THE 2 MEV ELECTRON COOLER FOR COSY

D. Skorobogatov, M. Bryzgunov, A. Goncharov, I. Gusev, M. Kondaurov, V. Kozak, A. Medvedko, V. Parkhomchuk, D. Pureskin, A. Putmakov, V. Reva, D. Senkov, BINP SB RAS, Novosibirsk

Abstract

The 2 MeV electron cooler for the COSY storage ring (FZJ) is being assembled at BINP. The electrostatic accelerating column generates a high-energy electron beam. The power supply for the accelerating column of the electron cooling system consists of 33 controlled modules distributed by the accelerating potential. Each module has a precision controlled voltage source for 60 kV, 1mA and an additional supply for the solenoids of the magnetic system with a maximum current of 2.5 A. All the systems are controlled through the wireless ZIGBEE network. This report presents the structure of the power system, its parameters, and the results of tests carried out at BINP.

INTRODUCTION

In 2009-2012, BINP was involved in the creation of an electron cooler for heavy ions to be installed on the COSY accelerator of the Jülich accelerator center (Germany) [1, 2]. The main parameters of the cooler are as follows: the electron energy is 25 keV to 2 MeV and the current is up to 3 A. The energy instability will not exceed 10 ppm. Besides, the installation was designed with a proper account of limitations associated with the fact that it will be installed on an already-existing accelerator ring in an earlier-built building.

The accelerating column, where the electron beam is accelerated and recuperated, is one of the main components of the installation.

The main parameters of the accelerator column of the cooler are presented in Table 1:

Table 1: Main parameters of the accelerator column of the COSY cooler

Parameter	Units	Value
Electron energy	MeV	0.025 - 2.0
Energy instability, less than		10^{-5}
Magnetic field of the transport line	G	500
Field instability		10^{-3}
External power supply	V	600
Carrier frequency	kHz	26.2
Power consumption	kW	30-40
Total height of the column	m	3.7

To meet the requirements of the installation we had to develop a power supply system which along with precision output parameters would have high reliability in a strong magnetic field and at strong electrostatic discharges.

STRUCTURE OF THE ACCELERATING COLUMN

The structure of the accelerating column is shown in Fig. (1).

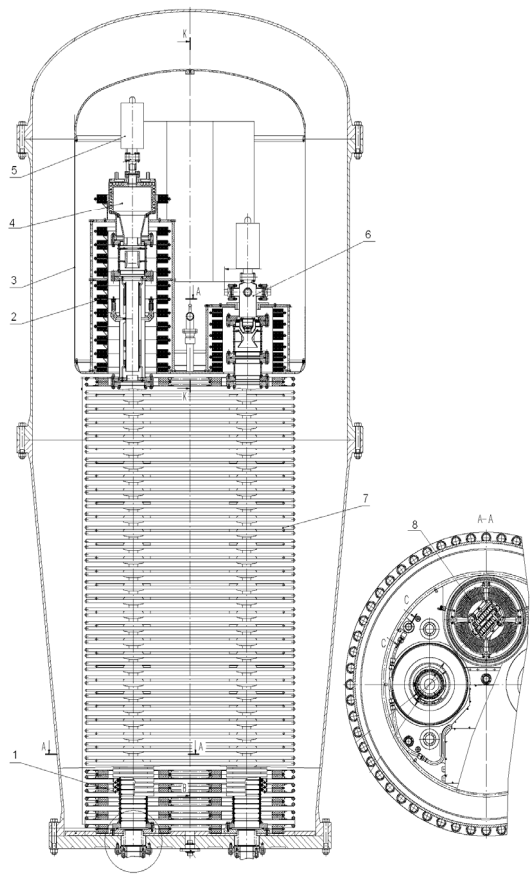

Figure 1: The structure of the accelerating column: 1 – accelerating tube; 2 – solenoid; 3 – high voltage terminal tank; 4 – collector; 5 – ion pump; 6 – electron gun; 7 – high voltage section; 8 – cascade transformer.

ISBN 978-3-95450-125-0

POWER SUPPLY SYSTEM OF THE PULSE BENDING MAGNET FOR THE LINEAR ACCELERATOR OPERATED AT THE MOSCOW MESON FACTORY

B.O. Bolshakov#, A.A. Budtov, A.V. Pozhenskiy, A.V. Popov,
D.V. Efremov Scientific Research Institute of Electrophysical Apparatus, Saint Petersburg, Russia
O.V. Grechov, V.N. Michailov, V.L. Serov, A.V. Feschenko,
Institute for Nuclear Research RAS, Moscow, Russia.

Abstract

To ensure simultaneous operation of the linear accelerator in the experimental and isotope production systems, a pulse (kicker) magnet with its power supply system (pulse modulator) has been designed and manufactured in the D.V. Efremov Institute by an order of the INR RAS. The pulse magnet with its power supply system has been installed in the INR RAS and adjustment works have been performed. In the paper are described a schematic and principle of operation of the pulsed magnet and modulator deflecting a part of proton macropulses to the isotope production system. The results of the adjustment works performed are presented in the paper.

INTRODUCTION

To widen the potentialities of simultaneous operation with the beams produced by the linear accelerator operating at the Moscow Meson Factory (Troitsk town), a special pulse electromagnet(kicker magnet) with a supply system (pulsed modulator) has been designed and manufactured. The magnet pulsed at a repetition rate of 50 Hz allows a deflection of a 100-160 MeV beam of H^+ или H^- ions by 13º to a target intended for production of isotopes. The rest macropulses intended for physical experiments pass without distortion of their trajectories.

REQUIREMENTS FOR KICKER MAGNET

The kicker magnet is intended to replace the used permanent electromagnet, therefore, overall and setting dimensions should be kept the same. In addition, the magnet was supposed to operate both in the pulse and continuous modes, and a sufficiently high induction in the magnet yoke, 0.85 T, was chosen. The pulse of the current passing through the magnet is of a half-sinusoidal shape; the current pulse length is 12 ms. The pulse repetition rate is 50 Hz. When a pulse ceases, the residual magnetic field should be minimum so that the second macropulse can pass without a deflection. When a 200 ms macropulse is passing, the magnetic field non-uniformity at the half-sinusoid top is 0.05%. To keep stable 13º bending of a proton macropulse, the long-term pulse-to-pulse reproducibility of the magnetic field should not exceed this value.

#Bolshakov.BO@luts.niiefa.spb.su

Table 1: Main Parameters of the Kicker Magnet

Parameters	Q-ty
Bending angle for 100-160 MeV proton beam	13º
Pole straight section length (uniform field), mm	350
Pole width (uniform field), mm	145
Gap height, mm	60
Magnet inductance, H	0.03
Magnetic half-sine pulse length, ms	12
Winding cooling	Water

PULSE MAGNET DESIGN

As the kicker magnet is pulsed at a repetition rate of 50 Hz, to reduce the eddy current heating of the magnet yoke it was assembled of 0.35 mm- thick laminations of electrotechnical steel 3413 previously thermally treated and with insulating coating [1]. Figure 1 shows the general view of the magnet.

Figure 1: The kicker magnet at a test facility.

ISBN 978-3-95450-125-0

SYSTEM OF VACUUM MONITORING OF SYNCHROTRON RADIATION SOURCES OF NATIONAL RESEARCH CENTRE KURCHATOV INSTITUTE

N. I. Moseiko, V.N. Korchuganov, Yu.V. Krylov, L.A. Moseiko, D.G. Odintsov, B.I. Semenov, A.V. Shirokov, National Research Centre Kurchatov Institute, Moscow, Russia

Abstract

The modernization project of the vacuum system of the synchrotron radiation source at the National Research Centre Kurchatov Institute (NRC KI) has been designed and is being implemented; it includes a change in the system to high-voltage power sources for NMD and PVIG–0.25/630 pumps. The system is controlled via the CAN bus, and the vacuum is controlled by measuring pump currents in a range of 0.0001–10 mA. The system ensures a vacuum of 10–7 Pa. The status is mapped and the data collected into the archive are processed on the MS SQL Server platform. The efficiency and reliability of the vacuum system is increased by this work, making it possible to improve the main parameters of the SR source.

INTRODUCTION

The vacuum system of the SR source (synchrotron) should ensure a vacuum of 10–7 Pa. In this case, NMD-type magnetic-discharge diode pumps with a pump capacity of 0.16 m3/s and 0.4 m3/s are placed on the small ring of the synchrotron. PVIG 250/620-type vacuum-ion-getter stations with a pump capacity of 0.25m3/s/630 l/s are placed on the large ring of the synchrotron.

EQUIPMENT OF THE VACUUM SYSTEM

Works on replacing outdated DIV-6 vacuum power sources with a 5-kV output voltage, used for energizing PVIG 0.25/630 pumps (800 pieces) in the BS storage of the synchrotron, are completed. The DIV-6 sources were replaced by new VIP-27 high-voltage four-channel power sources with a 5-kV/7-kV supply voltage [3]. The use of VIP-27 sources allowed us to increase pump capacity by 30% and reduce the time it takes to bring the system (after opening the chamber) to the operating conditions of the synchrotron by 10 h.

The VIP-27 source is controlled by BUP-27 units, which also measure the output voltages (*U*P) and currents of sources (*I*P) of the pumps (which used to be measured by outdated IVA-16 units). The VIP-27 power source with the BUP-27 control unit are placed in a standard 3U Euromechanics crate (Fig. 1). For powering 80 vacuum pumps of the large ring of the SR source, twenty crates with VIP-27 power sources and BUP-27 units are used. The SQL-server of the vacuum system controls the power source of all the pumps via a common CAN bus. Data on the pump currents (*I*P) obtained by it are transmitted to the main server of the SR source.

VIP-27 High-Voltage Power Source

Let us present the main technical characteristics of the VIP-27 source (Fig. 1) designed at OOO KBST (Vyborg). The VIP-27 source ensures the following: an open-circuit voltage of 5.0 ± 0.1 kV and 7.0 ± 0.1 kV, an output voltage no smaller than 4 kV with a load current of 4 mA and a setup open-circuit voltage of 5 kV, an output voltage no smaller than 6 kV with a current load of 4 mA and a setup open-circuit voltage of 7 kV, a short-circuit current of 10 ± 1 mA, and a remote switch to the START mode from the STOP mode and the other way around.

Fig. 1. VIP-27 power source.

Physically, the VIP-27 source is fulfilled in a 19" Euromechanics standard basket with a 3U height (133 mm), 84TE width (426 mm), and 300-mm depth. The basket contains six 12TE modules of equal width (60 mm), namely, four high-voltage modules, one power-supply module, and one BUP-27 interface control/diagnostic module. The power system consumption is no higher than 150 W.

ISBN 978-3-95450-125-0

CYLINDRICAL PHASED DIPOLES ARRAY FOR HYPERTHERMIA OF DEEP-SITUATED TUMORS

S.M. Polozov, A.M. Fadeev, V.N. Belyaev, National Research Nuclear University MEPhI, Moscow, Russia
E.A. Perelstein, JINR, Dubna, Moscow Region, Russia

Abstract

The treatment of deep-situated malignant tumors is often a difficult problem in which the purpose is to reduce the size of completely remove a tumor by using one or more modalities. The traditional methods are: radiation therapy, chemotherapy and surgery. Hyperthermia is another method which is used alone or coupled with other methods of cancer treatment. Hyperthermia is a heating of the tumor that makes it more sensitive to chemotherapy or radiation therapy and leads to it thermal damage. Temperature range for hyperthermia treatment is from 42.5 °C to 45 °C. It is important to prevent heating of healthy tissues and to produce sufficient heating at the site of a deep-situated tumor. This kind of hyperthermia is called the local hyperthermia. The electromagnetic field in 100-200 MHz frequency range is optimal for heating of deep-situated tumors. The system for local hyperthermia of cancer was simulated. This system is based on cylindrical phased array consisting of multiple dipole antennas with operating frequency 150 MHz. The electric fields and specific absorption rate distributions are calculated in cut of tissue-equivalent phantom. Shown that electric field can be focused in desirable region by means of varying of amplitudes and phases of each dipole. The advantages of using combined therapy of common hyperthermia with chemotherapy or radiation therapy are discussed.

INTRODUCTION

Hyperthermia is a good adjuvant for the common modalities such as surgery, radiation and chemotherapy. It is proved that cancer cells are dying under the heating and the main goal is to deliver heat into source of disease without damaging of nearby healthy tissues [1-3]. Also suitability of using hyperthermia combined with radiation and chemotherapy is proved [4, 5]. Efficiency required that temperature within tumor remain above 43 °C for 30 to 60 minutes, while limit temperatures in normal tissues has to be lower than 43 °C. Noninvasive heating of deep-situated malignancy is a difficult technical challenge. Electromagnetic field is more prior for creating higher level temperature in desirable volume than other methods of physical effect. High penetration ability of radiofrequency EM field into human body in comparison with other frequencies ranges makes using of radiofrequency promising for distance hyperthermia. As temperature increase occurs not at the expense of heat transfer from surface to inwards, but because of electromagnetic field absorption, danger of skin burns is decreasing. This fact makes fields in 100-200 MHz frequency range is optimal because wave length in human body is proportional with body's sizes. The thermal effect lead to lysosome activation, tissue breathing and protein synthesis inhibition, tissues pH decreasing, kariokynetic cycle modification, trans membrane transfer improvement, sensitization tumor cells to chemotherapy and growing up immunity. Moreover basic advantages of electromagnetic hyperthermia occurs on radio resistance tumors, in other words on cells with high reparation effect from radiation. First of all hyperthermia decelerates cell's reparation and secondly induces strong heat damage of zone with bad thermal sink, hypoxia zone.

PHASED DIPOLE ARRAY

Cylindrical phased dipole array is proposed for creating high level temperature inside patient body. In this paper we assume that phased array consists of eight dipole antennas arranged on an inner side of a cylindrical plastic shell. Dipoles are surrounding the patient body and the amplitude and phase of each antenna is under control of the operator as shown in Figure 1. The space between patient's body and dipoles is filled with deionized water (conductivity σ≈0). Hereby dipole antennas are squeezed between the high-permittivity medium inside the tank (ε≈80 for water) and the low-permittivity medium outside the tank. We assume to use flowing deionized water not for cooling only. Due to the electric field energy density ($1/2 \cdot ED$) inside the tank is higher by a factor ε (the relative dielectric constant of the medium) the E-field energy is extremely concentrated in the inner side of a tank. The frequency of operation is chosen to be 150 MHz.

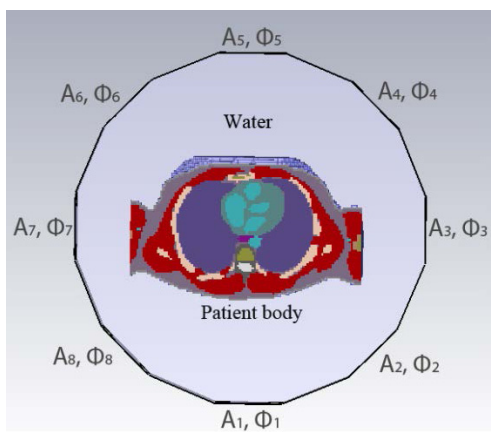

Figure 1: Patient body surrounded by phased dipoles array. Dipole antennas have amplitudes $A_1 \ldots A_8$ and phases $\Phi_1 \ldots \Phi_8$ respectively.

ISBN 978-3-95450-125-0

RF POWER AND CONTROL SYSTEMS FOR PHASED DIPOLES ARRAY SYSTEM FOR HYPERTHERMIA

S.M. Polozov, A.M. Fadeev, V.N. Belyaev, A. Blinnikov, National Research Nuclear University MEPhI, Moscow, Russia
E.A. Perelstein, JINR, Dubna, Moscow Region, Russia

Abstract

Cylindrical array of independently phased dipoles is suggested for hyperthermia of deep-situated tumors as a kind of treatment of cancer coupled with other methods such as radiation therapy and chemotherapy. It was proposed to focus the maximum of electromagnetic field at the site of tumor to produce high efficiency heating of tumor and to prevent overheating of surrounding healthy tissues. That's why we use system of independently fed dipole antennas. The operating frequency is 150 MHz. The independent feeding permits us to focus electromagnetic field producing by phased array in desirable area by means of changing of amplitudes and phases of each dipole. The RF power system schematic layout for 8 independently phased dipole antennas is presented. The control system of RF power system elements is considered. The software developing to provide the choosing of amplitude's and phase's values of dipoles are discussed.

INTRODUCTION

Many clinical and experimental studies have shown promising results in using of hyperthermia coupled with radiotherapy or chemotherapy for treatment of malignancies [1-3]. Treatment requires that temperatures within tumor remain above 43 °C during 30-60 min, while maximum temperature in normal tissues have to be lower than 42°C. Cylindrical phased dipole array is proposed to produce difference between temperature in healthy tissues and tumor. Range in 100-200 MHz of electromagnetic wave produced by dipoles is prior because wave length in human body is proportional with body's sizes. Phased array consists of eight dipoles arranged on inner side of plastic shell and surrounds patient body like it shown on Figure 1. Deionized water filling space between patient and array is for cooling outer side of body and for better matching. The E-field energy is extremely concentrated in the inner side of a shell due to the electric field energy density inside the shell is higher by a factor ε (the relative dielectric constant of the medium) than outside the shell.

Phased array provides desirable distribution of electromagnetic field inside of the patient body. The specific absorption rate (SAR) or absorbed power per unit mass (W/kg) is given by:

$$SAR(x,y) = \frac{\sigma E E^*}{2\rho}, \qquad (1)$$

where E is the total electric field at the point (x,y), E^* is the complex conjugate of E, σ and ρ are the electrical conductivity and the density of tissue respectively.

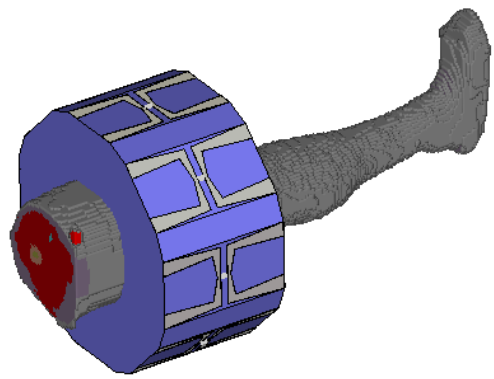

Fig. 1: Voxel model of leg inside phase array.

E_j is the E-field for antenna j scaled by the amplitude and phase take into account:

$$E_j = A_j E_{j0}(x,y) e^{i\Phi_j}, \qquad (2)$$

where E_{j0} is the complex field for $A_j = 1, \Phi_j = 0$, and $A_k = 0$ for $j \neq k$. A time variation of the form $\exp(-i\omega t)$ is dissembled.

Necessary distribution of E-field can be reached by means of independent feeding of each dipole that permits us to vary amplitudes and phases of electromagnetic field. In other words we can concentrate absorption energy of E-field and deliver therapeutic heat in tumor and at the same time prevent extra heating of normal tissues.

RF POWER SCHEME

As it was noted above, the RF power supply have to be independent for each dipole. The RF power system schematic layout is shown in Figure 2: 1 – driving generator with input signal's frequency range 100 – 300 MHz and input impedance 50 Ohm; 2 – 8-out power splitter (for example Mini-circuits ZBSC-8-82+); 3 – voltage-controlled phase shifter (Mini-circuits JSPHS-150) with frequency range 100 – 150 MHz, phase range 180°, control voltage 0 – 12 V; 4 - solid state amplifier (Mitsubishi RA60H1317M1A-101) with frequency range 135-175 MHz, output power – 60 W, supply voltage – 12.5 V, control gate voltage 12.5 V; 5 – 10 dB uni-directional coupler (Werlatone Model c7929, 100-

ISBN 978-3-95450-125-0

DATA PROCESSING AND QUANTITATION IN NUCLEAR MEDICINE*

E.D. Kotina, V.A. Ploskikh, St. Petersburg State University, St. Petersburg, Russia

Abstract

Accelerators of charged particles, radiation detectors are widely used in nuclear therapy and nuclear diagnostics. So there is necessity for diagnostic processing of data obtained using these devices. Nuclear diagnostics is based on analysis of radiation passing through the study object emitted from radiopharmaceuticals within the object or from external radiation source. First stage of data processing is presentation of detector signals in 2D or 3D image form. Further processing is based on mathematical modeling of processes within the investigated object. Mathematical modeling of static, dynamic and periodic processes is considered for quantitative analysis of studies in nephrology, osteology, endocrinology and cardiology. The data processing and quantitation software suite is presented. Clinical applications of the developed suite are discussed. Possibilities of software deployment in clinical centers are considered.

DATA ACQUISITION

The NM diagnostic methods study the activity distribution of object.

Nuclear imaging system consists of n_d logical detector units. Detector units need not correspond to physical detectors. Examples of detector unit are Anger camera projection bin at a particular projection angle ($n_d=n_x n_y n_\Theta$), a line of response in PET ($n_d=(n-1)n/2$, where n is a number of detector crystals). Radiation detection hardware registers emission radiation of radiopharmaceutical and forms the flow of registration events. The event carries information about detector unit and time of registration. Registration software during the time of acquisition accumulates events in a projection data array. Exact structure of the array depends on the hardware type and operating mode.

Discrete formulation of the projection problem reads:

$$p=Hx,$$

where x is a column vector of $n_x n_y n_z$ elements corresponding to activity distribution, p is projection data array and H is the system matrix. Each element H_{ij} of H is defined as the probability that emission event occurred in voxel j is detected by i-th logical detector unit.

Depending on studied process temporal nature three basic hardware operating modes can be distinguished [1, 2]:

Static. During the static acquisition it is assumed that the activity distribution function does not vary in time. The goal of static studies is to analyze spatial distribution of radiopharmaceutical.

Dynamics. During the dynamic scan several projection data arrays are formed in sequence. Dynamic studies used to analyze processes of radiopharmaceutical redistribution.

Gated acquisition. Gated acquisition is used in cardiac cycle analysis. The acquisition computer defines the number of time slots to divide the R to R interval of the patient's electrocardiogram. Electrocardiogram guides the acquisition so a projection data array is formed for each time slot.

After acquisition projection data should be corrected for various physical effects: attenuation, Compton scattering, Poisson noise, false coincidences et al.

Planar SPECT projection data is presented as sequence of 2D images. Projection data arrays of tomographic studies are subjected to reconstruction methods and presented as series of 3D data volumes.

For mathematical modeling purposes we consider these series of images as discrete representation of continuous radiopharmaceutical density distribution function $\rho(t, x)$. In 3D case the density distribution function coincides with the source activity distribution function. In 2D case the density distribution function is a projection of the source activity distribution to the detector plane.

DATA PROCESSING

Quantitative analysis is based on computation of various parameters for regions of interest (ROIs). The first step is to extract these ROIs from raw projection data.

Segmentation

In SPECT data processing various region extraction techniques are used. In most cases of static planar processing human-drawing ROI tools is the most simple and flexible method. This method also used in planar dynamic studies in conjunction with patient motion correction methods.

Specialized applications may use organ specific detection methods (fig. 1)

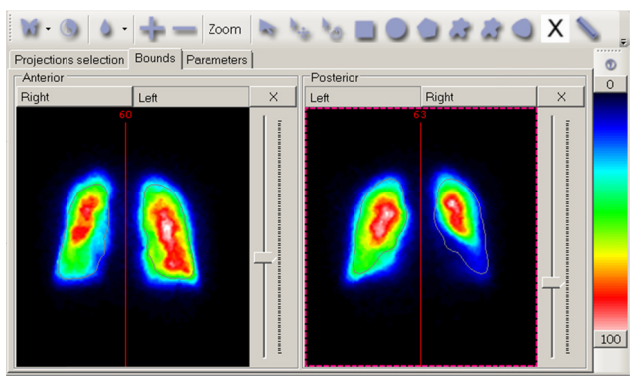

Figure 1: Automatic segmentation in lung perfusion.

*Work supported by SPbGU, grant 9.39.1065.2012

ISBN 978-3-95450-125-0

DESIGN PARAMETERS OF BIPERIODIC ACCELERATING STRUCTURE FOR MEDICAL LINAC WITH WIDELY VARIABLE ENERGY

Yu.V. Zuev#, M.A. Kalinichenko, V.V. Terentiev
D.V. Efremov Scientific Research Institute of Electrophysical Apparatus, Saint Petersburg, Russia

Abstract

Results on the simulation of the beam dynamics in an accelerating structure with the particle energy varied from 6 to 21 MeV are presented. The structure operating in the standing wave mode consists of two weakly-coupled substructures and resonates at closed frequencies f_1 and f_2. In-phased electromagnetic field oscillations take place in the substructures at the frequency f_1, whereas anti-phased oscillations occur at the frequency f_2. Main features of the accelerating structure are electronic control of the beam energy and possibility to form narrow energy spectrum at both frequencies.

OPERATION PRINCIPLE OF THE STRUCTURE

Different methods are used to vary the energy of electrons in standing wave accelerators [1]-[3]. In the paper, we consider a biperiodic accelerating structure with inner (axial) coupling cells to be used in a medical accelerator. The method of energy variation was suggested in [4]. The accelerating structure consists of two substructures A and B with an odd (N_A and N_B) number of resonator cells tuned to the same frequency f_0. In each separate substructure, π/2-oscillations are excited at the frequency f_0. By joining substructures A and B through a small hole in a diaphragm, a structure, consisting of an even ($N_A + N_B$) number of cells, is formed to resonate at frequencies close to f_0:

$$f_1 = f_0(1 - k_{AB}/(N_A + N_B)),$$
$$f_2 = f_0(1 + k_{AB}/(N_A + N_B)) \quad (1)$$

where k_{AB} is the coupling coefficient of substructures. At the frequency f_1, in-phased π/2- oscillations occur in substructures A and B, and these oscillations are anti-phased at the frequency f_2. As a consequence, either acceleration of electrons in the substructure A and deceleration in the substructure B or acceleration in both of these substructures is possible. Switching from one mode to another is realized by change in frequency f_G of the generator, which drives the structure; this produces maximal variation of the beam energy. For “fine tuning" of the beam energy, the power of the RF generator is additionally varied.

FEATURES OF THE STRUCTURE DESIGN AND OPERATING MODE

Similar to the prototype [4], the considered structure consists of sixty six cells, N_A=39 and N_B=27. First ten (cylindrical) cells form a cascade buncher. The remaining elements are standard Ω-shaped accelerating and cylindrical coupling cells, which are uniform in size with exception for two (or four) cells located at the joint of substructures [5]. The axial length of these cells has strong influence on the beam dynamics, therefore their dimensions like the buncher cell dimensions are specially designed. The RF power is supplied to the substructure A through the wave converter cell.

In contrast to the prototype-structure [4], the resonance frequency of separate cells, f_0, has been changed from 2856 to 2998 MHz. The dependence of the input VSWR of the structure with the beam off on the generator frequency is shown in Fig. 1. Frequencies f_1 = 2997.693 MHz and f_2 = 2998.307 MHz correspond to operating modes of the structure. Fig. 2 shows an axial distribution of the amplitude of the electric field excited at the frequency f_1 in the cold structure. Practically the same field distribution was obtained in computations performed at the frequency f_2.

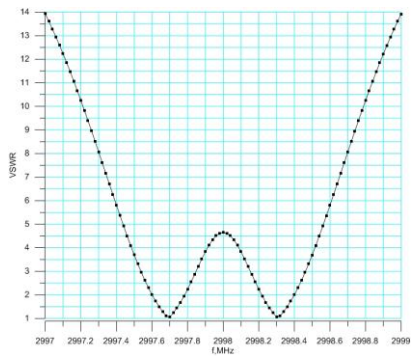

Figure 1: The dependence of the input VSWR of the structure with the beam off on the generator frequency.

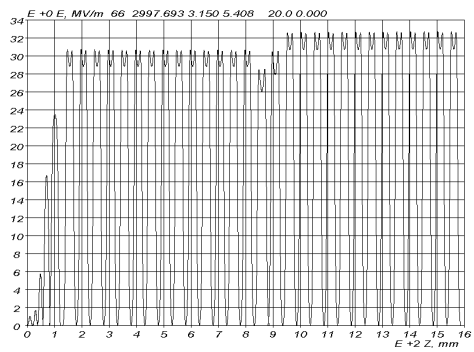

Figure 2: An axial distribution of the amplitude of the electric field excited at the frequency f_1 in the cold structure

#yuri_zuev@mail.ru

ISBN 978-3-95450-125-0

POSITRON ANNIHILATION SPECTROSCOPY AT LEPTA FACILITY

P. Horodek, A. Kobets, I. Meshkov, V. Pavlov, A. Rudakov, A. Sidorin, S. Yakovenko,
JINR, Dubna, Russia

Abstract

At the moment Positron Annihilation Spectroscopy (PAS) unit is being created as a part of LEPTA project at JINR in Dubna. A slow positron beam, dedicated to creating a positronium atom in flight, will also be used for material research related to detection of point defects under the surface. For this purpose Doppler broadening of annihilation line spectrometer is being made. Basis of the method, operational principle, plans and current state of works, are all presented in this article.

INTRODUCTION

Positron Annihilation Spectroscopy method is sensitive to presence of defects in materials. Its currently highly developed measurement techniques enable detection of imperfection of crystal lattice the size of a lattice constant. Vacancies, concentrations of vacancies, pores and dislocations can be spotted in this way. Since late 1960s, when it was discovered that a positron interacts with defects, PAS method has been developing. At the moment it has got solid theoretical basis. A growing interest in this method in condensed matter research and materials engineering in recent years resulted not only in new results but also in a search for increasingly sophisticated measuring techniques. Research on monoenergetic positron beams and positron microscopy are the current trends in this department.

POSITRONS IN THE MATTER

Positron, antiparticle of an electron, coming from β^+ decay in PAS experiments is implanted into the tested sample directly after emission from isotope or into a specially formed beam.

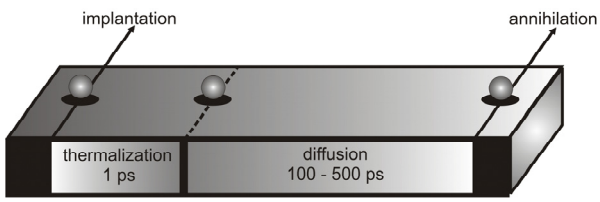

Figure 1: Stages of positron implantation into the matter.

As it possesses both energy and charge, it reacts elastically and non-elastically with ions and electrons, and to a lesser degree with phonons and impurities. Thus, after circa 1 ps it reduces its energy to thermal oscillation energy i.e. about 25 meV [1]. This stage is called thermalization. Next, anti-electron, which at this stage is in a state of thermodynamical balance with its environment starts free diffusion, which is a random walk over the area occupied by 10^7 atoms. Such state lasts from 100 to 500 ps and it ends with an encounter with an electron. The process of annihilation into two gamma quanta of energies that equal about 511 keV occurs in over 99% cases [2].

Therefore, the process of positron-electron annihilation does not occur immediately after positron appears in the matter. The fact that in different stages (schematically marked in Fig.1) it spends a certain time in the material, is significant from PAS point of view.

In the central mass system annihilation quanta are emitted in the exactly opposite direction (see Fig. 2). In a laboratory system a certain deviation from this collinearity will be observed, expressed by

$$\Delta\theta = \frac{p_\perp}{mc} \qquad (1),$$

where m is electron's mass, c is speed of light in a vacuum and $p_\perp$ is a perpendicular component of the momentum of the annihilating pair. A deviation from 180° will be bigger, the bigger momentums of a positron and an electron. The momentum additionally manifests itself in gamma quanta energies, which are changed as a result of Doppler effect

$$E_\gamma \cong mc^2 + E_B \pm \frac{p_\parallel c}{2} \qquad (2)$$

where E_b is the energy of positron-electron pair coupling and $p_{||}$ is a perpendicular component of the pair's momentum. It is worth emphasising that positron's momentum is negligibly small in relation to electron's momentum, therefore it usually omitted in deliberations.

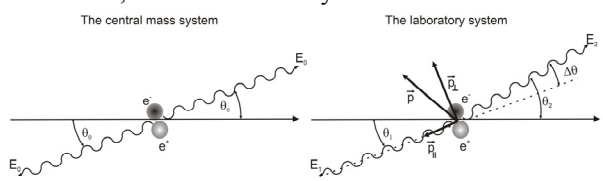

Figure 2: The annihilation processes in the two systems.

During its random walk a positron may encounter places which have a modified electron density. Those place are structural defects such as vacancies, inside of which a positron may be located. Electron density in such traps is smaller in comparison with the defect's environment. This inevitably is reflected in deviation from collinearity of annihilation quanta and in their energies, which are then respectively smaller, as well as in an average life time of a positron in a defect, which is longer than outside of it.

Observations of angular correlations of annihilation quanta, changes of energies or life times are operational basis of the three basic measuring PAS techniques. The technique of observation of Doppler broadening of annihilation gamma line is going to be more widely discussed further in the article.

ISBN 978-3-95450-125-0

RF PHOTOINJECTOR PARAMETERS OPTIMIZATION

T.V. Bondarenko, S.M. Polozov,
National Research Nuclear University (MEPhI), Moscow, Russia

Abstract

Sources of high-power electromagnetic radiation in THz band are becoming promising as a new method of a low activation introscopy. Research and development of accelerating RF photoinjector for THz source are reported. The photoinjector is based on disk loaded waveguide (DLW). Photoinjector consists of two accelerating structures: widespread 1.6 cell DLW structure and travelling wave resonator structure based on 9 cells traveling wave accelerating structure. The resonant models of these structures and the structures with power ports were designed. Electrodynamics characteristics and electric field distribution for all models were acquired. Electrodynamics models were tuned to the resonant frequency of 3000 MHz. Magnetic field coupling between cells of accelerating structure and optimization of the diaphragms sizes were analyzed to enlarge the structures efficiency. Diaphragms windows profiles were optimized to decrease the overvoltage on the windows edges and to eliminate the breakdown possibility.

INTRODUCTION

RF photoinjectors are accelerating structures and electron guns at the same time. The main work principle of photoinjector is based on photoemission electron generation type. Photoinjectors are used is applications that requires femto-picosecond time resolution beam such as free electron lasers that demand short bunches for generation of monochromatic radiation.

One of interesting applied usage of photoinjectors is a source of high intensity THz radiation based on Cherenkov irradiating capillary channel that can be used in the field of cargo introscopy [1]. This source implies travelling of about 5 MeV beam in the capillary with sub-mm transverse sizes.

Such facilities can be used not only in introscopy system as well as in biology, medicine, chemistry, solid state physics, radio astronomy, homeland security, environment monitoring, spintronics, advanced spectroscopy, and plasma diagnostics.

ACCELERATING STRUCTURES

The photoinjector must be formed of accelerating structure with one or two sections for achieving of the demanded beam energy, laser system for beam generation from the photocathode and focusing system for beam shape preserving.

RF power source feeding the photoinjector is based on 2.5 MW pulse power magnetron with 2.995-3.005 GHz working frequency. Hence the accelerating system must be formed of two accelerating structures – standing wave structure emitting and preliminary accelerating the electron beam and travelling wave structure proceeding acceleration to the final energy.

Accelerating structures geometry was tuned to provide advanced operating mode of the structures and from here to reach the maximum possible efficiency of the structures.

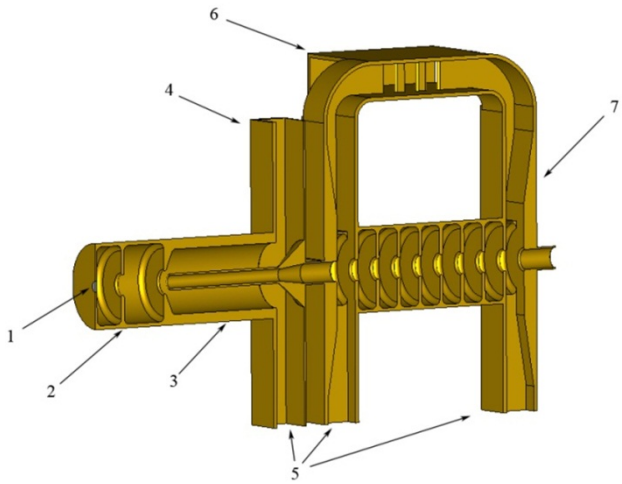

Fig. 1. General layout of accelerating system: 1 – photocathode, 2 – 1.6 cell DLW structure, 3 – coaxial wavetype transformer, 4 – RF power input, 5 – vacuum ports, 6 – directional coupler, 7 – travelling wave resonator structure.

Standing Wave Structure

1.6 cells accelerating structure was computed for 3000 MHz operational frequency. The general view of the accelerating system with MW power port is represented in Figure 2. The photocathode will be arranged in 0.6 cell's sidewall, therefore accelerating field on the sidewall's surface must be as high as possible. That is the reason of making half-cells length equal to 0.6 of full sized cell. Zero and π modes are excited in this structure, mode with $\mu = \pi$ phase shift per cell is the operating mode. The structure is characterized by the positive normal dispersion.

Iris profile was made rounded to eliminate the possibility of breakdown. This was done to reduce the electric field in the window's aperture because of high-rate accelerating fields in 1.6 cells accelerating structure that can lead to electrical breakdown. The ratio of iris window to the wavelength was set to 0.1. This value is a trade-off between the wish to get maximum amplitude of accelerating field and except probable beam loses on the iris. The structure performance was also increased by rounding of shells edges. The rounding radius value was chosen to provide the highest possible shunt impedance.

ISBN 978-3-95450-125-0

OPERATIONAL EXPERIENCE WITH 55 MEV PULSED RTM

A.N.Ermakov, V.V.Khankin, N.I.Pakhomov, V.I.Shvedunov, SINP MSU, 119992 Moscow, Russia
A.I.Karev, V.G.Raevsky, P.N.Lebedev Physical Institute, RAS, 119991 Moscow, Russia

Abstract

Operational experience with 55 MeV pulsed race-track microtron (RTM) is reported. The upgrade of the accelerator after the commissioning and some results of the physical experiments with a beam of the RTM are presented.

INTRODUCTION

The 55 MeV RTM [1] was designed and manufactured in framework of the contract between Lebedev Phisical Institute (Russia) and Lawrence Livermore National Laboratory (USA). The purpose of the work consists in development of an effective photonuclear detector of hidden explosives [2].

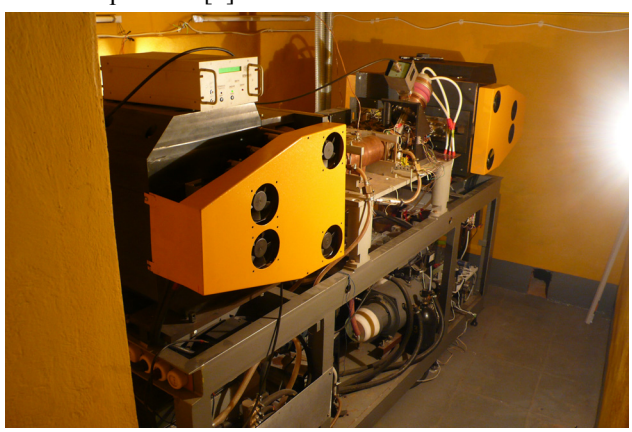

Figure 1: RTM photo.

Table 1: RTM parameters

Output energy	55 MeV
Output pulse current	Up to 10 mA
Repetition rate	6.25 – 50 Hz
Number of linac passages	11
Energy gain / turn	5 MeV
Current pulse length	6 μs
Operating frequency	2856 MHz
End magnet field	1.0 T
Maximum RF power	6 MW
Orbit circumference increase / turn	1 λ

RTM has been built following a classical scheme with two 1 T end magnets and a standing wave linac between them providing 5 MeV energy gain per pass. A 50 keV beam from an electron gun is injected into linac through a 45^0 magnet and a solenoidal lens. The 5 MeV electron beam after the first acceleration is reflected by the end magnet field back to the linac axis and is accelerated up to 10 MeV - the energy sufficient to bypass the linac at the next turn. The beam is extracted from the last orbit with a dipole of 17.5^0 deflecting angle. The RF system is based on a 6 MW multibeam klystron KIU-168 [3]. A pumping port, a vacuum window, and a circulator are installed between the linac and the klystron. Parameters of the vacuum window and the circulator during commissioning restricted the maximum RF power transported to the linac by 2.5 MW and thus restricted a maximum exit pulsed beam current. To simplify the RF system we use a auto-oscillation mode of klystron operation with accelerating structure in a feed-back loop [4]. More details about the RTM systems can be found in [1].

RTM commissioning had been conducted at temporary place at SINP MSU accelerator hall and temporary solutions had been used for some RTM systems. During commissioning the first physical experiment also had been conducted with RTM beam after which the work to install RTM at designated area with final solutions for its systems has been done. The main RTM parameters are listed in Table 1.

UPGRADE OF THE RTM SYSTEMS

Since the last report [1] part of the RTM systems have been upgraded, specifically: RF system, gas system, system of high voltage power supply, control system and beam diagnostics. The accelerator has been moved to specially built bunker in order to reduce background radiation in experimental hall. Photo of RTM in bunker is shown at Fig. 1.

RF System

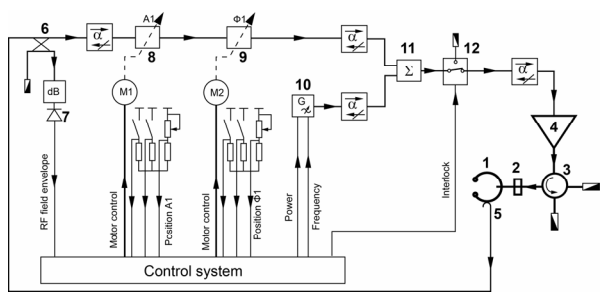

Figure 2: RTM RF system. 1 - accelerating structure, 2 - vacuum window, 3 - circulator, 4 - klystron, 5 - RF antenna, 6 - directional coupler, 7 - RF diode, 8 - attenuator, 9 – phase shifter, 10 - RF generator, 11 - RF power combiner, 12 - RF switch.

Upgraded RTM RF system is shown in Fig. 2. Klystron operation in auto-oscillation mode has several advantages as compared with traditional scheme with excitation from external generator, the most important is automatic following of the oscillations frequency to frequency of accelerating structure. However in pulsed mode the RF

ISBN 978-3-95450-125-0

STATUS OF 1 MEV 25 KW CW ELECTRON ACCELERATOR

D.S. Yurov, A.S. Alimov, B.S. Ishkanov, N.I. Pakhomov, V.P. Sakharov, V.I. Shvedunov, Skobeltsyn Institute of Nuclear Physics, Lomonosov Moscow State University, 119992 Moscow, Russia

Abstract

Status of 1 MeV 25 kW continuous wave (CW) linear electron accelerator for radiation technologies which is under construction at SINP MSU is described. Driven by 50 kW CW klystron on-axis coupled standing wave accelerating structure was optimized, manufactured and tuned. The results of accelerating structure measurements and tuning are presented. RF system, high voltage, vacuum and control systems of the accelerator are described.

INTRODUCTION

Industrial CW linear electron accelerator with beam energy 1.0 MeV and maximum beam power 25 kW is under construction at SINP MSU using as a prototype the two-section accelerator with 1.2 MeV energy and 50 kW maximum beam power [1]. Accelerator general view is shown in Fig. 1, main parameters are listed in Table 1.

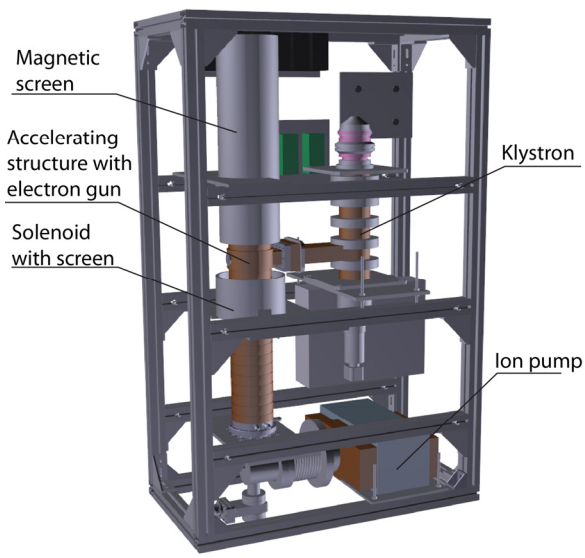

Figure 1: Accelerator general view.

Advantages of the proposed accelerator are its compactness and low weight which allows to use local radiation shielding and to incorporate the accelerator into operating material production lines which need radiation processing. The accelerator power supply system has no voltages exceeding 15 kV therefore operates without high voltage discharges.

The accelerator will be used at SINP MSU for the following purposes [2]:

- Electronics radiation stability testing.
- Solar batteries radiation degradation testing.
- Obtaining new data on variations of mechanical properties, surface structure, phase composition and microstructure of model and construction materials for nuclear reactors and nanostructure objects.
- Investigations of radiation resistance of optical materials with bremsstrahlung beam.
- Investigations of radiochemical processes.

Table 1: Project parameters of the accelerator

Beam energy	1,0 MeV
Beam current	0 - 25 mA
Maximum beam power	25 kW
Gun /Klystron high voltage	15 kV
Operating frequency	2450 MHz
Klystron power	50 kW
Electric power consumption	~75 kW
Efficiency	~33%
Dimensions	500x900x1400 mm3

ELECTRON GUN

15-keV electron gun with two intermediate anodes providing current regulation from 0 to 250 mA has been designed and manufactured (Fig. 2). The electron gun is joined directly to the input accelerating section flange without any drift space, standing alone pre-bunching cavity, and focusing elements between the gun and the accelerating section.

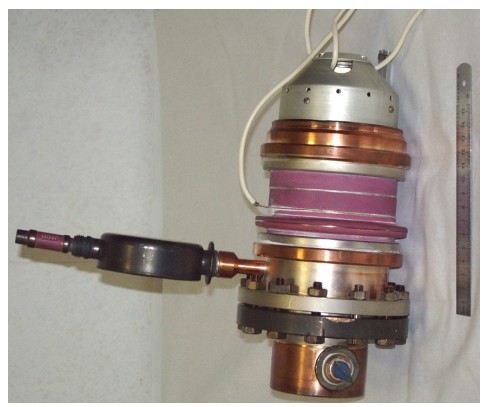

Figure 2: Electron gun after manufacturing.

ACCELERATING STRUCTURE

The accelerating structure is a standing wave bi-periodic on-axis coupled structure. As it is described in [3,4] the first accelerating cell acts as a buncher cavity while the second cell increases the beam energy to level sufficient for further acceleration in low strength field inherent to CW operation. This approach permits to get

ISBN 978-3-95450-125-0

PROTON CHANNEL THAT PROVIDES SIMULTANEOUS INDEPENDENT OPERATION OF A TREATMENT ROOM OF PROTON THERAPY AND NEUTRON SOURCES OF THE EXPERIMENTAL COMPLEX INR RAS

M.I. Grachev, E.V. Ponomareva, S.V. Akulinichev, L.V. Kravchuk, INR RAS, Moscow, Russia
V.N. Zapolsky, IHEP, Protvino, Russia

Abstract

During 2012 we have developed the system for beams separation, based on the splitter magnet, for simultaneous work of neutron source RADEX and a treatment room of the complex of proton therapy (CPT).

This set up also allows for an independent change of protons energy in the channel of proton therapy in a wide range from 209 MeV to 70 MeV.

The system is an extension of the main channel of the proton and H^- beams, previously described in [1]. Main channel carries out the simultaneous transportation and elevation of the beams H^- and protons in the experimental hall of INR RAS.

BEAMS SEPARATION AND UPGRADE OF THE CHANNEL TO RADEX

Figure 1 depicts the layout of the beams separation the beams line. After magnet 4MC the main beams line (protons and H^-) from Linac distributes to three beam lines as shown in Fig.1. Magnet 2MC2 [1] has been replaced by a pair of magnets 4MC and 4M.

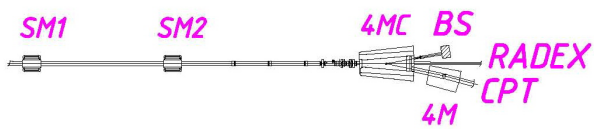

Figure 1: Layout of the beams separation: SM1, SM2 – steering magnets, 4MC – Lambertson magnet, 4M – bending magnet, BS – beam stopper, RADEX – neutron source, CPT – complex proton therapy.

A pair of magnets of this scheme provides a correction in the position of the deflected beam at its axial passage through the hole without the field of magnet 4MC.

The poles of magnet 4MC were developed by NIIEFA as part of the design Lambertson Septum Magnet for the proton storage ring. Coil of the magnet 4MC have been manufactured from the radiation-resistant water-cooled cable of PYROTENAX type.

The block of water-cooled poles is placed in the thin walled vacuum stainless steel chamber. There are the apertures in the upper and lower poles.

Wall thickness between the aperture and the gap is about 1 mm. Fig.2 and Fig.3 represent the photos of magnet 4MC (downstream and upstream respectively).

Detailed description of this magnet will be presented in the next paper.

Figure 2: 4MC magnet assembly view downstream.

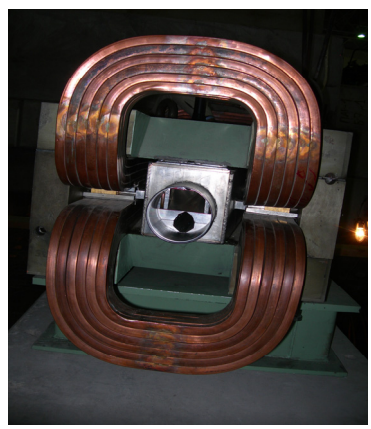

Figure 3: 4MC magnet assembly view looking upstream.

Wall thickness between the hole and the pole is about 1 mm. Detailed description of the magnet will be presented in the next paper.

In front of the magnet 4MC a thin foil is installed, with aperture of different diameters, to control the intensity of the beam H^-. The thickness of the foil is sufficient for a recharge H^- in protons. Protons from distribution tails are deflected after recharging in the BS - beam stopper.

Due to the fringe fields, especially at the exit of the magnet, the direct beam experiences a deflection on some mrad. The set of doublet lenses L31-L32 is installed in order to fix the position of the beam on the target of the neutron source RADEX. These lenses focus the centre of magnet 4MC on the target centre (Fig.4).

ISBN 978-3-95450-125-0

BEAM SCANNING SYSTEM OF LINEAR ACCELERATOR FOR RADIATION PROCESSING

M.I.Demsky, V.V.Krotov, D.E.Trifonov, CORAD Ltd., Saint-Petersburg, Russia

INTRODUCTION

Company CORAD Ltd. has elaborated the beam scanning system for irradiation of opposite sides of the boxes during one pass. This system will be useful for irradiation of products which are difficult to rotate on 180 degrees mechanically and as alternative instead of a mechanical rotation system.

SYSTEM DESCRIPTION

Beam scanning system is shown at Fig.1 has two windows for the irradiation of products from two opposite sides.

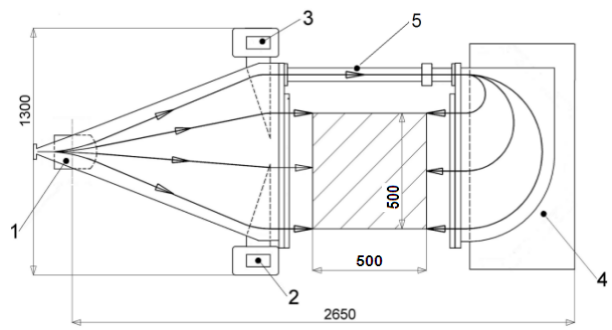

Fig.1. Beam scanning system scheme.

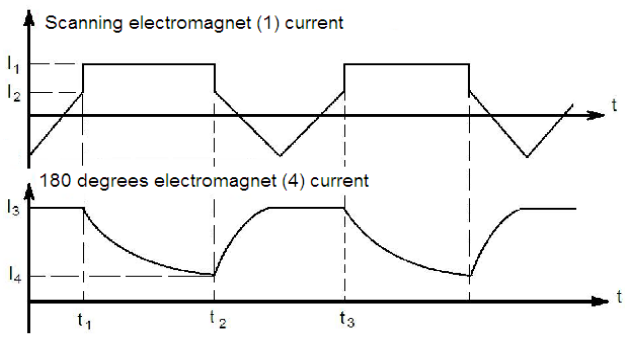

Fig.2. Electromagnets currents.

This device consists of two vacuum chambers, connected by electron beam channel (5), which is placed sideways from an irradiated product. Electron beam is scanning in vertical strip of 500 mm length by means of the scanning electromagnet (1) with the saw-tooth shape of a current in a winding as shown at Fig.2 in the time period t_2- t_3. The beam moves from the top to bottom and back along the first extraction window, and afterwards jumps up to input of bending electromagnet (3) and transits in the second 180 degrees electromagnet (4) through the electron beam channel, due to the abrupt change of a current in a scanning electromagnet (1) to the given constant value I_1. The beam moves from the top to the bottom along the second extraction window due to the changing current in the electromagnet (4) from value I_3 up to value I_4 and the product is irradiating from the opposite side. The field in a scanning electromagnet (1) jumps sharply to the value corresponding to the top position on the first window I_2 and process is repeating again. Electromagnets (2) and (3) allow improving parallelism of the beam, which comes out of the first extraction window. The computer control system produces the required hyperbolic shape of current in the time period t_1- t_2 and quite linear saw-tooth shape of current in time period t_2- t_3 in order to achieve the necessary homogeneity of dose along both scanning windows.

EXPERIMENTAL RESULTS

This system has been tested on the linear electron accelerator UELR-10-15S2 with the electron energy of 10 MeV and up to 15 kW of the beam power. This accelerator was made on the base of standing-wave accelerating structure made by NIIEFA (St.Petersburg, Russia) with use of the klystron TH2173F made by Thales Electron Devices S. A. (France). The photo of this system is shown at Fig.3.

Fig.3. Beam scanning system photo.

ISBN 978-3-95450-125-0

THE IDK-6/9MEV LINEAR ELECTRON ACCELERATOR AND ITS APPLICATION IN THE CUSTOMS INSPECTION SYSTEM

V.P. Malyshev#, A.V. Sidorov, P.O. Klinovskiy, K.V. Kotenko, B.O Bolshakov., V.S. Smekalkin, D.V. Efremov Scientific Research Institute of Electrophysical Apparatus, Saint Petersburg, Russia.

Abstract

A linear electron accelerator IDK-6/9MeV has been designed for operation as a source of ionizing radiation in a customs inspection system intended for inspection of large-scale cargos. The main operating mode of the accelerator is the X-ray mode with an energy of 6 MeV, which ensures the penetrability more than 300 mm (for steel). The operating mode of the accelerator can be quickly changed for 9 MeV, which allows the objects under study to be discriminated based on the organics/non-organics criterion using the "two energies" method.

A triode electron source with cathode and grid modulators is applied in the accelerator. A system of collimators located at the output of the accelerating device serves to form a fan-shaped X-ray beam in the vertical plane with an opening angle of 46^0 directed towards the detector line. The accelerator is equipped with a computerized system of protective interlocks and control, which makes possible its operation both in the setting mode and as a component of the whole customs inspection system.

IDK-6/9MEV LINEAR ELECTRON ACCELERATOR

Up-to-date equipment for inspection of the cargos transported abroad are nowadays a mandatory requirement to ensure a high throughput, efficiency and quality of inspection at customs checkpoints. Customs inspection of large-scale containers and trucks is the most complicated procedure as it involves labor and time – consuming handling operations. Design features of vehicles can also be used to hide smuggled goods. An X-ray customs – inspection system allows an image necessary for the identification of a large-scale container or vehicle to be obtained within several minutes. In the case of any suspicious goods observed on the obtained image or non-compliance of the actual cargo with that described in the cargo customs declaration, a manual inspection can be assigned.

The linear electron accelerator IDK-6/9MeV has been designed as a source of ionizing radiation to be used in a customs inspection system intended for inspection of large-scale cargos and vehicles (Fig. 1).

Figure 1: The IDK-6/9ÌeV accelerator in a customs inspection system.

#npkluts@niiefa.spb.su

ISBN 978-3-95450-125-0

UPDATING OF THE "ELECTRON-3M2" ACCELERATOR IN THE LINE FOR RADIATION CURING OF POLYMER COATINGS

V.P. Ovchinnikov#, I.V. Druzgalckiy, V.P. Maznev, M.P. Svinin,
D.V. Efremov Scientific Research Institute of Electrophysical Apparatus, Saint Petersburg, Russia
O.V. Borisov, V.V. Koltsov, A.I. Seleznev,
JSC "Admiralty Shipyards", Saint Petersburg, Russia

Abstract

More than thirty years ago the «Electron-3M» accelerator was delivered to FSUE "Admiralty Shipyards" to be operated in the line for radiation curing of polymer coatings. In 2008-2009, works on updating the machine were performed to increase its reliability and make much easier its maintenance in the process of operation. After obtaining nominal parameters on the updated accelerator «Electron-3M2», the intensity of bremsstrahlung on the surface of the accelerator shielding was measured; the obtained data confirmed its compliance with corresponding normative documents. Measurements of parameters of the accelerator electron radiation field have demonstrated that the uniformity coefficient of the beam current linear density is 5%, and the symmetry coefficient amounts to 1%. The beam current and accelerating voltage instability during one hour of operation does not exceed 1%. After the updating, the lifetime of the accelerator will be not less than 10 years.

High voltage «Electron-3» accelerators and their modifications manufactured in NIIEFA in 1975-1985 [1, 2, 3] have been widely used in various research and industrial radiation-processing facilities. More than fifteen similar machines have been manufactured including 12 accelerators to be used in the shipbuilding industry. Inspection of these machines performed after the end of the planned 10-year operation period have demonstrated that major components, in particular, high voltage generator, electron source and accelerating structure remained in good working condition. However, a series of units and systems needed replacement because of depreciation and obsolescence.

The «Electron-3M1» accelerator was put into operation in 1977 in the JSC "Admiralty Shipyards". In 2001-2002, works on its updating were performed. In the process of the updating the following devices and systems were designed, manufactured, adjusted and put into operation:

- scanning device with a bellows branch pipe, which allowed the non-uniformity of the beam current distribution in the irradiation zone to be reduced;
- independent closed water cooling system;
- systems to control the filament current of the electron source and to stabilize the accelerator beam current by using fiber-optics lightguides;
- system for automatic control of the accelerator based on an industrial computer.

#ovchinnikov@luts.niiefa.spb.su

High-vacuum pumps were also replaced with pumps of higher pumping capacity.

To meet the requirements of the new Principal Sanitary Radiation Safety Rules (OSPORB-99), means of radiation monitoring have been replaced and thickness of the radiation shielding has been increased.

In the updated accelerator, there was used an extraction window with a supporting grid made with wedge ribs with a variable inclination angle α (see Fig. 1), which transparency coefficient for the electron beam K is higher than its optical transparency (see Table 1).

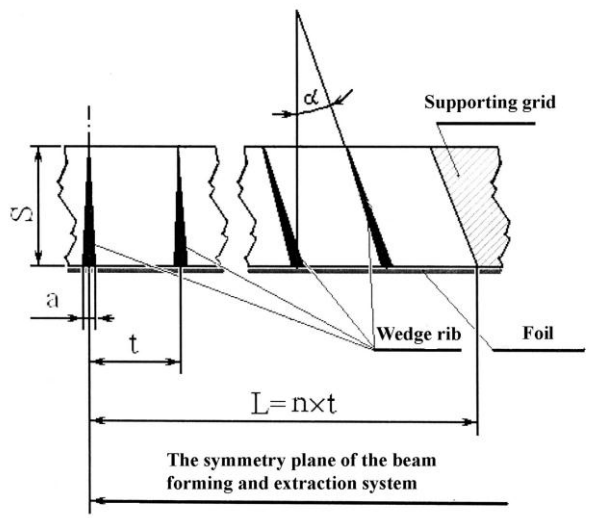

Figure 1: Fragment of the extraction window with the supporting grid (the cross-section along the window long side): "L" is the maximum beam deviation from the plane of symmetry; "S" is the thickness of the supporting grid; "t" is the distance between ribs; "a" is the rib thickness.

Table 1: Measurement of the beam current passed through the extraction window.

Distance from the beam absorber to the diaphragm, mm	Supporting grid	Current recorded by the beam absorber, mA	*K*
50	Without grid	0.80	0.95
	With grid	0.76	
105	Without grid	0.76	0.93
	With grid	0.71	

ISBN 978-3-95450-125-0

HIGH EFFICIENCY [F18]FLUORIDE TARGET SYSTEM FOR THE EFREMOV INSTITUTE CC-18/9 CYCLOTRON

D. Sysoev, V. Zaytsev, M. Mostova, O. Shtukovskiy, RRCRST, Saint-Petersburg, Russia

Abstract

Positron emission tomography (PET) is a nuclear medicine imaging technique that produces a three-dimensional image or a picture of functional processes in a body. The system detects pairs of gamma rays emitted indirectly by a positron-emitting radionuclide (tracer), which is introduced into the body on a biologically active molecule.

If a biologically active molecule chosen for PET is FDG, 2-deoxy-2-[18F]fluoro-D-glucose, an analogue of glucose, concentrations of the tracer imaged then give tissue metabolic activity in terms of regional glucose uptake. Use of this tracer, to explore the possibility of cancer metastasis (i.e., spreading to other sites), results in the most common type of the PET scan in the medical care (95% of current scans).

Due to the short half-lives of the most positron-emitting radioisotopes, the radiotracers have traditionally been produced using a cyclotron in close proximity to the PET imaging facility. The half-life of fluorine-18 is long enough for manufacturing radiotracers labeled with fluorine-18 commercially at offsite locations and transporting to the imaging centers. Since radiochemistry lab in the RRCRST produces FDG for needs of our PET-center and also for two PET-centers in Saint-Petersburg (currently), it is of major importance to produce sufficient amount of fluorine-18 and to obtain FDG with a high radiochemical yield.

The aim of this work was to develop and construct a highly efficient target system for producing fluoride-18 with the Efremov CC-18/9 cyclotron, which is a negative ion system that accelerates 18 MeV ions. The maximum achievable beam current is 100 μA. The beam profile measured with a scanner indicates that approximately 95% of the beam is distributed within a 20 mm diameter circle.

The former fluoride-18 target system for this cyclotron, supplied by the cyclotron producer, the Efremov Institute, had insufficient productivity, not greater than 1 Ci of fluorine-18 during 2 hour irradiation, and didn't allow achieving high radiochemical yields in producing radiopharmaceuticals due to contamination of irradiated water with metallic impurities from target body.

TARGET CONTRUCTION

The major demerits that caused poor performance were inadequate heat transfer rate of the target body and an inadequate water layer. Since the heat input exceeded the heat removal capability of the target, excessive voiding occured in the target water. Protons of a given energy have a characteristic range in water which is inversely related to the water density. Since the water density decreases with the void fraction, the operating void fraction dictates the necessary target depth to prevent the beam from penetrating to the target rear surface. If the proton beam penetrates the water volume and deposits heat in the back wall of the target, the fluoride-18 yield will be reduced due to less proton interactions in the water. Interactions between the beam and the target surface can also release metal ions into water, which react with the ionic fluorine-18 and cause further reduction of the yield.

To prevent the proton beam from striking the back wall of the target, the target must be range thick. The target depth should exceed the range of the protons in the saturated mixture. The range of protons with incident energy between 0 and 18 MeV in water has been determined using the Stopping and Range of Ions in Matter program (SRIM), presented in fig. 1. A 5 mm depth of the target chamber was chosen to provide full functionality with 65/35 % water/vapour mixture (at 8 bar).

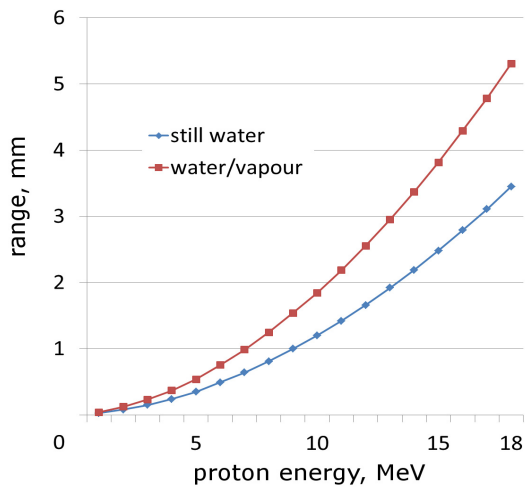

Fig.1. Proton range in water (SRIM).

Niobium has been chosen as a material for the target body, since it is a proper and well-known interface material due to its excellent chemical compatibility. Unfortunately, niobium suffers from a relatively low thermal conductivity. To overcome this problem, heat exchange mechanisms other than simple water-metal-cooling water conduction have to be considered. The new target has been designed to allow boiling in the target chamber to take advantage of the high rate of heat transfer. Heat deposition in the water causes boiling and results in formation of voids or bubbles. The buoyancy

ISBN 978-3-95450-125-0

IMPROVING OF UNIFORMITY OF THE ELECTRON-BEAM TREATMENT OF MATERIALS BY ELV ACCELERATORS

N.K. Kuksanov, S.N. Fadeev, D.A. Kogut, BINP SB RAS, Novosibirsk, Russia

Abstract

The problem of the absorbed dose distribution during the EB treatment by ELV accelerator is considered. The value of the absorbed dose is determined by the speed of scanning electron beam along the accelerator exit window (i.e. the movement across the conveyor). It is determined both by the shape of scanning current and by the geometry of scanning magnets. A simple way to improve the dose distribution near the edges of the extraction device of accelerator is suggested. It allows to provide the non-uniformity less 4%.

INTRODUCTION

ELV accelerators produced by the Budker Institute of Nuclear Physics (Novosibirsk), has the leading position among the proposed equipment for radiation processing of materials. High performance, wide range, covering almost all the needs of modern industrial technology, reliability and relative ease of use and maintenance form the strong demand for this product in tough market conditions. The technology development radiation modification increases the requirements for the parameters of industrial accelerators produced by stimulating the creation of more powerful and energy efficient models [1]. In a number of industrial applications emerge and increased demands on other characteristics ELV accelerators, such as the stability of the energy of the beam current, the uniformity of the irradiation and etc. The condition of uniform dose distribution to be no more than 4% of the length of the material is an example of such a requirement. It occurs when you use the extended length of the output window, as in the modernization of the accelerator, which took place in spring 2012.

THEORETICAL PART

The dose of radiation is determined by the current density and linear scanning speed of the beam along the axis of the output device. In Figure 1 shows the trajectory of the electron beam in the deflecting magnets in the form of unlimited axis x band width l (the using of cylindrical poles, that takes into account the effect of the edge focusing, is shown in Figure 2) and the calculated reduced velocity (V) of a beam and reduced radiation dose (D ~ 1 / V) as a function of deflecting magnets current. These formulas are obtained by taking into account that

$$\sin(\varphi) = \int_l Hdl \Big/ (H\rho)$$

where $H\rho$ – given the relativistic momentum of the electron, and the integral can be written as

$$\int_l Hdl = K \cdot I(t), K = Const.$$

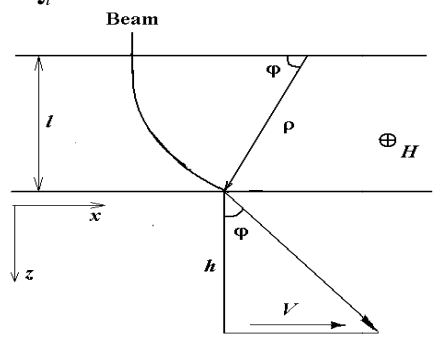

$$Y_V = \frac{V(\varphi)}{V(\varphi = 0)} = \frac{1}{\cos^3(\varphi)}; Y_D = \cos^2(\varphi)$$

Figure 1: Forms of the scanner current in case of the unlimited axis x magnetic field band.

Thus obtain the following formula for the rate and dose

$$V = h \cdot \frac{K}{(H\rho)} \cdot \frac{1}{\cos^3(\varphi)} \cdot \frac{dI}{dt}; D \sim \frac{1}{V} \cdot \frac{1}{\cos(\varphi)} = \cos^2(\varphi)$$

and similarly for Figure 2 –

$$V = h \cdot \frac{K}{(H\rho)} \cdot \frac{\cos^2(\varphi/2)}{\cos^2(\varphi)} \cdot \frac{dI}{dt}; D \sim \frac{\cos(\varphi)}{\cos^2(\varphi/2)}$$

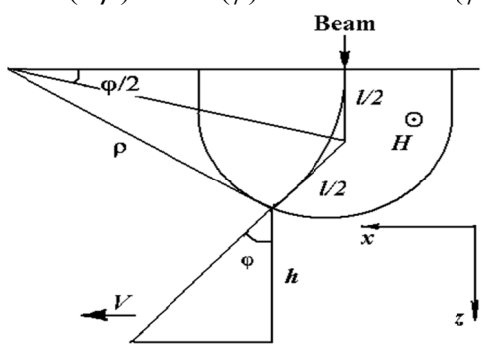

$$Y_V = \frac{V(\varphi)}{V(\varphi = 0)} = \frac{\cos^2(\varphi/2)}{\cos^2(\varphi)}; Y_D = \frac{\cos(\varphi)}{\cos^2(\varphi/2)}$$

Figure 2: The trajectory of the electron beam and the horizontal velocity and dose formula.

In Figure 3 shows graphs of the calculated dose distribution and the actual measurements made by different energies. Differences are due to the scattering of the electron beam as the output device in the foil, and in the air. Contribute to the actual shape also makes scanning electromagnets, which real view (Figure 4) differs from the above described cases and have the form closer to Figure 1.

ISBN 978-3-95450-125-0

CALIBRATION TESTING OF THE STRIPPING TARGET OF THE VACUUM INSULATED TANDEM ACCELERATOR

A. Kuznetsov, V. Aleynik, I. Sorokin, S. Taskaev, M. Tiunov, I. Shchudlo,
BINP SB RAS, Novosibirsk, Russia

Abstract

Presented work is aimed on modernization of the gas stripping target that is used in the Vacuum Insulated Tandem Accelerator (VITA) to recharge negative hydrogen ions into protons. The target was modernized to get higher efficiency of the beam transportation and to raise the current of the accelerated proton beam. The design of the modernized stripping target, the calculated data on the gas flow rate and recharge effectiveness, also the results of experimental measurement of transported current depending on the gas flow rate are presented. The method of the target thickness determination and the procedure to adjust the regime of the gas flow rate to get the required recharging effect were suggested.

INTRODUCTION

The Vacuum Insulated Tandem Accelerator (VITA) was developed in the Budker Institute of Nuclear Physics [1] to produce epithermal neutrons for boron neutron capture therapy in the ^{7}Li(p,n)^{7}Be reaction. The parameters of the generated radiation allow us to carry out in vitro and in vivo investigations of BNCT. In present moment the modernization of the facility elements is carrying out to meet the parameters required for clinical usage.

The design of the VITA facility is shown at figure 1. The principle of the tandem accelerating scheme is accelerating of the negative hydrogen ions to the 1 MeV energy determined by the high voltage electrode potential, recharging the ions into protons in the gas stripping target and then accelerating to the 2 MeV energy by the same accelerating potential. The vacuum insulation of the electrodes, the circumstance that the feedthrough insulator is located at significantly big distance to the accelerating gaps and the gas pumping realized through the electrode shutters allows us to believe in capability of the VITA to produce a high current proton beam.

The optimal stripping target is supposed to be the argon gas target constructed as a cooled tube with the gas injection in the middle of the tube [2]. The tube length is 400 mm, inner diameter was made 10 mm, and from 2011 year the diameter was increased to 16 mm. The photo of the new target is shown at the figure 2.

The protons equilibrium yield is 99.9880%. The beam charged components and the full current in the output of the stripping target in dependence on the linear density of the argon in the target are presented at figure 3. The gas consumption for the 16 mm tube with length 400 mm and 300 K temperature is in linear dependence on the target density and described as an equation:

$$Q\ [10^{18}\ s^{-1}] = 2.63\ nl\ [10^{16}\ cm^{-2}],$$
$$\text{or } Q\ [mTorr\ l\ s^{-1}] = 75\ nl\ [10^{16}\ cm^{-2}].$$

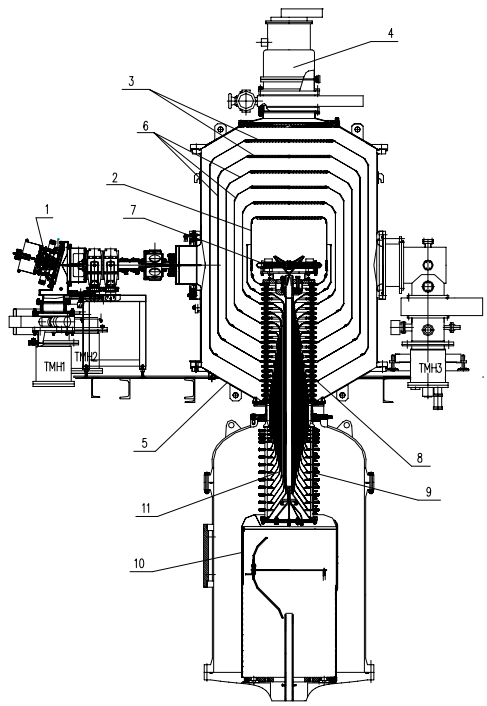

Fig. 1. Scheme of the VITA facility. 1 – ion source (H^-); 2 – high voltage electrode; 3 – electrode shutters; 4 – cryo pump; 5 – accelerator vacuum volume; 6 – intermediate electrodes; 7 – stripping target; 8 – feedthrough insulator (vacuum part); 9 – feedthrough insulator (gas part); 10 – high voltage source; 11 – coaxial feeding tubes.

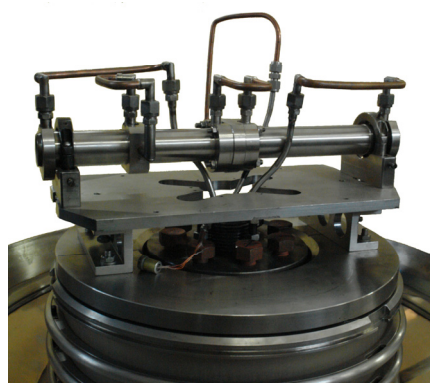

Fig. 2. New Ø16-mm stripping target placed on the feedthrough insulator.

ISBN 978-3-95450-125-0

ELECTRON BEAM IMAGE VISUAL MONITORING

V.N. Boriskin, V.V.Zakutin, N.G.Reshetniak, S. K. Romanovsky#, V.P.Romasko, A.Eh. Tenishev, V.J.Titov, I.A.Chertishev, V.A. Shevchenko, I.N. Shlyakhov, V.L. Uvarov,
NSC KIPT, Kharkov, 61108, Ukraine

Abstract

The system for visual monitoring of the electron beam was developed and implemented. The technique is based on registration of optical radiation, which is generated under object-beam interaction. The system comprises image transferring channel, remote-controlled digital photo-camera, connected with PC by USB-interface as well as proper software. The images obtained give information on the beam density distribution over the surface of the object being irradiated. 40 KeV and 10 MeV electron beams were researched.

VISUAL MONITORING OF ELECTRON BEAM WITH ENERGY OF 40 KEV IN VACUUM

Tubelike electron beam was formed by magnetron gun with a secondary-emission 40 mm aluminium cathode [1] providing 40 kV and 50 A pulse of 40000 nS in width. The beam hit an eight-segment Faraday cup (see Fig. 1).

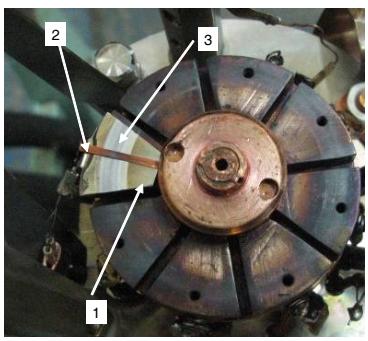

Figure 1: Faraday cup with electron beam traces. 1- target, 2- calibration strip, 3- beam image.

One of its segments has a stainless steel cover with calibration strip. For visual control, electron beam image is taken out by system of mirrors and lenses (see Fig. 2) and fixed with a digital camera controlled by PC.

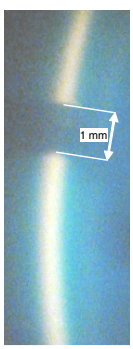

Figure 2: Electron beam image of magnetron gun with 40 keV electron energy at the target.

romanovsky@kipt.kharkov.ua

Processing of images is provided using program Origin7.5 (see Fig. 3).

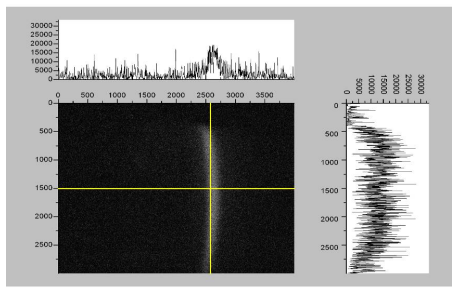

Figure 3: Image of beam profile at the target.

VISUAL MONITORING OF ELECTRON BEAM WITH ENERGY OF 10 MEV IN ATMOSPHERE

The system was created for visual monitoring of the objects being irradiated on LUE-10 LINAC (see Fig. 4) as still as fixed and moved by transfer conveyor[2].

Figure 4: LINAC LUE-10 with conveyor and supercritical water convection loop.

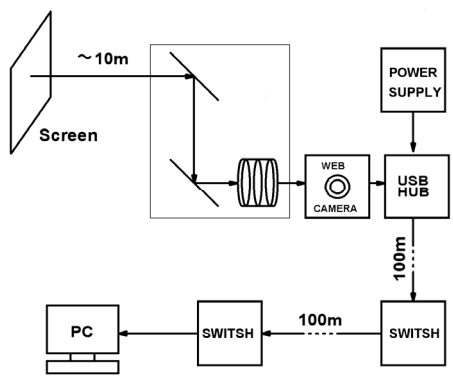

Fig. 5. Functional chart of the system for visual monitoring of electron beam at LINAC LUE-10.

ISBN 978-3-95450-125-0

EXPERIMENTAL CHANNEL FOR PROTON BEAM WITH ENERGY 9 GEV

Mark Kats, ITEP, 25, B.Cheremushkinskaya, Moscow, Russia

Abstract

It was described one of possible version of experimental channel for proton beam with energy 9GeV for ITEP. It based on proton beam after quick extraction, on existing experimental hall and on existing quadrupoles.

INTRODUCTION

For investigation of inner design of different target it is possible to use proton beam which can pass through the target and specific channel for transport scattered beam between the target and equipment for measurement shape of the beam at the end of the channel. Now in ITEP there is such channel for proton beam with energy 0.8GeV. This report is devoted to one of possible version of new channel on extracted from ITEPs synchrotron proton beam with energy 9GeV. New channel will be able investigate more thick targets with more high resolution.

OPTICAL SOLUTION

It was suggested to use optical scheme of channel with minimal angular sizes of the beam at the target, and with focus of the beam by two symmetrical parts (like triplets of quadruples). The first triplet focus initial (without scattering into the target) beam in middle point. Scattered beam can be collimated in this point according angle of scattering. The second triplet focus initial beam in both planes on equipment for measurement its profile with magnification -1. So, scattered in any point of the target proton beam will be focus at the equipment with magnification -1. It was suggested to use 8 quadrupoles ML15 (L=0.9m, D=0.15m, B<0.7Tl), which are free now in ITEP. Optical properties of the channel were calculated by TRANSPORT in second order.

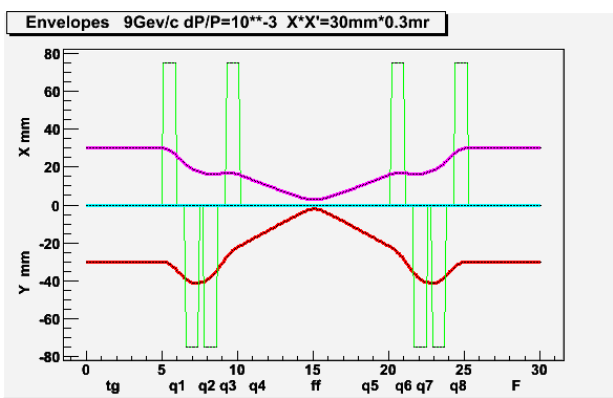

Figure 1. Scheme of proton beam envelopes into the cannel for beam without scattering in the target

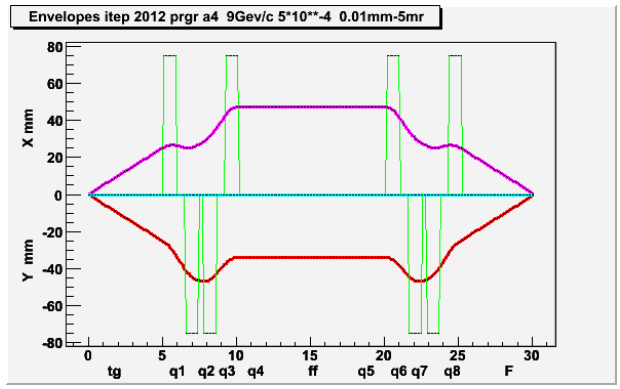

Figure 2. Scheme for beam envelopes for protons scattered in the target at angles 5mrad.

R11=R33=-1.0 magnifications are -1.0 in both planes. R116=R336=10^{-6}. Across sizes of the target have small influence on precision of measurements.

Chromatic aberration, which has strong influence on resolution, can be estimated in both planes as multiplication of those coefficients on angular sizes X' or Y' of scattered beam and on momentum spread dP/P of the scattered beam. According of calculations R126 = R346 = 30m. For dP/P=10-3 and X'=Y'≤5mrad limit of resolution according of chromatic aberration is like 0.15mm, for dP/P=10-4 and X'=Y'≤2mrad the same limit is like 0.006mm. Angular sizes of the beam in channel at measurement depend on initial angular sizes of the beam, on initial energy of protons, on properties of the target (length and material) and on collimation of the beam in middle point of the channel.

PRELIMINARY TRANSPORT OF EXTRACTED BEAM

Extracted proton beam at energy 9GeV has momentum spread in interval $10^{-3} < dP/P < 10^{-4}$, its phase volumes are less 10mmmrad. If the target can change its properties quickly (10^{-6}sec) steel window with thickness like 10mm must be installed on the beam direction in 1m after 303 magnet of accelerator. Such window scattered protons on angles like 1mrad. At this condition sizes of beam for its transport to the target can be estimated 3mm*mrad < XX' < 16mm*mrad. Input proton beam at the target must be with diameter like 60mm and with minimal angular sizes. 4 existing quadrupoles 20K100 can be used for this aim.

ISBN 978-3-95450-125-0

SIMULATIONS AND DESIGN OF THZ WIGGLER FOR 15-40 MEV FEL

E.M. Syresin, N.A. Morozov, R.S. Makarov, S.A. Kostromin, D.S. Petrov
Joint Institute for Nuclear Research, Dubna, Russia

Abstract

The electromagnetic wiggler is applied for narrow-band THz radiation in the 30 μm to 9.35 mm wavelength range. This is a planar electromagnetic device with 6 regular periods, each 30 cm long. The end termination pattern structure is +1/4,-3/4,+1,…,-1,+3/4,-1/4. This structure is more appreciable for compensation of the first and second fields, especially, to provide the small value of second integral of 500 G×cm^2. The peak magnetic field is up to 0.356 T, it is defined by large wiggler gap of 102 mm and a capacity of water cooling system of 70 kW. The parameter is varied in the range K=0.5- 7.12 corresponding to a field range B=0.025- 0.356 T peak field on axis. The wiggler is used in 15-40 MeV. The bunch compression scheme allows the whole wavelength range to be covered by super-radiant emission with a sufficient form factor. The wavelength range corresponds to 217 μm-9.35 mm at electron energy of 15 MeV, it is equal to 54 μm-2.3 mm at electron energy of 30 MeV and it is 30 μm-1.33 mm at electron energy of 40 MeV. The 3D Opera simulations of THz wiggler is under discussion.

INTRODUCTION

The design of THz wiggler and technical solution at its construction are based on FIR FLASH undulator constructed in JINR [1-5].

Table 1: Summary of wiggler technical data.

Parameter of THz wiggler	value
period length, mm	300
number of full periods	7
number of poles including end-pieces	14+4
maximum wiggler parameter K_{RMS}	7.12
peak field on axis, T	0.356
height of magnetic axis above floor level, m	1.4
minimum clear gap, mm	102
position accuracy of magnetic axis, mm	0.5
angular precision of magnetic axis, mrad	0.5
field flatness at ±20 mm off-axis (horizontally), %	-0.1… +0.5
first field integral I1, G×cm	50
second field integral I2, G×cm^2	500
stability and reproducibility of magnetic axis, mm/μrad	±0.1/ ±50

The second peculiarity of wiggler is related to the trim coils. The four trim coils with individual power supply should be installed in wiggler. These trim coils permit to compensate on the full wiggler length the first and second integrals. However it does not permit to compensate integral on period length. The first integral on period length should be smaller than 50 G×cm and also very low second integral 500 G×cm^2. To provide both these requirements it is propose to install in each regular coil an additional correction coil. The individual correction coils should compensate imperfection of wiggler mechanical construction and errors in coil position. In the parallel to each individual correction coil a variable resistance divider will be installed. As a result through each individual correction coil will pass the individual optimal correction current; however for all 7 pairs of correction coils will use only 1 power supply system.

The 3D wiggler simulations at its full scale were performed by TOSCA code (Fig.1). The maximal available magnetic field corresponds to 0.356 T at number of Ampere×turns of $I_W=1.85\cdot10^3$. An increase of the number of Ampere turns up $I_W=2.1\cdot10^3$ permits to linearly increase the magnetic field up the value of 0.375 T (Fig.1, Table 1.).

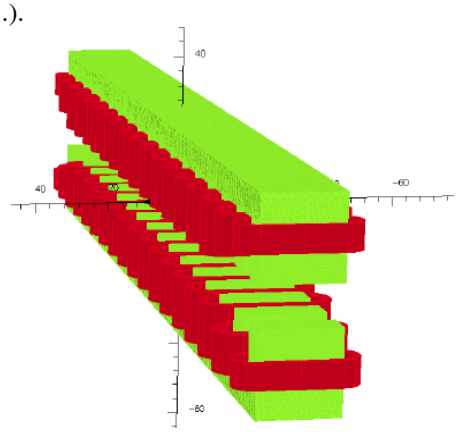

Figure 1: TOSCA 3D simulation of THz wiggler.

The 3 layer coil at the magnetic field of 0.356 T corresponds to following water cooling system parameters: dissipated power of 70 kW, water cooling flow of 2.6 l/min through one coil (about 94 l/min for 36 coils) and temperature rise of 12^0. So the maximum available magnetic field is defined by water cooling system. The increase of the magnetic field up to 0.375 T is required an increase of dissipated power up 96 kW and temperature up 16^0.

The diffraction spot size of radiation defines the diameter of vacuum chamber and wiggler gap. The diffraction angle and spot radius of wiggler radiation are equal to

ISBN 978-3-95450-125-0

DIAGNOSTIC TECHNIQUE WITH FEMNTO SECOND RESOLUTION APPLIED FOR FEL ELECTRON BUNCHES

O. Brovko, A. Grebentsov, R.Makarov, N.Morozov, A.Shabunov, E. Syresin#, M. Yurkov,
Joint Institute for Nuclear Research, Dubna, Russia

Abstract

Diagnostic technique applied for FEL ultrashort electron bunches is developed at JINR-DESY collaboration within the framework of the FLASH and XFEL projects. Photon diagnostics developed at JINR-DESY collaboration for ultrashort electron bunches are based on calorimetric measurements and detection of undulator radiation. The infrared undulator constructed at JINR and installed at FLASH is used for longitudinal bunch shape measurements and for two-color lasing provided by the FIR and VUV undulators. The pump probe experiments with VUV and FIR undulators provide the bunch profile measurements with resolution of several femtosecond. The MCP based radiation detectors are effectively used at FLASH for VUV pulse energy measurements. The new three MCP detectors operated in X-ray range are under development now in JINR for SASE1-SASE 3 XFEL.

FLASH MCP-BASED PHOTON DETECTOR

The free electron laser FLASH has been in operation at DESY since the year 2000. The maximal electron energy since 2007 up 2009 was equal 1 GeV, rms bunch length is 50 μm, the FWHM radiation pulse duration is about 30 fs, the normalized emittance is 2 π·mm·mrad, the bunch charge is 0.5 nC, the peak power is up to 1 GW, the peak brilliance is of 10^{28} ph/s/mrad^2/mm^2/(0.1%bw). In 2010 FLASH was upgraded to maximum electron energy 1.25 GeV and third harmonic RF system was installed which provides by few times longer the VUV pulse radiation comparing with the previous FLASH operation.

Successful operation of FLASH strongly depends on the quality of the radiation detectors. The key issues are: the wide wavelength range 4-100 nm, the wide dynamic range (from the spontaneous emission level to the saturation level), and the high relative accuracy of measurements which is crucial for detection of radiation amplification and characterization of statistical properties of the radiation.

The key FLASH photon detector developed by the JINR-DESY collaboration is a micro-channel plate (MCP) detector intended for pulse energy measurements [1-4]. The MCP detector is used for measurement of statistical properties of the radiation allowing determination of the pulse length. Key element of the detector is a wide dynamic MCP which detects scattered radiation from a target. With four different targets and MCPs in combination with optical attenuators, the present FLASH detector covers an operating wavelength range 4 -100 nm, and a dynamic range of the radiation intensities, from the level of spontaneous emission up to the saturation level of SASE FEL.

The gold target is perfect for the wavelength range above 10 nm, however its reflectivity falls dramatically for shorter wavelengths, and different targets and geometries of the detector are used. We added three more targets to gold mesh: two iron meshes, and one copper mesh. This helps us to operate the detector in a range below 10 nm.

For tuning SASE at very short wavelengths we use movable MCPs directly facing photon beam. Light intensity variation by a factor of 50 is controlled by a mechanical attenuator of light located in the target unit. To have full control of light intensity in a wide range we installed a side MCP which detects radiation reflected by the iron mirror. The mirror serves for two purposes. One is to deflect the photon beam off- the axis, which allows placing the MCP in better background conditions.

The FLASH bunch has non-Gaussian longitudinal distribution of electrons at operation in 2007-2009. The bunch edge or so named leading spike has a high peak current that is cable of driving the high intensity lasing process. Energy in radiation pulse and integrated spectral density fluctuate accordance with the gamma distribution with an energy width σ_w. Parameter $M=1/\sigma_w^2$ characterizes the number of modes in the radiation pulse. This parameters corresponds to a ratio of the electron bunch leading spike length σ_z to the coherence time τ_c at a saturation of the radiation in the SASE mode: $M=\sigma_z/c\tau_c$. The measurements of the integrate spectra density in radiation pulse permit to define the VUV pulse duration.

The r.m.s. VUV radiation pulse length was equal to $\tau_{VUV}= 8\pm1$ fs at the end of the regime of exponential growth for wavelength radiation of 13.7 nm and bunch charge 0.5 nC at electron energy 1 GeV [1]. After 2010 upgrade the r.m.s. VUV pulse radiation time corresponds to $\tau_{VUV}= 41\pm8$ fs at electron energy 1.25 GeV and bunch charge 0.5 nC [5].

DESIGN OF THE XFEL MCP DETECTOR

An important task of the photon beam diagnostics at the European XFEL is providing reliable tools for measurements aiming at the search for and fine tuning of the FEL creating SASE process. The problem of finding SASE amplification is crucial for the XFEL because of a large synchrotron radiation background. This requires a detector with a wide dynamic range, controllable tuning to the required wavelength range, and suppression of the unwanted radiation background. The JINR-XFEL

#syresin@nusun.jinr.ru

ISBN 978-3-95450-125-0

LONGITUDINAL STABILITY OF ERL WITH TWO ACCELERATING RF STRUCTURES

Ya. V. Getmanov#, O. A. Shevchenko, Budker INP, Novosibirsk, Russia
N. A. Vinokurov, Budker INP,Novosibirsk, Russia and KAERI, Daejeon, Korea

Abstract

Modern ERL projects use superconductive accelerating RF structures. Their RF quality is typically very high. Therefore, the RF voltage induced by electron beam is also high. In ERL the RF voltage induced by the accelerating beam is almost cancelled by the RF voltage induced by the decelerating beam. But, a small variation of the RF voltage may cause the deviations of the accelerating phases. These deviations then may cause further voltage variation. Thus, the system may be unstable. The stability conditions for ERL with one accelerating structure are well known [1, 2]. The ERL with split RF structure was discussed recently [3, 4]. The stability conditions for such ERLs are discussed in this paper.

INTRODUCTION

The scheme of an ERL with two accelerating structures is shown in Fig. 1.

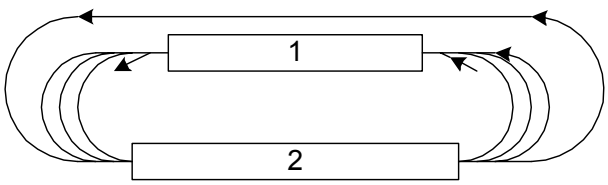

Figure 1: Scheme of ERL with two linacs.

Electrons are injected to the linac 1. After two passes through linac 1 and linac 2 they are used, for example, in undulators. After that electrons are decelerated.

There are four electron beams in each linac simultaneously. Each beam induced large voltage in the linac, but the sum is not so large. If the phases of the beams vary, the sum voltage also varies, and initially small phase deviation may increase due to the dependence of flight times through arcs on the particle energy. This longitudinal instability is considered in our paper.

THE VOLTAGE EQUATIONS

To simplify the picture, consider each linac as one RF cavity. Its equivalent circuit is shown in Fig. 2.

The gap voltage expression $U = L\,d\left(I_b + I_g - C\,dU/dt - U/R\right)/dt$, I_b and I_g are the currents of the beam and of the RF generator, leads to the standard equation

$$\frac{d^2U}{dt^2} + \frac{1}{RC}\frac{dU}{dt} + \frac{1}{LC}U = \frac{1}{C}\frac{d}{dt}\left(I_b + I_g\right) \qquad (1)$$

Taking the effective voltage on the linac with number α in the form $\mathrm{Re}(U_\alpha e^{-i\omega t})$ (ω is the frequency of the RF generator), one obtains:

$$\frac{2}{\omega}\frac{dU_\alpha}{dt} = \frac{i\xi_\alpha - 1}{Q_\alpha}U_\alpha + \rho_\alpha(I_{b\alpha} + I_{g\alpha}), \quad (2)$$

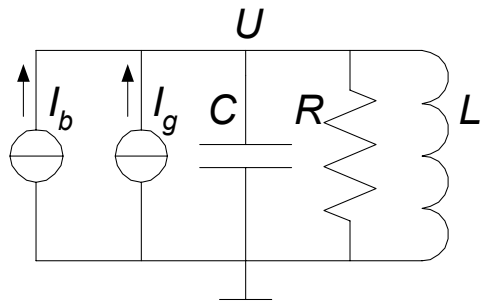

Figure 2: Equivalent circuit of the RF cavity.

where $\omega_\alpha = 1/\sqrt{L_\alpha C_\alpha} = (1 - \xi_\alpha/2Q_\alpha)\omega$ is the resonant frequency, $Q_\alpha = R_\alpha/\sqrt{L_\alpha/C_\alpha} >> 1$ is the loaded quality of the cavity, $\rho_\alpha = R_\alpha/Q_\alpha = \sqrt{L/C}$ and R_α are the characteristic and the loaded shunt impedances for the fundamental (TM_{010}) mode, and $I_{b\alpha}$ and $I_{g\alpha}$ are the complex amplitudes of the beam and (reduced to the gap) generator currents correspondingly. We are interested in the case of constant $I_{g\alpha}$. The beam currents $I_{b\alpha}$ depend on all U_α due to phase motion. Linearization of Eq. (2) near the stationary solution

$$U_{0\alpha} = \frac{R_\alpha}{1 - i\xi_\alpha}\left[I_{b\alpha}(\mathbf{U}_0) + I_{g\alpha}\right] \qquad (3)$$

gives:

$$\frac{2}{\omega}\frac{d\delta U_\alpha}{dt} = \frac{i\xi_\alpha - 1}{Q_\alpha}\delta U_\alpha + \qquad (4)$$

$$+ \rho_\alpha \sum_\beta \left(\frac{\partial I_{b\alpha}}{\partial\,\mathrm{Re}\,U_\beta}\mathrm{Re}\,\delta U_\beta + \frac{\partial I_{b\alpha}}{\partial\,\mathrm{Im}\,U_\beta}\mathrm{Im}\,\delta U_\beta \right)$$

Strictly speaking, I_b depends on the values of U at previous moments of time, so Eq. (4) is valid only if the

ISBN 978-3-95450-125-0

VERTICAL SIZE OF AN ELECTRON BEAM AT SIBERIA-2

A.G.Valentinov, V.N.Korchuganov, Yu.V.Krylov, Yu.L.Yupinov, NRC Kurchatov Institute, Moscow, Russia

Abstract

Brightness of the synchrotron radiation light sources is defined by electron beam sizes at radiation point. Horizontal size depends mainly from designed magnetic structure. Vertical size is defined by two processes: first, betatron coupling between vertical and horizontal motions and second, presence of vertical dispersion function at bending magnets. Vertical dispersion creates non-zero vertical emittance even without coupling.

The report is dedicated to methods of vertical beam size decreasing at SIBERIA-2 storage ring. There are two families of skew-quadrupoles on the ring, one lens of every family in each of 6 cells of the magnetic structure. After analyzing of betatron coupling coefficient equation we stayed only two lenses in each family. As a result power supplies' currents for coupling compensation became much lower.

In order to decrease vertical dispersion a special algorithm was developed and tested. Vertical dispersion on beam position monitors (BPM) azimuths was corrected by vertical displacements of chromaticity compensating sextupoles. Maximal value of the dispersion became four times lower. It leaded to prominent vertical beam size decreasing.

INTRODUCTION

The vertical size of the electron beam in storage ring SIBERIA-2 is mainly determined by two factors. Firstly, there is a vertical emittance ε_z, which is generated by the vertical dispersion function η_z in the places, where the electrons radiate energy - similar to the way that the horizontal dispersion function leads to the appearance of the horizontal emittance. Vertical dispersion occurs in the presence of any horizontal fields on the orbit, such as fields of vertical corrective magnets, fields due to deviation of the beam from the centers of quadrupoles and sextupoles, any parasitic fields. In addition, there are the inevitable errors in the position of the magnetic elements, which may lead to the distortion of vertical orbit. Secondly, there is a coupling of vertical and horizontal betatron. It appears in the presence of skew-quadrupole fields on a closed orbit. These fields can be a consequence of the rotation of quadrupole lenses along their longitudinal axis, as well as errors in the upright position of the sextupole lenses. The betatron coupling leads to the periodic transfer of energy between the horizontal and vertical betatron oscillations.

Other mechanisms to increase the vertical size of the beam, such as multiple internal scattering of electrons in the bunch (the Toushek effect), and the interaction of a beam with the currents, induced on the walls of the vacuum chamber, give negligibly small contribution to the vertical size of the beam at SIBERIA-2 at 2.5 GeV.

To decrease the vertical size of the beam it is necessary to control the vertical dispersion function, as well as the coupling of betatron oscillations.

VERTICAL DISPERSION FUNCTION CONTROL

In the case of small connection between transversal betatron oscillations an equation for the vertical dispersion is written as

$$\eta_z'' + K_1\eta_z = K_2 z_c \eta_x - K_{1s}\eta_x + K_1 z_c - \frac{1}{\rho_z} = F \qquad (1)$$

where η_x - horizontal dispersion function, K_1, K_2, K_{1s} - normalized power of quadrupoles, sextupoles and skew-quadrupoles respectively, z_c - vertical deviation of a closed orbit, ρ_z is the radius of rotation in vertical plane [1]. The solution to this equation has the same form like for a closed orbit:

$$\eta_z = \frac{\sqrt{\beta_z(s)}}{2\sin\pi\nu_z}\int_s^{s+C}\sqrt{\beta_z(y)}\cos(\phi_z(s)-\phi_z(y)+\pi\nu_z)F\,dy \qquad (2)$$

where ν_z - vertical betatron frequency, C – ring circumference, β_z - vertical β-function.

For us the important thing here is that η_z is described by exactly the same formulas as the vertical closed orbit. This means that η_z, as well as the orbit, can be corrected to obtain its acceptable view. As for correction of the closed orbit, the goal is to decrease the value of RMS η_z deviations from zero: $\sigma_{\eta z} \rightarrow 0$. Magnetic elements contributing to the function F can be used as correctors. In fact, with already adjusted closed orbit, one can affect only the second term in the expression for F, because in this case the following conditions are satisfied: z_c = const and ρ_z = const. Thus, only the magnetic elements with skew-quadrupole component in the field can influence on the vertical dispersion without the distortion of the orbit. They must be located inside achromatic bend with a non-zero η_x. It is preferable to have skew-quadrupole lenses with independent power supplies inside each achromatic bend. There are no that kind of lens at SIBERIA-2, but we can use sextupole lenses for natural chromaticity correction as correctors for η_z. We can get skew-quadrupole field K_{1s} from sextupole vertical displacement Δz: K_{1s}= -K_2·Δz. Impact on the closed orbit is small enough, because components of the field arising from sextupole moving ΔB_z and ΔB_x are proportional, respectively, to z_c·Δz and x_c·Δz, where z_c and x_c - vertical and horizontal orbit distortions at sextupoles' azimuths. Each of the z_c, x_c and Δz does not exceed 1-2 mm, and the

ISBN 978-3-95450-125-0

ENERGY RAMPING AT SIBERIA-2

A.G.Valentinov, V.N.Korchuganov, Yu.V.Krylov, Yu.L.Yupinov, NRC Kurchatov Institute, Moscow, Russia

Abstract

Siberia-2 storage ring has great difference between injection energy 0.45 GeV and working energy 2.5 GeV. Beam lifetime at injection energy is equal to approximately 1 hour. In order to minimize beam losses of the stored beam it is necessary to accelerate energy ramping process. It is not very simple because power supplies of bending magnets, quadrupole lenses and sextupoles have different response time and behavior after changes in regulated current level. Magnetic elements are manufactured from non-laminated iron. It leads to slower field/gradient increasing at high current values.

Complicated algorithm with 9 intermediate regimes (collections of power supplies' settings) was developed to produce fast and efficient energy ramping. First, correction of closed orbit, betatron tunes and chromaticity is accomplished in each regime in static conditions. Special file is used to provide acceleration or deceleration of power supplies in dynamic conditions. This scheme allows to compensate betatron tune shifts during energy ramping. Power supplies are not stopped on intermediate regimes; speed of current changing is continuous function of time. This algorithm allowed decreasing ramping time down to 2 minutes 40 seconds. Beam losses are not exceeding 2 – 3%; betatron tune shifts as a rule are lower than 0.01. The algorithm can easily be modified to stop in any intermediate regime.

INTRODUCTION

Synchrotron radiation source SIBERIA-2 [1] has a big difference between injection energy (450 MeV) and working energy (2.5 GeV). Beam lifetime at energies below 1 GeV is small and does not exceed 1.5 hours. To avoid losses of electrons, immediately after the accumulation of the necessary current energy should be increased as soon as possible. The process of energy ramping consists in proportional change of magnetic field in bending magnets, field gradients in quadrupole and sextupole lenses. The difficulty lies in the fact that different magnetic elements have different curves of magnetization, that is, the dependence of the field/gradient on supply current. In addition, power supplies of the magnetic elements have different speed of reaction on change of nominal current. Magnetic elements are manufactured from nonlaminated iron, which leads to delay of the field in the working gaps of the magnets and lenses. As a result, betatron tuneshifts arise after the start of energy ramping. Too large shifts can lead to losses of the current on the closest resonances. Also chromaticity can change, resulting in additional losses due to a decrease of the dynamic aperture or the occurrence of instabilities in the beam.

To solve all these problems a unique algorithm for energy ramping was developed and implemented.

DIFFERENCIES IN MAGNETIZATION CURVES

Magnetic system of SIBERIA-2 includes one family of bending magnets, 6 families of quadrupole lenses, two families of sextupole lenses for chromaticity correction. The supply current of the bending magnets varies from 1270 A up to 7200 A, it determines the machine energy. The currents of the quadrupole power supplies vary from 80 A up to 760 A depending on the energy and number of the family, the currents of sextupole power supplies vary from 0.4 A up to 8 A. As a result saturation of iron exists at high energy, while residual magnetization manifests at low energies. The magnetization curve of the bending magnets is also influenced by busbar layout near current sensor. Thus, a simple proportional increase of the currents will lead to the betatron tuneshifts during energy ramping.

To facilitate the energy ramping process, 9 intermediate regimes were introduced at a distance of 10 - 20% in energy one from another. The regime means list of power supply settings. Magnetic measurements were conducted to determine right currents for all power supply families in each regime. Field in bending magnets was measured with an accuracy of 10^{-5} using NMR sensor. For the quadrupole lenses measurements were carried out by Hall effect sensor with an accuracy of 10^{-3}. Relative changes of the field gradients in each family in all intermediate regimes were measured. According to the results of measurements a correction of the setpoint currents was carried out so the relations of the gradients in different families in each regime remained the same as at the injection energy. Some of the results after this correction are shown in Fig. 1.

For more accurate reproduction of the results standard demagnetization cycle was introduced. After the work on the energy of 2.5 GeV currents of power supplies of the magnetic elements rise above the maximum working value, then gradually, over 80 seconds, fall below the minimum values of the injection energy, then regime of injection is restored. In every state a 30 seconds pause is maintained. The practice showed that after this demagnetization cycle betatron tunes returned to its initial values with a good accuracy of about 0.003.

TRANSIENT PROCESSES IN POWER SUPPLIES AND MAGNETIC ELEMENTS

Power supplies of the SIBERIA-2 magnetic elements have different speed of reaction to the change of current settings. In addition, magnets and lenses are manufactured

ISBN 978-3-95450-125-0

MEASUREMENT OF SPEED OF LIGHT EMITTED BY ULTRARELATIVISTIC SOURCE*

A.I. Stirin#, P.A. Aleksandrov, V.N. Korchuganov, National Research Center Kurchatov Institute, 123182 Moscow, Russia
E.B. Aleksandrov, Ioffe Physical–Technical Institute, Russian Academy of Sciences, 194021 St. Petersburg, Russia
V.S. Zapasskii, St.Petersburg State University, 198504 St. Petersburg, Russia

Abstract

The paper focuses on the results of experiments on direct measurement of speed of the light emitted by an ultrarelativistic source. The source of synchrotron radiation (SR), electron storage ring Siberia-1 at the Kurchatov Institute, was used as a pulsed source of light. Experiments were made on the visible part of the SR emitted by ultrarelativistic electron bunch moving along a curved trajectory in the magnetic field of the bending magnet.

The measured velocity is within 0.3 % of the standard speed of light in a vacuum.

INTRODUCTION

The statement that "the speed of light is independent of the velocity of the source" was put forward by Einstein as the second postulate of special relativity [1]. In the last century, many astronomical observations and experimental studies have been devoted to accrediting this postulate, see, e.g., recent review [2]. During this time, the validity of this postulate was questioned many times with regard to the insufficient accuracy of the measurements, which was usually due to the low velocity of the source v compared to the speed of light *c*. In this work, we directly measured the speed of the light emitted by a source moving with an ultrarelativistic velocity and found that this speed does not differ from the standard speed of light in a vacuum, which is in agreement with Einstein's postulate.

SETUP AND THE IDEA OF THE EXPERIMENT

The experiment was based on the use of synchrotron radiation from a bunch of relativistic electrons moving at a velocity very close to the speed of light *c* along a curved trajectory in the magnetic field of the bending magnet of the electron storage ring. Under these conditions, it is easy to measure the speed of the emitted light in a very high laboratory vacuum.

According to the Newton–Ritz corpuscular ballistic hypothesis [3–5], which is most popular among opponents of special relativity, the speed of the light emitted by an electron bunch in the forward direction at a tangent to the trajectory should be twice as high as the speed of the light emitted by a source at rest. If this very large effect existed, it could easily be detected without special tricks in view of a high intensity of the synchrotron radiation.

The general layout of the experiment is shown in Fig. 1. The magnetic system of the electron storage ring Siberia-1 forming a closed orbit of electrons consists of four 90° bending magnets M1–M4 separated by four 60-cm-long rectilinear segments and forms a closed orbit of electrons. The radius *R* of the stationary orbit of electrons in the bending magnets is 1 m.

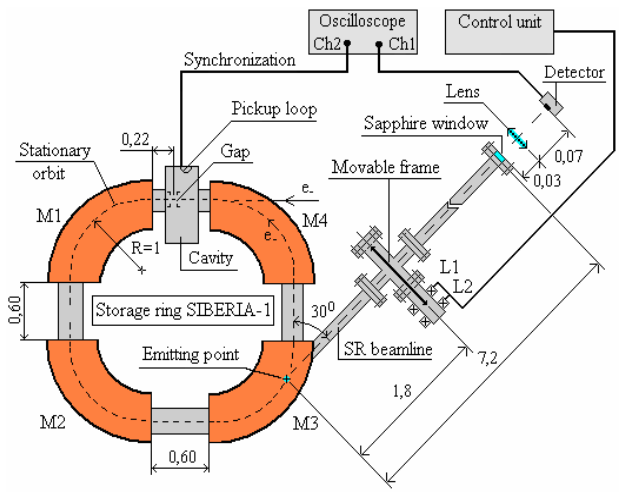

Figure 1: Layout of the experiment: L1, L2-magnetic drive coils of carriage; M1-M4 - bending magnets. Distances are given in meters.

The magnetic flux density on the stationary orbit is 1.5 T at a nominal electron energy of 450 MeV. Synchrotron radiation emitted by relativistic electrons in bending magnets covers a wide spectral range from infrared to X-ray with a characteristic wavelength of 61.3 Å. This emission leads to a 3.69 keV energy loss of each electron per round trip.

To compensate for these losses, a high-frequency cavity was placed in the first segment of the storage ring. Due to the high-frequency power supplied to the cavity, a voltage with an amplitude of 15 kV and a frequency of

*The work was supported by the Russian Foundation for Basic Research under Project No. 11-02-00538-a.
staxiv@mail.ru

ISBN 978-3-95450-125-0

STUDY OF TWO CAVITIES ACCELERATING MODULE AT SR SOURCE SIBERIA-2

V. Korchuganov, V. Moiseev, A. Smygacheva, A. Vernov, RNC KI, Moscow, Russia.

Abstract

SR source Siberia-2 RF system includes an accelerating module consisting of two 181 MHz cavities powered by one amplifier. Some problem occurred now is the accelerating voltage instability under high beam currents conditions. The phase shift between the voltages at cavities causes the asymmetry in beam loading and detuning of cavities. To study the performances of accelerating module, the analytical description has been developed. The whole system can be characterized by seven parameters. These base parameters give the relations of voltages and currents in system. Measurements determine the real values of the base parameters. Set of non linear equations received can be reduced to the voltages and currents in system as the functions of beam current and energy. The results can be applied to injection and ramping in Siberia-2.

ANALYTICAL DESCRIPTION

Accelerating Cavity with Beam

Accelerating cavity with beam can be described by four parameters (see Fig. 1): cavity impedance Z, reflectivity Γ at any cross section of feeder and two coefficients k and m for the same cross section.

.

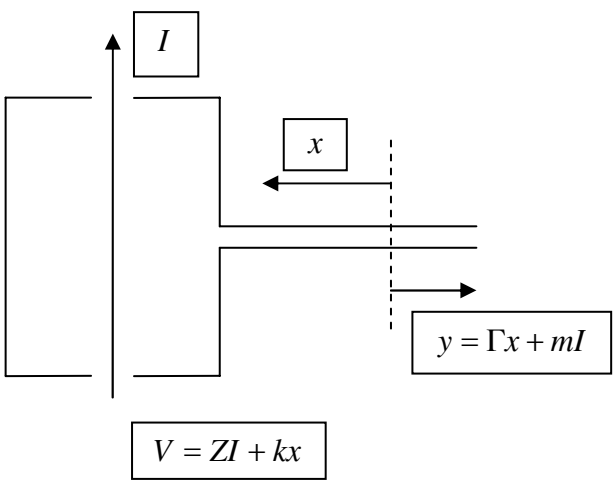

Figure 1: Accelerating cavity with beam (I - the main harmonic of the beam current, V - complex amplitude of accelerating voltage, x and y - complex amplitudes of normalized waves in feeder).

The energy conservation requirements for any beam current harmonic I and any wave x from generator give the relations:

$$4|m| = k,$$
$$-2|m|^2 = \frac{|Z|^2}{R_{sh}} + \mathrm{Re}\,Z, \quad (1)$$
$$-2m^*\Gamma = k\left(\frac{Z^*}{R_{sh}} + \frac{1}{2}\right),$$

where R_{sh} is the shunt impedance of the cavity.

For two fields exited in cavity by beam and by generator, Lorenzt lemma gives additional to (1) relation:

$$-4m = k. \quad (2)$$

The expression for impedance Z can bee written in conventional form:

$$Z = -\frac{R_{sh}}{1+g+i\eta}, \quad (3)$$

where g is the cavity coupling with feeder and η is the cavity detuning. The system (1), (2) and (3) can be reduced to expressions for coefficients k and m:

$$k = \frac{k_0}{|k_0|}\sqrt{8R_{sh}g}\,\frac{1}{1+g+i\eta},$$
$$m = \frac{m_0}{|m_0|}\sqrt{\frac{R_{sh}g}{2}}\,\frac{1}{1+g+i\eta}.$$

The phase factors

$$\frac{k_0}{|k_0|} = -\frac{m_0}{|m_0|}$$

depend on position of equivalent representation cross section in feeder.

Simpler cavity description (see Fig. 2) can be reached by using the beam loading parameter

$$M = \frac{IR_{sh}}{V}. \quad (4)$$

It can be seen that real part of this parameter

$$\mathrm{Re}\,M = \frac{\frac{\mathrm{Re}\,IV^*}{2}}{\frac{|V|^2}{2R_{sh}}} = \frac{P_{beam}}{P_{walls}}$$

and imaginary part $\mathrm{Im}\,M$ presents the cavity detuning by beam. At Fig. 2,

ISBN 978-3-95450-125-0

STANDING WAVE RF DEFLECTORS WITH REDUCED ABERRATIONS *

V. Paramonov†, L. Kravchuk, P. Orlov, INR RAS, Moscow, Russia
K. Floettmann, DESY, Hamburg, Germany

Abstract

Deflecting structures are now widely used for bunch phase space manipulations either to rotate a bunch for diagnostics purposes or in emittance exchange concepts. Even though the field of the synchronous harmonic is aberration free, the higher spatial harmonics provide nonlinear additions to the field distribution, leading to emittance growth during phase space manipulation. For short deflectors Standing Wave (SW) operation is more efficient. The criterion to estimate the field quality is developed and applied in order to minimize aberrations in the total deflecting field. The solution for dispersion correction together with the optimization of the end cells is described too.

INTRODUCTION

Deflecting Structures (DS), originally introduced for bunch deflection and particle separation [1], are now mainly used to rotate a bunch either for short bunch longitudinal diagnostics, [2], or in emittance exchange optics or to increase the luminosity. For deflection the bunch center crosses the DS at the maximal deflecting field, i.e. $\phi = 0$, while for bunch rotation $\phi = 90^o$ is used.

Modern DS applications are transformations of particle distributions in six-dimensional phase space. A tool for a transformation should provide as minimal as possible distortions of the original distribution.

The framework for the treatment of deflecting fields has been laid in the 60's by introducing the basis of hybrid HE and HM waves, [4], [3], and some results and conclusions, with certain assumptions and approximations, have been derived.

Even the synchronous harmonic of a deflecting field is inevitably nonlinear. The nonlinearity vanishes with $\beta \to 1$ and the aberration free, ideal case is reached for $\beta = 1$ only. But in the total DS field are always higher spatial harmonics which are by their nature nonlinear. The nonlinear terms lead to emittance growth during phase space manipulations, which can become important for precise measurements of very low emittance beams, or in case of multiple DS crossing.

FIELD DISTRIBUTIONS ANALYSIS

A recipe for estimates of field aberrations can be based on the general properties of periodicity and linearity, [5].

In any periodical structure the distribution of each field component $E_j(r,z)$ in the beam aperture can be represented in the complex form

$$E_j(r,z) = \widehat{E_j(r,z)}e^{i\psi_j(z)} = \sum_n^n a_{jn}(r)e^{\frac{-i(\Theta_0+2n\pi)z}{d}}, \quad (1)$$

where $\widehat{E_j(r,z)}$ and $\psi_j(z)$ are the amplitude and phase distributions, $d = \frac{\Theta_0\beta\lambda}{2\pi}$ is the structure period, $a_{jn}(r)$ is the transverse distribution of the n-th spatial harmonics and Θ_0 is the phase advance. Spatial harmonics are essential at the aperture radius $r = a$ while higher harmonics attenuate toward the axis as

$$a_{jn}(0) \sim a_{jn}(a) \cdot exp(-\frac{4\pi^2 n}{\beta\Theta_0} \cdot \frac{a}{\lambda}), \quad |n| \gg 1, \quad (2)$$

where λ is the operating wave length. To estimate the harmonics in detail and 'in total', we use the parameters $\delta\psi_j(z)$ and Ψ_j at the axis $0 \le z \le d, r = 0$, [5]

$$\delta\psi_j(z) = \psi_j(z) + \frac{\Theta_0 z}{d}, \quad \Psi_j = max(|\delta\psi_j(z)|). \quad (3)$$

The total force on a charged particle - the Lorenz force

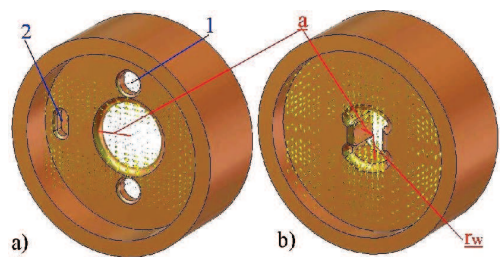

Figure 1: Structures with the minimized E_d aberrations, the optimized DLW structure (a) with holes for deflecting plane stabilization (1) and slots for dispersion correction (2) and the decoupled structure (b).

$\vec{F}^L$ - can be split in Cartesian coordinates into the longitudinal eE_z and the transverse eE_d components, assuming deflection in x direction,

$$\vec{F}^L_{z,x} = eE_z\vec{z}_0 + eE_d\vec{x}_0, E_d = E_x - \beta Z_0 H_y, Z_0 = \sqrt{\frac{\mu_0}{\epsilon_0}}. \quad (4)$$

Parameter Ψ_j can be used to estimate the level of harmonics (aberrations) both in the longitudinal eE_z, Ψ_z and in the transverse eE_d, Ψ_d force component.

The structures, obtained by optimizing aberrations, are shown in Fig. 1. Besides the well-known Disk Loaded Waveguide (DLW), Fig. 1a, a decoupled deflecting structure has been optimized. This structure follows the design idea of separated functions, see [6] for details.

* Work supported in part by RBFR N12-02-00654-a
† paramono@inr.ru

ISBN 978-3-95450-125-0

INVERSE COMPTON SOURCES ON THE BASIS OF ELECTRON ACCELERATORS WITH BEAM ENERGY RECOVERY

V.G.Kurakin, P.V.Kurakin, Lebedev Physical Institute, Moscow, Russia

Abstract

In inverse Compton Source, photons in Roentgen range originate from visible light laser photons scattered back on electrons with the energy of dozens MeV. Several schemes are suggested in the paper, beam energy recovery conception being the common idea of all of them. The first one is based on synchrotron with flat part of guiding magnetic field. Being accelerated, electron bunch interacts with photon bunch of free electron laser mounted on straight paths of the accelerator, then is decelerated during falling down period of magnetic field cycle, and extracted at low energy from synchrotron to absorb in beam dump. This measure decreases background that originates from bremsstrahlung of lost electrons inherent to classical schema with linear accelerator and storage ring. Two other schemes use superconducting linac that produces relativistic electron bunches which energy is recovered after use, free electron laser (FEL) driven by bunches from linac being used to produce photons bunches for source. In one scheme the same electron bunches are use to drive FEL and inverse Compton Source, while in the other one beam splitting technique is suggested. It is based on beam energy modulation with subsequent separation of successive bunches. The expected self excitation inverse Compton sources parameters are estimated followed by critical issues discussion for all schemes suggested.

INTRODUCTION

They say that back Compton scattering takes place when part of electromagnetic radiation is reflected backward by relativistic electron moving in the direction opposite to electromagnetic wave flow. In spite of low cross section of this process the devices based of this phenomenon find practical applications due to narrow spectrum of the radiation. The maximum energy of back scattered photons scales as square of electron energy thus allowing the radiation in Roentgen wave range obtaining scattering visible light on the electron bunch with the energy of several dozens of MeV. The availability of power lasers as well as charged bunch formation technique that came from accelerator based technique makes it possible Compton sources developing with intensities quite sufficient for applications.

Classical scheme of the light source based on the back Compton scattering represents optical cavity and electron storage ring arranged in such a way that these have an interaction point [1], one turn time circulations of electron bunch in storage ring and photon bunch in the cavity being synchronized to cross this point at the same moment. This arrangement is complemented by electron linac with injection system and a laser with appropriate cavity excitation system. The project based on this scheme had already realized successfully and might serve as prove of principle. It seems quite natural in further study and the development of such Roentgen source to move from oscillator scheme to self oscillator, and one of the main elements of existing equipment namely electron accelerator might be a basis for similar extension.

In this paper, we discuss the possibility to develop back Compton scattering source on the basis of free electron laser (FEL) and the energy recovery accelerator that drives this FEL. Three schemes are studied, one of these being built on the basis of electron synchrotron while two others on the basis of superconducting rf linac. In these schemes, electron bunches from an accelerator are used to drive FEL and to be a target for photons generated in the FEL. The critical issues of all schemes as well their advantages and shortcomings are discussed.

THE MAIN FEATURES OF FEL AND BACK COMPTON SCATERING

Fig.1 illustrates schematically back Compton scattering process. There is an incident electromagnetic wave of frequency ω with the energy density U_{ins} and relativistic electron with relative energy γ moving towards electromagnetic wave.

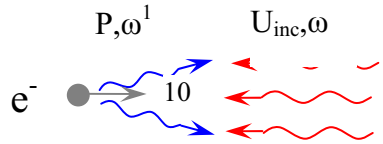

Fig.1 Back Compton scattering

The following formulae take place

$$\omega' \cong 4\omega\gamma^2,\ P \cong \frac{4}{3}\sigma_T c\gamma^2 U_{inc}. \qquad (1)$$

Here P is scattered wave power calculated per one electron, ω' is the frequency of scattered wave, c is light velocity and σ_T is so called Thomson cross section of an electron:

$$\sigma_T = \frac{8\pi}{3}\left(\frac{e^2}{m_e c^2}\right)^2 \approx 6{,}65\times 10^{-25}\,см^2, \qquad (2)$$

where e, m are the electron charge and its mass.

It follows from the above formulae that inferior limit of the total number of scattered photons might be represented in the form

$$N \cong \frac{\sigma_T}{3\sigma_{ph}} N_{ph} N_e, \qquad (3)$$

ISBN 978-3-95450-125-0

HELICAL 1T×1CM PULSED INSERTION DEVICES FOR PRODUCTION OF INTENSE POLARIZED X- & GAMMA-RAYS

A.V. Smirnov, RadiaBeam Technologies Inc., Santa Monica, CA 90404, USA

Abstract

Two types of high-field, pulse undulators are revisited as non-coherent or partially coherent sources capable of undulator factor approaching unity at substantial gap-to-period ratios exceeding 0.4 not achievable with conventional technology. One type is a microwave guide, smooth-wall undulator powered by wake-fields extracted with CLIC-type scheme adapted for the two-beam undulator (TBU). Another novel ID is represented here by a bifilar transmission line energized by a high voltage, ~ns-pulse, solid-state generator. These two devices fit well future linear colliders based on high-gradient microwave linac technology and radiation facilities respectively.

INTRODUCTION

Development of electron–positron colliders requires a source of intense polarized positron beams. Polarized positrons can be produced from polarized γ-rays irradiating a thin target (a fraction of radiation length [1]). One way is using of SC helical undulator having at least hundred meters length, limited period (<1.2cm), sufficient gap (>4–5mm), and field magnitude (>0.7T). Existing helical undulator technology is not failure-free and viable enough as requires close to critical currents (for SC undulators), has too small gaps (~1mm) implying bypassing, very limited section length because of low vacuum conductivity, gas bremstrahlung and radiation-induced desorption. Normal-conducting, pulse-current option is limited by heat deposition and pulsed power supply. Unique Cornell design [2] employs sophisticated ferrofluid cooling system and operates at <30Hz rep rate (12μs pulse length), whereas a normal-conducting linear collider operates at higher rep rates (about 100Hz).

Another possibility is photon backscattering on energetic electrons. The polarization of backscattered gammas is determined entirely by the polarization of incident electromagnetic radiation and changes a little with scattering angle or gamma-photon energy. A terawatt laser produces a deflecting force equivalent to several tens of Tesla of undulating field. However, the interaction length is limited by diffraction to about a centimeter [3]. Substantial problems [4] are related to multistaging, jitter, sustainability of optical elements, synchronized timing, dramatic reduction of the polarized gamma-photons yield for off-axis electrons.

Somewhat similar problems are related to development of IDs for intense polarized synchrotron radiation sources, applied, e.g., for circular dichroism studies.

In this paper, two novel concepts of a helical undulator are proposed: a microwave undulator powered by a microsecond- range wakefield extractor (two-team undulator, TBU), and a pulse-line undulator (PLU) powered by a ns-pulse, high-voltage source.

MICROWAVE UNDULATOR AS A PULSED, POLARIZED RADIATION SOURCE

A microwave undulator is especially suitable for long radiators of spontaneous X- and γ-ray emission. Such a waveguide-based ID does not need tapering (unlike FEL), can have shorter period and much better active/physical length ratio due to shorter interruptions (if any) compared to any conventional magnetic undulator. One can also provide a larger gap that exceeds considerably the equivalent undulator period (or operating wavelength in an oversized, open mm-wave guide [5]). It may have side openings (using open type structure) or evanescent slots/holes for better pumping and insertion of wakefield BPMs. The microwave undulator is perfectly compatible with superimposed focusing/correcting elements (quadrupoles and sextupoles). For a normal-conducting linear collider active cooling of the waveguide undulator is not a challenging problem due to larger aperture and lower power deposition than pulsed electromagnetic undulator (for the same pulse rate). Fore example, the ferrofluid-cooled, 1mm aperture, 1m length undulator consumes about a half kW power at 30Hz pulse rate [2], which is comparable to that for the two-wave undulator considered here at higher rep rates and much larger $5.6\times5.6\text{mm}^2$ cross-section at about the same peak field. Bypassing can be eliminated due to enlarged aperture and enhanced vacuum conductivity, super-imposed focusing, reduced period, and absence of undulator fields in the idle mode. That also means that the undulator physical length can be reduced from ~790m [1] down to ~150m making the physical and active undulator lengths equal.

And finally a waveguide undulator to be more robust and easier in manufacturing as the smooth-wall square or elliptical pipe tolerances are determined only by minimal reflection and insertion losses (about 1 mill tolerance at 30GHz) and the bremstrahlung radiation is less dangerous for the waveguide unlike magnetic undulators subjected to quench and/or degradation of the insulation undergoing to enormously high mechanical stress at strong X-ray and gamma-radiation background (~100MRad dose) and extremely low (for SC ID) or elevated temperatures (NC ID). On the other hand, the waveguide bremstrahlung may seed high–order multipactor to be taken into account in the design (including external magnetic fields).

ISBN 978-3-95450-125-0

HTS WIGGLER CONCEPT FOR A DAMPING RING

A. Mikhailichenko, Cornell University Ithaca, NY 14853, USA
A.V. Smirnov, RadiaBeam Technologies Inc., Santa Monica, CA 90404, USA

Abstract

Magnetic design proposed for a damping ring (DR) is based on second generation HTS cabling technology applied to the DC windings with a yoke and mu-metal-shimmed pole to achieve ~2T high-quality field within a 86 mm gap and 32-40 cm period. Low levels of current densities (~90-100A/mm^2) provide a robust, reliable operation of the wiggler at higher heat loads, up to LN_2 temperatures with long leads, enhanced flexibility for the cryostats and infrastructure in harsh radiation environment, and reduced failure rate compared to the baseline SC ILC DR wiggler design at very competitive cost.

INTRODUCTION

Damping rings (DR) play a crucial role in producing the beams of sufficient quality and stability in achievement both peak and integrated luminosity in a Linear Collider. The baseline technology choice for the ILC damping ring [1], but based on the design developed for the CESR-c program [2,3,4]. However, the low temperature superconducting (LTS) DR wiggler is subject to failures caused by the cryogenics, power supplies, control system, and by quench. Normal-conducting alternative appears to be the most robust against long-term radiation effects. However, it would require enormously high electrical power of MW order [5]) even for small 25-mm gap TESLA DR wigglers [5,6].

Hybrid, permanent magnet ILC DR wiggler prototype having 56mm gap and ~1.7T amplitude was designed [7]. The analysis showed technical feasibility to build a prototype of such a failure-free wiggler at zero maintenance cost. Cryogenic variant of the hybrid design may sustain much higher radiation levels and also substantial heat loads, [8]. The problem is mass production: the total amount of rare-earth material required for 160-200 m wiggler (76-172 tons dependently on grade and cooling) is comparable with global year production (~130 tons in 2010 and up to 250 tons in 2015 [9]).

High Temperature Superconducting (HTS) winding made from 2nd generation wires are considered here (Figure 1). With energy cost rising and conductor cost falling, HTS magnets operating in the 20-77 K° temperature range are gaining renewed interest for the lower cost of ownership (capital and operation). Moreover, in a few low to medium field R&D applications, HTS magnets not only provided a better technical solution but also proved to be less expensive to build and test than the magnets made with conventional LTS. In addition, HTS magnets can tolerate large energy and radiation loads and can operate with a simpler cryogenic system [10].

Bismuth Strontium Calcium Copper Oxide (BSCCO) HTS wire is referred to as Generation 1 conductor [11,12]. BSCCO wire requires relatively expensive batch production process and relatively high quantities of silver (<10% of the cost). Manufacturers are transitioning to and scaling up manufacturing capacity to produce YBCO coated conductors in a semi-continuous process [13,14]. The Generation 2 technology utilizes epitaxial growth, where films deposited on a prepared structure can assume the substrate's crystal orientation. Manufacturers planning large volume price reduction in to 50% to 20% of BSCCO. That would make it competitive with copper in many large industrial applications, putting aside the cost of cooling [15].

State-of-the-art Gen.-II wire (e.g., Amperium™ [14]) presents significant leap in technological improvements to build magnets. Engineering properties exhibit good fit to the ILC damping ring wiggler needs due to high strength and stability, hermetical solder fillets at the edges, high strength, and enhanced electrical stability, sufficient robustness, mechanical strength and bend tolerance. The 1.1-1.5cm bending radius of the wire tape is perfectly small enough to be used in 32 cm-period wiggler (though too large for some other insertion devices like short-period undulators).

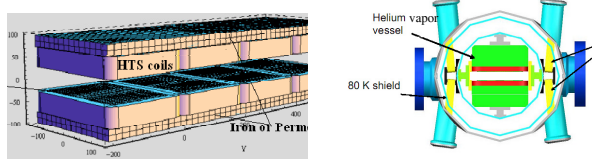

Figure 1: On the left: conceptual design of two periods of HTS wiggler. On the right: the cryostat schematics with a two phase Helium in the central chamber.

Robustness also means better sustainability to harsh radiation environment than conventional SC coils. Several HTS magnets (see, e.g., [16,17]) or insertion devices having HTS leads have been implemented [18]. Radiation-resistant dipole and quadrupole HTS magnets were developed for Rare Isotope Accelerator (RIA) [19].

MAGNETIC DESIGN

Different modifications of the Figure 1 design to accommodate both field-gap requirements (1.97T, 86mm) and HTS limits have been analyzed to achieve engineering (bulk coil) current density J in HTS wires, which is ~100A/mm^2 [20,21]. Permendur–based variant provides a viable design (see Table 1). Further

ISBN 978-3-95450-125-0

DUBNA-MINSK ACTIVITY ON THE DEVELOPMENT OF 1.3 GHZ SUPERCONDUCTING SINGLE-CELL RF-CAVITY

N.Azaryan#, J.Boudagov, D.Demin, G.Shirkov, JINR, Dubna, Russia
M.Baturitsky, V.Karpovich, N.Liubetsky, S.Maximov, V.Rodionova, BSU, Minsk, Belarus
S.Kolosov, A.Kurayev, A.Sinitsyn, BSUIR, Minsk, Belarus
V.Petrakovsky, I.Pobol, A.Pokrovsky, S.Yurevich, A.Zhuravsky, PhTI NASB, Minsk, Belarus
S.Demyanov, E.Kanyukov, SSPA SPMRC NASB, Minsk, Belarus
B.Kephart, L.Ristori, FNAL, Batavia, USA

Abstract

In 2011 Dubna-Minsk collaboration started an activity on the development and manufacture the series of superconducting niobium cavities in the enterprises in Belarus. First results of this work are presented.

Simulation code was developed to compute EM characteristics, and to calculate the shape and geometric dimensions of SC niobium RF-cavity taking into account higher order oscillations modes. The calculations of a single-cell and 9-cell cavity were made: the found ratio of the maximum electric field on the cavity axis to an average accelerating field is 2 within 1%; the found geometric factor equals 283 Ohm.

Half-cells will be made by hydraulic deep drawing and welded by electron-beam (EBW). A stamping tool for hydraulic deep drawing of the half-cells and a set of technological tools for probing of EBW of two half-cells have been designed. Mechanical properties of niobium and model material (Cu, Al) were investigated.

Cryogenic system for low temperature RF tests of the SC single-cell cavity was successfully tested at 4.2 K.

Coupling device for RF measurement of the single-cell SC niobium cavity was synthesized and manufactured – the measured standing wave ratio is about 1.01-1.07. Warm RF tests with etalon single-cell cavity were made: fundamental frequency – 1.273 GHz, quality factor (warm) – $28 \cdot 10^3$.

INTRODUCTION

Since 2007 Joint Institute for Nuclear Researches officially joined the ILC project and proposed Dubna site for ILC accelerator [1]. The key technology of the ILC is the accelerator that uses superconducting RF cavities for acceleration of electrons and positrons. R&D in superconducting radio-frequency technology is of a high priority and makes a global technical challenge for the R&D organizations worldwide.

Nowadays, in the framework of the ILC project, JINR laboratories perform several tasks. One important task is creation of series of superconducting niobium cavities in tight collaboration with the leading research centers of Republic of Belarus. First production series of 1.3 GHz superconducting niobium single-cell cavities will be manufactured in Minsk by 2015. After the tests in Minsk and Dubna these cavities will be presented to international ILC community for the expertise.

#azaryan@jinr.ru

COMPUTER SIMULATIONS

Group of specialists from Belarus State University of Informatics and Radioelectronics has developed a program package CEDR [2] for simulations and optimization of electrodynamic processes in non-regular RF systems including ohmic losses in the surface. The package allows finding all the electromagnetic characteristics of the single-cell and multi-cell RF cavity, and obtaining its optimal geometry and dimensions.

Table 1: Calculated EM characteristics of the cavity

Parameter	ILC requirements	BSUIR results
f_0	1.3 GHz	1.3 GHz
E_{peak}/E_{acc}	2	2.026
B_{peak}/E_{acc}	4.26 mT/MV·m	4.731 mT/MV·m
G	270 Ω	283 Ω
k_{sell}	1.87 %	1.94 %

RF-calculations of the main electromagnetic characteristics of a single-cell and a nine-cell cavity were made and higher order oscillation modes were investigated [3-5]. Thus, using the package, one can find the optimal shape of the cavity which provides maximum accelerating gradient on the cavity axis with minimal electric and magnetic field on the surface. The results of these computer simulations along with the ILC requirements [6] are presented in Table 1. In the Fig.1 we present the conceptual sketch of the calculated half-cell being the base detail for cavity manufacturing.

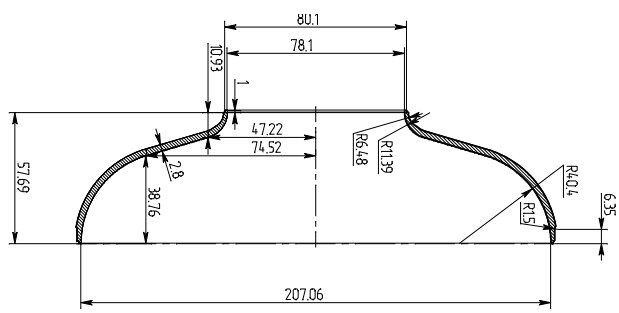

Figure 1: Conceptual draw of the half-cell.

ISBN 978-3-95450-125-0

THE QUENCH DETECTION SYSTEM FOR SUPERCONDUCTING ELEMENTS OF NUCLOTRON ACCELERATION COMPLEX

E.Ivanov, A. Sidorin, G. Trubnikov
JINR, Dubna, Moscow Region

Abstract

New quench detection system for Nuclotron is described. The system provides highly effective detection of quenches in superconducting elements of Nuclotron. Full information about quench element is transmitted to control room. Diagram of analogue quench signal could be displayed on screen for further analysis. The system performs scheduled self-test diagnostics in real time and controls power elements of energy evacuation.

INTRODUCTION

Cryogenic magnetic system of the Nuclotron accelerator facility consists of the Nuclotron ring and measurement superperiod [1]. The last one includes four dipole and four quadrupole (two focusing and two defocusing) magnets. The Nuclotron ring includes 96 structural dipole magnets, 64 structural quadrupole magnets, two lambertson magnets and four quadrupole magnets of slow extraction system, inflector magnet of the injection system and a few tens of dipole, sextupole and oqtupole corrector magnets. Quench protection of the corrector magnets is provided by individual low current supply units. Quench protection system of all other elements is based on energy evacuation system including thyristor power switches and dump resistors. Status of the magnets is monitored by quench detectors based on a bridge scheme. For main part of the magnets the arms of the bridge are formed by inductivity of the coils of nearest identical magnets (dipole, quadrupole or lambertson), the balancing resistor is located outside the cryostat (Fig. 1).

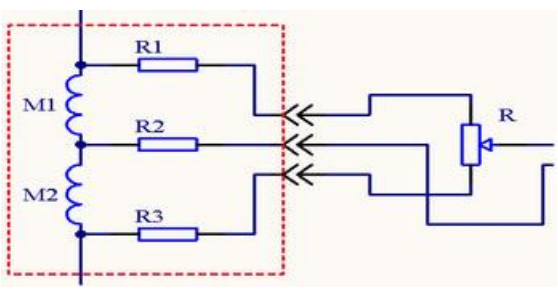

Figure 1. Scheme of the Voltage comparison: M1 and M2 – coils of nearest identical magnets, R1 – R3 – protective resistors, R – balancing resistor.

Currents of four structural dipole magnets, which are used to provide an orbit bump in the slow extraction area, are adjusted by additional suppliers. The quadrupole magnets of the slow extraction system are supplied individually also. For these magnets, and for inflector magnet of the injection system, the bridge arms are formed by two halves of the magnet coil using potential feed through.

First quench detection system at the Nuclotron was created in the end of 80-th. In reality it was full scale prototype which was in operation during about 15 years without serious modifications. The system of the quench detector monitoring and control became outdated and obsolescent. In 2007 the modernization of the accelerator facility was started in order to prepare the Nuclotron as an element of an injection chain of heavy ion collider creating in the frames of the NICA project [2]. One of the goals of the Nuclotron upgrade was to provide safe and stable operation at maximum design magnetic rigidity, that corresponds to 2 T field of the dipole magnets. New power supply and energy evacuation systems are successfully tested at this field during the Nuclotron run #42 (December 2011) [3]. Creation of new quench detection system is in the final stage now. This system based on modern technical and design solutions is described in this paper.

DESCRIPTION OF THE SYSTEM

The new quench detection system was designed on the basis of serial interfaces: all the detectors are connected to the common CAN bus used for information exchange. This solution permits to change operatively number of detectors, to work uniformly with group and individual detectors and realize total reservation of the line controlling the energy evacuation system. The system provides monitoring of current status of all its elements, signals testing of external systems and indication of malfunctions. Such a design requires more complicated electronics but sufficiently simplifies operative service and improves reliability of the operation.

General element of the system is quench detector aiming to compare two signals in order to detect a change of one of them due to appearance of active component of resistance after loss of the superconductivity.

Peculiarity of the quench detector design relates to the requirement that each detector has to be galvanically insulated from common ground circuits as well as from other detectors. Parasitic leakages in the electrical circuits of the accelerator have to be avoided as well. Accordingly the detector consists of two constructive parts: insulated from the ground, which detects and amplifies an input signal, and grounded part, at which the obtained signal is processed, analyzed and so on. Insulated and grounded parts are connected using insulated analog amplifier.

ISBN 978-3-95450-125-0

BEAM POSITION MONITOR SYSTEM FOR 2 MEV ELECTRON COOLER FOR COSY

E.A. Bekhtenev, V.P.Cherepanov, G.V. Karpov, V.B. Reva, E.I.Shubin, D.N. Skorobogatov
Budker Institute of Nuclear Physics, Novosibirsk, Russia

Abstract

The 2 MEV electron cooler for COSY storage ring FZJ is assembling in BINP. Beam position monitor (BPM) system for orbit measurements has been developed and fabricated at BINP. The system contains 2 BPMs inside the cooling section and 10 BPMs in transport channels. Continuous electron beam is modulated with a 3 MHz signal for capability to get signals from pickup electrodes. The beam current modulation can be varied in the range of 0.3-1.5 mA. The BPMs inside the cooling section can measure both electron and proton beams. It is achieved by means of switching the reference signals inside the BPM electronics. The BPM electronics provides highly precise beam position measurements. Position measurement error doesn't exceed 1 micron. Design features of the BPM system, its parameters and testing results are presented in this paper.

INTRODUCTION

The 2 MEV electron cooler for COSY storage ring FZJ has been designed and assembled in BINP [1, 2]. Beam position monitor (BPM) system consists of 12 BPMs and electronics. 2 BPMs are located inside the cooling section. 10 BPMs are located in transport channels. Continuous electron beam current is modulated with a ~3 MHz signal for capability to get signals from BPM electrodes. Some parameters of cooler and main BPM system requirements are presented in Table 1.

Table 1: Main requirements to BPM system

Electron current	0.1-3 A
Modulation amplitude of electron current	0.3-1.5 mA
Proton current	0.1-2 mA
COSY RF frequency	~0.5-1.5 MHz
Position measurement error	less than 100 μm
Measurement rate	0.1-1 sec

To achieve the best cooling effectiveness electron and proton beams must be aligned inside the cooling section with accuracy better than 100 μm. This condition requires simultaneous measurements of electron and proton beams position by 2 BPMs located inside the cooling section. 10 BPMs in the transport channels measure only electron beam position. A new feature of the gun four-sector control electrode allows measuring not only electron beam position but the beam shape and rotation [2].

SYSTEM STUCTURE

The structure chart of the BPM system is presented in Fig. 1.

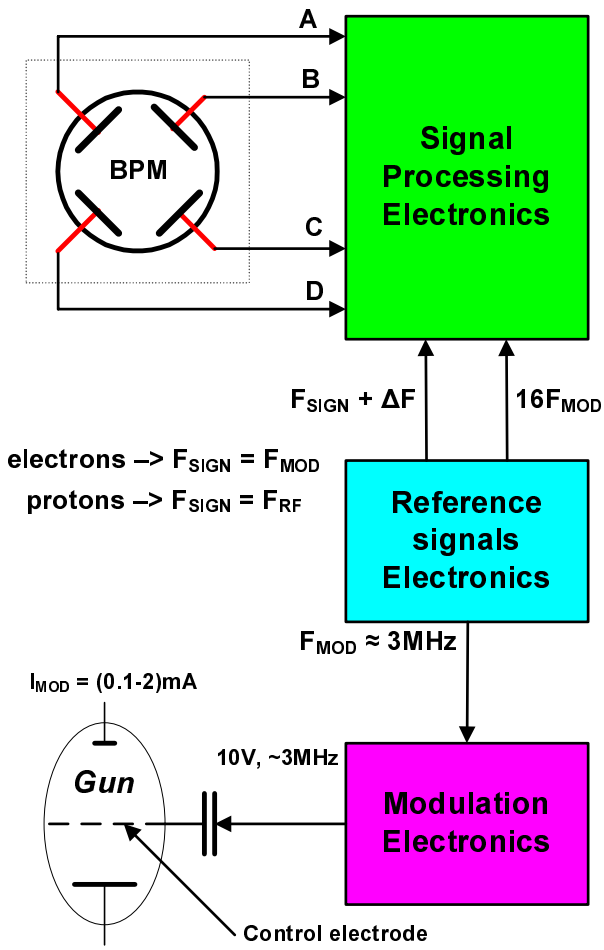

Fig.1. The structure of the BPM system.

The system consists of 12 BPMs, Signal Processing Electronics, Modulation Electronics and Reference signals Electronics. The four-electrode electrostatic BPM for transport channels is represented in Fig.2.

Modulation Electronics provides electron beam current modulation with frequency F_{MOD} ~3 MHz. Signal Processing Electronics measures the beam signals amplitude at each of four BPM electrodes. The measurement is based on synchronous detecting of the BPM signal with frequency F_{SIGN}, which equals F_{MOD} for electron beam and F_{RF} for proton beam. The sinusoidal

ISBN 978-3-95450-125-0

FAST TUNE MEASUREMENT SYSTEM

E.A. Bekhtenev, V.P.Cherepanov, G.V. Karpov, A.S.Styuf
Budker Institute of Nuclear Physics, Novosibirsk, Russia

Abstract

Tune measurement system developed in Budker Institute of Nuclear Physics provides fast and accurate measurements of fractional part of betatron tunes in electron-positron storage rings and accelerators.

The tune measurements rate can achieve 1 kHz. It is especially important for electron-positron accelerators to have tunes measurement data for each phase of accelerating cycle.

The developed system is planned to be installed at the NSLS-II Booster Synchrotron. The system can perform up to 330 measurements during 300ms time interval of Booster energy ramping. The kicking technique is used as measurement method. The kicks are carried out by a radio frequency (RF) pulses. Each RF pulse contains two frequencies and thus can simultaneously excite the horizontal and vertical betatron oscillations.

All signal processing including FFT is performed inside FPGA. The tune measurement accuracy is better than 0.0005.

The developed system was put into operation at the February 2011 in VEPP-3 electron-positron storage ring at BINP.

INTRODUCTION

Booster synchrotron for third generation synchrotron light source NSLS II is presently under construction in BNL, USA [1]. The Booster main parameters are given in Table 1.

Table 1: Main parameters of the NSLS II Booster

Beam energy injection/extraction	200 MeV/3 GeV
Repetition rate	1 Hz (2 Hz)
Revolution frequency F_0	1.894 MHz
RF frequency	499.68 MHz
Betatron tunes: ν_x/ν_y	9.6455 / 3.4105
Beam current	1-30 mA
Energy ramping time	300 (150) ms

Requirements to Tune measurement system (TMS) for the Booster synchrotron are:

- Tune measurements rate has to be up to 1 kHz
- Tune measurements accuracy has to be better than 0.5×10^{-3}.

TMS satisfied to these requirements has been designed and fabricated at BINP. The system includes two identical sets of of four 50-Ω striplines and TMS electronics. One set is a Kicker for beam excitation; another one is a Pickup for measurement of a beam response signal.

The system uses the kicking method for tunes measurement. The beam is excited by radio frequency (RF) pulse with the frequency f_e close to $f_B = (1 - \nu_{x,y})f_0$, where f_0 is the revolution frequency, $\nu_{x,y}$ – is the fractional part of the horizontal (vertical) tune. Duration of the RF pulse is 100-200 μs. The measurements are possible when the difference between frequency f_e and betatron frequency $(1 - \nu_{x,y})f_0$ does not exceed $(0.01\text{-}0.02)f_0$. In this case, the signal of the beam betatron oscillations is received by the stripline pickup after the end of the exciting RF pulse. Then the signal is transferred to the signal processing electronics, where it is sampled by ADC and is processed by a Field Programmable Gate Array (FPGA) circuit. The result of signal processing is the values of $\nu_{x,y}$.

SYSTEM STUCTURE

The structure chart of the Tune measurement system is presented in Fig. 1.

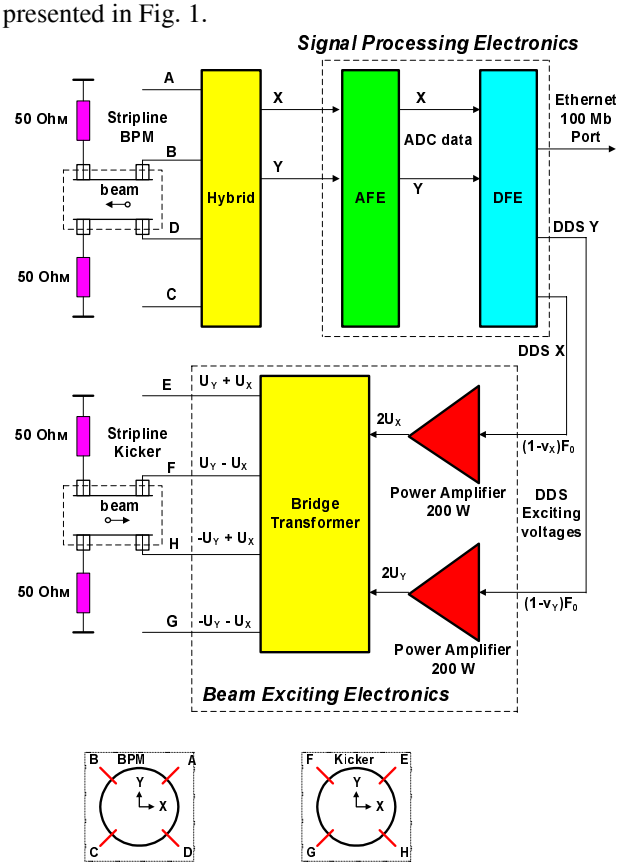

Fig.1. The structure of the Tune measurement system.

The system consists of Pickup, Kicker, Hybrid, Signal Processing Electronics and Beam Exciting Electronics. The Pickup and Kicker stripline electrodes are mounted at

ISBN 978-3-95450-125-0

NEW BEAM POSITION MONITOR ELECTRONICS FOR VEPP-5 PREINJECTOR

G.V. Karpov, A.S.Styuf, Budker Institute of Nuclear Physics, Novosibirsk, Russia

Abstract

A new beam position monitor (BPM) electronics has been designed, manufactured and tested in VEPP-5 preinjector. Preinjector BPM system measures position of single electron and positron bunches for each injection cycle. New BPM electronics provides more high sensitivity with respect to existing one developed in 2004. The system can measure the position of bunches with 10^8 - 10^{10} particles per bunch. The resolution of measurements of single bunch is better than 10 μm for 10^{10} particles per bunch. The features of BPM electronics design, the main parameters and results obtained in VEPP-5 preinjector are presented.

INTRODUCTION

It is planned to put VEPP-5 preinjector [1] into regular operation in 2012. The preinjector produces electron and positron bunches with main parameters given in Table 1.

Table 1: Main parameters of the preinjector

Number of electrons in a bunch	$(2\text{-}3)\times10^{10}$
Number of positrons in a bunch	$(2\text{-}3)\times10^{8}$
Longitudinal bunch size	4 mm
Repetition rate for electrons for positrons	 1 Hz 50 Hz

The preinjector includes 300 MeV electron linac, conversion system and 510 MeV positron linac [1]. Existing Beam position monitor (BPM) system developed and fabricated in 2004 consists of 14 stripline BPMs and electronics [2]. The main problem with this system operation is insufficient position measurement accuracy of the positron bunches due to low signal-to noise ratio caused with interferences on the cables connecting BPMs with electronics. New BPM electronics developed in 2012 has signal-to noise ratio at least in one order better than old one. This improvement is achieved with help of two main changings:

- increasing of processing electronics bandwidth;
- decreasing of the timing circuit jitter.

Signal processing used in both new and old systems is low pass filtering. Signal amplitude at the Low Pass Filter (LPF) output U_{LPF} strongly depends on the LPF cut-off frequency F_{LPF}. In Fig.1 calculated dependence of the U_{LPF} value on the F_{LPF} for our sripline BPM signal is represented. In low frequency domain the signal amplitude grows with increasing of F_{LPF} almost as square of F_{LPF} value whereas the noise r.m.s. amplitude grows as square root of F_{LPF}.

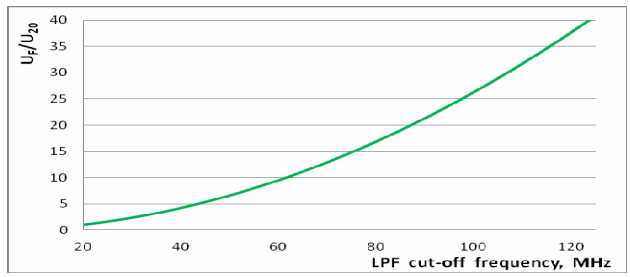

Fig.1. Calculated dependence of the relative signal amplitude in the LPF output U_F / U_{20} on the F_{LPF}.

In new electronics we have chosen F_{LPF} = 120 MHz. It is in 6 times more compare with old electronics. It gives a gain in signal-to-noise (S/N) ratio approximately in 15 times. Taking into account that main part of interference power is located in frequency domain 1-20 MHz total increasing of S/N ratio is more considerable. But increasing of the signal processing bandwidth imposes more hard requirements to jitter of the ADC clock signal. Therefore main efforts were applied to this aspect.

BPM ELECTRONICS STRUCTURE

A functional diagram of the new BPM electronics is presented in Fig. 2.

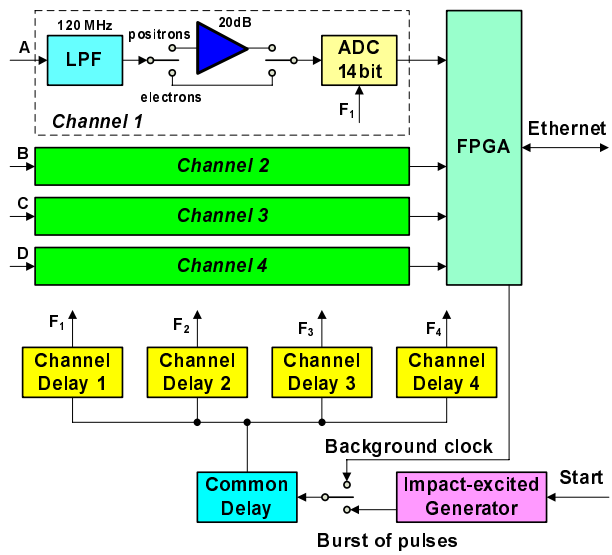

Fig.2. A functional diagram of the new BPM electronics.

The Electronics consists of four identical signal processing channels, timing circuit and FPGA. Signal processing channel contains LPF, switched amplifier and 14-bit ADC. The BPM signals are amplified by fixed gain

ISBN 978-3-95450-125-0

MULTIMODE DIGITAL INTEGRATORS FOR PRECISE MAGNETIC MEASUREMENTS

A. Batrakov, A. Pavlenko, D. Shickov, BINP, Novosibirsk, Russia
P. Vagin, DESY, Hamburg, Germany

Abstract

Increasing demands of the accelerator techniques and modern electronics capabilities stimulate the creation of more accurate and fast instrumentation, based on the induction method. This report describes multimode integrators VsDC2 and VsDC3 (**V**olt-**s**econds to **D**igital **C**onverter), intended for precise measurements of the magnetic fields, both pulsed and constant. These integrators utilize new, digital integration method, which allows reaching accuracy close to the 10^{-5}.

INTRODUCTION

The induction method of magnetic measurements is the most important, widely used and oldest measurement method for particle accelerator magnets. This method generally requires integration of an input signal. In recent years, two types of the integrators have been developed in Budker INP (Russia). These devices are based on the digital integration method. Integrators provide high accuracy both for the constant magnetic field measurements using movable coils and for the pulsed measurements also. It is possible to achieve relative accuracy better than the 10^{-4} and even better than the 10^{-5} in special cases.

DIGITAL INTEGRATION METHOD

The digital integration method is shown in Figure 1.

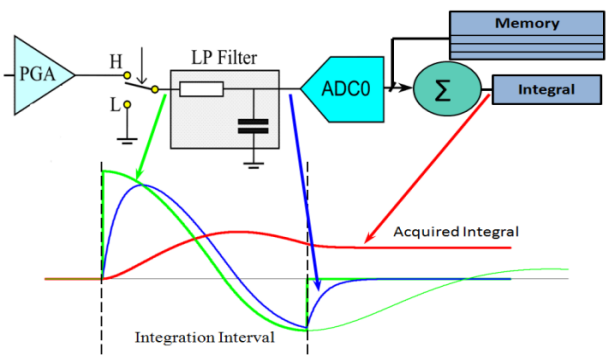

Figure 1: Digital integrator stricter and signal passing.

An input signal is converted to appropriate scale by preliminary amplifier with programmable gain (PGA). The integration interval is determined by the fast analog switch. During integration interval the scaled input signal passes through the switch to the low pass (LP) filter input. Remaining time LP filter is connected to ground. The required integral equals to volt-second square of the signal shaped by the analog switch. After LP filtering the signal is converted to the digital form by the ADC.

Let's mention, that similar structure one may found out in the device FDI2056 [1], but the last one doesn't contain the fast switch and LP filter, which are principal elements in the described integrators.

It should be noted that LP filter does not change integral of the incoming signal. Let's show it. Suppose that input signal *f(t)* is non-zero only in the interval from 0 to τ. This signal spectrum equals to:

$$S_{in}(\omega) = \int_{-\infty}^{\infty} f(t)\cdot e^{-j\omega t}dt = \int_{0}^{\tau} f(t)\cdot e^{-j\omega t}dt\ .$$

Note that spectral component at zero frequency equals to required integral. It is known that the LP filter output is given by:

$$S_{out}(\omega) = K(\omega)\cdot S_{in}(\omega)\ .$$

Where $K(\omega)$ is the filter transfer function. So the output integral equals to the required one if the LP filter has unity transfer function value at zero frequency:

$$\int_{0}^{\infty} f_{out}(t)dt = S_{out}(0) = S_{in}(0) = \int_{0}^{\tau} f(t)dt\ .$$

Digital integration method implies that the signal integral is calculated by summing ADC samples multiplied by the ADC time quant. Consider now the accuracy of continuous integral interpolation by the sum of discrete samples. Suppose that the LP filter limits the incoming signal spectrum to half the ADC sampling frequency. Therefore, according the Kotelnikov theorem [2], the continuous input can be precisely interpolated by a digital string as:

$$f(t) = \sum_{n=-\infty}^{n=+\infty} f(nT_s)\,\mathrm{sinc}\left(\pi\frac{(t-nT_s)}{T_s}\right).$$

Hence, for input signal integral we can write:

$$\int_{-\infty}^{+\infty} f(t)dt = \int_{-\infty}^{+\infty} dt \sum_{n=-\infty}^{n=+\infty} f(nT_s)\,\mathrm{sinc}\left(\pi\frac{(t-nT_s)}{T_s}\right).$$

Changing summing and integration order and integrating we obtain:

$$\sum_{n=-\infty}^{n=+\infty} f(nT_s)\int_{-\infty}^{+\infty}\mathrm{sinc}\left(\pi\frac{(t-nT_s)}{T_s}\right)dt = \sum_{n=-\infty}^{n=+\infty} f(nT_s)\cdot T_s$$

i.e. in the case of the ideal filter and infinite discrete sequence the required integral exactly equals to the digital sum.

It is impossible to satisfy these conditions strictly in the real device. Therefore, high theoretical accuracy of digital

ISBN 978-3-95450-125-0

THE SYSTEM FOR CONTROL OF AN ELECTRON BEAM WELDING MACHINES

V.V. Repkov, E.A. Kuper, A.U. Protopopov, A.A. Zharikov,
Budker Institute of Nuclear Physics, Novosibirask, Russia

INTRODUCTION

A cathode unit of electron beam welding is a device that generates beams of electrons of required intensity.The report examines the main issues, that had to be overcome in developing this unit.

-the electronics of the unit is under cathodic potential of the accelerating voltage (60kV), therefore it required solving the problem of power transmission and control signals.

- the volume of the device had to be minimized as the room to put the electronics was limited.

- the electronics must be resistant to high voltage breakdowns as when breakdowns there may be a voltage pulse of 60 kV with energy to 20 J in any electrode of the cathode unit.

- to control the current of the electron beam (welding current), a linear amplifier, which produces the voltage on the control electrode in the range 0 – 4kV, was developed. The amplifier bandwidth is 1 kHz.

- to control the current beam, current intensity, and to control the parameters of the gun, a specialized controller was developed. The connection of the controller with a computer is carried out with the help of optical links.

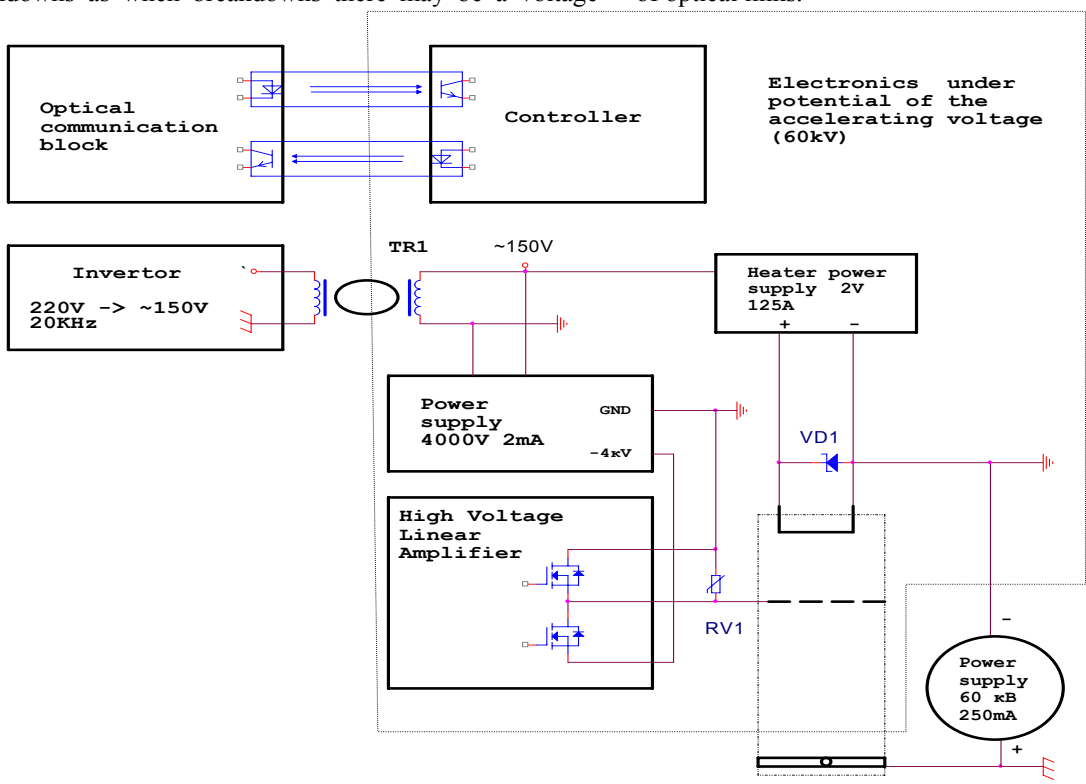

Figure 1: Block diagram of the electronics of the cathode unit.

TRANSFORMER

Power required to operate the power supply is passed through a special isolation transformer TR1. Voltage of isolation between the primary and secondary windings of the transformer is 100kV.

Transmission capacity is up to 300W. The transformation ratio is 1:1. It should be noted that the voltage between the primary and secondary windings is 60 kV, so structurally transformer consists of two cores. The primary winding was wound on one core, the secondary winding is on the other one. Coupling between cores is carried out by the volume coil. It is easier to provide high-voltage isolation.

CONTROLLER

Management of all parts of the unit is carried out by a specialized controller made with a microprocessor ADUC 842.

The controller sets the following parameters:

- The current gun (welding current), is set during the welding process in the range of 0 - 250 mA. The

ISBN 978-3-95450-125-0

OPTIMIZATION OF THE NEGATIVE HYDROGEN ION BEAM INJECTION INTO THE TANDEM ACCELERATOR WITH VACUUM INSULATION

A. Makarov#, V. Aleynik, A. Kuznetsov, I. Sorokin, S. Taskaev, M. Tiunov,
BINP SB RAS, Novosibirsk, Russia,
Bashkirtsev, I. Shchudlo, Novosibirsk State Tehnical University, Russia

Abstract

The beam of negative hydrogen ions is injected into the tandem accelerator with vacuum insulation in order to obtain high-current proton beam. To accurately direct the beam into the accelerator the magnetic focusing lenses are used. In this paper it is described the design of the special beam detector mounted in front of the first accelerating electrode and intended to measure beam profile and the current density. The results of measurements of the dependence of the current density on the power of the magnetic focusing lenses are shown. The parameters of the beam resulting in the best agreement of calculation and experiment are specified. The optimum focusing mode to inject the negative hydrogen ions into the accelerator is determined.

INTRODUCTION

Negative hydrogen ions are injected into the accelerator and accelerated up to 1 MeV by potential applied to the electrodes, then H^- turn into protons in the charge-exchange target and at last the protons are accelerated up to 2 MeV by the same potential [1].

Although the accelerator is designed to obtain a 5 mA proton beam, but in the experiments carried out in 2008-2010 we usually got the proton beam currents of hundreds of microamperes, and occasionally for a short time - a few milliamps. Such a current was enough to demonstrate the generation of neutrons [2] and monochromatic gamma-quanta [3], but it is clearly not sufficient for the thorough BNCT research and other applications.

To clarify current-limiting reasons, a detailed study of the transportation of negative hydrogen ions have been carried out using multichannel detector mounted in front of the first accelerating electrode of the accelerator.

EXPERIMENTAL SETUP

The scheme of the experiment is shown on Fig.1. Negative ion beam with energy of 21 keV, current up to 5 mA and angle distribution of 100 mrad is created by surface-plasma source with Penning discharge and hollow cathode. After turning at an angle of 15 degrees the peripheral part of the beam is cut off by 28mm cone diaphragm and the rest center of the beam enters into the transport channel.

Next, the expanding beam is focused by two magnetic lenses. Each of the magnetic lenses is powered by an independent power supply and currents of lenses may be different, but in our experiments they were set the same and opposite. For a typical current of 50 A maximum magnetic field on the axis of the lens has a value of 2.1 kG. Following the lenses it is installed magnetic corrector. Each of the two elements of the corrector consists of two pairs of coils, powered by independent power sources. The angular displacement of the beam from each pair of coils is characterized by 10 mrad/A.

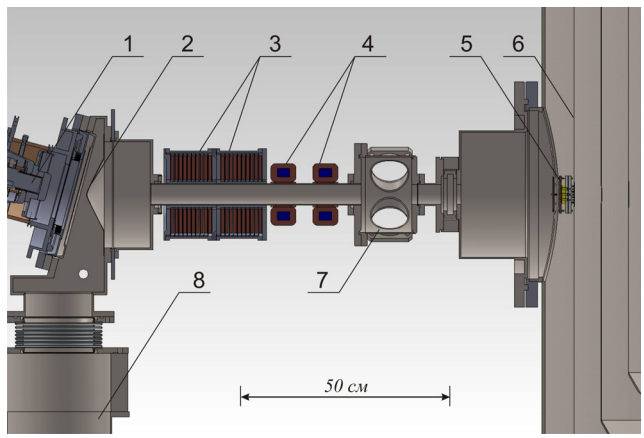

Fig. 1. Experimental setup: 1 - the source of negative hydrogen ions, 2 - cone aperture, 3 - magnetic focusing lenses, 4 - corrector, 5 - beam detector, 6 - the first electrode of the accelerator, 7 - diagnostic chamber, 8 - TM pump.

Focused and corrected the beam then strikes the detector mounted in front of the accelerator so the surface of the beam receiver is 47 mm in front of the surface of the first electrode. The detector is centered along the transporting channel using a laser (Fig. 2).

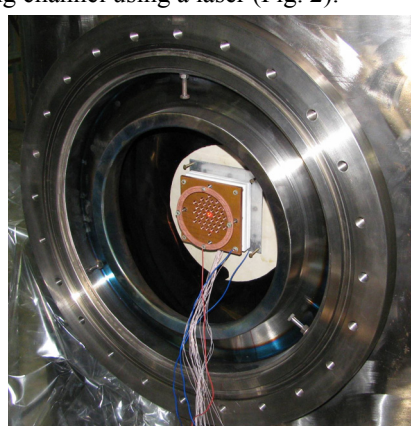

Fig. 2. Photo of the beam detector.

ISBN 978-3-95450-125-0

DEVELOPMENT OF THE NEW CONTROL SYSTEMS FOR JINR e- LINAC ACCELERATOR TEST-BENCH

M.A. Nozdrin#, N.I. Balalykin, V.F. Minashkin, V.Yu. Schegolev, G.D. Shirkov, G.V. Trubnikov,
JINR, Dubna, Russia

Abstract

Linear accelerator test-bench in the Joint Institute for Nuclear Research is based on the part of the accelerator complex which was transferred to the possession of JINR by The National Institute for Subatomic Physics (NIKHEF, Amsterdam). Analysis of the transferred accelerator equipment has shown that full re-engineering is required for its control systems; all other systems are in good condition and have considerable endurance. Results of development and creation of the Electron Gun Control System (EGCS), Video and Analog Signals Control System (VASCS) and Automatic System of Radiation Safety Control (ASRSC) are presented. These systems allowed achieving a commissioning of the first accelerator section of the bench with current of 3 mA in 1 μs pulse and at beam energy of 23-25 MeV.

INTRODUCTION

JINR linear accelerator test-bench is based on the so-called Medium Energy Accelerator (MEA) equipment. MEA [1] was developed by Haimson Research Corporation (USA) in 1969-1974, built in 1975-1978 and put into operation in 1978. In the end of 1990s the accelerator complex was transferred to JINR.

A set of projects for realization of the base of the test-bench is proposed:

- Free electron lasers (FEL) complex. Test-bench construction allows beam extraction with energy of 15 to 200 MeV. Beam with such energy can be used for infrared to ultraviolet FEL radiation generation with wavelength of 300 μm to 200 nm. First undulator of the IR range (transferred to JINR by NPO of automatic systems, Samara; E = 25 MeV, λ = 18.7 μm) is going to be installed.
- Testing of the accelerating structures and diagnostics, e.g. intensity monitors for short-pulse facilities like ILC [2]. This issue may require replacement of the current gun by the photocathode gun.
- Volume FEL with centimetric to infrared energy range creation [3].
- Experiments with RF gas discharge in quasi-optical cavity to confirm nuclear fusion in resonant streamer. [4]

At the present time the injector (composed of electron gun, chopper, prebuncher and buncher) and the first accelerating section are assembled and put into operation. Schematic view of this setup is presented in Fig. 1.

Most of the transferred control systems were obsolete and complete renewal of control equipment was needed. Results of the development of the new control systems are described in this paper.

ELECTRON GUN CONTROL SYSTEM

Triode type DC electron gun [5, 6] with an impregnated thermionic cathode (W with 20% Ba, Ca and Al oxides) is being used at the test-bench. Gun focusing system consists of extractor electrode and 15 anodes with forced resistive (R = 200 MΩ) potential distribution (about 30 kV per interval). The voltage of the first focusing electrode can vary from 12 to 30 kV. Electron gun control system (Fig. 2) consists of following components:

- ICT (Insulating Core Transformer) power supply unit provides cathode voltage of -400 kV with stability of $10^{-4} – 10^{-5}$.
- Cathode electronics unit allows remote control of the gun.
- Computer with the GunCtrl program provides interface with the cathode electronics.
- Communication line consists of protocol converters and fibre-optic cables.

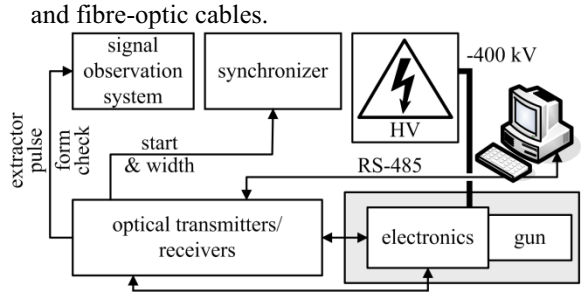

Figure 2: Scheme of the Electron Gun Control System.

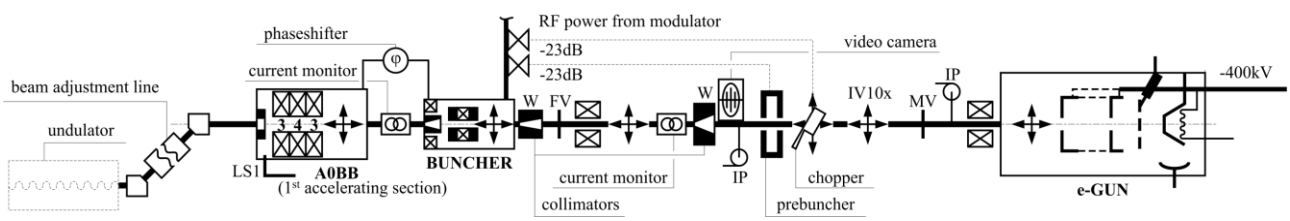

Figure 1: Schematic view of the injector and 1st accelerating section.

#nozdrin@jinr.ru

ISBN 978-3-95450-125-0

PRECISION THERMOSTATIC CONTROL FOR LUE-200 ACCELERATOR SECTION

V.N. Zamriy, A.P. Sumbaev, JINR, Dubna, Russia

Abstract

A two-loop thermostating system for the accelerating section of the S-band electron linac has been developed. To provide the required heatsink path and an opportunity of re-changing the section while altering the acceleration mode, the temperature in the system of the thermostat and the cooling water channel in the external contour are regulated. To achieve the required precision and stabilization time of the temperature of the thermostat having extended waterways (~70 m), the method of proportional-integral-derivative (PID) control has been applied. The programmed controller allows one to adapt the system for several operating modes: the fast warming up, operated establishment of temperature and thermostabilization, change of the preset temperature of the thermostat. It provides the reduction of setting time of the thermostatting regime, and also of minimization of errors and power consumption of the thermostat.

INTRODUCTION

The LUE-200 linac based on the traveling wave (2856 MHz) is used in IREN installation as the driver of a pulse photoneutron source [1]. For the LUE-200 thermal energy losses on RF-warming up of walls of the accelerating structure are about 30% of RF-power reached from the klystron, and in dependence on the repetition rate of cycles the losses can reach 10÷12 kW. The change of a of the accelerating structure temperature mode leads to displacement of its resonant frequency that results in the following: decreasing the mean energy of the accelerated electron beam, increasing the beam energy spread out and, eventually, decreasing the intensity of the neutron flux of the source. Influence of fluctuations of the temperature on the electron beam and, as a result, on the intensity of neutron flux is illustrated in Figs. 1 and 2, that was observed while adjustment of the accelerating section. Fluctuations of intensity of the neutron flux (Fig. 2) correlate on time with temperature deviations ±0.3°C (Fig. 1), repeating with a period of time of ~10 minutes.

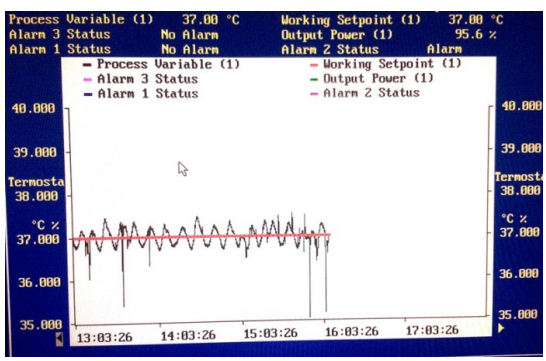

Figure 1: Fluctuation of the thermostat temperature.

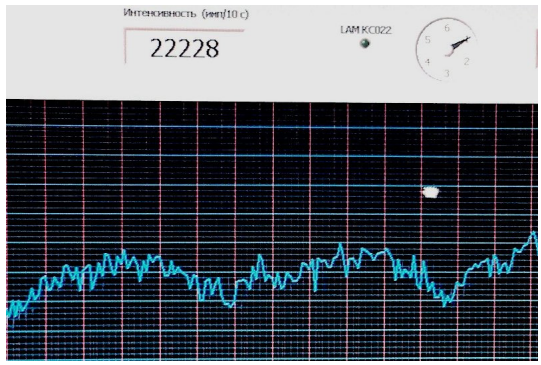

Figure 2: Fluctuations of neutron intensity.

THERMOSTATIC CONTROL SYSTEM

The Structure Chart of the Thermostatic Control

The structure of system of the thermostabilized cooling for the accelerating section is presented in Fig. 3.

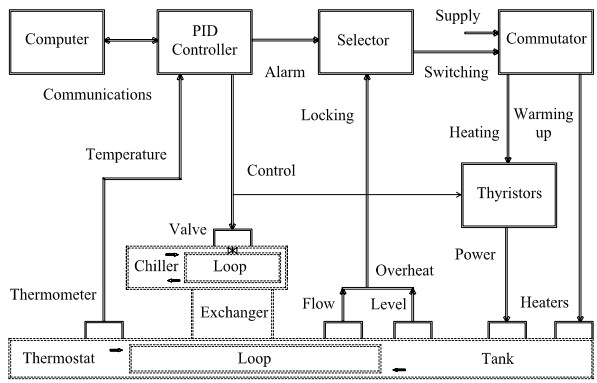

Figure 3: The system of thermostatic control.

The thermostat loop connects a tank of water heating, the thermostat, the heat exchanger, and also the built-in detector showing the lack of the water flow. The thermometer is installed at the exit of the pumped water from the thermostat. In the tank there are heaters and sensor controls of emergency overheating and the water level. The cooling loop joins a linac chiller and the heat exchanger, and, also, the built-in valve and the electric drive. Besides, the equipment for water mains has casual valves, pumps, etc.

The PID-controller (type 906S Eurotherm Controls) has measurement lines with the Pt-resistance thermometer and a control line. At the length of lines (~ 70 m) under the conditions of high-intensity noises the raised interference protection of the control unit is provided. The

ISBN 978-3-95450-125-0

ACCELERATION OF LOW-CHARGE KRYPTON IONS IN THE CYTRACK CYCLOTRON

Yu. N. Denisov, G. A. Karamysheva, O. V. Karamyshev
Joint Institute for Nuclear Research, Dubna, Russia

Abstract

The basic results of numeric simulations of krypton ion motion with decreased charge in the CYTRACK cyclotron are presented. CYTRACK is the world's first industrial cyclotron dedicated to the production of track membranes. Computer modeling confirms the possibility of ion acceleration in the magnetic field with an increase in the level of the magnetic field by 1.6% on the 6 harmonic of the accelerating system. The beam energy will be sufficient for the exposure of a film with a thickness of 10 μm.

INTRODUCTION

The CYTRACK cyclotron [1], designed to irradiate polymer films used in the production of separating and filter elements for medical, industrial, and domestic purposes, was devised and manufactured at the Joint Institute for Nuclear Research. This cyclotron is intended for the acceleration of heavy ions with $A/Z \approx 5$ up to the energy 2.4 MeV/nucleon.

CYTRACK was commissioned in August 2002: a beam of Ar_{40}^{+8} ions was accelerated and ejected [2,3]. The world's first industrial cyclotron for track membrane production has become the basic facility of NPK ALFA, which manufactures medical equipment for membrane plasmapheresis. Nowadays NPK ALFA is a unique research and production complex that stock produces track membranes (with a pore diameter of 400 nm) as well as medical apparatus for plasmapheresis. The track membrane is a polymer film made of lavsan (polyethylene terephthalate) or polycarbonate 10 to 25 μm thick in which there is a system of through pores.

To improve the quality of the membranes to extend the field of application, it is necessary to irradiate a film with heavier ions, especially with accelerated krypton ions. The currently operating ECR source does not produce krypton of the needed charge size. In this paper we analyze the possibility of accelerating krypton ions with a charge below the design one, namely 11+ and 12+.

CYTRACK PARAMETERS

The CYTRACK accelerator is an isochronous cyclotron with an azimuthal variation of magnetic field (a four sector structure), an axial ion injection, a high frequency accelerating system, and an electrostatic ejection system. The main specifications of the CYTRACK cyclotron are presented in Table 1. The general view of the accelerator is shown in Fig. 1.

Table 1: Cyclotron parameters

Accelerated ions	Ar_{40}^{+8}
Initial energy, MeV/nucleon	0.003
Final energy, MeV/nucleon	2.4
Final acceleration radius, mm	730
Operating vacuum, Torr	3×10^{-7}
Magnet overall dimension, m^3	$3.7 \times 2 \times 1.65$
Magnetic field level, T	1.48
Dees voltage, kV	40
Resonant frequency, MHz	18.25
Acceleration ratio	4

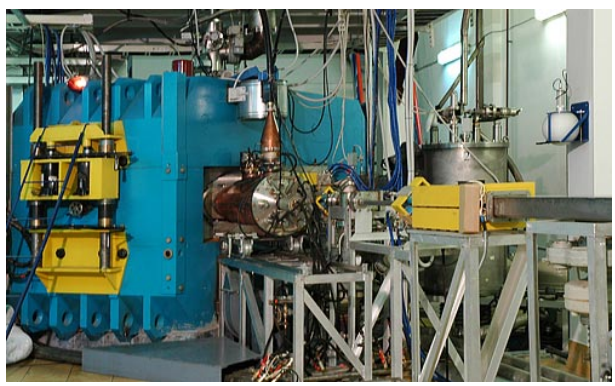

Figure 1: General view of the accelerator.

The ECR type ion source produces 3 keV/nucleon ions; the intensity of an argon beam on the Faraday cup placed in the diagnostic unit at the beginning of the injection line is on the order of 10 μA. The injection system incorporates a buncher. It also includes an ion guide, an analyzing and a turning two section magnet, and beam focusing and adjustment elements.

A spiral electrostatic inflector is used to turn the ion beam from the vertical to the horizontal plane of the CYTRACK cyclotron. A device is designed that allows the inflector to rotate around its axis (±8°) to adjust the ion trajectory to the starting radius and starting angle in order to optimize the initial conditions for ion acceleration in the cyclotron. The ions are injected into the cyclotron's chamber at a radius of 5.3 cm.

A radio-frequency accelerating system tuned to a fixed frequency is used to accelerate ions in the cyclotron's magnetic field. The RF system consists of two quarter wave resonators with accelerating electrodes in the form of dees. The RF resonators assure a frequency range from 18.250 to 18.600 MHz. The two dees of the accelerating system have an azimuthal extent of 45° and are located in the opposite valleys of the magnetic system.

ISBN 978-3-95450-125-0

VACUUM AUTOMATIC CONTROL SYSTEM (ACS) FOR NICA PROJECT

A.Bazanov, A.Butenko, A.Galimov, H.Khodzhibagiyan, A.Nesterov,
R.Pivin#, A.Smirnov, G.Trubnikov, JINR, Dubna, Russia
P.Hedbavny, Vacuum Praha, Praha, Czech Republic
J.Moravec, FOTON, Nova Paka, Czech Republic

Abstract

Upgrade of the Nuclotron [1] is the first step in the Nuclotron-based Ion Collider fAcility [2] project. A modernization of the Nuclotron vacuum system leads to decreasing of the heavy ion losses due to scattering on the rest gas. The successful realization of the modernization takes possibility to use Nuclotron as a part of NICA project. It's impossible to image the modern vacuum system without the automation control system (ACS). The goal of ACS at Nuclotron is to manage about 70 units of the vacuum system and the data acquisition.

VACUUM SYSTEM MODERNIZATION

Modernization of the Nuclotron high vacuum system had the aim to increase the beam lifetime which is the necessary condition for the using of Nuclotron for the NICA project. For this work it was chosen non-oil pumps such as ion pump, turbo pump and forvacuum pump "Pfeiffer Vacuum" company (Figure 1). It allowed to reach the pressure about 10^{-10} Torr. Mass-spectrometer PrismaPlus were installed to rest gas composition definition.

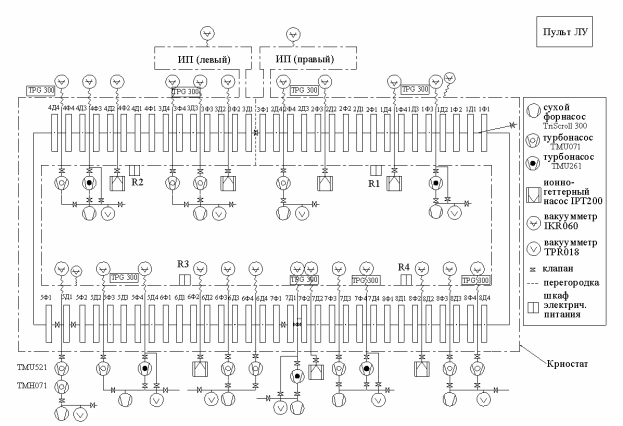

Figure 1. The scheme of the Nuclotron high vacuum system.

First step of the modernization includes the mounting of new turbo pumps. It permits to decrease a vacuum pressure about ten times. Problem vacuum parts also were reconstructed, measurement units were added.

Second step includes the installation of the tandem with two turbo pumps at each parts of the ring (22 points) and scrappers which are used for the lost ions absorption.

THE CONTROL SYSTEM FOR THE VACUUM OPERATION

Structure

ACS system consists of two main parts:

- Master controller (PLC), touch-panel and PC in the control room;
- Four Racks in the center of Nuclotron and units at the experimental hall.

PLC (Figure 2) works at the main controller and defines system logic. RS485 protocol is used for communication between units.

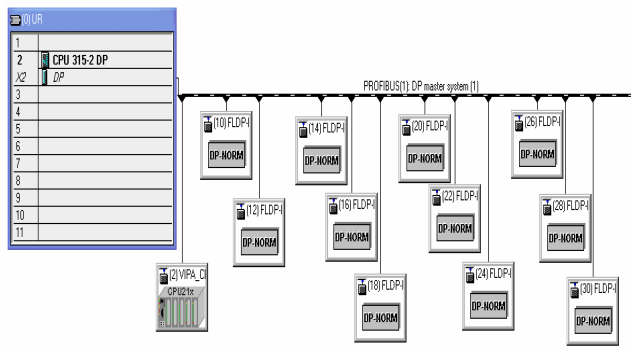

Figure 2. PLC controller with Profibus protocol.

The touch-panel (Figure 3) is placed on the central rack, creates visual interface for vacuum system components and hand mode provides.

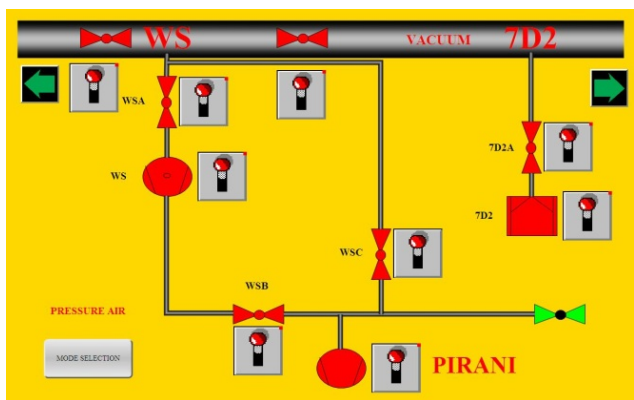

Figure 3. Touch-panel of control system.

#pivin@jinr.ru

ISBN 978-3-95450-125-0

CONCEPT OF THE SOFTWARE FOR ITEP-TWAC CONTROL SYSTEM

P. Alekseev, F. Sizov, ITEP, Moscow, Russia

Abstract

The work is in progress on development of new control system for ITEP accelerators complex. All software for the system should be developed from very beginning. Core element of new software is PostgreSQL object-relational database management system. All interactions between programs on device side and on operator side are made utilizing the database functionality. The database is also provides storage space for all configuration data, operational modes, logs and so on.

INTRODUCTION

ITEP accelerators complex is located in several buildings in the area of the institute. Control functions should be available for staff located at main control room and at local control panels of subsystems. In addition, diagnostic signals and some control parameters should be accessible from outside the complex. Therefore, the control system will be distributed and multiuser.

Common architecture of the control system is shown on Fig. 1. Offered structure allows connecting to the system almost any equipment with any known control interface. Supposed that the equipment may be industry manufactured or self designed.

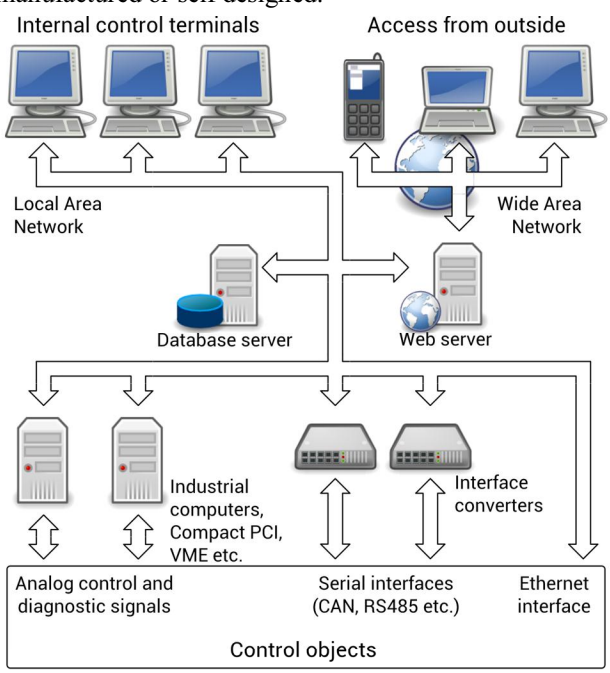

Figure 1: Common control system structure.

Front-end programs that user interacts with, may be called from the LAN or even from internet using the web server. Back-end software that interacts with control objects, executes on industrial PCs or on the database server.

The investigation of capabilities of various software products was made relative to our problem. The results coupled with existing resources and expertise allows to offer configuration of software described below.

Control of data flows between front-end and back-end software is implemented by PostgreSQL database. In addition, the database is used to store all the information related to the control system. Main functions of the database are illustrated in Fig. 2.

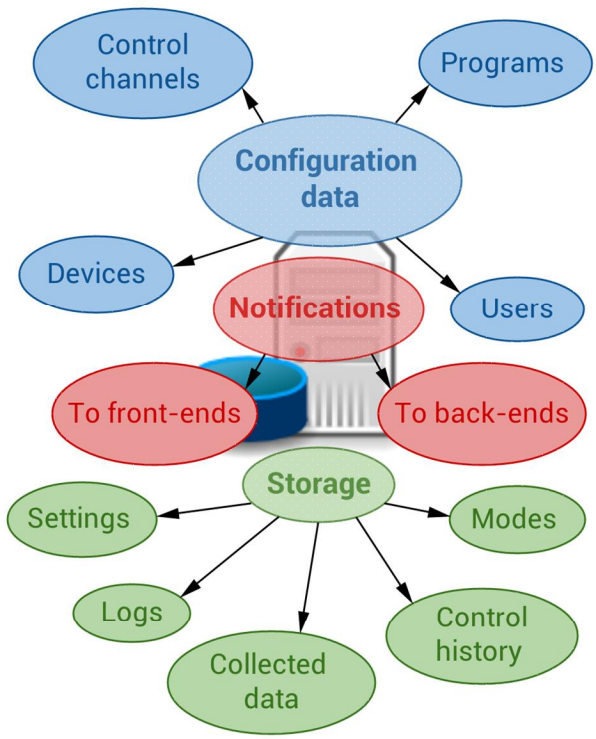

Figure 2: Database functions.

DATABASE STRUCTURE

There are three types of objects are used to describe the control system structure. These are daemons, devices and channels. Database table DAEMONS contains data about all back-end programs of the control system. Equipment of the control system should be described in the DEVICES data table. Each device such as communication port, dac board, peripheral module etc. has its own database record.

All the physical parameters of the control system are presented as channels. Database table CHS contains an information that used by front-end programs to configure control elements. Each channel should be linked to device that operates with it.

A set of tables that are used in the database to describe all the objects of the control system are shown in Fig. 3.

ISBN 978-3-95450-125-0

DEVELOPING OF THE SYNCHRONIZATION SYSTEM FOR ACCELERATION-STORAGE FACILITY ITEP-TWAC

A. Orlov, P. Alexeev, S. Barabin, D. Liakin, SSC RF ITEP Moscow, Russia

Abstract

The renovation of the ITEP-TWAC synchronization system is a complex and challenging matter. This system must provide a full-scale timing signal set for all existing and foreseeing modes of operation of the two-ring accelerator facility. The workflow of the complete design covers all levels of a design management hierarchy like decision concerning, the new system architecture or basic electronic modules development. In this article we present a description of most critical elements of the synchronization system.

INTRODUCTION

Two general rules were formulated before starting the design of the novel synchronization system. Those rules are following:

- New elements must be compatible with existing system. Partly they are replacing obsolete components giving them where it is necessary a new functionality. A principle of organization of the synchronization system in ITEP-TWAC accelerating complex could be illustrated by Fig.1.

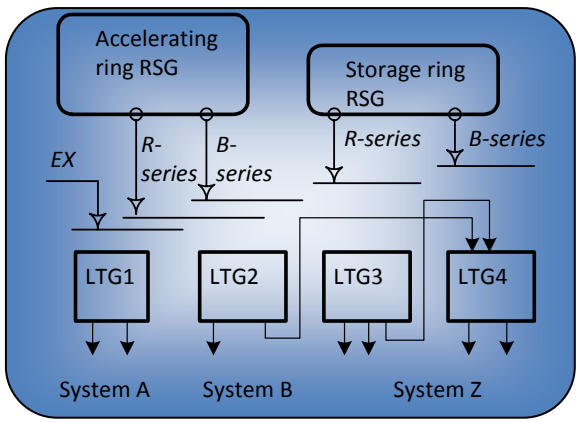

Figure 1.A structure of the synchronization system of the ITEP-TWAC accelerating complex.

- Reference signal generators (RSG) issue so called B- and R- sequences of control pulses which are synchronized with magnetic field strength (B) and RF oscillations(R). The system also accepts external synchronization signals (EX) from independent or adjusted installations like injector and target systems. A general module of the local timing generator LTG is an assembly of logical modules, programmable time-delay modules and signal duplication modules.
- New elements provide possibility to upgrade to the new principles of organization of the synchronization system, namely using serial timing bus (STB) for building synchronization system. A principle of organization of the synchronization system based on STB shown on Fig.2.

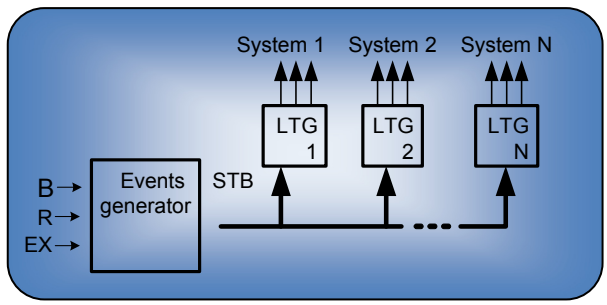

Figure 2. A principle of organization of the synchronization system based on serial timing bus architecture - STB.

STRUCTURE OF THE DEVICES

There are two families of devices, which require for building of the synchronization system with serial timing bus. The first type is a master or event generator shown in Fig.3. The master analyses incoming events of different format on B,R and EX lines and generates unified data frames on the serial bus. The second type is a service module shown on Fig.4.

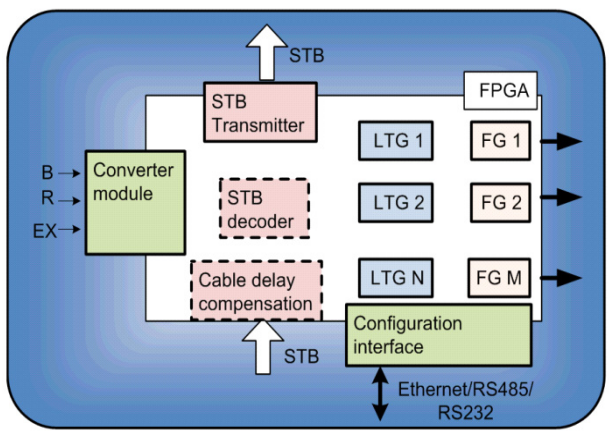

Figure 3. The block scheme of the events generator.

The differences between those two types of devices are nominal because the logical structure of the STB transmitter(master) can be completely realized inside FPGA, except the physical interface of the STB. A service module also can be logically implemented inside FPGA, except the schematic of the input signal converter. Both modules can be realized in the same hardware, therefore

ISBN 978-3-95450-125-0

OPTIMIZATION OF THE DETECTOR GEOMETRY AND DATA PROCESSING ALGORITHMS FOR FAIR CR BPMs

A.Orlov, S.Barabin, D.Liakin, SSC RF ITEP, Moscow, Russia
F.Becker, GSI, Germany

Abstract

A beam diagnostic is an important part of all FAIR accelerators and storage rings. A small flux of antiprotons in the collector ring CR (10^8 particles in a store ring) as well as dominated at first turns p-meson component of a beam require careful design for all elements of the beam position monitoring system. To increase a BPM resolution and sensitivity we propose a compact multi-electrode design of the position detector, matched low-noise electronics in connection with dedicated enhanced digital data processing algorithms. Here we present a comprehensive set of aspects of a preliminary design of the BPM system for FAIR CR.

SYSTEM OVERVIEW

The antiproton and rare isotopes collector ring (CR) is a specific component of FAIR. It is designed for conditioning of crude assemblies of particles with large initial transversal emittance and wide energy spectra. The estimated beam intensity for antiprotons is 10^8 particles in the ring. For rare isotopes only the highest intensity is specified as 10^{10} stripped ions in the ring. Geometrical constrains of the beam position monitor chamber are shown on 0. This figure shows the possible beam profiles and their envelope. Due to the limited space BPM chambers must be installed inside of quadrupole magnet so the chamber's outline must follow the inner shape of the yoke.

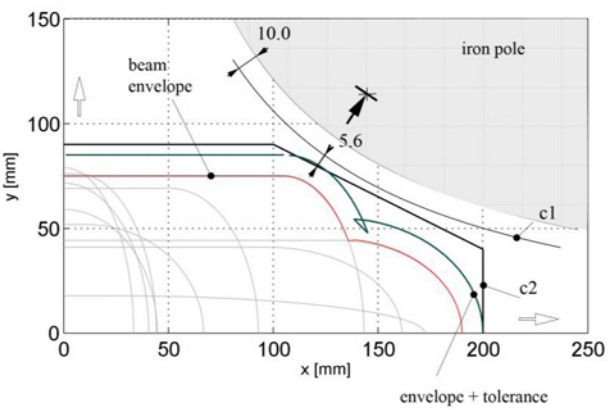

Figure 1. Geometrical constrains for the BPM chamber and electrodes design. c1 – the inner surface of the vacuum chamber, c2 – electrodes.

NUMERICAL MODEL OF THE BPM CHAMBER

A detailed investigation of the BPM antenna has been performed by numerical simulation. An electrostatic and low frequency AC approaches had been chosen according to operating frequencies and characteristic length of the system. A general 3D CAD model used for simulation of the BPM chamber is shown on 0. In this model electrodes are presented as a conducting surfaces connected to the circuit with defined impedance. A high-Z preamplifier, impedance transformer and direct 50-ohm cable connection were investigated.

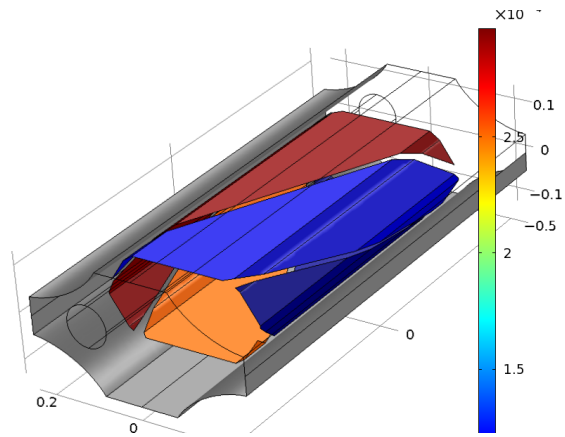

Figure 2. A 3D simulation model of the BPM chamber.

The beam of charged particles was simulated by space charge distribution. Generally the distribution is uniform in longitudinal direction and limited by volume of the circular or elliptical cylinder as it is shown on 0. Practically the charge density used in simulation was given by formula

$$Q = A(1-r)^2;\ r^2 = \left(\frac{x}{a}\right)^2 + \left(\frac{y}{b}\right)^2;$$

where a and b are semi axes of the cylinder crossection, A is a normalisation coefficient.

THE TOPOLOGY OF ELECTRODES

The signal strength and therefore signal to noise ratio important for low current measurements directly depend on effective length of pick-up electrodes. 0 on bottom schematically shows a classical design with separate electrodes for vertical and horizontal measurements. Such two modules are placed in space allotted for the BPM. The length of each section is about 40% of full dedicated length taking into account the gap required for decoupling of the vertical and horizontal sections. To obtain a higher sensitivity for CR BPM we consider a combined topology of the BPM. Because of digital signal processing it is possible to use more comprehensive algorithms for beam position detection. Particularly it allows dynamic 'reconfiguration' system consisting of four or even more

ISBN 978-3-95450-125-0

DIGITAL DELAY-LINE PERIODIC FIR FILTER LAYOUT OF TRANSVERSE FEEDBACK IN THE U70

O. Lebedev, N. Ignashin, S. Ivanov, and S. Sytov
Institute for High Energy Physics (IHEP), Protvino, Moscow Region, 142281, Russia

Abstract

A novel architecture of the wide-band transverse feedback system was successfully beam-tested in the U70 proton synchrotron of IHEP-Protvino. It employs a finite-time impulse response (FIR) non-recursive filter layout based on 3 (or 4, optionally) variable (–10%) multi-turn digital delay lines. Apart of using these natural-to-DSP components, the configuration involved has, at least, two operational advantages: (1) A single beam-pickup layout plus acceptability of an arbitrary betatron phase advance between pickup and kicker. (2) A straightforward rejection of hampering DC and higher rotation frequency harmonic signals from beam position raw readouts. The latter occurs due to a periodic notch nature inherent in the amplitude-frequency in-out open-loop feedback transfer function. The paper reports on technical solutions implemented, problem-oriented R&D, and beam observations.

PREHISTORY

The inventory of transverse beam feedbacks available in the U70 is outlined in Ref. [1].

Layout of the existing wide-band feedback is plotted in Fig. 1. Its two pickups (PU) are located in straight sections (SS) #107 and #111. In the U70, azimuth Θ of SS#*n* is 2π*n*/120. A properly weighted sum of beam position readouts produces a virtual pickup located 33 (an odd number) quarter betatron wavelengths upstream of the fast EM kicker (deflector) K in SS#90. A variable (–10% ca) delay line matches open-loop delay rime τ to beam time-of-flight between pickups and kicker.

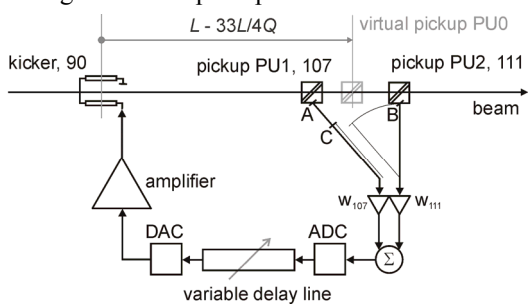

Figure 1: Layout of the existing wide-band feedback.

Suppression of closed-orbit offset signal at $\omega = k\omega_0$, with DC ($k = 0$) included, is accomplished via a variable electrical center of a pickup biased with balance amplifiers. Here, ω_0 is circular beam rotation frequency, integer $k = 0, \pm1, \pm2, \ldots$ is rotation harmonic number.

A single-delay-line layout of Fig. 1 is inherited from the earlier, all-analog implementation of the circuit. Indeed, in the analog world, a 5–20 μs variable delay line is by itself a sufficiently intricate device to preclude any use of a multiple number of them.

To be on the safe side in running the U70 and get experience with the DSP techniques, we have first converted the proven layout of Fig. 1 to a fraction-of-turn digital 1-delay-line version. The outcome is reported in Ref. [1].

In an attempt to better suppress (reject) the persisting closed-orbit offset signal at $\omega = k\omega_0$, a supplementary option using a one-tap periodical (with a period ω_0) digital notch FIR filter in the feedback path was also tested.

Thus, de facto, the U70 has got a digital transverse feedback employing the key techniques of (1) weighted summation of beam signals, (2) two digital delay lines (delays $\tau < 2\pi/\omega_0$ and $\tau + 2\pi/\omega_0$).

Next self-suggesting step was to arrange a more straightforward and promising single-pickup option with 3 (or 4, optionally) variable delay lines shown in Fig. 2.

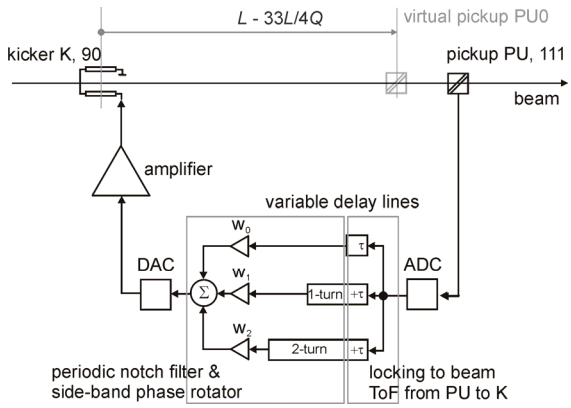

Figure 2: Layout of the new wide-band digital feedback (here, with 3 delay lines).

FIR FILTER LAYOUT

This topology was put forward in Refs. [2, 3]. Its attractive features are:

1. Use of natural-to-DSP circuits, esp., variable delay lines realized, say, as FIFO shift registers clocked by the higher (16^{th}) harmonic of (the U70) acceleration frequency ($\omega_{RF}/2\pi$ = 5.516–6.062 MHz).
2. A single beam-pickup layout that saves a room on the orbit.
3. An arbitrary betatron phase advance between pickup and kicker.
4. A natural built-in rejection of (unwanted) steady-state DC and higher rotation frequency harmonic signals present in raw beam position monitor readouts.

The latter occurs due to in-out open-loop feedback transfer function that is synthesized as a periodic notch filter.

ISBN 978-3-95450-125-0

THE OPTIMIZATION OF RF DEFLECTOR INPUT POWER COUPLER

A. Smirnov, O. Adonev, N. Sobenin,
NRNU MEPhI, Moscow, 115409, Kashirskoe sh., 31, Russia
A. Zavadtsev, NanoInvest, Moscow, Russia

Abstract

This paper concerns the investigation of different types of input power cell for S-band RF electron deflector. This device serving for slice emittance diagnostics is a disc-loaded waveguide which operates with TE_{11}-like wave in travelling wave regime with 120 deg phase shift per cell. Since this deflector meets the restriction on its length and has to provide high enough deflecting potential to a particle during its flight time it is significant to increase the transversal field strength in coupling cell or to shorten it so that the deflecting potential remains constant. The total structure consists of 14 regular cells and two couplers. As it is now all cells have the same length equal to D=33.34 mm and the field in couplers is lower than that of regular cells. In this paper different lengths are considered and numerically simulated in order to choose the best one.

INTRODUCTION

A deflecting voltage seen by a particle travelling along the axis of a disc-loaded waveguide driven with dipole TE_{11} (Fig. 1) mode can be calculated using transversal values of on-axis electric and magnetic fields or using longitudinal value of the electric field at some offset from the axis (Panofsky-Wenzel theorem) [1].

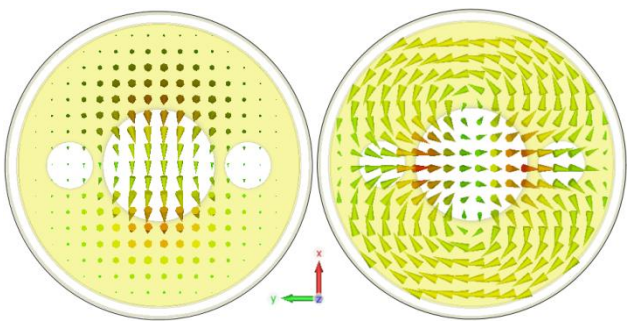

Figure 1: Electric (left) and magnetic (right) fields of TE11 mode

In the first method, we can use x-component (vertical) of E-field and y-component (horizontal) of H-field distributions along the axis z, since the particle experiences actions from both fields. Electric and magnetic fields are orthogonal to each other. The equivalent transversal deflecting field can be derived from the expression of Lorentz force $F_L=eE_d=e(E_x\pm vB_y)$:

$$\dot{E}_d(z)=\dot{E}_x(z)\pm\mu_0\beta c\dot{H}_y(z)\,, \qquad (1)$$

where (and further on) the sign '±' refers to the interplay of the particle and the wave propagation directions. According to time dependence of field components as $\exp(i[\omega t+\theta])$, this gives the equation for the transversal potential that is gathered by electron on a path from z=0 to z=L (structure length):

$$V_d(\theta)=\int_0^L\Re\left(\dot{E}_d(z)\right)dz=$$

$$=\int_0^L\left|\dot{E}_d(z)\right|\cos\left(\varphi_{E_d}(z)\pm\frac{2\pi}{\lambda}z+\theta\right)dz\,, \qquad (2)$$

where λ=c/f is the wavelength and θ is the initial phase of the deflecting voltage with respect to particle. Now by varying θ through the range from 0 to 2π one can find the maximal value of the deflecting voltage V_{dmax}.

An approach through Panofsky-Wenzel theorem requires longitudinal component of the electric field only, which is taken at some small enough vertical offset from the structure axis a – $E_z(z, x=a)$. The transverse deflecting field in this case is

$$\frac{\lambda}{2\pi}\left.\frac{\partial\dot{E}_z(z)}{\partial x}\right|_{x=0}\approx\frac{\lambda\dot{E}_z(z,x=a)}{2\pi a} \qquad (3)$$

due to the fact that longitudinal on-axis field $E_z(x=0)$ is nil for hybrid waves. And the corresponding potential V_{dmax} can be found from the following expression by varying θ from 0 to 2π:

$$V_d(\theta)=\frac{\lambda}{2\pi a}\times$$

$$\times\int_0^L\left|\dot{E}_z(z,x=a)\right|\cos\left(\varphi_{E_z}(z,x=a)\pm\frac{2\pi}{\lambda}z+\theta\right)dz. \qquad (4)$$

Both dependencies (2) and (4) are sin-shaped and shifted with 90^0, which is result of Maxwell equations.

TRANSVERSE DEFLECTING STRUCTURE

The structure layout [2] is presented on Fig.2. Cell irises have two additional holes used both for coupling between the cells and for stabilization of the mode polarization plane. The deflector consists of 14 regular cells with length of D=33.34mm (required for a phase shift of 120^0 per cell) and two power couplers, therefore

ISBN 978-3-95450-125-0

SOFTWARE FOR VIRTUAL ACCELERATOR ENVIRONMENT

N. Kulabukhova*, St.Peterburg State University

Abstract

The article discusses appropriate technologies for software implementation of the Virtual Accelerator. The Virtual Accelerator is considered as a set of services and tools enabling transparent execution of computational software for modeling beam dynamics in accelerators on distributed computing resources. Control system toolkits EPICS (Experimental Physics and Industrial Control System), realization of the Graphical User Interface(GUI) with existing frameworks and visualization of the data are discussed in the paper. The presented research consists of software analysis for realization of interaction between all levels of the Virtual Accelerator.

INTODUCTION

In order to control large-scale accelerators efficiently, a control system with a virtual accelerator model was constructed by many facilities [1, 2]. In many papers by the words Virtual Accelerator an on-line beam simulator provided with a beam monitor scheme is mean. It works parallel with real machine. The machine operator can access the parameters of the real accelerator through the client and then feed them to the virtual accelerator, and vice versa. Such a virtual machine scheme facilitates developments of the commissioning tools; enable feasible study of the proposed accelerator parameters and examination of the measured accelerator data. That is the common scheme of virtual accelerators used in different laboratories [3]. Until now there is no virtual accelerator working without real machine. Our goal is to construct virtual accelerator application can be used independently from any machine.

CONCEPT OF THE VIRTUAL ACCELERATOR

The model of Virtual Accelerator like any other model is standard. As it is shown on the figure 1 first comes the approximation model where all necessary options are determined. Further, the theoretical models are constructed. On them computational models are build. After that the time for testing and verifying comes.

The key idea of Virtual Accelerator (VA) concept is beam dynamic modeling by the set of several packages, such as COSY Infinity, MAD, etc., based on distributed computational resources, organized on Grid- and Cloud-technologies. Simulation beam dynamics by different packages with the opportunity to match the results (in case of using different resources for the same task) and the possibility to create the set of tasks when the results of using

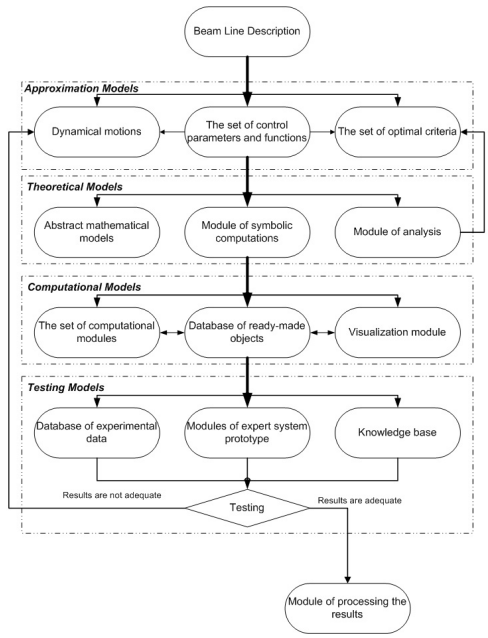

Figure 1: The total circle of computational experiment

one package can be sent to the input of another is the main use of VA [6]. Users will get the access to VA resources by unified interface including GUI on different platforms. Figure 2 shows the scheme of VA

The natural parallel and distributed structures of beam physics problems allow the use of parallel and distributed computer systems. But the usual approaches based on traditional numerical methods demand using the resources of supercomputers. This leads to the impossibility of using such multiprocessing systems as computational clusters. There are two classes of problems in beam physics which demand very extensive computer resources. The first class includes long-time evolution problems, the second is concerned with the computer realization of optimization procedures for beam lines. Examples of the first type of problem include multi-turn injection and extraction of the beam in circular accelerators. Usually, these problems do not consider space charge effects. For advanced applications it is essential to study beam dynamics in high-intensity accelerators. Such machines are characterized by large beam currents and by very stringent uncontrolled beam loss requirements. An additional difficulty of numerical simulation is connected with long-time beam evolution that requires the computation of hundreds of thousands or millions of turns. It requires the use of high-performance computers for beam evolution study. The problems of similar multi-turn evolution such as transverse stability with

* kulabukhova.nv@gmail.com

ISBN 978-3-95450-125-0

APPROXIMATE METHOD FOR CALCULATION OF FIELD OF CHARGED PARTICLE MOVING THROUGH DIELECTRIC OBJECT*

Ekaterina S. Belonogaya#, Sergey N. Galyamin, Andrey V. Tyukhtin,
Saint Petersburg State University, Saint Petersburg, Russia

Abstract

Cherenkov radiation is widely used for particle detection. As well, it is prospective for particle bunch diagnostics. Therefore, it is actual to elaborate methods for calculation of the fields of bunches moving in the presence of different dielectric objects. We offer the approximate method based on calculation of the field in unbounded medium and accounting of boundary influence with help of geometrical optics. First, we consider the problem concerning the field of charge crossing a dielectric plate. This problem has an exact solution. It is used as a "test" problem for estimation of precision of the approximate method. Computation of the field is performed using both methods and the results have a good agreement. Further, we analyze the cases of more complex objects, in particular, a dielectric cone. Note that the offered method allows to obtain wave fields using neither complex analytical transformations nor laborious numerical calculations.

INTRODUCTION

Problems of radiation of charged particles in the presence of dielectric objects are of interests for some important applications in the accelerator and beam physics. It can be mentioned for example a new method of bunch diagnostics offered recently [1]. For realization of this method, it is necessary to calculate the field of radiation outside a dielectric object. As a rule the form of object in such problems does not allow obtaining an exact analytical solution. Computer simulation of electromagnetic field is also very cumbersome. Therefore development of approximate analytical methods for analyses of radiation in such problems is an actual task. One of such methods will be offered and developed in this paper.

BASIS OF THE METHOD

The method offered here concerns problems which are characterized by some large geometric parameters. Let a charged particle bunch move in some dielectric or magnetic object. It is possible as well that the charge moves in a vacuum channel in the object, and radius of the channel can be arbitrary. In addition, the case of charge moving along one of borders of object can be considered, and in such case the distance from this border to the charge trajectory can be arbitrary. Anyway we assume that the sizes of the object are much more than wave lengths under consideration. Therefore, the Cherenkov radiation (CR) excited by the bunch runs inside the object some distance which is much more than wave lengths.

Under such conditions we can apply the following approach. At first, we calculate analytically the field of the charge in the infinite medium without "external" border. It is important that we can take into account such peculiarities of the problem as a vacuum channel (if the charge moves into the object) or finite distance from trajectory to the object's border (if the charge moves along the object). We underline that a lot of such problems have been solved in the literature.

The second step is approximate calculation of radiation going out of the object (sometimes it is named "Cherenkov-transition radiation" (CTR) [2]). The idea of this calculation is related to Fok's method of analysis of reflection of waves from arbitrary surfaces [3] but we deal with transmission instead of reflection. The incident field is multiplied by the Fresnel transmission coefficient, and then we should take into account decrease of the radiation because of spreading of a ray tube in the external medium. Thus we obtain the first of refracted rays of CTR. Probably, this will be enough for the majority of applied problems. If it will be necessary, multiple reflections and refractions on the object borders can be taken into account.

TESTING OF THE TECHNUQUE FOR DIELECTRIC LAYER

For testing the method, we use the problem about the field of point charge flying through the dielectric layer with permittivity ε placed at $0 < z < d$. The charge density is set in the form $\rho = q\delta(x, y, z - Vt)$. Such a problem has exact solution [4] which has been proved by us independently. We compare computations performed with use of exact formulae and approximate ones. Some results concerning the magnetic strength Fourier component $H_{\phi\omega}$ are given in Fig. 1. Note that approximate curves have a break on the boundary of "the light bar". Naturally, the exact solution is continuous everywhere (excepting the layer boundaries).

One can see that some agreement takes place even for $d \sim \lambda_2 = 2\pi c / \left(\omega\sqrt{\varepsilon}\right)$ if the distance from the plate is $\sim \lambda_2$ as well. In the case when $d \sim 10\lambda_2$ we have very good agreement for the most part of "the light bar". This result is very encouraging, and it stimulates applying the

*Work was supported by Saint Petersburg State University, the Dmitry Zimin "Dynasty" Foundation and Russian Foundation for Basic Research (Grant No. 12-02-31258)
ekaterinabelonogaya@yandex.ru

ISBN 978-3-95450-125-0

MODERNIZATION OF THE AUTOMATED CONTROL SYSTEM IN THE KURCHATOV SYNCHROTRON RADIATION SOURCE

E. Kaportsev, A. Valentinov, V. Dombrovsky, V. Korchuganov, Yu. Krylov, K. Moseev,
N. Moseiko, Yu. Yupinov, RRC Kurchatov Institute, Moscow, Russia
Yu. Efimof, CJSC RTSoft, Moscow, Russia

Abstract

The running cycle of Kurchatov Synchrotron Radiation Source (KSRS) includes the injection of electrons with energy 80 MeV from the linear accelerator in the booster storage ring Siberia-1, the accumulation of a electron current up to 400 mA and, then, electron energy ramping up to 450 MeV with the subsequent extraction of electrons in the main ring, storage ring Siberia-2, and accumulation there up to 300 mA, and at last the energy ramping up to 2.5 GeV. [1]

The current automated control system (ACS) of KSRS «SIberia» – synchrotron radiation source and the center of communities, NRC Kurchatov institute, was founded over 20 years ago on the basis of control equipment in the CAMAC standard. It is physically and morally outdated and does not meet modern requirements for speed, accuracy and data transmission.

This paper presents some options for replacing the old control system of KSRS with modern components, high-speed CPUs, standard VME, and high-speed industrial network CAN.

OPERATIONAL MANAGEMENT OF THE COMPLEX

The network consists of a machine operator workstations running Windows, connected with the local network Ethernet. [2] Applications obtain the diagnostic information from the database server based on MS SQL Server, where it comes from the application server. The database server and application server are located within one computer. The ADC and DAC integrated into CAN-network. The application server executes the control program and collecting data from sensors and diagnostics. We have three servers: Canserver, CAMAC messaging server и Vacuum server. [3]

Canserver, used to control the DAC and ADC via CAN network. The application server runs specialized programs that support communication with the CAN-network actuators, K167 controllers, RF generators and power systems. [4]

Messaging Server CAMAC organizes communication with controllers that have not adapted to the standard CAN. [5]

The management server of the vacuum system is located directly in the vacuum console. It has its own database, which stores the archive of the currents of vacuum pumps. [6]

The most important disadvantage of the control system is outdated equipment, made on a hardware platform CAMAC. Currently, developed in BINP (Novosibirsk), controllers and control modules are Non-Repair, due to obsolete element base and removed from the production of most parts, which have no analogue in the free distribution. Due to the failure of most modules of the control system, there was an urgent need to replace outdated equipment with modern, easily upgradeable and scalable.

Canserver server used to control the DAC and ADC via the CAN network. On the application server run specialized programs, which support communication on CAN-network with executive devices, such as high-frequency generators and power of magnetic systems. [3]

Messaging Server CAMAC [4] organizes the exchange of data with CAMAC crate controller with CAN interface type of K167 [5].Through it passed all the information from the controllers and modules that have not yet adapted to the standard CAN.

Management server of vacuum system is directly in the vacuum control room. It has its own database that stores the archive currents of vacuum pumps. [6]

UPGRADED ACS

Upgraded ACS of KSRS (further - UACS) will be a multi-level structure, conventionally divided into upper and lower level, server level and peripherals (fig.1). UACS structurally divided into five branches of management: control of the injection part of the complex (linear accelerator and small storage ring “Siberia-1”), management of large storage ring (“Siberia-2”), diagnostic of beam in accelerators, vacuum control and temperature control.

Lower Level of UACS

Lower level of UACS must be made on the basis of bus-modular equipment in the standard VME and control equipment with embedded processors, running under operating systems like Lynxos. At this level should be gathered diagnostic information and perform control algorithm of the complex systems. This equipment is connected to a server level with Ethernet or CAN.

Server Level of UACS

Server level of UACS includes application servers and a database management system (DBMS). At this level, to be implemented:

- general algorithm for management and monitoring of the KSRS;
- communication with the VME standard CPUs;
- communication with the CAN-controller;

ISBN 978-3-95450-125-0

NEW ELECTRON BEAM REFERENCE ORBIT MEASUREMENT SYSTEM AT DEDICATED SYNCHROTRON RADIATION LIGHT SOURCE SIBERIA-2

Ye. Fomin, V. Korchuganov, N. Moseiko, A. Valentinov, NRC Kurchatov Institute, Moscow, Russia
R. Hrovatin, P. Leban, Instrumentation Technologies, Solkan, Slovenia

Abstract

The paper focuses on the project of the electron beam closed orbit measurement system at SR source SIBERIA-2 realizing at present time at Kurchatov Institute.

The main purpose of new closed orbit measurement system creation is an improvement of the electron beam diagnostic system at storage ring. In addition, it will be a part of fast feedback system which will damp the distortions of the closed orbit at SIBERIA-2. This system provides continuous measurements of the electron beam closed orbit during storing, ramping and operation for users. Besides, with the help of the system it is possible to carry out turn-by-turn measurements of the electron beam trajectory during injection process.

The paper describes the new orbit measurement system, the principle of operation and its technical characteristics.

INTRODUCTION

The electron beam reference orbit measurement system which is currently operating at SIBERIA-2 is obsolete and outdated. The initial part of the orbit measurement system consists of 24 beam position monitors (4 pickups at one superperiod) and the preliminary signal processing electronic device located near each beam position monitor (BPM). The main purpose of this electronic devices are preliminary signal processing to transmit its to main control room for final processing and calculating electron beam horizontal and vertical positions (X and Z). Into the main control room all 96 signals from each button of BPM consecutively are digitized with the help the switch and one ADC made into the CAMAC standard bus. Control of the switch and the ADC as well as the beam center of gravity position calculation and results display are performed by micro controller Odrenok. As a result, the process of the electron beam reference orbit measurement takes a lot of time – 5 s.

Due to very slowly orbit measurement process it is possible to measure the electron beam orbit only in stationary accelerator operation mode. It is not possible to perform correct measurement of the beam trajectory during electron beam injection or acceleration process. It would also like to note the electron beam reference orbit correction process takes a lot of time - up 1 hour.

Now the synchrotron radiation light source SIBERIA-2 is being upgraded and the synchrotron radiation beam quality is being improved. New synchrotron radiation sources (superconductive and normal conductive wigglers), new synchrotron radiation beam lines and experimental stations are constructed. So both the synchrotron radiation and electron beam requirements will be only become stronger. Some electron beam parameters at storage ring SIBERIA-2 are presented at Table 1.

Table 1: Electron beam parameters at SIBERIA-2

Beam current, mA	1 - 200
Revolution frequency, MHz	2.4152
Beam emittance, nm·rad	98
Lifetime at 160 mA current, h	~ 20
Number of bunches	1 - 75
Bunch sizes, mm: σ_x, σ_z, σ_s	0.34, 0.059, 20.0

In the nearest future the existing electron beam reference orbit measurement system and the global orbit feedback system will be not able to provide required photon beam quality for all synchrotron radiation users.

NEW ELECTRON BEAM ORBIT MEASUREMENT SYSTEM

New electron beam reference orbit measurement system at dedicated synchrotron radiation source SIBERIA-2 is being created based on the electron beam position processor Libera Brilliance units developed by Instrumentation Technologies company, Slovenia. In all respects the new system is better the old one.

The architecture of the new orbit measurement system is looking like the old one. 24 Libera Brilliance processors are used to process the signals from BPMs. These processors are combined into 4 groups with the help of 4 Clock Splitter units and 4 ethernet switches. Each device group (6 Libera Brilliance units, 1 Clock Splitter and 1 Ethernet switch) is installed into one rack. The all 4 racks are mounted at the equal distance (one quarter of the accelerator circumference) from each other on the inner side of the shielding wall of the storage ring at a 1.5 m height from accelerator median plane. Such arrangement of racks with the equipment is allowed to reduce radiation background to the equipment. Measured radiation background at the place of racks location does not exceed the maximum radiation level for normal equipment operation.

ISBN 978-3-95450-125-0

SOME ASPECTS OF THE CAVITY RESONANT FREQUENCY CONTROL SYSTEM HEATER OPERATING POINT CHOICE

V.V. Grechko, G.I. Yamshikov, INR RAS, Moscow, Russia

Abstract

To adjust and to stabilize a resonant frequency of the accelerating cavities INR Linac comprises a Cavity Resonant Frequency Control System (CRFCS). The main final control element of the system is an electric heater (EH). Operating point of EH determines power consumption of the system and rf power feed in duration. Electromagnetic noise originated from thyristor regulators of the heaters and influencing linac electronics also depends on the operating point. One of the most sensitive systems is Fast Beam Interlock System (FBIS) intended for prevention of excessive activation and damage of linac components. To exclude false responses of FBIS and to decrease power consumption of CRFCS operating point of the heater has been shifted to a range of smaller power. This approach has been tested during several beam runs with the following results: no false responses of FRIB were observed; the quality of frequency stabilization during beam runs remained at the same level; relatively rare restarts of RF channels did not increase a downtime to beam time ratio; CRFCS power consumption was decreased twice. The rf power feed in duration increased insignificantly.

INTRODUCTION

The cavity resonant frequency control system (CRFCS) is intended for:

- warming up of cavity to the resonant temperature and its stabilizing before to begin rf power feed in (rf feeding) both at primary rf channel switching on and at the unauthorized switching off rf generator or system on the whole;
- providing of attenuating transient process in the system at rf power feed in (according to principle of Ljapunov - the stability "in large");
- stabilizing of cavity resonant frequency during beam run (stability "in small").

All these tasks are solved by the change of temperature of desalted water circulating in closed contour. A heat-exchanger with the regulated efficiency of heat exchange and power regulated electric heater (EH) with a corresponding measuring and regulating equipment allow to support the required thermal balance in any mode of CRFCS operation.

The circuit of EH power (current) control contains sensors measuring the regulated coordinate (cavity temperature or cavity phase off-tuning), corresponding threshold sensors, null device, PID-regulator, block of the signal transformation and fixing of EH operation point (OP) and also the thyristor regulator with the changeable angle β of thyristor switching on. Here under a concept "EH OP" the following is implied: bipolar signal of CRFCS unbalance from the PID – regulator should be transformed in unipolar ones before signal giving in the control unit RNTO-250 or ROT-250 type of thyristor regulator. Electric heater OP is point on the regulation curve, corresponding to CRFCS off-tuning $\xi = 0$.

Fronts of thyristor switching on have duration about tens of microseconds and cause appearance of noise affecting near-by located electronic equipment, and choice of angle $\beta = \pi/2$ leads to the increasing of noise amplitude to the maximally possible value. (Angle $\beta = \pi/2$ at unbalance in CRFCS $\xi = 0$ was chosen at tuning of CRFCS as providing the best condition of rf power feed in).

It should be noted the high intensity of noise: firstly, EHs are energized from the network of 220V 50Hz, that at antiparallel on of thyristors gives 100Hz frequency noise, secondly, at the present state of accelerator up to 20 channels can be involved in operation.

AFFECT OF NOISE ON FBIS AND OTHER ELECTRONIC EQUIPMENT OF LINAC

Fast beam interlock system (FBIS) is intended for prevention of the excessive activation and thermal damages of linac components. In the system there are 74 detectors of the secondary radiations located on length of linac tunnel and electronics racks behind of shield in control rooms and PS gallery. Constructively detectors are executed as plastic scintillator connected by light guides with photomultipliers. On the area of beam turn with energy of 160 MeV PM is used as a detector directly. Synchronized with linac operation electronic part of FBIS is a threshold device reacting on external signals only during the beam acceleration. FBI system produces a signal "Prohibition of FBIS" and injection of beam in linac is terminated if permissible beam losses and corresponding threshold level (~10 ÷ 20 mV) are exceeded. The reset of "Prohibition of FBIS" is performed by either an operator or automatically. During this a beam in linac is absent ~ 0.5 sec.

FBIS forms a false response "Prohibition of FBIS" and stops the acceleration of beam if attending linac work noise is coming at time gate of beam loss registration and threshold level is exceed. The losses of beam run time may reach a few percents, and on occasion - to block the work of accelerator fully.

To find the source of noise during working linac and at the regular mode and complete volume of FBIS equipment different parts of linac were independently switched on: injector, rf channels, equipment of CRFCS, pulse magnet, equipment of accelerator control system, etc. As a result the high degree of correlation between false responses of FBIS and value of EH current of CRFCS was revealed.

Further researches allowed:

ISBN 978-3-95450-125-0

EMITTANCE MEASUREMENTS AT THE EXIT OF INR LINAC

P. Reinhardt-Nickoulin, S. Bragin, A. Mirzojan, I. Vasilyev, O. Volodkevich, Institute for Nuclear Research of RAS, Moscow, Russia
A. Feschenko, S. Gavrilov, Institute for Nuclear Research of RAS, Moscow, Russia and Moscow Institute of Physics and Technology, Moscow, Russia

Abstract

Emittance measurements at the exit of INR linac are of importance for proper beam matching with the beam line of the downstream experimental facility. Emittance ellipses are reconstructed from beam profile data obtained with three wire scanners and one ionization beam cross section monitor (BCSM). A possibility of quadrupole gradients adjustment not only increases the reconstruction accuracy but also enables to find emittances with BCSM data only. The latter provides completely transparent measurements and can be done within a wide range of beam currents. The results of measurements by wire scanners and BCSM are presented and compared, the reconstruction procedure features are discussed.

INTRODUCTION

Accelerated proton beam of INR linac is used on the experimental facility of Neutron Studies Laboratory, proton therapy complex of Medical Physics Laboratory, facility for dibaryon resonances study and on other experimental targets.

Neutron Studies Laboratory experiments are carried out on the beams of 0.3 to 200 μs duration at repetition rate of 1 to 50 Hz with a pulse current up to 15mA, i.e., the average current can be as high as 150 μA, while for the proton therapy complex one should apply an average current of about 10 nA. The beam energy can be varied from 70 to 209 MeV. So each experiment requires specific values of beam energy, intensity, duration, and matching of these parameters with the characteristics of beam channels at INR experimental complex.

For INR proton linac operation in wide dynamic range of beam parameters one has to carry out proper retuning and matching procedures according to the features of the experiments. This in turn requires more attention to the dynamic range of the beam measuring system to ensure reliable diagnostic abilities for different beams.

Last years the linac diagnostics has been supplemented and upgraded. In particular, the system of wire scanners (WS) was developed. Besides the ionization beam cross section monitor was installed [1], which allows to measure transverse beam profiles at the linac exit.

Beam cross section monitor (BCSM) of accelerated protons provides possibility to observe the following beam parameters during adjustment and operation of the linac: protons distribution in beam cross section (BCS), beam centre position and its displacement relative to linac axis. The transverse beam profiles can be obtained from the beam cross section distribution too.

In process of linac tuning various interactive procedures are used [2]. They give the possibility to carry out transverse matching of the beam, centre correction and minimization of beam losses. Description of the equipment at the linac exit is presented. The emittance measurement procedures, as well as a comparison of the results obtained by different methods are discussed.

BEAM INSTRUMENTS AT LINAC EXIT

The measuring area at the linac exit for transverse beam matching and centre correction is shown in Fig.1a. The following equipment is installed at this area:

- 8 quadrupole magnetic doublets D106 ÷ D113. Their windings are supplied from a common current source;
- beam current transformer;
- 4 quadrupole magnetic doublets D114 ÷ D117. Their windings are supplied from different current sources;
- 3 wire scanners. They are installed downstream the doublets D113, D114, D115. Each scanner consists of two mutually perpendicular wires of 0.1 mm, which are parallel to horizontal and vertical axes.
- BCSM is installed upstream the doublet D114.

Procedures of transverse beam matching and correction are realized using the profiles obtained by WS at the same time with BCSM.

High sensitivity of BCSM allows to extract profiles from beam cross-sections measurements in very wide dynamic range of beam intensities for high- and low-current beams, while WS measurements are effective only in limited range of beam pulse currents due to noises induced on electronics and cables.

PROFILE AND EMITTANCE MEASUREMENTS

Linac tuning is performed strictly with 1 Hz pulse frequency to avoid excessive equipment activation and damage due to overheating of linac equipment in the point of significant beam losses.

Profile measurement with BCSM during linac tuning is also executed with 1 Hz beam frequency. Single pulse of 100 μA÷10 mA with 100 μs duration is sufficient to obtain profile. However, it is possible to measure beam profiles with pulse current lower than 100 μA using higher beam frequency e.g. 10÷50 Hz. In former case average proton beam current would be smaller than 10 mA of 100 μs pulse current with 1 Hz repetition rate. Low current beam Profiles are generally measured by BCSM using averaging over multiple pulses.

ISBN 978-3-95450-125-0

DEVELOPMENT OF INR LINAC BCT SYSTEM

P. Reinhardt-Nickoulin, S. Bragin, V. Gaidash, O. Grekhov, Yu. Kiselev, N. Lebedeva,
A. Mirzojan, A. Naboka, I. Vasilyev, O. Volodkevich.
Institute for Nuclear Research of RAS, Moscow, Russia

Abstract

New electronics of automatic BCTs system was developed to improve beam parameters measurements along INR Linac. BCT electronics details are described. The available results of beam pulse measurements are given.

INTRODUCTION

At proton beam acceleration process in initial part of INR linac from 750 keV to 100 MeV high level of interference and hum are produced in measuring channels on beam current transformers (BCT), preamplifiers (Preamp); cables between Preamps and Main modules of amplification (AMP) and calibration (CLB), that are installed in control room of initial part.

These low frequency (LF) and high frequency (HF) interference distort the BCT measurement results with single channel Preamp [1].

Besides that at time of proton acceleration in initial part, when beam from RFQ is accelerated from 750 keV to 20 MeV in first drift tube linac (DTL) tank, the amplitude of beam pulse is decreased from 23÷18 to 12÷10 mA approximately in process of the accelerating beam formation. But significant level of interference and hum don't permit to estimate with sufficient accuracy the rate of beam losses in first DTL tank and in another DTL tanks of linac initial part. Therefore, efforts were made to improve of resolution ability of BCT measuring system in initial part.

In the past two years system has been expanded with a new BCT on ferrite core and two differential Preamp circuits of two types, that enable to reduce interference and hum from high-power devices of linac.

Upgraded BCT system provides reliable and stable beam parameters representation along the linac in high level of activation of the equipment also.

THE STRUCTURE OF INITIAL PART BCT SYSTEM

Block-scheme of automated BCT system [2] for initial part of linac is shown on Fig. 1. The beam is injected from the RFQ in the initial part, which consists of five tanks (R1÷R5) of DTL type. After acceleration to 100 MeV, beam is injected into the main part of the linac, consisting of 27 accelerating sections of disk and washers (DAW) types.

BCT's and Preamps are installed on the exits of each DTL tanks excluding R2. Preamps are located in linac tunnel 1.5 m away from corresponding BCT. Analog pulse signals from Preamps are fed inputs of amplifiers (AMP) by RF cables. Generator of calibration pulses CLB is combined with appropriate AMP in common module MAC. All MAC's are installed in control room of linac initial part. CLB signals are fed to corresponding BCT. AMP output signals are fed on ADC inputs of corresponding servers (PC1÷PC5), installed in each of 5 sectors of linac. All ADC's are built into server computers of corresponding sectors of linac (PC1÷PC5). Servers are built into control system of linac (CSL).

The programs for data acquisition and processing are on the servers and remove the remnant distortions due to hum and interference. Processed data are transmitted into CSL. The final results of treatment are represented on computers of linac central control room.

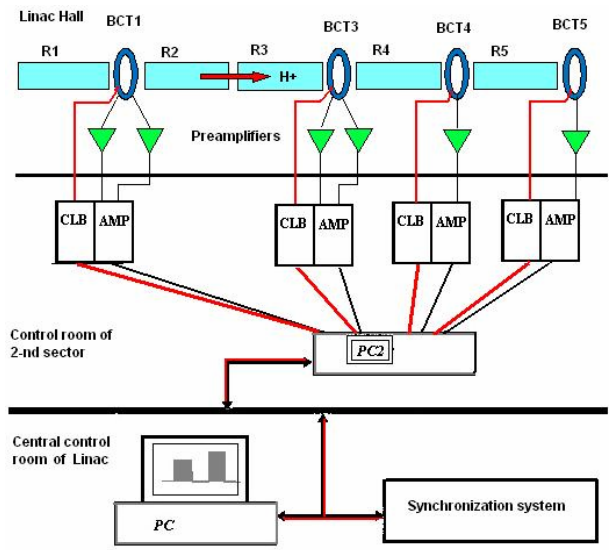

Fig. 1. Block diagram of automated BCT system of linac initial part.

BEAM LOSSES AND RADIATION CONDITIONS ON INITIAL PART OF INR LINAC

Currently, INR linac proton pulses have the 10÷12 mA pulse amplitudes, up to 200 μs pulse duration and 1÷50 Hz pulse repetition frequency. The beam amplitude formation is produced into first DTL tank.

RFQ, operating on the frequency of initial part 198.2 MHz, injects in R1 the beam of ions with 200 μs duration, consisting from $4*10^4$ bunches of 0.8 ns duration. The number of particles in bunches is decreased in R1 in process of formation of more short bunches at acceleration.

ISBN 978-3-95450-125-0

COMMISSIONING OF NEW DIAGNOSTIC DEVICES AT PITZ

D. Malyutin, M. Krasilnikov, J. Meissner, F. Stephan, G. Vashchenko, DESY, 15738 Zeuthen, Germany
K. Kusoljariyakul, S. Rimjaem, Department of Physics and Materials Science, Faculty of Science, Chiang Mai University, Chiang Mai, 50200, Thailand

Abstract

The Photo Injector Test facility at DESY, Zeuthen site (PITZ) is the test stand of the electron source for the European X-ray Free Electron Laser (XFEL). The main goal of the facility is the detailed characterization of the electron bunch parameters produced by the RF photo-cathode gun. Characterization of the bunch longitudinal properties such as bunch length or longitudinal phase space earlier was done using a streak camera, which measures the Cherenkov light produced by electron bunches passing through aerogel radiators. Recently, a Transverse Deflecting Structure (TDS) and a Second High Energy Dispersive Arm (HEDA2) were installed in the PITZ beamline. They will enable time resolved measurements of the electron bunch with much better time resolution than the streak camera system.

The first results of the commissioning of the HEDA2 section at PITZ are presented in this contribution.

INTRODUCTION

PITZ develops and optimizes electron sources for Free-Electron Lasers (FELs) like FLASH and the European XFEL in Hamburg (Germany). The main goal is to produce high brightness electron bunches whose quality fulfills the stringent requirements of these FELs [1].

A schematic layout of the current PITZ beamline is shown in Fig. 1. The main components are: the RF photo gun as electron source, an accelerating cavity Cut Disk Structure – CDS booster, three dipole spectrometers, three Emittance Measurement SYstems (EMSYs), a transverse deflecting structure (TDS) and a phase-space tomography module (PST). The three dipole spectrometers are located in the low energy section downstream the gun (Low Energy Dispersive Arm – LEDA), in the high energy section downstream the booster cavity (First High Energy Dispersive Arm – HEDA1) and at the end of the PITZ beam line (Second High Energy Dispersive Arm – HEDA2). A slit scan [2] is the standard technique for the projected emittance measurement at PITZ. The longitudinal phase space of the electron bunch is measured at PITZ with Cherenkov radiators in dispersive sections [3] up to now. The most recent upgrade of the PITZ facility included the installation of the TDS and the HEDA2. The TDS cavity is a multipurpose device, which is expected to provide a significant improvement in time resolved measurements. Beside measurements of the bunch length, the TDS is planned to be used in combination with HEDA2 for measurements of the longitudinal phase space. The main goals and working principles of the TDS and the HEDA2 are described in this paper. First results of the HEDA2 commissioning at PITZ are presented.

TRANSVERSE DEFLECTING STRUCTURE

The TDS cavity was designed and manufactured by the Institute for Nuclear Research (INR, Troitsk, Russia) as a prototype for the European XFEL [4]. The basic operation principle of the TDS is illustrated in Fig. 2.

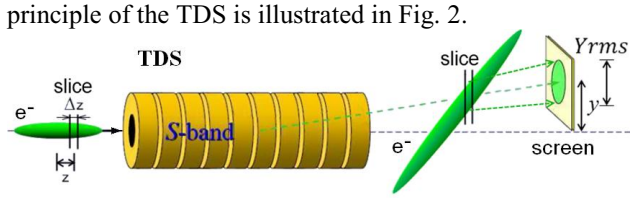

Figure 2: TDS working principle.

The structure deflects electrons vertically in linear dependence on their longitudinal coordinates within the bunch, which as a result enables measurements of the longitudinal bunch properties. An electron bunch propagates from left to right, passing through the deflecting structure. After a drift space, it is imaged on a screen. In case the bunch length is much shorter than the RF wavelength and if the bunch center propagates through the structure in the "zero" RF phase, then the

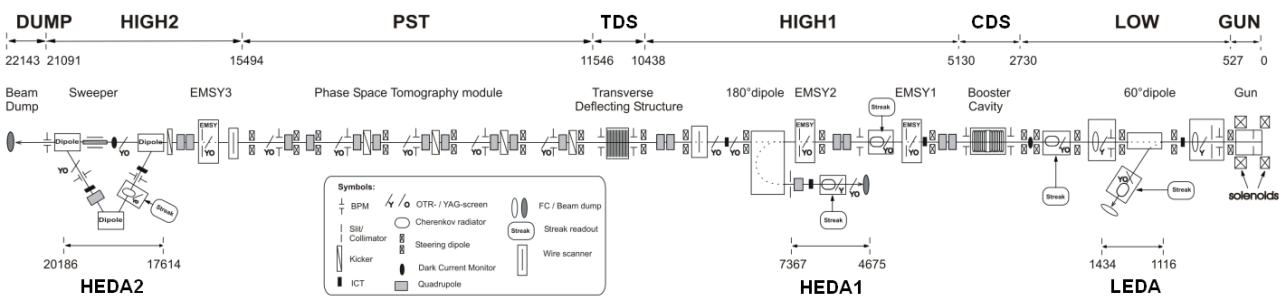

Figure 1: Current PITZ beamline layout.

ISBN 978-3-95450-125-0

AIRIX MEASUREMENT CHAIN OPTIMIZATION FOR ELECTRON BEAM DYNAMIC AND DIMENSIONAL CHARACTERISTICS ANALYSIS

F. Poulet, V. Bernigaud, C. Chollet, H. Dzitko, J. Kranzmann, C. Noel, O. Pierret
CEA, DAM, DIF, Bruyères le Châtel, F-91297 Arpajon, France

Abstract

AIRIX is a linear accelerator dedicated to X-ray flash radiography at CEA's hydrotest facility. It has been designed to generate an intense X-ray pulse using a 2 kA, 19 MeV and 60 ns electron beam.

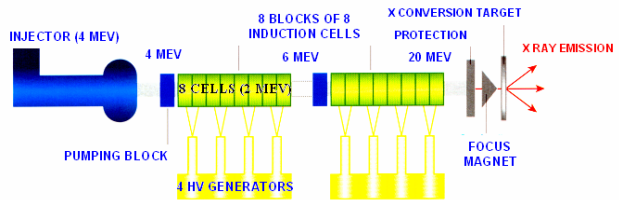

Figure 1: AIRIX accelerator

The electron beam transport in the accelerator is insured by the knowledge of the dynamic and dimensional characteristics of the beam created downstream the injector. These characteristics are assessed from a measurement chain, established by adapted optics and an intensified camera, aiming at observing the Cerenkov radiation produced during the interaction of electrons with a mylar target placed in the beam. This paper deals with the characterization, and comparison with the previous model, of a new intensified camera which was experimentally tested on AIRIX during an injector characterization campaign. This allowed to define profile and emittance beam characteristics. The obtained results are promising and revealed very interesting properties in particular in term of dynamic, temporal resolution, linearity and signal-to-noise ratio.

INTENSIFIED CAMERAS THEORETICAL CHARACTERIZATION

This characterization was achieved in laboratory, both on the intensified camera PROXITRONIC (NANOCAM HF4-S-5N model) currently set up on AIRIX, and on the new PRINCETON camera (PIMAX3 model).

Table 1: General characteristics

Parameters	PROXITRONIC	PRINCETON
Type	Analog	Numeric
CCD captor cooling	No	Down to -25°C air cooled
CCD format	512 x 512	1024 x 1024
Digital conversion	8 bits	16 bits
Gate width	5 ns to 65 ms	2 ns to 20 s
CCD pixel size	11.2 x 11.6 µm²	12.8 x 12.8 µm²
Image area	8.7 x 6.5 mm²	13.1 x 13.1 mm²
MCP-captor coupling	O.F – reducing cone – O.F	O.F – O.F
Usual configuration	Black level : 30% Video Gain : 90% MCP Gain : 90%	

Signal Base Line Adjustment

For PROXITRONIC camera, a "Black Level" parameter allows the adjustment of the signal base line. With a homogeneous pulsed DEL source, we estimate the signal base line mean level relatively to the "Black Level" variation, and we note that decreasing Black Level of 10% reduces the pixel level of 20 ADU. Finally, in the PROXITRONIC camera usual configuration, pixels which are lower than 48 ADU are reduced to 0 (threshold effect). For new PRINCETON camera, the signal base line and video gain can not be changed.

Linearity

The tests are achieved with a 532 nm nanosecond LASER and an integral sphere of 40 mm diameter. By convention, we reach camera sensitivity saturation when linearity defects are higher than ±5%. For the PROXITRONIC camera (figure 2), we note a beginning of sensitivity saturation around 130 ADU/pixel. In linear mode, the ±10% dispersion is representative of the weak signal to noise ratio.

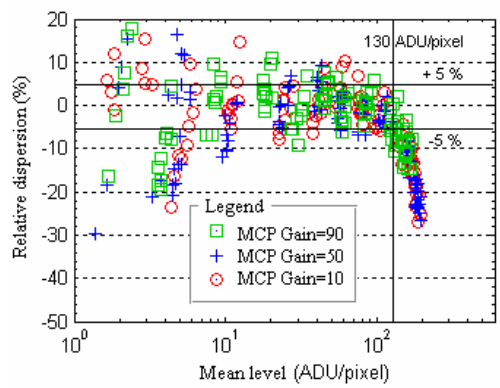

Figure 2: PROXITRONIC camera linearity defects

As for the new PRINCETON intensified camera (figure 3), sensitivity saturation defects are observed around 8000 ADU/pixel. We remark a weak dispersion level in linear

ISBN 978-3-95450-125-0

DISTRIBUTED CONTROL SYSTEM FOR AN INDUSTRIAL ELECTRON BEAM ACCELERATOR

Vijay Sharma*, S. Acharya, & K.C. Mittal
Electron Beam Centre, BARC, Mumbai-400085, India

Abstract

A PCVM type 3MeV DC Electron beam accelerator has been developed at Electron Beam Centre, BARC, Mumbai, India. A PLC based distributed control system has been incorporated for the control of the accelerator. A touch screen user interface (HMI) has been provides for single point control of the entire accelerator. The accelerator operation/fault related data is stored in the memory Flash card of the HMI. The Accelerator has many subsystems such as scan magnet supply to scan the electron beam, Chiller unit to supply the chilled water to the accelerator for cooling, vacuum system to maintain the vacuum inside the beam tube, high voltage unit to generate the EHV for electron acceleration and other support system. All the above subsystems have to be controlled from the central location in order to operate the accelerator safely. Each of the subsystem has been controlled by an independent PLC controller with all the safety features and control flow controlled by the program logic algorithm written into the PLC. After each of the subsystem has been tested separately all the PLCs are connected to the central PLC on Modbus TCP-IP. The main central PLC has been programmed to fetch the processed data from the individual subsystems PLCs and provides control and monitoring of the accelerator. In auto mode of operation setting the accelerator parameters operates all the subsystems automatically.

INTRODUCTION

The electron beam accelerator has various subsystems. All the subsystems have to work together in a defined sequence to generate the desired accelerated electron beam from the accelerator. All the subsystem such as vacuum system, sweep scan magnet unit, high voltage unit, chiller water unit, air circulation unit, search-secure, safety, interlock unit, steering/focussing magnet unit has to be controlled. Each group of similar units has been provided with a PLC controller in order to perform the fully automatic operation of that its subsystem. Finally all the PLCs are connected together on Modbus TCP-IP network to achieve a single point control of the accelerator. A touch screen panel has been provided at the control panel as an institutive user interface.

SYSTEM OPERATION

The 3 MeV electron beam accelerator is an industrial accelerator developed for the various industrial electron beam processing applications. The accelerator control system has been designed using industrial PLC in such a way that an operator with short duration training can operate the accelerator. The control system has been equipped with the self diagnostic features for quick finding of faults in the failed subsystem. This feature reduces the down time of the accelerator by giving type and location of fault hence helps in quick recovery of the accelerator.

All the PLCs of the various subsystems are connected to the main PLC. All the subsystem PLCs, operate their subsystems in the desired sequence in the pre-defined control flow. All the operate/control trip limits are set by the operator. Each of the subsystem PLC reports about the current state of operation to the main PLC. The main Master PLC initiates the inter-PLC operation based on its program to start the next subsystem operation when the previous stage operation gets over. For example after the desired vacuum has been achieved in the system the electron gun can be started. All these operations are performed automatically by the control system. The failure of any subsystem is reported on the control panel for the notice of the operator.

The control panel has three levels of control privileges as ‘Engineer’, ‘Supervisor’ and ‘Operator’ in their decreasing order of privileges. There are three login password based on the type of privileges. Log-in as an ‘Engineers’ allows the user to access/modify all the information related to each of the subsystem. Engineer also has the freedom to operate all the subsystem in manual mode instead of predefined sequence. This operator (Engineer) also has the privilege to bypass certain soft interlocks. This helps him in modifying the process or debugs the system fault. Login as supervisor allows him to access all the information related to accelerator operation, fault timings, system fault locations etc but he cannot modify the process or bypass any interlock. Operator login has only one mode of operation ‘AUTO MODE’. The Auto mode is also called as ‘operator mode’ of operation. This is the simplest mode of operation designed for the regular operation of the accelerator. In auto mode operation, the operator has to set the desired accelerating voltage and current and press start button. The control system starts the mains stabilizer to energize all the power supplies. Switches ON the electron gun filament then waits for it to heat up. Starts the HVDC supply and set the accelerating voltage to the set value by making incremental changes in the HVDC. When the set accelerating voltage is reached, the ‘Accelerator Ready’ is displayed’ on the HMI. During the automatic operation when any type of severe fault occurs say high voltage arc fault or over heating fault occurs, the accelerator high voltage is tripped automatically besides displaying and

* vijay9819420563@gmail.com

ISBN 978-3-95450-125-0

DESIGN AND SIMULATION OF A NEW FARADAY CUP FOR ES-200 ELECTROSTATIC ACCELERATOR

E. Ebrahimibasabi, S.A.H. Feghhi, M. Khorsandi, Department of Radiation Application, Shahid Beheshti University, Tehran, Iran

Abstract

Faraday Cups have been used as diagnostic tools to measure the charged particle beam current directly. Up to now, different designs have been introduced for this purpose. In this work, a new design of Faraday Cup has been performed for ES-200 accelerator, a proton electrostatic accelerator which is installed at SBU. FC's dimensions and desirable material have been considered Based on the ES-200 beam characteristics (maximum energy of 200 keV and maximum current of 500 μA). Thickness and dimensions of FC has been calculated by SRIM and MCNPX codes according to the range of proton and induced electrons. The Appropriate FC geometry specifications have been simulated by using CST Studio package. In addition, the heat power generated by proton collision with FC material has been calculated analytically and then required cooling system has been designed by ANSYS. The results showed that the new designed Faraday Cup has a good performance to measure the proton beam current in ES-200 ion accelerator.

INTRODUCTION

An electrostatic accelerator is a type of accelerator that uses static electric field to accelerate charged particles. ES-200 is a 200 keV electrostatic proton accelerator at Shahid Beheshti University (SBU), which has four main components as shown in Fig (1). In this accelerator; RF ion source is positioned inside the high voltage terminal and injects protons into the accelerating tube. A variable high voltage is used to create a 200 kV potential difference between the ion source and the high voltage terminal. Within the accelerating tube is a strong uniform electric field which accelerates protons toward the target. The vacuum system lowers the pressure of the accelerating tube down to at least 10^{-5} Torr to ensure that the accelerated protons have no interaction with air molecules and energy loss [1]. This machine will require ultra-sensitive instrumentation for its proper operation. So a new design of Faraday Cup (FC) will be considered to do more precise measurement of accelerator beam current.

DESIGN CONCEPTS

FCs are used as a destructive instrument, which can provide accurate information on the beam current in a very straightforward manner [2]. Designing proper cooling system, determining the optimal dimensions of a FC and backscatter loss reduction techniques (including: Geometry-based techniques, Electromagnetic techniques, and using of a low-Z material) are a number of issues that need to be considered for designing a FC [3].

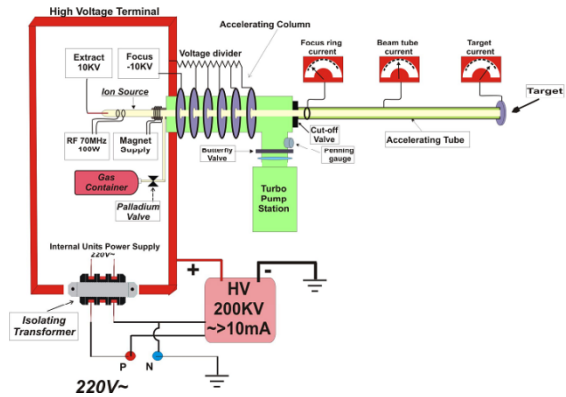

Figure 1: Electrical Schematic of 200keV Electrostatic System [1].

As is shown in Fig (2) heavy charged particles such as proton interact with matter primarily through coulomb forces between their positive and negative charge of the orbital electrons within the absorber atoms [4]. Although nuclear interaction of the charged particle with material (as in Rutherford scattering) is also possible at high energies, but because of the low energy of proton beam in ES-200, forward and backward distribution of electrons due to nuclear interactions could not be possible. The energy spectrum of the secondary electrons, has a peak at a few eV with a spread at half height of the same order of magnitude, thus about 80-95% of emitted particles are below 100 eV [5]. This behaviour may indicate that the emission of low-energy electron is indeed due to the cascade process. High-energy part of the spectrum reflects the direct energy transfer process from the impinging ion to an electron within the matter.

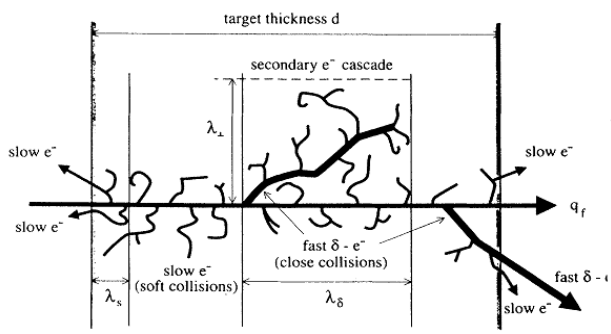

Figure 2: Ionization of the mater by ions and process of electron emission [6].

ISBN 978-3-95450-125-0